MODELLING AND MEASUREMENTS ON A CONDENSING COUNTER-FLOW HEAT EXCHANGER

MAHDI BIN ABDUL WAHAB

Doctor of Philosophy

THE UNIVERSITY OF ASTON IN BIRMINGHAM

June 1989

THE UNIVERSITY OF ASTON IN BIRMINGHAM

MODELLING AND MEASUREMENTS ON A CONDENSING COUNTER-FLOW HEAT EXCHANGER

MAHDI BIN ABDUL WAHAB

Thesis submitted for degree of Doctor of Philosophy

1989

THESIS SUMMARY

Experimental investigations and computer modelling studies have been made on the refrigerant-water counterflow condenser section of a small air to water heat pump. The main object of the investigation was a comparative study between the computer modelling predictions and the experimental observations for a range of operating conditions but other characteristics of a counterflow heat exchanger are also discussed.

The counterflow condenser consisted of 15 metres of a thermally coupled pair of copper pipes, one containing the R12 working fluid and the other water flowing in the opposite direction. This condenser was mounted horizontally and folded into 0.5 metre straight sections. Thermocouples were inserted in both pipes at one metre intervals and transducers for pressure and flow measurement were also included. Data acquisition, storage and analysis was carried out by a micro-computer suitably interfaced with the transducers and thermocouples.

Many sets of readings were taken under a variety of conditions, with air temperature ranging from 18 to 26 degrees Celsius, water inlet from 13.5 to 21.7 degrees, R12 inlet temperature from 61.2 to 81.7 degrees and water mass flowrate from 6.7 to 32.9 grammes per second.

A fortran computer model of the condenser (originally prepared by Carrington[1]) has been modified to match the information available from experimental work. This program uses iterative segmental integration over the desuperheating, mixed phase and subcooled regions for the R12 working fluid, the water always being in the liquid phase. Methods of estimating the inlet and exit fluid conditions from the available experimental data have been developed for application to the model.

Temperature profiles and other parameters have been predicted and compared with experimental values for the condenser for a range of evaporator conditions and have shown that the model gives a satisfactory prediction of the physical behaviour of a simple counterflow heat exchanger in both single phase and two phase regions.

Keywords: condenser, counter-current, heat transfer, heat pump, model

ACKNOWLEDGEMENTS

I would like to thank the followings:

Firstly, to Mr.George Pearce for supervision, encouragement, guidance and much advice.

Secondly, to Dr.Paul Cooper, Mr.Mike Wrenn, Dr.Roy Andrew Summers and Dr.David Hetherington for all useful criticisms, suggestions, encouragement and interest shown throughout the course of this project.

Thirdly, to Mr.Howard Arrowsmith, and Mr.Dick Blunt, the workshop technicans for their help in the early stage of this project. Mr.Andrew Abbot and Mr.R.Bassi, the technicans for their help and guidance in technical work.

Fourthly, Universiti Pertanian Malaysia and Malaysian Public Service Department (JPA) for their financial support throughout the course and stay in England. Malaysian Student Department in London (MSD) for the service and coordination.

Finally, to my wife Halimah, my daughter Masleena, and my sons Hadzrin, Hadzron and Haikal for their support, understanding and sacrifice throughout the last four years.

LIST OF CONTENTS

LIST OF TABLES

LIST OF FIGURES

LIST OF PHOTOGRAPHS

NOMENCLATURE

Symbol	Descriptions and quantities	Units
A	Cross-sectional area	m^2
A_l	Cross-sectional area of liquid flow	m^2
A_r	Cross-sectional area of the freon pipe	m^2
A_v	Cross-sectional area of vapour flow	m^2
A_{wr}	Cross-sectional area of the water pipe	m^2
a	External acceleration	ms^{-2}
a	Calibration coefficients for temperature and pressure	-
C	Constant in Blasius-equation for friction factor in Eqn.2.52	-
C_p	Specific heat at constant pressure	J/(kg.°C)
C_{pr}	Specific heat of freon	J/(kg.°C)
C_{pwr}	Specific heat of water	J/(kg.°C)
COP	Coefficient of performance	-
D	Internal pipe diameter or average diameter of the fluid flow	m
D_l	Average diameter of liquid flow	m
D_v	Average diameter of vapour flow	m
dz	Thickness shown in Fig.2.2.1	m
E_{inb}	Condenser energy inbalance, where $E_{inb} = Q_{freon}-[Q_{water}+Q_{loss}]$	W
F	Force	N
F_f	Shear stress due to frictional effect	$N.m^{-2}$
F_g	Shear stress due to gravitational effect	$N.m^{-2}$
F_l	Shear stress in liquid state	$N.m^{-2}$
F_m	Shear stress due to momentum effect	$N.m^{-2}$
F_o	Wall shear stress	$N.m^{-2}$
F_v	Shear stress in vapour side	$N.m^{-2}$
f	Friction factor, $f=\Delta P(D.\rho/2.G^2.L)$	-
f_{la}	Friction factor in laminar flow	-
f_{lost}	Overall percentage of heat lost from condenser	%
f_p	Pressure correction factor defined in Eqn.4.13	bar

f_t	Temperature correction factor defined in Eqn.4.11	°C
f_{tu}	Friction factor in turbulent flow	-
G	Mass velocity, G=(m/A)	$kg.s^{-1}.m^{-2}$
Gr	Freon mass velocity, Gr=(mr/Ar)	$kg.s^{-1}.m^{-2}$
Gw	Water mass velocity, Gw=(mw/Aw)	$kg.s^{-1}.m^{-2}$
g	Gravitational acceleration	ms^{-2}
H	Convective heat transfer coefficient	$W/m^2.°C$
HR	Freon convective heat transfer coefficient	$W/m^2.°C$
HW	Water convective heat transfer coefficient	$W/m^2.°C$
h	Specific enthalpy	J/kg
h_f	Specific enthalpy of liquid component	J/kg
h_{fg}	Latent heat of vapourization or condensation	J/kg
h_g	Speciic enthalpy of vapour component	J/kg
hr	Specific enthalpy of freon	J/kg
hw	Specific enthalpy of water	J/kg
I,i	Line numbers used in model, (I from 1 to 152)	-
Idr	Internal diameter of the freon pipe	m
Idw	Internal diameter of the water pipe	m
J	Defined in Eqn.2.74,[97]	-
j_g	Dimensionless gas velocity defined in Eqn.2.41	-
k^+	Dimensionless height, $k^+=(\varepsilon.u_z)/\nu$ in Eqn.2.26	-
L	Length of condenser	cm,m
L_i	Length between the measured points outside the condenser and condenser last point, defined in Eqn.4.10 and Fig.4.5.1	cm,m
L_{in}	Length, measured at the freon entry between the measured pressure point outside the condenser end and the inlet effective point, defined in Eqn.4.12	cm,m
L_{nth}	Length between the two point, i->(i+1)	cm,m
L_{out}	Length measured at the freon exit between the measured pressure point outside the condenser and the effective point, Eqn.4.12	cm,m cm,m
Mom	Momentum	$kg.m.s^{-1}$
$\dot{m}$	Mass flowrate	gs^{-1},kgs^{-1}
$\dot{m}r$	Freon mass flowrate	gs^{-1},kgs^{-1}
$\dot{m}_l$	Liquid mass flowrate	gs^{-1},kgs^{-1}

$\dot{m}_v$	Vapour mass flowrate	gs^{-1}, kgs^{-1}
$\dot{m}_W$	Water mass flowrate	gs^{-1}, kgs^{-1}
Ntu	Number of transfer units	-
Ntu_r	Number of transfer units for freon side	-
Ntu_{wr}	Number of transfer units for water side	-
Odr	Freon outer pipe diameter	m
Odw	Water outer pipe diameter	m
P	Pressure	bar
$P_{o,cond}$	Measured pressure at the point outside the condenser, Eqn.4.12 and Fig.4.5.1	bar
PR	Pressure for freon side	bar
PT	Pressure or pressure transducer	bar
PW	Pressure for water side	bar
Q	Quantity of heat per unit time	W
$\dot{Q}_{freon}$	Total thermal power rejected by freon from condenser	W
$\dot{Q}_{lost}$	Thermal power loss from condenser	W
$\dot{Q}_{water}$	Total thermal power picked-up by water	W
q	Quantity of heat being transfered	Js^{-1}
R	Pipe radius	m
R_i	Inside radius of pipe	m
R_{ir}	Inside radius of the freon pipe	m
R_{iw}	Inside radius of the water pipe	m
R_o	Outside radius of pipe	m
R_{or}	Outside radius of the freon pipe	m
R_{ow}	Outside radius of the water pipe	m
RT	Room temperature or thermocouple for sensing room temperature	°C
r	Elemental radius or radial distance from rotation axis	m
r_o	Volumetric radius	m
S	Circumference	m
S_l	Circumference in liquid side	m
S_v	Circumferemce in vapour side	m
s	Specific entropy	J/(kg.°C)
T	Temperature	°C
$T_{o,cond}$	Measured temperature at the points outside the condenser, Eqn.4.10 and Fig.4.5.1	°C
Th_{wall}	Thickness of the pipe	m

TR	Freon temperature	°C
TW	Water temperature	°C
$TW_{m,exit}$	Water outlet temperature measured manually	°C
t	Time	s
U	Velocity	ms^{-1}
U_L	Overall heat transfer coefficient	W/m.°C
$U_{L,12}$	Overall heat transfer coefficient from point 1 to point 2, defined in Eqn.5.23	W/m.°C
$U_{L,23}$	Overall heat transfer coefficient from point 2 to point 3, defined in Eqn.5.23	W/m.°C
$U_{L,34}$	Overall heat transfer coefficient from point 3 to point 4, defined in Eqn.5.23	W/m.°C
$U_{L,45}$	Overall heat transfer coefficient from point 4 to point 5, defined in Eqn.5.23	W/m.°C
u or u_{mean}	Fluid velocity	ms^{-1}
u_l or U_l	Liquid velocity	ms^{-1}
u_m	Mean velocity	ms^{-1}
u_t	Friction velocity, $u_t=(\tau_w/\rho)^{1/2}$, defined in Eqn.2.21 and Eqn.2.22	-
u_v or U_v	Vapour velocity	ms^{-1}
u_{vi}	Vapour velocity at the vapour liquid interface	ms^{-1}
u_z	Velocity in the direction of z	ms^{-1}
u^+	Dimensionless velocity, $u^+=(u/u_t)$	-
V	Voltage	mV,V
V	Volume	m^3
V_{wr}	Volume of water	cc,m^3
v	Specific volume	m^3/kg
$\dot{V}_{wr}$	Water volumetric flowrate	cc/s,m^3/s
W	Work done	J,kJ
W_o	Weight of empty measuring cylinder	g,kg
W_{o+wr}	Weight of empty container plus weight of water	g,kg
W_{wr}	Weight of water	g,kg
X	Dimensionless Martinelli-parameter	-
x	Dimensionless vapour quality or quality	-
x_e	Dimensionless exit vapour fraction, Eqn.5.35	-
x_i	Dimensionless inlet vapour fraction, Eqn.5.35	-
x_m	Average quality at the inlet and exit of the test-section, eqn.2.56	-
x^+	Dimensionless $x^+=(1/Gz)$ defined in Eqn.2.13	-

y	Distance shown in Fig.2.2.4(a), or cartesian coordinate across the flow cross-section distance measured from the pipe wall	m
y^+	Dimensionless distance, $y^+=(y.u_t/v)$	-
z	Length in the direction of freon flow or location in the condensing length	m
Δf_p	Error in f_p	bar
Δf_t	Error in f_t	°C
Δh	Difference in the specific enthalpy	J/kg
Δhr	Difference in the freon specific enthalpy, $\Delta hr=(h_{g,1}-h_{f,16})$	J/kg
Δhw	Difference in the watter specific enthalpy, $\Delta hw=(hw_1-hw_{16})$	J/kg
Δmw	Error in water mass flowrate, mw	gs^{-1}, kgs^{-1}
ΔP	Difference in pressure or pressure drop	bar
ΔP_l	Pressure drop for liquid flow alone	bar
ΔP_v	Pressure drop for vapour flow alone	bar
ΔPR	Pressure drop in the freon side	bar
ΔPT	Pressure drop between two points outside the condenser, Eqn.4.12 or pressure transducer	bar
ΔPW	Pressure drop in the water side	bar
$\Delta(\Delta P)$	Error in the pressure drop	bar
$(\Delta P/\Delta z)$	Pressure gradients or pressure drop per unit length	bar/m
$(\Delta P/\Delta z)_l$	Pressure drop per unit length due to liquid flowing alone	bar/m
$(\Delta P/\Delta z)_{tpf}$	Pressure drop per unit length in two-phase flow	bar/m
$(\Delta P/\Delta z)_v$	Pressure drop per unit length due to vapour flowing alone	bar/m
ΔT	Difference in temperature	°C
ΔT_j	Difference between temperature at point outside and inside the condenser, Eqn.4.10 and Fig.4.5.1	°C
ΔT_m	Log mean temperature difference	°C
ΔTR	Difference in the freon temperature	°C
ΔTW	Difference in the water temperature	°C
Δt	Error in time, t	s

ΔW_{wr}	Error in measuring the weight of water, W_w	g,kg
Δx	Distance shown in Fig.5.4.2(a)	m
Δz	Elemental length or the length between point i and point (i+1)	m

<u>Dimensionless symbols</u>

Gz	Graetz number, $Gz=(Re.Pr.D)/L$	
Nu	Nusselt number, $Nu=(H.D/\kappa)$	
Pr	Prandtl number, $Pr=(\rho.u.D)/\mu = (\nu/\alpha) = (\mu.Cp/\kappa)$	
Re	Reynolds number, $Re=(G.D/\mu) = (D.u/\nu)$	
Re_{d+}	Reynolds number based on displacement thickness, δ^+, $Re_{d+}=(\delta^+.u/\nu)$	
Re_ε	Reynolds number based on pipe roughness, ε, $Re_\varepsilon=(\varepsilon.u_t/\nu)$	
Re_l	Reynolds number based on the liquid portion of the two-phase flow, $Re_l=G(1-x)D/\mu_l$	
Re_{ro}	Reynolds number based on r_o, $Re_{ro}=(r_o.u/\nu)$ defined in Eqn.2.26	
Re_v	Reynolds number based on the vapour portion of the two-phase flow, $Re_v=(G.x.D)/\mu_v$	
Re_z	Reynolds number based on distance z defined in Eqn.2.26, $Re_z=(z.u)/\nu$	
St	Stanton number, $St=Nu/(Re.Pr)$	
St^+	Stanton number, $St^+=H/(\rho_l.u^+.Cp_l)$	

<u>Greek symbols</u>

α	Void fraction	-
α	Thermal diffusivity, $\alpha=(\kappa/\rho.Cp)$	m^2s^{-1}
β	Fluid viscosity-temperature parameter defined in Eqn.2.73	^oK
δ	Thickness of the laminar sublayer or thickness of liquid film in two-phase flow	m
δ^+	Dimensionless thickness defined in Eqn.2.26 and Eqn.2.38	
ε	Roughness elements of the pipe or pipe roughness	-
ε	Heat exchanger effectiveness (dimensionless)	-
ε_H	Thermal eddy diffusivity (or eddy conductivity) and ε_H analogus to thermal diffusivity, α	m^2s^{-1}

ε_M	Eddy diffusivity of momentum (or eddy viscosity) and analogus to kinematic viscosity	$m^2 s^{-1}$
ε_r	Effectiveness of the freon side	-
ε_{wr}	Effectiveness of the water side	-
θ	Dimensionless temperature defined in Eqn.2.66 and Table 2.7	-
κ	Fluid thermal conductivity	W/m.°C
κ_{bond}	Thermal bonding conductance for copper	W/m.°C
μ	Dynamic viscosity	kg/m.s
ν	Kinematic viscosity, $\nu=(\mu/\rho)$	$m^2 s^{-1}$
ρ	Fluid density	kgm^{-3}
τ_o	Shear stress defined in Eqn.5.39	$N.m^{-2}$
τ_w	Wall shear stress	$N.m^{-2}$
φ	Angle that flow vector makes with horizontal	°
Φ	Function depending on Martinelli-parameter, X correlating two-phase ΔP (dimensionless)	-
Φ_l	Function depending on X, if liquid flowing alone in two-phase region (dimensionless)	-
Φ_v	Function depending on X, if vapour flowing alone in two-phase region (dimensionless)	-

<u>Short form</u>

ADC	Analogue-digital converter
AS	Optical sensor for air speed measurement
CH	Channel number in ADC
CN	Channel number used in data acquisition program
DCCC	Double coupled counter-current flow condenser
DN	Device number used for ADC
FF	Freon flowrate sensor
FID	Fixed input data
FRO	Full range output used in ADC
FV	Frequency-voltage converter
HP	Heat pump
IEEE	Institute of Electrical and Electronic Engineers
IRJ	internal reference junction
LM	Lockhart-Martinelli correlation
OR	Order of reading during Run, Fig.4.4.1
PKN	Prandtl-Karman-Nikuradse correlation

PROC	Procedure statement in BASIC language
R11	Trichloromonofluoromethane
R12	Dichlorodifluoromethane
R22	Chlorodifluoromethane
TEV	Thermostatic expansion valve - heat pump component
TS	Thermocouple
VID	Variable input data
WF	Water flowrate sensor
WM	Optical sensor for Watt-meter measurement

<u>Subscripts</u>

a	point shown in Fig.4.5.1, Fig.5.2.5 and defined in Eqn.4.10
b	bulk condition or point shown in Fig.4.5.1, Fig.5.2.5 and defined in Eqn.4.10
bend	180°-bend pipe condition
bond	bonding used for κ_{bond} of the pipe
c	critical condition or point shown in Fig.5.2.5
cond	condensing condition or condensing region
cp	constant-property condition
desup	desuperheating region
dew	dew condition used in temperature
diff	difference
ε	at the pipe roughness condition
e	condenser exit condition
eff	effective condition
evap	evaporating condition
exit	exit condition
f	frictional effect
f	liquid component condition in two-phase flow
fg	liquid and vapour component in two-phase flow
fs	free stream flow condition
g	gas component condition in two-phase flow
g	gravitational effect
higher	higher condition in Eqn.2.1
i	number 0,1,2,3,.... or position at the test-sections concerning TR,TW,PR and PW
i	condenser inlet condition, Eqn.5.19
in	inlet condition

ir	inside of the freon side
iw	inside of the water side
L	based on length used in overall heat transfer coefficient
l	liquid condition or liquid component of two-phase flow
la	laminar
li	liquid condition at the vapour liquid interface
liq	liquid
lnth	between the two consecutive points
lower	lower condition in Eqn.2.1
m	momentum effect
m	mean or average value
max	maximum
min	minimum
n	numbers defined in Eqn.4.2
o	outside, defined in Eqn.5.19
or	outside of the freon side
out	outlet condition
ow	outside of the water side
R or r	freon condition
r	given by Deissler and Prester in Table 2.7
ref	reference
s	smooth condition
sat	saturated condition
st	straight
sub	subcooling-region
tpf	two-phase flow condition
tran	transition flow condition
tt	turbulent liquid and turbulent vapour
tu	turbulent
tv	turbulent liquid and viscous or laminar vapour
v	vapour component in two-phase flow
v or vap	vapour or gas condition
vi	vapour condition at vapour-liquid interface
vt	viscous or laminar liquid and turbulent vapour
vv	viscous or laminar liquid and viscous or laminar vapour
W or wr	water
w or wall	at wall condition
x	at vapour quality condition
z	in the direction of z-axis or direction of freon flow

Superscripts

a	exponent
b	Blasius exponent defined in Eqn.5.28 or other exponent
m, n	exponents

CHAPTER 1

INTRODUCTION

1.1: General introduction

The thesis consists of seven chapters, divided between three major sections; a literature survey (including heat transfer and pressure in chapter 2), the main project research including the heat pump system (equipment and system operations in chapter 3 and 4), and computer model application including experimental results and predictions (chapter 5 and chapter 6).

In this chapter, a general view of the literature surveys, programmes of work and objective of the research is presented. The final chapter discusses the overall conclusions from the results, and further suggestions for future work are also included. A brief outline of each chapter will be presented later in the chapter.

In summary, the primary concern of the research is to test the model devised by Carrington,[1] concerning a laboratory freon to water heat pump condenser. The condenser comprises of a 15 meter long double-pipe, thermally coupled, in which freon and water flow in opposite directions. The physical properties of the working fluids (temperatures and pressures) are detected by the sensors which are placed at various test-points. The thermocouples for sensing both of the fluid temperatures are fixed, opposite each other at one meter intervals, while four pressure transducers are placed at the inlet and at the exit of the heat pump evaporator and condenser. The pressure transducers which are fixed at the inlet and outlet of the condenser are of prime importance in this project. The third primary parameter is the water mass flowrate which is measured manually.

These parameters are the basis for calculating secondary parameters including the thermodynamic and other physical properties of the fluids, performance of a counter flow heat exchanger, and other thermodynamic and physical behaviour of the flow during the process.

Heat transfer and pressure drop processes are the main issues highlighted in the research, which can be considered as the effect of the single-phase and two-phase flow. These effects are represented and correlated in terms of dimensionless Nusselt number and friction factor respectively, adapted from established findings, with some modifications to suit the present situations.

A numerical method for integration is used to calculate the fluid temperatures at the test-points by dividing the heat exchanger into 150 segments of equal length of 0.1 meter, which corresponds to a total length of 15 meter. From here, other parameters at the test-points (pressure, vapour quality, heat transfer coefficient and wall temperature) can be predicted. The temperature distribution over the 15 meter long condenser can be directly compared with the temperature profile predicted by the model.

A brief outline of each chapter follows.

1.1.1: Chapter 1

In this chapter, a general idea of the thesis covering the programme of the research, literature reviews and the aim of this project is briefly presented.

A general picture of the research, including the experimental work, data-acquisition system and data analysis. Sets of experimental data are used as the basis to test the model at particular operating conditions.

1.1.2: Chapter 2

A literature survey was focused on the heat transfer and pressure phenomena in both single-phase and two-phase flow regimes, which are separately discussed in brief in the chapter.

Convective heat transfer is the study of heat transport processes between the layers of a fluid when the fluid is in motion, or between a fluid in motion and a boundary surface in contact with it, when they are at different temperatures. In fact, heat flow is a vector in the sense that it is in the direction of the negative temperature gradient (from higher to lower temperatures). The science of heat transfer is based upon the foundations comprising both the theory and experiment.

The pressure drop for fluid flow in smooth (for laminar flow) and rough (for turbulent flow) circular tubes (greatly influenced by the friction factor which is normally determined experimentally), is also presented in this chapter.

The final part of the chapter discusses the reviews which correlate the effect of temperature-dependent properties upon the Nusselt numbers and friction factors of a single-phase fluid flow. For liquid, the ratios (Nu/Nu_{cp}) and (f/f_{cp}) are empirically correlated to the ratio of bulk fluid viscosity to the fluid viscosity at the wall (see Eqn.2.62). For vapour, the correlation is with temperature ratio rather than viscosity (see Eqn.2.63).

In the model, these correlations, with minor modifications to suit the present system are applied to evaluate heat transfer and pressure parameters.

1.1.3: Chapter 3

A laboratory air to water heat pump system is discussed in general. It comprises four major components (a reciprocating compressor, a 15 meter-long double-coupled condenser, an evaporator and a thermostatic expansion valve). In addition, the miscellaneous components such as water regulator, sight glass, pressure system analyser, fan and refrigerant filter drier attached to the system are also discussed.

The chapter mainly explains the work done on the system which can be classified as follows:

1.System: 35 thermocouples, 4 pressure transducers, 2 flowrate sensors, and 2 opto-switches for sensing air speed through an evaporator and power consumption are used in the system. Each of the last four sensors were connected to frequency-voltage converters before connecting to an analogue-digital converter. The details of the lay-out of these sensors are explained in this chapter.

2.Analogue-digital converter: Two types of analogue-digital converters (two of PCI 1001 versions and one of PCI 1002 version), each supplied with 16 channels (each channel provided with its own operational amplifier) were used in the system. Analogue signals from the sensors are converted to digital form. An IEEE interface was used to communicate with the computer system for acquiring data.

3.Computerized data-acquisition system: A personal BBC computer was employed to store data on floppy disc and to display data on screen.

1.1.4: Chapter 4

The experimental procedure and data analysis is discussed in this chapter.

The first part of the chapter explains the transducer calibration. It also discusses the conversion of ADC bits to temperature and pressure. Over 25 sets of calibrating-experiments (thermocouples and pressure transducers) and over 50 sets of heat pump test-experiments using R12 as a working fluid have been carried out before considering the final set of data.

Over 100 Runs have been recorded in the range of 7.58-12.32 bar for freon pressure, 60.2-81.7 ^{o}C for freon inlet temperature, 13.2-21.7 ^{o}C for water inlet temperature and 6.72-32.86 gs^{-1} for water mass flowrate. The condenser outer pipe diameter for freon and water flow is fixed at 5.75 mm and 7.65 mm respectively. Only 68 Runs with operating conditions 7.63-12.14 bar for freon inlet pressure, 61.2-81.7 ^{o}C for freon inlet temperature, and 6.72-32.86 g/s for water mass flowrate had been recorded in the thesis.

Water mass flowrate was measured manually and was used to calculate freon mass flowrate using the condenser energy balance equation.

The second part of the chapter discusses the analysis and evaluation of the experimental data. An effective value of the inlet and outlet temperature and pressure for each Run (estimated by the linear extrapolation method), was used as input data to initiate the calculation in the model. The errors made during the measurements, and the experimental problems encountered are also described.

1.1.5: Chapter 5

A counter flow heat exchanger model in which freon and water flow in opposite directions in two pipes coupled together, proposed by Carrington,[1] is used to predict the heat transfer and pressure drop parameters in the single-phase and two-phase flow regimes. These parameters are then used to predict other fluids properties over a length of condenser.

The details of the model are described, consisting of the following items; a numerical integration and iteration programme (main program), input data, output results, and subroutines for calculating heat transfer coefficient, pressure drop and thermodynamic and physical properties of the fluids (corresponding to the particular flow mechanism).

Empirical correlations used in the model are adapted from various investigators, with some modifications to suit the present system. In the single-phase flow, the correction factors analysed from the temperature-dependent fluid properties and the influence of pipe roughness are considered to evaluate the Nusselt number and friction factor. Laminar, transitional and turbulent flow are treated separately.

An annular flow model for condensation inside a long tube is considered in the two-phase region to determine the Nusselt number based on the Martinelli-parameter. The Lockhart-Martinelli method for predicting two-phase pressure drop in turbulent-turbulent case is applied.

1.1.6: Chapter 6

In this chapter, experimental and predicted results are presented and discussed. The main discussion compares the temperature distribution along the condenser tube, measured in the experiment, to that predicted by the model. Variation of pressures, fluid mass flowrates and temperatures at given conditions, with freon inlet pressures are also explained.

The results predicted by the model, including the fluid thermodynamic and physical properties in three separate regions (subcooling region, condensing region and desuperheating region), and other profiles (pressure, quality, water and freon linear heat transfer coefficient, and overall heat transfer coefficient) are also described.

Summary of range of evaporator conditions (based on predicted results) is discussed, assuming certain values of isentropic efficiencies. In this section, the possible refrigeration cycle can be predicted by assuming there is no pressure drop across the evaporator, isentropic compression work, and the specific enthalpy at the subcooled liquid is taken to be the same with the specific enthalpy at the evaporator entry (isenthalpic). The final part is to predict the possible coefficient of performance of the heat pump system.

1.1.7: Chapter 7

The final chapter describes the possible conclusions from the research, and the suggestions for future work. Conclusions are made based upon the model within the operating conditions recorded in chapter 6 by considering all possible assumptions explained in chapter 5.

The main objective of this research is to test the model by comparing it with the experimental data. Two very important fields gained from the research, widely used in physical and engineering application are heat transfer and pressure drop, which are greatly application are heat transfer and pressure drop, which are greatly influenced by the Nusselt number and friction factor respectively. Since these parameters are empirically correlated, a careful study to simplify the correlations based on the available data is essential.

To summarize, the following block diagram shows relationships between the chapters (chapter 1 is not included).

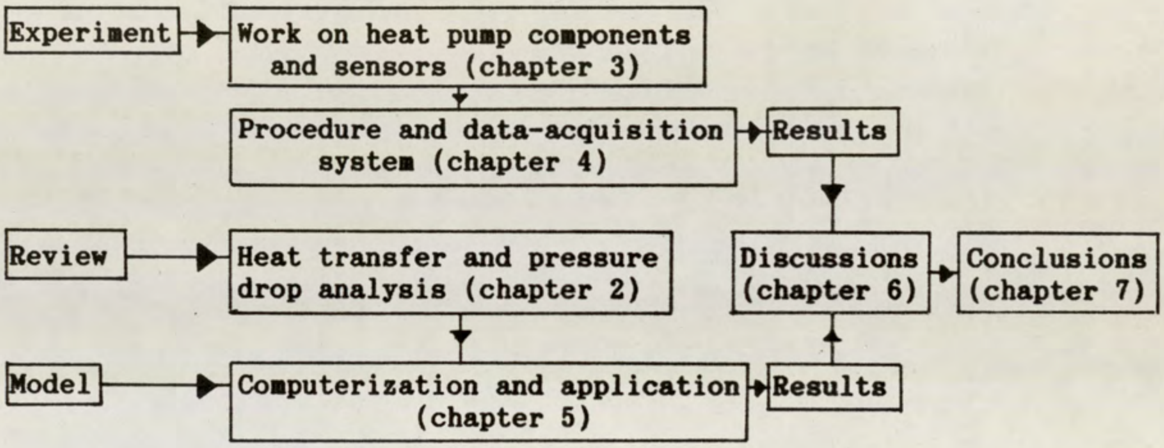

Fig.1.1.1: Relationship between the chapters

1.2: Literature review

The sources of knowledge concerning the present research can be classified as follows:

1.**Text books**: Majority of the reviews were taken from the handbooks, conference papers and edited papers which can be further subdivided to heat pump system, heat transfer and pressure analysis, theoretical and experimental heat exchanger, computer programming, and other auxiliary texts.

2.**Manual,maintenance and manufacturer specifications**: Most of these references are available in chapter 3, where equipments used in the system were supplied by various companies or appointed agents. Some of the important specifications and technical notes were also included in appendices at the end of this thesis.

3.**Papers and journals**: Over 300 papers have been collected, some of which are useful for the present research. The papers are classified as follows; heat pump theory and applications, heat transfer and pressure drop (single-phase and two-phase), and heat exchangers.

Two important sections briefly discussed in general are the heat pump system as the basis for the project and heat transfer in the heat pump condenser as the main research interest.

1.2.1: A brief review of heat pumps

The invention of the heat pump was initially started when the interest of pumping heat to a higher temperature was introduced by Joule,[60]. He demonstrated the principle of changing the temperature of a gas by altering its pressure. The theoretical concept was described by Carnot in 1824 and the following year Thomson,[60,61] was the first to propose a practical heat pump system (he called it heat-multiplier) for cooling and heating of buildings.

Until 1940, the development of vapour compression machines using ether, ammonia, methyl chloride and halocarbon refrigerants as working fluids was in rapid progress. Haldane,[60] was the first to install a heat pump using outside air as a heat source to provide space heating and water heating, where he recommended the use of reversible heat pump.

The oil prices increase in early 1970 led to a rapid growth of interest in heat pump research,[60] including compressor, heat exchanger surface, control system, refrigerants, basic thermodynamic properties, performance, reliability, economic assessements and heat pump in general. Ambrose,[62] has discussed the thermodynamics of the Carnot and Rankine refrigeration cycle,including heat sources, heat sinks, typical configuration and applications, and energy estimation method for heat pump.

Edison Electric Institutes's final report ,[3] has described the effort of improving electric heat pump efficiency and reliability. Hise,[4] has discussed the seasonal performance and provided a critical comment on some of the literature data. The report on the reliability, life cycle cost, market prospects, institutional factors and resource energy efficiency of heat pump for residental and commercial applications is discussed in [5,6].

Finally, it was estimated that, by early 1990, total annual sales will be reaching 2 to 3 million units, especially in Japan and United State of America, for residential and commercial sectors,[7]. For further information on heat pump theory and its applications, see references, [63,64,65,78,79].

1.2.2: Development of heat transfer in general

A knowledge of convective heat transfer (from historical background) can be divided into two periods of time,[9]. Firstly, the foundations for a systematic and coherent body of heat transfer knowledge were laid in 1880-1930, initiated by Osborne Reynolds. Reynolds's studies provide a guideline for the correlation of experimental results in the heat transfer processes until now. The other earlier pioneer in the heat transfer studies is Wilheim Nusselt, who used a knowledge of dimensional analysis and energy transport equations to relate the heat transfer coefficients of an ideal constant property of fluid,

$$H = C(\kappa_w/D)(\rho.u.D/\mu)^m(\mu.C_p/\kappa)^n \qquad \text{Eqn.1.1}$$

where C denotes a constant, κ the thermal conductivity, u the velocity of the fluid, subscript w refers to wall condition, and m and n are the exponents obtained from energy equations.

The second period is between 1930 to 1980, where the contributions were applied to an ever widening variety of situations as new technical developments were encountered. The two earlier investigators associated with this period of time are William H.McAdam, who has collected, screened and correlated the available information on heat transfer processes in his book,[81] in 1933, and Llewellyn M.K. Boelter,[10] in his famous lecture note on 'Heat Transfer Notes' in early 1930,[80].

Raymond Constantine Martinelli (1914-1949) is the man who discovered a well known parameter (Martinelli-parameter) which is widely used as the basis to predict the two-phase pressure drop,[11]. There are a few other pioneer contributors not included in this brief introduction.

1.3: Aim and objective of the research

The main goal of this research is to test the model by comparing it with the experimental data. In this case, the research was focused on the study of a counter flow heat exchanger such as heat pump condenser. The main primary parameters obtained from the experiment that can be directly used for comparison with the model are temperature distribution along the condenser (measured at one meter intervals), water and freon mass flowrate, and freon outlet pressure (measured at the condenser exit). The temperature profiles predicted by the model are more detailed along the condenser axis, because the numerical integration was based upon the 150 point-segments. The predicted temperatures were calculated for every 0.1 meter along the condenser but the results were printed for every 0.2 meter. The results at each meter interval could be compared with the experimental measurements.

Other parameters predicted by the model which cannot be directly compared with the experiment are also studied and discussed. Assuming the basic predicted parameters (for comparison) are in good agreement, a behavioural study of these parameters in a counter flow heat exchanger is important to generalise a conclusion which can be used as a guideline in the study of heat transfer and pressure drop. In this case, the objectives are based upon the following studies:

1. Fluids thermodynamic properties.

2. Counterflow heat exchanger performance.

3. Characteristics of heat exchanger in three regimes (subcooling, condensing and desuperheating).

4. Other secondary parameter profiles such as pressure, quality, number of transfer units and heat transfer coefficients at given operating conditions.

5. Freon and water thermal power during the process from enthalpy and entropy points of view.

It is also possible to predict the refrigeration cycle of the laboratory heat pump system using available parameters calculated in the model. This will help to give a guide for better performance in designing an air-water heat pump system, especially in the industrial sectors, for domestic use.

To achieve those aims, the work is observed from two angles; experiment and model.

1.3.1: Experiment

Following is the list of work done during the research:

1. Sensors: Thermocouples and pressure transducers are carefully designed, calibrated and mounted in the test-sections to give accurate measurements. Various thorough tests, checks and modifications were also carried out to ensure performance, reliability and consistency.

2. Heat pump system: Each of the components in the system had been thoroughly tested and checked before conducting any experiment. The sensors should give a correct measurement at the correct position in the test-sections.

3. Experimental measurements: Data were acquired by means of a computer. It was also important to ensure that correct sets of data were measured at the given operating conditions. In this case, duplicated Runs at approximately the same operating conditions as before were organized for counter checks.

1.3.2: Model

As discussed earlier, the model is based upon the theory of heat transfer and pressure drop in a single-phase and a two-phase flow. The parameters acquired from above phenomenon were used to determine other parameters discussed at the beginning of this section.

The list of work associated with the model is as follows:

1. Review some of the useful literature by previous workers, so that it can be applied to the present model.

2. Modification of the Carrington-model using appropriate correlations to match the experimental data, especially in the calculation of Nusselt numbers and friction factors for various flow regimes.

3. More attention was given to the area of heat transfer and pressure drop in a single-phase and a two-phase flow by considering the effect of fluid temperature-dependent properties, pipe roughness, constant wall temperature and heat flux, boundary conditions, three-layer model in the turbulent flow, and an annular model for condensation inside a long tube.

4. Application of 3 (above) to evaluate other characteristics of the heat pump condenser.

5. Using available data to test the model before storing the final sets of data for analysis.

1.4: Programmes of work

In this section, the whole programme of the research starting from the basic concept of a heat pump system to the model application is outlined. The programme of work is discussed to give a rough idea for the readers to follow what has been done in the research.

It was divided into five categories as briefly listed in the following:

1. Heat pump theory: To gain an understanding and perception of the basic concept of a heat pump (heat pump as a heat-pumping system, thermodynamic characteristics, and the functions of its

components and other auxiliary components), especially an air source heat pump. A practical vapour-compression cycle for refrigeration system is applied to the present laboratory air to water heat pump.

2. Experiment: This concern the study of experimental rig and laboratory heat pump in operations. The experimental data were acquired using data-acquisition system via an analogue-digital converter, an IEEE interface and a personal mini-computer.

3. Computerization: In this case, the computational study was divided into two areas; data-acquisition method where the programme is written in BASIC and computer-modelling where the programme is written in FORTRAN-77. The scope of research was narrowed to the behavioural study of heat transfer and pressure in heat pump condenser, which is applicable to the present experimental rig. Its application is extended to the heat exchanger performance, thermodynamic and physical properties of the fluids at various flow regimes and characteristic and behaviour of a counter flow heat exchanger, and the possible refrigeration cycle by varying range of evaporator conditions.

4. Model: The heat transfer and pressure processes in single-phase and two-phase flow are complicated. The theoretical study including the literature search had been carried out to relate the empirical correlations discovered by previous workers to the present model. It is important to ensure the correct correlations applied to the correct situations and conditions of the present system.

In general, the programme of work in 4 (above) can be subdivided as follows; input data, heat transfer and pressure drop process (the main body of the model), application to other related characteristic of a counter flow heat exchanger and output results.

5. Application and results: An appropriate set of input data, measured in the experiment; freon inlet pressure, freon and water inlet temperature, pipe dimensions (fixed value) and an estimated total thermal power of the freon were used in the model. Different sets of input data were introduced, corresponding to appropriate operating conditions. The predictions of the model for various Runs were then compared with the appropriate experimental data.

CHAPTER 2

HEAT TRANSFER AND PRESSURE DROP ANALYSIS

2.1: Introduction

This chapter mainly explains the heat transfer and pressure drop analysis for single-phase and mixed-phase flow, reviewed from the texts, papers, journals and other sources discovered by other workers. In addition, the effect of the temperature-dependent fluid properties in circular tube flow are also presented.

The application of the analysis will be discussed in chapter 5 where the heat transfer and pressure drop characteristics will be directly used to calculate other related physical and thermodynamic properties of the fluid. These also include the temperature distribution and the effectiveness of the condenser in counter flow.

Basically, heat can be transferred from one place to another, either by interaction with the internal structure of the body (conduction), removal by a fluid (convection), or by radiation. The first two mechanisms to move heat from a higher temperature region to a lower temperature region across a temperature gradient between the points are considered in this thesis. The heat transferred by radiation is negligible. Attention is focused on the macroscopic effects of the heat transfer, its principles and applications to the model.

The heat transfer process can be described by equations which relate the heat energy to be transferred in unit time to various physical properties of the fluids and the system used. Temperature is the most important parameter, heat only flowing when there is a temperature gradient. A knowledge of temperature distribution is essential to design heat exchangers such as the heat pump condenser, which is controlled by the combined effects of the heat transfer mechanisms just mentioned.

The second part of the chapter discusses the pressure distribution in the condenser. In the case of flow in pipes, the research is primarily concerned with the pressure gradients due to the friction and momentum. The pressure gradient due to gravity is assumed to be zero, since the pipe was fixed horizontally. The method of predicting the pressure drop in a straight pipe both in the single-phase and mixed-phase flow is also outlined.

The final part considers the fluids thermodynamic and physical properties to identify the temperature distribution along the condenser tube, performance of the counter flow heat exchanger and other related heat exchanger parameters which will be discussed in chapter 5.

The analysis is based on the counter flow heat exchanger where freon and water flow in opposite directions. If the flow is in the single-phase, the same heat transfer and pressure drop phenomena for both R12 and water using appropriate correlations is applied. On the other hand, if the freon flow is a mixture of liquid and vapour, the analysis in the two-phase flow regime is considered and treated separately from that in the single-phase flow.

Although in practice, the single-phase and two-phase region cannot be separated (they are in one single long tube), for simplicity, the heat transfer problems can only be solved by treating these regions separately. The boundary conditions between each region are also considered to ensure the correct equations are applied to the correct regimes.

In the single-phase region, the types of flow mechanism (laminar, transition and turbulent flow regimes) are also treated separately. The Lockhart-Martinelli (LM) correlation,[12] concerning the pressure drop in the two-phase region is of great importance in the model application.

2.2: Convective heat transfer and pressure drop in a circular duct

In this section, we wish to examine the method of predicting the heat transfer coefficient,H which requires an energy balance along with an analysis of the fluid dynamics. The influence of the flow on the temperature gradients is the key to the determination of heat transfer coefficients.

From Newtons-Law of Cooling, a general equation to describe convective heat transfer,H can be written as,

$$q = H.A(T_{higher}-T_{lower}) = H.A.\Delta T_m \qquad \text{Eqn.2.1}$$

where H varies for different flow regimes, fluid properties and temperature differences. Because of many complexities, the convection problems cannot be easily solved by mathematical correlation. A dimensionless technique along with the experimental correlations is introduced to solve the problems.

The most popular dimensionless parameter to relate the heat transfer processes is the Nusselt number,Nu where H can be related by

$$Nu = H.D/\kappa \qquad \text{Eqn.2.2}$$

where D is the internal pipe diameter and κ is the fluid thermal conductivity.

Many investigators have established empirical correlations of the Nusselt number with other dimensionless groupings such as Reynolds number,Re and Prandtl number,Pr. Some authors have also included the length and the internal diameter of the tube,

$$Nu = f(Re,Pr,D,L) \qquad \text{Eqn.2.3}$$

In single-phase flow, the empirical formula for calculating Nusselt number depends on the types of flow mechanism; laminar, transition and turbulent. It is also influenced by the duct flows; fully developed, hydrodynamically developed, thermally developed and simultaneously developed,[83]. In addition, to interpret the heat transfer problems accurately, the thermal boundary conditions imposed on the pipe wall are essential when treating the singly connected tube in the heat pump condenser.

Looking back at the factors stated above, the heat transfer becomes more complicated to solve. The heat transfer empirical correlations presented in the model are adapted from various authors findings by considering all possible conditions described above related to the experimental condenser.

The heat transfer problems in the two-phase region are far more complicated where the Nusselt number is not only a function of Reynolds number and Prandtl number but also depends on the fluid properties evaluated both in the liquid and vapour by apparently assuming the liquid and the vapour are to flow alone. In this case, the fluid is regarded as flowing separately. A mathematical correlation called Martinelli-parameter,X_{tt} is introduced to relate those properties.

It is difficult to imagine the flow in the liquid-vapour mixture of the two-phase region where in general they do not move at the same velocity. Considering the length of the condenser used in the system is long enough for the flow to become annular, with the vapour occupying the middle of the tube and the liquid layer at the periphery of the wall, an annular model inside a long horizontal tube is employed to determine the heat transfer coefficients.

2.2.1: Single-phase heat transfer and pressure drop

The process of heat transport in a fluid is the combined action of the heat conduction and fluid motion. It involves heat transfer within the layers of a fluid and between the fluid and the wall surface of the pipe when they are in contact. The flow mechanism is influenced by the diffusion and the transport of thermal energy via fluid motion.

The fluids are said to flow in the single-phase when there is no change in the phase; either purely liquid or vapour. When dealing with such flows, many factors affect the heat transfer; nature of the flow, mechanism of the flow, properties of the fluids, ducting systems, flow arrangement and heat transfer mechanism. These factors can be summarized in Table 2.1.

Factors	Remarks
Nature of flow	Steady- and unsteady-compressible flow and steady- and unsteady-incompressible flow.
Mechanism of flow	Laminar, turbulent and transition flow.
Fluid properties	Constant- and variable-property of the fluid.
Ducting systems	a. <u>General features</u> Straight or non straight piping system. The cross-section; circular, rectangular, flat, triangular, elliptical, square and annular (both concentric and eccentric). b.<u>Transfer process</u> Direct or indirect contact type with the compact or non-compact surface. c. <u>Construction</u> Tubular, plate, extended surface and regenerative. These included double-pipe, shell-and-tube, spiral tube, plate fin, tube-fin and rotary.
Flow arrangement	Single-pass and multi-pass; counter, parallel and cross flow in the single-pass.
Heat transfer mechanism	Single-phase convection on both sides and one side, two-phase convection on other side and both sides,and combination of convection and radiation.

Table 2.1: Factors affecting the heat transfer

Based on **Table 2.1**, the transfer processes encountered (in the model) in single-phase flow are steady-compressible, constant wall temperature and heat flux, constant and variable property of Newtonian fluid which is temperature-dependent, all possible flow mechanisms, smooth and rough pipe (smooth for laminar flow and rough for turbulent flow), counter flow of the fluids in direct contact and the single-phase convection on both sides of the tube.

Having summarized the heat transfer process, the next step is to investigate the flow mechanism involving the laminar, transition and turbulent regimes by considering the effect of fluid properties which can be represented by mathematical expression.

Laminar flow at constant property

a. Pressure drop

To evaluate the model pressure drop, one should investigate the velocity distribution in a fully developed laminar flow. For a long pipe at steady flow and fully developed velocity distribution, there is a pressure differential sufficient to balance the viscous resistance.

Considering a fluid elemental radius, r ($r<R$) and the thickness of dz as shown in Fig.2.2.1, the viscous and pressure forces are balanced if (assuming the pressure gradient is constant),

$$(\partial u/\partial r) = (1/2\mu)(dP/dz).r \qquad \text{Eqn.2.4}$$

On integration and then taking boundary conditions at $u=0$ and $r=R$ (at the pipe wall), we obtain

$$(u/u_{mean}) = 2[1-(r/R)^2] \qquad \text{Eqn.2.5}$$

where $u_{mean} = -(1/8\mu)(dP/dz)R^2$. Eqn.2.5 is known as the Hagen-Poiseuille parabolic profile which can be further rearranged as,

$$-(dP/dz) = (32.u_{mean}.\mu/D^2) \qquad \text{Eqn.2.6}$$

On further integration and taking boundary conditions at $P=P_{z=0}$, $z=0$ and $P=P_{z=L}$, $z=L$, we get the pressure drop per unit length,

$$P_{z=L} - P_{z=0} = \Delta P = (32.u_{mean}.\mu/D^2) \qquad \text{Eqn.2.7}$$

From dimensional analysis for the Reynolds number, Eqn.2.7 can be rearranged in term of Reynolds number,

$$\Delta P = 2(16\mu/D)(1/D)u_{mean} = 2(16\mu/G.D)(G/D)(G/\rho) \qquad \text{Eqn.2.8}$$

where $(\mu/G.D)=1/Re$ and $G=(\dot{m}/A)$. More generally,

$$\Delta P = 2f(G^2/\rho.D) \qquad \text{Eqn.2.9}$$

where $f=(16\mu/G.D)=16/Re$.

At constant mean velocity, with approximately constant pipe internal diameter, as the Reynolds number increases, the friction factor,f is decreased and there is a decrease in the pressure drop. The effect of fluid variable properties in laminar flow will be discussed later in the section.

Bhatti and Shah,[82] have quoted from Churchill regarding the friction factor in laminar flow, the following correlation covering laminar, transition and turbulent regimes,

$$2/f = \{1/[(8/Re)^{10}+(Re/36500)^2]^{1/2} + [2.21Ln(Re/7)]^{10}\}^{1/5} \qquad \text{Eqn.2.10}$$

This equation is in good agreement with the value of f described above but looks a bit complicated.

b. <u>Heat transfer</u>

The heat transfer is evaluated from the temperature profile. At uniform wall temperature, fully developed flow, non dissipative flow in the absence of flow work, thermal energy source and fluid axial condition, Shah and Bhatti,[83] have obtained the laminar Nusselt number as,

$$Nu = 3.657 \qquad \text{Eqn.2.11}$$

which is independent of the Reynolds number and Prandtl number.

In reality, it is possible to include the influence of the entrance effect of a pipe in term of Graetz number,Gz [70], given by Hausen using oil as a working fluid,

$$Nu = 3.657 + \frac{0.0668Gz}{(1+0.04Gz^{2/3})} \qquad \text{Eqn.2.12}$$

where $Gz=(Re.Pr.D/L)$.

Eqn.2.12 can be applied to the case where heating begins beyond the entrance of the tube and velocity profiles become fully developed. It approaches a constant value of 3.657 when the tube is sufficiently long.

On further analysis, Shah and Bhatti,[83] have differentiated Eqn.2.12 with respect to x^+ to study the effect of fluid axial conduction in the Graetz solution, where $x^+=1/Gz$; giving,

$$Nu = 3.657 + \frac{0.0018}{(x^+)^{1/3}[0.04+(x^+)^{2/3}]^2} \qquad \text{Eqn.2.13}$$

It was found that, Eqn.2.12 and Eqn.2.13 give values from 14% higher for $x^+<10^{-4}$, to 0% for x^+ tending to infinity, compared with the values calculated by Shah and London,[66] at circumferentially and axially constant wall temperature (T_w=constant and the wall thermal resistances are negligible).

In the model, Eqn.2.12 was modified by Carrington,[1] for long tube at constant wall temperature to suit the working fluids as,

$$Nu = 3.66 + \frac{0.057Gz}{(1+0.04Gz^{4/5})} \qquad \text{Eqn.2.14}$$

which is slightly less then the value calculated from Eqn.2.12. For a very long pipe, both equations give Nu roughly 3.66. These values are taken as the mean value and the dimensionless grouping in the second term of the equation is evaluated at the bulk temperature.

<u>Transition flow at constant property</u>

As the flowrate increases, the streamline becomes unstable, transition from laminar to turbulence taking place at roughly $Re=2x10^3$. Until now, there is no definite value for the upper critical Reynolds number but most researchers agree, taking lower critical Reynolds number between $2.0x10^3$ to $2.3x10^3$.

Bhatti and Shah,[82] in their reviews, have reported that Reynolds, Lindgren and other investigators had agreed that the transition is not a sudden process but occurs over a range of Reynolds number, starting at the duct core region rather than the duct wall.

The summary of the critical Reynolds number limit in the transition regime is tabulated in Table 2.2.

Investigators	Reynolds number $Re_{c,min}$	$Re_{c,max}$	Observations
Reynolds(1883)	3.8×10^3	1.2×10^4	Verified by other authors but confusing since Re_c covers a range of 2.0×10^2 to 5.1×10^4.
Ekman	-	-	Experimenting Reynolds's work by eliminating all source of disturbances but concluded with no upper critical limit.
Pfenninger	-	1.001×10^5	Confirmed Ekman's finding.
Schiller(1921)	2.32×10^3	-	Accepted Ekman's idea of no upper critical limit.
Simonek	2.295×10^3	-	Agreed with Schiller and other researchers's idea.
Prengle and Rothfus	1.225×10^3	2.5×10^4	Perform a correlation corresponding radial distance from the centre of the tube to the edge of laminar sublayer. As Re goes infinity, the laminar sublayer vanishes.

Table 2.2: Transition critical Reynolds number adapted from some investigators

The Reynolds number between 2.1×10^3 to 7.1×10^3 (inclusive) is used in the present model to represent the flow in the transition regime.

a. Friction factor for pressure drop

The general equations 2.8 and 2.9 are applied to calculate the pressure drop in this region, which is greatly dependent on the friction factor, f.

There have been some attemps to calculate the friction factor for the Reynolds number in the range of 2.3×10^3 to infinity,[82], spanning the laminar, transition and turbulent flow regimes. In their reviews, Wilson and Azad and Barr developed a numerical correlation using Re as a linking parameter but ended with a complex analytical expression. Churchill has developed the correlation in Eqn.2.10 for $Re<2.1\times10^3$ and $Re>4.0\times10^3$ (transition cum turbulent flow), the values are in good agreement with the values solved from Eqn.2.9. The Colebrook-equation for $4\times10^3<Re<10^7$ can be written as,

$$(1/f^{1/2}) = 1.5635\text{Ln}(Re/7) \qquad \text{Eqn.2.15}$$

which is within ±1% of the classical Prandtl-Karman-Nikuradse correlation (PKN). For $2.1\times10^3 \ll Re \ll 4.0\times10^3$, Eqn.2.10 gives a fair agreement with the available experimental data.

The other correlations are listed as follows,

Researchers	Friction factor	Reynolds Numbers	Observations
Hrycak and Andrushkiw	$-3.1\times10^{-3} + 7.125\times10^{-6}Re - 9.7\times10^{-10}Re^2$	2.1×10^3-4.5×10^3	Within +3% to -9% of Eqn.2.10.
Bhatti and Shah	$C + B/Re^{1/m}$	$Re<2.1\times10^3$	C=0,B=16,m=1 (laminar flow)
		$2.1\times10^3<Re<4.0\times10^3$	$C=0.0054, B=2.3\times10^{-8}, m=-2/3$ (Transition flow).
		$Re>4.0\times10^3$	$C=1.28\times10^{-3}, B=0.1143, m=3.2154$ (turbulent flow).
Blasius(1913)	$0.079/Re^{1/4}$	4.1×10^3-10^5	Covering the portion of transition flow regimes. Within 2.0% to -1.3% of Eqn.2.10.
Drew et.al.	$0.0014 + 0.125Re^{-0.32}$	4.0×10^3-5.0×10^6	Within 3% of Eqn.2.10 (covering the portion of the transition flow regimes).
PKN	$1/f^{1/2} = 1.7372\text{Ln}(Re/f^{1/2}) - 0.3946$	4.0×10^3-10^7	Covering the portion of transition flow regimes. Within +2% of the experimental measurements.

Table 2.3: Friction factor in transition and transition cum turbulent flow

The basic correlation of Eqn.2.9 can be used to calculate the pressure drop using appropriate value of the friction factor discussed earlier.

b. Nusselt number

Similarly, the heat transfer coefficients are greatly influenced by the Nusselt number (Eqn.2.2). The heat transfer results are rather uncertain in the transition region where a large number of parameters is required to characterize the heat being affected by the flow. A combination of laminar and turbulent Nusselt numbers is needed to analyse the heat transfer coefficients in the region.

Churchill,[82] has developed a correlation for Prandtl numbers from zero to infinity and $2.1\times10^3 \ll Re \ll 10^6$ (spanning laminar, transition and turbulent flow regimes) for the constant wall temperature,

$$Nu^{10} = Nu_{la}^{10} + \left\{ \frac{\exp[(2200-Re)/365]}{Nu_{la}^2} + \frac{1}{Nu_{tu}^2} \right\}^{-5} \qquad \text{Eqn.2.16}$$

where $Nu_{la}=3.657$ and $Nu_{tu}=Nu_w + \dfrac{0.079(f/2)^{1/2}Re.Pr}{(1+Pr^{4/5})^{5/6}}$, $Nu_w=4.8$ and f is chosen from Eqn.2.10. He claimed that, for $2.1\times10^3 \leqslant Re \leqslant 10^4$, the Nusselt number is on a par with the experimental measurements.

Most authors found difficulty in evaluating the Nusselt number in transition flow. They discovered the Nusselt number in more wide range of Reynolds number which covered the spanning laminar,transition and turbulent flow. Some of the findings are listed below,

Investigators	Correlation for Nusselt number	Reynolds numbers	Observations
Nusselt	$0.024Re^{0.786}\ Pr^{0.45}$	10^3-10^6	Within 4.4% to -6.3% for Pr<1 of the Gnielinski-correlation.
Prandtl(1910) and Taylor (1916)	$\dfrac{(f/2)Re.Pr}{1+5(f/2)^{1/2}(Pr-1)}$	5×10^3-5×10^6	Within 14.9% to -11.1% for Pr<10 of the Gnielinski-correlation.
Dittus and Boetler	$0.024Re^{0.8}\ Pr^{0.4}$ $0.026Re^{0.8}\ Pr^{0.3}$	2.5×10^3-1.24×10^5	Variation of the fluid temperature for 0.7<Pr<120. For Re=2.5×10^3, predictions are unacceptable; 94% higher than the Gnielinski-correlation. Notes: The first equation is for heating fluid and the second one is for cooling liquid.

Table 2.4: Nusselt number in transition and transition cum turbulent flow

Turbulent flow at constant property

The analysis of turbulent flow is much more complicated than that in laminar flow because the streamlines of the flow are no longer parallel to each other. Theoretically, the turbulent boundary layer comprises three distinct regions; laminar sublayer (thin layer adjacent to the pipe wall in which laminar shear stress is dominant), buffer layer (viscous and turbulent shear stresses are equally important) and turbulent core at the centre where the fluids move in a totally disorder pattern.

In order to calculate pressure drop, the correlation concerning the friction factor must initially be performed. The velocity distribution in the three regions described above must be solved. For practical use, the roughness elements of the pipe,ε (assumed to exceed the thickness of the laminar sublayer,δ, see Fig.2.2.2), affects the velocity distribution. The problems become more complicated if the effects of roughness on the velocity profile are included.

Ozisik,[67] reported that Nikuradse identified the three flow regimes depending on the effect of roughness using sand grains glued onto the interior of the circular tube. The results are as follows,

(i). Hydraulically smooth regime, $0 \leqslant Re_\varepsilon \leqslant 5$; $f=f(Re)$.

(ii). Transition regime, $5 < Re_\varepsilon \leqslant 70$; $f=f(\varepsilon/D,Re)$.

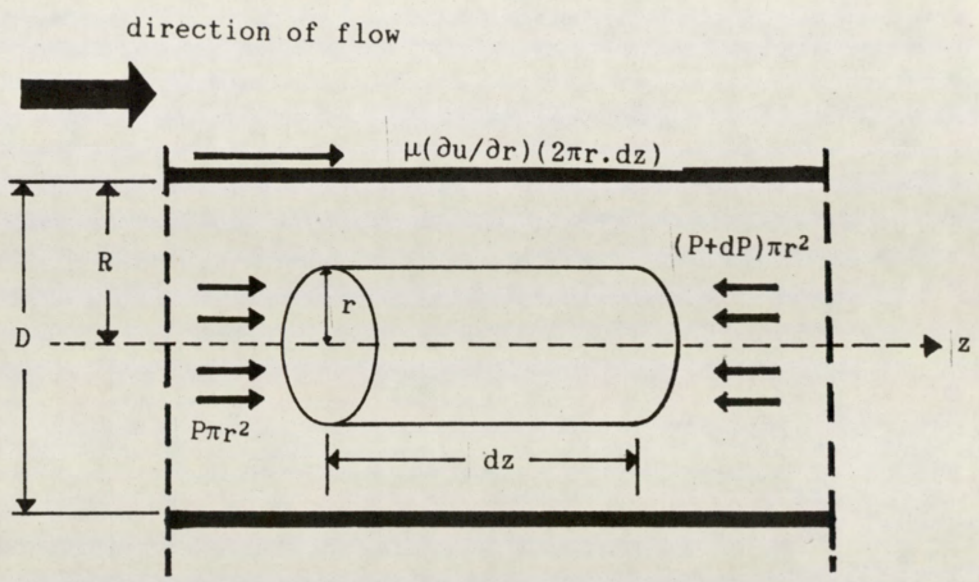

Fig.2.2.1: Control volume for flow in a circular tube

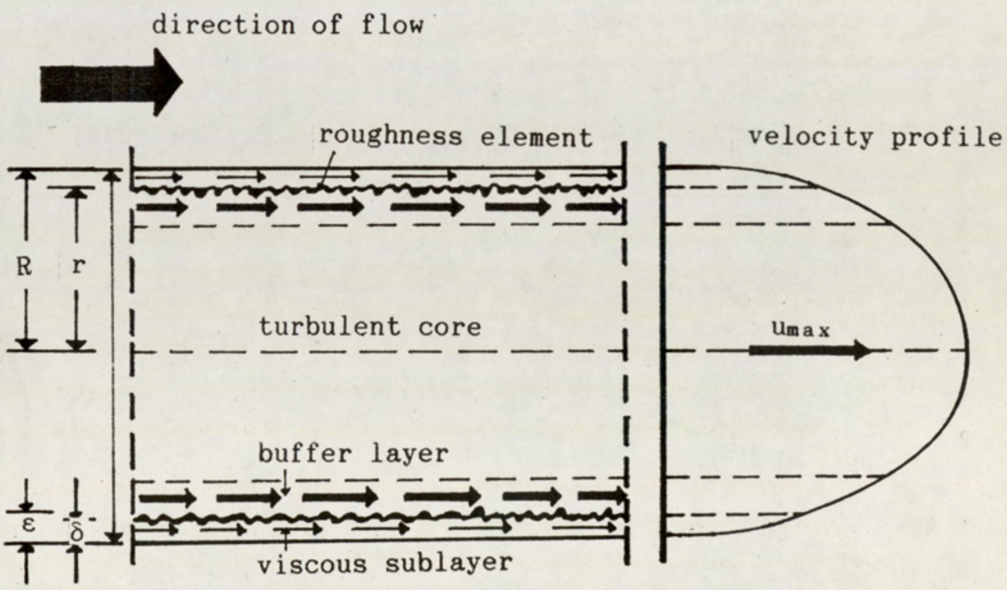

Fig.2.2.2: Fully developed turbulent flow showing three zones in rough tube

(iii). Completely rough regime, $Re_\varepsilon>70$; $f=f(\varepsilon/D)$.
where $Re_\varepsilon=(\varepsilon.u_t/\mu)$; u_t is the friction velocity and μ is the fluid's viscosity.

Roughness has no effect on a hydraulically smooth regime, but in the transition region, where sand grains are partly outside the laminar sublayer, some additional resistance is exerted on the flow. It is greatly influenced by the relative roughness and Reynolds number. For the fully rough case, where the sand grains penetrate the viscous sublayer the flow is only dependent on the size of the relative roughness,ε/D. The equivalent sand grain roughness experiments were also done by other authors, reported in [13,14].

For practical application, the Moody-charts for commercial duct surfaces are widely used (see also Fig.2.2.3). In the present model, ε was chosen to be 1.524×10^{-6} meter for drawn copper tubing. This is simply because the roughness used in the Nikuradse-experiment does not represent the type of roughness employed in the commercial duct surfaces.

In fact, for small diameter pipes, the roughness surfaces can have a significant effect on the turbulent flow even when the surface of the pipe is carefully prepared. In general, the roughness elements are not homogenous in size and distribution. Perkins and McEligot,[15] have introduced the scanning electron microscope method to evaluate the size and the distribution of the roughness elements, which they claimed to be far more complete, to characterize the flow in the heat transfer application.

The influence of surface roughness on the heat transfer rate will increase the tube surface area and heat transfer coefficients. The latter effect is brought about the change in the turbulent pattern close to the pipe wall.

Norris,[16] had developed a simple correlation to show the influence of roughness elements on the heat transfer in turbulent flow as,

$$(Nu/Nu_s) = (f/f_s)^n \qquad \text{for } (f/f_s)\leqslant 4 \qquad \text{Eqn.2.17}$$

where $n=0.68Pr^{0.125}$ in the range of $1<Pr<6$. For $(f/f_s)>4$, it has been observed that the Nusselt number is no longer increased. For higher Prandtl number, the effect of surface roughness is more pronounced because the thermal resistance is concentrated very close to the pipe wall. On the other hand, for lower Prandtl number, the thermal resistance is distributed over a large portion of the pipe cross-section.

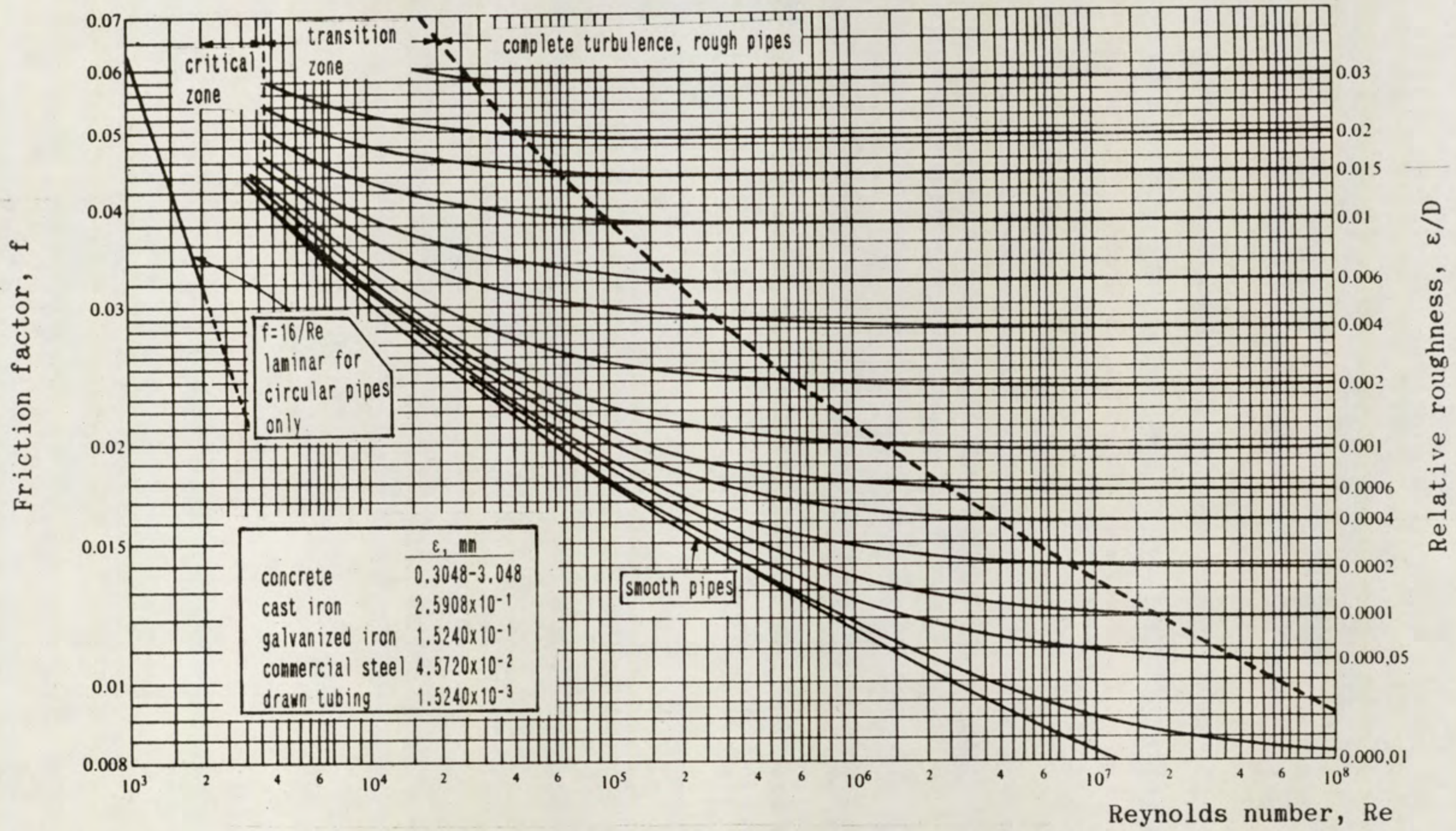

Fig.2.2.3: Friction factor for use in pressure drop for flow inside circular tubes (from Moody-diagram)

a. <u>Friction factor for pressure drop</u>

This section discusses the empirical correlations for friction factor in turbulent flow by considering the effect of roughness. At a given fluid temperature, the appropriate friction factor can be directly established from the Moody-charts in Fig.2.2.3, and then used to calculate the pressure drop over the length, L of a pipe of internal diameter D using Eqn.2.9.

As earlier mentioned, in rough duct flow where $\varepsilon>\delta$ (see Fig.2.2.4), the eddies caused by the roughness elements dominate the turbulent motion. The velocity distribution, u is given by

$$u = f(\tau_w,\rho,y,\varepsilon) \qquad \text{Eqn.2.18}$$

which can be solved using dimensional analysis in terms of,

$$[u/(\tau_w/\rho)] = f(y/\varepsilon) \qquad \text{Eqn.2.19}$$

Kay and Nedderman,[68] have expressed the velocity distribution (Eqn.2.19) in the wall layer in the form

$$u^+ = C_1 \, Ln(y^+/Re.\varepsilon) + C_2 \qquad \text{Eqn.2.20}$$

by considering the velocity gradient with respect to y^+ ($du/dy=u_t/\kappa.y$), where $C_1=1/\kappa$ and $\kappa=0.4$ in the case of smooth wall but a constant C_2 is adapted from the result of the Nikuradse's sand grain experiments ($C_2=8.5$).

For the central zone of the pipe, where friction factor can be defined in terms of the shear stress at the wall, τ_w and the mean flow velocity, u_m can be expressed as,

$$f = (2\tau_w/\rho.u_m^2) = 2(u_t/u_m)^2 \quad \text{or}$$
$$(u_m/u_t) = (2/f)^2 \qquad \text{Eqn.2.21}$$

The next step is to evaluate (u_m/u_t) in terms of Eqn.2.20. The mean flow velocity is defined as,

$$(u_m/u_t) = 1/R^2 \int_0^R [2(R-y)u^+]dy \qquad \text{Eqn.2.22}$$

Eqn.2.22 can be further rearranged by inserting Eqn.2.20. On

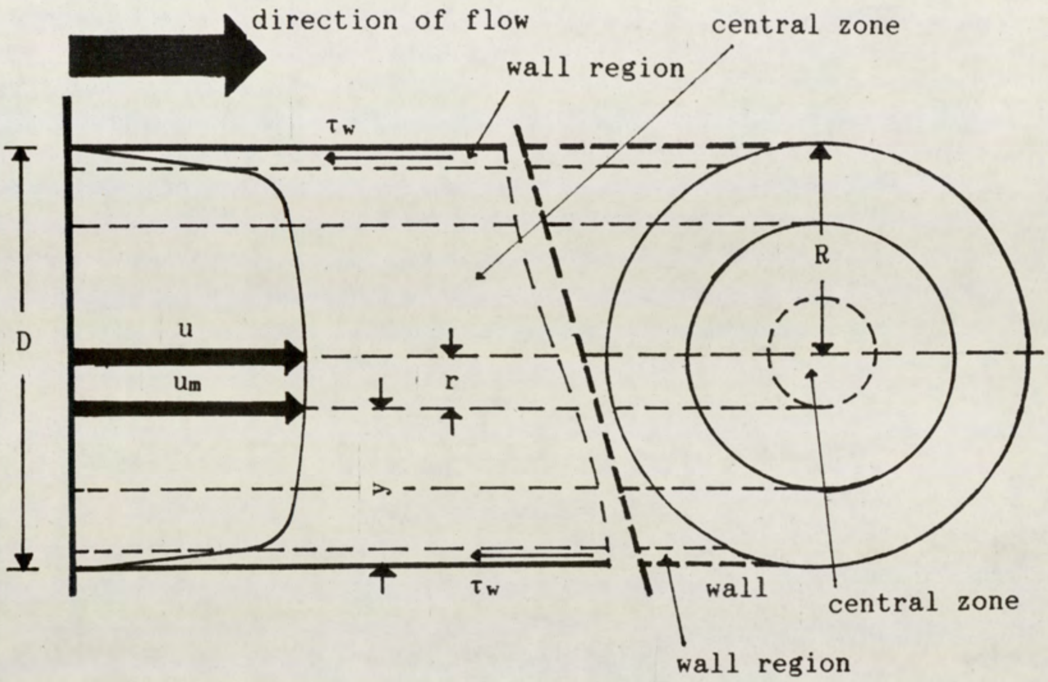

Fig.2.2.4(a): Velocity distribution in a circular duct

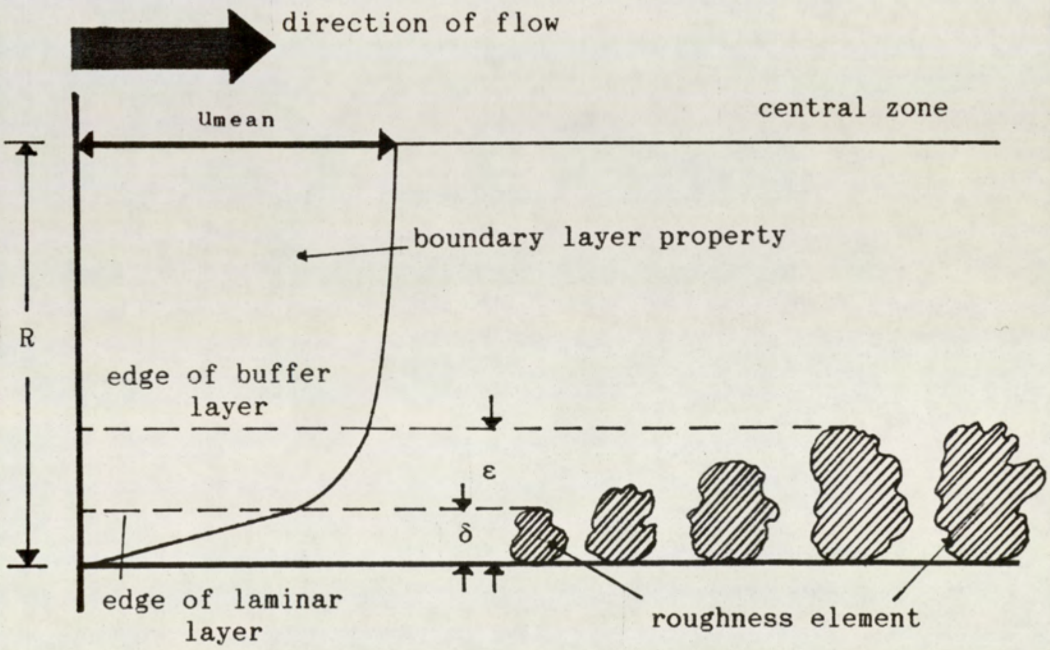

Fig.2.2.4(b): Effect of roughness element in turbulent flow

integration, taking boundary conditions and then insert Eqn.2.21 in term of friction factor, considering appropriate adjusted values for the constant, Karman,[82] has reduced Eqn.2.22 to

$$(1/f^{1/2}) = 3.36 - 1.763 \operatorname{Ln}(2\varepsilon/D) \qquad \text{Eqn.2.23}$$

For $Re_\varepsilon > 70$ in a fully turbulent rough regime, Eqn 2.23 is nearly close to the Nikuradse-correlation for the same conditions, which can be expressed as

$$(1/f^{1/2}) = 3.48 - 1.737 \operatorname{Ln}(2\varepsilon/D) \qquad \text{Eqn.2.24}$$

As $(2\varepsilon/D)$ decreases, the friction factor is also moderately decreased.

An empirical formula correlating the friction factor for $5<Re_\varepsilon<70$ established by Colebrook and White is reported in [82], and given by

$$(1/f^{1/2}) = 3.48 - 1.7372 \operatorname{Ln}[(2\varepsilon/D)+(9.35/Re.f^{1/2})] \qquad \text{Eqn.2.25}$$

As ε approaches zero, the formula transforms to the classical PKN-correlation (see Table 2.3) and for ε approaching infinity, it transforms to Eqn.2.24.

The Colebrook-White correlation seems to be more complicated to solve, because f appears on both sides of the equation. Many authors have established a simple correlation for the friction factor in a rough circular tube based on Eqn.2.25. Some of the findings are listed in Table 2.5.

Researchers	Correlations	Observations compared to Eqn.2.25 for $4x10^3 \leq Re \leq 10^8$ and $2x10^{-8} \leq (2\varepsilon/D) \leq 0.1$
Moody	$f=1.375x10^{-3}[1+21.544(2\varepsilon/D+100/Re)^{1/3}]$	Maximum deviation of -15.8%.
Wood	$f=0.08(2\varepsilon/D)^{0.225} +0.265(2\varepsilon/D)+ 66.69(2\varepsilon/D)^{0.4} Re^{-n}$ where $n=1.778(2\varepsilon/D)^{0.134}$	Maximum deviation of 6.25%.
Swamee and Jain	$(1/f^{1/2})=3.4769-1.7372 \operatorname{Ln}[(2\varepsilon/D)+ (42.48/Re^{0.9})]$	Maximum deviation of 3.2%.
Chen	$(1/f^{1/2})=3.48-1.7372 \operatorname{Ln}[(2\varepsilon/D)-(16.2426/Re)\operatorname{Ln} A_2]$ where $A_2=[(2\varepsilon/D)^{1.1098} /6.0983+(7.149/Re)^{0.8981}$	Maximum deviation of -0.4%.
Zigrang and Sylvester	$(1/f^{1/2})=3.4769-1.7372 \operatorname{Ln}[(2\varepsilon/D)-(16.1332/Re)\operatorname{Ln} A_3$ where $A_3=[(2\varepsilon/D)/7.4+(13/Re)]$	Maximum deviation of 0.96%.
Haaland	$(1/f^{1/2})=3.4735-1.5635 \operatorname{Ln}[(2\varepsilon/D)^{1.11} +(63.635/Re)]$	Maximum deviation of 1.21%.
Serghides	$(1/f^{1/2})=A_5-[(A_5-B_2)^2/(A_5-2B_2+C_1)]$ where $A_5=-0.8686 \operatorname{Ln}[(2\varepsilon/D)/7.4+(12/Re)]$ $B_2=-0.8686 \operatorname{Ln}[(2\varepsilon/D)/7.4+(2.51A_5/Re)]$ $C_1=-0.8686 \operatorname{Ln}[(2\varepsilon/D)/7.4+(2.51B_2/Re)]$	Maximum deviation of 0.14%,[46]
Serghides	$(1/f^{1/2})=4.781-[(A_5-4.781)^2/(4.781-2A_5+B_2)]$	Maximum deviation of -0.45% (Modification of previous equation).

Table 2.5: Fully developed turbulent flow friction factor correlation for rough circular tube

Vilemas and Adomaitis,[17] studied the velocity and temperature profiles in a boundary layer to obtain a reliable correlation for the heat transfer and friction factor of a heat generating rough cylinder in a longitudinal gas flow with variable physical properties within $Re_z=6x10^4$ to $3x10^7$, $Re_{ro}=2x10^4$ to $2x10^5$, $k^+=5$ to 200 and $(T_w/T_{fs})=1$ to 3. They established a correlation as,

$$(f/2)^{1/2} = 5.6\ Log(Re_{\delta+}\ /k^+)- (2.2\delta+/r_o) + 4.6 \qquad \text{Eqn.2.26}$$

where $Re_z=(z.u/\nu)$ is the local Reynolds number based on z, $Re_{ro}=(r_o.u/\nu)$ is the Reynolds number based on r_o, $Re_{\delta+}=(u.\delta+/\nu)$ is the Reynolds number based on dimensionless displacement thickness $\delta+$, where $\delta^+=r_o\{[(1 + 2/r_o)\int_o^R \{1-(\rho.u_m/\rho_{fs}.u_{fs})(r/r_o)dy-1\}]^{1/2}\}$, $u_z=(\tau_w/\rho)^{1/2}$, $k^+=(\varepsilon.u_z/\nu)$ is the dimensionless height and u is the free stream velocity.

b.Nusselt number

As earlier mentioned, the heat transfer coefficient is evaluated from the dimensionless Nusselt number which is determined from the turbulent temperature profiles. In turbulent flow, The Nusselt number can be expressed in general by

$$Nu = f(Re,Pr,f) \qquad \text{Eqn.2.27}$$

where for fully rough flow, f can be chosen from an appropriate correlation for the rough friction factor described earlier. The heat transfer coefficient (Eqn.2.2) in the rough-walled tube is higher than that in the smooth-walled tube because of the disturbance of roughness elements on the laminar sublayer.

Some authors have also established empirical equations for the Nusselt number directly from the rough flow regime phenomena in fully developed turbulent flow (direct method),[51,53]. Others investigators initially calculate the Nusselt number in the smooth flow regime and then use this to evaluate the rough flow regime Nusselt number (indirect method).

In dealing with the Nusselt number in the turbulent region, there are two established analogies which provide a satisfactory answer to heat transfer problems. Firstly, the Prandtl-Taylor analogy in which the turbulent flow consists of two layers; a laminar sublayer and a turbulent core. They performed an analysis based on the two-layers model (see

Fig.2.2.4) where the buffer layer was negligible. Combining the velocity and temperature distribution, the final solution can be expressed as,

$$Nu = \frac{(f/2)Re.Pr}{1+5(f/2)^{1/2}(Pr-1)} \qquad \text{Eqn.2.28}$$

Eqn.2.28 can be used to solve the heat transfer coefficient in the transition cum turbulent and turbulent flow. For $Pr \leqslant 10$ and $5x10^3 \leqslant Re \leqslant 5x10^6$, its predictions are within +14.9% to -11.1% of the Gnielinski-correlation.

Secondly, an extension of the Prandtl-Taylor analogy known as the von Karman analogy, based on the three-layers model; laminar sublayer, buffer layer and turbulent core (see Fig.2.2.4). Assumptions were made on the relative magnitude of the molecular motion and turbulent diffusivities of heat in the laminar sublayer and turbulent core similar to those in the Prandtl-Taylor analogy. In addition, the effect of buffer layer is included.

The velocity distribution within these layers is summarized below:

a. A laminar sublayer (the heat is transferred by molecular process),

$$u^+ = y^+ \qquad \text{for } 0 \leqslant y^+ \leqslant 5 \qquad \text{Eqn.2.29}$$

b. A buffer layer in which both molecular and eddy transfer processes occur

$$u^+ = 5\ Ln(y^+)-3.05 \qquad \text{for } 5 < y^+ \leqslant 30 \qquad \text{Eqn.2.30}$$

c. A turbulent core in which the eddy transfer process is dominant,

$$u^+ = 2.5\ Ln(y^+)+5.5 \qquad \text{for } y^+ > 30 \qquad \text{Eqn.2.31}$$

where $u^+=u/u_t$, $u_t=(\tau_w/\rho)^{1/2}$ is the friction velocity, $y^+=(y.u_t/\nu)$ is the wall coordinate and $\nu=(\mu/\rho)$ is the kinematic viscosity.

He obtained an expression for the Nusselt number as,

$$Nu = \frac{(f/2)Re.Pr}{1+5(f/2)^{1/2}\{(Pr-1)+Ln[(5Pr+1)/6]\}} \qquad \text{Eqn.2.32}$$

For $0.5 \leqslant Pr \leqslant 10$ and $10^4 \leqslant Re \leqslant 10^6$, its predictions are within 16.2% to -11.0% of the Gnielinski-correlation, where f is the friction factor selected from appropriate values discussed earlier.

Petukhov,[97] has considered the variation of the heat flux and shear stress along the radius of a tube. Several values of Nu and f were calculated and then the ratio of the corresponding values of Nu and f (for varying heat flux and shear stress) to the values at the wall has been studied for Pr from 0.5 to $2x10^3$ and Re from 10^4 to $5x10^6$, and described by,

$$Nu = \frac{(f/8)Re.Pr}{[K_1+K_2(f/8)^{1/2}(Pr^{2/3}-1)]} \qquad \text{Eqn.2.33}$$

where $f=[1.82\ Log(Re)-1.64]^{-2}$, $K_1=(1+3.4f)$ and $K_2=(11.7+1.8Pr^{-1/3})$. The values are within 1% with the available experimental data, except for the ranges $5x10^5 \ll Re \ll 5x10^6$ and $200 \ll Pr \ll 2000$, where it is within 1% to 2%. This equation is also applicable to a rough tube. He modified Eqn.2.33 to make it simpler by taking constant values of $K_1=1.07$ and $K_2=12.7$ and giving,

$$Nu = \frac{(f/2)Re.Pr}{[1.07+12.7(f/2)^{1/2}(Pr^{2/3}-1)]} \qquad \text{Eqn.2.34}$$

with an accuracy within 5% to 6% over the range of 10^4 to $5x10^6$ for Re and 0.5 to $2.0x10^3$ for Pr, and within 10% accuracy for $0.5<Pr<2.0x10^3$ and $10^4<Re<5x10^6$.

Sleicher and Rouse,[40] give a correlation based on analytical and experimental results for $0.1<Pr<10^5$ and $10^4<Re<10^6$,

$$Nu = 5 + 0.015Re_m{}^a Pr_w{}^b \qquad \text{Eqn.2.35}$$

where $a=0.88-[0.24/(4+Pr)]$ and $b=[(1/3)+0.5\ exp(-0.6Pr)]$. The subscripts m and w are evaluated at the average temperature, $T_m=(T_w+T_b)/2$ and at the wall temperature respectively.

The Gnielinski correlation was based on comparison with the experimental measurements. In this correlation, Eqn.2.34 has been modified and extended for Reynolds number from $2.3x10^3$ to $5x10^4$ giving

$$Nu = \frac{(f/2)(Re-1000)Pr}{[1+12.7(f/2)^{1/2}(Pr^{2/3}-1)]} \qquad \text{Eqn.2.36}$$

where $f=[1.58Ln(Re)-3.28]^{-2}$. For $0.5 \leqslant Pr \leqslant 2.0x10^3$ and $2.3x10^3 \leqslant Re \leqslant 5x10^6$, overall predictions compared with the experimental measurements are reported to be within -2% to +7.8%.

There have been attemps to improve the Nusselt number correlations in simpler forms in the range of $10^4<Re<5x10^6$ and $0.5<Pr<2.0x10^3$, reported in [18,19,20]. Most of them have studied the Nusselt number as a function of (Re,ε) and (ε) in the transition cum turbulent and turbulent flow regimes. Correlations were made either directly from experimental results or by using other researchers's experimental results to invent new correlations, or to simplify the established correlations by considering additional conditions. Their works covered a wide range of Reynolds numbers and Prandtl numbers.

2.2.2: Heat transfer and pressure drop in two-phase flow

Two-phase heat transfer is far more complicated than single-phase. In the case of a condenser, it concerns a mixture of liquid and vapour. If the vapour strikes a surface that is cooler than the corresponding saturation temperature at a particular pressure, the vapour will immediately condense into liquid-phase. If condensation continuously takes place over the wall surface, the condensed liquid at the surface is removed by gravitational motion but the surface is always covered by a thin layer of liquid. The film of condensate acts as a barrier to heat transfer from vapour to the pipe wall (resistance to the heat flow is from the vapour side).

The film tends to be thicker at the bottom of the tube than at the top but tends to be uniform over the length of the tube if the wall temperature is constant. For a very long tube, it is found that the flow becomes annular with vapour occupying at the centre of the pipe, and the liquid layer at the periphery of the tube. The process of condensation inside the tube is greatly affected by the frictional, momentum and gravitational forces.

a. Heat transfer

In the general case, the heat transfer in two-phase flow depends on a great number of different factors; heat flux, pressure, mass flowrate, quality, thermal properties of the fluid, wall materials and geometrical shape of the channel. The main parameters that determine the vaporization heat transfer are mass flowrate and quality.

A survey of the literature shows that no general heat transfer correlation exists that correlates correctly the effect of friction, momentum and gravity on the forced convection condensation process.

Akers, Deans and Crosser,[22] studied the effect of vapour velocity, liquid loading and physical properties of the fluids inside a horizontal tube, using propane and R12 as working fluids over condensing temperature from 63°C and 66°C respectively. Their correlations are expressed as ,

$$Nu = \begin{cases} 0.0265Pr^{1/3}Re^{0.8} & \text{for } Re>5x10^4 \\ 5.03Pr^{1/3}Re^{1/3} & \text{for } Re\leqslant 5x10^4 \end{cases} \qquad \text{Eqn.2.37}$$

They concluded that the shear stress due to the vapour velocity is dominant. In addition, the liquid loading and the temperature difference across the film has an effect upon the heat transfer coefficient at high vapour rates. The correlation is within about±20% with the experimental data.

Kunz and Yerazunis,[23] studied an annular two-phase flow inside a circular tube for Pr>1, liquid-vapour interface assumed to be smooth and the turbulent diffusion coefficients considered to be similar to those in single-phase flow. They used water inside the tube and arrived at a general correlation for the heat transfer coefficient,

$$[H/\kappa_l(\nu_l^2)^{1/3}] = Pr_l.St^+(\delta^+)^{1/3} = Pr_l[f(Pr_l,Re_l)][f(Re_l)^{1/3}] \qquad \text{Eqn.2.38}$$

where $St^+=(H/\rho_l.u^+.Cp_l)$ is the friction Stanton number and u^+ is the friction velocity, and $\delta^+=(\delta.u^+/\nu)$ is the dimensionless thickness of the liquid film.

Breber, Palen and Taborek,[24] investigated the heat transfer coefficients by estimating the types of flow pattern at various points along the tube. They discovered that the ratio of shear stress to the gravitational forces on the condensate film, and the ratio of the vapour volume to the liquid volume influence the flow patterns. In annular flow (for j_g>1.5 and X_{tt}<1.0), they correlate an expression for the heat transfer coefficient in forced convection as ,

$$H = H_l(\Phi_l^2)^m \qquad \text{Eqn.2.39}$$

where H_l is the convective heat transfer coefficient for the liquid phase determined from the boundary layer theory, and $\Phi_l^2=(\Delta P_{tpf}/\Delta P_l)$ can be obtained from the Lockhart-Martinelli pressure drop correlation and

X_{tt} is the Martinelli-parameter given by Eqn.2.40,

$$X_{tt} = (\Delta P_l/\Delta P_v)^{1/2} = [(1-x)/x]^{0.9} (\rho_v/\rho_l)^{0.5} (\mu_l/\mu_v)^{0.1} \qquad \text{Eqn.2.40}$$

and the dimensionless gas velocity, j_g can be expressed as,

$$j_g=\{G/[D.g.\rho_v(\rho_l-\rho_v)]^{1/2}\}[k/(X_{tt}{}^{1.111} +k)] \qquad \text{Eqn.2.41}$$

where $k=(\rho_v/\rho_l)^{0.555}(\mu_l/\mu_v)^{0.111}$ is a constant depending only on the physical properties of the fluids, G is the total mass velocity, x is the vapour quality, g is the gravitational acceleration and m is an exponent ranging from 0.4 to 0.5.

Altman, Norris and Staub,[25] correlate the average condensing heat transfer coefficient of the refrigerant in horizontal tubes in higher velocity ranges. The R22 flowrates were varied from 4.8 gs^{-1} to 37.9 gs^{-1} at saturation temperature, 5°C and 24°C. The inlet conditions to the test-section were varied from 20% to 99% by weight of the vapour. The experimental data for the exit-vapour quality below 90%, correlate the average heat transfer coefficient for R12 and R22 to within +10% and -20%.

Carpenter and Colburn, cited by Soliman at. el.,[21] used experimental data to obtain an average heat transfer coefficient using steam, methanol, ethanol, toluene and trichloroethylene (working fluids) inside a 11.66 mm internal diameter, 2.44 m long vertical tube. The experiments were limited up to 152 ms^{-1} of the inlet vapour velocity with the Prandtl numbers ranged from 2 to 5. They hypothesized that, due to the shear stress, the condensate layer becomes turbulent at a much lower value of the Reynolds number than that in the absence of vapour stress. The major thermal resistance occurs in the laminar sublayer of the condensate film. They obtained an expression for the heat transfer coefficient,

$$H = 0.043Pr_l{}^{1/2}[\kappa_l.\rho^{1/2}.F_o{}^{1/2}/\mu_l] \qquad \text{Eqn.2.42}$$

where F_o is the shear stress in the laminar sublayer (equal to the wall shear stress due to the assumption of a laminar velocity profile) which is affected by the gravity, momentum and friction, (or $F_o=F_g+F_m+F_f$). They claimed that the value of H is in fair agreement with the experimental data.

A careful analysis in [21] concerning the shear stress, F_o in Eqn.2.42 over a wide range of vapour velocities and Prandtl numbers from

1 to 10, based on the Carpenter-Colburn correlation, derives three separate expressions for F_g, F_m and F_f, which is explained in section 5.4.3 of chapter 5.

The force due to the friction, F_f was derived from the Lockhart-Martinelli data for Φ_v versus X_{tt}. The force due to the momentum, F_m, was considered by solving the effect of momentum changes in the vapour core, liquid in the condensate layer and vapour molecules. As it condenses, the velocity is reduced to the liquid film velocity. The last term (F_g) due to the gravitational force, was solved using Zivi-equation for the local void fraction. The heat transfer coefficient is then expressed as,

$$H = [0.036 Pr_l^{0.65} (\kappa_l . \rho^{1/2} . F_o^{1/2})]/\mu_l \qquad \text{Eqn.2.43}$$

This equation is in fairly good agreement with the experimental data in the range of Pr from 1 to 10, vapour velocity from 6 ms^{-1} to 305 ms^{-1} and a range of qualities from 0.99 to 0.03, shown in Fig.2.2.5. Fig.2.2.6(a) shows the theoretical heat transfer coefficient calculated from Eqn.2.43 compared with the available experimental data. The predicted heat transfer coefficient using the same experimental data proposed by Akers, et. al.,[22] is much lower and shown in Fig.2.2.6(b).

The heat transfer calculations just reviewed show that most correlations are long and complicated except for Eqn.2.37. This equation is applicable to R12 with a condensing temperature above 66°C, which is not suitable for the present heat pump condenser where the condensing temperatures are within the range of 35°C to 50°C.

In the annular model, where the condensation rate is high, the void fraction α is above 80% and vapour quality,x exceeds 5%, the condensation heat transfer coefficient is greatly influenced by the wall shear stress. Basically, the model is divided into two zones; vapour core and liquid film adjacent to the wall. Dealing with the heat transfer, one should consider three possible different solutions in the zones,

a. Liquid layer: There is a temperature difference across the film which is governed by the heat transfer rate and by the effective conductivity of the liquid-phase. The temperature profile is influenced by the velocity profile in which the conductivity can be affected by the laminar or turbulent flow.

b. Interface: At saturation temperature rate, assuming zero slip at the liquid-vapour interface (or $u_{vi}=u_{li}$), the molecules leave the

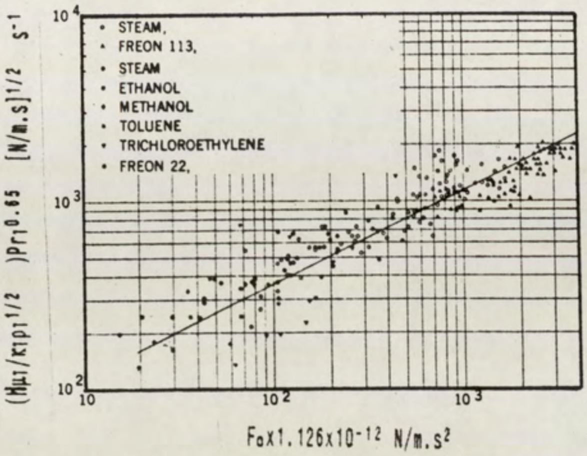

Fig.2.2.5: Heat transfer data for condensation inside tube- line represents Eqn.2.43

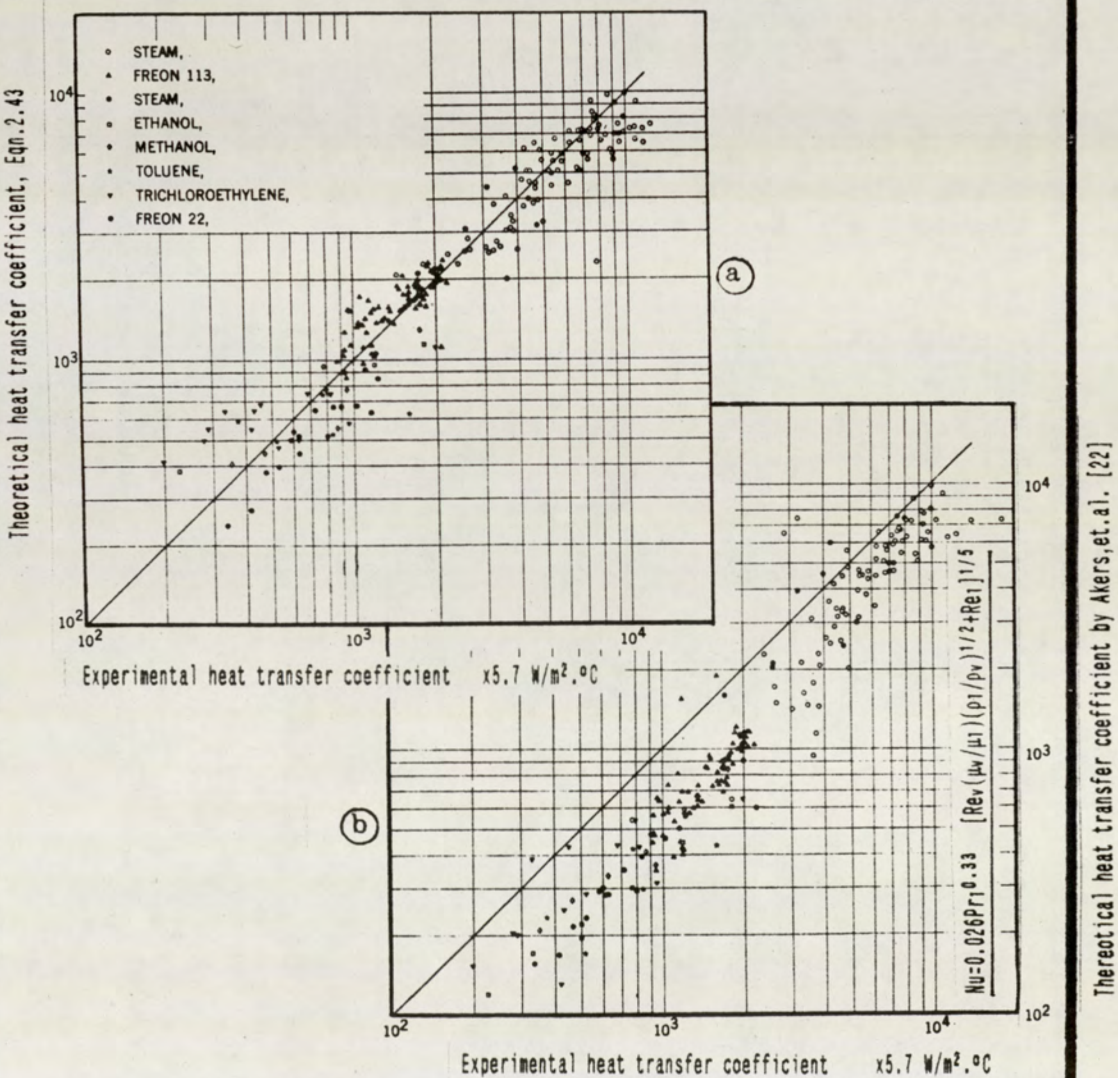

Fig.2.2.6(b): Comparison of correlation in [22] with experimental data from various sources

Fig.2.2.6(a): Comparison of Eqn.2.43 with experimental data from various sources surface at the same rate as they are deposited on the surface. These processes are dependent on the molecular thermal motion on either side of the interface.

c. Vapour core: In this case, the vapour phase will be approximately isothermal and have a temperature near to the saturation temperature.

More generally, we could write,

$$Nu = f(Re, Pr, F_w) \qquad \text{Eqn.2.44}$$

where F_w is the wall shear stress along the condenser, which depends upon the three forces mentioned earlier.

Assuming a turbulent condensate layer and a turbulent vapour core, the vapour shear stress is the result of the friction between the condensate film and the vapour core. The frictional effect, F_f can be best predicted by the Lockhart-Martinelli correlation, where the vapour shear stress is related to the two-phase pressure drop in an adiabatic system.

The momentum term is the combination of the three possible changes of momentum due to liquid-film, interfacial boundary and vapour core. The relationship between the interfacial velocity, u_{li} (or u_{vi}) and the average liquid velocity, u_l depends on the velocity distribution within the liquid layer.

Since the vapour and the liquid do not travel at the same speed, their velocities can be represented in term of vapour quality, x and void fraction, α,[55,56] respectively

$$u_v = (\dot{m}.x/\rho_v.\alpha.A) \qquad \text{and}$$

$$u_l = \dot{m}(1-x)/\rho_l(1-\alpha)A \qquad \text{Eqn.2.45}$$

where α can be obtained from [26], and expressed as,

$$\alpha = \frac{1}{\{1+[(1-x)/x](\rho_v/\rho_l)^{2/3}\}} \qquad \text{Eqn.2.46}$$

Finally, the gravitational term depends on the external acceleration ($a = g\sin\varphi$), void fraction, internal tube diameter and density evaluated both at the liquid and vapour portion. In the present system, the angle of inclination, φ is zero (horizontal pipe mounting system) and therefore F_g is taken to be zero.

In his work, Rohsenow,[87,89] has cited the Traviss-correlation concerning the two-phase Nusselt number. Eqn.2.47 is the combination of the flow effects described above in a simpler form,

$$Nu = [Pr_l . Re_l^{0.9} . \Phi_{tt}]/f_2 \qquad \text{Eqn.2.47}$$

where $\Phi_{tt}=[(1/X_{tt})+2.85/(X_{tt}^{0.476})]$, $X_{tt}=(\mu_l/\mu_v)^{0.1}[(1-x)/x]^{0.9}(\rho_v/\rho_l)^{0.5}$, and f_2 is defined by Eqn.5.31 of chapter 5. The relationship between terms Φ_{tt} and $(Nu.f_2/Pr_l.Re_l^{0.9})$ agrees quite well with the experimental data for R12.

b. <u>Pressure drop</u>

The two-phase pressure gradient is affected by the pipe diameter, liquid and vapour flowrate, viscosity and density of the liquid and vapour, quality and perhaps the shear stress of the liquid. These effects can be summarized as the effects of pressure gradient due to the friction, momentum and gravity. Mathematically, in an annular flow, the total pressure drop per unit length can be represented by,

$$(\Delta P/\Delta z)_{tpf} = (\Delta P/\Delta z)_f + (\Delta P/\Delta z)_m + (\Delta P/\Delta z)_g \qquad \text{Eqn.2.48}$$

The pressure analysis resulting from the simultaneous flow of a liquid and a vapour is firstly based on the static pressure drop for the liquid phase being equal to the static vapour-phase pressure drop, regardless of the flow patterns. Secondly, the sum of the volume occupied by the liquid and vapour at any instant must be equal to the total volume of the pipe.

The expressions of these postulates led Lockhart and Martinelli,[12] to the following equations for predicting two-phase pressure drop due to the liquid and vapour flow respectively,

$$(\Delta P/\Delta z)_{tpf} = \begin{cases} 2f_l(\rho_l . u_l/D_l) \\ 2f_v(\rho_v . u_v/D_v) \end{cases} \qquad \text{Eqn.2.49}$$

where D_l and D_v are the average diameter of liquid and vapour flow respectively. The two-phase pressure drop can also be expressed as,

$$(\Delta P/\Delta z)_{tpf} = \Phi_l^2 (\Delta P/\Delta z)_l \qquad \text{Eqn.2.50}$$

Eqn.2.50 is for the liquid-phase assumed to flow alone and if the vapour-phase is assumed to flow alone, we get

$$(\Delta P/\Delta z)_{tpf} = \Phi_v^2 (\Delta P/\Delta z)_v \qquad \text{Eqn.2.51}$$

Φ_l and Φ_v represent the functions depending on the Martinelli-parameter, X which is characterized by the two-phase flow parameters.

Eqn.2.49 to Eqn.2.51 are the basic equations to calculate $(\Delta P/\Delta z)_{tpf}$. The Martinelli-parameter is widely used in predicting the heat transfer parameters and pressure drop in the two-phase flow. The parameters differ from one flow condition to another depending upon the flow mechanisms (X_{tt}, X_{tv}, X_{vt} and X_{vv}) described in Fig.5.2.6 of chapter 5.

Lockhart and Martinelli give a general correlation,

$$X^2 = (Re_v^a/Re_l^b)(C_l/C_v)(\dot{m}_l/\dot{m}_v)^2(\rho_v/\rho_l) \qquad \text{Eqn.2.52}$$

where C_l and C_v are the constants in the Blasius-equation for the friction factor in liquid-phase and vaour-phase respectively while a and b are the exponents depending on the types of flow occuring in the pipe. This expression is equal to the ratio of liquid pressure drop to vapour pressure drop, assuming each phase flows separately.

$$X^2 = (\Delta P/\Delta z)_l/(\Delta P/\Delta z)_v \qquad \text{Eqn.2.53}$$

For simultaneous liquid-turbulent and vapour-turbulent flow, Eqn.2.52 can be rearranged and reduced to Eqn.2.40.

In their early paper, Martinelli at. el.,[27] studied the relationship between the two functions Φ and X concerning the two-phase pressure drop in four possible combinations of the flow mechanisms. Fig.2.2.7 shows the average values for all possible type of flows. At higher values of X, Φ_l approaches unity, and at lower values, Φ_v also approaches unity. The prediction for the two-phase pressure drop if both phases flow turbulently is within -30% to +30% compared with the experimental measurements shown in Fig.2.2.8. The complete correlation is rewritten as,

$$(\Delta P/\Delta z)_{tpf} = (\Delta P/\Delta z)_v[1+\alpha^{1/4}(\mu_l/\mu_v)^{0.083}\ (\rho_v/\rho_l)^{0.416} \times(\dot{m}_l/\dot{m}_v)^{0.75}\ ]^{2.4} \qquad \text{Eqn.2.54}$$

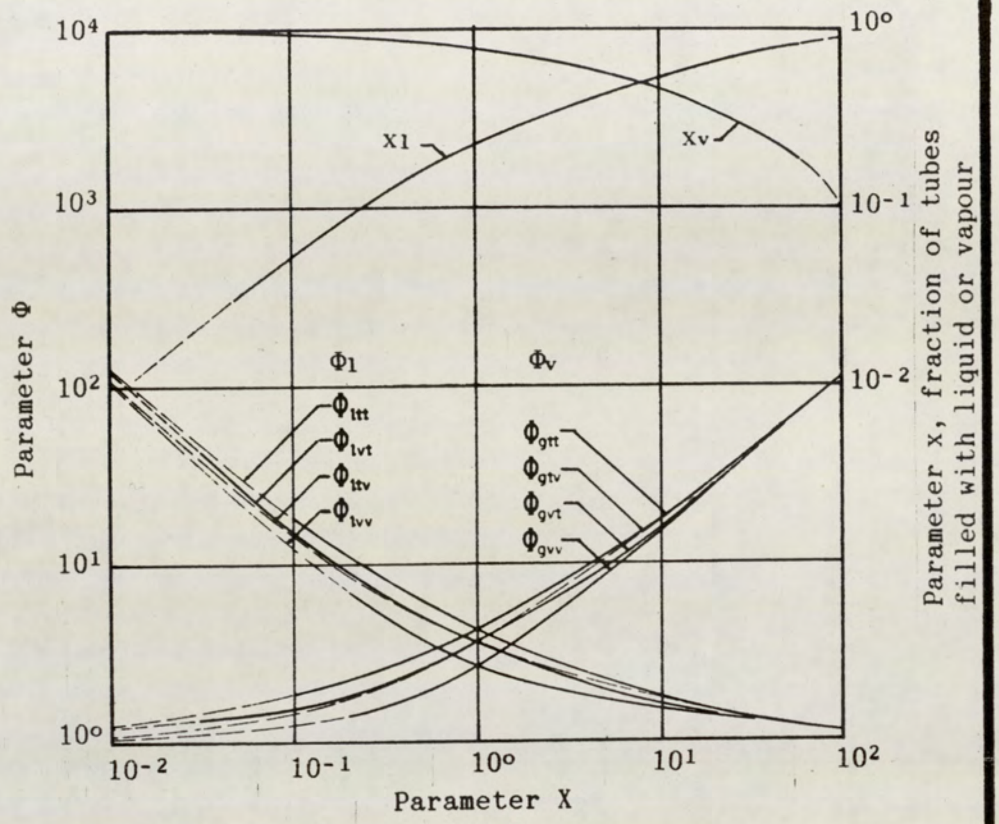

Fig.2.2.7: Relation between Φ_l, Φ_v, X_l and X_v for all flow mechanism (Φ_{tt}, Φ_{tv}, Φ_{vt} and Φ_{vv}) adapted from [12]

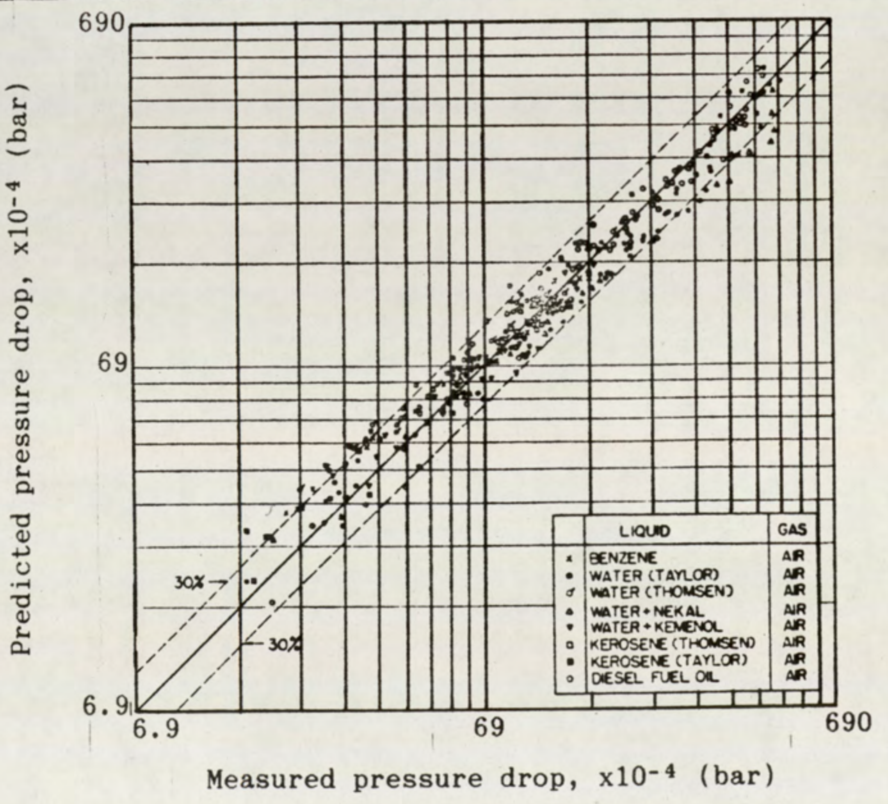

Fig.2.2.8: Comparison of predicted and measured ΔP_{tpf} for both liquid and vapour are turbulent,[27]

where $\alpha=[A_l/(\pi/4)D_l^2]$. On inspection of Eqn.2.51 and Eqn.2.54, the function Φ_{tt} can be expressed as,

$$\Phi_{tt} = [1+\alpha^{1/4}X_{tt}^{0.8325}]^{1.2} \qquad \text{Eqn.2.55}$$

where $X_{tt}=[(\mu_l/\mu_v)^{0.11}(\rho_v/\rho_l)^{0.555}\{(1-x)/x\}]$. The relationship between the Φ_{tt} and X_{tt} is shown in Fig.2.2.9 where Φ_{tt} approaches unity as $(X_{tt})^{1/2}$ approaches zero. At large value of $(X_{tt})^{1/2}$, Φ_{tt} has a constant value ($\Phi_{tt}=X_{tt}^{0.65}$).

Hatch and Jacobs,[28] have investigated the two-phase pressure drop in single-component fluid flow, both with and without heat transfer, expressed in terms of Lockhart-Martinelli parameters using R11 and hydrogen as working fluids. They used three sets of calculations to evaluate the friction factor and Reynolds number in the single-phase, equivalent length of upstream test-section and computation of the Martinelli-Nelson parameters in the two-phase flow. They correlate parameters Φ and $X^{1/2}$ and then expressed the following equation

$$X^{1/2} = (\rho_v/\rho_l)^{0.571} (\mu_l/\mu_v)^{0.148} [(1/x_m)-1] \qquad \text{Eqn.2.56}$$

where x_m is the average quality at the inlet and exit station test-points. It was graphically compared with the Martinelli-Nelson correlation.

The prediction from Eqn.2.56 was found to be within 10% to 30% lower than that predicted by the Martinelli-Nelson correlation, which is also based on the effect of friction and momentum . They assumed the liquid-phase and vapour-phase moves at the same velocity.

The majority of researchers use the Lockhart-Martinelli (LM) correlation as a basis to predict the pressure drop in two-phase single-component and two-component fluid flow. Some of them have also commented,[33,34] discussed and extended the application of this correlation in a wide range of flow mechanisms,[47] although in certain flow regimes it indicates deviation up to 200%. In most cases, the LM-correlation predicts a pressure drop slightly higher than the measured one. Other investigators,[29,30,31] compared their own correlations with the available data to simplify the calculation of pressure drop in two-phase flow (normally, the results are compared to those predicted by the LM-correlation).

Johannessen,[32] gives an equation for predicting the pressure drop

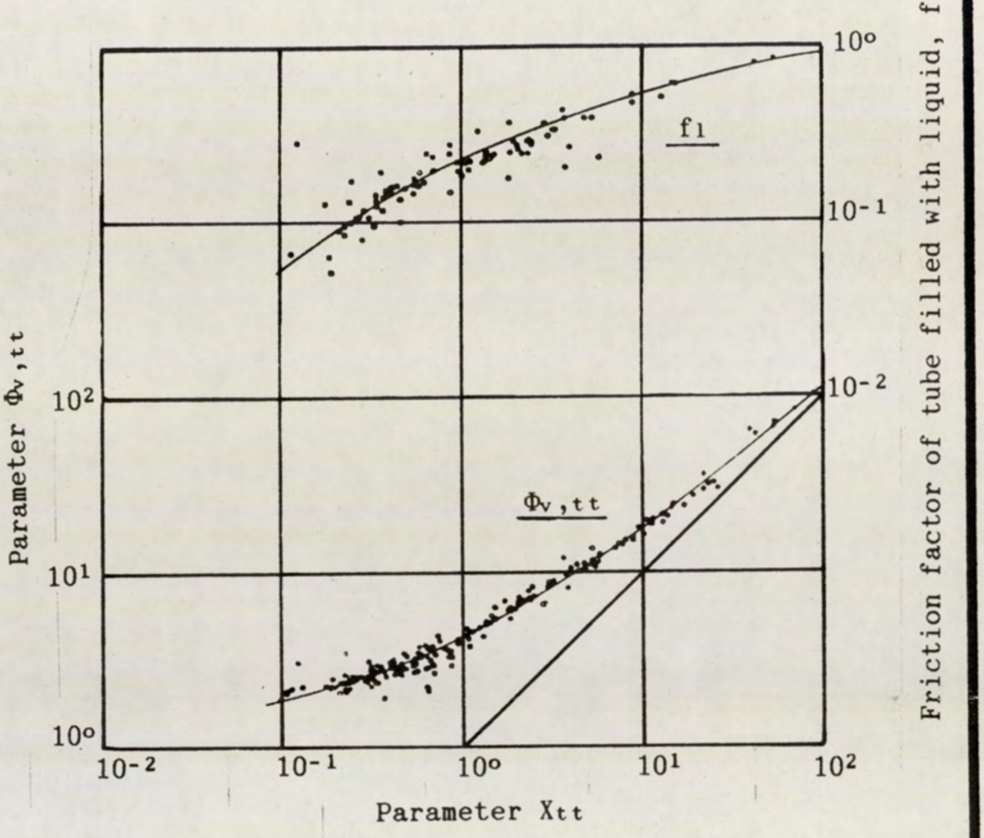

Fig.2.2.9(a): Relation between $\Phi_{v,tt}$, X_{tt} and f_l adapted from [12]

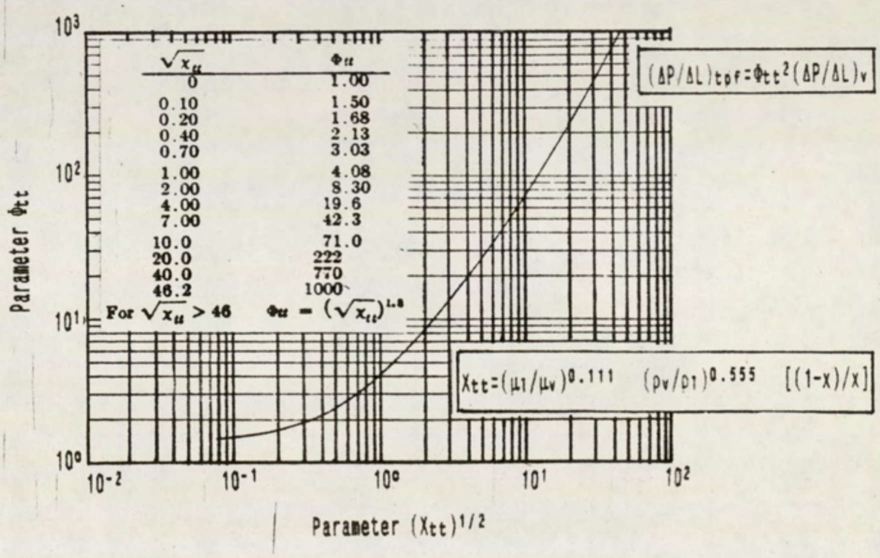

Fig.2.2.9(b): Φ_{tt} as a function of $(X_{tt})^{1/2}$ adapted from [27]

in the stratified and wavy two-phase flow based on the LM-correlation. The new correlation for X and Φ is compared with experimental data from other researchers. The predicted curve is lower than that predicted by the LM-correlation. For X between 0.3 and 2, the data points are evenly distributed about the theoretical curve, and for lower values of X (higher vapour mass flowrate), the theoretical curve is low.

Rouet,[33] has summarized a note on the LM-correlation in the turbulent-turbulent case, proposing,

$$\alpha = 1 - (m/2)X_{tt}^{2/(2-b)} - \{[1+(m/2)X_{tt}^{2/(2-b)}]^2-1\}^{1/2} \qquad \text{Eqn.2.57}$$

where α is the void fraction fitted by,

$$\alpha = [1 - (1/\Phi)] \qquad \text{Eqn.2.58}$$

where $\Phi^2 = [1 + (21/X_{tt})+(1/X_{tt}^2)]$, X_{tt} is the Martinelli-parameter given by Eqn.5.28 of chapter 5 and m denotes a dimensionless parameter to be fitted to the experimental data; m=0.054. The agreement is quite good, except for $x \to 0$ where the value calculated from Eqn.2.57 is too low, due to the unphysical singularities.

Kubie, and Oates,[31] used correlations derived by Chisholm,[75] to predict and correlate two-phase frictional pressure drop in pipe using n-butyl acetate and water as working fluids. They used,

$$\Phi_{tt}^2 = 1+(2/X_{tt})+(1/X_{tt}^2) \qquad \text{Eqn.2.59}$$

Fig.2.2.10 shows a relation between Φ_{tt} and X_{tt}, which they claimed, the maximum error is less than 3%. Fig.2.2.11 shows variation of acetate velocity and frictional pressure gradient at various volumetric water flowrates. At higher water flowrate, the pressure gradient is high.

Chen,[34] comments on the note on the LM-correlation in the turbulent-turbulent flow made by Rouet,[33]. He used the Chen-Spedding correlation for α,

$$\alpha = k(k+X_{tt}^{2/3}) \qquad \text{Eqn.2.60}$$

where k is function of a number of parameters including the pipe size; numerically, k is about 3.5 (almost identical to the LM-correlation). When comparing the X_{tt} and α calculated from Eqn.2.57 and Eqn.2.60

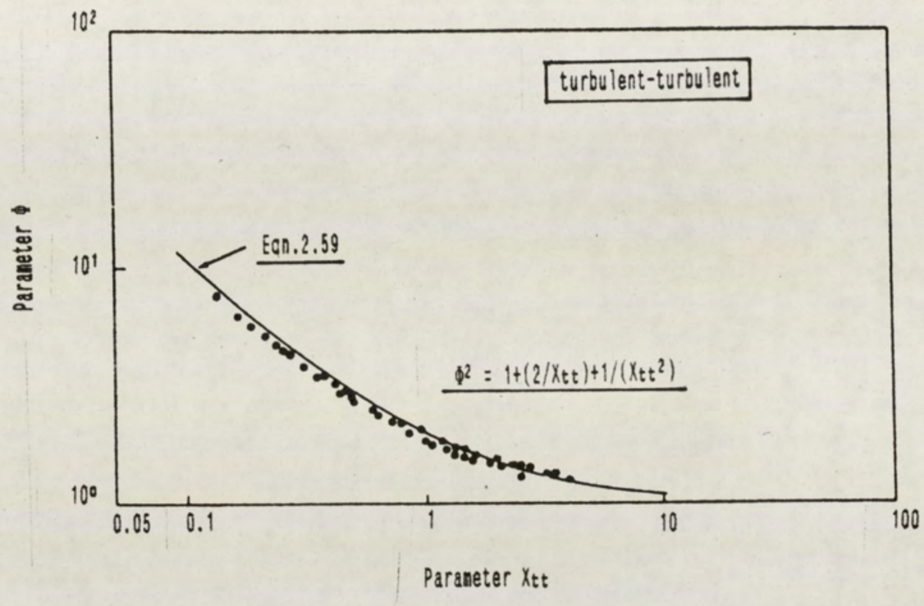

Fig.2.2.10: Comparison of the thereotical prediction and experimental data for turbulent-turbulent flow,[31]

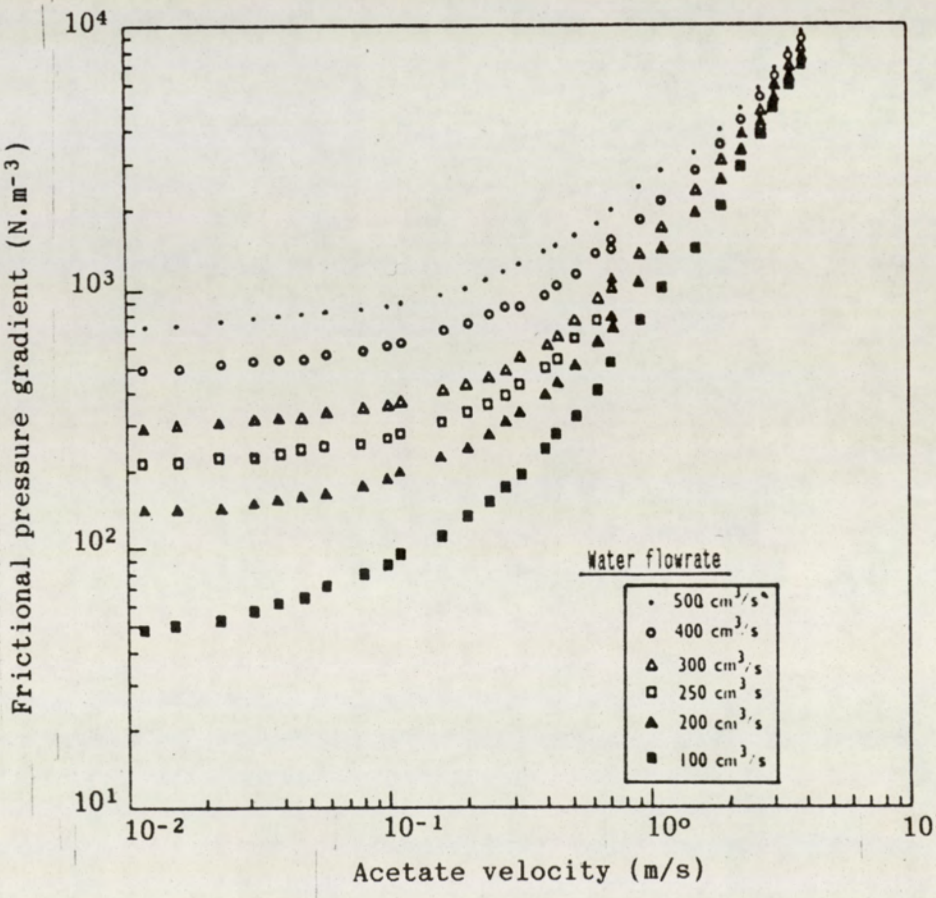

Fig.2.2.11: Frictional pressure gradient obtained from experiment for two-phase acetate/water flow

with the original LM-correlation at higher value of X_{tt}, the Chen-Spedding correlation of α maintains a good agreement with the LM-correlation, while the Rouet-correlation begins to deviate (more than 20% lower than that in the LM-correlation).

The total pressure drop in an annular flow is the sum of the pressure drop due to the friction, momentum and gravity (see Eqn.2.48). These effects have been simplified and reduced in the Traviss-correlation,[87]. The frictional and the momentum term are expressed in Eqn.5.34 and Eqn.5.35 respectively, while the gravitational term can be written as,

$$(\Delta P/\Delta z)_g = g\mathrm{Sin}\varphi[\alpha.\rho_v+(1-\alpha)\rho_l] \qquad \text{Eqn.2.61}$$

where α is the void fraction expressed in Eqn.2.46 and φ is the inclination angle of the tube from horizontal. For a horizontal tube mounting system, $\varphi=0$ and $(\Delta P/\Delta z)_g=0$.

The Martinelli method is recommended for predicting two-phase pressure drop in an adiabatic process involving fluids other than water at not very high pressure.

2.3: Effect of temperature-dependent fluid properties in a circular tube

The single-phase heat transfer solutions discussed earlier were generally for constant fluid properties. The constant fluid properties refer to the unchanged fluid properties (ρ,μ,C_p and κ) which are functions of temperature, at any temperature between the fluid and the wall at the particular test-point. When applied to practical heat transfer, where there is a temperature difference between the wall and the fluid, this assumption could cause errors. In general most fluids, including freon and water, vary with temperature, which influences the variation of velocity and temperature over the flow cross-section of a tube. In this section, the internal forced convection with the temperature-dependent properties are considered.

For most liquids, the specific heat, density and thermal conductivity is approximately temperature independent, but the viscosity decreases markedly with increasing temperature. In gases, density, viscosity and thermal conductivity all vary at approximately the same rate as the absolute temperature but the specific heat varies only slightly with the temperature; the Prandtl number does not vary significantly.

Considering these phenomena, the heat transfer and the friction factor will be greatly affected by the property variations, thus altering the velocity and temperature distribution. For practical applications, an appropriate correlation based on the constant-property assumption can be corrected when the variable-property effect becomes important.

Kakac,[84] has suggested the use of a property-ratio method where, for liquid, the variation of viscosity is dominant,

$$(Nu/Nu_{cp}) = (\mu_b/\mu_w)^n \quad \text{and}$$
$$(f/f_{cp}) = (\mu_b/\mu_w)^m \qquad \text{Eqn.2.62}$$

where Nu_{cp} and f_{cp} are the constant-property Nusselt number and friction factor respectively evaluated at the bulk temperature. The ratio of bulk temperature viscosity,μ_b to wall temperature viscosity,μ_w is dependent on the exponents n and m.

In the case of vapour, the Nusselt number and friction factor is corrected by the temperature ratio evaluated at the wall to the bulk expressed by,

$$(Nu/Nu_{cp}) = (T_w/T_b)^n \quad \text{and}$$
$$(f/f_{cp}) = (T_w/T_b)^m \qquad \text{Eqn.2.63}$$

The correlation for the constant-property Nusselt numbers and friction factors evaluated at the fluid bulk temperature can be taken from appropriate equations discussed earlier in the chapter.

2.3.1: Laminar flow

There are two possible types of flow that may encountered in this region; liquid-laminar and vapour-laminar. Most authors focus their investigations on the ratio of bulk temperature and wall temperature viscosity, except that the exponent values of n and m are different. Swearingen and McEligot,[35] report that the effect of fluid property upon the heat transfer was first discovered by Yamagata in 1940.

a. Liquid

In laminar flow of liquids, through a circular duct at constant heat flux Kakac,[84] has cited a numerical analysis proposed by Deissler for viscosity variation with temperature,

$$(\mu_b/\mu_w) = (T_b/T_w)^{-1.6} \qquad \text{Eqn.2.64}$$

He concluded that the effect of fluid-property variation was to decrease the Nusselt number by 22% and to increase the friction factor by 28% as (T_w/T_b) increases from 1.0 to 1.8. He also obtained n=0.14 for Pr>0.6. For exponent m in Eqn.2.62, he obtained m=-0.58 for heating and m=-0.50 for cooling in a fully developed flow.

Yang,[36] used an analytical solution for a fully developed region in a circular duct, with temperature-dependent viscosity to obtain an expression,

$$(\mu_b/\mu_w) = 1/(1+C.\theta) \qquad \text{Eqn.2.65}$$

where θ is the dimensionless temperature variable, defined by,

$$\theta = [(T_b-T_w)/(T_i-T_w)] \qquad \text{Eqn.2.66}$$

where T_i is the inlet temperature and C is a constant viscosity-variation parameter (positive for cooling and negative for heating of liquid).

Seven different values of C;9.0, 6.0, 3.0, 0, -0.3, -0.6, and -0.9 were used. As C increases from negative to positive, the Nusselt number is decreased , but at C=0, the Nusselt number is roughly equal to 3.70. His predictions for the inlet temperature boundary condition were correlated with n=0.11 (Eqn.2.62) and he concluded that the effect of thermal boundary conditions is small and the influence on the friction factors is substantial.

A simple empirical Sieder-Tate correlation,[84] for predicting average Nusselt number and friction factor at constant wall temperature can be re-written as,

$$Nu_b = 1.86[Re_b.Pr_b.(D/L)]^{1/3}(\mu_b/\mu_w)^{0.14} \text{ and}$$
$$f = (16/Re_b)(1/1.1)(\mu_b/\mu_w)^{0.25} \qquad \text{Eqn.2.67}$$

valid for $0.48 < Pr_b < 1.67x10^4$ and $4.4x10^{-3} < (\mu_b/\mu_w) < 9.75$. Based on this correlation, Test,[37] gives another correlation,

$$Nu_b = 1.4[Re_b.Pr_b.(D/L)]^{1/3}(\mu_b/\mu_w)^n \qquad \text{Eqn.2.68}$$

where n=0.05 for heating and n=0.333 for cooling, with the range of $(Re_b.Pr_b.D/L)>6x10^3$. The correlation for the friction factor is expressed by,

$$f = (16/Re_b)(1/0.89)(\mu_b/\mu_w)^{0.20} \qquad \text{Eqn.2.69}$$

For $Re_b>30$, it gives a fair result.

For fully developed flow, $Pr > 0.6$ and $(\mu_b/\mu_w)=(T_b/T_w)^{-1.6}$, it is recommended to use n=0.14 for both heating and cooling of liquid in the calculation of Nusselt number. For the friction factor, m=-0.58 for heating and m=-0.50 for cooling is recommended. These exponents are associated with the Eqn.2.62 concerning the heat transfer and pressure drop in liqiud-laminar flow.

b. Vapour

It has been reported in [84], that Diessler was the first to study the effect of variable-properties of air in laminar flow. Some idealizations had been made including the constant heat flux boundary conditions, negligible heat dissipation, entrance effects and heat conduction in the direction of flow (small, compared to radial conductivity), constant air specific heat, and both the viscosity and thermal conductivity is proportional to $T^{0.8}$. From the results, he concluded,

(i). For the Nusselt number, the evaluation of conductivity is at the reference temperature, $T_{ref}=T_b-0.27(T_w-T_b)$.

(ii). For the friction factor, the viscosity is at the reference temperature $T_{ref}=T_b+0.58(T_w-T_b)$.

Then, followed by Sze, who discovered the effect of temperature-dependent properties experimentally using the same conditions as before,but more generally. For the Nusselt number, he evaluated the conductivity at $T_{ref}=T_b-0.18(T_w-T_b)$ and the effect on friction factor is obtained by evaluating viscosity at the average temperature, $T_m=(T_w+T_b)/2$.

Both of them did not mention any further details regarding the application to the specific calculation of the Nusselt number and friction factor. The reasonably complete solution to a vapour flowing in a tube with temperature-dependent property variation was firstly initiated by Worsoe-Schmidt, cited in [38], using a finite difference method for fully developed flow. The results are as follows,

$$n = \begin{cases} 0 \text{ in the range of } 1<(T_w/T_b)<3 \text{ for heating} \\ 0 \text{ in the range of } 0.5<(T_w/T_b)<1 \text{ for cooling} \end{cases} \quad \text{and}$$

$$m = \begin{cases} 1 \text{ for heating, } 1<(T_w/T_b)<3 \\ 0.18 \text{ for cooling, } 0.5<(T_w/T_b)<1 \end{cases} \qquad \text{Eqn.2.70}$$

These equations are to be used together with Eqn.2.62 in both developing and fully developed regimes at constant wall temperature.

R12 and water are the fluids used in the present system where in laminar flow, they are assumed to be only present in the liquid-phase (the laminar vapour-phase does not exist). In such case, the vapour-phase of laminar Nusselt number and friction factor is not taken into consideration in the present model.

2.3.2: Turbulent flow

In laminar flow, the shear stress depends solely on viscosity, which is a fluid property and depends only on the temperature of the fluid. This situation is different in turbulent flow, where the effect of eddy viscosity is so dominant over a major portion of the flow. Eddy viscosity is a function of flow configuration which varies from one flow cross-section to another and is indirectly temperature-dependent.

The heat transfer in turbulent flow depends not only on the thermal conductivity which is temperature-dependent, but also depends on the thermal diffusivity, which is a function of Reynolds number and Prandtl number. An accurate prediction of the heat transfer and friction coefficients depends on the accurate relationship of the velocity distribution, eddy diffusivity of momentum (or eddy viscosity), ε_M , and thermal eddy diffusivity (or eddy conductivity), ε_H . In most of the analysis, it was assumed that $\varepsilon_M = \varepsilon_H$, so that $Pr = (\varepsilon_M/\varepsilon_H) = 1$, but the turbulent Prandtl number is not constant, it varies continuously from the wall to the centre of the tube. The Prandtl number, very close to the wall is just above unity. The turbulent Prandtl number was found to be above unity for most gases and between 0.8-0.9 for most liquids,[84].

Similarly, The temperature-dependence of the fluid properties can be classified as turbulent-liquid and turbulent-vapour. In turbulent-liquid, the Nusselt number and the friction factor depends on the ratio of viscosity (Eqn.2.62), while in the turbulent-vapour, it is directly influenced by the temperature ratio (Eqn.2.63). Both cases will be considered in the present model, where in the desuperheating region, R12 is assumed to be in the vapour-phase and in the subcooling region, it is in the liquid-phase. For water, the flow is assumed to be in the liquid-phase depending on the flow mechanisms.

The appropriate Nusselt number and friction factor at constant-property discussed earlier (Nu_{cp} and f_{cp} respectively) can be used to determine these parameters at variable-property as given in Eqn.2.62 and Eqn.2.63 by choosing the correct value of n and m.

a. Turbulent liquid

To choose the correct value of n, Petukhov,[97] has collected heat transfer experimental data corresponding to heating and cooling for several liquids; water, butyl alcohol, transformer oil and oil MS over a wide range of (μ_w/μ_b); 0.19-0.77, 0.08-0.45, 1.2-8.6 and 1.6-38 respectively. He found that the data is best correlated by,

$$n = \begin{cases} 0.11 \text{ for heating, } (\mu_b/\mu_w)>1 \\ 0.25 \text{ for cooling, } (\mu_b/\mu_w)<1 \end{cases} \qquad \text{Eqn.2.71}$$

which is applicable over a range of 10^4-$1.25\text{x}10^5$ for Re, 2-140 for Pr and 0.08-40 for (μ_w/μ_b). These equations are used together with Eqn.2.62 where Nu_{cp} is taken from Eqn.2.33.

He also collected data from various investigators for the influence of variable viscosity on the friction in water, for both heating and cooling, over a wide range of $1.3\text{x}10^4$-$2.25\text{x}10^5$ for Re and 1.3-8 for Pr, and suggested the following expression,

$$(f/f_{cp}) = \begin{cases} 1/6[7-(\mu_b/\mu_w)] \text{ for heating and } (\mu_b/\mu_w)>1 \\ (\mu_b/\mu_w)^{-0.24} \text{ for cooling and } (\mu_b/\mu_w)<1 \end{cases} \qquad \text{Eqn.2.72}$$

Eqn.2.72 is true over a range of 0.35-2 for (μ_w/μ_b), 10^4-$2.3\text{x}10^5$ for Re and 1.3-10 for Pr. An appropriate value of f_{cp} can be chosen from previous discussion.

Hanna and Sandall,[39] developed an analytical approximation to predict the effect of a temperature-dependent viscosity on liquid convective heat transfer in a fully developed turbulent pipe flow for Prandtl number from 2 to 10^5. They obtained the viscosity variation with the temperature as $\mu \propto \alpha\exp(\beta/T)$, where β is the fluid viscosity-temperature parameter in the range of $10^3 \leqslant \beta \leqslant 10^4$. Based on the same model used by Petukhov,[97], they give a correlation,

$$\frac{[St/(f/2)^{1/2}]}{[St/(f/2)^{1/2}]_{cp}} = [1-(1/C_1)]+\{J/[C_1(T_b-T_w)]\} \qquad \text{Eqn.2.73}$$

where $St=(Nu/Re.Pr)=(H/G.C_p)$, $C_1=1.08$ for cooling, $C_1=1.26$ for heating and

$$J = \begin{cases} T_b . C_2 & \text{for cooling} \\ -T_w \exp[\beta(1/T_b - 1/T_w)]C_2 & \text{for heating} \end{cases} \qquad \text{Eqn.2.74}$$

where $C_2=\{1-\exp[-(T_b/T_w - 1)(\beta/T_b +2)]\}/[(\beta/T_b)+2]$, f and f_{cp} is adapted from **Eqn.2.72**. They used $C_1=1.05$ for cooling and $C_1=2.4$ for heating, to compare the ratio of (St/St_{cp}) with the Petukhov-correlation. For the cooling case, in the range of $12.35 \leqslant (\mu_w/\mu_b) \leqslant 1.16$, their results are within -5% to 11%, and for the heating, in the range of $0.425 \leqslant (\mu_w/\mu_b) \leqslant 0.833$, are in good agreement.

Some other correlations for turbulent Nusselt numbers in forced convection for liquids with variable-properties and Pr>0.5 are summarized in Table 2.6.

Investigators	Liquid	Correlations	Remarks and limitations
Seider and Tate	-	$Nu=0.023Re^{0.8}\ Pr^{1/3}(\mu_b/\mu_w)^n$	$(L/D)>60$, $Pr>0.6$ for moderate (T_w-T_b) and $n=0.14$.
Norris and Sims	oil	$Nu=0.006Re.Pr^{0.2}\ (\mu_b/\mu_w)^n$	$3.5x10^3 \leqslant Re \leqslant 1.1x10^4$, $n=0.14$ and undeveloped velocity profiles.
Malina and Sparrow	H_2O,oil	$Nu=0.023Re^{0.8}\ Pr^{1/3}(\mu_b/\mu_w)^n$	$3<Pr<75$, $(L/D)=30$ and $n=0.05$.
Hufschmidt, Burck and Riebold	H_2O	$Nu=Nu_{cp}(Pr_b/Pr_w)^{0.11}$	$2x10^4<Re<6.4x10^5$, $0.1<(Pr_b/Pr_w)<10$, and use Eqn.2.33 for calculating Nu_{cp}.
Everett	-	$Nu=0.0225Re^{0.795}\ Pr^a(\mu_b/\mu_w)^n$ where $a=0.495-0.225Ln(Pr)$	$Re>4x10^3$, $n=(Re/8.7x10^5)^{0.84}$ for $Re<6.25x10^4$ and $n=0.11$ for $Re>6.25x10^4$.
Hackl and Groll	oil	$Nu=Nu_{cp}[0.645(\mu_w/\mu_b)+0.355$	$4x10^3<Re<1.1x10^4$.
Kuznetsova	oil	$Nu=0.013Re^{0.8}\ Pr^{0.4}\ (\mu_b/\mu_w)^n$	$2x10^3<Re<8x10^3$, $70<Pr<200$ and $n=-0.11$.
Oskage and Kakac	H_2O and 30% glycerine-water mixture	$Nu=0.023Re^{0.8}\ Pr^{0.4}\ (\mu_b/\mu_w)^n$	$1.2x10^4<Re<4x10^4$, $(L/D)>10$ and $n=0.262$ for water. $8.9x10^3<Re<2x10^4$, $(L/D)>10$ and $n=0.487$ for glycerine-water mixture.
Hausen	-	$Nu=0.0235(Re^{0.8}\ -230)(1.8Pr^{0.3}\ -0.8)$ $x[1+(D/L)^{2/3}](\mu_b/\mu_w)^n$	$n=0.14$.
Sleicher and Rouse	-	see Eqn.2.35	$(L/D)>60$, $0.1<Pr<10^5$, $10^4<Re<10^6$ and $T_m=(T_b+T_w)/2$.
		$Nu=0.015Re_m^{0.8}\ Pr_w^{1/3}$	$Pr>50$
		$Nu=4.8+0.015Re_m^{0.8}\ Pr_w^{0.93}$	$Pr<0.1$ for uniform wall temperature.
		$Nu=6.3+0.0167Re_m^{0.85}\ Pr_w^{0.93}$	$Pr<0.1$ for uniform heat flux.
Gregorig	-	$Nu=Nu_{cp}(Pr_b/Pr_w)^a$ where $a=[0.264(0.5-B)^{0.28}\ +0.0757]/[Pr^{0.05}\ Re^{0.02}\ (0.5-B)^{0.01}\ ]$ $b=[(Pr_m-Pr_w)/(Pr_b-Pr_w)]-(1/2)$ at $T_m=(T_b+T_w)/2$.	$(L/D)>70$ for cooling of liquid and $T_m=(T_w+T_b)/2$.

Table 2.6: Turbulent Nusselt number in circular tubes for liquid with variable-properties

b. <u>Turbulent vapour</u>

As earlier discussed, the physical vapour properties (ρ, C_p, κ and μ) were considered as given functions of temperature. The variation of density with pressure and energy dissipation is neglected, and the heat diffusivity,ε_H is taken to be equal to the momentum diffusivity,ε_M .

Petukhov,[97] had carried out the analyses over the following range of parameters;$0.37 < (T_w/T_b) < 3.1$ and $10^4 < Re < 4.3x10^6$ for air, and $0.37<(T_w/T_b)<3.7$ and $10^4<Re<5.8x10^6$ for hydrogen. He performed a correlation from analytical results to be used together with Eqn.2.63 as,

$$n = \begin{cases} +0.36 & \text{for cooling and } (T_w/T_b)<1 \\ -[0.3Log(T_w/T_b)+0.36] & \text{for heating and } (T_w/T_b)>1 \end{cases} \qquad \text{Eqn.2.75}$$

Eqn.2.75 describes the solution for air and hydrogen with an accuracy of ±4%. It is also suggested that, for simplicity, n can be taken as constant (n=-0.47) for heating gas, with an accuracy within ±6%. These results have been confirmed experimentally and can be employed for practical calculation in the range of $1\leqslant(T_w/T_b)\leqslant4$.

Comparing analytical results and experimental data for the prediction of friction factor for air and hydrogen in a fully developed turbulent flow, the exponent m for Eqn.2.63 is suggested as follows,

$$m = \begin{cases} -0.6+0.79Re_w^{-0.11} & \text{for cooling} \\ -0.6+5.6Re_w^{-0.38} & \text{for heating} \end{cases} \qquad \text{Eqn.2.76}$$

where $Re_w=(u_m.D.\rho_w)/\mu_w$ is the wall Reynolds number. This equation is applicable over a range $0.37<(T_w/T_b)<3.7$ and $1.4x10^3\leqslant Re_w\leqslant10^6$ with an accuracy within 2% to 3%.

In the Kutateladze-Leontiev correlation,[84] an analytical expression for the function describing the influence of variable physical properties in a turbulent vapour flow when Re goes very high is considered. The correlation can be expressed as,

$$(Nu/Nu_{cp}) = (f/f_{cp}) = \{2/[1+(T_w/T_b)^{1/2}]\}^2 \qquad \text{Eqn.2.77}$$

This correlation is also recommended for the finite values of Re, in which, the influence of varying physical properties depends weakly on Re. The accuracy for lower Reynolds number (the difference by using the value of n and m in Eqn.2.75 and Eqn.2.76 respectively into Eqn. 2.63) is less than 10%. For higher Re values, Eqn.2.77 is in good agreement with Eqn.2.76.

For gases, Sleicher and Rouse,[40] modified Eqn.2.35 for $0.6<Pr<0.9$ to find a better fit to the heating data,

$$Nu = 5+0.012Re^{0.83}\ [(Pr+0.29)(T_w/T_b)^n] \qquad \text{Eqn.2.78}$$

where $n=-[\text{Log}(T_w/T_b)^{1/4}]+0.3$, with the average deviation of the data within 4.2%. This equation is suitable for $10^4<Re<10^6$, $1<(T_w/T_b)<5$ and $(L/D)>40$, where as (T_w/T_b) increases above about 2, it correlates the data better.

A great number of experimental studies are available in the literature (cited in [54,58,59]) to investigate the heat transfer between the pipe wall and the vapour flow at large temperature differences when physical properties of the fluid cannot be considered constant. The majority of the works deal with the gas heating at constant wall temperature in a circular duct. Studies on gas cooling are limited. In addition, the vapour friction factor in a circular duct with larger temperature differences between the wall and the fluid has also been studied but they are not in agreement with each other. From Ilyin's experimental data, the value of **m** in Eqn.2.63 can be expressed as,

$$\mathbf{m} = \begin{cases} 0 & \text{for cooling vapour} \\ -0.58 & \text{for heating vapour} \end{cases} \qquad \text{Eqn.2.79}$$

where for heating vapour, it is in good agreement with the analytical results, but lower in the case of cooling vapour.

The results of heat transfer measurements at larger temperature differences between the wall and the gas flow are usually predicted in more general form,

$$Nu = C.Re^{0.8}\ Pr^{0.4}\ (T_w/T_b)^n \qquad \text{Eqn.2.80}$$

At the entrance region of the tube, coefficient C and exponent n varies with L/D. For larger ratio of L/D (L/D<40-100) in fully developed temperature and velocity profiles, far from the entrance region, C becomes constant and n becomes independent of L/D.

Some of the turbulent forced convection correlations for the Nusselt numbers in circular ducts for vapour with variable-properties are shown in Table 2.7.

Investigators	Gas	L/D	Rex10^3	$\theta=(T_w/T_b)$	Expressions accounting for the variable-properties influences.
Ilyin	Air	59,62	7-60	0.56-2.30	$Nu=C.Re^{0.8}\ \theta^n$ θ: 0.5-0.9 0.9-1.2 1.2-2.3 C: 0.0218 0.0212 0.0223 n: 0 -0.27 -0.58
Humble, Lowdermilk and Desmon	Air	30-120	7-300	0.46-3.50	$Nu=0.023Re^{0.8}\ Pr^{0.4}\ \theta^n$ for $(L/D)>60$ $n=0$ at $\theta<1$ (cooling) and $n=-0.55$ at $\theta>1$ (heating).
Taylor and Kirchgessner	He	60,92	3.2-60	1.60-3.90	$Nu_m=0.021Re_m^{0.8}\ Pr_m^{0.4}$ at $T_m=(T_b+T_w)/2$.
Bialokoz and Saunders	Air	29-72	124-435	1.10-1.73	$Nu=0.022Re^{0.8}\ Pr^{0.4}\ \theta^n$ $n=-0.5$
Weight and Walters	H_2	-	-	1.00-4.00	$Nu=0.021Re^{0.8}\ Pr^{1/3}\theta^n$ at large (L/D) and $n=-0.515$
McCarthy and Welf	H_2,He	21-67	5-1500	1.50-9.90	$Nu=0.045Re^{0.8}\ Pr^{0.4}\ (L/D)^{-0.15}\ \theta^n$, $n=-0.7$
Wieland	He,H_2	250	-	<2.80	$Nu_m=0.021Re_m^{0.8}\ Pr_m^{0.4}$ at $T_m=(T_b+T_w)/2$ and far from entry
Taylor	He,H_2	77	-	1.50-5.60	$Nu_m=0.021Re_m^{0.8}\ Pr_m^{0.4}$ at $T_m=(T_b+T_w)/2$
McEligot, Masee and Leppert	Air,He and N_2	160	-	1.10-2.50	$Nu=0.021Re^{0.8}\ Pr^{0.4}\ \theta^n$ $n=-0.5$
Kirillov and Malungin	N_2	138	7-160	1.10-2.30	$Nu=0.021Re^{0.8}\ Pr^{0.4}\ \theta^n$ and $n=-0.5$
Lelchuk,Elphimov and Fedotov	Air,CO_2 and Ar	77-206	14-600	1.10-2.70	$Nu=0.021Re^{0.8}\ Pr^{0.4}\ \theta^n$ at $(L/D)>50$ and $n=-0.5$
Vokov and Ivanov	Air	48-370	14-400	1.10-2.10	$Nu=0.0193Re^{0.8}\ Pr^{0.4}\ \theta^n$ at $(L/D)>100$ and $n=-0.55$
Petukhov,Kirillov and Maidanic	N_2	80-100	13-300	1.00-6.00	$Nu=0.021Re^{0.8}\ Pr^{0.4}\ \theta^n$ at $(L/D)>80$ and $n=-(0.9Log\theta+0.205)$
Deissler and Prester	Air,He,Ar and H_2	>60	>10	-	$Nu_r=(Re_r^{3/4})/31$ evaluated at $T_r=T_b+0.4(T_w-T_b)$
Gnielinski	Air,He,CO_2	-	-	-	$Nu=0.0214(Re^{0.8}\ -100)Pr^{0.4}\ \theta^n[1+(D/L)^{2/3}]$ for $0.5<Pr<1.5$ with $n=0.45$
Dalle-Donne and Bowditch	Air,He	18-316	10-100	-	$Nu=0.022Re^{0.8}\ Pr^{0.4}\ \theta^n$ $n=-[0.29+0.0019(L/D)]$
Perkins and Worsoe-Schmidt	N_2	160	18-280	1.30-7.50	$Nu=0.024Re^{0.8}\ Pr^{0.4}\ \theta^{-0.7}$, at $L/D>40$

* All values are evaluated at the bulk temperature unless stated in the subscript.

Table 2.7: Turbulent Nusselt number in circular ducts for vapour with variable-properties

In general, the exponent n and constant C in Eqn.2.80 described in the table varies depending on the range of (T_w/T_b).

CHAPTER 3

EXPERIMENTAL RIGS

3.1: Introduction

The air-water heat pump was originally designed and constructed by Hassan [41]. Later, Khan [42] modified the condenser from a helical configuration to one with 180 deg-bends at every half-meter to make up the total length of 15 meters (see Fig.3.1.1). The major focus of the work was to investigate the condenser. 32 thermocouples and 2 pressure transducers were placed at the test-point positions that will be discussed in detail in coming sections.

In general, the experimental data obtained from the heat pump system was digitised through analogue to digital converter (ADC) via an IEEE 488 interface and computer system (Fig.3.1.2). For simplicity, the term 'system' will refer to the combination of these components unless otherwise stated.

There are 35 thermocouples, with connecting lengths between 1.5-2.5 meter. 32 of them were positioned in the condenser, 2 were placed at the entry and exit of the heat pump evaporator and the final thermocouple was used for room temperature measurement. Originally, there were four additional sensors for measuring water flowrate, freon flowrate, power consumption and air speed through the evaporator. These were connected via frequency-voltage converters (FV) to the ADC, an IEEE interface and computer system, but owing to the severe fluctuations and instabilities of the readings these sensors were not used. The water mass flowrate was mechanically measured and used to calculate the freon mass flowrate from the energy balance equation. The electrical power and air speed measurement from the other sensors was completely ignored because of the reasons stated and in fact the model is based on the thermal power calculation. The exclusion of these measurements did not affect the performance of the model.

As mentioned earlier, the main focus of the research was the heat pump condenser, where 32 thermocouples and 2 pressure transducers had been attached. It comprises two copper pipes joined side by side of length 15 meter. The most important measurements are the temperatures at various positions in the condenser, and the pressure at the entry and exit of the condenser.

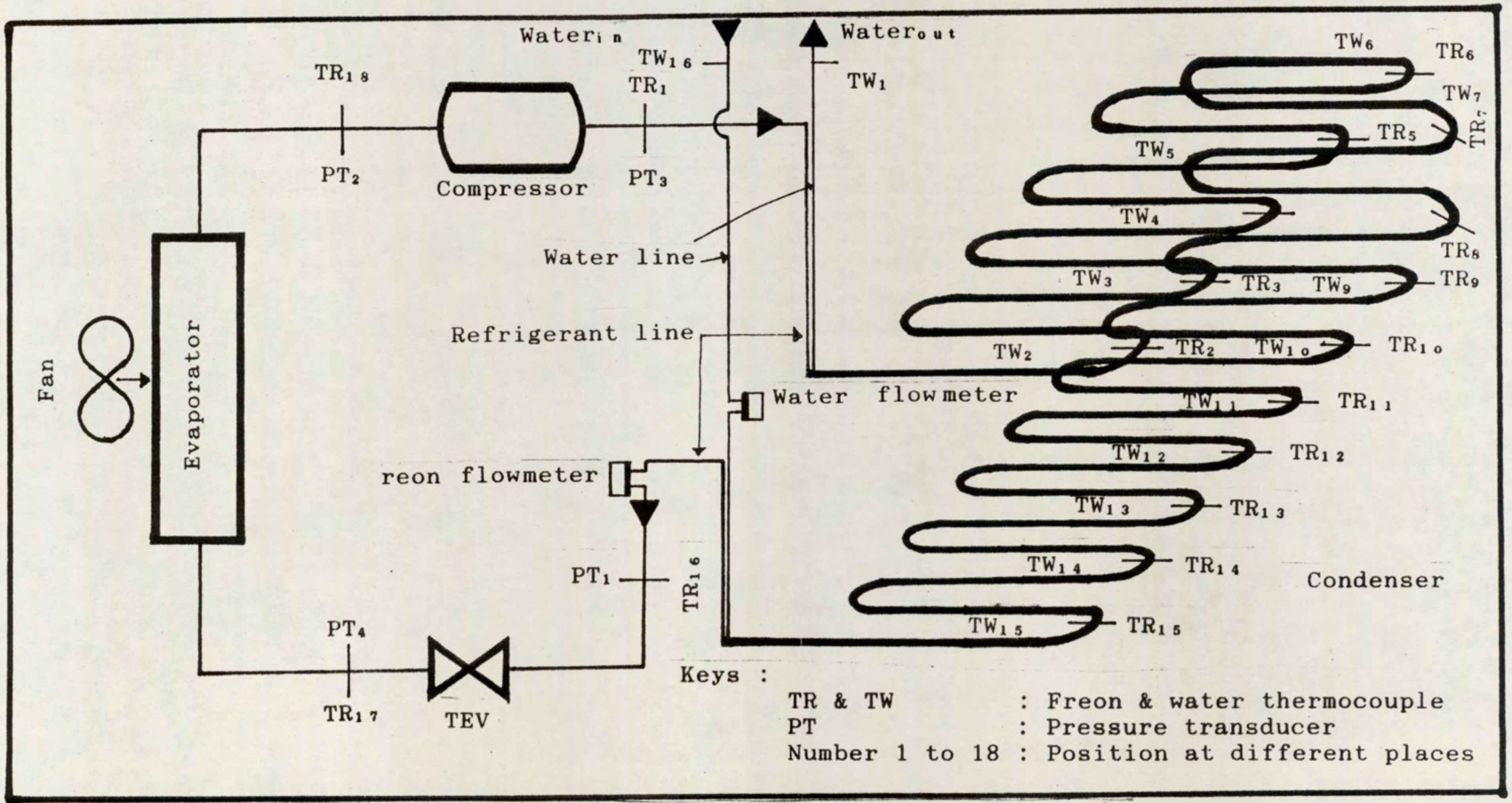

Fig.3.1.1: Block diagram showing the thermocouples and pressure transducers in heat pump system

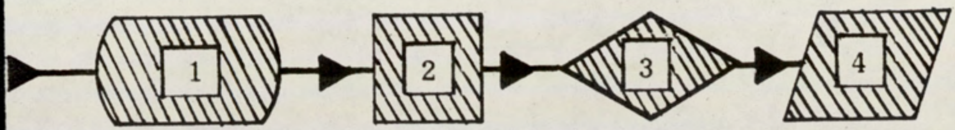

Keys :

1. Heat pump system
2. Analogue digital converter (ADC)
3. IEEE 488 interface
4. Computer system

Fig. 3.1.2 : Experimental protocol system

The final task was to develop a data-acquisition programme to enable the computer to respond to the sensors via the IEEE interface (Appendix A-2). The outputs were also displayed on screen, and stored on floppy disc for data analysis.

3.2: Air-water heat pump set up in laboratory

A small laboratory air-water heat pump with heat output in the region of 1.2 kW comprises of four major components: a compressor, an evaporator, a condenser, and a thermostatic expansion valve (TEV). Other related components to the system were also connected, which will be described later in the chapter (Fig. 3.2.1). Basically the refrigerating cycle can be divided into two parts; the higher-pressure side (high temperature and heat rejection) which includes the condenser, and the lower-pressure side (low temperature and heat extraction) which includes the evaporator. These two lines are separated and controlled by an expansion valve (see Appendix A-1.2 for detailed equipment specifications).

The heat can be pumped via the evaporating coil from a lower grade energy to a higher grade energy, so that its output becomes useful for heating purposes.The present experimental system is driven by a reciprocating compressor from a cold air heat source produced by a fan via evaporator, to a warmer water heat sink at the output of the water line in the condenser, (Fig. 3.2.2) using R12 as a working fluid.

3.2.1: Danfoss SC10H compressor

A compressor is a machine which is capable of increasing the pressure of the refrigerant gas by removing the vapour from evaporator so that discharge reed opens allowing the higher temperature and pressure gas to escape and enter the condenser whereby the condensation of vapour will produce usable heat.

The reciprocating compressor is designed for smaller heat pump systems, mainly for heating water. It is a hermetic type where the single-phase ac-motor and compressor is hermetically sealed in one casing. The compressor is also provided with an oil-cooling system (in the oil sump). Fig.A-1.2.1 shows a Danfoss SC10H compressor, with the technical dimensions at different view given by the manufacturer.

Fig.3.2.3 shows the compressor performance given by the manufacturer,[107]; at 0°C evaporating temperature and 45°C condensing temperature, where heat-output is 1120 W, and power consumption is 315 W, the coefficient of performance (COP) is claimed to be 3.55.

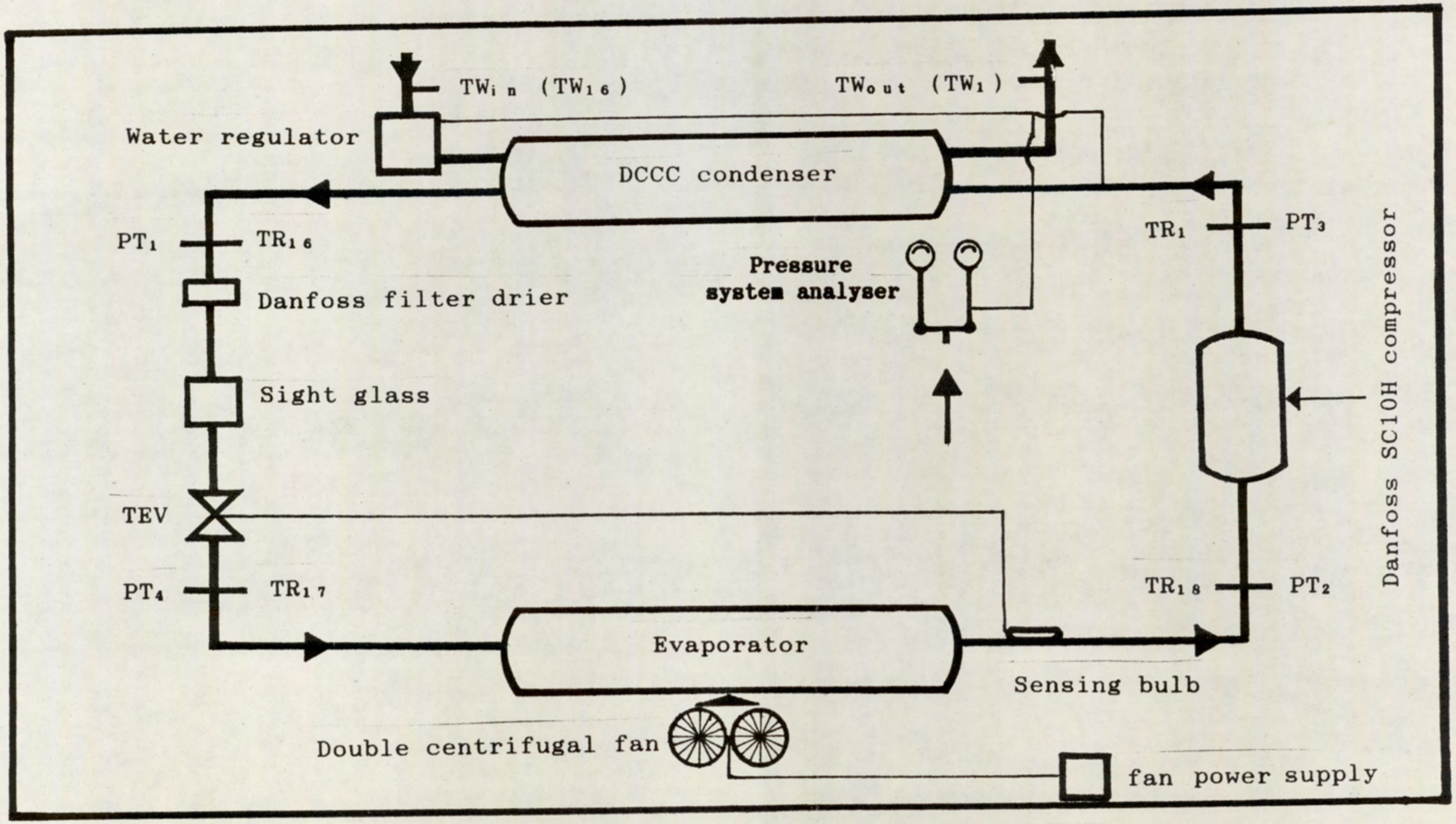

Fig.3.2.1 : Heat pump system and its components layout

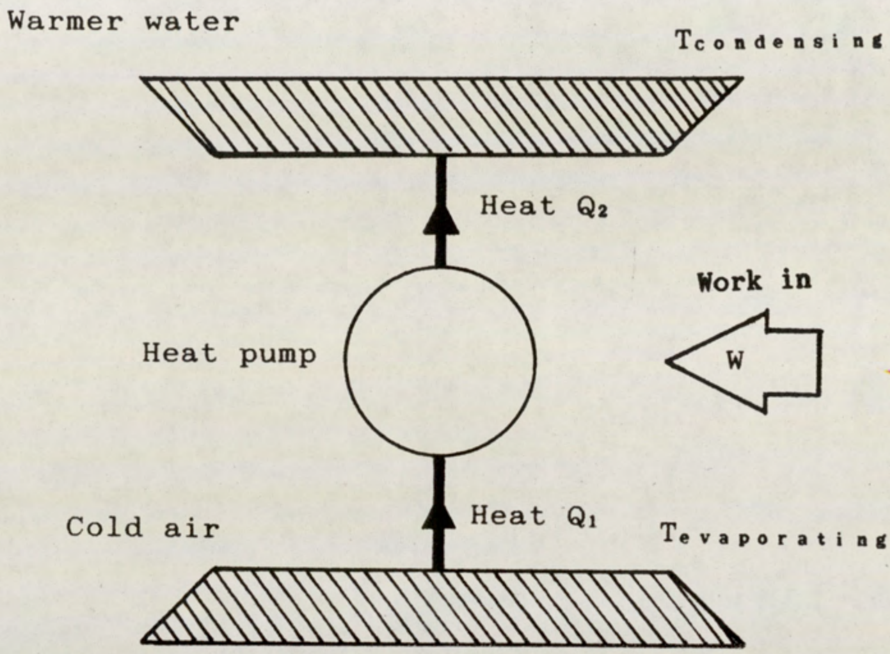

Fig.3.2.2: Schematic diagram showing cold air via heat pump system to warmer water

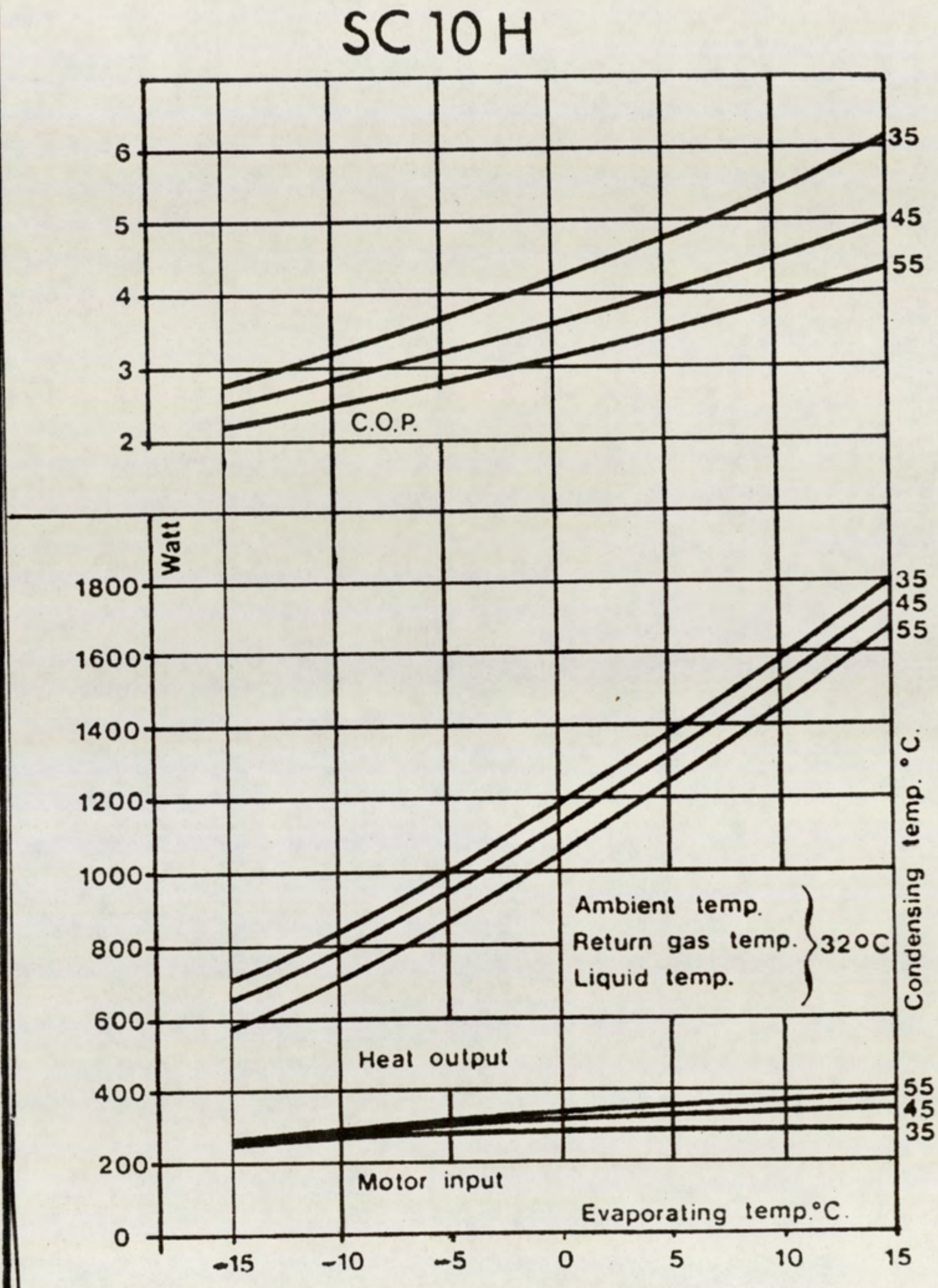

Fig.3.2.3: Danfoss SC10H compressor performance given by manufacturer

3.2.2: Thermostatic expansion valve (TEV)

The TEV is a pressure reducing device which separates the high and low pressure side of the vapour compression circuit as shown in Fig.3.2.4(b).The two major functions are to reduce the liquid refrigerant pressure and temperature, and to regulate its flow to the compressor. Fig.3.2.4(a) is a schematic diagram of the TEV showing the four principal parts of the valve:

a. A needle and a seat.

b. A diaphram connected to the needle.

c. A remote sensing bulb which is open to one side of the diaphram via a capillary tube.

d. A spring which can be adjusted by an adjustable-screw.

The TEV used in the system is supplied by Danfoss [108] (see Fig.A-1.2.2 for the manufacturer's specification). The operation is based on the interaction of the three forces (Fig.3.2.4(a)); evaporator-pressure ($P_{evap.}$), spring-pressure (P_{spring}), and the pressure exerted by the saturated liquid-vapour mixture in the sensing-bulb (P_{bulb}). The sensing-bulb is clamped to the suction line parallel to the refrigerant tube (outlet of the evaporator) which is responsive to the changes of the refrigerant vapour temperature. For practical purposes, this temperature is taken to be equal to the temperature of liquid-vapour mixture so that its pressure is always assumed to be the saturation pressure corresponding to the vapour temperature at the sensing-bulb contact.

The saturation pressure which is exerted on the diaphram through the capillary tube tends to push downwards and cause the valve to move in the opening direction (Fig.3.2.4(a)) while the combination of evaporator-pressure and the spring-tension (hand adjustable) tends to push the diaphram upwards and cause the valve to move in the closing direction. The valve is said to be in the equilibrium position when

$$P_{bulb} = P_{evap.} + P_{spring} \qquad \text{Eqn.3.1}$$

The position will be held until a change in the degree of suction superheat unbalances the forces and causes the valve to open or close. The suction superheat set by the manufacturer is 6°C (Appendix A-1.2). If the superheat is greater than 6°C, $P_{bulb} > P_{evap.} + P_{spring}$, the valve is open, thereby increasing the liquid flow into the evaporator. On the other hand, if the superheat is less than 6°C, $P_{bulb} < P_{evap.} + P_{spring}$, the

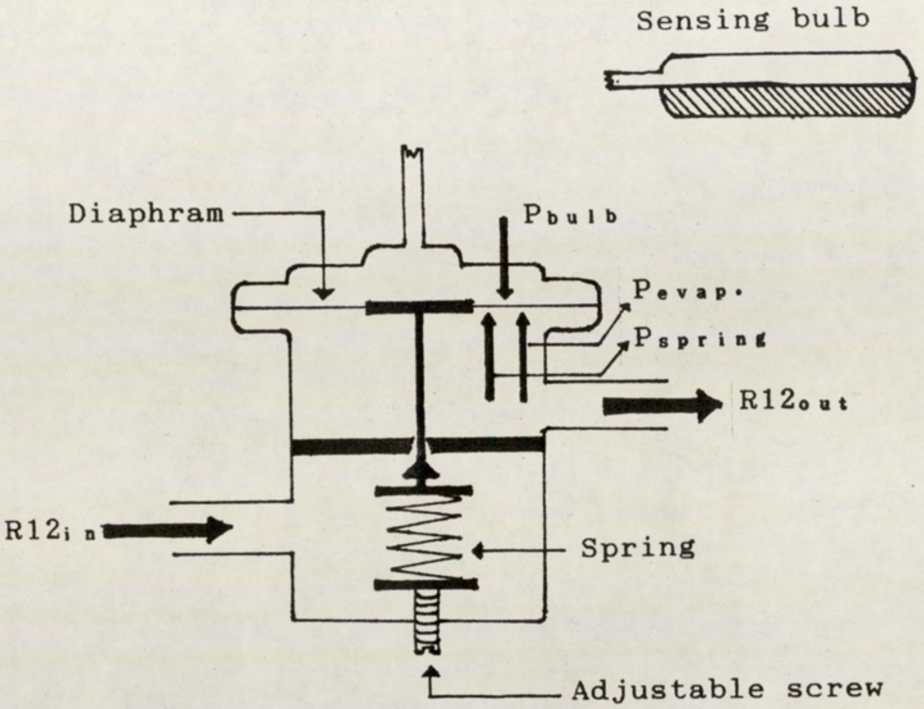

Fig.3.2.4(a): Schematic diagram showing the four parts of a TEV

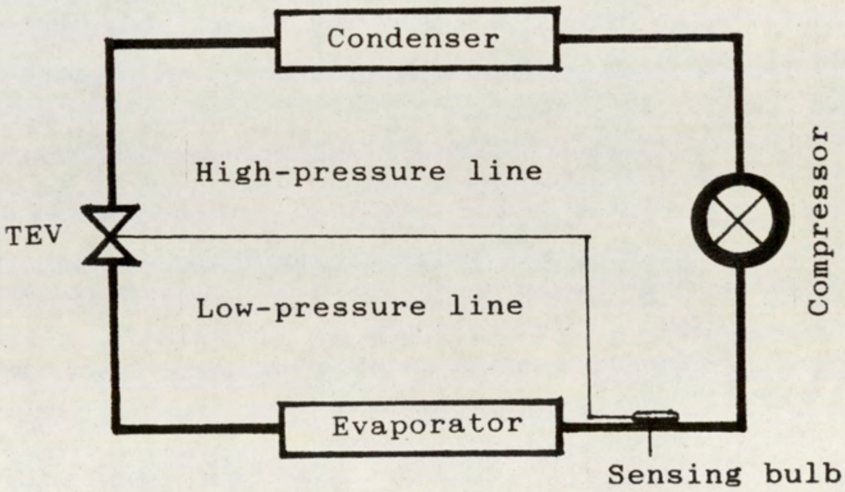

Fig.3.2.4(b): Vapour compression circuit control by TEV

valve is in the closing position, so throttling the liquid flow into the evaporator. This phenomenon will continue until the superheat is brought back to 6°C where the equilibrium position is attained.

3.2.3: Heat exchanger

The heat exchanger is an important device used in the heat pump system which acts as a medium of transferring heat. In the system, the heat exchanger is designed as a medium for heat to be collected from the outside cool air through an evaporator and also, as a medium for heat to be released to a higher grade energy in the condenser. Shah [92] has classified the design of heat exchangers according to transfer processes, surface compactness, construction features, flow arrangements, number of fluids, and heat transfer mechanism. In the present system, the focus is the heat pump condenser, where the behaviour of the fluid flows at given conditions is studied. The present evaporator was not the main interest of the research, but it was used as a medium, to collect cool air outside the system.

Evaporator

The present evaporator was salvaged from an air-conditioning unit manufactured by Versa Temp Air-Water Heat Pump Company,[41] (see also Appendix A-1.2 for detailed geometrical specifications).

A double centrifugal fan is used to circulate the air through the evaporator, which consists of wavy continuous fins with the tubes for freon flow in staggered positions, as shown in Fig.3.2.5 (see Photo 1 and Photo 3). The heat from the cool air which is driven through the fan will be picked up causing the liquid freon in the evaporator to evaporate by absorbtion of latent heat of evaporation. The fan is fixed parallel to the front surface of the evaporator so that the constant air circulation rate could be channeled directly to the evaporator. The air-speed is controlled by a variable power supply (variac), fixed at the bottom of the rig.

Condenser

Another type of heat exchanger present in the system is the condenser. It consists of two copper tubes, 15 meter long, with different diameters, brazed together side by side (see Appendix A-1.2 for the technical dimensions). The straight double tube is then bent through 180degrees every half-meter, as shown in Fig.3.1.1 to make it

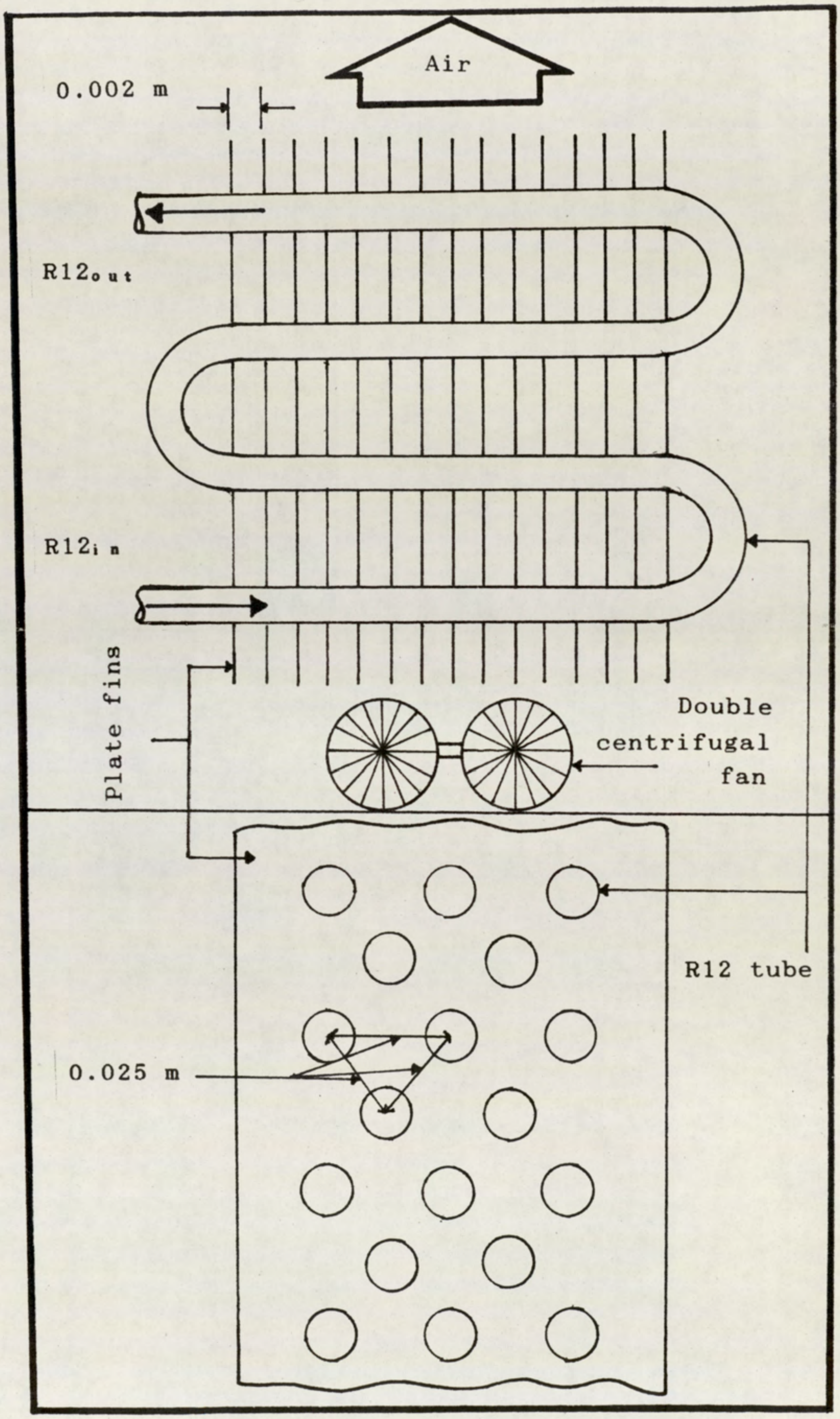

Fig.3.2.5: The cross-section of continuous fin evaporator used in the system

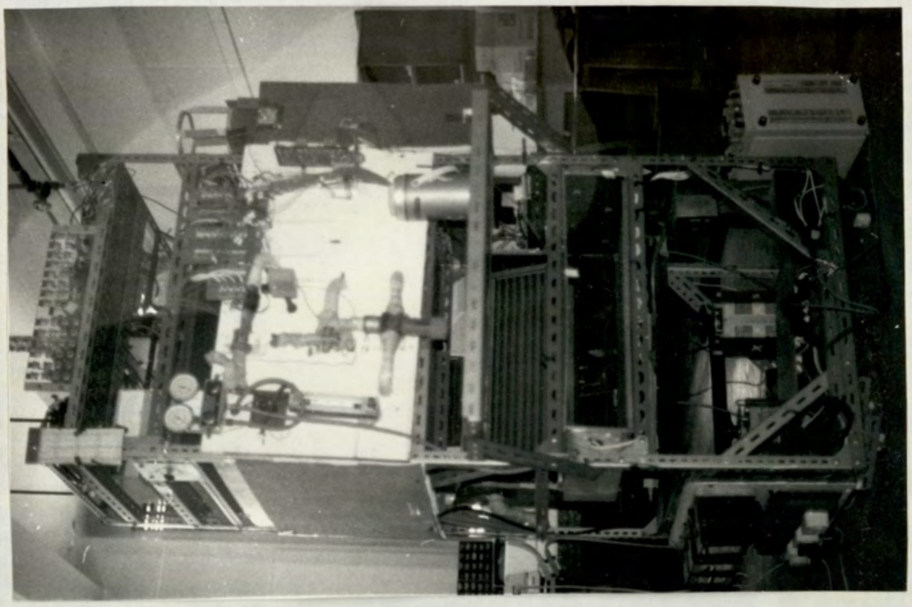

Photo 1:
The rear view of a laboratory air-water heat pump

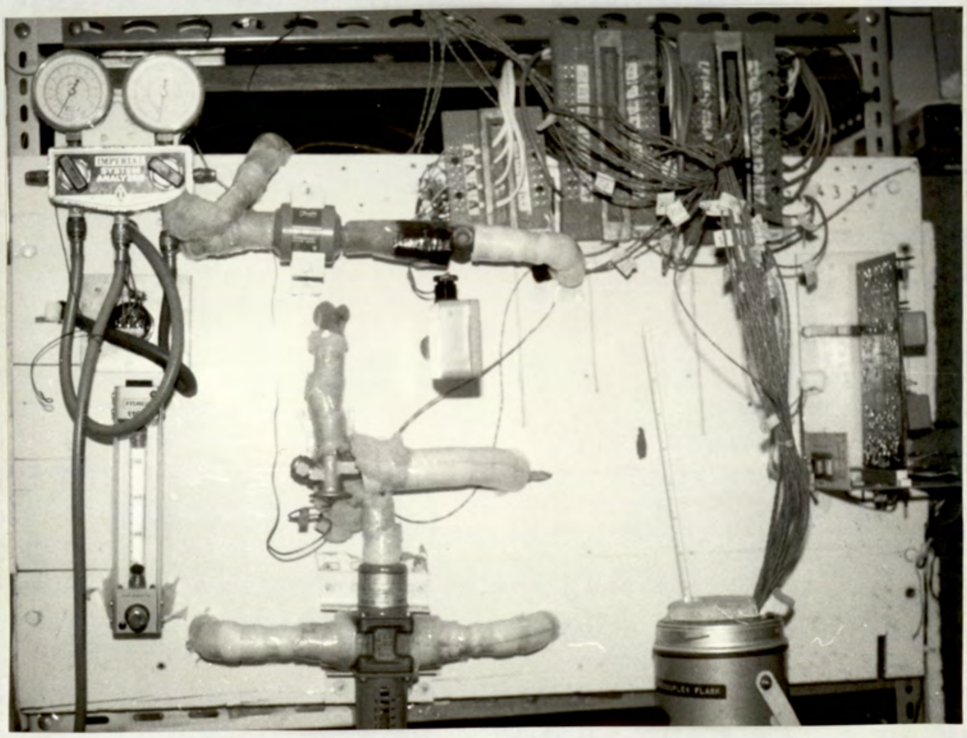

Photo 2: Reference junction and other heat pump components (closed-up of Photo 1)

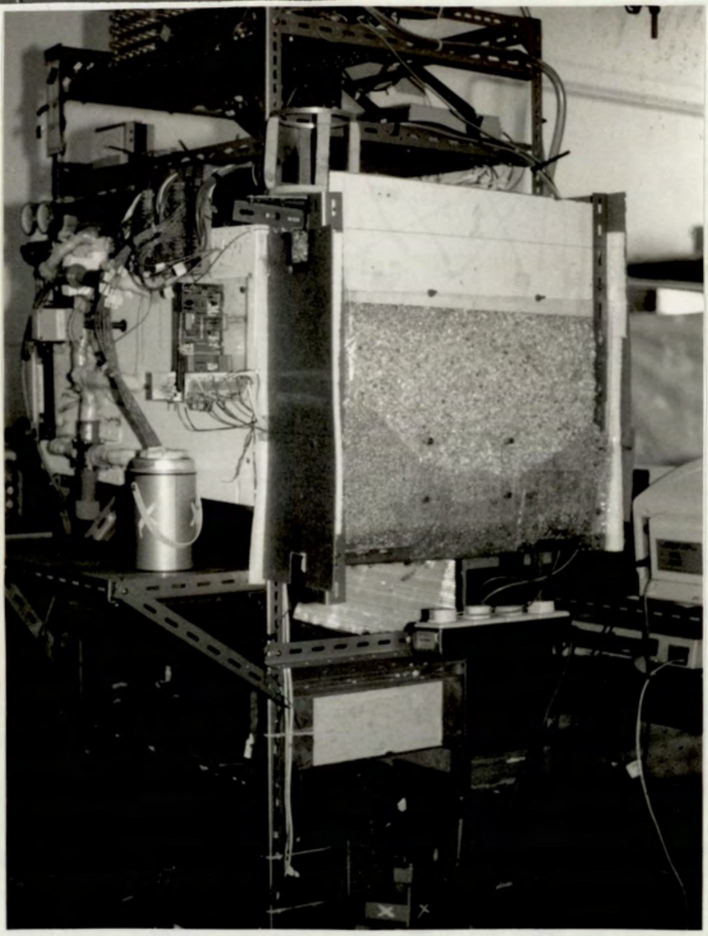

Photo 3: Side view showing the heat pump system

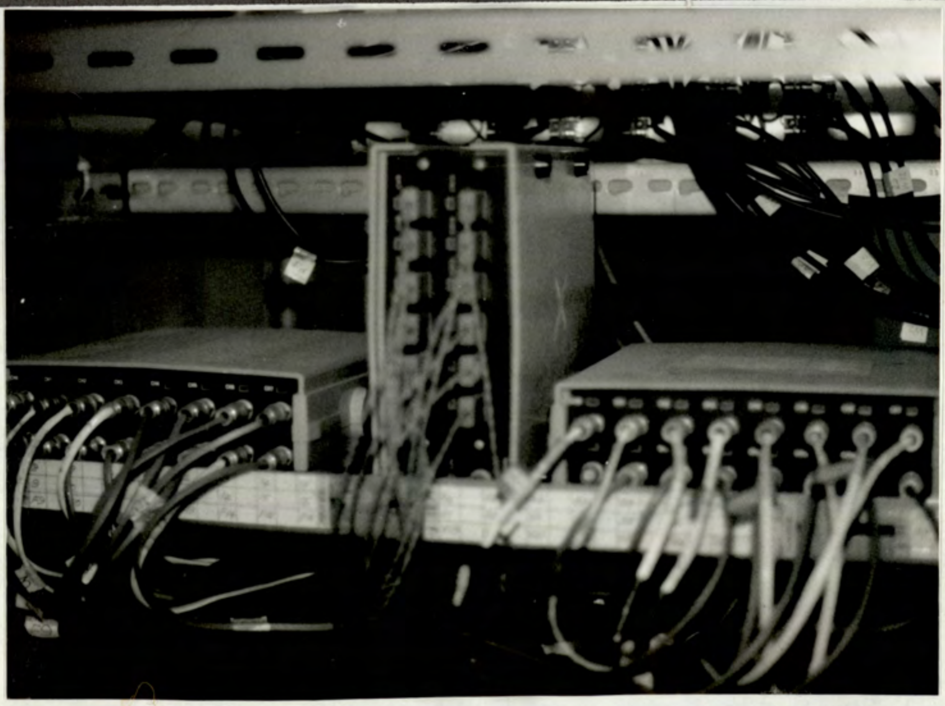

Photo 4: Photo showing the connection of sensors to analogue-digital converters

conveniently compact.

Fig.3.3.1 shows the cross-section of the condenser with R12 flow in the refrigerant tube and water flows in the water tube in parallel but opposite flow direction. In simple terms, the condenser is to referred to as a double coupled counter-current flow condenser or DCCC. The DCCC was lagged with pipe lagging insulation of 1.5 cm internal diameter, and fully covered by vermiculite insulating material to minimize heat loss to the surroundings. An accumulator made of a 0.25m long copper tube with 0.025m diameter was soldered at a point, 12m away from the refrigerant entry on the refrigerant tube, and the next 3m of the refrigerant tube was again soldered to the water tube. The possibility of liquid refrigerant flow back to the compressor was eliminated by the accumulator.

3.2.4: Miscellaneous refrigeration components

Fan

A double centrifugal fan with backward curved blades taken from the Versa Temp heat pump unit is fitted such that the outlet air is directly blown onto the front face of the evaporator. The fan ensures high operating efficiency by increasing the air circulation rate which is controlled by a variac. Fig.3.2.6 shows the layout of the fan attached to the evaporator.

Refrigerant filter drier

Moisture and contaminating particles that may enter during construction or during system operation can cause restriction of the liquid flow. A filter-drier was fitted in the refrigerant line just before the TEV. It consists of a very fine wire-gauzed filter to trap any contaminants, and silica gel as a drying agent in the form of small granules supplied by Danfoss (Fig.3.2.7).

Water regulator

The condenser water regulator is essential for varying the operating conditions. By turning the adjustable hand wheel in a clockwise direction, the water flowrate will be decreased causing the water outlet temperature to increase. The decrease in the water flowrate also increases the refrigerant condensing temperature and pressure (anticlockwise turning will reverse the condition).

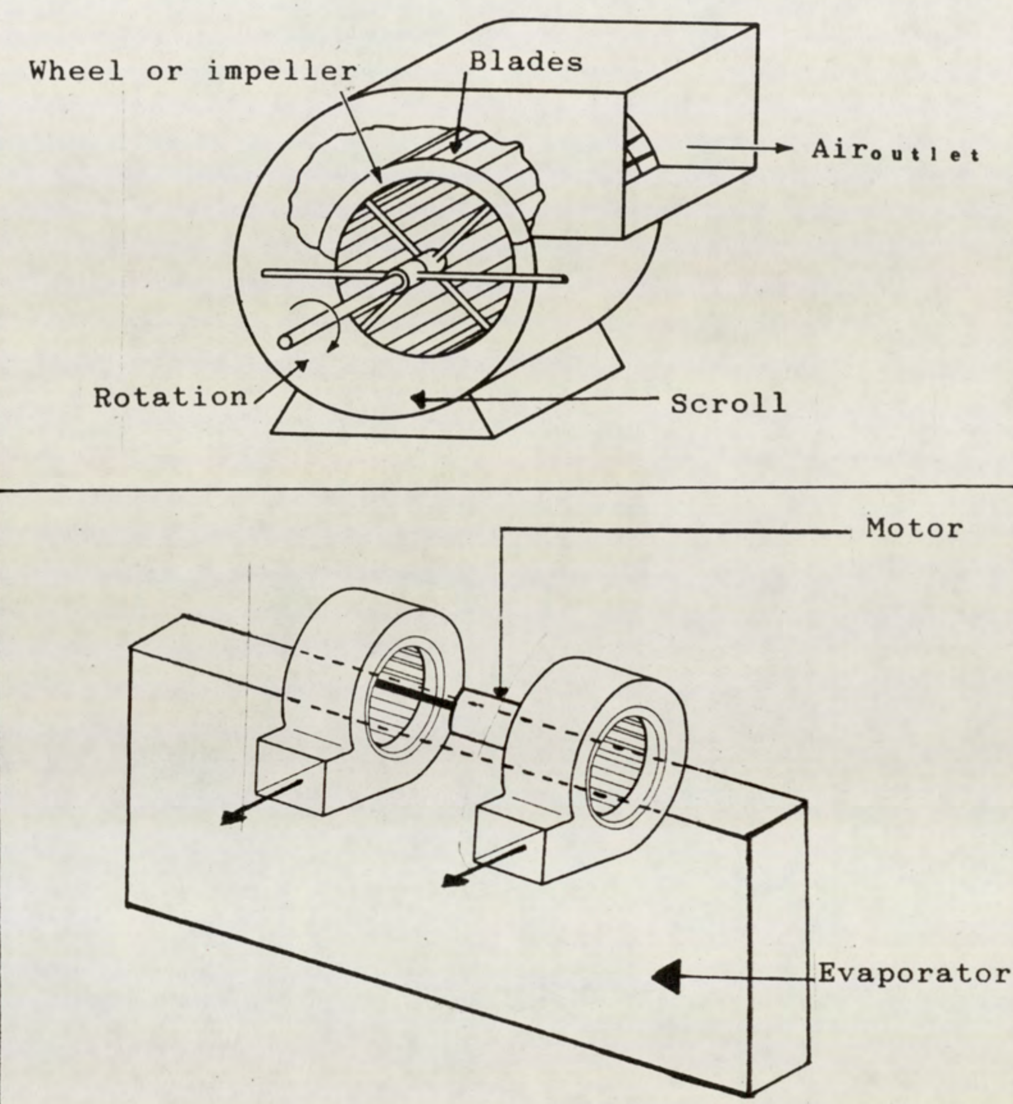

Fig.3.2.6: Positioning of the fan attached to heat pump evaporator

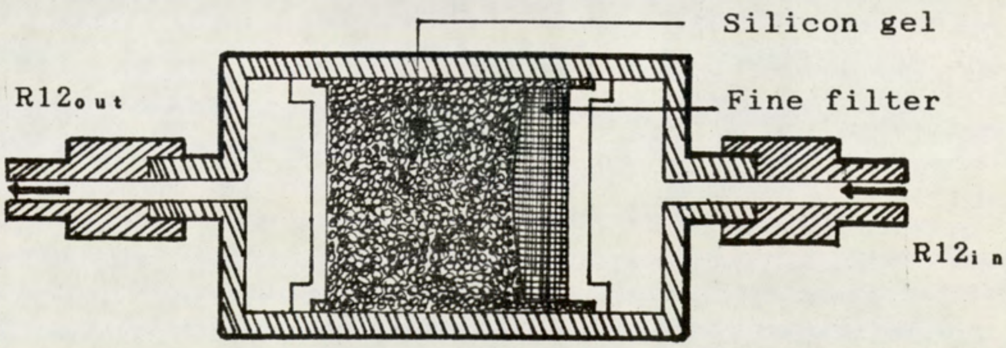

Fig.3.2.7: Schematic diagram of a Danfoss filter drier

Fig.3.2.8 shows a block diagram drawn not to scale of a typical Danfoss WVFX water regulator (see also Fig.A-1.2.3 for detailed internal instruction) which is fitted in the water line just before the water enters the condenser. A tube of inside diameter of 0.001m connects the valve to the discharge line outside the condenser. The discharge pressure could be maintained constant condition by varying water flowrate. The range of the working pressure and working flowrate in the experimental results is controlled by this unit.

<u>Sight glass</u>

A Danfoss sight glass was fitted in the liquid refrigerant line immediately after the filter drier to ensure complete condensation has occured before measuring the actual freon temperature and pressure. It consists of a brass body into which a glass window has been fitted at the centre,[109]. The system is said to be fully charged with freon when liquid freon is hardly seen through the glass window (only clear liquid could be seen). The presence of bubbles throttling rapidly in the glass indicates a shortage of freon in the system which may result in incomplete condensation. To ensure there is enough freon in the system, the sight glass should always be checked and refilling of freon must be done at once.

<u>Pressure system analyser</u>

A pressure system analyser which consists of the low-pressure scale and high-pressure scale is connected to the system. The main functions are to indicate whether there is sufficient freon in the system after each run, admitting freon into the system, and evacuation of the freon from the system by using a vacuum pump type BS 2400 (Appendix A-1.2).

3.3 : Experimental condenser

The main function of the condenser unit in the system is to remove heat from refrigerant. The refrigerant will change its state from vapour to liquid as it passes through the condenser. As the refrigerant enters the condenser (at discharge pressure), it consists of 100% vapour (the desuperheating region). In this case heat will be transferred to the cooler-surface area where the cooler water side of the DCCC will absorb heat from the refrigerant side, increasing the water temperature.

The process will continue until the refrigerant temperature at discharge pressure is below the saturated vapour temperature. The partly

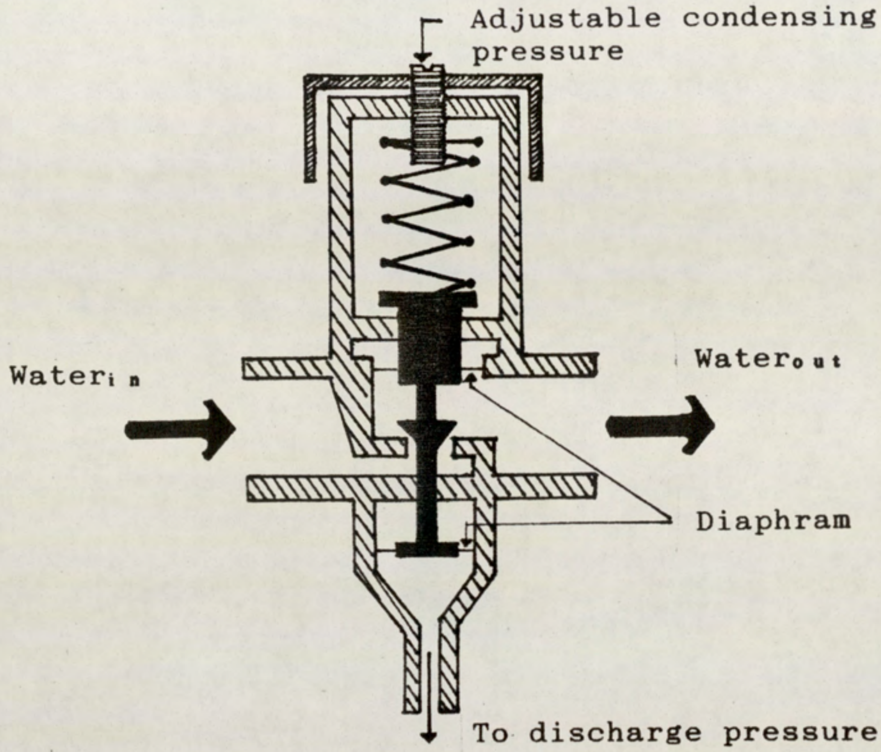

Fig.3.2.8: Schematic diagram showing the cross-section of a Danfoss WVFX water regulator

condensed vapour will form the mixture of liquid-vapour where the vapour fraction or quality (by its mass) will be reduced while the liquid fraction is increased. While vapour fraction is reducing from 1 to 0 the refrigerant is a two-phase fluid. The process will continue until complete condensation is attained, when all refrigerant vapour has changed its state to liquid (at x=0). The latent heat of vapourization at condensing temperature will be absorbed by the water side through the transferring area to cause water temperature higher than when it is in the single vapour region.

The fully condensed refrigerant liquid will be further cooled down in the single-phase subcooling region exiting as a sub-cooled liquid at the entrance to subcooling region. The liquid refrigerant expands through the TEV back to the evaporator.

To summarize, there are three distinct regions treated separately in the analysis:

a. The single-phase desuperheating region (vapour).

b. The two-phase condensing region (liquid-vapour mixture).

c. The single-phase subcooling region(liquid).

3.3.1: Layout of the condenser

The present condenser was designed such that the 15 meter long tube can be seen as in Fig.3.1.1 where it occupies a small area. The whole unit is supported by a 0.3x0.3x1.0 meter wooden frame with face 6 facing outwards left openable for filling with vermiculite insulation materials, as shown in Fig.3.3.2. Fig.3.3.1 shows the cross-section of the DCCC in which the thermocouples for sensing refrigerant and water temperatures are fixed opposite to each other at the bend. Two different sizes of pipe diameter are used, the refrigerant tube being smaller in diameter.

As mentioned, the bending and the soldering is done manually making it difficult to measure the pipe diameter accurately at the 180deg-bends, and the thickness of the soldering material used throughout the 15 meter long condenser. The pipe sizes given by the manufacturer were remeasured manually in order to suit the design of the condenser.

$$\text{Straight pipe diameter} > \text{Bending pipe diameter} \qquad \text{Eqn.3.2}$$

The above measurement was done at different points and an average value was considered in the analysis.

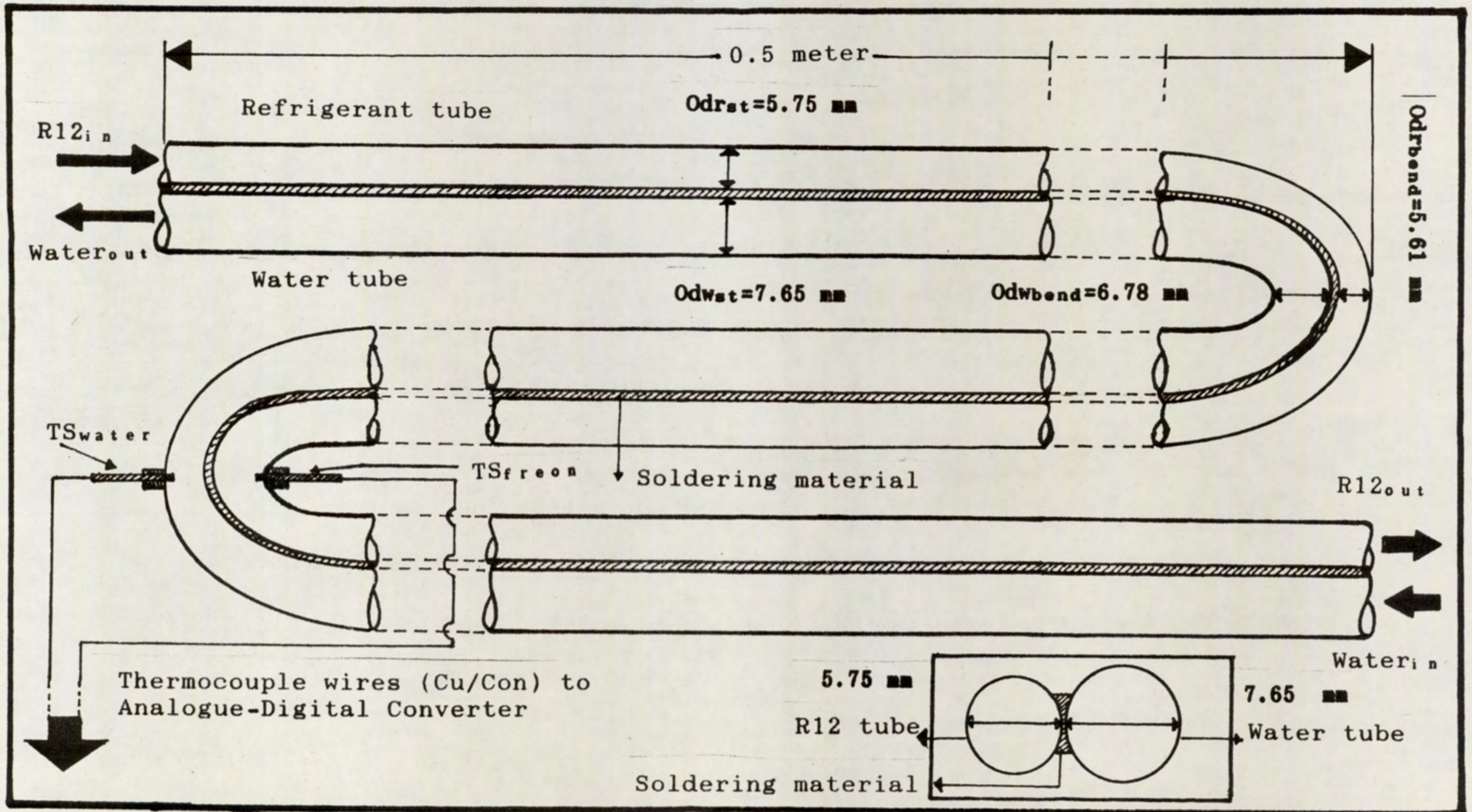

Fig. 3.3.1 : The partly cross-section (side view) of the DCCC condenser used in the heat pump system

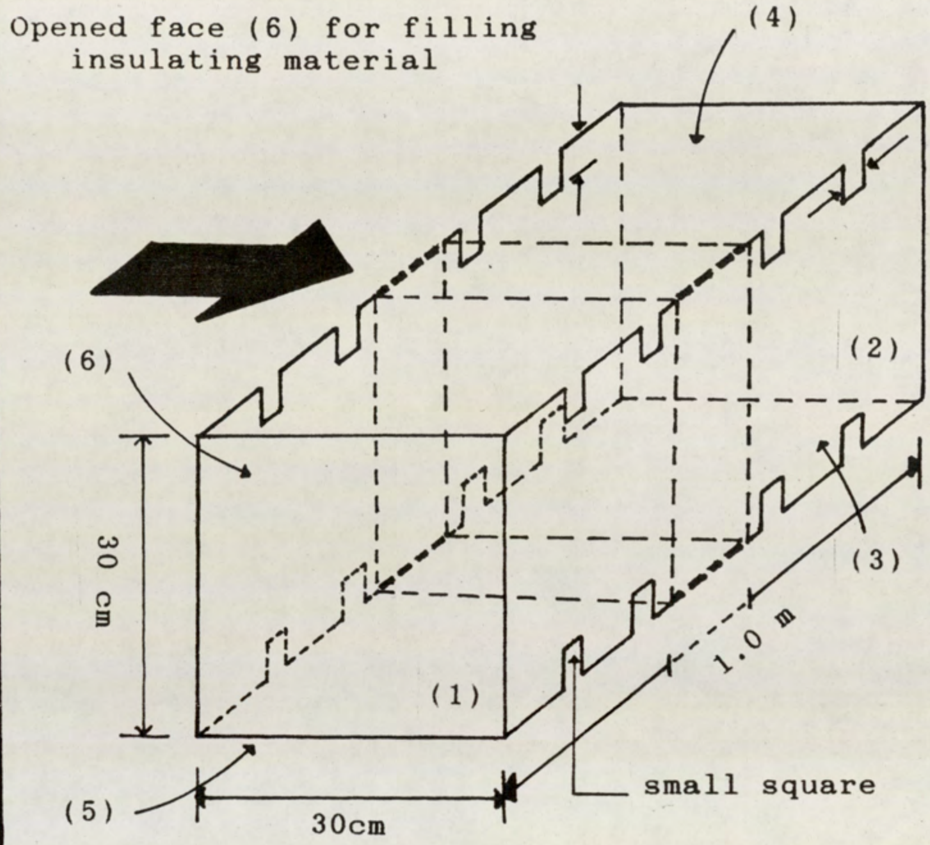

Keys :

i. Face 1 and 2 is closed by square shape of specified dimension .

ii. Face 3,4,and 5 is also closed by rectangular shape of specified dimension .

iii. Face 6 is uncovered .

iv. The copper tube is supported on the small square both in the upper and bottom faces .

Fig. 3.3.2 : A cuboid frame to support the copper pipe (DCCC) by the small square

3.4: Computerized data acquisition system

This section discusses how the information measured in the system is transferred to a mini computer via ADC and an IEEE interface. A BASIC program for data acquisition system was developed to store the data automatically on floppy disc and displayed it on the screen.

A delay time between each Run is set to enable the equilibrium condition be achieved before storing information onto the disc. The computer also does all the necessary calculations and conversions. The computer programme which has been developed for data acquisition system can be subdivided as follows; single-channel reading, all-channel reading, averaging -channel reading, and conversion-channel reading. Fig.3.4.1 shows a data acquisition system which enables the information be read and displayed on the screen. It comprises four major sections; sensors, analogue-digital converters, an IEEE interface, and a computer.

Its flowchart diagrams are also discussed later in this section (see also Appendix A-2 for full data acquisition computer programme and related programme).

3.4.1: Mini-computer

For sampling and storing the information read or measured from the system, a BBC 64K mini computer with a double disc drive was used. The output was displayed on a monitor connected to it (see Appendix A-1.3).

The unit is also used for experimental data analysis which is graphically displayed and printed by Epson LX-80 printer. The experimental data was used to compare with the model analysis and to use partly as input data to the model. For the model analysis, a BBC Master 128K supplied with a double disc drive, a hard-disc of 20 Mbytes, and a 32016 second processor was used (see Appendix A-1.3 for details).

3.4.2: IEEE 488 interface

The IEEE (Instituate of Electrical and Electronic Engineers) interface was originally developed by Hewlett Packard in 1975,[110]. It exchanges digital data in bit parallel, byte serial form between devices. It has the ability to send data (talker), receive data (listener) or both (talker-listener), and act as a controller. In the present system the IEEE interface acts both as a talker and listener.

The information which has been signaled to the ADC is then listened to by the interface which then communicates with the computer. Three

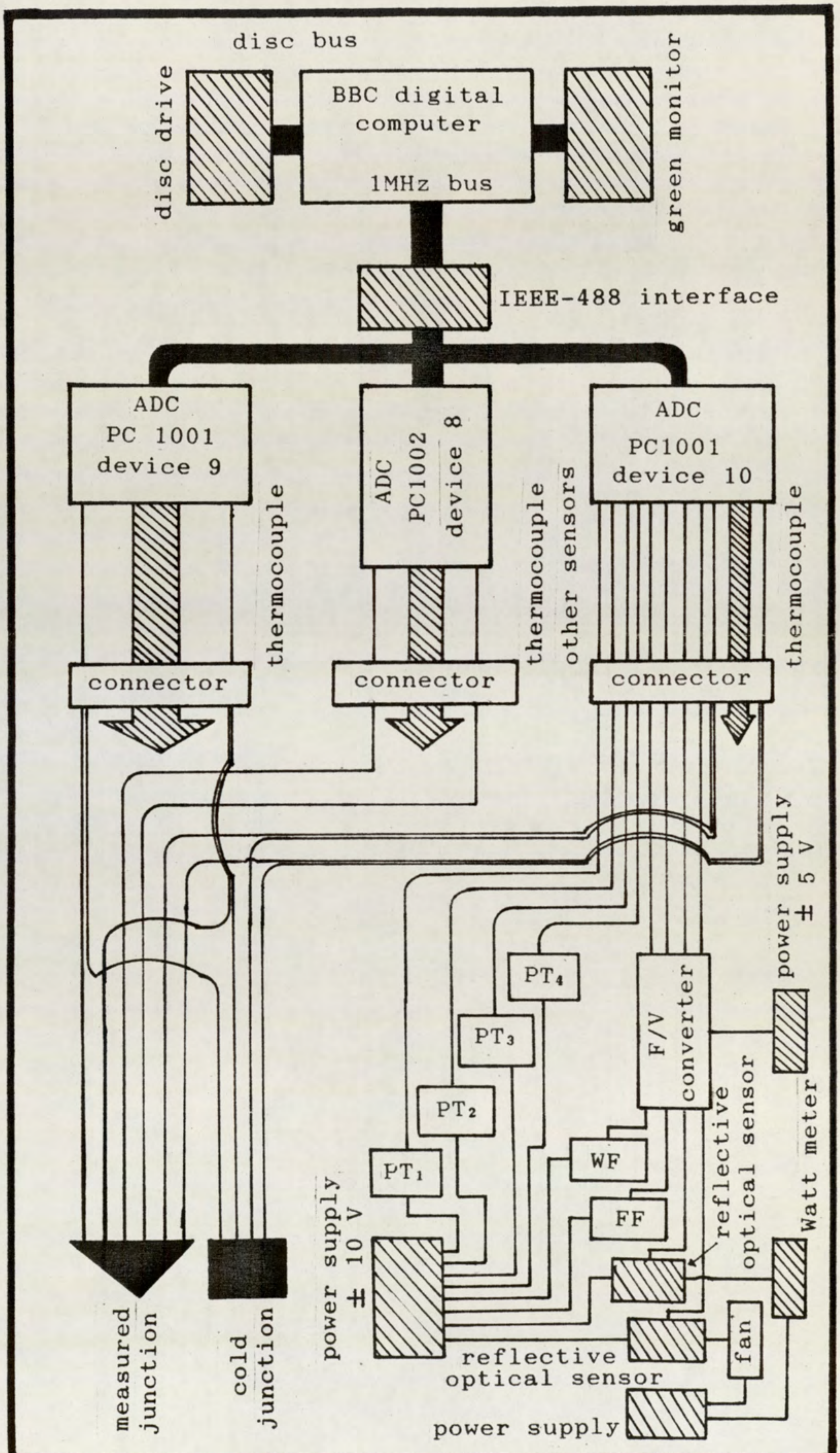

Fig.3.4.1: A block diagram showing data acquisition for the heat pump system

analogue to digital converters are connected to the IEEE interface which is linked to the 1Mhz bus port of the computer.

3.4.3: Analogue to digital converters

The computer can only recognise the information sent by the system in digital form. So, all information is digitised by the ADC and communicated through the IEEE interface to the computer. Two types of device have been used; ADC version PCI 1001 and PCI 1002 (see **Appendix A-1.3** for the specification).

As mentioned earlier, there were 43 sensors in the system. 4 of them were not used in the measurement but they were still connected to the system.

Three ADCs (2 of PCI 1001 and 1 of PCI 1002) supplied with 16 channels in each unit were used, shown in **Photo 4**. Out of 48 channels, 3 channels were unused. The sensors for measuring water and freon flowrate, air speed from the fan, and power from the Watt meter were also connected although they were not used in the data-analysis.

PCI 1001

Two ADCs of this type, as shown in **Fig.3.4.1**, were used to convert the analogue signals from the sensors. For sampling, a subroutine for the computer program was developed. The device number was selected in the range of 0 to 14 by means of 4 binary sequence dual in line switches, in this case numbers 9 and 10 were chosen as device numbers respectively for the units.

For full scale voltage input, the output should read 4000±1 bits. These units were been calibrated at 4000 bits FSD (full scale display) where overange occurs at +4097 bits and underange occurs at -4097 bits. With all inputs short circuited the outputs should read 0±1 bit,[111]. It is important to note that every channel should be within its operating range, otherwise cross-talk across the channel may occur. The unused channels were left open circuit, when the output will read approximately zero.

Each channel is provided with its own operational amplifier mounted inside the top cover with gain of 100 which is matched with 0.1% resistors accuracy. For full scale output, the input to the ADC section is 1.0 V so that the input to each channel must not exceed 10 mV dc. Some modifications in the gain of the unit were made to suit the individual signals from the sensors.

The modifications on device number 10 (SN17433) are as follows:

a. Channel 0 to 3: The gain was changed to unity for the water and freon flowrate, air speed from the fan, and power from the Watt mater measurements.

b. Channel 4 to 7: The gain was increased to 5 to suit the pressure transducer's operating limit, where maximum output is 200 mV dc corresponding to pressure 14.0 bar (1480.4 kPa).

c. Channel 8 to 15: These channels remain unchanged (as supplied by the manufacturer) supplied with the maximum input of 10 mV. For measuring temperature up to 210°C with the reference temperature of 0°C, these arrangements are suitable.

The operational amplifiers on device 9 were unchanged since they were only used for measuring temperatures. Table 3.1 shows the connections of the sensors to the input of the ADC, and the connections of the sensors via IEEE interface and ADC to the computer for sampling are shown in Fig.3.4.2.

PCI 1002

No modifications were made since the unit was only used to measure temperatures. It was designed for thermocouple wire type-T for temperature range between -270°C and +212°C with input range internally set to 10 mV. The inputs were scanned, displaying the output in bits for channels 1 and 2, and in temperature for channels 4 to 15, while channel 3 acts as a reference junction.

The operation channel selection was as follow:

a. Channel 0: Internally connected to a proportion of power supply voltage. Used to identify which range the unit has been set to, either approximately 400 bits for 100 mV or 1333 bits for 30 mV range or 4000 bits for 10 mV range.

b. Channel 1 and 2: Directly connected to the multiplexer with high level single ended input connections. The ranges are 10 mV, 30 mV or 100 mV.

c. Channel 3: Internally connected to the platinum resistance thermometer on the cold junction block. The cold junction temperature scaling is:

0°C - 100°C = 0 - 4000 bits (10 mV range)

0°C - 100°C $\simeq$ 0 - 1333 bits (30 mV range)

0°C - 100°C = 0 - 400 bits (100 mV range)

d. Channel 4 to 15: Connected via thermocouple material plugs and

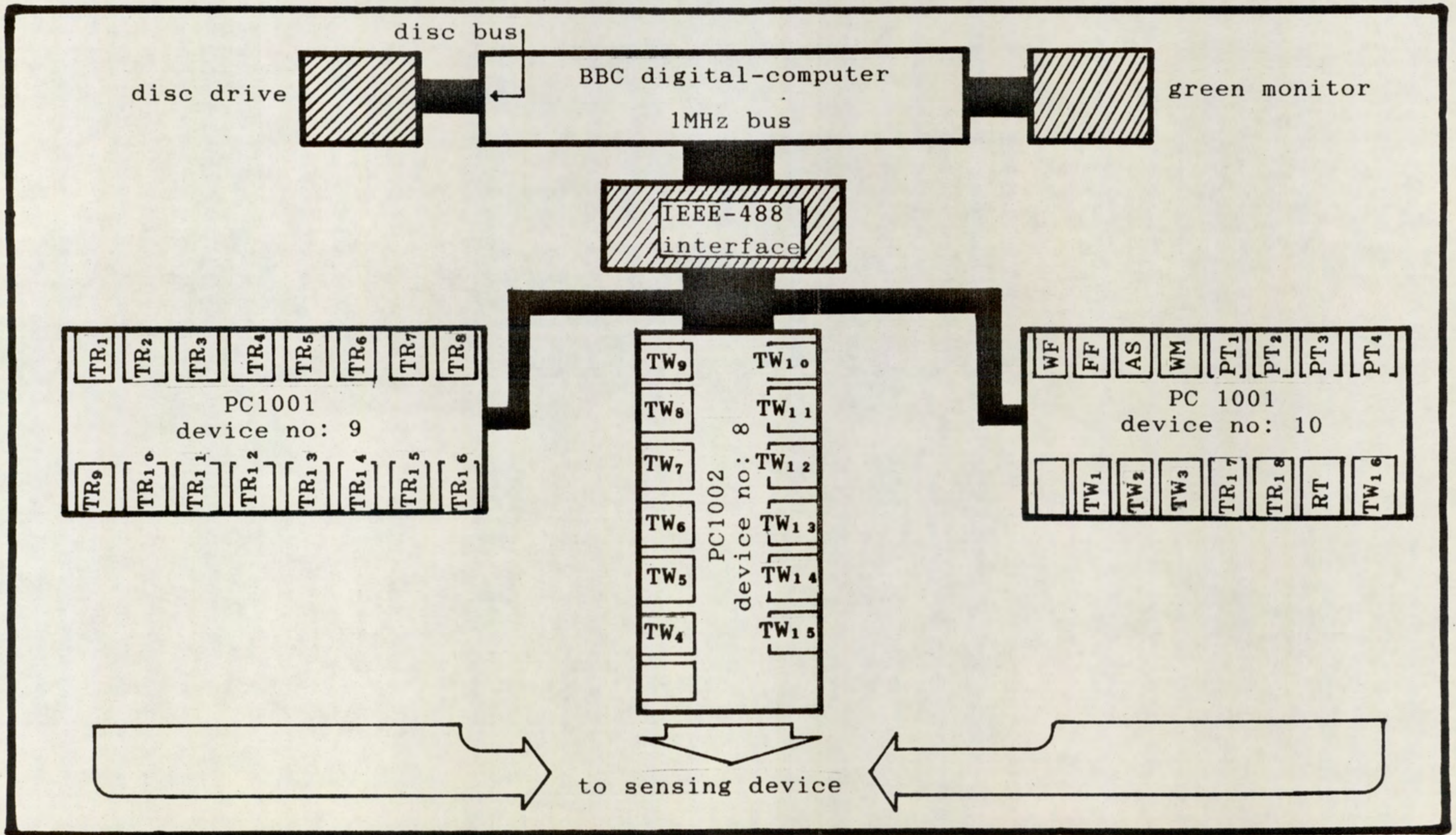

Fig.3.4.2: Sensors connecting via input ADC and an IEEE interface to digital-computer

sockets and cable to the cold junction block which is then fed to individual differential amplifiers of gain 100 and then to the multiplexer.

PCI 1002 produces data which is linear with microvolts rather than linear with the temperature. Linearisation is simply carried out by a polynomial expansion of fourth order.

$$T = \sum_i C_i V^i \qquad \text{Eqn.3.3}$$

where T is temperature in °C, V is voltage in mV, and C_i is selected from the type of the thermocouple wire and the input voltage range as given by the supplier,[112]. For practical purposes the conversion of reference bits in channel 3 to temperature, 10 mV input range was considered where it gives a maximum of 4000 bits corresponding to 100°C of the cold junction temperature, scaling has been approximated to 40 bits per °C.

$$T_{ref} = (Bit_{ref} \times 0.025)\ °C \qquad \text{Eqn.3.4}$$

The reference temperature in PCI 1001 was taken to be 0°C (T_{ref} = 0°C) since the cold junction was externally immersed in a flask of ice-water maintained at 0.0 ± 0.1 °C.

A summary of the sensors's arrangement connected to the ADC is given in Table 3.1 below:

Model PCI	1002			1001			1001	
Serial No.	17369			18352			17433	
Device No.	8			9			10	
Items	CH	CN	Items	CH	CN	Items	CH	CN
-	0	-	TR_1	0	1	WF	0	40
-	1	-	TR_2	1	2	FF	1	41
-	2	-	TR_3	2	3	AS	2	42
IRJ	3	0	TR_4	3	4	WM	3	43
TW_4	4	20	TR_5	4	5	PT_1	4	36
TW_5	5	21	TR_6	5	6	PT_2	5	37
TW_6	6	22	TR_7	6	7	PT_3	6	38
TW_7	7	23	TR_8	7	8	PT_4	7	39
TW_8	8	24	TR_9	8	9	-	8	-
TW_9	9	25	TR_{10}	9	10	TW_1	9	17
TW_{10}	10	26	TR_{11}	10	11	TW_2	10	18
TW_{11}	11	27	TR_{12}	11	12	TW_3	11	19
TW_{12}	12	28	TR_{13}	12	13	TR_{17}	12	32
TW_{13}	13	29	TR_{14}	13	14	TR_{18}	13	33
TW_{14}	14	30	TR_{15}	14	15	RT	14	34
TW_{15}	15	31	TR_{16}	15	16	TW_{16}	15	35

Table 3.1: Summary of sensors arrangement connected to analogue-digital converter

where Items: Thermocouple sensors or pressure transducers or flowrate sensors or optical sensors for air speed and Watt meter measurements.

CH: Channel number in analogue digital converter.

CN: Channel number for computer program and positioning of sensors in the system.

TR & TW: Freon and water sensor for temperature measurements respectively.

WF: Water flowrate sensor.

FF: Freon flowrate sensor.

AS: Optical sensor for air speed measurement.

WM: Optical sensor for Watt meter measurement.

PT: Pressure transducer for pressure measurement.

IRJ: Internal reference junction in PCI 1002.

RT: Sensor for measuring room temperature.

Numbers: Positioning of the sensors as illustrated in Fig.3.1.1.

3.4.4: Computer program

A simple BASIC program was developed to link the information to be stored and displayed on the screen. The main program for data acquisition reads the appropriate channel number corresponding to the sensor in the system as shown in Fig.3.4.3 by using control statements to the device number and desired channel number. As it passes the channel, the light indicator will flash.

The second part of the program is to display the output onto the screen. The program has the following objectives:

a. Single and all channel readings: Mainly for testing the single channel reading and all channel reading so that any faults in the sensors could be easily detected and repaired or replaced.

b. Averaging channel readings: Used for the purpose of temperature calibration by taking an average reading of 10 data sets. A complete set is the data from all channels from the beginning to the last channel. An average of 10 sets of readings are considered to make up one Run. It was found that the change in temperature during the readings was not significant.

c. Converting channel readings: This program displayed the average output data by converting to their actual values, and stored them onto the disc for each Run.

d. Miscellaneous programs: Included the program for pressure transducer calibration, graphical and pictorial representation of output

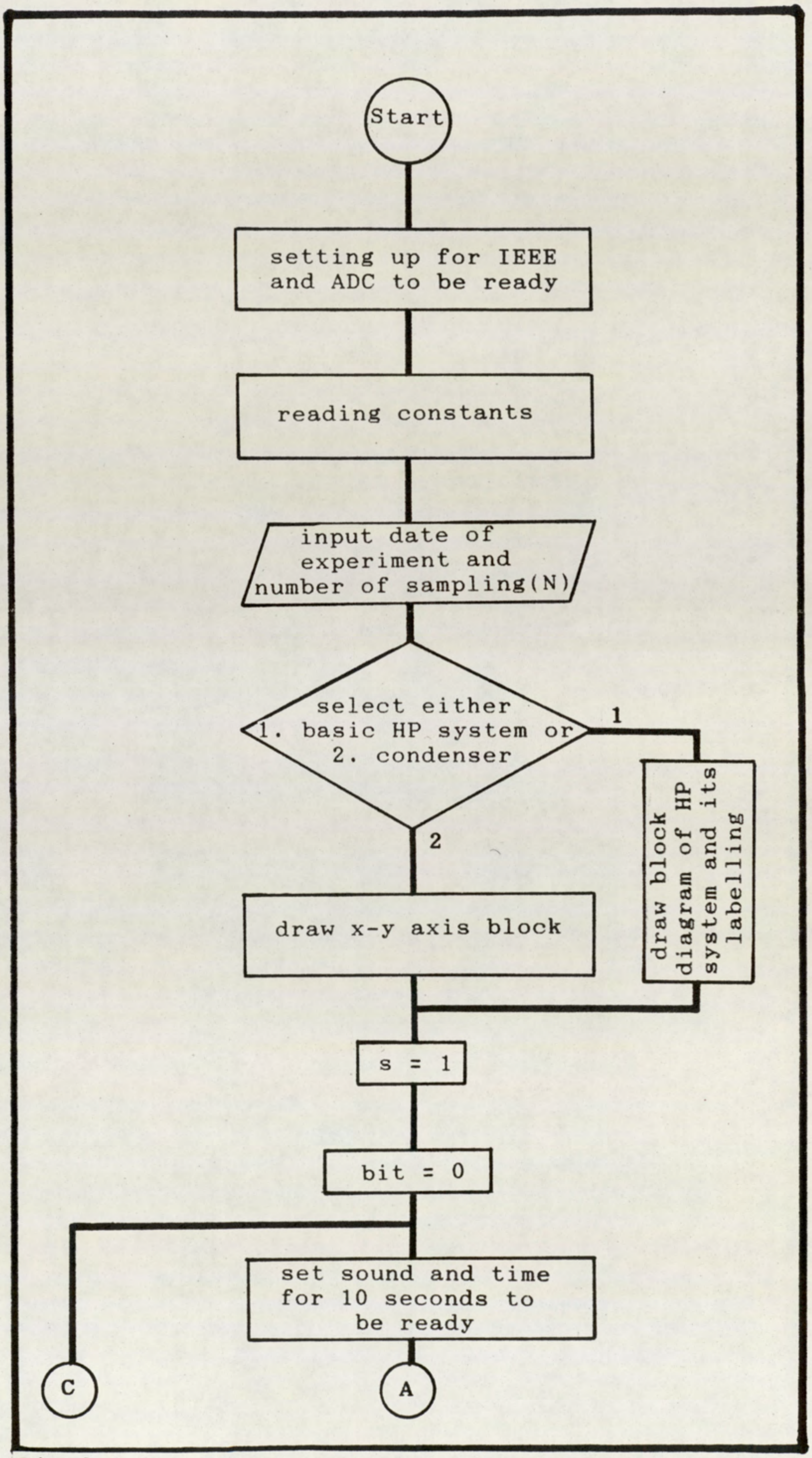

Fig.3.4.3 : Flowchart description for sampling data

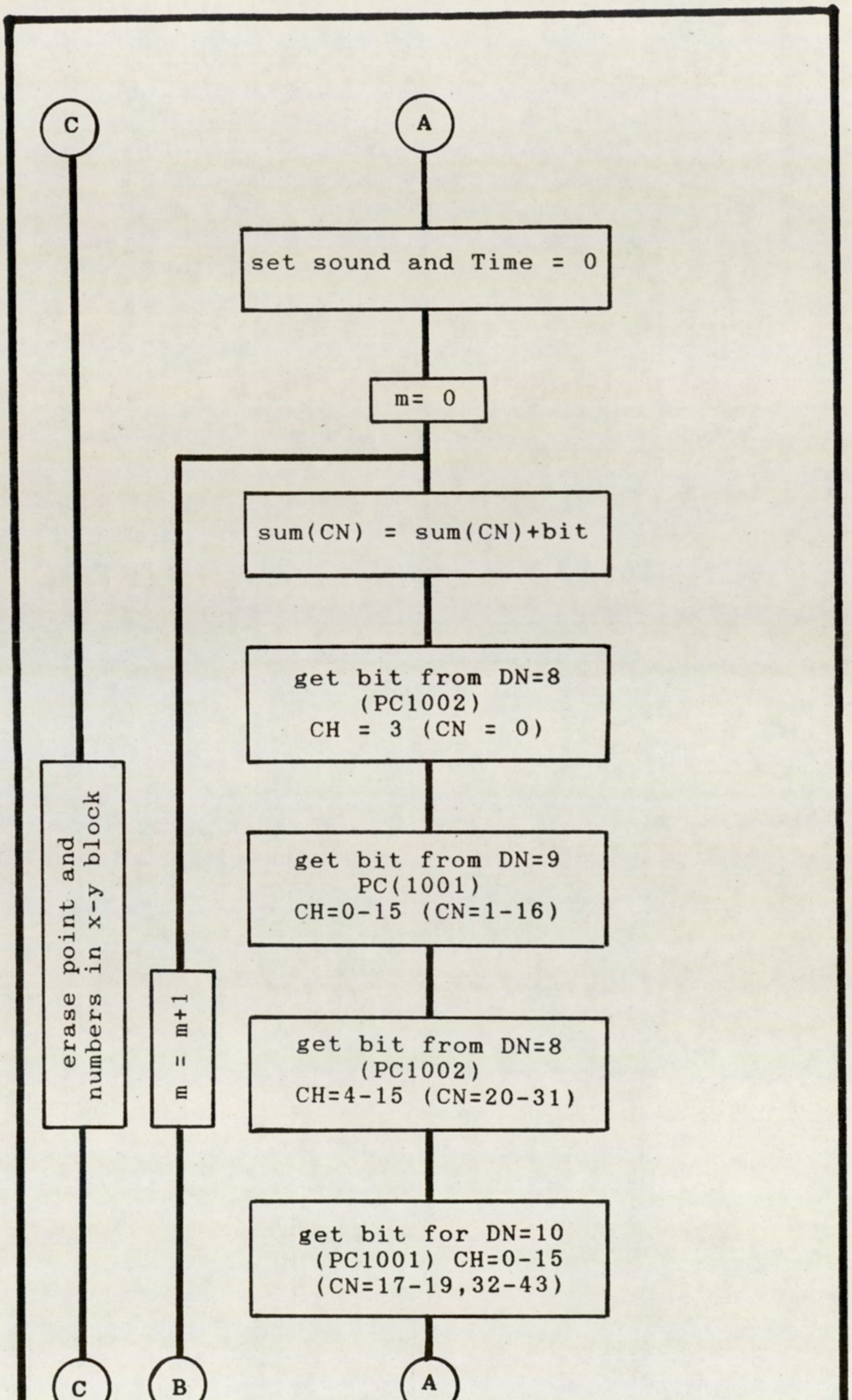

continue next page

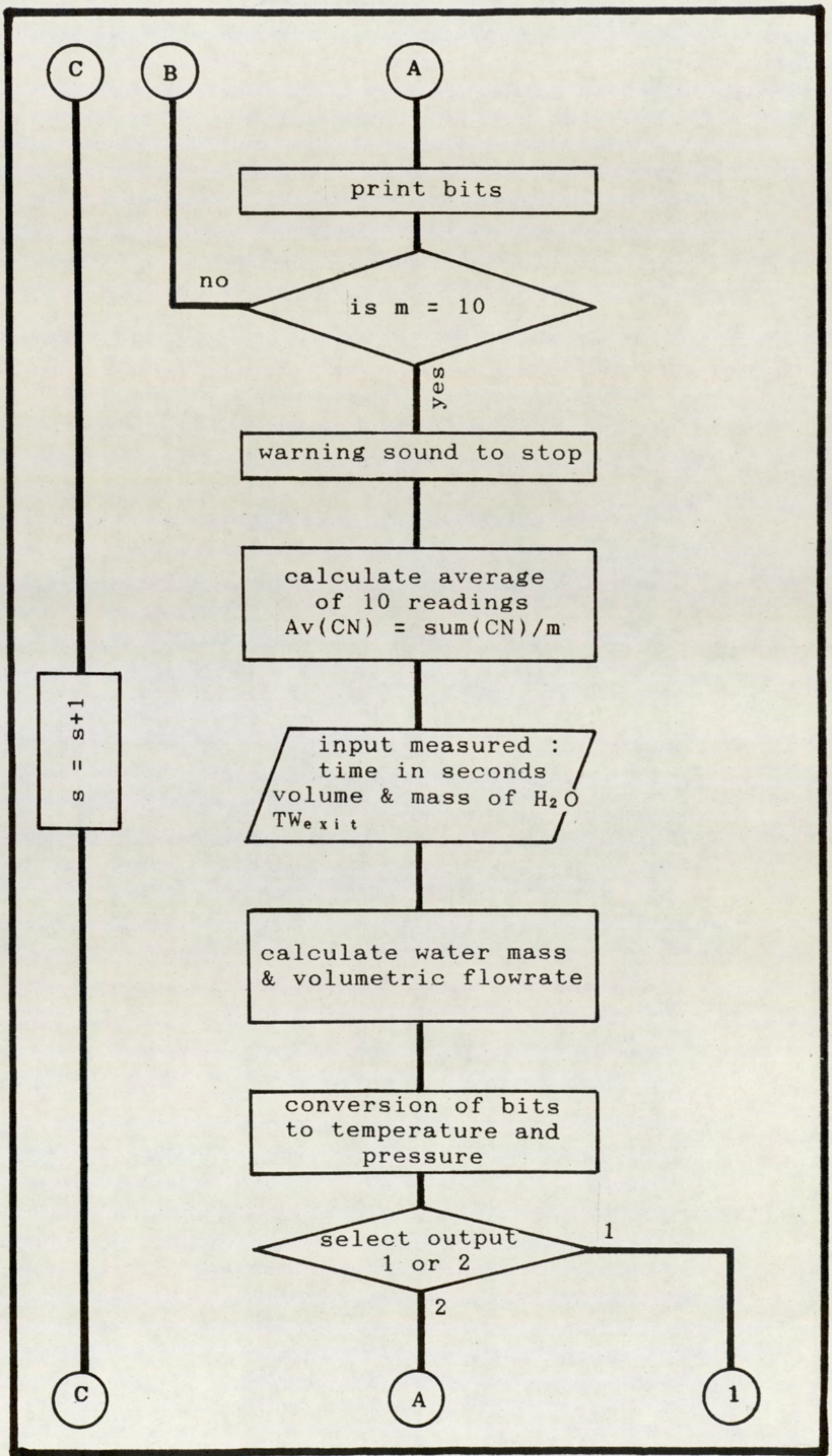

continue next page

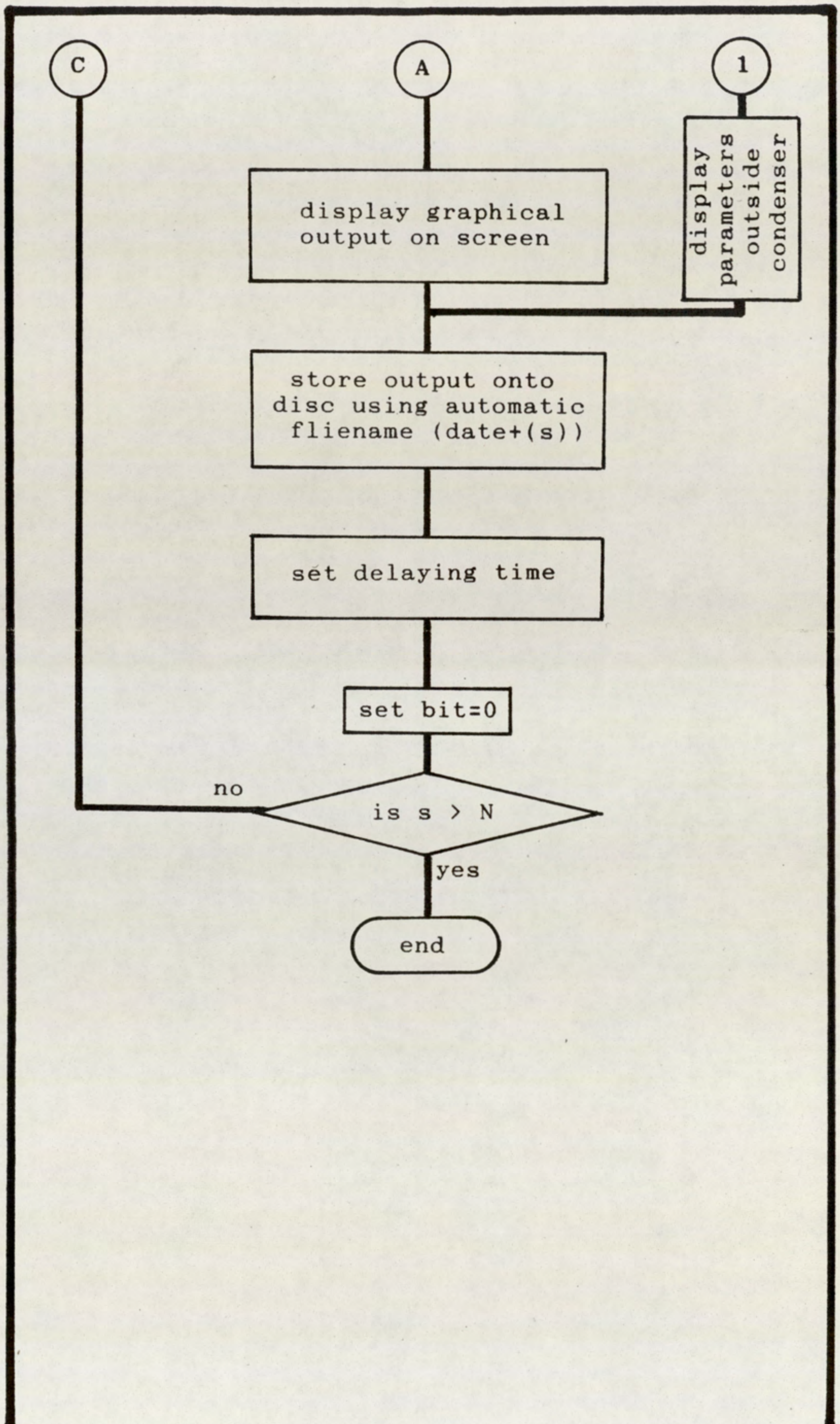
C
A
1
display graphical output on screen
display parameters outside condenser
store output onto disc using automatic flìename (date+(s))
set delaying time
set bit=0
no
is s > N
yes
end

data, and thermodynamic properties of R12 in the single-phase (liquid and vapour) and two-phase (mixture of liquid-vapour). The selected programs are shown in Appendix A-2.

The most frequent program used in sampling data is the one which consists of graphical and pictorial representation, listed in Appendix A-2 of section A-2.2. For the experimental data analysis, a program has been developed to read stored data and to calculate refrigerant thermodynamic properties in liquid, vapour, and liquid-vapour mixture. All calculations are based on the effective values of the temperature and pressure at the exit and entry of the condenser, since the placing of sensors at these points are outside the actual condenser. Fig.3.4.3 shows the sampling procedure flowchart description comprises two type of outputs.

a. Graphical output representing water and freon temperature profiles in the condenser included the flowrates as well as the discharge and suction pressure.

b. Block diagram showing the basic heat pump system where the physical properties outside the condenser are displayed.

In general, procedure statements (PROC) are used to avoid the confusion that may occur in between the line numbers since the programs are all written in BASIC. These statements are also much faster than Gosub or Goto.

3.5: Transducers

3.5.1: Introduction

A total of 39 sensors was employed throughout the system, comprising 35 thermocouples and 4 pressure transducers. In this section, the discussion will be mainly on the thermocouple sensors and pressure transducers.

The sensors are fixed perpendicularly to the pipe line either using cross-fitting or tee-fitting or straight-fitting connections. The thermocouple components are shown in Photo 5 and 6 comprising twisted type-T thermocouple wire, tensioning PTFE, brass nut, PTFE ring, thermocouple tip, thermocouple well, insulating bush, and brass socket.

Since two types of analogue to digital converter were used with the reference junction of type 1 externally connected (ice-water in a flask), while the reference junction of type 2 was internal, two types of connection to the junctions were necessary. The pressure transducer was a standard manufactured design, the output directly connected to the ADC

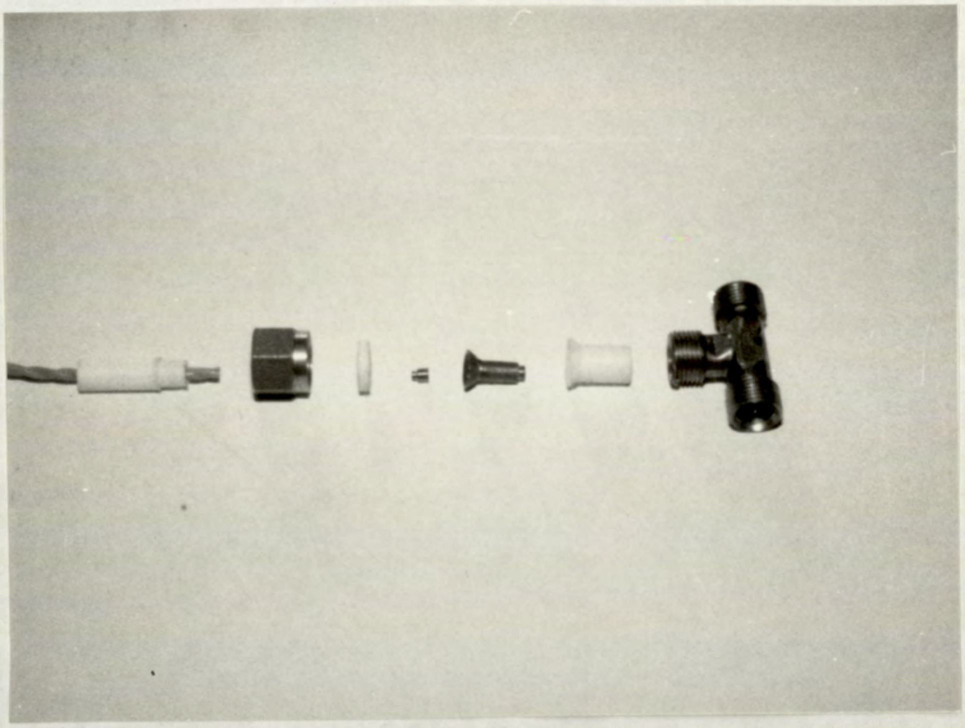

Photo 5: Thermocouple components

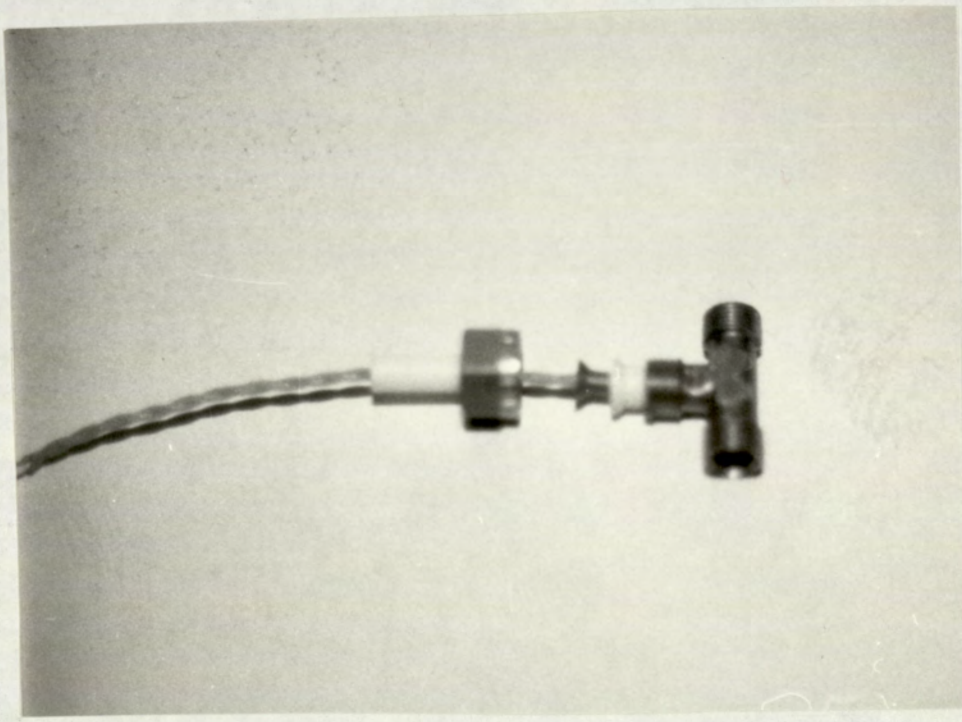

Photo 6: Thermocouple, in connection from Photo 5

input.

3.5.2: Transducer positioning in heat pump rig

Fig.3.1.1 shows the arrangement of the thermocouple sensors and pressure transducers including flowrate sensors and optical sensors. The positioning is summarized in Table 3.2.

Position	Number of sensor	Arrangement	Function to measure	Labelling	Remarks/Notes
THERMOCOUPLE					
condenser	28	TR and TW are oppositely fixed in refrigerant and water line respectively to each other with sensor cable facing outside	temperature	TR_2-TR_{15} TW_2-TW_{15}	-
just outside the condenser exit in R12 line	1	directly opposite to PT_1	temperature	TR_{16}	outlet R12 temperature
outside the condenser exit in water line	1	fixed directly to water pipe line	temperature	TW_{16}	inlet H_2O temperature
just outside the condenser entry in R12 line	1	directly opposite to PT_3	temperature	TR_1	inlet R12 temperature
outside the condenser entry in water line	1	fixed directly to the pipe line	temperature	TW_1	outlet H_2O temperature
between TEV and evaporator in R12 line	1	opposite to PT_4	temperature	TR_{17}	inlet evaporator temperature
between evaporator and compressor in R12 suction line	1	opposite to PT_2	temperature	TR_{18}	outlet evaporator temperature
outside the heat pump system	1	open place near the system	temperature	RT	room temperature
PRESSURE TRANSDUCER					
just outside the condenser exit in R12 line	1	opposite to TR_{16}	pressure	PT_1	liquid pressure or outlet condenser's pressure
just outside the condenser entry in R12 line	1	opposite to TR_1	pressure	PT_3	discharge pressure or inlet condenser's pressure
between TEV and evaporator in R12 line	1	opposite to TR_{17}	pressure	PT_4	inlet evaporator pressure
between evaporator and compressor in R12 suction line	1	opposite to TR_{18}	pressure	PT_2	suction pressure

Table 3.2: Summary of sensors employed in the system

Three additional thermocouple sensors measured by a calibrated electronic thermometer which can be removed to desired spot were also connected outside the system. These sensors were introduced for the following reasons:

1. To check the water temperature at three different places in a water tank (Fig.3.5.1(a)) during flowrate test-experiment and during the heat loss experiment by running water directly through the water line.

2. To be immersed at three different depths in the vermiculite insulation of the system as shown in Fig.3.5.1(b). The temperatures at different levels were measured for the purpose of calculating the heat loss from the system, as well as to check that the temperatures measured during the experiment do not raise very high.

3.5.3: Temperature measurements

The measurements were made with thermocouples, where the measuring junction is designed to be immersed in the stream of the flowing fluid while the reference junction is immersed in a flask of ice-water mixture or alternatively uses the built-in internal of PCI 1002. The complete thermocouple sensor comprises thermocouple wire, thermal well and the sensing tip (see Photo 5 and Photo 6 for separate thermocouple components). Fig.3.5.2 shows the construction of a thermocouple using twisted type-T wire.

<u>Layout of the sensors into the stream of fluid</u>

The temperature sensors for both water and refrigerant were designed so that the tip of the thermowell, which is placed in a tight copper-bored well filled with heat sink compound for better heat transfer performance, was about 1 mm to 2 mm immersed in the stream of the moving fluid. Fig.3.5.3(a) shows the mounting system of the thermocouples in water and refrigerant lines.

It is important to ensure the connection to the line is leak-tight so that no fluid can flow back or diffuse through the joint or within the layers. The design ensures that the sensors are thermally insulated from the pipe or compression fitting body; the main goal is contact of the thermowell with the flowing fluid. Following is a summary thermocouple construction (see also Fig.3.5.2 and Fig.3.5.3):

a. Insulated copper and constantan cable with twisted-teflon insulating material at the outside.

b. The second layer is covered by heat shrinkable sleeving material

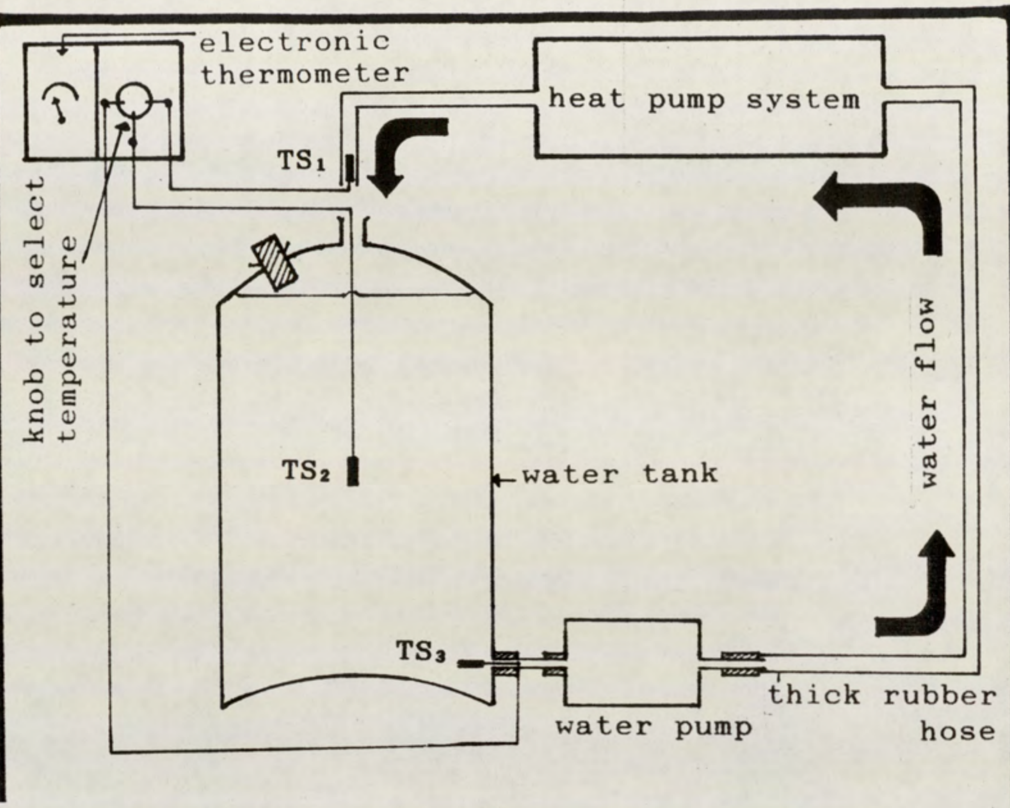

Fig.3.5.1(a): Schematic diagram showing three additional thermocouples in water tank via heat pump system

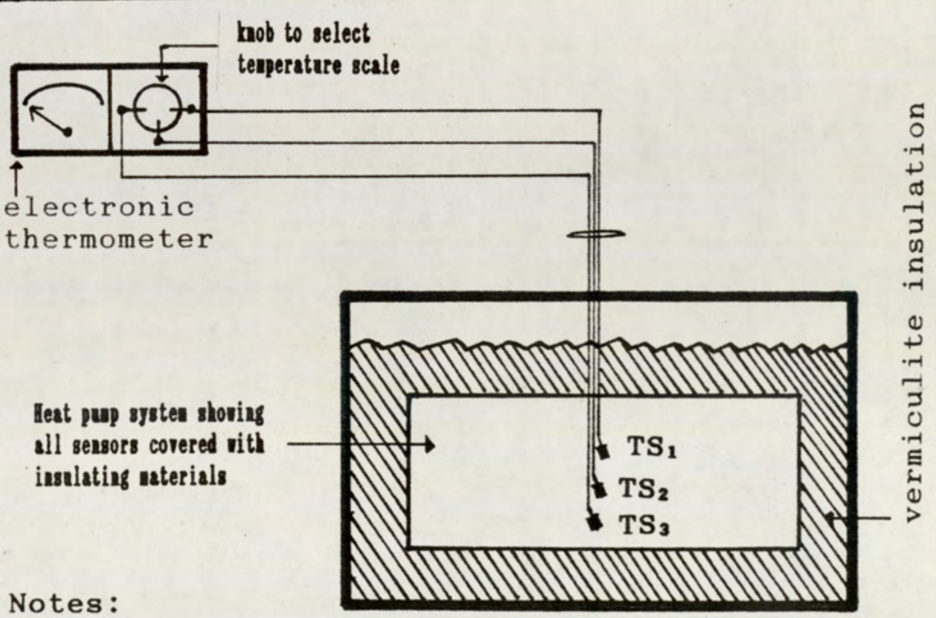

Notes:

Thermocouples TS_1 ,TS_2 and TS_3 are at different depth ;can be removed to other spot

Fig.3.5.1(b) :

Front view showing three additional thermocouples immersed in vermiculite insulating material

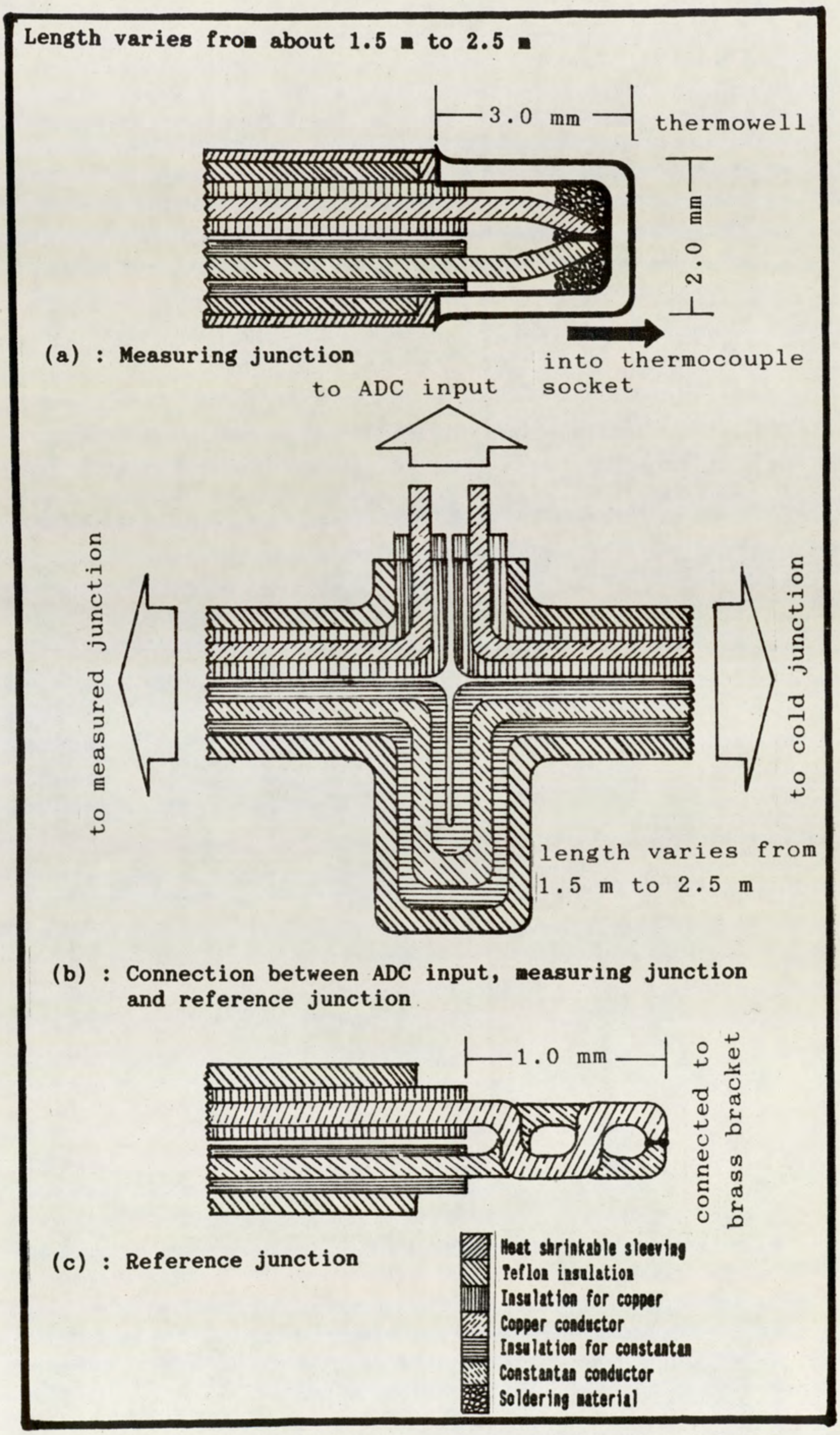

Fig.3.5.2: Construction of a thermocouple using twisted type-T wire (not in scale)

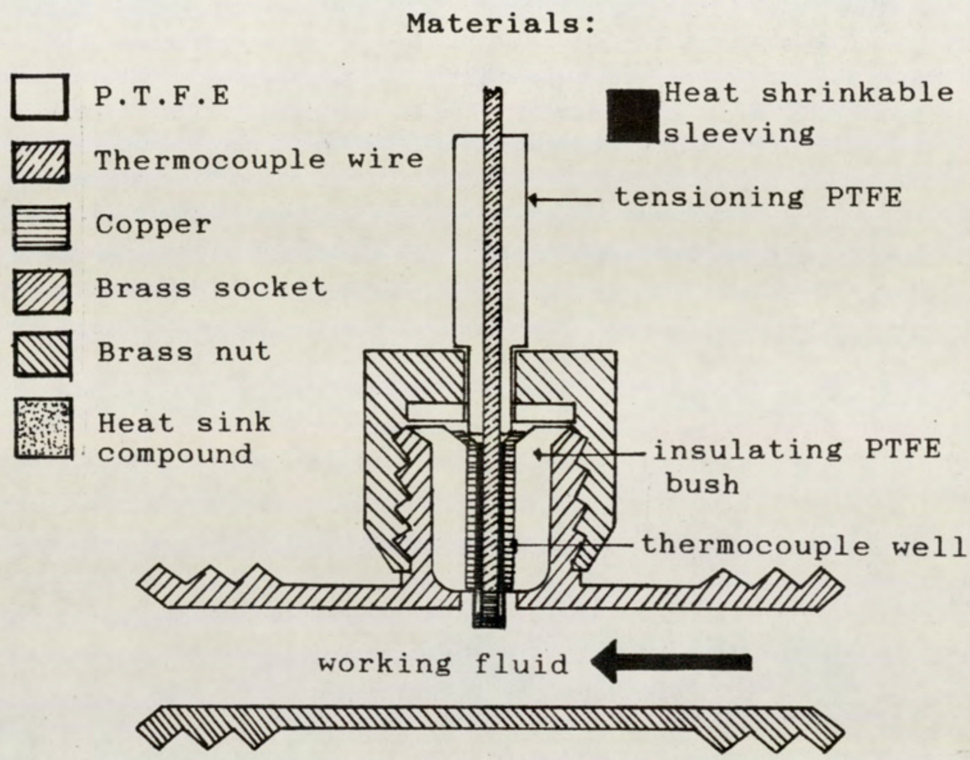

Fig.3.5.3(a) : Thermocouples mounting system in water and refrigerant line

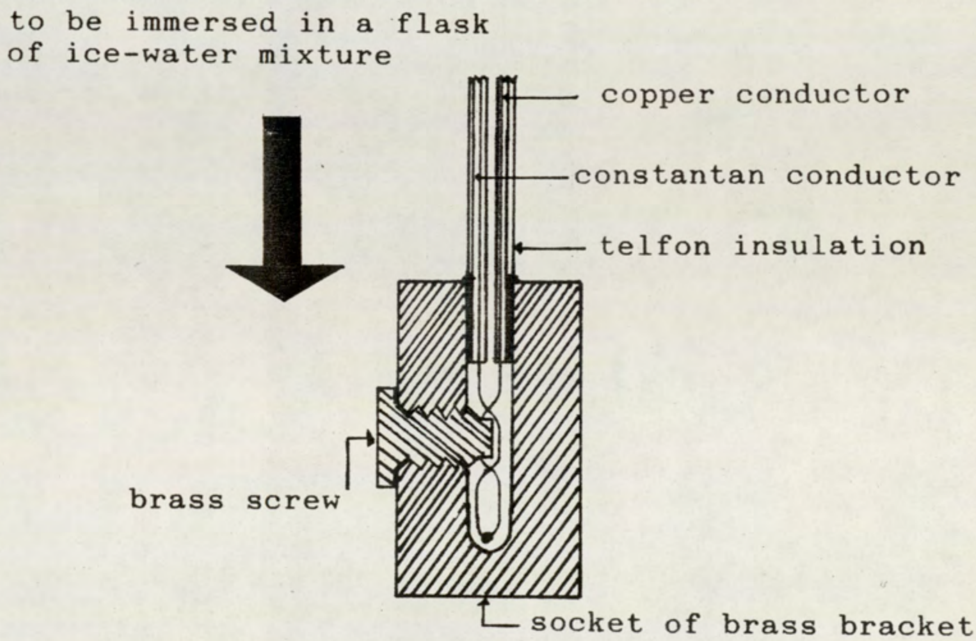

Fig.3.5.3(b) :

Fluid's reference junction mounting system

(about 2.5 cm in length) up to the opening mouth of the thermowell.

c. PTFE cylindrical shape tightly fitted to the brass nut which is internally covered by PTFE ring so that the sensor would stand up-right. A small amount of Araldite epoxy-resin was glued between the nut and the PTFE cylindrical shaped.

d. The sensing well directly touches the tip of the copper-bored well by introducing heat sink compound in between the contact. It was then put into PTFE sleeve before putting into a brass fitting-socket which is then screwed by a brass fitting-nut.

The reference junctions were directly connected to individual small holes of a brass block of dimension roughly 2x4x6 cm and secured by screws. The whole brass block was immersed in a flask of ice-water mixture covered with a round polystyrene-lid as shown in **Fig.3.5.3(b)**.

3.5.4: Pressure measurement

The P102 solid state transducer is a standard pressure measuring device consist of an integrally machined, precipitation hardened stainless steel body and pressure sensing diaphram,[113]. In a full wheatstone bridge configuration the transducer translates pressure induced strain to an electrical signal which is directly proportional to the applied pressure. It is also claimed that the semiconductor strain gauge transducer operates at typically 1/2 to 1/3 of the normal operating stress of a conventional transducer with corresponding benefits in fatigue life, linearity and sensitivity.

There were 4 pressure transducers fitted in the refrigerant circuit with PT_1 and PT_3 in the higher pressure side before and after the condenser. The other two, PT_2 and PT_4 were in the lower pressure side, fixed before and after the evaporator as shown in **Fig.3.1.1**. They were directly connected to the refrigerant line by 6mm compression cross-fittings while the other end of the transducer was plugged-in to the respective channel input of the device number 10. The transducers were supplied with their own calibration data, some of them are listed in **Table A-1.1**. **Fig.A-1.4.1** shows the external features and the dimensions of a P102 transducer.

<u>Pressure transducer mounting system</u>

All pressure transducers employed in the system are fitted opposite to the freon thermocouples in the refrigerant line. **Fig.3.5.4** shows the pressure transducer mounting system, comprising three main sections (see

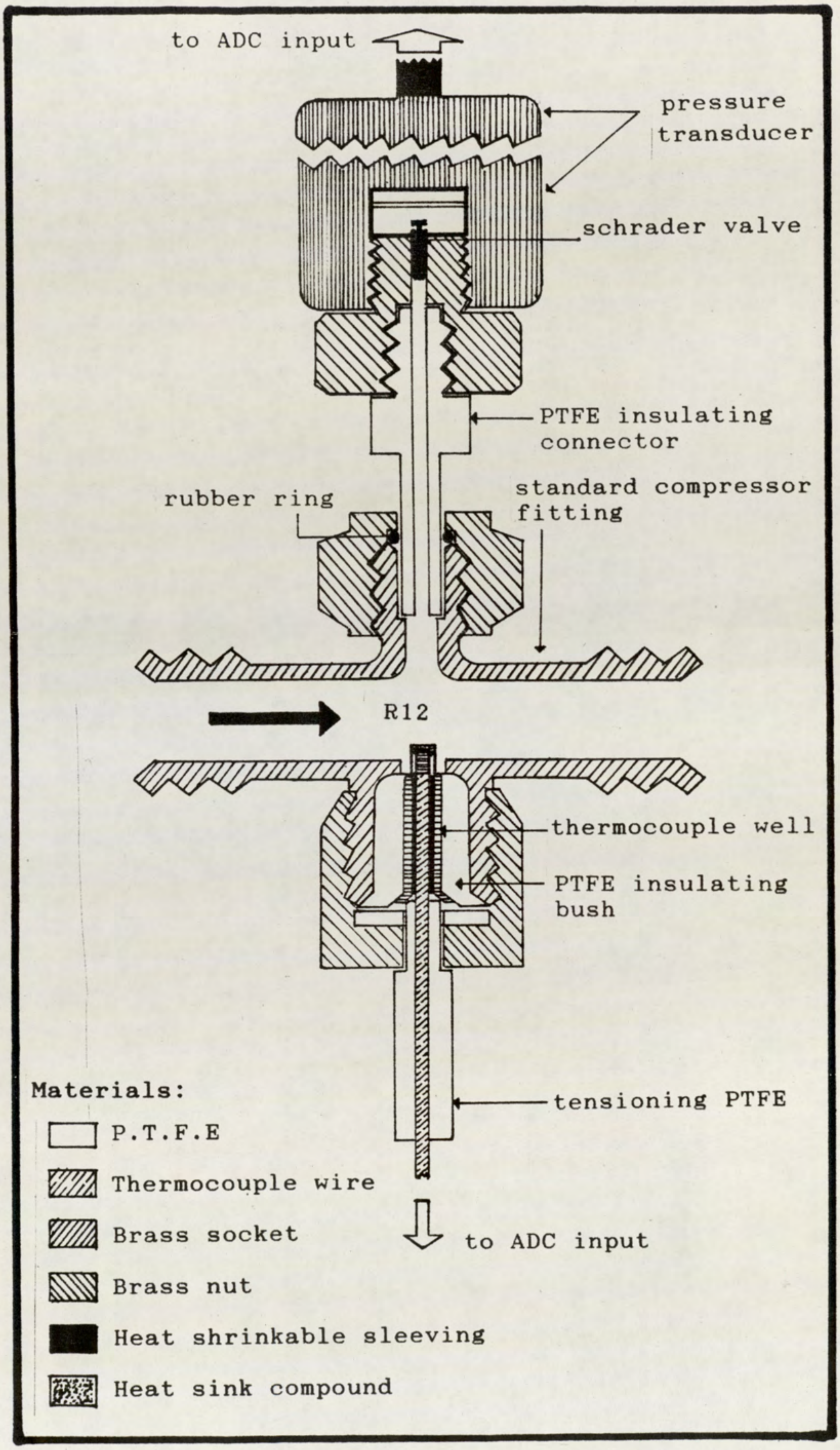

Fig.3.5.4: Static pressure transducer in line with the thermocouple mounting system in R12 line

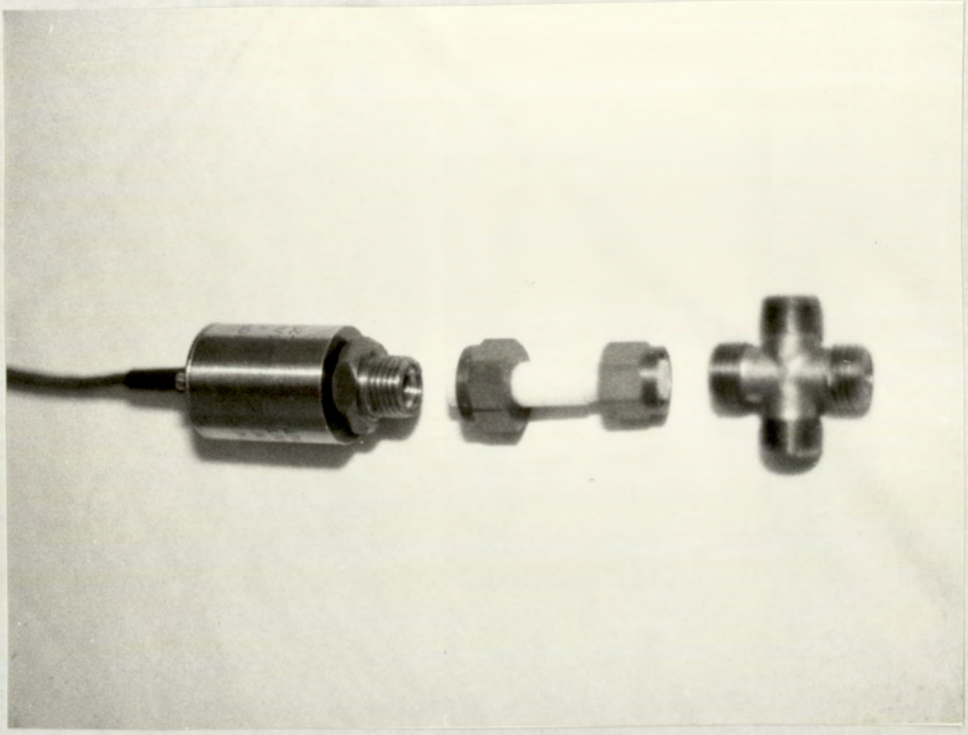

Photo 7: Pressure transducer components

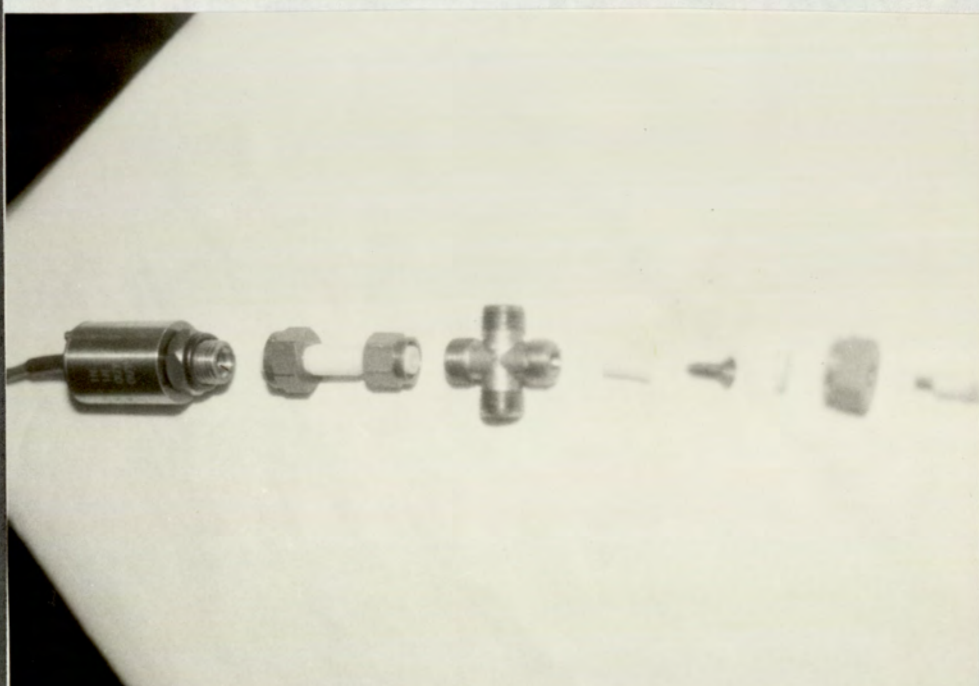

Photo 8: Thermocouple and pressure transducer connected opposite each other (at condenser entry and exit)

also Photo 7 and Photo 8):

a. The transducer body is fitted with a schrader valve. The other end is connected to a PTFE insulating connector.

b. The small hollow PTFE thermally insulating connector was designed to fit both the transducer input and the refrigerant line's brass socket. The length of the connector is roughly between 4 to 5 cm.

c. The final section was to fit the other end of the connector to the standard compression fitting.

The measured pressure is assumed to be at the same point as the measured temperature of a particular position in the refrigerant line.

3.5.5: Flow measurement

Turbine type flowmeters both for measuring water and freon flowrate were originally introduced in the system but proved to be unreliable and difficult to calibrate. A set of experiments was carried out by circulating water in the water pipeline at slow, moderate and fast rates. In this test, the water regulator was temporarily bypassed by a short thick rubber hose. The test was continuously carried out for 50 to 60 minutes before recording the steady-state flowrate for 5 minutes on the monitor. The output variation of bits and the number of counts within the period of time was printed in Fig.3.5.5(a and b).

The same procedure was also carried out for testing the freon flowmeter where water was kept circulating in the refrigerant line. The electrical signals from the meter were converted to pulses in the frequency-voltage converter which were then digitised by the ADC. The output was displayed on the screen and on a D54 oscilloscope. It was found that;

a. Water flowmeter (channel 40): At constant water rate the readings for 1876 counts are between 614-673 bits which is roughly ±29 bits deviation from the averaged value.

b. Freon flowmeter (channel 41): At constant water rate the readings vary from 1067-1097 bits in 1838 counts which gives ±15 bits deviation from the averaged value.

Finally, it was decided to measure the water flowrate manually during the Run by recording the time, volume and mass of water for each Run. The freon flowrate is then calculated from the condenser energy balance equation.

3.5.6: Air speed and power measurement

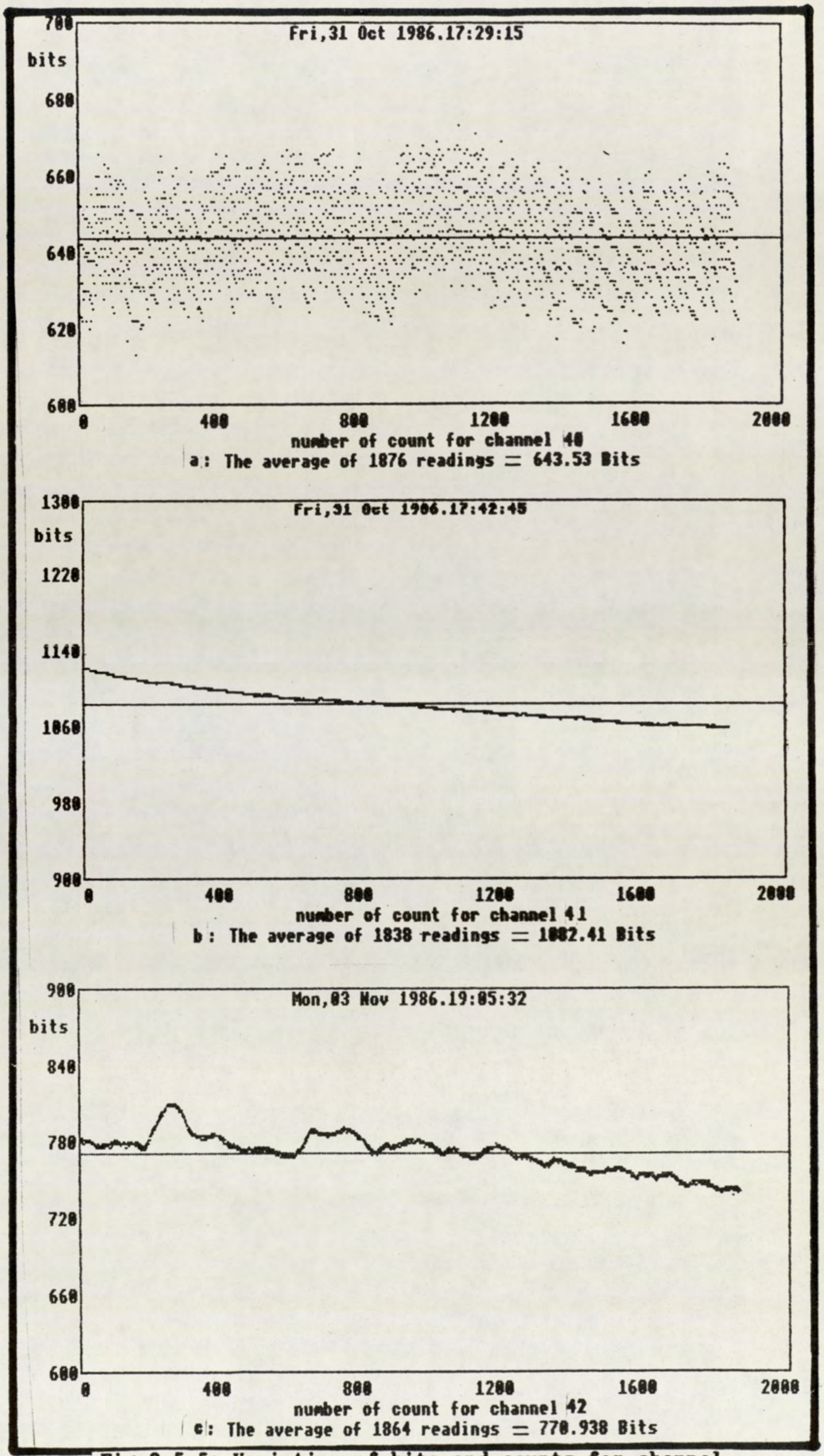

Fig.3.5.5: Variation of bits and counts for channel 40,41 and 42 during test-experiment

The air speed test-experiment was controlled by a variac. One side of a fan blade was marked in black and the optical device (reflective opto switch,[114]) was directly clamped so that the reflective surface faced the marked point during rotation. The output of the optical sensor was connected to a frequency-voltage converter so that the signals could be converted to pulses before being fed to an ADC.

The test was carried out at different circulating rates for about 5 minutes. An example of the test is shown in **Fig.3.5.5(c)**, where at the constant air flowrate the bits fluctuated from 734-808 bits in 1864 counts ($\pm$37 bits away from the average value).

It was decided that the measurement of air flowrate and electrical power would not be included. To this stage, the test for electrical power measurement was not carried out.

CHAPTER 4

EXPERIMENTAL PROCEDURE AND DATA ANALYSIS

4.1: Introduction

The main objective of the experimental runs was to obtain sets of data over a wide range of operating conditions to compare with the predictions from the theoretical model. It should be noted that the purpose of this project was to study the heat pump condenser rather than the performance of the heat pump. In this chapter, the methodology employed to acquire data will be outlined.

The following definitions will be used thoroughout this thesis:

Set of readings: One complete reading consists of 43 pieces of data taken at a particular operating condition.

Set of data: The average of 10 **sets of readings** of data (temperature, pressure and etc.) at a operating condition.

Time interval: A time delay of 30 minutes between each **Run**.

Run: An experiment during which a **set of data** is taken.

Duplicated run: A duplicated Run at approximately the same operating condition.

Single channel reading: A continuous reading taken from a selected channel number at particular operating condition.

All channel reading: A continuous **set of readings**.

Working pressure: Discharge pressure or the freon pressure at the condenser entry.

The experiment was done by varying the water regulator and the air circulation rate through the heat pump evaporator so that the working pressure could be varied from 7.6-12.3 bar. These variations would also effect the water and the freon flowrate, condensing temperature,inlet freon temperature, outlet water temperature and other related temperature profiles in the condenser. Duplicated runs were also done by repeating the operational conditions as close as possible.

The heat pump operating modes will be discussed. The step of the experimental procedure leading to the storing of data from each Run will also be discussed. Over 100 Runs have been recorded, only some of which will be shown and analysed in this thesis. The Runs were selected to cover the working pressure range.

4.1.1: Experimental working modes

Three possible working modes are summarized in Table 4.1.

Mode	Function
1	a. Viability test for the heat pump components and the sensors employed in the system. b. Rig test at small, moderate and full charge of freon. c. Sensors calibrating experiments. d. Heat loss experiment.
2	Heat pump experimental-Runs with variation of operating conditions. a. Increase or decrease of the discharge pressure with fixed water flowrate. b. Variation of the water flowrate at fixed pressure.
3	Duplicated Runs of mode 2 (above) with about the same operating conditions.

Table 4.1: Summary of working modes

In mode 1, a considerable time was spent to make sure all heat pump components and the sensors were satisfactory. Other important tests were testing the freon line and checking for contamination before any experimental runs could be carried out. The heat pump system was initially evacuated by a vacuum pump before any calibration and heat loss experiments could be done.

The duplicated Runs were organised in two ways:

1. The duplications were made immediately after each Run in mode 2 on the same day.

2. Close adjustment of operating conditions so that operating conditions in mode 2 could be repeated approximately as in mode 3 experiment on a different day.

4.1.2: Heat pump operational ranges

The operating conditions were purely pressure dependent, the pressure control device being varied to suit the working pressure range given by the manufacturer. At the same time, the effect of pressure variations will also alter the water flowrate. The amount of heat being transferred in the evaporator could be varied by slowing down or speeding up the air circulation rate. The slower the rate, the colder the air output, causing the possibility of frost formation. To avoid these situations, the air speed was fixed at a suitable rate by varying the fan speed.

To summarize, the following factors had a great influence on the experimental operating conditions:

1. Variation of pressure-controlled water valve.
2. The control of water flow in the system.
3. The control of air circulation rate.

The majority of the output Runs analysed were taken in 1987. Table 4.2 is a summary to show the number of experiments, with operating conditions done during the course.

Date of experiment	Number of Runs	Delaying time between each Run (minute)	Range of working pressure bar	Room temperature (°C)	Range of working temperature (°C) TR_{in}	TW_{in}	Range of water flowrate (g/s)	Remarks
02-12-1986	35	10	7.62-14.63	20.7-21.5	59.9-83.8	-	7.91-16.10	Test-experiment for sensor modification
13-05-1987	14	20	7.85-10.87	19.4-20.2	60.2-75.1	13.2-14.9	9.94-10.64	Test-experiment for sensor calibration
18-05-1987	14	30	7.66-11.45	18.5-20.8	61.2-75.9	13.5-15.5	6.72-17.46	Using polystyrene insulating materials
08-06-1987	10	30	7.97- 9.09	19.6-20.2	62.7-69.4	15.7-17.2	12.97-19.76	Using vermiculite insulating materials
09-06-1987	14	30	9.22-11.08	19.8-20.5	69.9-77.6	16.8-17.6	8.15-11.64	Continued from 08-06-1987
07-07-1987	12	30	7.58- 9.23	24.4-24.7	66.5-73.6	19.2-20.2	13.74-32.86	-
13-07-1987	14	30	8.85-11.49	23.8-26.2	65.7-77.3	19.0-21.4	10.65-19.25	-
14-07-1987	14	30	10.37-12.14	24.5-26.1	71.9-79.2	19.5-21.7	9.47-12.52	-
06-01-1988	10	30	9.98-12.32	20.0-20.3	72.8-81.7	14.1-18.8	7.50-11.13	-

Table 4.2: Experimental runs and their operating conditions taken during the course

Over 100 Runs were recorded during the course of the research, with the first set of Runs dated 02-12-1986 being done for checking and testing the heat pump components and the sensors. It took almost six months to reconstruct, recalibrate and repair the thermocouples and the pressure transducers. The second part of the table shows the actual Runs using two types of insulating materials used to minimise heat loss from the condenser. Vermiculite was used in the latest experiments.

To generalise, the following table shows the overall operating ranges adapted from Table 4.2.

Working pressure (bar)	Working temperature (°C) TR$_{in}$	TW$_{in}$	Range of water flowrate (g/s)	RT (°C)
7.58-12.32	60.2-81.7	13.2-21.7	6.72-32.86	18.5-26.2

Table 4.3: Overall operating mode summarized from Table 4.2

To acquire data, the heat pump operation was controlled in two ways with fixed air flow (see Fig.4.1.1).

a. The discharge pressure-controlled water valve was fixed at a certain level; the data were recorded for approximately the same levels of discharge pressure by repeating the same conditions.

b. On the other hand, the pressure-controlled water valve was slowly varied for different levels of discharge pressure.

4.2: Transducer calibration

It is very important to make sure that all the sensors are in good condition. All ADC channels were checked one at a time by shorting the input connector while other channels remain connected. The average zero reading was recorded to be 0±2 bits.

Three types of calibrating-experiments were carried out, depending on the type of sensors to be calibrated.

a. Thermocouple calibration to convert ADC bits to temperature in °C.

b. Pressure transducer calibration to convert ADC bits to absolute pressure in bar.

c. Flowrate measurement by conventional method to calculate water mass flowrate in g/s. In this case, the water flowrate was separately measured in each Run.

These basic primary parameters would be used to calculate the following secondary parameters introduced in the model.

1. Freon flowrate, total thermal power in each Run, condenser energy balance and the effective value of the inlet and outlet pressure and temperature, to be introduced as input data in analysing each Run.

2.(a) Thermodynamic properties of R12 and water at given pressure and temperature.

(b) Other physical properties of the fluid such as heat transfer

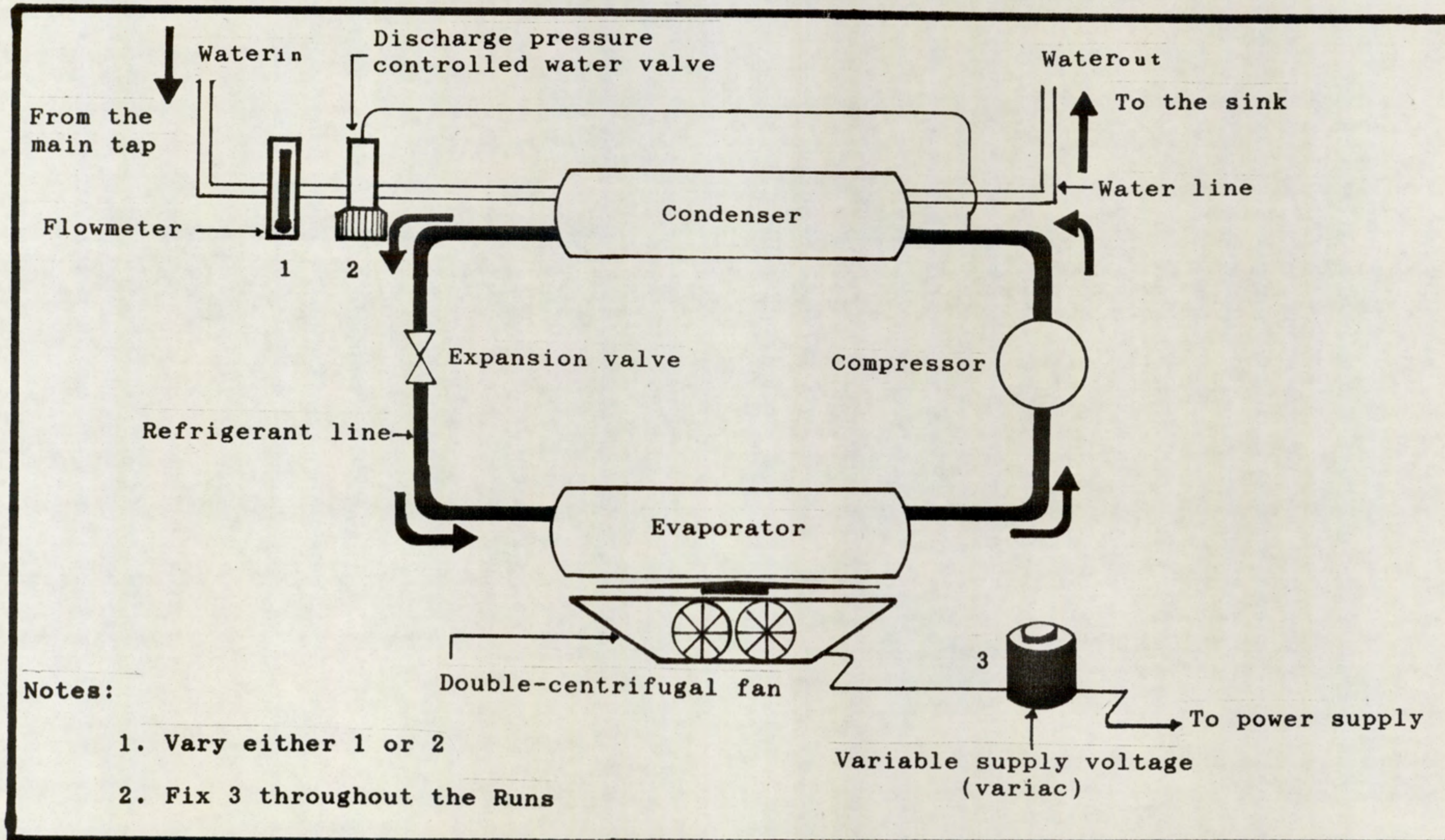

Fig.4.1.1: Experimental control method

coefficients, pressure at the test-stations etc.

4.2.1: Test experiments

Over 50 sets of thermocouple test-experiments were carried out to make sure the readings were within the acceptable range. The tests were done in three different experimental procedures.

Water tank-experiment

The water was circulated through the water pipeline of the system to maintain a uniform temperature distribution (see also Fig.3.5.1(a)). All the 35 measuring junctions were three-quarters immersed in the tank. The brass block holding the cold junctions was immersed in a flask of ice-water mixture. The measuring junctions were separately fitted into the cylindrical-shaped holes of the size of the thermowell's outer diameter. Fig.4.2.1 shows the measuring junctions being fitted to a block of insulating PTFE constructed with small holes. This experiment was useful for checking the performance of the thermocouples. The water temperature in the tank could be increased by an electrical immersion heater. For the thermocouple calibrating-experiment this arrangement is not suitable because it takes a longer time to heat the water in the tank evenly, if the variation of the temperatures is from 0°C to 100°C.

Flask of water-experiment

A PTFE block carrying the measuring junctions was immersed into a flask of water covered with a polystyrene lid with the cold junctions maintained at 0°C. The water temperature could be easily increased by pouring hot water at desired temperature.This method was frequently employed in the thermocouples calibrating-experiment; the temperature drop over 5 to 7 minutes was small.

Test-point experiment

The water was continuously circulated from the mains through the water pipeline of the system (there was no water or freon flow in the refrigerant line at this time) with the thermocouples fixed individually at their respective test-points. In the test, the temperature recorded in the refrigerant line should be expected to be slightly higher than the temperature in the water line. The output from each thermocouple was recorded; each Run taking roughly one minute.

Fig.4.2.2 and Fig.4.2.3 shows some of the outputs recorded from

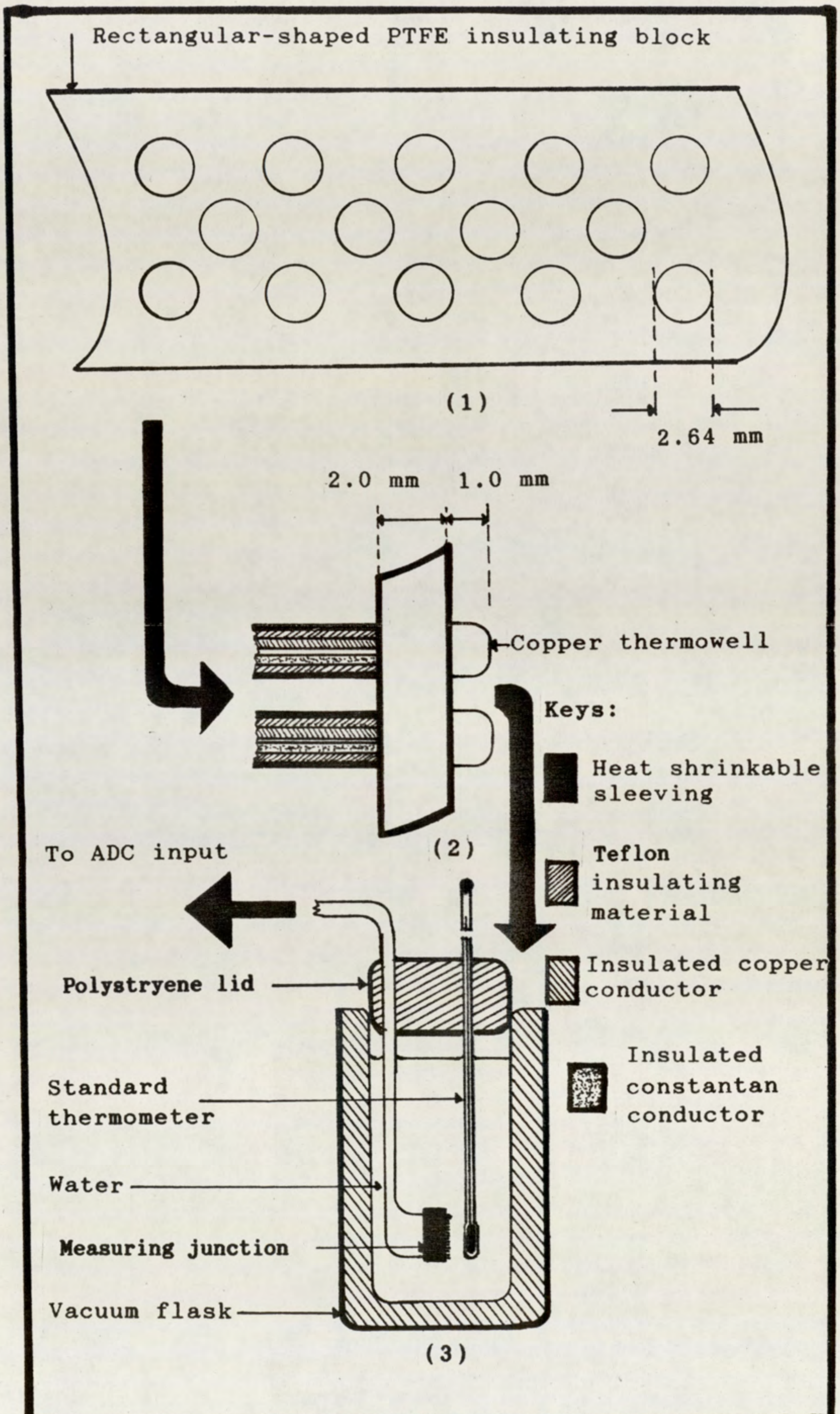

Fig.4.2.1: The thermocouple's measured junction fitted into a block of PTFE insulating material (drawn not in scale)

the test-point experiment at constant water flowrate (see also Fig.3.4.3 in chapter 3). In this experiment, the sensors were placed roughly at one meter apart. It is easier to check the drop in the bits when comparing the bits drop in the first two experiments mentioned above, where the measured junctions were all in one block. From this test, the following conclusions could be drawn.

1. Fig.4.2.2 (typical results for the freon line): The ADC readings were found to be within ±0.5% of the average value.

2. Fig.4.2.3 (typical results for the water line): The readings in the water line were also found to be within ±0.5% of the average value.

4.2.2: Thermocouple calibration

Since temperature is a dominant parameter in the research, careful calibration is essential to ensure that the correct fluid temperatures are measured. The temperature of water (water is used as a calibrating fluid) in the region of the PTFE block is assumed to be the same as the temperature of the junctions. The experiments were carried out many times. Only that done on the 28-04-1987 is shown and discussed. The calibrating coefficients for each thermocouple were treated separately and automatically stored onto floppy disc for later use. The calibrating temperatures ranged from 0°C to 90°C.

Experimental procedure

35 measuring junctions were fitted into respective hollow cylindrical-shaped holes of a rectangular-shaped PTFE block with about 1.0mm of the thermowell tip left outside the hole as illustrated in Fig.4.2.1. The PTFE block was then immersed to three-quarter depth in a flask of water. The water temperature in the flask was kept constant during the Run by steady stirring. A standard thermometer with an accuracy of 0.1°C ranged from -5°C to 105°C was employed to check the temperature. The bottom part of the thermometer was placed approximately at the same level as the PTFE block. The vacuum flask was covered with the polystyrene lid to minimise the heat lost from the flask. 11 Runs were conducted in the range of 0°C to 90°C with about 30-45 minutes interval between each Run. The measurements were recorded at each constant temperature and automatically stored.

The cold junctions which were fitted into a brass block (see also Fig.3.5.3(b)) were immersed in a vacuum flask of ice-water mixture (covered with the polystyrene lid) maintained at 0.0±0.1°C. For CN=20 to

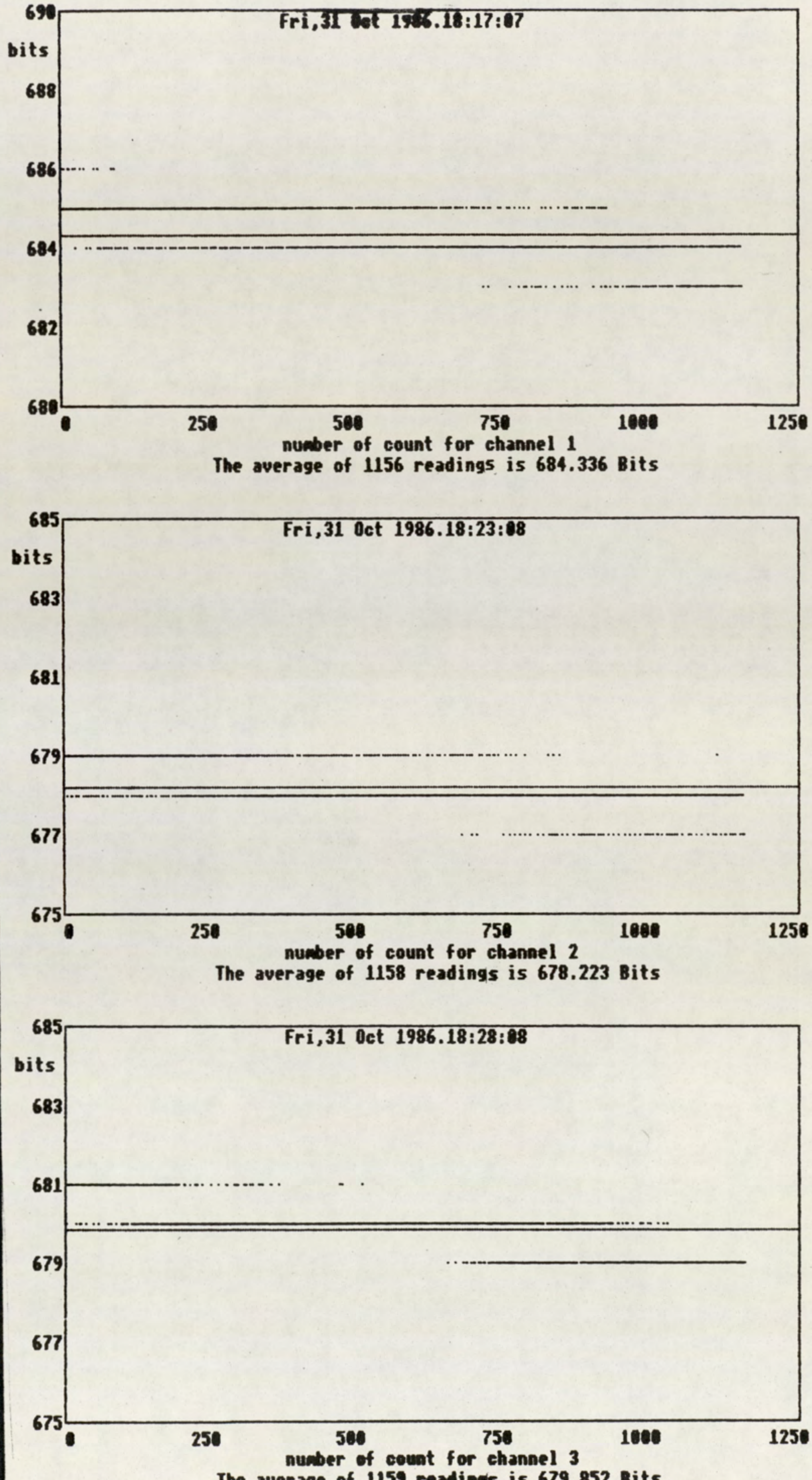

Fig.4.2.2: The test-experiment outputs for the freon line

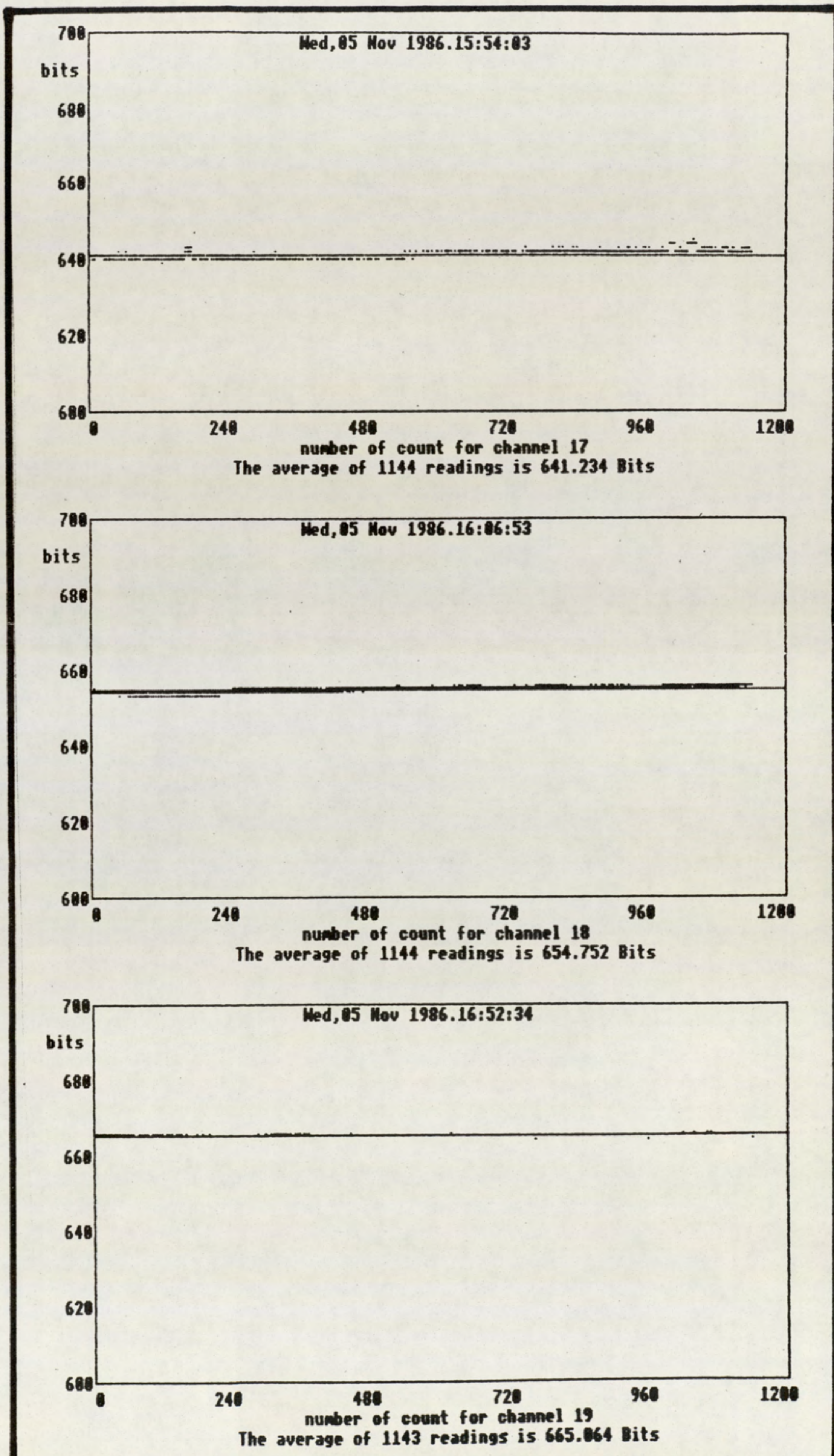

Fig.4.2.3: The test-experiment outputs for water line

CN=31, the internal reference junction in device 8 was directly used. During the Run and the interval, the temperature at the reference point was continuously checked. The outputs were only recorded when temperatures in both flasks were steady.

Output results

Two types of output which had been recorded depending on the reference point are tabulated in Table 4.4 and Table 4.5. The complete readings for each channel at different temperature are shown in Table A-1.2.

1.External reference junction (PCI 1001)

Measured temperature (°C)	Range of bits recorded from respective channel; CN=1 to CN=19 and CN=32 to CN=33 in bits	
	bit_{min}	bit_{max}
0.0	-8	7
9.0	130	145
20.7	312	327
31.4	487	504
39.5	622	641
44.8	709	728
52.3	835	857
62.1	1000	1022
69.5	1131	1156
76.4	1252	1274
90.7	1512	1540

Table 4.4: The temperature-bits calibration from PCI 1001

The bits recorded in each channel at a particular measured temperature were different from each other. The minimum reading was found in CN=13, while the maximum was in CN=2. The differences in the readings would not affect measurements because each channel had its own calibrating coefficients. The bits versus temperature is shown in Fig.4.2.4(a).

2. Internal reference junction (PCI 1002)

The reference bits were also recorded in each Run, which when multiplied by a factor of 0.025 (Eqn.3.3) yields the reference temperature in a particular Run where $T_{ref} \neq 0$. The difference between the measured and reference temperature represents the actual fluid temperature, measured at that point.

$$\Delta T = (T_{measured} - T_{ref}) \qquad \text{Eqn.4.1}$$

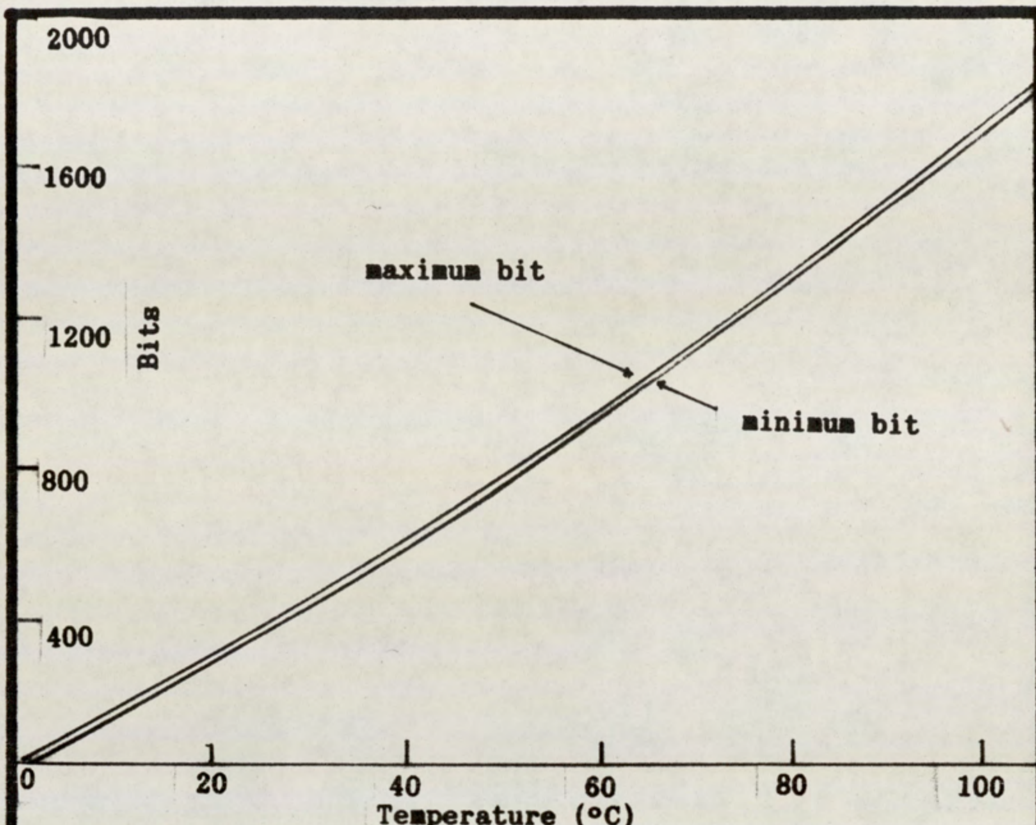

Fig.4.2.4(a): Measured temperature versus bits for CN=1 to CN=19 and CN=32 to CN=35(PCI 1001)

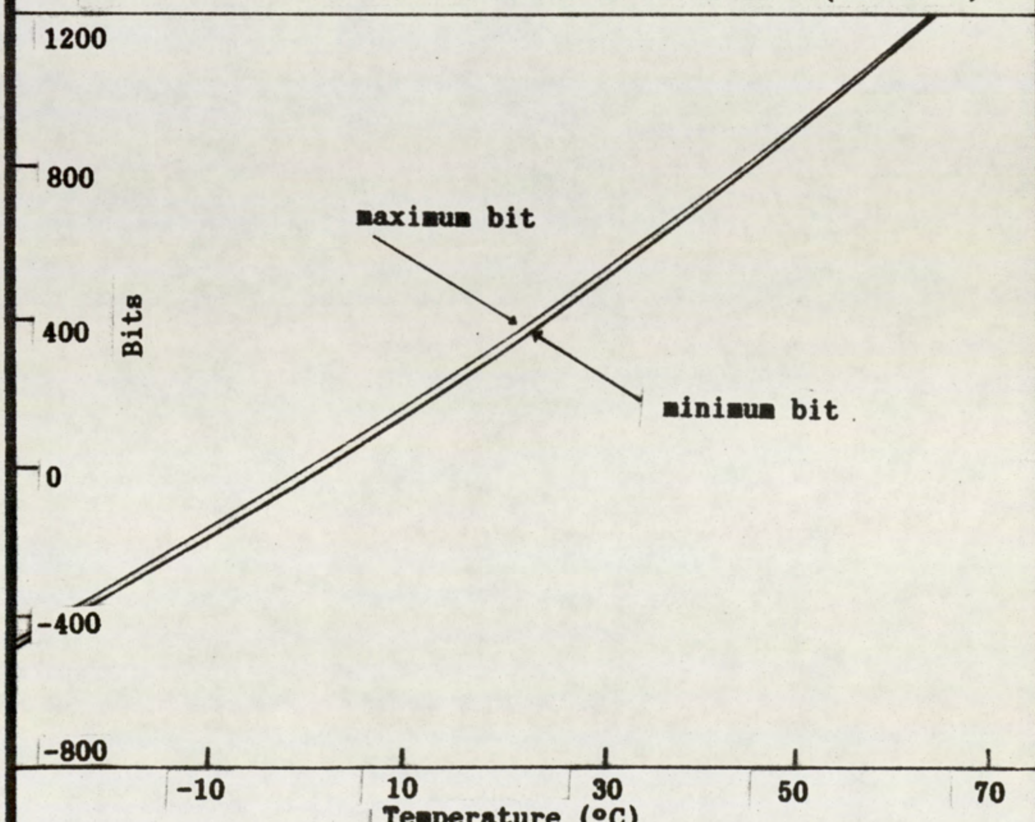

Fig.4.2.4(b): Measured temperature versus bits for CN=20 to CN=31 (PCI 1002)

Table 4.5 shows the temperature-bits relations for CN=20 to CN=31 for the water temperature sensors, after multiplying the reference bit by a factor of 0.025 in the range of -32.4°C to 58.5°C (or 0.0°C to 90.7°C if reference temperature is zero). In the case of PCI 1001, T_{ref} is zero. The range is suitable for water temperatures between 10°C to 55°C.

Measured temperature TW_4-TW_{15} (°C)	Reference temperature T_{ref} (°C)	Bits from channel 3 bit_{ref}	Range of bits taken from respective channel; CN=20 to CN=31 in bits bit_{min}	bit_{max}
0.0	32.4	1294	-503	-481
9.0	32.4	1294	-363	-342
20.7	32.4	1294	-179	-159
31.4	32.3	1293	-3	16
39.5	32.3	1292	134	156
44.8	32.3	1291	222	241
52.3	32.2	1289	351	370
62.1	32.1	1284	519	537
69.5	32.2	1288	652	674
76.4	32.2	1289	772	788
90.7	32.2	1289	1038	1055

Table 4.5: The temperature-bits calibration from PCI 1002

Similarly, the minimum and the maximum readings occured in CN=21 and CN=25 respectively. The temperature-bits calibration is shown in Fig.4.2.4(b).

The basic relationship between the bits and the temperatures could be written as

$$\text{bits} = \sum_{i}^{n} a_i \, \Delta T^i \qquad \text{Eqn.4.2}$$

where n and i=0,1,2, 3,4,.... .
For simplicity, a polynomial of the second order was considered to evaluate the coefficients. A least squares curve-fitting program was used to calculate the calibration coefficients a_o,a_1 and a_2. Table A-1.3 shows individual coefficients for CN=1 to CN=35 saved under "Ca28487". These had been tested and will be used for the bit-temperature conversions.

Coefficient a_1 could be assumed to be equivalent to the slope of a straight line equation if a_2 is considered to be very small compared to a_o and a_1. Table 4.6 is the analysis of coefficient a_1 taken from each device.

Device number	Coefficients $a_{1,min}$	$a_{1,max}$	Average value
8	16.450	16.483	16.466 ± 0.016 (± 0.1%)
9	15.057	15.358	15.208 ± 0.150 (± 1.0%)
10	15.209	15.351	15.280 ± 0.071 (± 0.5%)

Table 4.6: Analysis of a_1 taken from each device

The solution of Eqn.4.2 up to the second order yields

$$\Delta T = \frac{-a_1 \pm \sqrt{a_1^2 - 4a_2(a_0 - \text{bits})}}{2(a_0 - \text{bits})} \qquad \text{Eqn.4.3}$$

with $\Delta T = (T_{measured} - T_{ref})$,

where $T_{ref} = \begin{cases} 0 \text{ for CN=1 to CN=19 and CN=32 to CN=35} \\ \text{bit}_{ref} \times 0.025 \text{ for CN=20 to CN=35} \end{cases}$

and bit_{ref} is an internal reference point read from channel 3 of PCI 1002 at the beginning of each Run. Since the thermocouples were individually calibrated, Table 4.7 ((a)and (b)) shows a comparison between the measured temperatures (taken to be the same during calibration) with the calculated temperatures using Eqn.4.3. Fig.4.2.4(c) and Fig.4.2.4(d) show the calibration curve drawn for CN=1 to CN=19 and CN=32 to CN=35, and CN=20 to CN=31 respectively. These figures illustrate the minimum and maximum values of calculated temperatures taken from Table 4.7(a) and Table 4.7(b).

Over 50 test-experiments for the temperatures were conducted by running water in the water pipeline while the freon pipeline was left empty. Each of the experiments took between 30 minutes and 120 minutes, each point representing an average of 10 readings. The bit-tempereature conversions were calculated using the coefficients just discussed. Fig.4.2.5 shows some of the examples taken for CN=1 to CN=32. For simplicity, the outputs recorded in the final minute of the Run are summarized in Table 4.8.

Figure 4.2.5	Temperature in °C T_{min}	T_{max}	$T_{average}$	Duration of Run (minutes)
a	20.4	20.7	20.5 ± 0.1	35
b	42.1	42.3	42.2 ± 0.1	60
c	63.6	63.7	63.6 ± 0.1	120

Table 4.8: The output temperatures summarized from Fig.4.2.5

	Measured temperature (°C)										
	0.00	9.00	20.70	31.40	39.50	44.80	52.30	62.10	69.50	76.40	90.70
CN	Calculated temperature for CN=1 to CN=19 and CN=32 to CN=35 in °C										
1	0.06	8.97	20.53	31.39	39.66	44.85	52.42	61.98	69.54	76.21	90.80
2	0.07	8.98	20.49	31.38	39.67	44.85	52.43	61.97	69.57	76.19	90.79
3	0.10	8.96	20.45	31.35	39.70	44.90	52.43	61.98	69.58	76.14	90.81
4	0.09	8.99	20.43	31.35	39.71	44.89	52.45	61.97	69.59	76.11	90.82
5	0.08	9.00	20.44	31.36	39.71	44.88	52.42	61.96	69.58	76.17	90.80
6	0.06	9.02	20.44	31.38	39.70	44.87	52.40	61.98	69.56	76.18	90.80
7	0.04	9.02	20.49	31.39	39.68	44.86	52.39	62.00	69.52	76.21	90.80
8	0.07	8.98	20.48	31.39	39.70	44.86	52.41	61.99	69.53	76.19	90.81
9	0.07	8.98	20.48	31.40	39.68	44.87	52.40	61.99	69.54	76.20	90.80
10	0.07	8.99	20.45	31.39	39.69	44.87	52.40	61.99	69.56	76.18	90.80
11	0.08	8.97	20.49	31.39	39.67	44.86	52.38	61.97	69.55	76.26	90.77
12	0.04	9.00	20.53	31.38	39.66	44.86	52.38	61.96	69.54	76.26	90.78
13	0.04	8.99	20.55	31.40	39.63	44.87	52.35	61.99	69.51	76.32	90.75
14	0.03	8.99	20.54	31.44	39.63	44.87	52.37	61.98	69.47	76.31	90.78
15	0.05	8.98	20.53	31.42	39.65	44.87	52.36	61.99	69.50	76.28	90.78
16	0.03	9.01	20.51	31.43	39.64	44.86	52.36	62.00	69.50	76.29	90.77
17	0.00	9.02	20.60	31.38	39.65	44.84	52.31	62.01	69.53	76.31	90.76
18	0.02	9.02	20.54	31.38	39.66	44.85	52.36	62.01	69.56	76.22	90.79
19	0.04	9.01	20.54	31.37	39.66	44.84	52.36	62.01	69.56	76.23	90.78
32	0.02	9.03	20.51	31.43	39.64	44.84	52.35	62.00	69.51	76.30	90.76
33	0.03	8.99	20.56	31.44	39.62	44.84	52.33	62.00	69.49	76.35	90.75
34	0.02	8.97	20.67	31.42	39.57	44.82	52.30	62.02	69.47	76.43	90.72
35	0.01	8.98	20.65	31.41	39.60	44.84	52.31	61.99	69.46	76.44	90.72

Table 4.7(a): Comparison between the measured and the calculated temperatures for CN=1 to CN=19 and CN=32 to CN=35

	Measured temperature in °C										
	0.0	9.0	20.7	31.4	39.5	44.8	52.3	62.1	69.5	76.4	90.7
CN	Calculated temperature for CN=20 to CN=31 in °C										
20	0.06	9.07	20.63	31.37	39.63	44.86	52.35	61.89	69.54	76.22	90.76
21	0.04	9.07	20.67	31.38	39.62	44.85	52.31	61.89	69.50	76.33	90.73
22	0.08	9.06	20.63	31.35	39.63	44.87	52.35	61.89	69.54	76.27	90.73
23	0.09	9.06	20.57	31.33	39.67	44.88	52.38	61.90	69.58	76.13	90.78
24	0.09	9.05	20.58	31.35	39.66	44.89	52.36	61.89	69.59	76.13	90.78
25	0.09	9.05	20.58	31.36	39.65	44.89	52.36	61.90	69.58	76.14	90.78
26	0.05	9.07	20.61	31.39	39.65	44.84	52.34	61.92	69.55	76.16	90.79
27	0.07	9.09	20.57	31.35	39.67	44.84	52.37	61.94	69.54	76.17	90.77
28	0.10	9.05	20.55	31.35	39.67	44.89	52.38	61.91	69.56	76.12	90.79
29	0.10	9.06	20.54	31.36	39.68	44.89	52.36	61.90	69.56	76.15	90.78
30	0.10	9.06	20.54	31.34	39.67	44.90	52.39	61.88	69.57	76.15	90.78
31	0.09	9.06	20.59	31.34	39.64	44.87	52.38	61.91	69.56	76.21	90.77

Table 4.7(b): Comparison between the measured and the calculated temperatures for CN=20 to CN=31

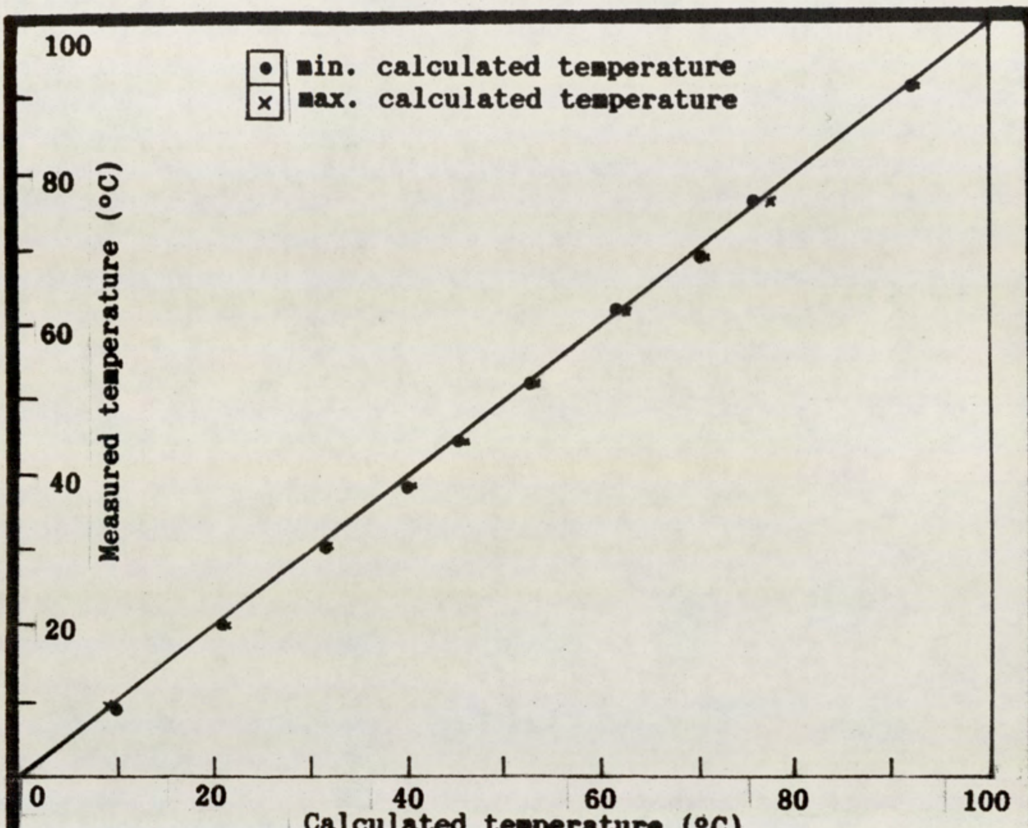

Fig.4.2.4(c): Calibration curve for temperature (CN=1 to CN=19 and CN=32 to CN=35 - PCI 1001)

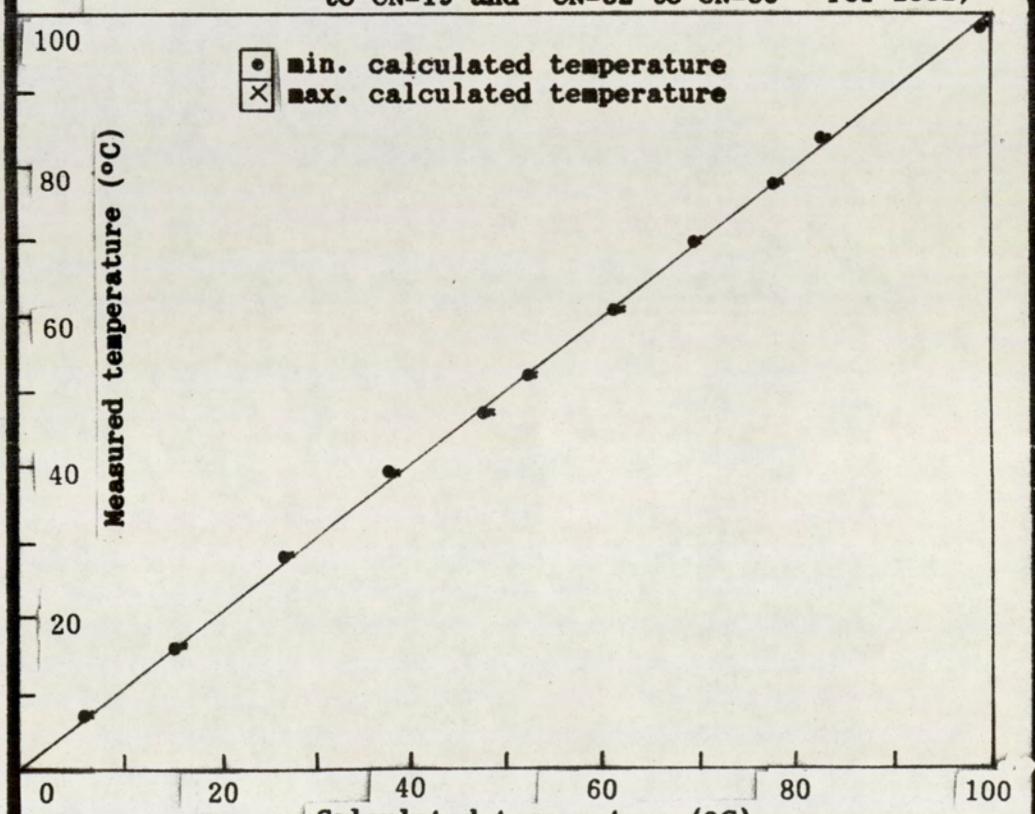

Fig.4.2.4(d): Calibration curve for temperature (CN=20 to CN=31 - PCI 1002)

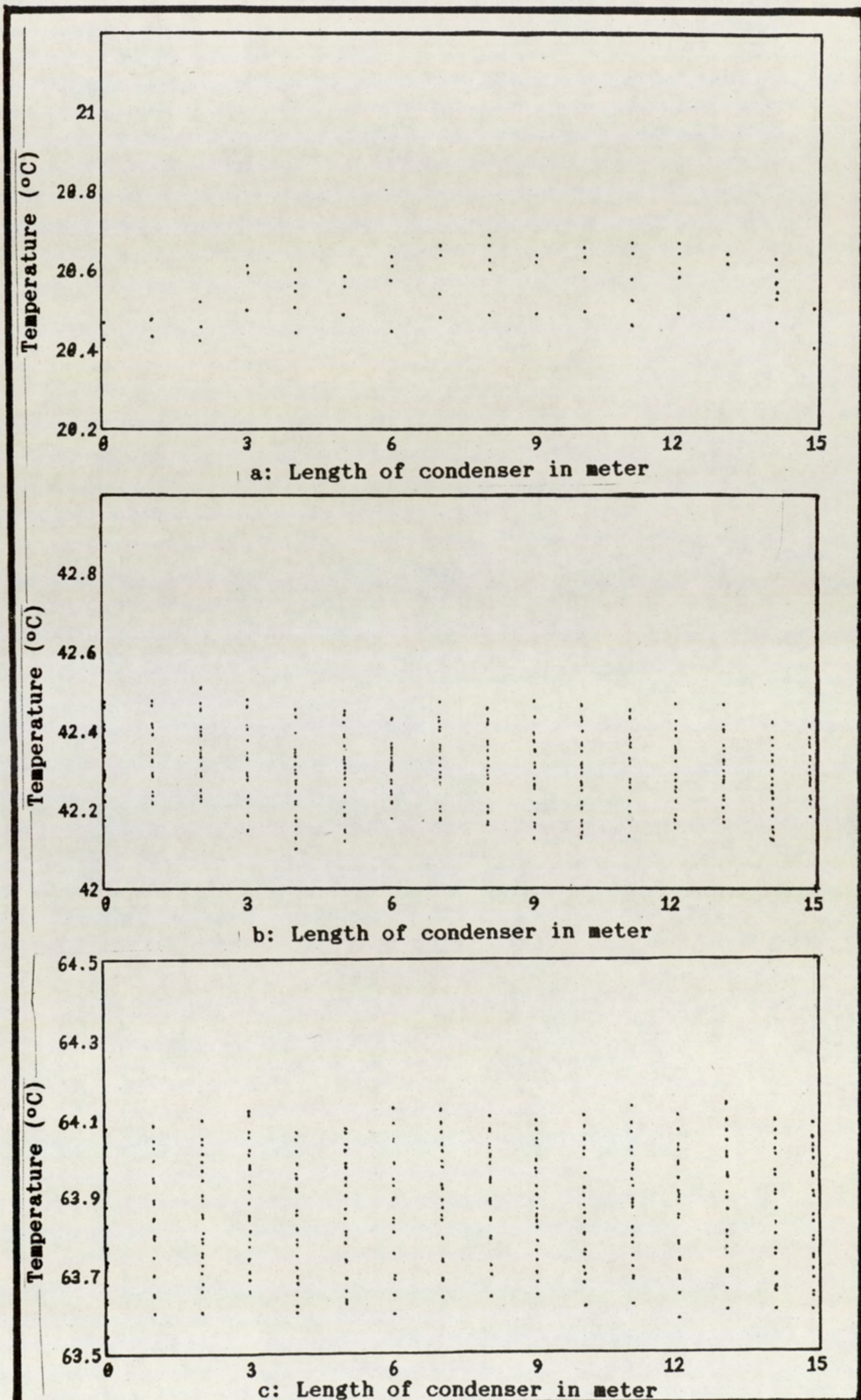

Fig.4.2.5: Bits-temperature conversion experiment using calibration coefficients Ca28487

4.2.3: Pressure transducer calibration

The four pressure transducers attached to the heat pump system were temporarily removed for calibration. The transducers were calibrated separately. A straight line fitting program to analyse the calibrating outputs was developed. Several experiments were carried out to make sure the readings were consistent. The following discussions are based on the experiment done on 28-04-1987.

Calibrating setting-up

Fig.4.2.6 shows the procedure for transducer calibration. The transducers were connected to a rectangular metal base joined to a pressure calibrator device (Budenberg SN:7607/279). Oil was poured into the calibrator until it could be seen in the thick rubber tube which was then connected to the transducers. In this experiment, it was important to ensure there was no oil leaking from either the pump or the transducers.

The dead-weight, equivalent to a pressure of 1 bar to 14 bar in steps of 1, was placed on the pump turntable, the computer recording the pressure readings in bits. The four transducers were calibrated simultaneuosly. An average of 20 readings was recorded by rotating the turntable slowly just before the experiment began to avoid any kind of frictional resistance that might be added to the measured pressure during calibration.

The outputs

A linear relationship between the bits and the pressures was considered in this case,

$$P = a_0 + a_1.\text{bits} \qquad \text{Eqn.4.4}$$

where P is the pressure in bar, a_0 and a_1 are the constants to be determined. The summary of the coefficients computed from Eqn.4.4 for CN=36 to CN=39 is shown in Table A-1.3.

The measured pressure and the calculated pressure was then compared and illustrated in Fig.4.2.7 (a) and Fig.4.2.7(b) taken from Table 4.9.

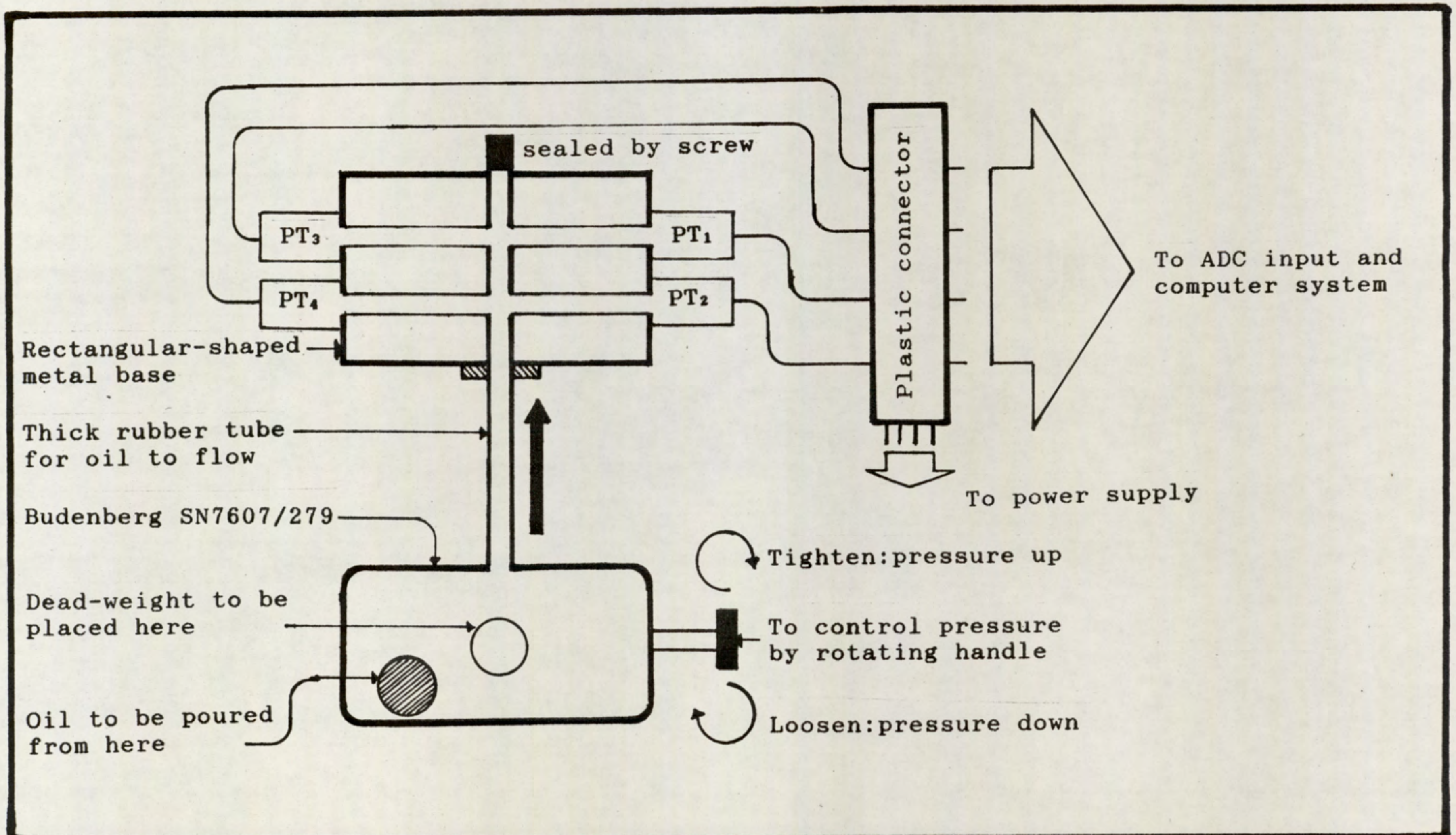

Fig.4.2.6: The calibrating experiment for pressure transducer

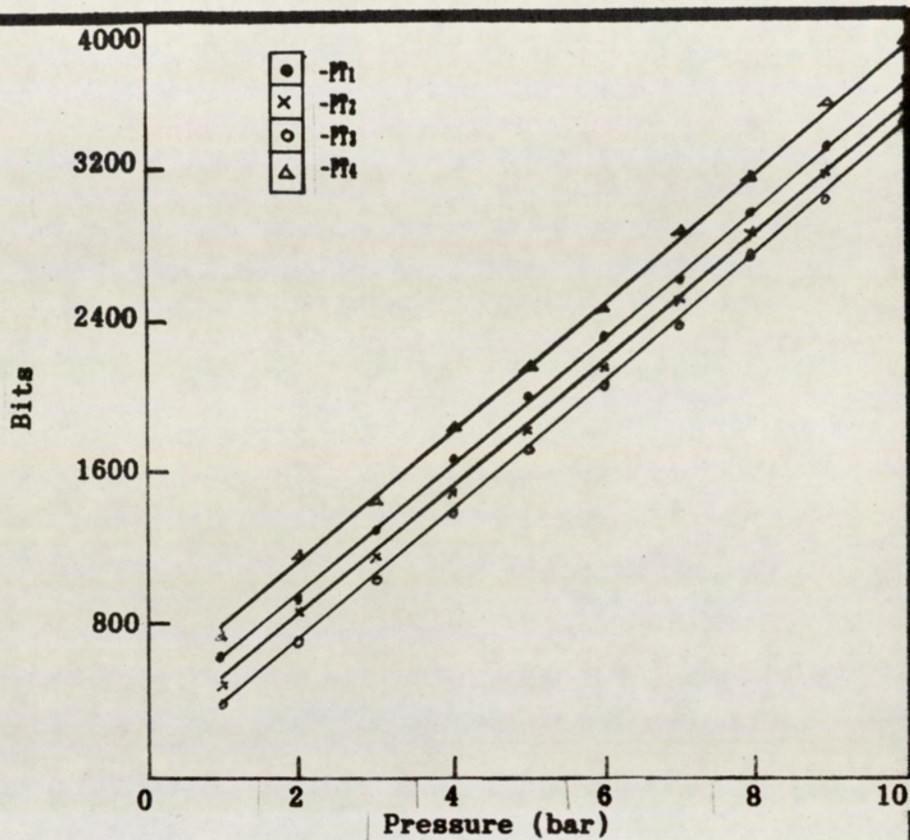

Fig.4.2.7(a): Calibration curve; bits versus pressure

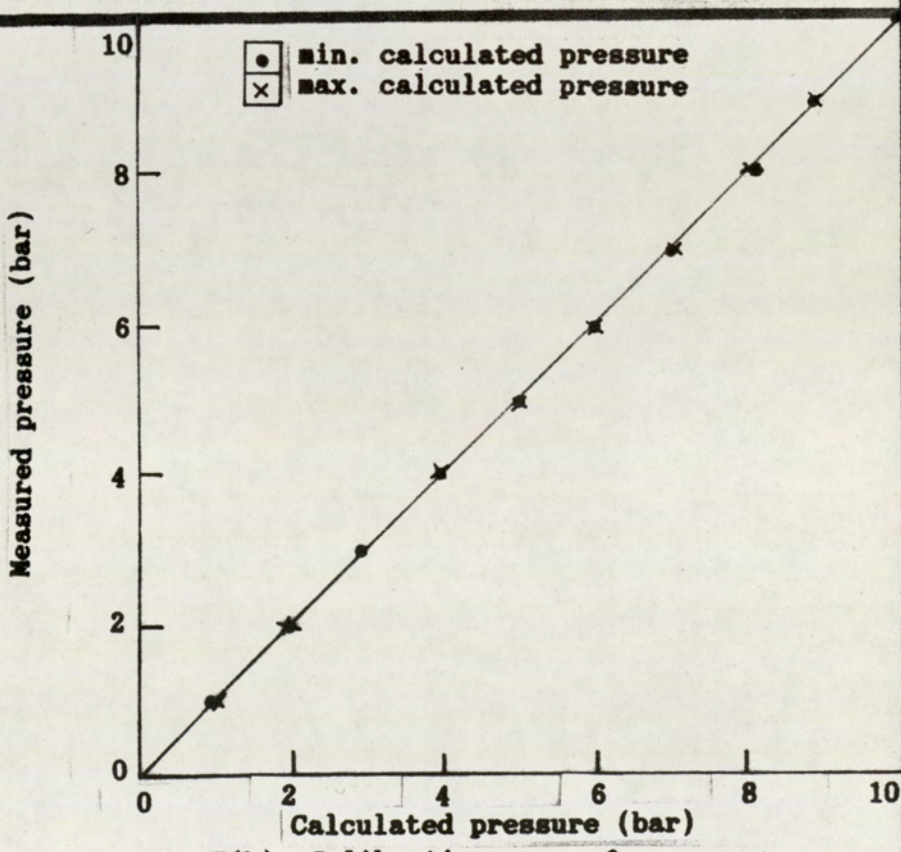

Fig.4.2.7(b): Calibration curve for pressure

Measured pressure (bar)	Calculated pressure from equation 4.4							
	PT_1 (CN=36)		PT_2 (CN=37)		PT_3 (CN=38)		PT_4 (CN=39)	
	bits	bar	bits	bar	bits	bar	bits	bar
1	635	0.9975	447	1.0011	327	0.9989	771	1.0000
2	977	2.0002	789	1.9987	670	1.9990	1164	2.0002
3	1318	2.9999	1132	2.9993	1013	2.9992	1457	3.0001
4	1659	3.9996	1475	3.9998	1356	3.9993	1800	3.9999
5	2001	5.0022	1818	5.0003	1700	5.0023	2143	5.0003
6	2342	6.0019	2161	6.0008	2043	6.0024	2486	6.0007
7	2683	7.0016	2504	7.0014	2386	7.0025	2829	7.0011
8	3024	8.0013	2846	7.9990	2728	7.9997	3172	8.0001
9	3364	8.9981	3185	8.9995	3021	8.9998	3575	9.0003
10	3705	9.9978	3532	10.0000	3413	9.9970	3858	10.0000

Table 4.9: Measured and calculated pressure compared

These coefficients were added to Ca280487 for CN=36 to CN=39 and were used in the bits-pressure conversion.

4.2.4: Error in measurements

The differences between the actual value of the parameters measured at the particular position, the value computed from the calibration coefficients and the bits reading from ADC are the basic errors occuring in the measurements.

There are two main sources of error encountered in this measurement. Firstly, calibrating error due to human error in reading from the conventional device or in the calibration device itself in registering of measured parameters. Secondly, the digitizing error that may occur during the analog-digital conversion.

<u>Calibrating error in measurement</u>

1. Thermocouples

The thermometer used to measure temperature in the thermocouples calibration was capable of measuring to an accuaracy of 0.1°C. It is quite difficult to visualize exactly between the steps marked on the thermometer glass, that would bring to a maximum of ±0.2°C error in the measurement. These errors would be obtained in measuring the temperature both at the measured point and at the cold point.

The other error that may appear could be from the thermocouples themselves. The errors may include the following:

a. The presence of the sensor itself may alter the temperature field at that particular location; we shall call this an installation error.

b. Any heat being transferred from (or to) the sensing element to (or from) either the body or the fluid may cause the temperature at the sensing element to be slightly different from the temperature of the body or the fluid at that location. There is a small temperature drop between them which results in error.

c. The depth of immersion of the sensing element into the stream of the fluid for each thermocouple may not be the same. This could cause the point in the fluid at which sensings were made to be different.

d. The distribution of the temperature in the sensing element and in the fluid at that region may not be the same.

$$T_{sensing\ element} \neq T_{fluid} \qquad \text{Eqn.4.5}$$

e. The properties of the insulation used in the system.

It is difficult to estimate numerically this factor. In this work these errors were assumed to be small compared to the errors caused by the thermometer's reading, and hence it was neglected.

2. Pressure transducer

The pressure calibration device has a claimed accuracy of ±0.05% of the pressure being measured. At the higher pressure range encountered (≃16 bar-Absolute) this would correspond to an uncertainity error of ±0.008 bar, and at the lower pressure (≃3 bar-Absolute) to an uncertainity error of ±0.0015 bar.

The uncertainty varies depending on the pressure being measured, but for simplicity, an average error of ±0.0048 bar was considered in any range of pressure measurements.

3. Digitizing error during analog-digital conversion

The ADC employed in the system is a 12-bit device with the full scale input voltage from -1V to +1V, represented digit by bits from -4096 bits to +4096 bits. At 0°C cold junction, the thermocouple generates 46µV/°C at 100°C (mentioned in chapter 3). Table 4.10 illustrates the digitizing errors occuring in the measurement of temperatures.

ADC	Sensor	Sensitivity	Digitizing error
Differential-input	Thermocouple	19.0 bits/°C	0.05 °C/bit
Channel 3 of PCI 1002 (differential-input)	Internal cold junction	40.0 bits/°C	0.025 °C/bit
Differential-input	Pressure transducer	290 bits/bar	0.0034 bar/bit

Table 4.10: Thermocouple and pressure transducer digitizing error

These errors may regarded as very small and negligible compared to the thermometer reading error of ±0.2°C. It was estimated that the total error in temperature measurement was ±0.2°C.

The total parameter error in the measurement of pressure was the sum of an average pressure calibrating device error and the pressure digitizing error which yields ±0.0082 bar.

4.3: Heat pump in operation

Before conducting an experimental run, the following steps were taken.

Firstly, the freon line was evacuated using a rotary vacuum pump before filling the refrigerant line of the system with freon. The system was kept running during the filling process. The system is fully charged when clear liquid could be seen to occupy the whole area of the sight glass window. A data acquisition program was set to display the output.

Secondly, The pressure-controlled device was fixed at the lowest marked level with the water flow rotameter fixed so that the float was constantly floating. The cold junction was checked to be at about 0°C, while the system was allowed to run continuously for at least 2 hours until it reached a steady-state condition before data could be taken into consideration. The profiles of the test-point temperatures as a function of time revealed the period of time necessary to reach steady state.

4.3.1: Mode 2 and mode 3 experiment

In mode 2, data was taken every 30 minutes. Water mass flowrate was measured manually over the duration of data acquisition period (see also Fig.3.1.1 and Fig.3.2.1). The discharge pressure was slowly increased at the end of each Run. About 60 seconds was needed to read one complete Run. At the end of each Run, the following steps were carried out.

a. The pressure was increased.

b. The freon level was checked. The freon should be topped up at once and a steady-state condition attained before recording any experimental output if there is lack of freon.

c. To check the temperature at the external cold junction is 0°C.

d. To measure manually the outlet water temperature at the sink.

e. To measure the mass, volume and the time of water being collected during data acquisition period.

f. Inserting of item 4 and 5 (above) to the computer, whereby the average value of bits, water mass flowrate and the water volumetric flowrate would be computed. The flowrate was assumed to be constant in each Run.

The apparatus for measuring flowrate was cleaned and dried during each interval. The empty measuring cylinder was then reweighed for the next Run. Usually, it took at least 9 hours to acquire 14 Runs. The pressure was slowly decreased at the end of each Run with the water flow rotameter fixed. The rest of the procedure was exactly the same as above.

In mode 3, the same procedure was employed except the pressure-controlled device and the water flowrate was set to be approximately the same as experiments in mode 2.

4.3.2: Measurement of water flowrate

The outlet water at the sink was collected in a one-litre measuring cylinder marked in the steps of 10 cc. The time for water to be collected during data acquisition period was also measured by a stop watch marked in the steps of 0.2 second. A triple beam balance with a marked scale of 0.1 g was introduced to weigh the mass of water. The complete method to measure condenser water flowrate is shown below.

Time taken to collect water	$= t$	s	($\pm$0.2s)
The weight of empty container	$= W_o$	g	($\pm$0.1g)
The weight of empty container + water	$= W_{o+wr}$	g	($\pm$0.1g)
The weight of water only, W_w	$= W_{o+wr} - W_o$	g	($\pm$0.1g)
The volume of water	$= V_{wr}$	cc	(+10cc)

The water mass flowrate, $\dot{m}_w$ $= W_{wr}/t$ g/s

$$= \frac{(W_{o+wr} - W_o)}{t} \text{ g/s} \qquad \text{Eqn.4.6}$$

The water volumetric flowrate, $\dot{v}_{wr}$ $= (V_{wr}/t)$ cc/s Eqn.4.7

Error in the measurement

The chief source of error encountered was the measurement due to human error in reading. The other possible technical errors, difficult to quantify numerically, were as follows.

a. The time set by the computer at the beginning and end of the water collection did not occur exactly at the same time with the time measured by the stop-watch.

b. There was a possibility of water sticking around and wetting the wall of the cylinder.

c. The possibility of the weighing machine and the cylinder not being really clean and dry could result in a small extra weight being added, since the machine can measure to an accuracy of ±0.1g.

The possible maximum error $\Delta\dot{m}w$ solved by Eqn.4.6 could be analysed by taking partial derivatives of $\dot{m}w$ with respect to each dimension yields

$$\left|\Delta\dot{m}w\right| = \dot{m}w(\Delta W_{wr}/W_{wr} - \Delta t/t) \qquad \text{Eqn.4.8}$$

where ΔW_w and Δt are the uncertainty errors revealed in W_w and t respectively. Inserting the typical values,

W_{wr} =	1978.2 g	ΔW_{wr} =	± 0.1 g
t =	59.8 s	Δt =	± 0.2 s
$\dot{m}w$ =	32.86 g/s	$\Delta\dot{m}w$ =	?? g/s

yields a fractional error of water mass flowrate of 0.10824 g/s which is 0.33% of the typical value.

4.4: Software for data acquisition program

The same program described in section 3.4.4 was used for all Runs except that for experimental data analysis. Because of the quasi-static nature of the experimental run, it was essential to time-average the data for each Run. To acquire one Run, the readings from the thermocouples and the pressure transducers were read sequentially and an average of 10 sets of readings were taken to be the final reading.

The time for acquiring data and the quantity of water being collected at the sink during data acquisition period was recorded for water flowrate calculation. The time taken to complete one Run was approximately 60 seconds.

4.4.1: Input statements

The date on which the experiment was carried out was automatically used as a filename. The maximum number of sampling in the Run in one experiment was also included as an input statement. The allocation of time was primarily considered to ensure that the Runs should be completed for the day. As an example, at least 10 hours were needed to acquire 14 Runs.

At the end of each Run, the necessary parameters for calculating condenser water flowrate were also inserted.

4.4.2: Reading and average of bits

The sequence of channels being read shown in Fig.4.4.1 could be summarized starting from the top to the bottom illustrated in Table 4.11.

CN	Device number	Items to be read
0	8	Reference bit
1-16	9	Temperatures of freon in condenser
17-19	10	Temperatures of water in condenser
20-31	8	Temperatures of water in condenser
32-33	10	Freon's temperatures outside condenser
34	10	Room temperature, RT
35	10	Water inlet temperature
36-39	10	Pressure
41-43	10	Water and freon flowrate, air speed and Watt meter respectively

Table 4.11: Reading of bits in order

For information, the whole set of the freon and the water temperatures at the test-points were read sequentially. An average of 10 sets of readings (one Run) was computed at the end of the tenth set of readings.

4.4.3: Output results

The bits and the bit-parameter conversions were all automatically stored for analysis. The measured water flowrate was also saved by adding channel numbers from CN=44 to CN=46, where

CN=44: Water volumetric flowrate

CN=45: Water mass flowrate

CN=46: Water outlet temperature, $TW_{m,exit}$

$TW_{m,exit}$ was included to compare with the outlet water temperature at the condenser, TW_{16} where TW_{16} should be slightly higher than $TW_{m,exit}$.

The outputs displayed could be either represented by the temperature

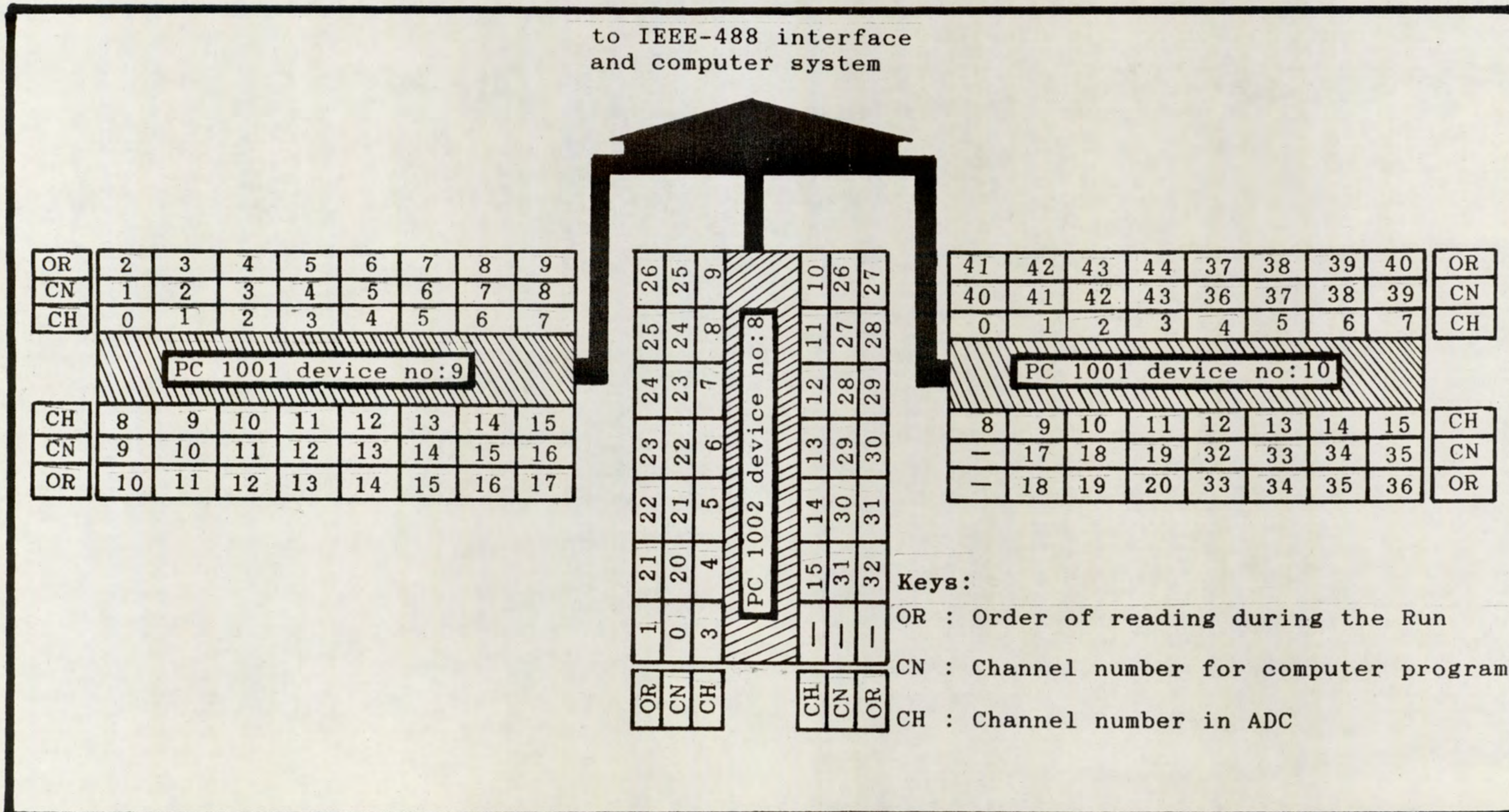

Fig.4.4.1: Sequence of channel readings via IEEE interface to computer

profile or by a block model of heat pump, shown in Appendix A-2.

The maximum permissible pressure for the pressure transducer is 14 bar, therefore a controlled-statement ($PT<14$) to avoid overanged pressure was also included in the program.

4.5: Analysis and evaluation of experimental data

In this section, an analysis is made of the secondary parameters which were not directly acquired from the experiment. These parameters were computed from the primary parameters, measured experimentally, such as temperature, pressure and water flowrate. The possibility that primary parameter errors influence the secondary parameters is also considered. Further, the secondary parameters are used to compute thermodynamic properties of the freon and water at given pressure and temperature, and other related physical properties of the fluid.

The second part of the section considers the usefulness of data taken from various Runs for different aspects of model verification. This assessment is important because of the experimental problems occurring during experiment, where the experiment does not completely represent the model being tested.

4.5.1: Estimation of model input data

Since the thermocouples for measuring fluid outlet and inlet temperature were placed at the point where the tubes are no longer brazed together (single pipe), an estimate of the fluid temperature at the last points of the joined pipe was taken to be the effective temperature. The estimate was also applied to the freon inlet and outlet pressure, where the pressure transducers were placed opposite to the corresponding thermocouples for sensing freon inlet and outlet temperature.

The effective values were calculated by linear interpolation from the values measured at point 1 and 2 at the condenser entry and at point 15 and 16 at the condenser exit, illustrated in Fig.4.5.1. An estimate was made for the temperature and pressure at point a and b. Assuming the temperature drop and rise, and pressure drop between these two points (1 and 2, and 15 and 16) are linear with the distance between them, an estimate for the temperature and pressure at point a and b could be made. The length between point a to point 1 and 2, and between point b to point 15 and 16 were measured manually to an accuracy of ±0.1 cm by a meter-ruler.

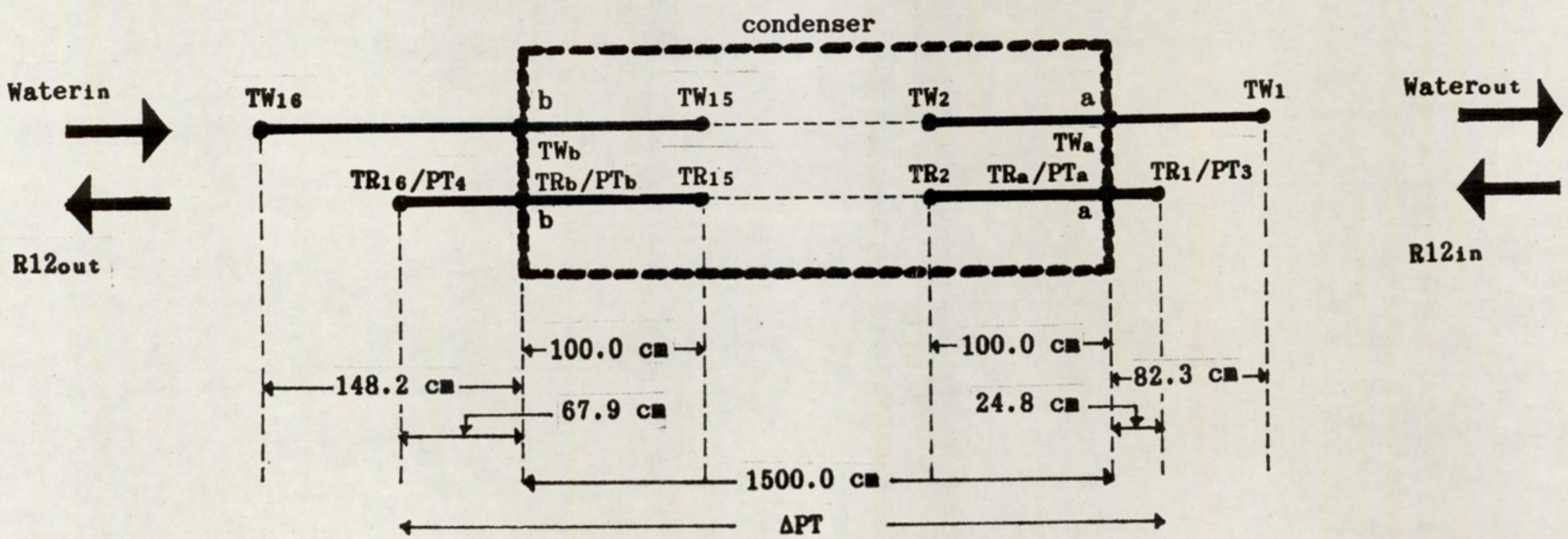

Notes:

1. TR and TW represent the temperature in the freon line and water line respectively. PT is the pressure
2. TW_1, TW_2, TW_{15}, TW_{16}, TR_1, TR_2, TR_{15}, TR_{16}, PT_3, and PT_4 are the measured temperatures (°C) and pressures (bar) respectively
3. TW_a, TW_b, TR_a, TR_b, PT_a and PT_b are the temperatures and pressures respectively to be determined

Fig.4.5.1: Effective parameters at the condenser inlet and outlet

Effective temperatures

The general formula to calculate the effective temperatures were estimated as (refer to Fig.4.5.1),

$$T_{eff} = T_{o,cond} \mp \left\{ \frac{L_i . \Delta T_j}{(100.0 + L_i)} \right\} \qquad \text{Eqn.4.9}$$

where T_{eff} = Effective temperature at point a and b to be determined in °C.

$T_{o,cond}$ = Measured temperatures at the points 1 and 16 in °C.

L_i = The length between the measured points (1, 2, 15, and 16) and the estimated points (a and b) in cm.

ΔT_j = The temperature difference between points 1 and 2, and between points 15 and 16 in °C.

where negative and positive sign (immediately after $T_{o,cond}$ of Eqn.4.9) represents the temperature drop and rise respectively.

The second term of Eqn. 4.9 is the correction factor depending on the lengths and the differences in the temperature, yields

$$T_{eff} = \begin{cases} TR_a \text{ for } L_i = 24.8 \text{ cm}, \ \Delta T_j = (TR_1 - TR_2), \ T_{o,cond} = TR_1 \\ TR_b \text{ for } L_i = 67.9 \text{ cm}, \ \Delta T_j = (TR_{15} - TR_{16}), T_{o,cond} = TR_{16} \\ TW_a \text{ for } L_i = 82.3 \text{ cm}, \ \Delta T_j = (TW_1 - TW_2), \ T_{o,cond} = TW_1 \\ TW_b \text{ for } L_i = 184.2 \text{ cm}, \ \Delta T_j = (TW_{15} - TW_{16}), T_{o,cond} = TW_{16} \end{cases} \qquad \text{Eqn.4.10}$$

where TR_a, TR_b and TW_b are the effective input values introduced in the model, while TW_a is the effective condenser exit water temperature, to be compared with the value computed by the model.

The error in the calculation is the sum of errors contributed from the measured temperature and the temperature correction factor of Eqn. 4.9. The temperature correction factor error yields

$$\left|\Delta f_t\right| = f_t(\Delta L_i/L_i + \Delta(\Delta T_j)/\Delta T_j - \Delta(100.0+L_i)/(100.0+L_i)) \qquad \text{Eqn.4.11}$$

where $f_t = L_i . \Delta T_j/(100.0+L_i)$. Inserting typical values to give a maximum possible correction factor error,

$$L_i = 148.2\ \text{cm}\ ;\ \Delta L_i = 0.1\ \text{cm}$$

$$\Delta T_j = 35.1\ ^oC\ ;\ \Delta T_j = 0.2\ ^oC$$

$$(100.0+L_i) = 248.2\ \text{cm}\ ;\ \Delta(100.0+L_i) = 0.1\ \text{cm}$$

$$f_t = 21.0\ ^oC\ ;\ \Delta f_t = ??\ ^oC$$

yields 0.14°C (± 0.68% of specified f_t).

The total possible maximum error of the effective temperature contributed by the temperature correction error was ±0.34°C.

<u>Effective pressures</u>

Similarly, the effective pressures could be writen as (refer also to Fig.4.5.1 for explaination),

$$P_{eff} = P_{o,cond} \mp \left\{ \frac{\Delta PT.L_i}{(1500.0+L_{in}+L_{out})} \right\} \qquad \text{Eqn.4.12}$$

where L_i = L_{in} ; The length between points 1 and **a** of the freon side in cm.

L_{out}; The length between points 16 and **b** of the freon side in cm.

ΔPT = The pressure drop between points 1 and 16 of the freon side in bar.

The maximum uncertainty occured in the second term of **Eqn. 4.12** contributed by the pressure correction factor, f_p yields

$$|\Delta f_p| = f_p \left[\frac{\Delta(\Delta PT)}{\Delta PT} + \frac{\Delta L_i}{L_i} - \frac{\Delta(1500.0+L_{in}+L_{out})}{(1500.0+L_{in}+L_{out})} \right] \qquad \text{Eqn.4.13}$$

where $f_p = \Delta PT.L_i/(1500.0+L_{in}+L_{out})$. Inserting the maximum typical values,

$$\Delta PT = 4.74\ \text{bar};\ \Delta(\Delta PT) = 0.0015\ \text{bar}$$

$$L_i = 67.9\ \text{cm}\ ;\ \Delta L_i = 0.1\ \text{cm}$$

$$(1500.0+L_{in}+L_{out}) = 1592.7\ \text{cm}\ ;\ \Delta(1500.0+L_{in}+L_{out}) = 0.1\ \text{cm}$$

$$f_p = 0.202\ \text{bar};\ \Delta f_p = ??\ \text{bar}$$

yields the pressure correction factor error of 0.00037 bar (±0.18%). Thus, the total maximum error calculated from estimated values was ±0.0019 bar.

In this case, PT_a and PT_b was assumed to be effective pressure where

PT_a will be used as input data for the model and PT_b used to compare with the value computed by the model.

The effective parameters described above could be concluded lying in the following order

$$TR_{16} < TR_b < TR_{15} < TR_2 < TR_a < TR_1$$
$$TW_{16} < TW_b < TW_{15} < TW_2 < TW_a < TW_1$$
$$PT_4 < PT_b < PT_a < PT_3 \qquad \text{Eqn.4.14}$$

4.5.2: Determination of freon mass flowrate

Freon mass flowrate was determined from consideration of the condenser energy, flowrate being assumed to be constant. From condenser energy balance, where the total thermal energy released from the freon side of the condenser is the sum of thermal energy picked up by the water side and the heat lost from condenser we obtain

$$\dot{Q}_{freon} = \dot{Q}_{water} + \dot{Q}_{loss}$$

$$\dot{m}r = \frac{[\dot{m}w.C_{pw}.\Delta TW + Q_{loss}]}{\Delta hr} \qquad \text{Eqn.4.15}$$

where Δhr = $(h_{g,1} - h_{f,16})$ in JKg^{-1}

$h_{g,1}$ = Specific enthalpy of vapour component at point 1

$h_{f,16}$ = Specific enthalpy of liquid component at point 16

$\dot{m}w$ = Total water mass flowrate in Kgs^{-1}

C_{pwr} = Specific heat capacity of water, 4.1833 $Jg^{-1}{}^{o}C$

ΔTW = $(TW_1 - TW_{16})$ in ^{o}C

TW_1 = Condenser outlet water temperature in ^{o}C

TW_{16} = Condenser inlet water temperature in ^{o}C

$\dot{Q}_{loss}$ = Heat loss from condenser in Watt

$\dot{Q}_{water}$ = Condenser total water thermal power in Watt

The first term of Eqn.4.15 is the total thermal power picked up by the water side across the condenser; and the second term is the total heat loss from condenser.

The specific enthalpy of R12 at points 1 and 16 was assumed to be in the vapour region and liquid region respectively. These secondary parameters are functions of the effective pressure and temperature evaluated in section 4.5.1. The effective water temperature difference estimated at points 1 and 16 across the condenser was the main parameter in the determination of freon mass flowrate.

The condenser water total thermal power, $\dot{Q}_{water}$ and the heat loss from the condenser, $\dot{Q}_{loss}$ was employed as input data to the model to determine freon and water mass flowrate.

4.5.3: Determination of condenser energy inbalance

An energy-balance calculation on the condenser indicates the accuracy of various measured parameters and derived parameters. This also reveals whether a particular Run represents a steady-state condition. The condenser energy inbalance, E_{inb} taken from Eqn.4.15, yields

$$E_{inb} = \dot{Q}_{freon} - (\dot{Q}_{water} + \dot{Q}_{loss}) \neq 0 \qquad \text{Eqn.4.16}$$

The determination of E_{inb} was based on the total estimated condenser thermal energy between points 1 and 16 and the total heat loss from condenser; it is difficult to measure experimentally the heat loss between the two consecutive test-points in the condenser.

4.5.4: Evaluation of experimental data

Certain experimental problems encountered raise the question of whether or not the measured data can be properly applied to the model.

Experimental difficulty 1: The primary measurements at the condenser inlet and outlet were not at the actual condenser end points. The actual values must be estimated from the measurements. Secondary parameters such as freon mass flowrate, freon specific enthalpy at the condenser inlet and outlet and the total water thermal power between these points are calculated from these estimated values. The other positions at which temperatures were measured in the condenser were those at which temperatures were computed by the model.

Experimental difficulty 2: This concerns the heat transfer from the freon side to the water side, assumed to be perpendicular to the fluid flow. Referring to Fig.4.5.2(a), there is a possibility of a temperature gradient existing across the tube ($T_a > T_b > T_c > T_d$). In this case, there is a temperaure drop between points a and b (freon side), between points b and c (wall), and between points c and d (water side). In practice, it is difficult to measure the bulk or average temperature for the freon and water side, with two known temperatures (at points a and d). In fact, the thermocouples may not be measuring the bulk or average

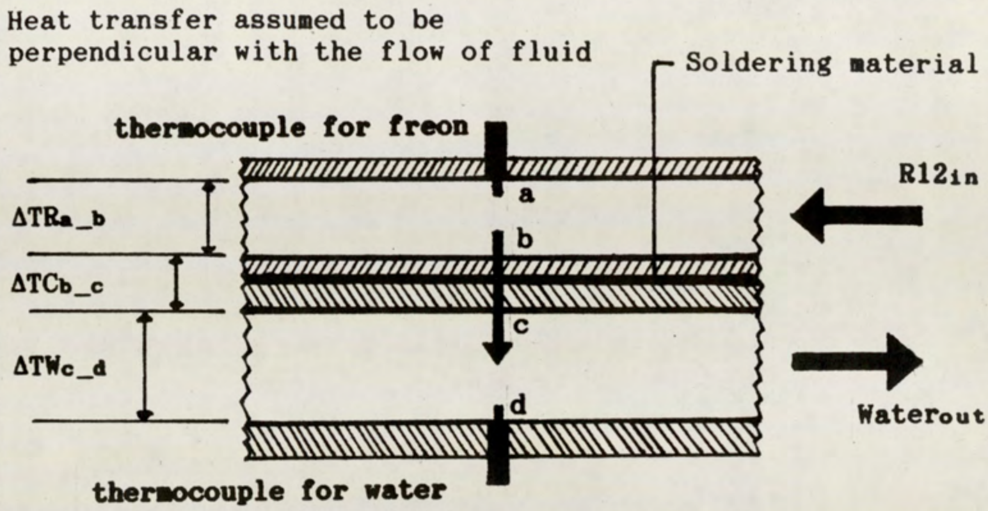

(a) The existence of temperature profiles across the tube

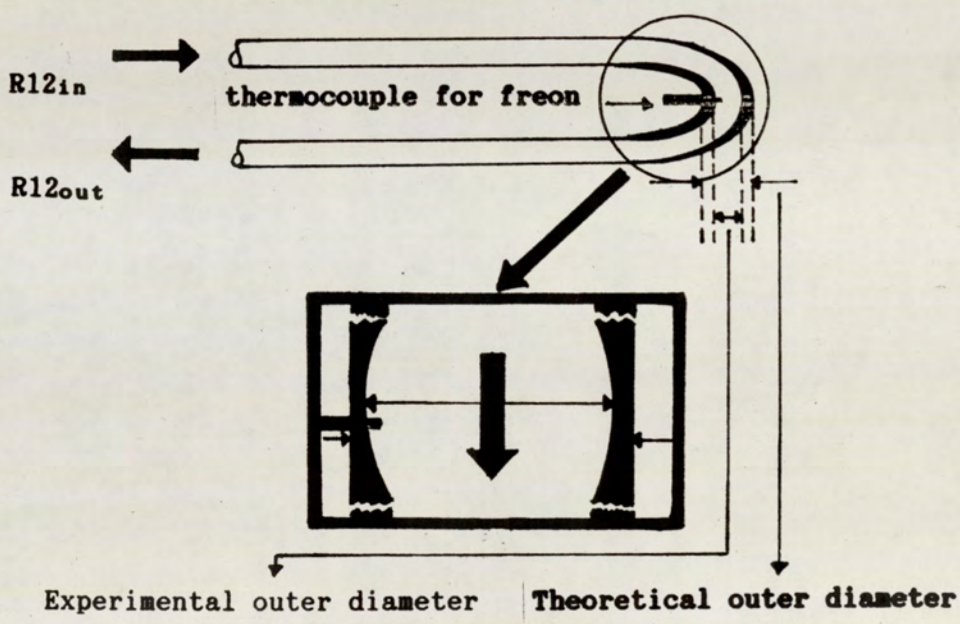

(b) The outer pipe diameter at the bend

Keys:

1. ΔTR_{a_b} : Freon temperature drop from point a -> b
2. ΔTC_{b_c} : Conductor temperature drop from point b -> c
3. ΔTW_{c_d} : Water temperature drop from point c -> d

$$TW_d < TW_c < TC_c < TC_b < TR_b < TR_a$$

Fig.4.5.2: Experimental difficulties ocurring during the Run

temperature. In the model, the measured temperature was assumed to be the bulk temperature.

Experimental difficulty 3: The problem, previously mentioned concerns the difficulty of achieving steady-state conditions in duplicating mode 3 experiments, where considerable alteration of the variables was required to achieve the required conditions. This results in a greater change in the operating conditions over the data-acquisition period in mode 3.

Experimental difficulty 4: This problem is associated with the measurement of the pipe diameters. As previously mentioned, the thermocouples in the condenser were fixed at the bends, where the effective bent pipe diameter was found to be smaller than the straight pipe. Referring to Fig.4.5.2(b), the bend was not smooth enough, which may result in higher values of heat transfer coefficients and pressure drop.

These problems affect the calculation of the heat transfer data. Since all heat transfer modelling requires a knowledge of freon temperatures and water temperatures within the condenser with the correct value of pipe diameter, the model verification may not be very accurate.

<u>Experimental input data used in modelling</u>

This concerns the use of experimental data to initiate the model. Two types of input data are introduced; variable input data and fixed input data.

1. Variable input data (VID)

The VID are the effective four primary parameters (TR_1, TR_{16}, TW_{16} and PT_3) calculated from the measured parameters. The other VID taken from secondary parameters are water thermal power and heat loss from the condenser.These values vary from one Run to another. All temperatures were assumed to be bulk temperatures.

2. Fixed input data (FID)

The diameter and the thickness of the freon pipe and water pipe was measured once and assumed to be the same for all sets of data analysis.

These relations can be summarized in Fig.4.5.3, which shows the effective temperatures and pressures employed to initiate the model.

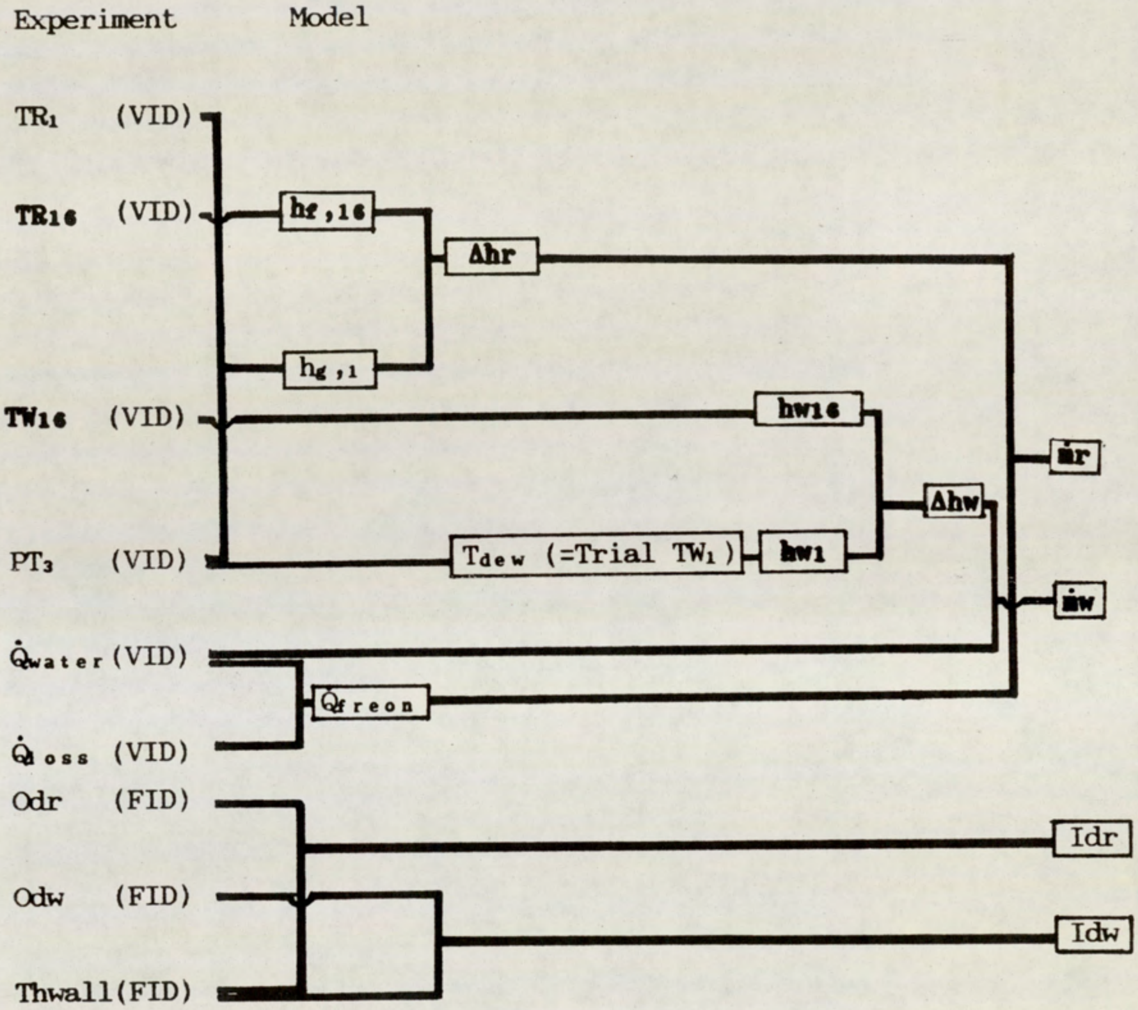

Fig.4.5.3: Input data taken from experiment related to model pre-calculation

CHAPTER 5

COMPUTER MODELLING AND MODEL APPLICATION

5.1: Introduction

This chapter mainly discusses the model provided by Carrington [1] which has been modified to suit the availability of the experimental data and also discusses its application within the experimental operating ranges. A detailed description of the model, together with the heat transfer phenomena and the pressure drop within the condenser at different regions is also presented. The second part of the chapter, discusses the model empirical correlations, the performance of the condenser using ε-Ntu method and the related fluid thermodynamics properties.

The model was modified to suit the available experimental data so that a comparison between experimental and predicted behaviour could be made. In general, the model predicts the behaviour of a counterflow heat exchanger which comprises two tubes thermally coupled. The thermal gradient that may occur between point a and b of Fig.4.5.2(a) was ignored in the single-phase region, and the two-phase region was treated separately. A subroutine originally written by Hickson [44] to compute refrigerant and water thermodynamic properties was also used. In addition, the temperature dependence of the fluid properties such as viscosity, conductivity, heat capacity and density taken from ASHRAE data book [105,106] was also considered.

The overall performance of the model is in agreement with the ASHRAE values and Dupont data but could be suspect near the critical point.

5.1.1: General idea of the main program

As previously mentioned, the model predicts the behaviour of a straight 15-meter long condenser including the thermodynamic and the physical properties of the fluid. The main idea is to predict both the temperature and the pressure of the fluid at consecutive points along the condenser using a numerical integration method.

The basic parameters computed are the pressure drop, and the heat transfer coefficients of the fluids in different regions. The main program can be divided into three major sections outlined as follows.

Input data: This concerns the variable input data (VID) and fixed input data (FID) as discussed in section 4.5.4 of chapter 4. The VID are temperature and pressure of entering hot refrigerant gas, exit temperature of condensed liquid freon, temperature of water entering condenser, and total thermal power to be transferred to water.

The FID are thickness of wall of the two tubes, outside diameter of the freon and water tube, total length of the condenser, and conductivity of thermal bond between tubes. These values were used for different sets of runs. The VID and FID were read from a subroutine.

It was also included the readings of reduced parameters, and the calculation of internal coil descriptions, integration increment, freon mass flowrate, and dew temperature at given initial pressure.

Main program: The calculation of heat transfer phenomena and pressure drops at each integrating point was done separately depending on whether the point lay in a single-phase region or in the mixed-phase region of the heat exchanger. The aim is to determine the exit water temperature. Subroutines for calculating thermodynamic and physical properties of the fluids in different flow mechanisms were also used.

To obtain the correct exit water temperature, other properties of the fluids at different regions, and profiles of some properties of the fluids along the heat exchanger integration, must initially be determined. The possible simple refrigeration cycle, by varying of evaporator conditions at different compressor isentropic efficiency were also presented in the main program.

Output data : This concerns the outputs predicted by the model, which can be classified to thermodynamic and physical properties of the fluids at separate regions, profiles of some fluids properties along the heat exchanger, and the summary range of evaporator conditions to predict simple refrigeration cycle.

The complete listing of the model program is shown in Appendix A-3 of section A-3.2.

5.1.2: Subroutines and functions

The subroutines and the functions associated with the main program were compiled and linked together, we shall call these Routine 1 and Routine 2.

Routine 1

The objectives of this routine are to compute thermodynamic and physical properties of the fluids which can be broken down as follows,

a. Effective input data, estimated from experimental data (subroutine).

b. The calculation of vapour and liquid heat transfer coefficient and pressure drop for laminar flow, turbulent flow and transition flow (subroutine).

c. The physical properties of the fluid as a function of temperature (function).

d. The thermodynamic properties of saturated and superheated freon as a function of temperature, pressure and vapour quality (function).

Routine 2

This concerns the freon properties at the condenser inlet and outlet. The general properties of the freon at various states at given parameters are also described.

a. The freon properties at the inlet and outlet of the condenser of the heat pump system in general (subroutine).

b. The pre-calculation of thermal and physical properties of the freon at different states as a function of pressure and temperature, associated with the Routine 1 (function).

A subroutine can be called at any time by the main program during integration process. The inter-calls between the subroutines are also possible (routine 1 calls routine 2 or vice versa). There are 12 subroutines and 15 functions associated with the main program. The complete listing of the program for routine 1 and 2 are shown in Appendix A-4 and A-5 of section A-4.2 and A-5.2 respectively.

5.2: Condenser modelling and its limitations

This section deals mainly with the mathematical calculations used in the model, which employ an iterative method to calculate the thermal and physical properties of freon and water in each region, and in each point of the integration. In addition, the properties of freon at the condenser inlet and outlet, and at the evaporator inlet and outlet are also presented.

To satisfy the requirement of the experiment, it is essential to outline the model assumptions, otherwise the experimental problems become too complicated to solve. The limitation of the model is also presented in this section.

5.2.1: Model iterative method and segment integration

The model simulates a counter-flow heat exchanger, in which water and freon flow in opposite directions, and uses numerical integration and iteration to solve the equations. The line integration was divided to 150 line segments, equivalent to 0.1 meter between each point. An integration through the heat exchanger, point I, shown in Fig.5.2.1 increases in the direction of refrigerant flow. Position I is at the start of the segment I, number 1 in the program (see Appendix A-3 of section A-3.2) being at the start of the refrigerant entry end. Simultaneously, for the water side, position (151-I) which is equivalent to position I in the freon side is the start of the segment (151-I) , with number 150 at the start of the refrigerant entry end. In the direction of freon flow, I increases in the freon side but decreases in the water side. This process seems to be equivalent with the counter-flow where the flow of freon starts at the condenser entry when I=1, and increases towards the direction of freon flow, and at the same time, the flow of water starts at I=(151-1)=150, equivalent to the length of 15 meter at the condenser exit, decreases. Position I=1 in the water side which is equivalent to position I=150 in the freon side indicates the condenser exit end.

The integration is said to be complete if all the segmental lengths have been covered, unless unsuitable input data has been introduced, in which case, the integration will be terminated and a new input value is reset to restart a new loop. One complete cycle of integration consists of a 150 line segment integration and is the same as one complete iteration. If there is an inbalance in the calculation, a new cycle of integration in the second iteration will proceed by re-estimating a new trial water exit temperature. The process will be carried on until all the conditions are satisfied. A smaller number of iterations indicates a faster convergence.

The main objective of the iteration is to determine the correct value of water exit temperature, TW_{exit} (=TW_{16}) which enables the counter-flow heat exchanger modelling in general. The initial trial water exit temperature is calculated from the freon saturated vapour temperature at given inlet pressure. All other parameters are computed during the iterating process.

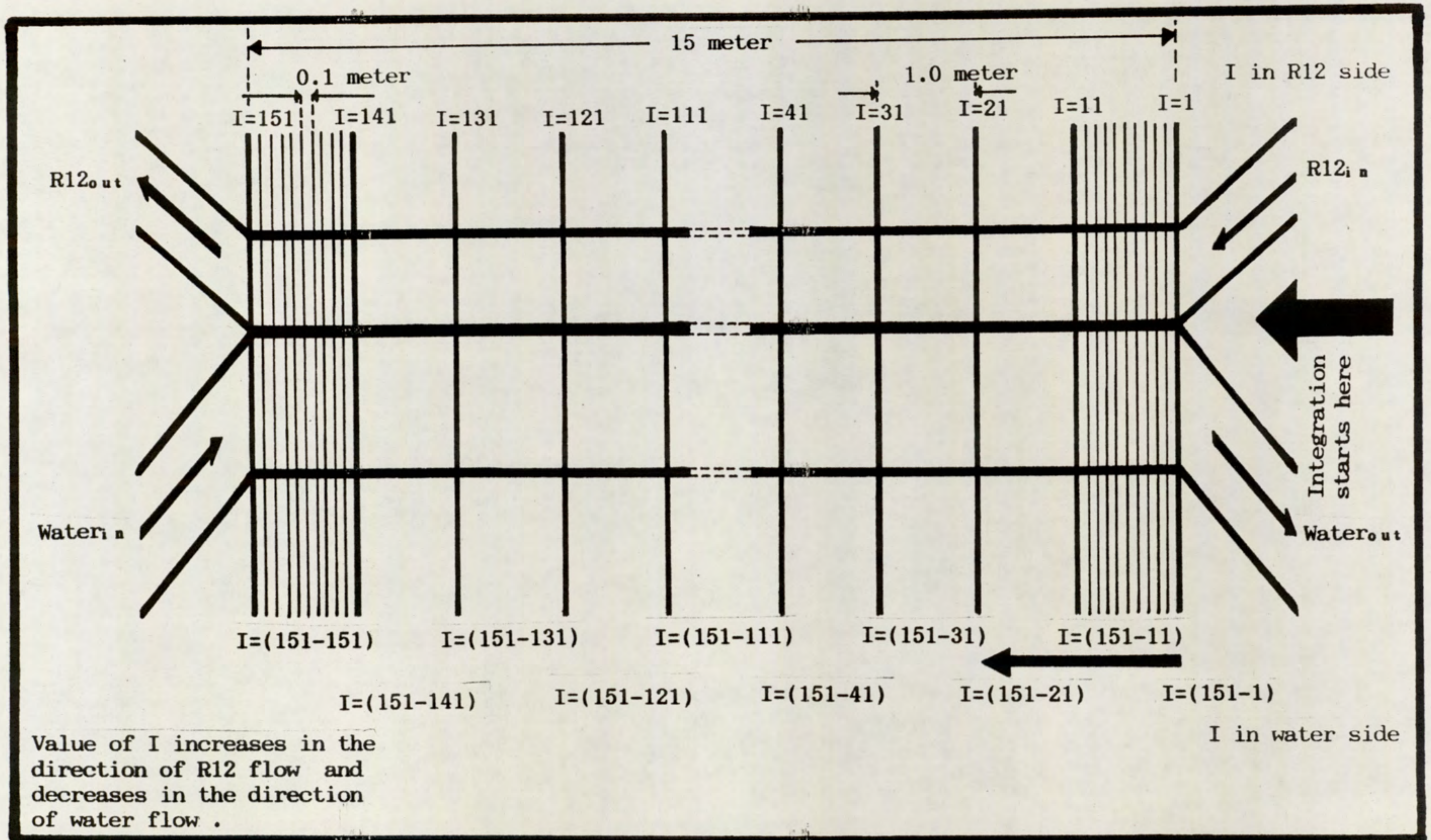

Fig. 5.2.1: Integrating process through a heat exchanger tube

Model calculation outside the iteration

Three parameters initially calculated outside the loop are summarized in Table 5.2.

Parameter	Calculated from	Function
T_{dew}	PR_1	As trial water exit temperature at the beginning of the loop.
$\dot{m}r$	$Q_{freon}/\Delta hr$; $\Delta hr=(h_{g,1}-h_{f,16})$	To calculate heat transfer coefficients and pressure drops during integration.
Idr/Idw	Odr, Odw and Th_{wall} (measured)	To be used together, to evaluate heat transfer coefficients and pressure drops in the iteration.

Table 5.1: Initial parameters calculated outside the iteration loop

These parameters would not affect the calculations within the loop.

Model calculation inside the iteration

This concerns the calculation of actual water exit temperature, leading to other temperatures of the freon and the water at consecutive points to form a temperature profile in the condenser. The general relationship between the water exit temperature and other parameters calculated within the iterative loop, is shown in Fig.5.2.2.

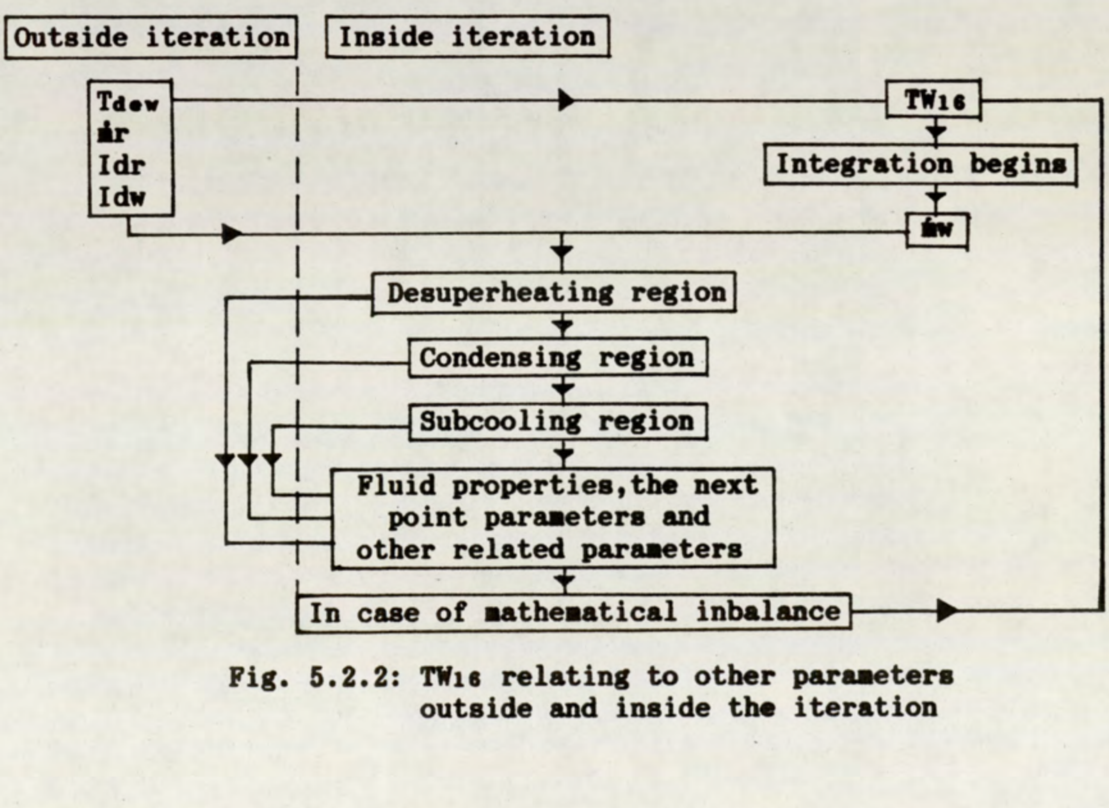

Fig. 5.2.2: TW_{16} relating to other parameters outside and inside the iteration

5.2.2: Condenser integrating control system

The complete condenser model was approached by solving for the desuperheating region, condensing region and subcooling region separately. Since the model predicts the behaviour of the freon and water in a heat pump condenser with the existence of three regions, it is very important to check the occurence of these regions on a pressure-enthalpy (p-h) diagram of R12 as shown in Fig.5.2.3.

It is assumed that the freon inlet temperature,TR_i is always in the vapour region, with PR_i as the freon inlet pressure. The saturated freon vapour temperature was calculated at that pressure (with all values in reduced units) where

$$T_{sat} = f(PR_{sat}) \qquad \text{Eqn.5.1}$$

For simplicity, this temperature was used as a trial water exit temperature where in this case TR_i is always above the TW_{exit}. Iteration becomes faster if trial TW_{exit} is closer to the actual TW_{exit}.

Referring to the p-h diagram of Fig.5.2.4(a), at given pressure and temperature one could test whether a point (P,T) lies either in the vapour region or in the mixed region or in the liquid region. The following conditions represent the above phenommena by considering the saturated pressure at given temperature.

a. Point A(P_{vap},T) lies in the vapour region for $P_{vap}<P_{sat}$.

b. Point B(P_{cond},T) lies in the mixed region for $P_{cond}=P_{sat}$.

c. Point C(P_{liq},T) lies in the liquid region for $P_{liq}>P_{sat}$.

On the other hand, by fixing the pressure, one could also determine from the given temperature at the line of isobar, the position of the point in various regions as illustrated in Fig.5.2.4(b), by initially calculating its saturated temperature.

a. Point A(P,T_{vap}) lies in the region of vapour for $T_{vap}>T_{sat}$.

b. Point B(P,T_{cond}) lies in the mixed region for $T_{cond}=T_{sat}$.

c. Point C(P,T_{liq}) lies in the liquid region for $T_{liq}<T_{sat}$.

During the integrating process, the conditions are set whether the point lies in the vapour region, the condensing region or the liquid region.

In the model, at given PR_i where (PR_i,TR_i) is at the starting point was used to evaluate $TR_{i,sat}$. This is exactly the same situation as in Fig.5.2.4(b) The various conditions are as shown in Fig.5.2.5; where TW_i should always be smaller than TR_i.

Condition 1 : At given pressure, the predicted freon

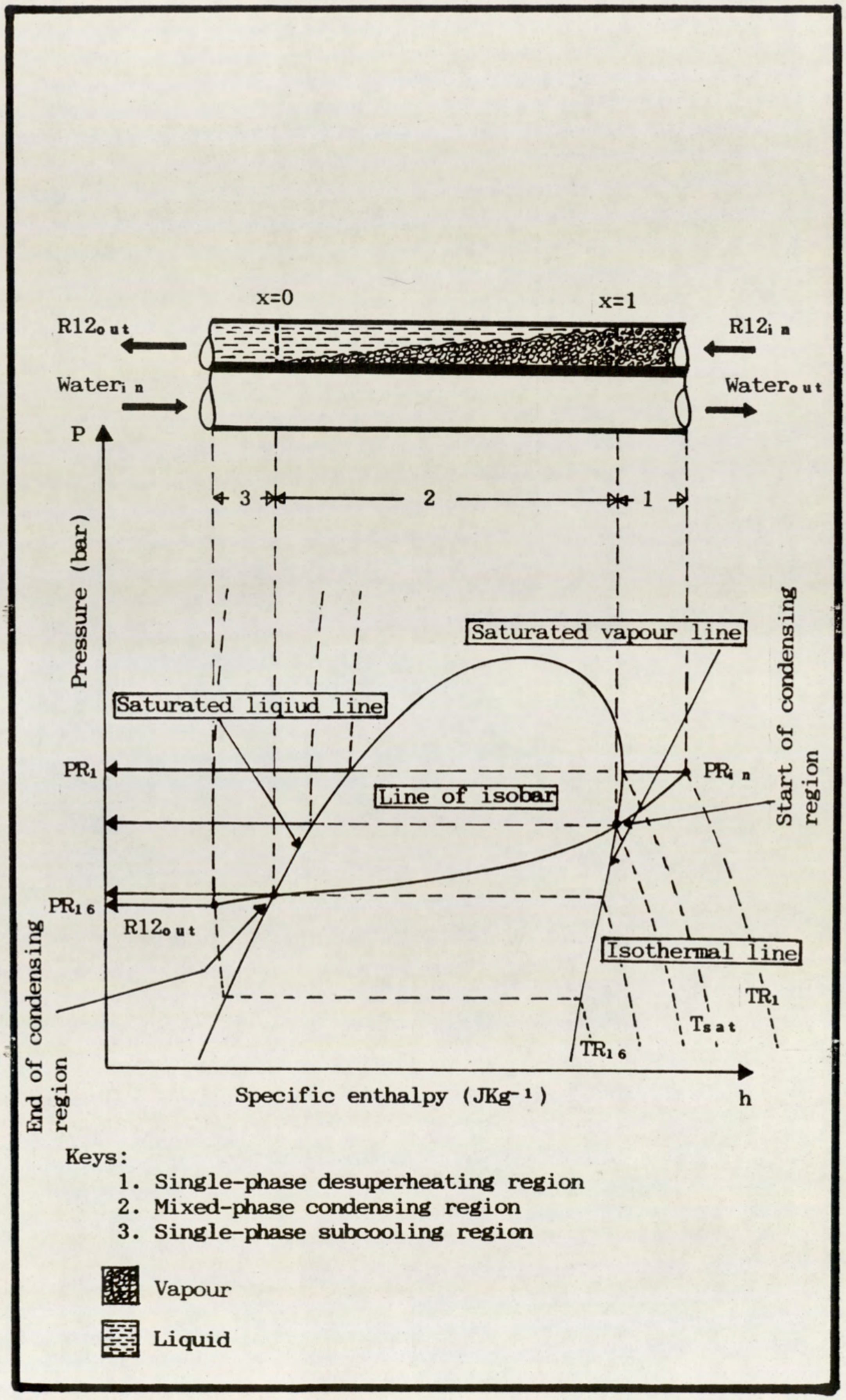

Fig. 5.2.3: P-h diagram showing three regions in condenser

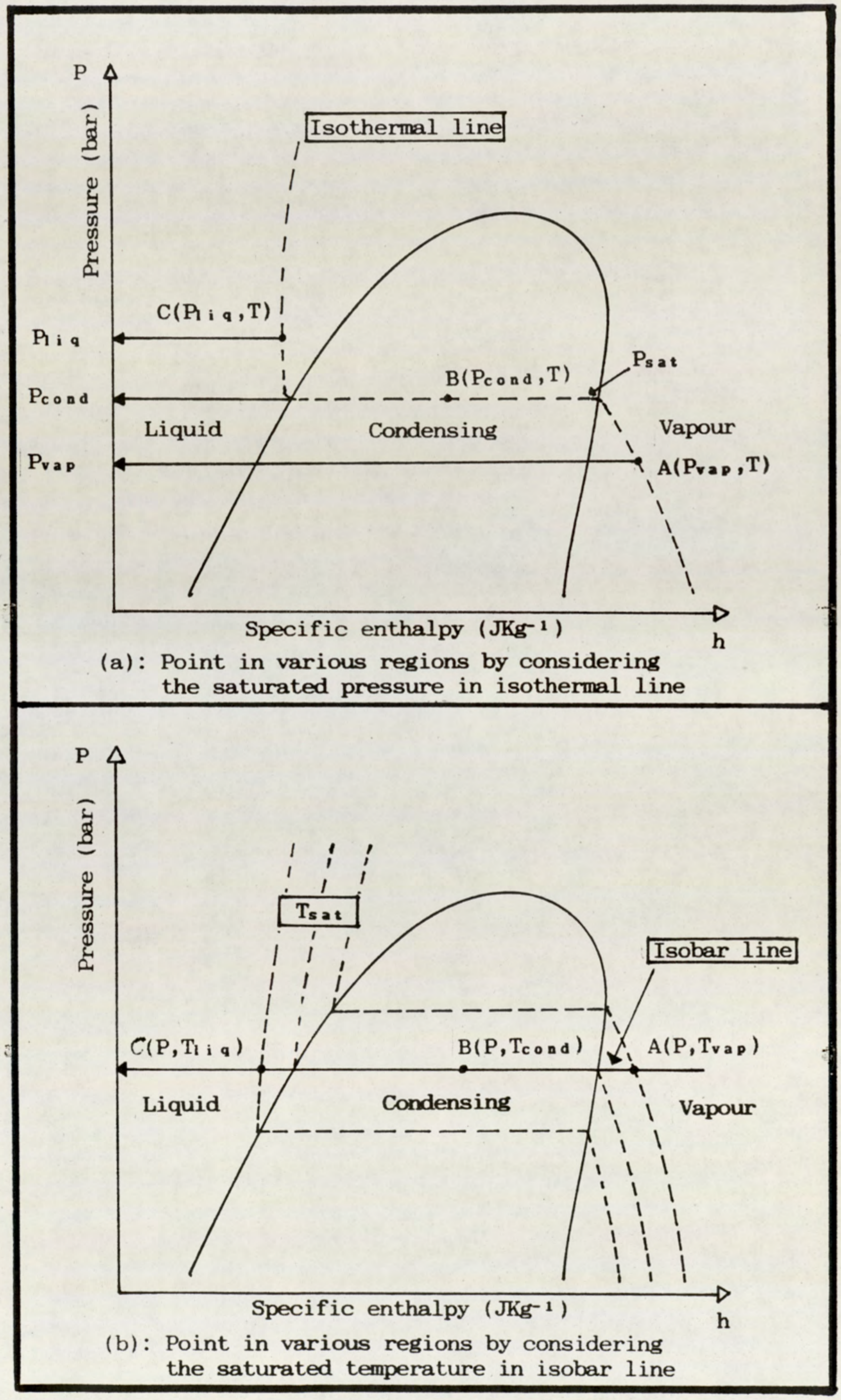

Fig. 5.2.4: P-h diagram testing the point in various regions

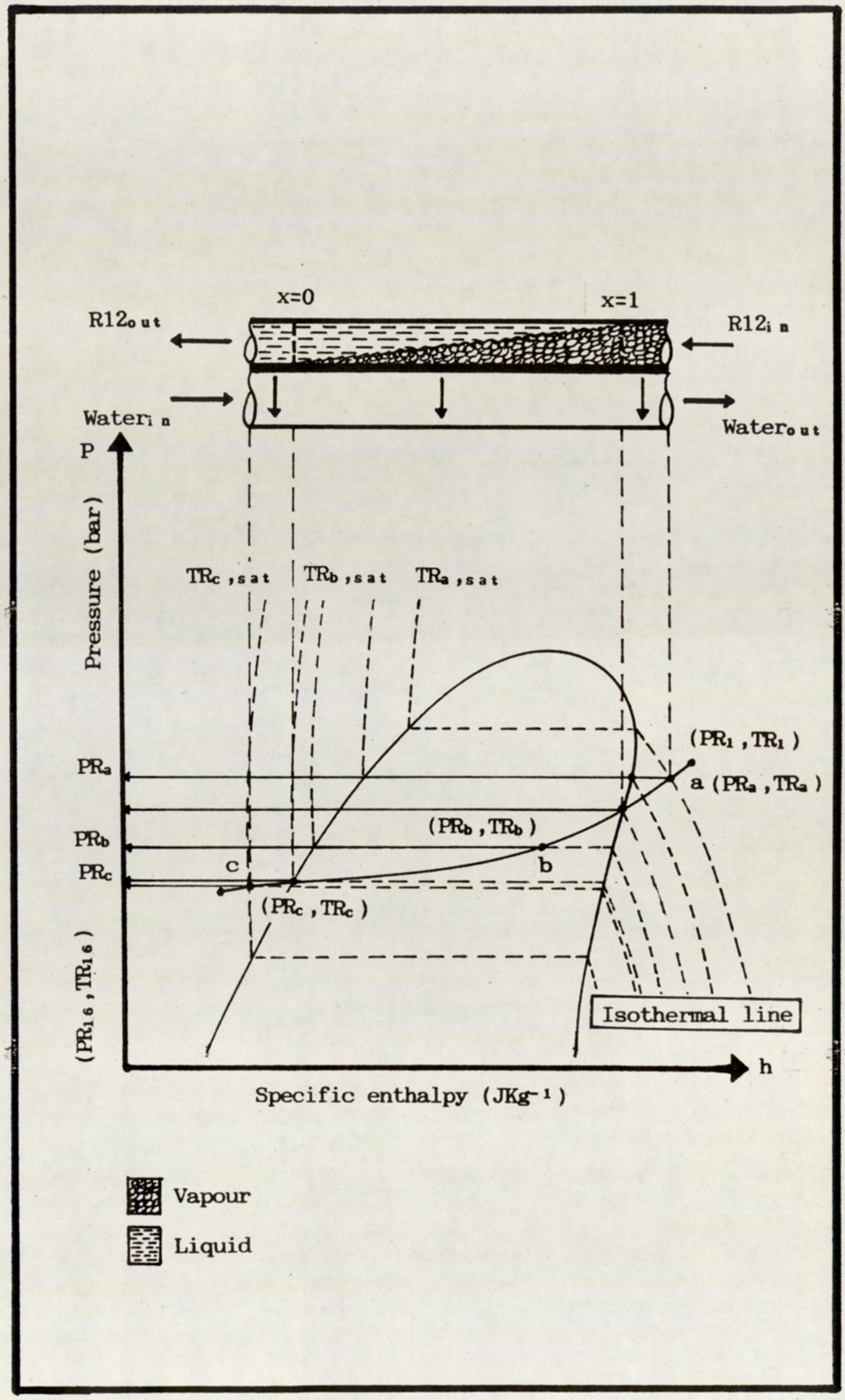

Fig.5.2.5: P-h diagram showing the conditions used in the model

temperature,TR_i and its saturated temperature,TR_{sat} should satisfy the following inequality,

$$TR_i > TR_{i,sat} \qquad \text{Eqn.5.2}$$

where in this condition, the point lies in the vapour region. In this region, the quality of vapour, x was assumed to be unity. For $TR_i < TW_i$, the trial water exit temperature will be readjusted by the monitoring program.

Condition 2 : At given pressure, at any situation, if condition 1 cannot be satisfied, where $TR_i < TR_{i,sat}$, the point could either be in the mixed region or in the liquid region. The point could only be in the two-phase region if

$$TR_i \leqslant TR_{i,sat}$$
$$0.0 < x < 1.0 \qquad \text{Eqn.5.3}$$

In the calculation, it is difficult to obtain the condition where $TR_i = TR_{i,sat}$ (see also Fig.5.2.5), therefore, another condition in the two-phase region, vapour fraction x calculated from the freon thermodynamic properties was introduced to supplement the condition.

Condition 3 : In this region, the freon is in the liquid-state where at given pressure,

$$TR_i < TR_{i,sat}$$
$$x = 0.0 \qquad \text{Eqn.5.4}$$

5.2.3: Model limitations and assumptions

As previously mentioned, the model did not satisfy all the experimental requirements. The following table summarized the assumptions employed in the model.

Items	Model assumption
Pipe description	Straight pipe of 15 meter long; the outer diameter at which sensors were placed (in the experiment, this position is at the bend) was assumed to be smaller than the diameter of straight pipe.
Temperature	1. The bulk or average temperature was encountered. 2. The pipe wall thermal gradient was ignored. 3. The fluid properties considered to be temperature dependent.
Pressure	The discharge pressure in the system was considered as an initial entry pressure in the integration.
Model input data	The input data were taken from the experimental estimated effective values calculated in the model subroutine.
All regions for all specified working fluids	Single-phase and two-phase treated separately by ignoring the boundary properties at the interface of the regions.
Superheated vapour region of R12 side (single-phase)	1. Assume a rough long length of uncoiled tube. 2. Fully developed turbulent flow was considered by neglecting the effect of dew formation on the pipe's wall.
Condensing region of R12 side (mixed-phase)	1. Annular flow model in a long condensing horizontal tube was adapted. 2. Employing Lockhart-Martinelli method in two-phase region with Martinelli parameter,X_{tt}. For $x<0.015$, X_{tt} is out of range, the single-phase heat transfer was adapted in this case. 3. The flow mechanism encounted is turbulent-turbulent.
Subcooled region of R12 side (single-phase)	1. For laminar flow, $Re<2100$, a long smooth tube, temperature dependent was considered. 2. For turbulent flow, $Re>7100$, a long rough tube, temperature dependent was considered.
Water side	1. The water was assumed to be in the liquid-state throughout the project. 2. The other consideration was the same as in the subcooled region of R12 (above).
Transition region	1. The transition was assumed to occur for $2100\leqslant Re\leqslant 7100$. 2. The heat transfer phenomena were predicted from a pro-rata mixture of the laminar and the turbulent values.

Table 5.2: Model assumptions

In the R12 vapour single region, The Reynolds numbers in the selected Runs show that $Re>7100$ therefore the flow was considered to be turbulent. The heat transfer coefficients and the pressure gradient either in the laminar flow or in the transition flow was completely ignored in this case.

For the single region of liquid freon and water, it was found that, the Reynolds numbers covered both the laminar flow, transition flow and turbulent flow, therefore, all of the flow mechanisms were considered.

Finally, the Reynolds numbers in the freon liquid-vapour mixture show that the turbulent-turbulent flows should be adapted.

5.2.4: Modelling overview

The main goal is to predict the freon and the water temperature profiles at the test-points along the condenser length. The steps and the theoretical relations leading to this aim could be classified as follows,

Firstly, concerning the physical and thermodynamic properties of the fluids: for freon, the properties in the state of vapour, saturated vapour, liquid-vapour mixture, saturated liquid and liquid should be treated separately; the properties of water were considered in the liquid-state only. A standard equation of state concerning the thermodynamic characteristics of R12 (using a subroutine by Hickson[44]) was employed. The other properties of the fluids were also considered.

Secondly, the determination of heat transfer coefficient and pressure drop of the fluids at the specified segmental length require a knowledge of single-phase and two-phase fluid flow mechanisms, which are summarized in Figure 5.2.6.

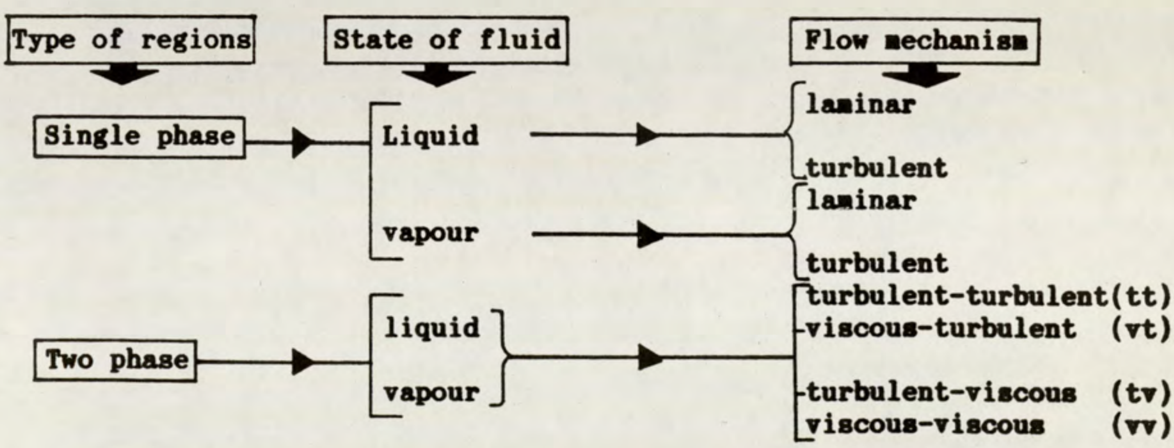

Fig.5.2.6: Flow mechanism in single and two phase region

The liquid water, assumed to be single-phase, is much easier to deal with. On the other hand, the freon could be either in the single liquid-state region or in the single vapour-state region or in the liquid-vapour mixture region, which is far more complicated. A separate empirical correlation was used to solve the problems in various regions.

Finally, the computation of the temperature at the consecutive points requires the effectiveness of the condenser at that point to relate the properties of the fluids, using number of transfer units method. The process will be sequentially carried out until the last temperature at the condenser exit is determined by satisfying all the required conditions.

5.3: Program description

In this section, the computer model program is sub-divided into the program-control statements and the program mathematical correlations, which are inter-related to each other.

The former case can now be further divided as follows,

a. **Monitoring program**: To determine whether iteration has converged, or the calculated water temperature at given a point exceeds the freon temperature, or the water temperature falls below the actual input water temperature in the subcooling region. The other function is to compare the calculated temperature with the actual entry temperature to see if the next temperature should be higher or lower than the previous one.

b. **Physical condition statements**: This detects whether the point-segments are in the vapour region or in the liquid-vapour mixed region, or in the liquid single region. The other test is to check whether condensation has either completed or prematurely completed.

c. **Mathematical condition statements**: The type of flow mechanism involved at various points is either laminar or turbulent or in between laminar and turbulent. It is necessary therefore to identify whether the fluid is in the liquid-state or vapour-state or mixture of liquid-vapour state.

In general, empirical correlations, based on available experimental data taken from established workers are used in the model, with some modification. There are also semi-empirical correlations to relate the physical behaviour of the fluid at certain condition and the experimental data employed in the model.

5.3.1: Model description in general

The program can be broken down into three main sections, one of which can itself be further divided into four major parts shown in a flowchart diagram in Fig.5.3.1.

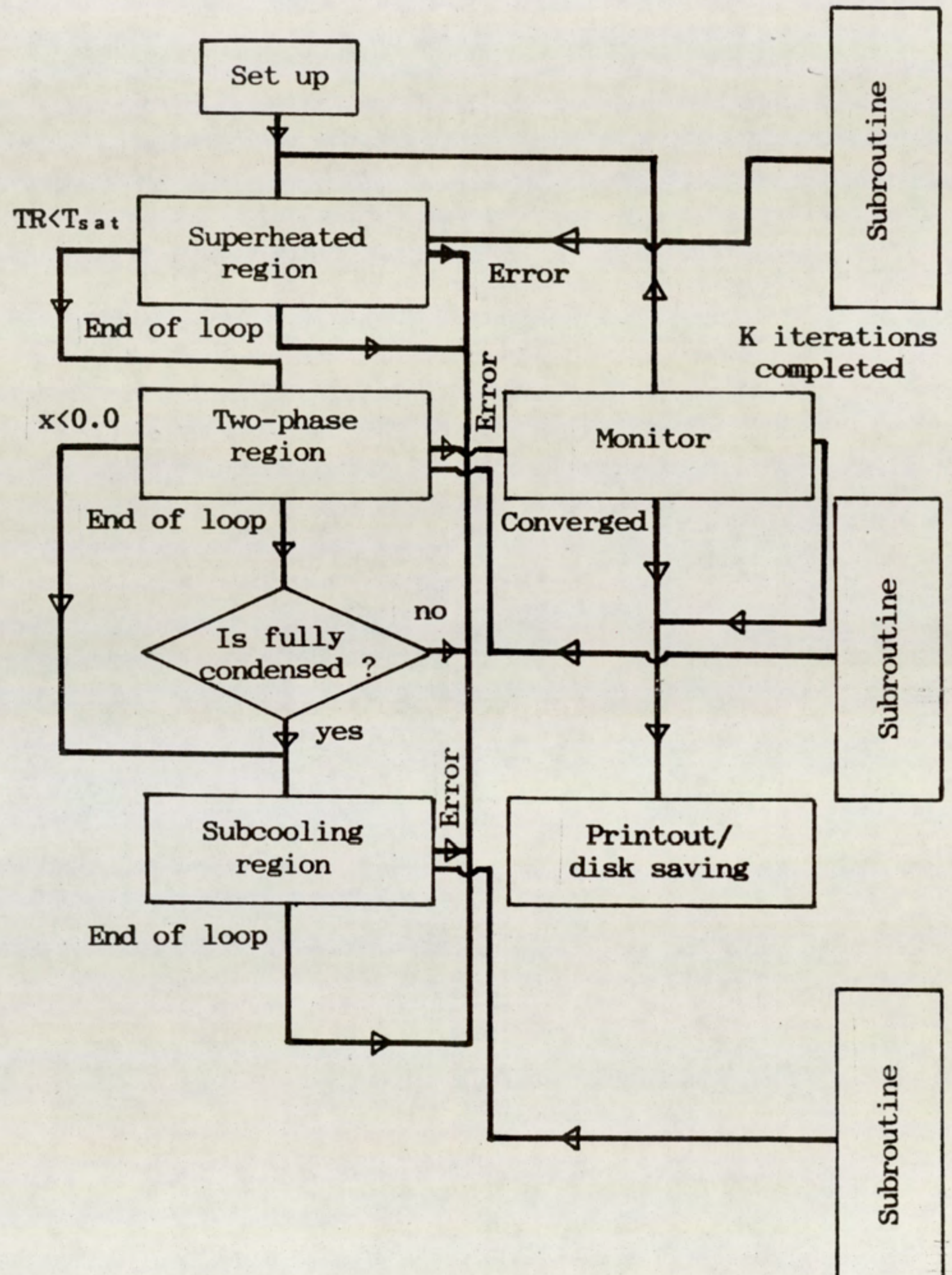

Fig. 5.3.1: Flowchart diagram showing overall model program in general

The first section deals with the character type of declarations, initialising arrays, reading in the input data and setting constants and other tasks included the calculation of freon dew temperature at given input pressure, freon mass flowrate, coil internal diameters and integration increment. This section is performed outside the iterative loop.

The second part of the program contains the iterative routine. A total of 150 points are divided between the desuperheating region, the two-phase region and the subcooling region of the condenser tube. The distance between the points is equivalent to an actual length of 0.1 meter.

The integration starts in the desuperheating block by estimating the water exit temperature (using calculated T_{dew} as trial water exit temperature) at the output of the heat exchanger, then working backwards through the freon and the water calculating the next point parameters of both the fluids. At various points checks are made on the iterative program. If an error condition occurs anywhere during the integrating process, a new estimate of water temperature is made and the iteration restarts. If the process has reached the far end of the tube (water entry or freon exit end), the calculated water entry temperature is compared with the input entry temperature. If the two do not agree, the program chooses a new trial water exit temperature and restarts the iteration. The program will proceed to the printout section if the two temperatures are within an acceptable distance of each other. A monitoring program is automatically called to check this kind of situation.

The final section sends the results of the iteration to either the printer or disk or both. This part also closes any open files and exits from the program cleanly. The results of the iteration in the printout statement can be broken down to separate outputs for the three regions, the parameter profiles and the summary of a possible simple cycle. The format statements for the outputs are also included in the main program. The listing of the main program are shown in Appendix A-3 of section A-3.2.

5.3.2: Single-phase desuperheating region

Fig.5.3.2 shows a flowchart description in the desuperheating region. This section of the heat exchanger is the region where the freon temperature is above its saturation point temperature at given inlet

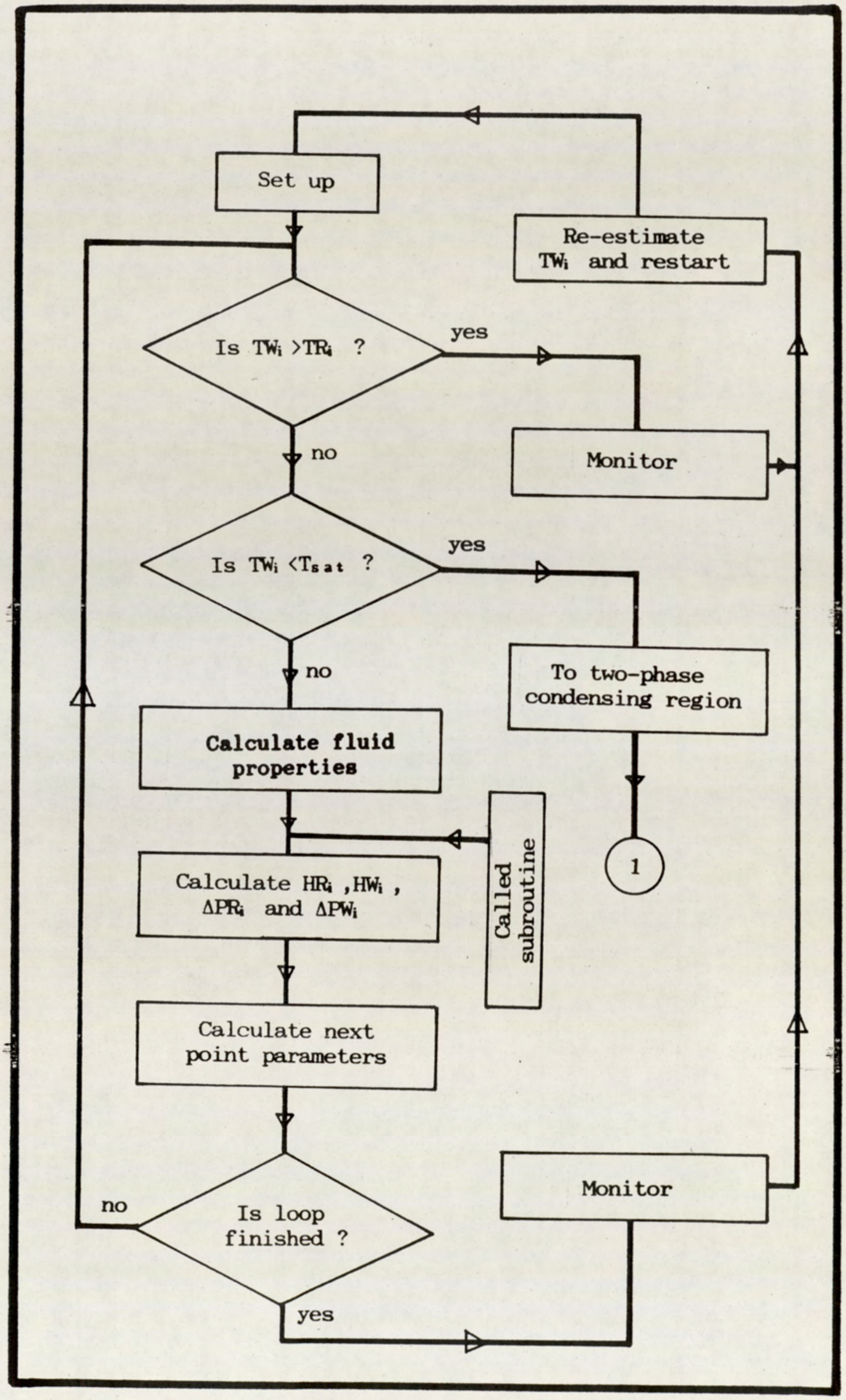

Fig. 5.3.2: Flowchart diagram showing the single-phase desuperheating region

pressure. It is the first part of the condenser to be considered by the program.

The program also checks if the water temperature at that point is above the temperature of the freon ($TR_i < TW_i$). If so, the exit water temperature set by the monitor was too high and the monitor is called to reset the new value.

The next decision made by the program is to check if the freon temperature has dropped below its saturation temperature at the given pressure. If it has, then the program jumps to the beginning of the two-phase region. If neither of these conditions has occured, the calculated properties of freon and water will be used to evaluate the heat transfer coefficient and the pressure drop at that point by calling subroutines. By this time, the computer has already calculated the next point parameters. If the loop has not finished, a jump is made back to the beginning of the loop.

The 150-segments have all been used if the loop does terminate at the end of the region. This means, the estimated water entry temperature was too low, in which case the monitoring program will be called to re-estimate the value and restart the iteration. If the calculated pressure of the freon is negative (in practice, this situation would not happen), the process will be abandoned and a new set of input data should be considered.

5.3.3: Two-phase condensing region

The program for the two-phase region is called from the desuperheated section when the temperature of the freon drops below the saturation temperature at the given pressure. The loop that moves the point under consideration is restarted from where it finished in the desuperheating region.

Fig.5.3.3 shows the whole process regarding the two-phase section. The vapour quality is firstly calculated in this region and is used to calculate whether any more vapour remains in the refrigerant tube. If there is no more vapour present in the tube, where $x=0.0$, a jump is made to the beginning of the single-phase subcooling region.

If the water entry temperature TW_i is above the refrigerant temperature, TR_i at the particular point, the monitor program is called to re-estimate the entry water temperature and restart the iteration.

On the other hand, if TW_i is still lower than TR_i, the properties of the freon liquid and vapour based on the vapour fraction are

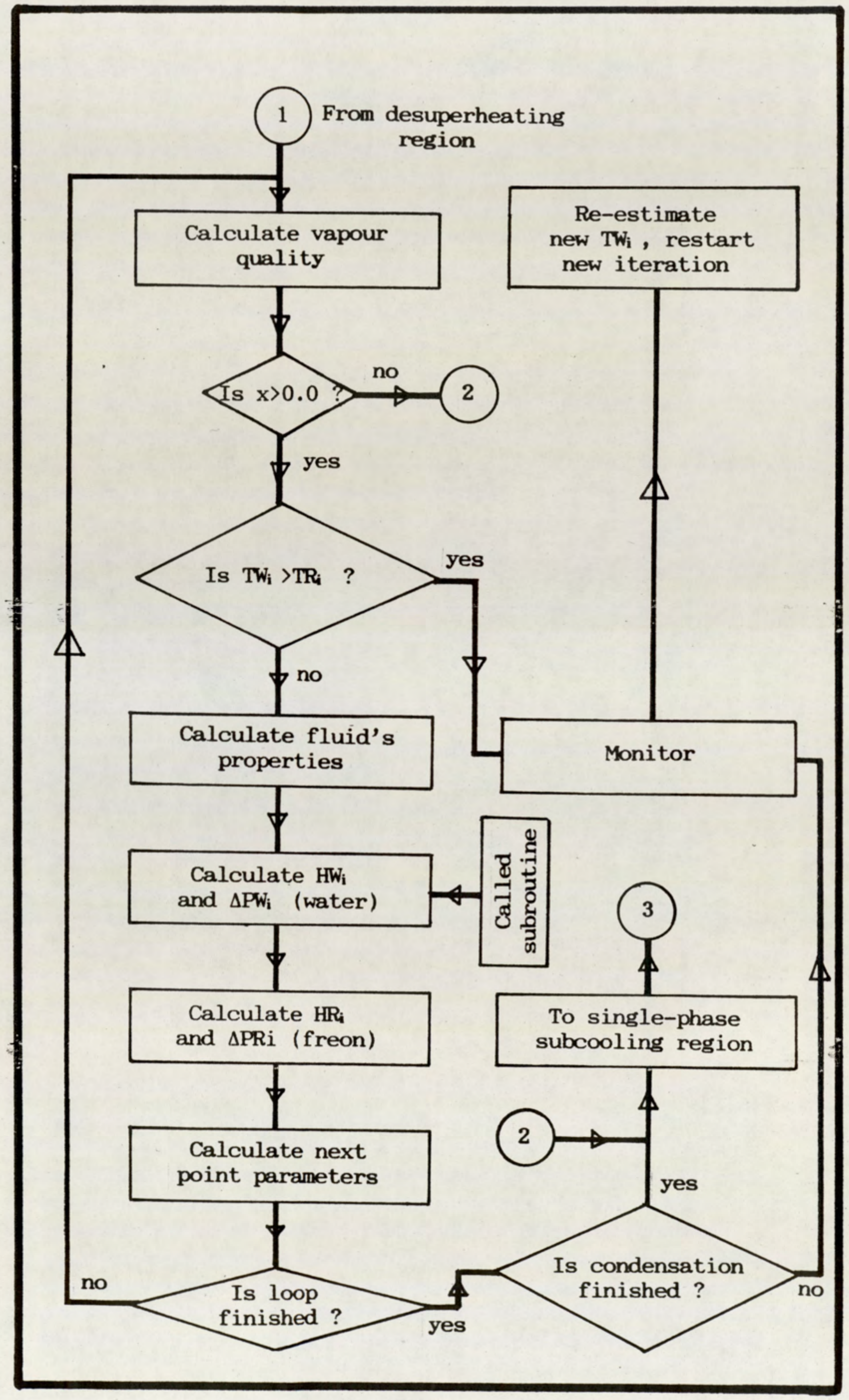

Fig. 5.3.3: Flowchart diagram showing the mixed-phase condensing region

calculated. Similarly, the properties of water, the heat transfer coefficient and the water pressure drop are found by calling subroutines. The heat transfer coefficient and the pressure drop of freon at that point is evaluated using an empirical correlation which will be discussed later in the chapter. The temperature and the pressure at the next point along the tube is then found and the loop is re-entered. The condensation of the freon is checked, if it has completed.

If the loop has not finished the monitor program is called, otherwise a jump to the beginning of the subcooling region is made.

5.3.4: Single-phase subcooling region

The loop that moves the calculation through the tube is restarted at the beginning of this section, when the vapour fraction calculated in the mixed region drops to zero. The water temperature is then checked to ensure that it has not dropped below the actual water entry temperature given by the datafile, or risen above the refrigerant temperature. In either of these two cases, the monitor program is called to readjust the estimated water entry temperature and restart the iteration. Fig.5.3.4 shows the process involving the subcooling region.

The properties of the two liquid fluids are calculated and again, the subroutine is called to evaluate the heat transfer characteristics and the pressure drop at the point under test. The program proceeds to calculate the temperature and the pressure at the next point along the tube. If the loop has finished, the monitor program is called to check if the iteration has converged, else a jump to the beginning of the section is made to restart the loop.

5.3.5: Monitoring program

This program checks if any conditions in various regions described in the previous section are disobeyed. The program can be called at any time during the process either from the end of each loop in various regions (water entry end) or from some point within the considered region. The whole monitoring process is shown in Fig.5.3.5.

<u>Program called from water entry end</u>

The iteration has converged if the actual water entry temperature (given by the datafile) is the same as the calculated water entry temperature. For modelling purposes, the absolute maximum difference between this value is taken to be 0.2°C, ($|TW_i - TW_{in}| < 0.2$). If the condition is satisfied, then the printout section is called.

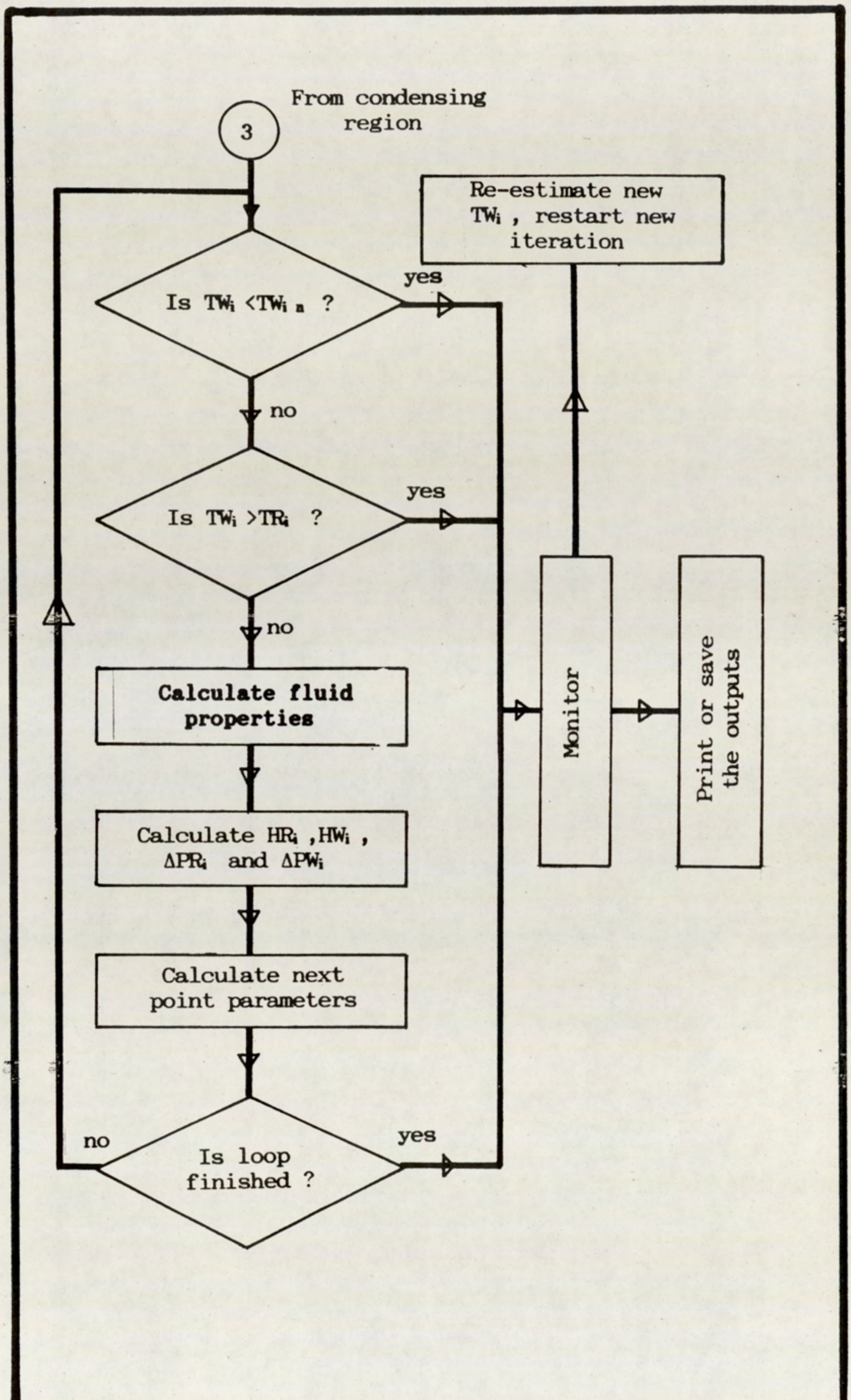

Fig. 5.3.4: Flowchart diagram showing the single-phase subcooling region

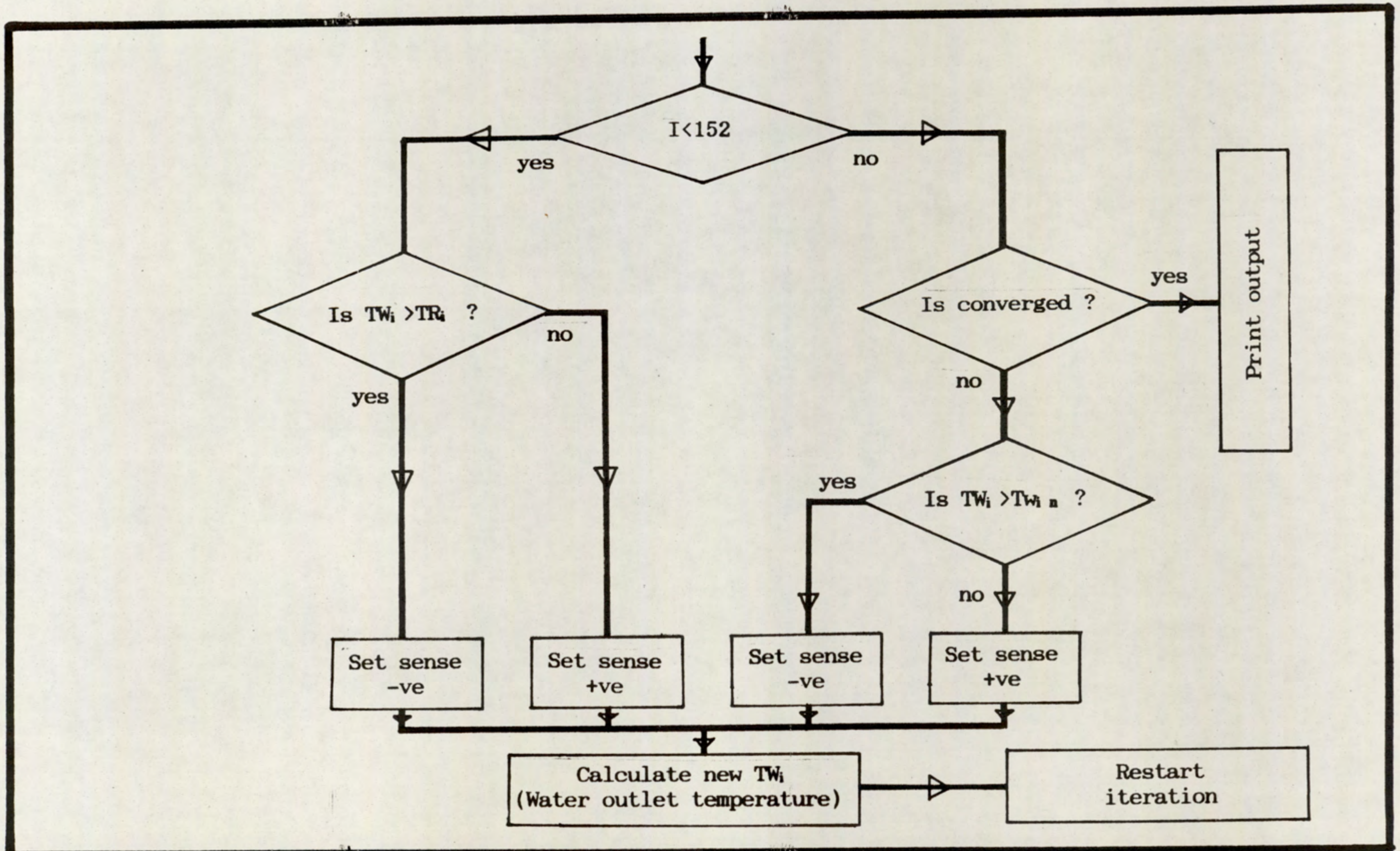

Fig. 5.3.5: Flowchart diagram showing monitoring program

The value of calculated temperature is compared with the actual water entry temperature to see if the next point temperature should be higher or lower than the previous one if the program has not reached a conclusion.If the estimated temperature is to be decreased a sense variable is set to -1, otherwise it is set to +1. The program then calculates the new water exit temperature and starts a new iteration.

Program called before condenser exit end

This situation occurs for some point before the end of the heat exchanger, which is less than the total considered point. The monitor is called due to the calculated water temperature at given point exceeding the freon temperature or due to the water temperature falling below the actual input water temperature in the subcooling region. The value of a sense variable is set to -1 in the former case and +1 in the latter case. Similarly, the new water outlet temperature is re-estimated and the new iteration is then restarted.

The sense variable is introduced to adjust the water exit temperature to either increase (positive sense) or decrease (negative sense).

5.4: Heat transfer phenomena

This section concerns the heat transfer in both single-phase and mixed-phase freon flow. The heat transfer parameters in various regions are dealt separately by considering the relationship betaween the Reynolds number (Re) and Prandtl number (Pr), evaluated at the fluid bulk temperature with the Nusselt number (Nu). Nusselt number is the basic heat transfer parameter which can be used to calculate heat transfer coefficient. Considering the fluid temperature-dependent properties, Nusselt numbers are calculated from the Nusselt numbers at constant-property. The general Nusselt number correlation at the fluid temperature-dependent property (some authors call as variable-property) can be summarized as

$$Nu_{cp} = f_1(Re, Pr, L, Idr \text{ or } Idw) \quad \text{and}$$
$$Nu = Nu_{cp} . f_2(\mu_b, \mu_w \text{ or } T_b, T_w) \qquad \text{Eqn.5.5}$$

where f_1 is a function of some variables, with Re and Pr evaluated at the fluid bulk temperature, and f_2 is a function of two fluid properties; viscosity (μ) and temperatures (T) evaluated at the bulk and at the wall temperature, with subscript b and w are the bulk and the wall condition respectively. The constant property of the fluids are denoted by subscript cp.

The overall heat transfer coefficient which is calculated from the Nusselt number is the key to the calculation of temperature and pressure at point (I+1) (see also Fig.5.2.1) in the condenser, which generally can be written as

$$U_L = f(HR, HW, \kappa_{bond}) \qquad \text{Eqn.5.6}$$

where HR = f(Nu,κ,Idr), HW = f(Nu,κ,Idw), κ_{bond} is the conductivity of thermal bond between tubes (copper), κ is the fluid conductivity, and Idr and Idw are the internal diameter of the freon and water tube respectively.

5.4.1: Introduction

The understanding of laminar and turbulent flow in the single-phase region is fairly clear, but the transition flow is still doubtful. In fact many investigators found it difficult to predict a definite value of the upper limit of the critical Reynolds number, $Re_{c,max}$. Most authors agreed taking Re=2100 as the lower limit of the critical Reynolds number, $Re_{c,min}$.

In the model, the $Re_{c,max}$ suggested by Carrington [1] was 7100. Any Reynolds numbers calculated within this range is considered to indicate flow in the transition regime; otherwise flow is considered to be either laminar or turbulent.

The heat transfer in the mixed-phase is far more complicated because it involves the liquid-vapour mixture in which the vapour fraction (by mass) should initially be evaluated. It is also important to find out what type of flow mechanism occurs in this region. The thermodynamic properties of the liquid and vapour freon in the mixture were treated separately. Both the liquid and the vapour in this model, were assumed to flow turbulently.

The condensation inside a long tube with annular flow was considered in this phase, where the flow regime becomes annular with a vapour core at the middle separated by the thin liquid layer. Due to the gravitational force, the liquid layer tends to be thicker at the bottom of the horizontal tube. The Martinelli parameter for turbulent-turbulent flow was considered to calculate heat transfer coefficients with the Reynolds number and Prandtl number evaluated at the liquid portion.

Similarly, the heat transfer parameters were determined from the Nusselt number,

$$Nu = f(Re_l, Pr_l, X_{tt}) \qquad \text{Eqn.5.7}$$

where $X_{tt}=f(\mu_l,\mu_g,\rho_l,\rho_g,x)$ is the Martinelli parameter for liquid and vapour flow turbulently, $\mu_l=f(v_{sat,vap},(P,T_{sat}))$, $\mu_g=f(v_{sat,liq},T_{sat})$, and x is the vapour quality.

Similarly, the overall linear heat transfer coefficient is found from Eqn. 5.6 with the properties determined for the liquid phase.

5.4.2: The flow of fluid in the single-phase region

The flow in the single-phase region (desuperheating and subcooling) is now discussed by considering that freon vapour flows turbulently in the desuperheating region, and the flow of the liquid freon is either laminar, turbulent or transitional.

The water, which is regarded as liquid water by assuming there is no formation of mixtures of ice-water or steam-water during the process, will be treated as a single-phase flow. The flow may be laminar or turbulent or transitional.

In the general case, the possible single-phase flow mechanisms (see also Fig.5.2.6) considered in the model are laminar-liquid, turbulent-liquid and turbulent-vapour. The regimes of the flow were divided according to the Reynolds numbers:

a. $Re<2100$: Laminar flow which is normally in liquid-state.

b. $2100<Re<7100$: Transition flow.

c. $Re>7100$: Turbulent flow, which occurs both in the liquid-state and vapour-state.

For the refrigerant side, where freon can be either in the liquid-state or vapour-state covers the three flow regimes described earlier. The calculation of heat transfer parameters in the liquid freon, single-phase regime are only focused in the subcooling region, where laminar, transition, and turbulent flow could occur. For the freon vapour in the single-phase regime, only turbulent flow are considered in the desuperheating region. The boundary layer at the interfacing regions are omitted.

The flow parameters in this region could be classified as follows,

1. Fluid properties of liquid-water, liquid-freon and vapour freon: These properties concern the thermodynamic and physical characteristics

of the fluids as a function of pressure only or a combination of pressure and temperature, or temperature only. These parameters will then be employed to calculate the heat transfer coefficient of the fluids at the particular test-point.

2. **Overall heat transfer coefficient:** This concerns the calculation of an average overall heat transfer coefficient evaluated from individual fluid heat transfer coefficients of liquid water, liquid freon and vapour freon depending on the point in the test-region (either in the subcooling region or desuperheating region). If it is in the subcooled-regime, the overall heat transfer coefficient is found from the heat transfer parameters of liquid water and liquid freon, otherwise the combination of liquid water and vapour freon is adapted.

3. **Temperature and pressure at the next test-point:** Before considering the end product of the modelling, the number of transfer unit and the effectiveness of the heat exchanger should be determined from 2 (above).

The temperature difference between the wall and the fluid (assumed to be bulk temperature) is large, so that a constant property assumption could cause an error. As previously discussed in chapter 2, the fluid transport properties vary with temperature and influence the distribution of heat transfer coefficients over the flow along the tube if variable-property is taken into consideration.

The property-ratio method taken at the bulk temperature with all other variable-properties effects are put into a function of the ratio of one property evaluated at the wall to that one property calculated as a bulk parameter, summarized in Eqn. 5.8.

$$Nu/Nu_{cp} = \begin{cases} (\mu_b/\mu_w)^n & \text{for liquid} \\ (T_w/T_b)^n & \text{for vapour} \end{cases} \qquad \text{Eqn.5.8}$$

where n is the ratio exponent adapted from recommended sources. Table 5.3 summarizes the heating and cooling modes used in the model.

State	Value of n in Eqn 5.8 <1	>1	Fluid
liquid	cooling liquid	heating liquid	freon and water
vapour	heating vapour	cooling vapour	only freon

Table 5.3: Fluid property influencing the heating and the cooling modes

The laminar and turbulent flow in the single-phase was considered to be fully developed, and the wall temperature at the circumference and at the axis was assumed constant (T_w=constant).

Laminar flow (Re<2100)

In a long tube, a forced convection in laminar flow is a process involving a moving fluid that carries away the heat, with the flow stream lines almost parallel, and heat is transferred radially from the wall of the pipe towards the centre of the fluid.

The heat transfer coefficient can be conveniently expressed in terms of a dimensionless Nusselt number,

$$H = (Nu_{cp}.\kappa)/D \qquad \text{Eqn.5.9}$$

where Nu_{cp} is evaluated at the constant property.

The Nusselt number is empirically correlated by

$$Nu_{cp} = 3.66 + (0.057Gz)/(1 + 0.04Gz^{0.8}) \qquad \text{Eqn.5.10}$$

where Gz = Re.Pr.D/L is the Graetz number and see **Table 5.4** for other related properties of the fluid used in the model.

Fluid	Re	Pr	L
Freon	$\frac{G_r.Id_r}{\mu_r}$; $G_r=\dot{m}_r/A_r$	$\frac{\mu_r.Cp_r}{\kappa_r}$	$I.L_{inth}$
Water	$\frac{G_w.Id_w}{\mu_{wr}}$; $G_w=\dot{m}_w/A_{wr}$	$\frac{\mu_{wr}.Cp_{wr}}{\kappa_{wr}}$	$(152-I).L_{inth}$

Table 5.4: Summary of Eqn.5.10 for other related properties of the fluid

For a sufficiently long pipe, where the second term of Eqn. 5.10 approaches zero, the Nusselt number is almost constant (Nu_{cp}=3.66) which is similar to the constant heat-flux analysis.

In laminar flow, a long smooth tube was considered, therefore the effect of the pipe roughness is ignored in this case. The value of n in Eqn. 5.8 was choosen to be 0.14 for both cooling and heating the liquid as suggested by Diessler, which was cited by Kakac [84], for Pr>0.6. In this case, the Nusselt number is calculated as an average value with the wetted perimeter of the pipe taken to be at the circumference of the inner pipe.

Therefore, the Nusselt number, by considering the temperature dependence, both for cooling and heating liquid becomes

$$Nu = Nu_{cp}(\mu_b/\mu_w)^{0.14} \qquad \text{Eqn.5.11}$$

where Nu_{cp} is given by Eqn.5.10.

Eqn.5.11 is used to calculate the Nusselt number in the range of Re<2100 for the liquid freon in the subcooling region and liquid water in all regions. For most liquids [84], the specific heat, thermal conductivity and density are nearly independent of the temperature but the viscosity decreases with increasing temperature.

In the direction of freon flow, as the distance along the freon tube increases, the second term of Eqn.5.10, is small compared to the first term. The Nusselt number is still in the region of 3.66. When applying to Eqn.5.11, the Nusselt number at variable properties is still slightly above 3.66.

<u>Turbulent flow (Re>7100)</u>

The calculation of heat transfer parameters in turbulent flow is more complicated than in laminar. In the model, the single-phase flow of turbulent liquid and turbulent vapour of the freon in subcooling and desuperheating region respectively are considered. Only turbulent liquid is considered in the water side.

In turbulent flow, the effect of eddy viscosity, (which is a function of flow configuration, varies with the flow cross-section area and indirectly dependent on temperature), plays an important role in the flow. It is not only depend on the thermal conductivity which is a temperature-dependent function of physical properties of the fluid, but also on the eddy diffusivity, which is a function of Reynolds number and Prandtl number.

For fully developed turbulent flow in a rough pipe, the above situations were correlated mathematically to the Nusselt number, yielding,

$$Nu_{cp} = f_5(Re,Pr,f) \qquad \text{Eqn.5.12}$$

where f is a friction factor.
Eqn.5.12 and Eqn.5.8 are then combined to evaluate the average Nusselt number by using the recommended value of exponent n, relating with the heating and the cooling of either vapour or liquid.

The calculation of Nusselt number in this flow is done separately. Firstly, the turbulent liquid involving the liquid freon in the subcooling region and liquid water in corresponding region was put in separate subroutine. Secondly, the turbulent vapour which involves the freon vapour in the desuperheating region was put in another subroutine.

1. **Turbulent liquid:** The calculation of Nusselt number at constant property was taken from an empirical correlation postulated by Petukhov and Popov,[45], which can be expressed as

$$Nu_{cp} = \frac{Re.Pr.(f/2)}{[1+(13.6f)]+[9.0(f/2)^{1/2}(Pr^{2/3}-1.0)]} \qquad \text{Eqn.5.13}$$

where $f=[1.58\ Ln(Re)-3.28]^{-2}$ adapted from Filonenko, cited by Bhatti and Shah [82], with a slight modification made by Carrington [1].

All values are evaluated at the bulk temperature with the assumption that the flow is fully developed with the constant heat flux boundary in the range of $7.1x10^3<Re<5.0x10^5$ and $0.5<Pr<2x10^3$. It was claimed that the accuracy is within 1% error.

The complete correlation taking account of the influence of viscosity, and the value of n of Eqn.5.8 recommended by Petukhov,[97], corresponding to heating and cooling for fully developed turbulent liquid flow, $7.1x10^3<Re<5x10^6$, $2<Pr<140$ and $0.025<(\mu_b/\mu_w)<12.5$ is rewritten as

$$Nu = Nu_{cp}(\mu_b/\mu_w)^n \qquad \text{Eqn.5.14}$$

where $n = \begin{cases} 0.25 \text{ for cooling liquid freon, } (\mu_b<\mu_w) \\ 0.08 \text{ for heating liquid water, } (\mu_b>\mu_w) \end{cases}$

2. **Turbulent vapour:** For fully developed turbulent vapour flow, the following correlation for calculating the Nusselt number in the desuperheating region is considered by assuming that freon vapour physical properties, ρ, μ, κ and C_p vary with the temperature. The Eqn.5.8 for the vapour-state is again introduced to calculate the Nusselt number.

The Nusselt number recommended by Petukhov [97], at constant property is

$$Nu_{cp} = \frac{(f/8).Re.Pr}{K_1 + K_2(f/8)^{1/2}(Pr^{2/3}-1)} \qquad \text{Eqn.5.15}$$

where $f=[1.82 \, Log(Re)-1.64]^{-2}$

and $K_1=(1.0+3.4f)$ and $K_2=(11.7+1.8Pr^{-1/3})$

calculated over the range of $10^4<Re<5x10^6$ and $0.5<Pr<2000$, within 1% error.

The turbulent vapour flow only concerns the freon desuperheating region where freon vapour is cooling down. The variable properties of Eqn.5.8 recommended in Kutateladze-Leontiev correlation in a circular tube for variable physical properties of gases, cited by Kakac [84], were considered, where

$$Nu = Nu_{cp}\left\{\frac{2}{[1 + (T_w/T_b)^{1/2}]}\right\}^2 \qquad \text{Eqn.5.16}$$

Similarly, the Reynolds number and the Prandtl number are evaluated at the bulk temperature. For larger Re, Eqn.5.8 is in good agreement with Eqn.5.16.

<u>Transition flow ($2.1x10^3 \leq Re \leq 7.1x10^3$)</u>

As previously mentioned, it is difficult to predict the heat transfer properties in this region. The Nusselt number in the specified range was calculated from the laminar Nusselt number, Nu_{la} and the turbulent Nusselt number, Nu_{tu} calculated at variable properties.

Fig.5.4.1 illustrates the calculation of transition Nusselt number, Nu_{tran} employed in the model. Let point A be the Reynolds number in the transition region denoted by Re_{tran}, where $Re_{c,min} \leq Re_{tran} \leq Re_{c,max}$; $Re_{c,min}=2.1x10^3$ and $Re_{c,max}=7.1x10^3$, yields

$$Nu_{tran} = \left\{\frac{(Re_{c,max}-Re_{tran})Nu_{la}}{Re_{c,diff}} + \frac{(Re_{tran}-Re_{c,min})Nu_{tu}}{Re_{c,diff}}\right\} \qquad \text{Eqn.5.17}$$

where $Re_{c,diff}=(Re_{c,max}-Re_{c,min})=5.0x10^3$.

The laminar Nusselt number and the turbulent Nusselt number is calculated from Eqn.5.11 and Eqn.5.14 respectively.

For Reynolds number very close to the lower limit, the Nu_{tran} is simply equal to the laminar Nusselt number. On the other hand, for Reynolds number approaching the value of the upper limit, the transition Nusselt number approaches the turbulent Nusselt number.

In general, the model predicts the transition Nusselt number to be between the laminar and the turbulent Nusselt number.

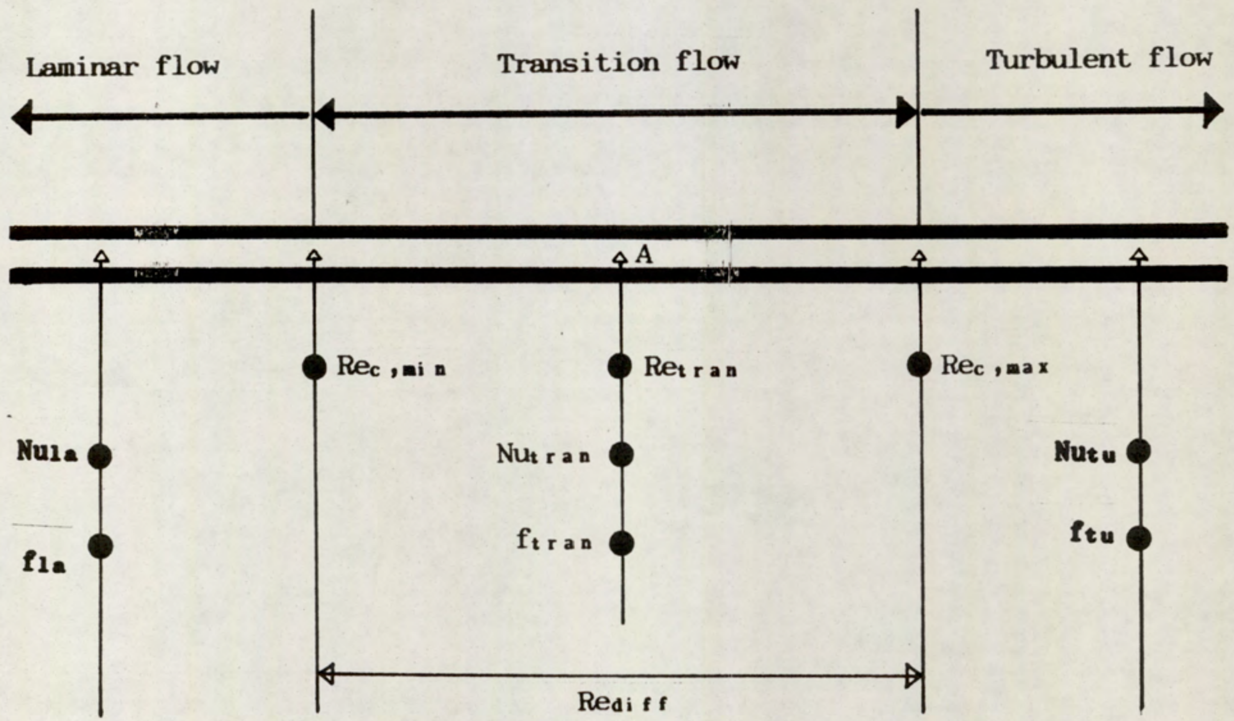

Fig.5.4.1: Nusselt number and Fanning friction in liquid transition region

Overall heat transfer coefficient

The calculation of overall heat transfer coefficient is based on the transfer of heat in forced convection and conduction. Referring to Fig.5.4.2 (a), the heat is assumed to flow in a straight line from point 1->2->3->4->5 corresponding to convection, conduction, conduction and convection. The flow of heat is from the higher temperature in the freon side to the lower temperature in the water side, assuming the wall temperature is constant; any temperature between point 2 and point 4 in the direction of flow is considered to be equal or $T_{iw,2}=T_{ow,3}=T_{iw,3}=T_{ow,4}$ (isothermal wall surface).

The heat transfer in convection and conduction is dealt with separately as follows,

a. Conduction

Fourier's Law of conduction (see Fig.5.4.2 (b)) states that the heat flow is

$$q = -\kappa . A_r . (dT/dr) \qquad \text{Eqn.5.18}$$

where $A_r=2\pi RL$; the surface-section area of the tube in m^2

dT/dr=Temperature gradient and κ=Thermal conductivity in W/m.K

Integration of Eqn.5.18 to calculate the total heat transferred by taking boundary conditions,

$$r=R_i \; ; \; T=T_i \quad \text{and} \quad r=R_o \; ; \; T=T_o \qquad \text{Eqn.5.19}$$

yields
$$q = \left\{ \frac{2\pi\kappa L(T_{in}-T_{out})}{Ln(R_o/R_i)} \right\}$$
$$= U_L \, .L.\Delta T \qquad \text{Eqn.5.20}$$

where $U_L = \left\{ \frac{1}{Ln(R_o/R_i)/2\pi\kappa} \right\}$ is the linear heat transfer coefficient.

The calculated U_L is for the heat transferred from point 2 to point 4 illustrated in Fig.5.4.2 (b).

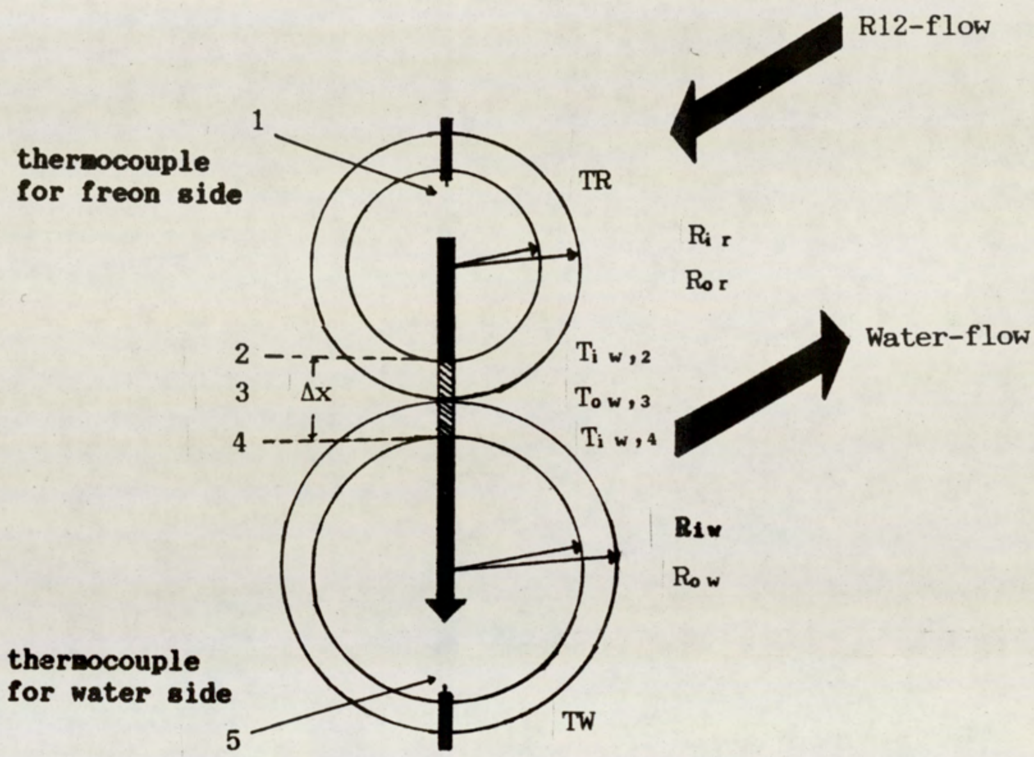

Fig.5.4.2(a): Overall heat transfer coefficient from point 1 to point 5

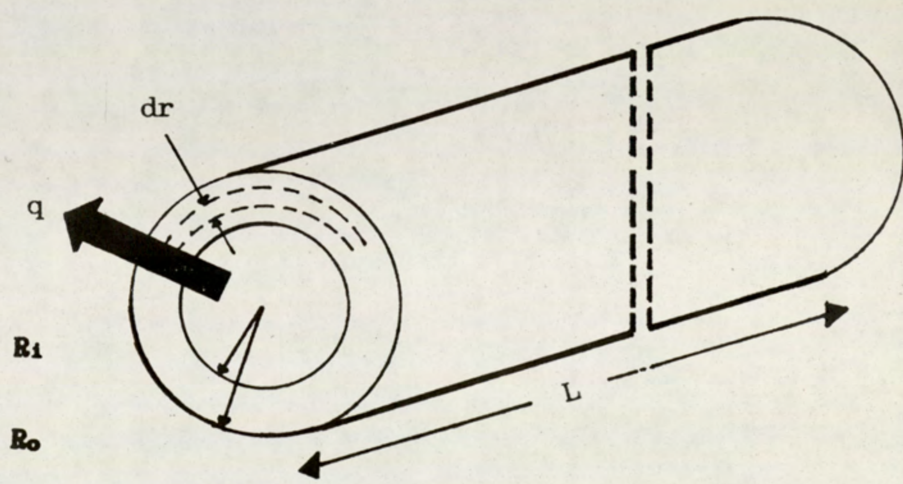

Fig.5.4.2(b): Thermal conductivity through the thickness of the pipe

b. Convection

This concerns the heat being carried away by the fluids from point 1 to point 2 and from point 4 to point 5 shown in **Fig.5.4.2(a)**. Similarly, the flow is from a point of higher temperature to a point of lower temperature and assumes the amount of heat being transferred from one medium to another medium is the same. From the convection equation, the total amount of heat can be expressed as

$$q = H.A(TR-T_{iw,2}) = H.A(T_{iw,4}-TW) \qquad \text{Eqn.5.21}$$

where H is the convective heat transfer coefficient, and A is the surface area of the pipe.

By inserting the boundary conditions and rearranging Eqn.5.20 and Eqn.5.21 in terms of model parameters, the relations can be shown in Table 5.5,

Direction of flow	Equation for heat transfer q	Method for heat being transferred
1->2; from inside to outside	$HR.A_r(TR-T_{iw,2})$	Convection
2->3; from inside to outside	$\frac{2\pi\kappa L(T_{iw,2}-T_{ow,3})}{Ln(R_{or}/R_{ir})}$	Conduction
3->4; from outside to inside	$\frac{2\pi\kappa L(T_{ow,3}-T_{iw,4})}{Ln(R_{iw}/R_{ow})}$	Conduction
4->5; from outside to inside	$HW.A_w(T_{iw,4}-TW)$	Convection

Table 5.5: The amount of heat transfer from point 1 to 5 associated with Fig.5.4.2

Rearrange the equations of **q** in **Table 5.5** by bringing the temperature difference to the left hand side of the equation and then, by adding all the equations, one should get

$$q = \frac{L(TR-TW)}{[U_{L,12} + U_{L,23} + U_{L,34} + U_{L,45}]} = U_L .L.\Delta T \qquad \text{Eqn.5.22}$$

where $\Delta T = (TR-TW)$; $U_L = 1/[U_{L,12}+U_{L,23}+U_{L,34}+U_{L,45}]$

$U_{L,12} = 1/(HR.\pi.Idr)$; $U_{L,23} = Ln(R_{or}/R_{ir})/2\pi\kappa_{bond}$

$U_{L,34} = Ln(R_{iw}/R_{ow})/2\pi\kappa_{bond}$; $U_{L,45} = 1/(HW.\pi.Idw)$

The convective heat transfer coefficient of freon and water is calculated from the Nusselt number described earlier. The thermal bonding for copper, K_{bond} was taken somewhat arbitrarily as 500 W/m.°C.

The overall heat transfer coefficient, U_L is greatly dependent on the radius of the tube, which has a fixed value, and also the Nusselt number. The greater the value of the Nusselt number, the larger is the value of the overall linear heat transfer coefficient.

5.4.3: Fluid flow mechanism in two-phase region

The two-phase flow is far more complicated than single-phase flow because it involves the flow of liquid-vapour mixture. In a general case, the heat transfer of the two-phase depends on a great number of factors such as mass flowrate, vapour quality, thermal properties of the saturated fluid (both liquid and vapour), wall material, heat flux and coil description. To solve the freon heat transfer problems, the main parameters to observe are the mass flowrate and the vapour quality.

This section is primarily concerned with the prediction of condensing heat transfer coefficients, and pressure drop in the two-phase regime. It is assumed that the tube is long enough for the flow regime to become annular, so that an annular model for condensation in a long tube could be applied. The Martinelli parameter by assuming turbulent liquid and turbulent vapour case was adapted. An empirical correlation adapted from Rohsenow [87], with minor modification to acquire condensing heat transfer coefficient was applied. For vapour quality dropping below 15%, the Martinelli parameter X_{tt} goes out of range; in such cases, single-phase heat transfer discussed earlier is considered. It is also assumed that annular flow occurs when the void fraction is greater than about 80%, or the vapour quality is above 5%.

Annular model for long horizontal tube

The two-phase annular flow is characterized by vapour flow in the middle region, separated from the thin liquid layer at the periphery of the tube as shown in **Fig.5.4.3(a)**. The liquid is assumed to flow as an annulus. In addition, the flow is also assumed to be one dimensional steady-state, no radial pressure gradient exists, and the annular flow is established as soon as condensation begins.

By integrating the momentum equations for the annular vapour and liquid layer, employing the Martinelli two-phase flow pressure drop correlation and then by analogy, the heat transfer coefficient could be determined.

The momentum equation states that the summation of the forces acting on a vapour control volume in the direction of flow along the condensing length (z-direction) is equal to the difference between the momentum leaving and entering the control volume,

$$\Sigma F_z = \Sigma Mom_{z,out} - \Sigma Mom_{z,in} \qquad \text{Eqn.5.23}$$

The application of Eqn.5.23 to both the element of vapour core and element of liquid layer is shown in Fig.5.4.3(b) and Fig.5.4.3(c), where the direction of flow is denoted by the big arrows while the small arrows represent the possible forces acting in the direction of flow and the forces opposing the direction of flow. The variation of cross-sectional area A_l and A_v is negligible over element Δz. In addition, zero slip between the vapour and the liquid at the vapour-liquid interface is assumed, where $F_v = F_l$.

The momentum equation for vapour core can be expressed as,

$$-\Delta(PA_v)-(F_v.S_v.\Delta z)\pm(\rho_v.a.A_v.\Delta z) = \Delta(\dot{m}_v.U_v)-(\Delta\dot{m}_v.U_{vi}) \qquad \text{Eqn.5.24}$$

and the equation for the liquid layer is

$$-\Delta(PA_l)+(F_l.S_v.\Delta z)-(F_o.S.\Delta z)\pm(\rho_l.a.A_l.\Delta z) = \Delta(\dot{m}_l.U_l)-(\Delta\dot{m}_l.U_{vi}) \qquad \text{Eqn.5.25}$$

These two equations are the general correlation for the annular flow. The solution of Eqn.5.24 and Eqn.5.25 can be summarized as follows,

$$F_o = F_f + F_m + F_g \qquad \text{Eqn.5.26}$$

where $F_f = F_v.(S_v/S)[1 + (A_l/A_v)]$ represents the effect of the two-phase friction,

$F_m = (A_l/S.A_v).\Delta(\dot{m}_v.U_v)_z - [\Delta(\dot{m}_l.U_l)_z/S] + (U_{vi}/S)[\Delta(\dot{m}_l)_z - (A_l/A_v)(\Delta\dot{m}_v)_z]$ is the effect of momentum changes,

and $F_g = (a.A_l/S)(\rho_l - \rho_v)$ is the effect of the gravitational field on the wall shear stress, assumed to be zero, since the flow is horizontal.

An analytical analysis for predicting F_f can be derived from the Lockhart-Martinelli correlation [12], where

$$(\Delta P/\Delta z)_{tpf} = \Phi_{tt}^2(\Delta P/\Delta z)_v \qquad \text{Eqn.5.27}$$

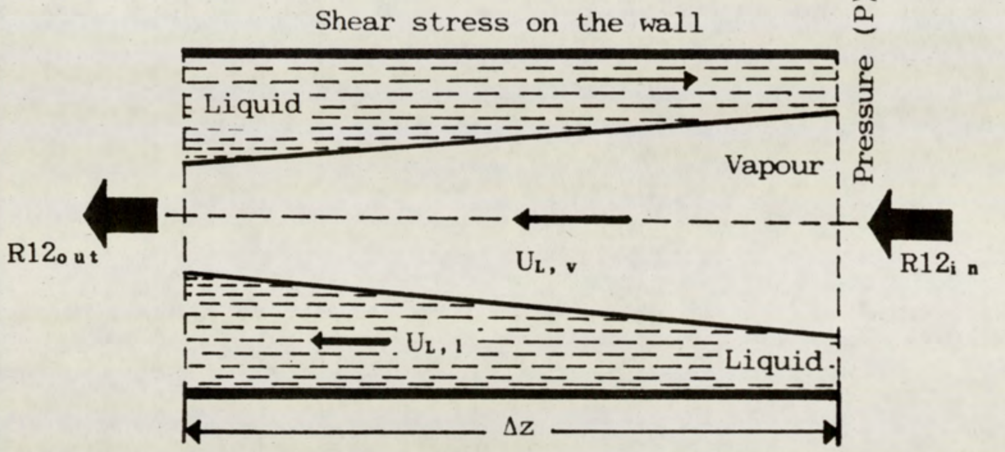

Fig.5.4.3(a): Annular model control volume for long condensation tube

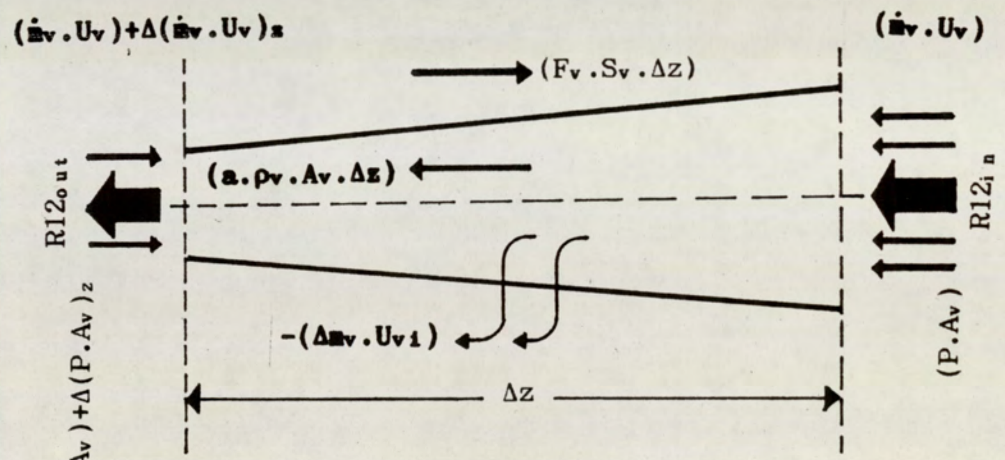

Fig.5.4.3(b): Differential element of vapour core

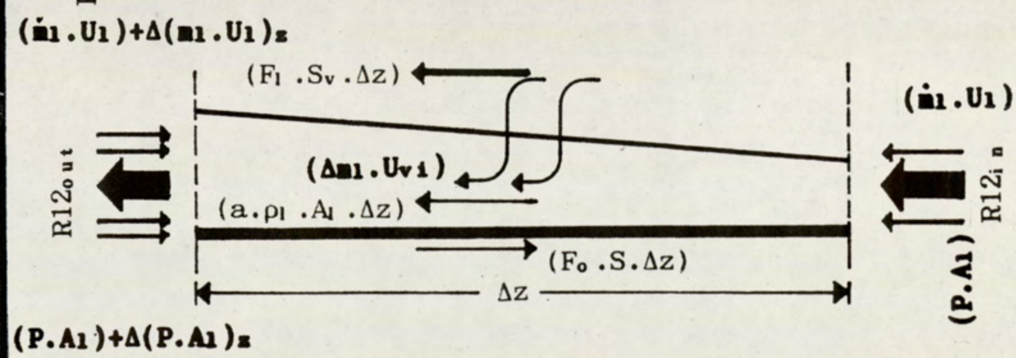

Fig.5.4.3(c): Differential element of liquid layer

where $\Phi_{tt}=f(X_{tt})$ and $X_{tt}^2=(\Delta P/\Delta z)_l/(\Delta P/\Delta z)_v$; X_{tt} is the Martinelli dimensionless parameter for turbulent vapour and turbulent liquid. This parameter is defined by

$$X_{tt} = (\rho_v/\rho_l)^{1/2} \ (\mu_l/\mu_v)^{b/2} \ [(1-x)/x]^{(2-b)/2} \qquad \text{Eqn.5.28}$$

where b is the Blasius exponent taken to be 0.2 as suggested by Rohsenow [87] with the physical properties evaluated at the liquid-state and at the gas-state. The complete empirical correlation is rewritten as,

$$\Phi_{tt} = 0.15[(1/X_{tt}) + 2.85/(X_{tt}^{0.467})] \text{ and}$$
$$X_{tt} = (\rho_v/\rho_l)^{0.5} \ (\mu_l/\mu_v)^{0.1} \ [(1-x)/x]^{0.9} \qquad \text{Eqn.5.29}$$

<u>Heat transfer coefficient</u>

In this case, the Nusselt number can be written more generally as,

$$Nu = f(Pr, Re, \Phi_{tt}, f_2) \qquad \text{Eqn.5.30}$$

where f_2 is a function of Reynolds number and Nusselt number. All properties are evaluated at the liquid-portion of the mixture,[89];

$$f_2 = \begin{cases} 5Pr_l + 5Ln(1+5Pr_l) + 2.5Ln(0.0031Re_l^{0.812}) & ;Re_l>1125 \\ 5Pr_l + 5Ln[1+Pr_l(0.09636Re_l^{0.585} - 1)]; & 50 \leqslant Re_l \leqslant 1125 \\ 0.707[Pr_l.Re_l^{0.5}]; & Re_l<50 \end{cases} \qquad \text{Eqn.5.31}$$

For vapour quality less than 1.5%, a single-phase heat transfer is adapted. The Nusselt number is then written as,

$$Nu = (HR.Idr)/\kappa_l = \begin{cases} [Pr_l.Re_l^{0.9}.\Phi_{tt}]/f_2; & \Phi_{tt}<1 \\ [Pr_l.Re_l^{0.9}.\Phi_{tt}^{1.15}]/f_2; & 1 \leqslant \Phi_{tt}<20 \end{cases} \qquad \text{Eqn.5.32}$$

where $Re_l=(4.\dot{m}r/\pi.Idr).(1-x)/\mu_l$ and $Pr_l=(\mu_l.Cp_l)/\kappa_l$. For any value of Φ_{tt} outside the range, again the single-phase calculation is introduced.

The overall heat transfer coefficients are calculated from Eqn.5.22, where the liquid water heat transfer coefficient is determined using the single-phase flow.

Pressure drop in annular flow

The Lockhart-Martinelli method [12], is employed to calculate the pressure drop in the two-phase regime. As described earlier in the annular model, the pressure drop for both the liquid and the vapour turbulentl flow is associated with the general correlation of **Eqn.5.27.**

The pressure drop in the two-phase flow is greatly influenced by the effects of the two-phase friction,the momentum changes and the gravitational field on the wall shear stress if the flow is not horizontal,where

$$(dP/dz)_{tpf} = (dP/dz)_f + (dP/dz)_m + (dP/dz)_g \qquad \textbf{Eqn.5.33}$$

where in this case, $(dP/dz)_g=0$. The empirical correlation adapted from Rohsenow [87] is derived from the first two term of **Eqn.5.33.**

1. Frictional term

$$(dP/dz)_f = 0.09[1 + 2.85.X_{tt}^{0.523}]^2\left[\frac{\mu_v.(Gr.x)^{1.8}}{\rho_v.Idr^{1.2}}\right] \qquad \textbf{Eqn.5.34}$$

where $Gr=(mr/Ar^2)=4/\pi[\dot{m}r/(Idr)^2]$ and X_{tt} is evaluated as in **Eqn.5.29** .

2. Momentum term

$$(dP/dz)_m = (Gr^2/\rho_v)(\Delta x/\Delta z)[2x + (1-2x)(\rho_v/\rho_l)^{1/3} + (1-2x)(\rho_v/\rho_l)^{2/3} - 2(1-x)(\rho_v/\rho_l)] \qquad \textbf{Eqn.5.35}$$

where $(\Delta x/\Delta z)=(x_i-x_e)$, Δz is the length between the segment of integration and x_i, x_e are the inlet and the exit vapour fraction respectively.

Therefore the total pressure drop is simply the sum of the pressure gradient due to the friction and the momentum.

Heat transfer and pressure drop parameters

The following steps outline the method for evaluating the heat transfer coefficients and pressure drops in the two-phase flow used in the model.

Heat transfer calculation: At any quality along the tube, the following steps are taken, with all values evaluated in reduced units,

a. To calculate vapour quality from latent heat of vaporization at given saturated temperature by assuming TR drops below T_{sat}, where

$$x = 1 - \left\{ \frac{C_{pr}[T_{sat} - TR]}{h_{fg}} \right\} \qquad \text{Eqn.5.36}$$

b. To calculate all other parameters evaluated at the saturated liquid and the saturated vapour included the specific volumes, densities, viscosities, thermal conductivities and specific heat at constant pressure.

c. The Reynolds numbers and the Prandtl numbers are calculated at the liquid portion of the mixture,

$$Re_l = (1-x).Gr.Idr/\mu_l$$
$$Pr_l = (\mu_l.C_{pr,l})/\kappa_l \qquad \text{Eqn.5.37}$$

d. The Martinelli parameter from Eqn.5.29 using known evaluated parameters in step 3 are then considered.

e. Finally, to calculate the Nusselt number and the heat transfer coefficient from Eqn.5.32.

The final product is then used together with the water heat transfer coefficient to evaluate the overall heat transfer coefficient.

Pressure gradient: Similarly, the same freon properties evaluated above are employed in this calculation,

a. To calculate the frictional term of Eqn.5.34 and the momentum term of Eqn.5.35 using known parameters.

b. To calculate the total pressure drop with respect to the length at that particular point.

The final step is to determine the pressure at the next point by considering the drop in the freon pressure in the direction of flow downstream the tube, where

$$PR_{i+1} = PR_i - \Delta PR \qquad \text{Eqn.5.38}$$

5.5: Pressure drop calculation

This section concerns the pressure drop analysis in the single-phase flow. The pressure drop in two-phase has been described in section 5.4.3, where it is much greater than that in the single-phase flow.

The same situations as in the single-phase heat transfer phenomena, the single-phase pressure drop in the vapour regime is also treated separately from the pressure drop in the liquid regime. Similarly, the liquid pressure drop in laminar and turbulent flow are evaluated separately in the subcooling region of the freon side. The vapour pressure drop in turbulent flow is calculated only in the desuperheating region. For the water side, only liquid pressure drop is effected, depending on whether the flow is laminar, turbulent, or transitional.

The flow is still assumed to be fully developed under steady-conditions. A simple relationship between the Fanning-factor,f and the pressure drop,ΔP over a length,L of a long pipe under steady-condition can be represented by a control-length shown in Fig.5.5.1. Assuming that, under fully developed steady flow conditions and no acceleration of the fluid, at equilibrium, the force due to the pressure gradient must be balanced with net force due to the wall shear stress,

$$(\Delta P).A = 2\pi.R.\Delta z.\tau_w \qquad \text{Eqn.5.39}$$

where $\tau_w = f.1/2(\rho.U^2) = f.(\dot{m}/A)^2.(1/2\rho)$.
Substituting for τ_w in Eqn.5.39, the pressure gradient over a length of L can rewritten as,

$$(\Delta P/L) = 2.f.G^2/D.\rho \qquad \text{Eqn.5.40}$$

where f is the Fanning-factor coefficient recommended from established sources and $G=(\dot{m}r/A_r)$ or $(\dot{m}w/A_{wr})$.

For all types of flow in the single-phase, the effect of variable properties is considered when calculating the pressure frictional factor f. The same situations as in the single-phase heat transfer discussed in section 5.4.2 are applied. In turbulent flow, the roughness of the pipe,ε is encountered when calculating friction coefficients.

In general, the friction factor is a function of the Reynolds number and also depends on the wall roughness. For very high Reynolds numbers and relative roughness, the friction factor becomes independent of the Reynolds numbers in a fully rough flow regime. The influence of the wall roughness on the laminar flow has little effect, but there is a strong effect on the turbulent flow.

5.5.1: Liquid friction factor

This concerns the friction factor in the liquid region, involving the freon subcooling region and the water region. The calculation is also based on the variable properties by firstly, evaluating the friction factor at the constant properties as discussed earlier. The variation of viscosity at the bulk temperature and wall temperature is responsible for the property effects. From the property-ratio method, the correlation can be expressed as,

$$f = f_{cp}(\mu_b/\mu_w)^m \qquad \text{Eqn.5.41}$$

where m is the exponent adapted from established data. The following discussion is based on the constant property.

Laminar flow ($Re<2.1\times10^3$)

For fully developed laminar flow in the long tube, the pressure drop given by Eqn.5.40 is compared with the Hagen-Poiseuille Law concerning laminar flow in a long tube, by analogy, the friction factor at constant properties can be written as,

$$f_{cp} = 16/Re \qquad \text{Eqn.5.42}$$

The complete equation including variable properties can be expressed as,

$$f = f_{cp}[\mu_b/\mu_w]^m \qquad \text{Eqn.5.43}$$

where
$$m = \begin{cases} -0.50 \text{ for } (\mu_b/\mu_w)<1, \text{ cooling liquid freon} \\ -0.58 \text{ for } (\mu_b/\mu_w)>1, \text{ heating liquid water} \end{cases}$$

adapted from Deissler, cited by Kakac [84] for fully developed and constant heat flux boundary condition at $Pr>0.6$ in a smooth tube.

The pressure gradient is then calculated from Eqn.5.40 where the drop is increased as the Reynolds number decreases with all other parameters evaluated at the bulk temperature.

Turbulent flow ($Re>7.1\times10^3$)

The wall roughness is considered in this case, by taking $\varepsilon=1.524\times10^{-6}$ meter adapted from Moody-diagram for drawn copper tubing. The roughness elements would strongly affect the friction factor in which the factor could be regarded as an apparent wall shear stress. It is related to the pressure forces generated by the faces of the roughness elements normal to the direction of flow (see Fig.5.5.2).

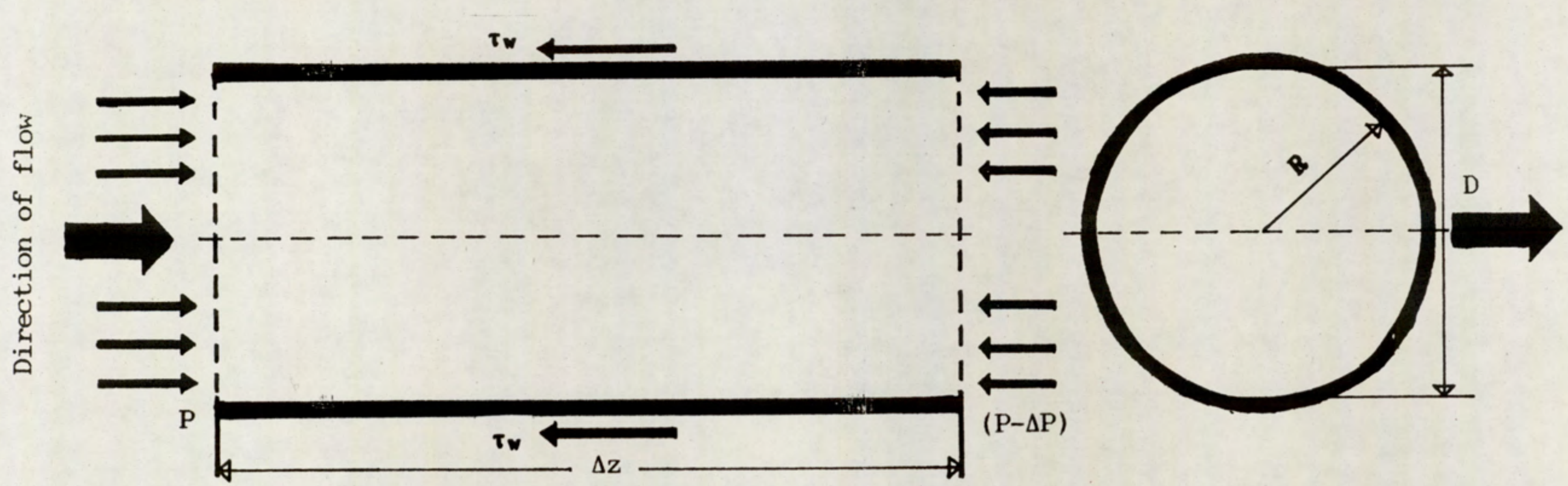

Fig.5.5.1: Force balance for steady single-phase flow

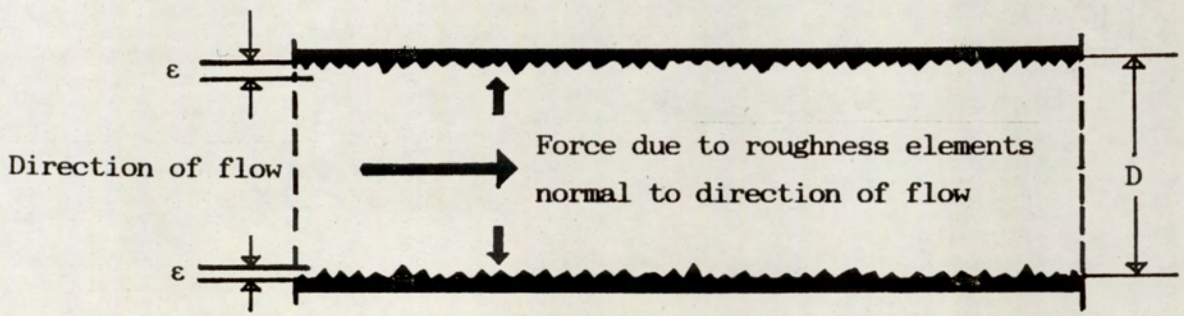

Fig.5.5.2: Roughness elements influencing the friction factor

An empirical correlation relating the friction factor at the constant property in liquid turbulent for fully developed flow in a rough tube originally established by Colebrook and White, modified by Serghides,[46] is employed,

$$f_{cp} = \frac{1}{[C_3 - [(C_3-C_2)^2/(C_3-2C_2+C_1)]]^2} \qquad \text{Eqn.5.44}$$

where
$$C_3 = -0.8686Ln[(\varepsilon/3.7D)+(12/Re)]$$
$$C_2 = -0.8686Ln[(\varepsilon/3.7D)+(2.51C_3/Re)]$$
$$C_1 = -0.8686Ln[(\varepsilon/3.7D)+(2.51C_2/Re)]$$

and ε is the pipe roughness in meter and D is the internal diameter of the tube in meter. The above equation is for the Reynolds number within the range $4.0x10^3 \leqslant Re \leqslant 10^8$ and $2.0x10^{-8} \leqslant (\varepsilon/D) \leqslant 5.0x10^{-2}$ in a complete rough regime.

Eqn.5.44 can also be used to calculate the friction factor in the transition region within the range of $4x10^3 < Re < 7.1x10^3$. For very large Reynolds numbers, the friction factor is only dependent on the relative roughness (independent of Re). On the other hand, for small Reynolds number, it is greatly influenced by the relative roughness and the Reynolds numbers.

For Re within the range of $2.1x10^3 \leqslant Re \leqslant 4.0x10^3$, the correlation suggested by Kakac [82] for the transition flow is rewritten in the form of,

$$f_{cp} = C_1 + (C_2/Re^{1/m}) \qquad \text{Eqn.5.45}$$

where $C_1=0.0054$, $C_2=2.3x10^{-8}$ and $m=-0.667$ which is claimed to be on par with the Churchill-equation. In this calculation, the roughness elements are ignored by assuming the flow is close to the laminar flow pattern.

The complete relation of Eqn.5.41 by considering the variable properties can be written as,

$$f = \begin{cases} f_{cp}(\mu_b/\mu_w)^{-0.24} & \text{for } (\mu_b/\mu_w)<1 \\ f_{cp}.(1/6)[7.0 - (\mu_b/\mu_w)] & \text{for } (\mu_b/\mu_w)>1 \end{cases} \qquad \text{Eqn.5.46}$$

<u>Transition flow ($2.1x10^3 \leqslant Re \leqslant 7.1x10^3$)</u>

Eqn.5.44 and Eqn.5.45, for $4.0x10^3 < Re \leqslant 7.1x10^3$ and $2.1x10^3 \leqslant Re < 4.0x10^3$ respectively is employed to calculate the friction

factor at the constant properties. Employing Eqn.5.46, the complete friction coefficients are determined by considering the effect of variable properties of the liquid.

5.5.2: Vapour friction factor

This section deals with the freon flows in the desuperheating region where the turbulent freon vapour with the Reynolds numbers above $7.1x10^3$ is considered.

For most gases, the variation with absolute temperature is approximately the same for the viscosities and conductivities, while specific heat capacities vary slightly with the temperature, therefore Prandtl numbers do not vary significantly.

For fully developed vapour flows, by neglecting the effect of dew formation on the wall, the Kutateladze-Leontiev correlation associating with the friction factor at the variable properties can be expressed as,

$$f = f_{cp}\left\{\frac{2}{[1+(T_w/T_b)^{1/2}]}\right\}^2 \qquad \text{Eqn.5.47}$$

where f_{cp} is the friction factor at the constant properties to be determined (see also Eqn.5.16).

In the vapour flow, the f_{cp} is chosen from the Colebrook-White correlation cited by Bhatti and Shah [82] for fully developed turbulent flow in a rough tube, $1.0x10^{-8} \leqslant (2\varepsilon/D) \leqslant 5.0x10^{-2}$ and $4x10^3 \leqslant Re \leqslant 10^8$ can be expressed as,

$$(1/f_{cp}^{1/2}) = 3.48 - 1.7372Ln[(2\varepsilon/D) + 9.35/(Re.f_{cp}^{1/2})] \qquad \text{Eqn.5.48}$$

To solve for f_{cp} which appears on both sides of the equation, a Newton-Raphson iterative method,[74] for numerical integration is adapted by considering f_{cp} in Eqn.5.44 as an initial value.

The value of f calculated in Eqn.5.47 is introduced to evaluate the pressure gradient using Eqn.5.40 in the test-section of the condenser with L representing the length between the two test-points.

5.6: Heat exchanger effectiveness and next point parameters

The number of transfer units method, ε-Ntu is adapted to determine the heat exchanger performance which is a measure of heat transfer area,[69,76].

A parameter effectiveness is defined as,

$$\varepsilon = \frac{\text{Actual heat transfer}}{\text{Theoretical maximum heat transfer}} \qquad \text{Eqn.5.49}$$

where the theoretical limit to the heat transfer is determined by the maximum and minimum of the temperature encountered.

The two methods described above, are compared to calculate the temperature at the consecutive points by assuming the heat lost by the freon between the two points is the same (by heat lost percentage).

In this case, the heat capacity of the freon, ($\dot{m}r.Cp_r$) is found experimentally always to be less than the water heat capacity, ($\dot{m}w.Cp_{wr}$). In the condensing region, the temperature assumed stays essentially constant, in which case, it has infinite specific heat, where the heat capacity ratio, ($\dot{m}r.Cp_r/\dot{m}w.Cp_{wr}$) tends to approach zero. In such case, the performance is maximised for the particular Ntu value.

5.6.1: ε-Ntu method in counter flow

Referring to Fig.5.6.1, from definition in Eqn.5.49,

$$\varepsilon_r = \frac{(\dot{m}w.Cp_r)[TR_i - TR_{i+1}]}{(\dot{m}r.Cp_r)[TR_i - TW_{i+1}]} = \frac{(TR_i - TR_{i+1})}{(TR_i - TR_{i+1})} \quad \text{and}$$

$$\varepsilon_{wr} = \frac{(\dot{m}w.Cp_{wr})[TW_i - TW_{i+1}]}{(\dot{m}w.Cp_{wr})[TR_i - TW_{i+1}]} = \frac{(TW_i - TW_{i+1})}{(TR_i - TW_{i+1})} \qquad \text{Eqn.5.50}$$

where ε_r and ε_{wr} are the effectiveness in the freon and water side respectively.

The heat transfer through an elemental length dz can be expressed as,

$$dq = -(\dot{m}r.Cp_r).dTR = -(\dot{m}w.Cp_{wr}).dTW = U_L\,.dz(TR-TW) \qquad \text{Eqn.5.51}$$

On integration, and taking the boundary conditions for $(\dot{m}r.Cp_r)<(\dot{m}w.Cp_{wr})$,

$$TR = TR_i \quad ; \; TW = TW_i \quad ; \; z = z_i \quad \text{and}$$
$$TR = TR_{i+1} \quad ; \; TW = TW_{i+1} \quad ; \; z = z_{i+1} \qquad \text{Eqn.5.52}$$

yields,

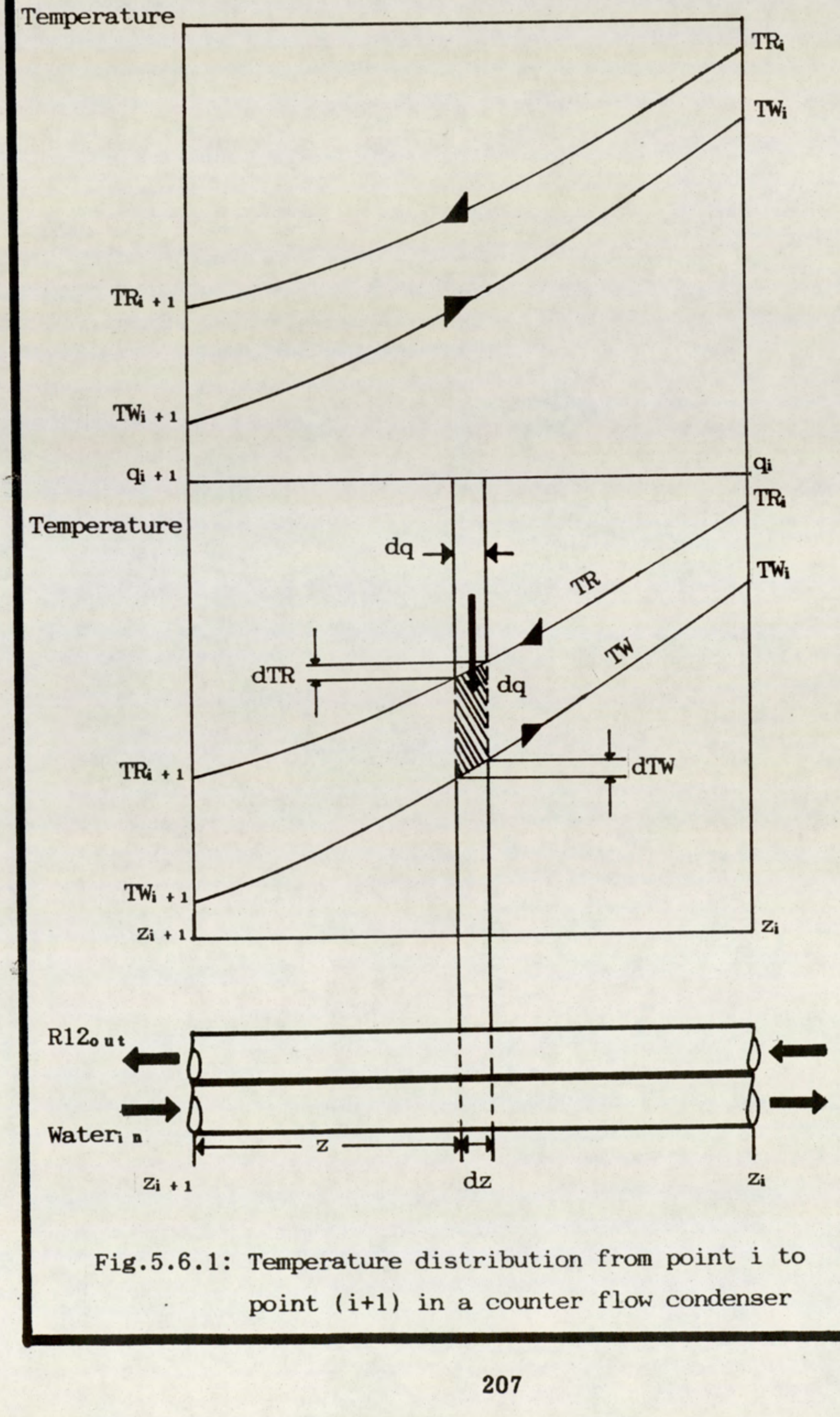

Fig.5.6.1: Temperature distribution from point i to point (i+1) in a counter flow condenser

$$\left\{\frac{(TR_{i+1} - TW_{i+1})}{(TR_i - TW_i)}\right\} = \exp[-Ntu_r + Ntu_{wr}] \qquad \text{Eqn.5.53}$$

where $Ntu_r=(U_L.L_{inth})/\dot{m}r.Cp_r$, $Ntu_{wr}=(U_L.L_{inth})/\dot{m}w.Cp_{wr}$ and $L_{inth}=(z_i-z_{i+1})$ is the distance between the two test-points.

The terms, Ntu_r and Ntu_{wr} are called the number of transfer units which indicates the size of heat exchanger.

5.6.2: The next point parameters in the single-phase

In the single-phase counter flow, to determine the temperature at the next point, an ε-Ntu method described above is employed by considering the heat capacity rate ratio ($\dot{m}r.Cp_r<\dot{m}w.Cp_{wr}$).

By eliminating the temperatures in Eqn.5.50 and Eqn.5.53 and then rearrange these equations in term of effectiveness, ε_r and number of transfer units, Ntu, we get,

$$\varepsilon_r = \frac{[1 - \exp(-Ntu_r+Ntu_{wr})]}{1 - (Ntu_r/Ntu_{wr})[\exp(-Ntu_r+Ntu_{wr})]} \qquad \text{Eqn.5.54}$$

This equation is only dependent on the heat capacities of the fluids. The effectiveness on the water side, ε_{wr} can be related by the energy balance equation from point i to point (i+1), which yields,

$$\varepsilon_{wr} = (1-f_{lost}).\varepsilon_r.(Ntu_r/Ntu_{wr}) \qquad \text{Eqn.5.55}$$

where f_{lost} is the overall percentage of heat lost from condenser.

Combining and rearranging Eqn.5.50, and then by substitution of Eqn.5.54 and Eqn.5.55, the temperature at the point (i+1) can be expressed as,

$$TW_{i+1} = \left\{\frac{TW_i - \varepsilon_r.TR_i}{(1 - \varepsilon_{wr})}\right\} \text{ and}$$

$$TR_{i+1} = TR_i + \varepsilon_r(TW_{i+1} - TR_i) \qquad \text{Eqn.5.56}$$

Similarly, the pressure at point (i+1) can be written as,

$$PR_{i+1} = PR_i - \Delta PR.L_{inth} \text{ and}$$

$$PW_{i+1} = PW_i + \Delta PW.L_{inth} \qquad \text{Eqn.5.57}$$

The above equations are used to calculate other unknown parameters in single-phase freon for the desuperheating and subcooling regions.

5.6.3: The next point parameters in condensing region

As earlier mentioned, the capacity rate ratio tends to approach zero, when condensing effectiveness is reduced to

$$\varepsilon_r = 1 - \exp(-Ntu_r) \qquad \text{Eqn.5.58}$$

Eqn.5.56 is again introduced to calculate the temperature of water at point (i+1) with the effectiveness given by Eqn.5.58.

The pressure drops calculated earlier in the section are employed together with Eqn.5.57 to determine the pressure at the next point both for the freon and water.

On further analysis, the freon pressure at this point is used to calculate the freon temperature at point (i+1) by assuming the temperature exits as a saturated temperature. Fig.5.6.2 shows a P-h diagram to illustrate these calculations where,

$$T_{sat} = TR_{i+1} = f(PR_{i+1}) \qquad \text{Eqn.5.59}$$

calculated from equation of state,[71,116] (see Appendix A-5 for the solution of thermodynamic properties of freon at various state).

The final major parameter considered is the vapour quality, x calculated from

$$x = h_{i+1} - \left\{\frac{h_{sat}(0, TR_{i+1})}{h_{fg}}\right\} \qquad \text{Eqn.5.60}$$

where h_{i+1} is the specific enthalpy at point (i+1) calculated from energy balance equation, $h_{sat}(0,TR_{i+1})$ is the specific enthalpy at saturated TR_{i+1} with x=0 (saturated liquid line), and h_{fg} is the latent heat of vaporization evaluated at TR_{i+1} between x=0 and x=1.

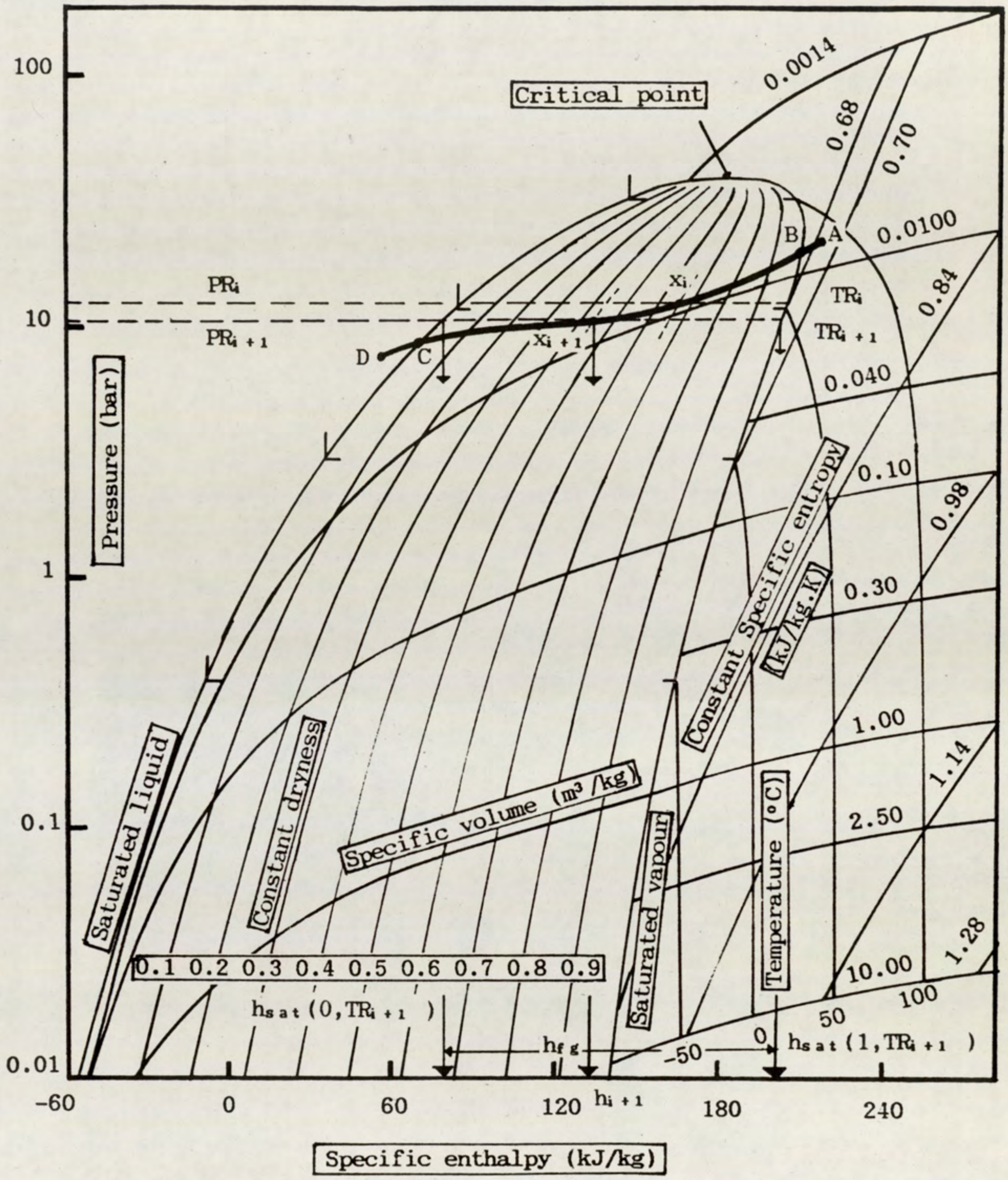

Fig.5.6.2: P-h diagram snowing freon properties at point (i+1) in condensing region, B→C

CHAPTER 6

RESULTS AND DISCUSSION

6.1: Introduction

In this chapter, experimental and predicted results are presented and discussed. The temperature profiles along the condenser tube, measured in the experiment are compared with the temperature distributions predicted by the model. The predicted temperature profile is calculated at 0.1 meter intervals by numerical integration, while the thermocouples were placed at one meter apart. The temperatures evaluated at every meter can then be compared with the corresponding temperature.

The other parameters to be directly compared with the model are the condenser inlet and outlet pressure (also known as discharge and liquid pressure respectively, in the heat pump system), freon and water mass flowrate, and freon and water inlet and outlet temperatures. Variations of these parameters at given conditions are shown and discussed later in the chapter. The primary parameters (mentioned above) are directly measured by experiment, and known as experimental data.

The second part of the chapter discusses the results predicted by the model, including the thermodynamic and physical properties of the fluids in three separate regions (subcooling-, condensing- and desuperheating-regime) and other parameter profiles (pressure, quality, water and freon linear heat transfer coefficient, and overall heat transfer coefficient) are also described.

The inlet pressure was varied from 7.6 bar to 12.3 bar. Variations of freon and water Reynolds number, linear heat transfer coefficient, number of transfer units, temperature, pressure, specific enthalpy and specific entropy, and condenser effectiveness are also discussed. The average or the total possible values of parameters described above are tabulated and shown for particular operating conditions.

Parameter profiles (other than the temperature profiles) which are not measured in the experiment but predicted by the model are important to study the thermodynamic and physical behaviour of the heat exchanger. The summary of the thermal power analysis discussed from the enthalpy and entropy point of views is also presented.

The final part describes the summary of possible range of evaporator conditions by assuming certain values of compressor isentropic efficiency.

In this case, the possible refrigeration cycle of the heat pump system (assuming there is no pressure drop across the evaporator) is predicted. The possible energy capacity across the evaporator, work done by the compressor and the heat pump coefficient of performance are also presented.

To summarize, the results and discussions are divided into two major sections; experimental results and predicted results.

6.1.1: Experimental results

The results are based on the 39 sensors attached to the system. These include 35 sensors for measuring temperatures, 16 for the water temperatures and 16 for the freon temperatures, 2 thermocouples for measuring freon temperature at the inlet and outlet of the heat pump evaporator, and the final thermocouple is to measure the room temperature. 4 transducers measure the pressure at the inlet and outlet of the heat pump condenser and evaporator. The two of them which are attached at the inlet and outlet of the condenser are normally used in the present analysis.

As discussed earlier in chapter 4 and 5, six parameters (TR_1,TR_{16}, TW_1,TW_{16}, $PR_{discharge\ gas}$ and $PR_{condenser\ exit}$) were measured at points which are not exactly at the condenser entry and exit. An estimation was done by interpolation to overcome this problem. These values are used either for comparison with the model or as input data to initiate the calculation in the model.

Fig.6.1.1(a and b), shows an estimate of the freon inlet and outlet temperature. The freon inlet temperatures were estimated to be lower by between 4.9°C to 5.8°C than the measurements. The freon outlet temperatures were estimated higher than those in the measurement between 0.2°C and 3.1°C.

Similarly, the water inlet and outlet temperature (TW_{16} and TW_1 respectively) were estimated in the same way. From the results, the water outlet temperatures were slightly lower, between 0.4°C to 1.2°C than the measured temperatures. For the water inlet temperature, where the sensor was placed quite far away from the condenser exit, the estimate is between 1.1°C to 7.5°C higher than those in the measurements. Fig.6.1.2(a and b) shows the deviations from the actual measurement.

The freon inlet and outlet pressures summarized in Fig.6.1.3(a and b) were estimated higher in both cases. The deviation from the measurement was estimated between 0.2-0.3 bar for the freon inlet pressure

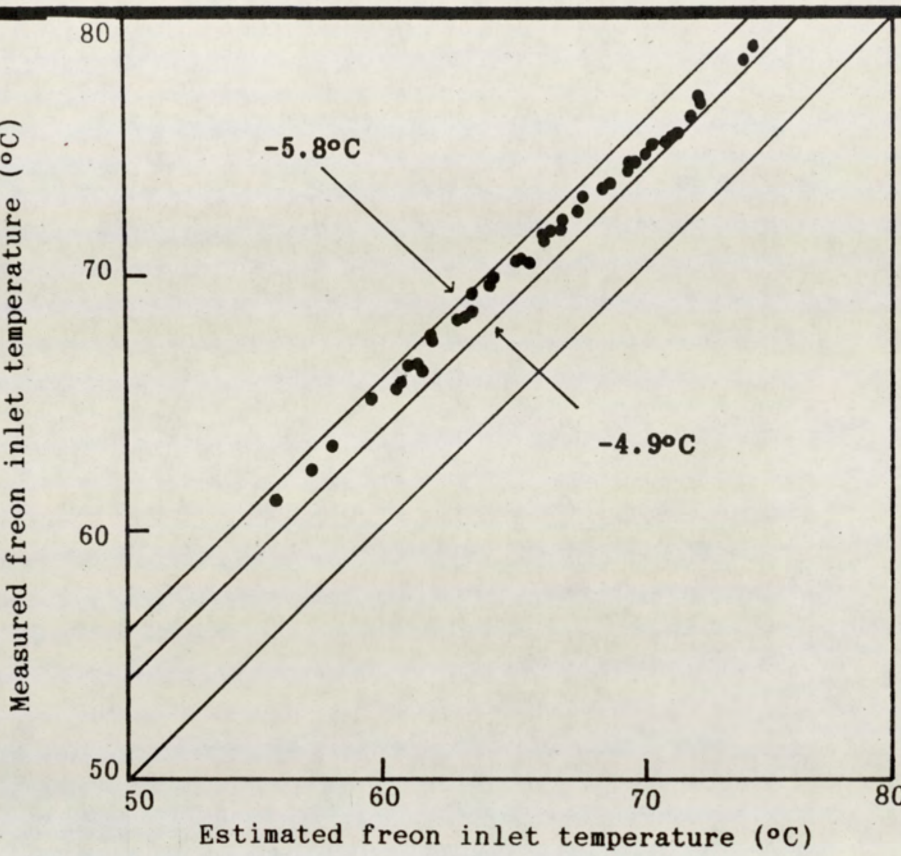

Fig.6.1.1(a): Estimated and experimental freon inlet temperature based on experimental measurement

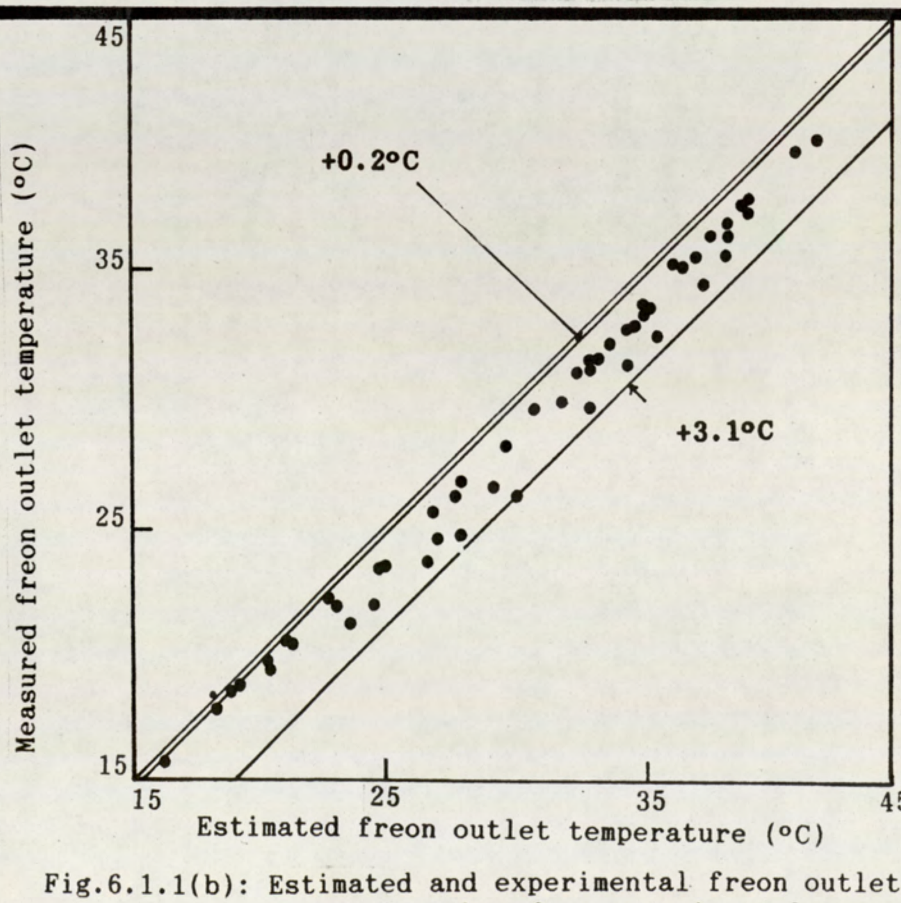

Fig.6.1.1(b): Estimated and experimental freon outlet temperature based on experimental measurement

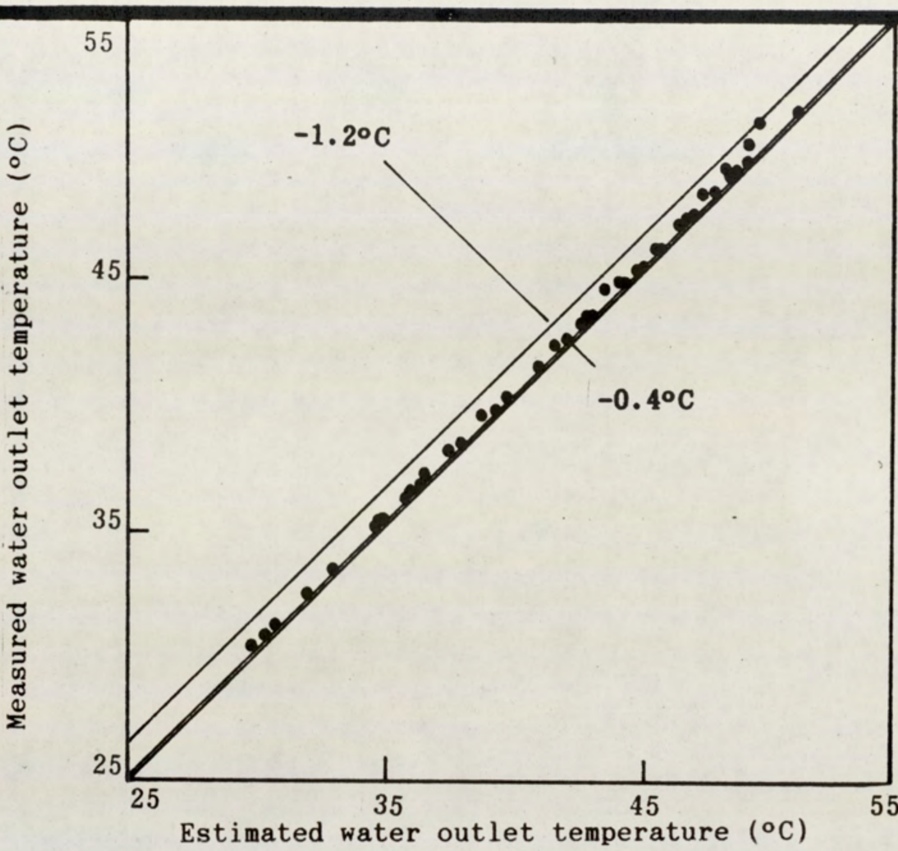

Fig.6.1.2(a): Estimated and experimental water outlet temperature based on experimental measurement

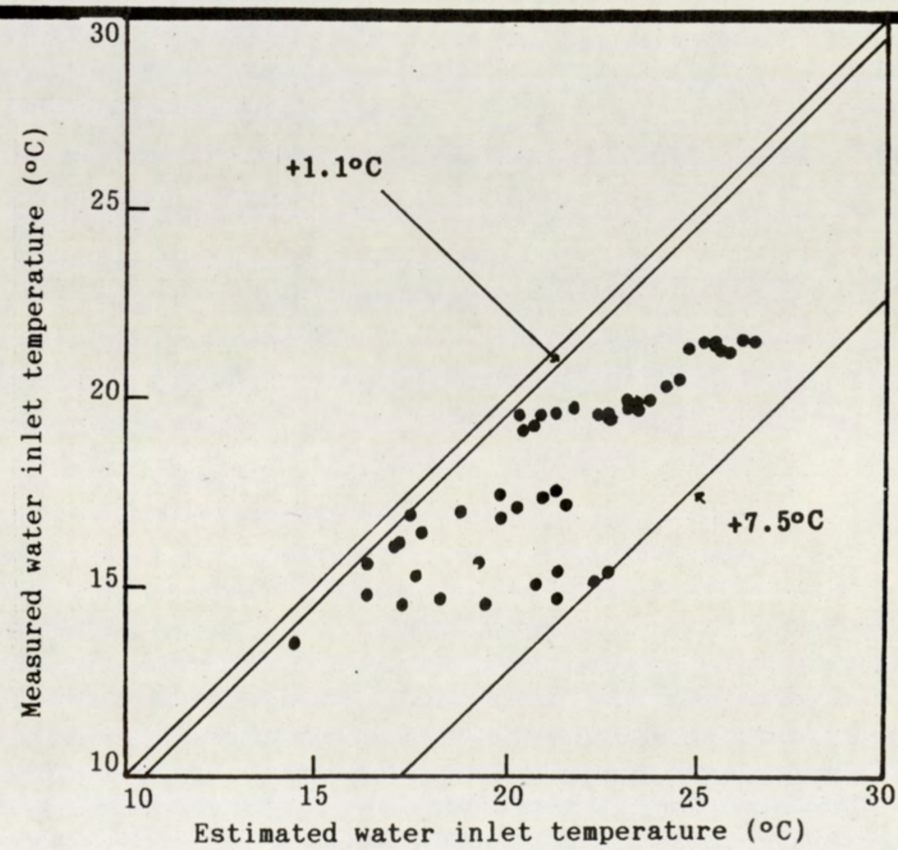

Fig.6.1.2(b): Estimated and experimental water inlet temperature based on experimental measurement

and 0.5-0.8 bar for the outlet pressure.

As discussed earlier, water mass flowrate which is measured manually is introduced to evaluate the average freon mass flowrate using condenser energy balance equation. In the system, the water and freon mass flowrate are assumed to be constant throughout the Run for particular conditions.

Each Run, which consists of 41 primary parameters, we shall call a set of experimental data. At given operating conditions, each Run is used to compare with the results predicted by the model. 32 temperatures at the test-sections in the heat pump counter flow condenser are the basic parameters to be compared with the predicted temperatures at the same position and operating conditions. At the same time, other parameters such as freon and water outlet temperature, freon outlet pressure, and freon and water mass flowrate are also used to supplement the comparison at given operating conditions. Other parameters which do not directly participate in the comparison will be discussed later in the predicted results.

6.1.2: Predicted results

The results predicted by the model can be discussed in four different sections as follows:

Three separate regions: In this section, the results are further divided thus; thermodynamic and physical properties of the fluids, heat exchanger performances using ε-Ntu method, and thermal power analysis of the fluids during the process.

The temperature and pressure at the interface (between each region) are also described. Fig.6.1.4 shows the possibility of the three separate regions in the heat pump condenser where the pressure and temperature are at the boundary zone except for the inlet and outlet condition,

$$TR_a = TR_{in}$$
$$TW_a = TW_{out}$$
$$PR_a = PR_{in} \qquad \text{Eqn.6.1}$$

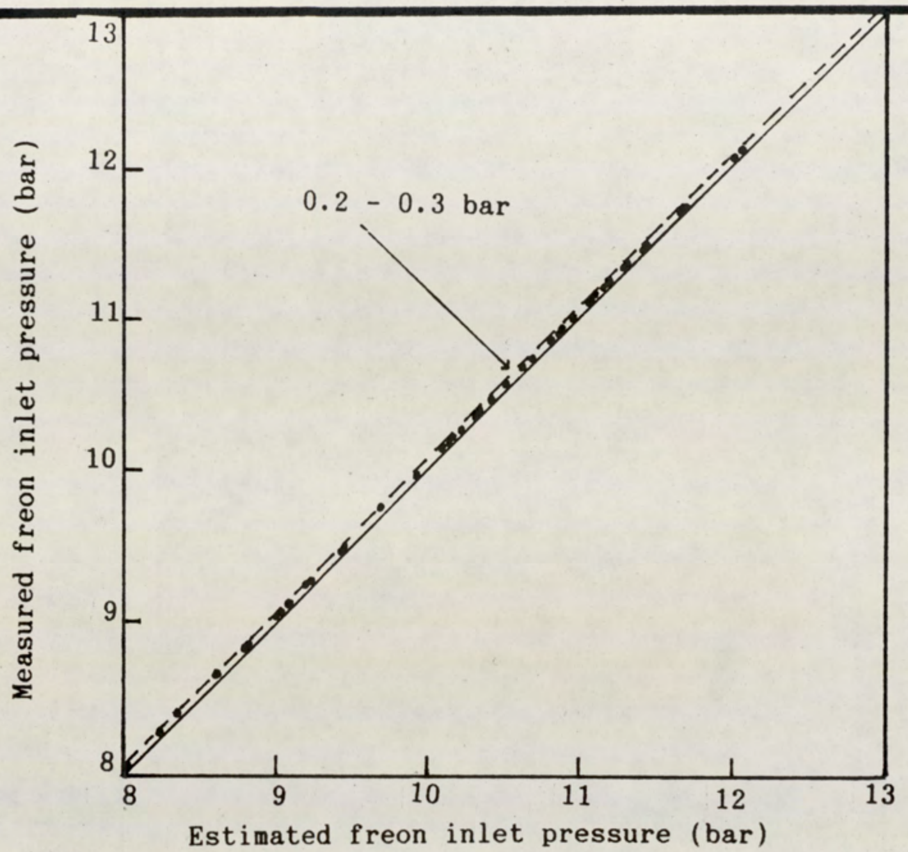

Fig.6.1.3(a): Estimated and experimental freon inlet pressure based on experimental measurement

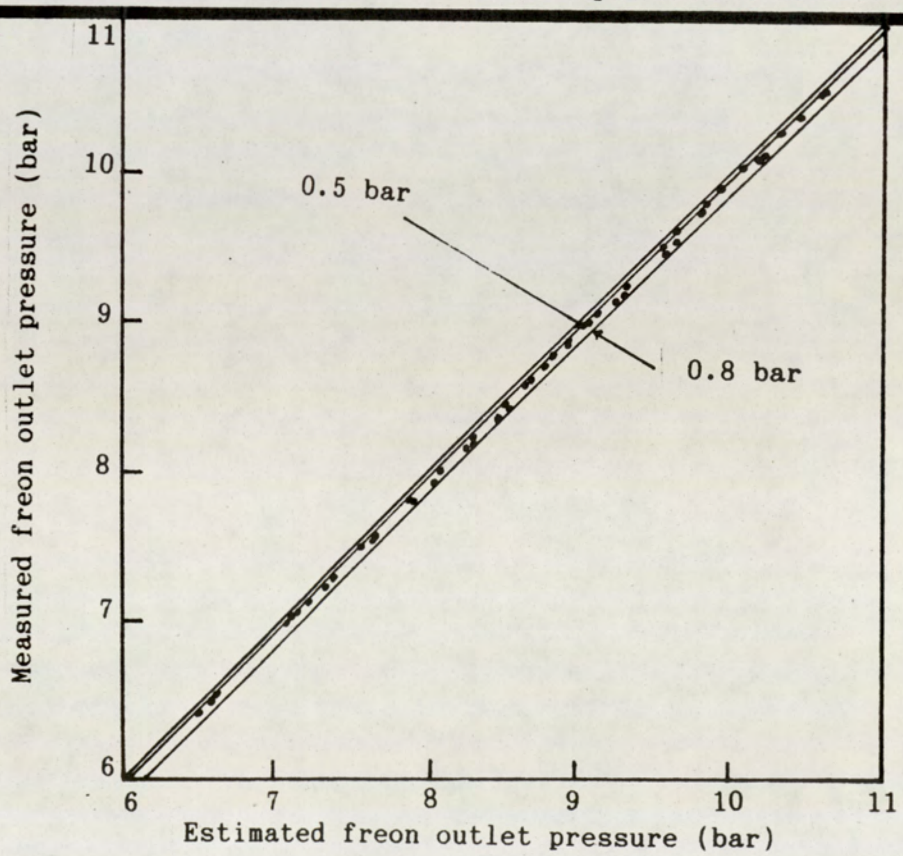

Fig.6.1.3(b): Estimated and experimental freon outlet pressure based on experimental measurement

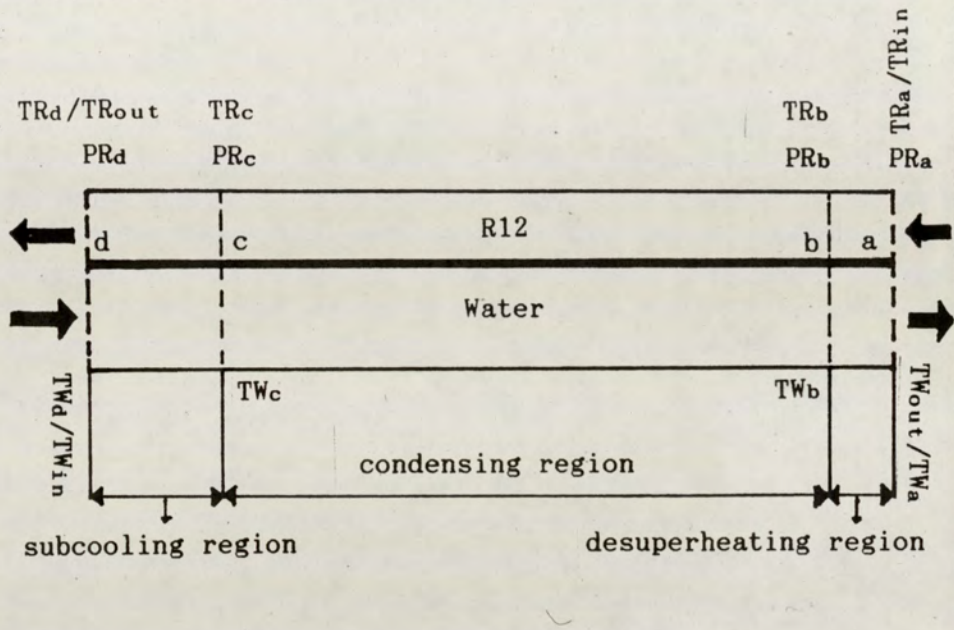

Fig.6.1.4: The possible three-separate regions in the present condenser (not in scale)

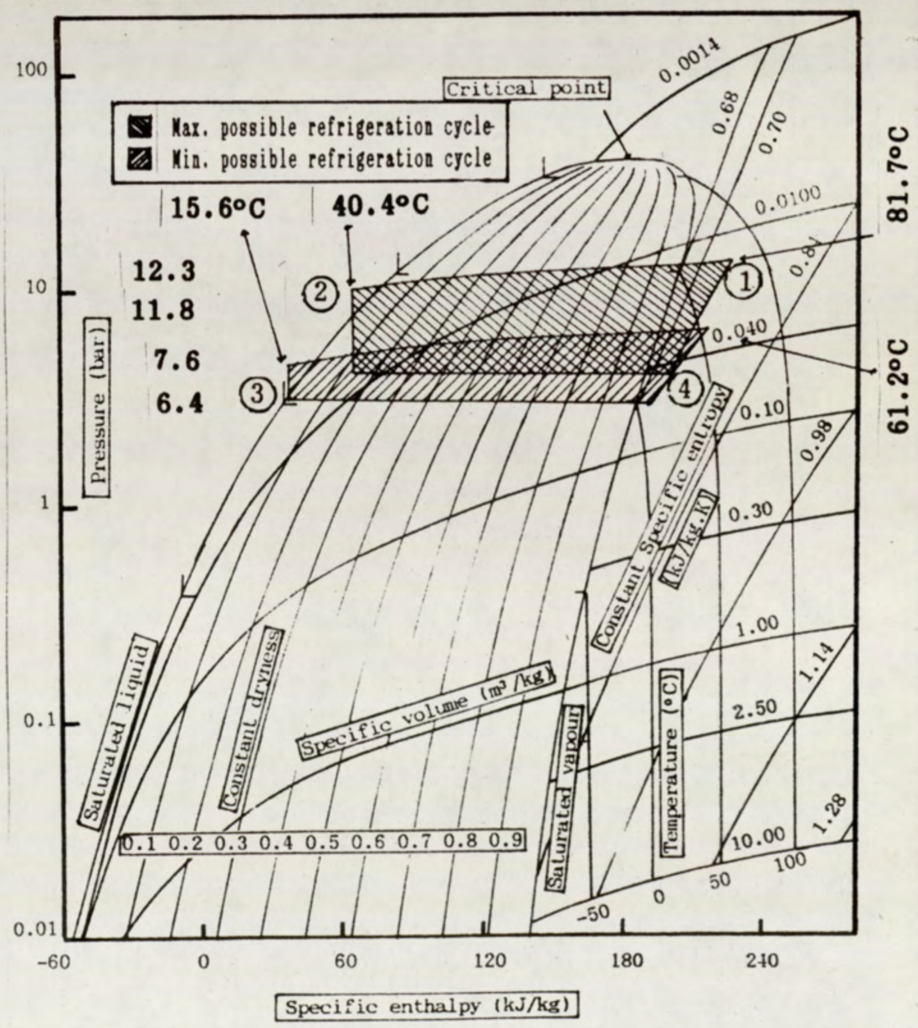

Fig.6.1.5: P-h diagram showing the possible maximum and minimum refrigeration cycle taken from Run 1 to Run 68

where TR_{in} is taken to be equal to the freon entry temperature measured in the experiment and TW_{out} is the outlet water temperature calculated in the model. The freon pressure at point a, PR_a taken to be equal to the freon inlet pressure, is the freon inlet pressure (or discharge pressure) measured in the system.

The temperature and pressure at point b, which represents the exit condition of the desuperheating region and the inlet condition of the condensing region,

$$TR_{b,desup} = TR_{b,cond}$$
$$TW_{b,desup} = TW_{b,cond}$$
$$PR_{b,desup} = PR_{b,cond} \qquad \text{Eqn.6.2}$$

are assumed to be equal. These parameters are calculated by the model (not found in the experiment, unless the point where the sensor is placed in the experiment coincides with the point in the model).

The temperature and pressure at point c, which represents the outlet condition of condensing region and inlet condition of the subcooling region can be written,

$$TR_{c,cond} = TR_{c,sub}$$
$$TW_{c,cond} = TW_{c,sub}$$
$$PR_{c,cond} = PR_{c,sub} \qquad \text{Eqn.6.3}$$

The freon outlet temperature and pressure, and water inlet temperature associated with the temperature and pressure at point d can be expressed as,

$$TR_d = TR_{out}$$
$$TW_d = TW_{in}$$
$$PR_d = PR_{out} \qquad \text{Eqn.6.4}$$

Eqn.6.4 can be directly compared with the experimental results.

Parameter distribution: The parameter distributions considered along the condenser are freon and water temperature and pressure, wall temperature, vapour quality, freon and water linear heat transfer coefficient, freon and water number of transfer unit, and overall heat transfer coefficient.

In a counter flow heat exchanger, the temperature distribution along the flow-axis decreases in the direction of R12 flow where heat is released from the freon side, and increases in the direction of water flow where heat will be picked-up from the freon. In general, the drop in the freon temperature is more pronounced in the single-phase regions (desuperheating-region and subcooling-region) than in the condensing-region (two-phase flow). This is also true for the drop in the water temperature.

The experimental temperature profiles are directly compared with those predicted by the model. Other profiles are also discussed. The behavioural study of these profiles along the specified length of a counter flow heat exchanger from one operating condition to another can be investigated.

Thermal power analysis: This concerns the analysis of the overall thermal power; gained and lost from the freon side and water side respectively, based upon the enthalpy and entropy phenomenon.

In this analysis, the energy inbalance of the specified power, the net rate of entropy flow through the system, thermal entropy creation, and overall effectiveness in term of number of transfer units are presented and discussed.

Summary of range of possible evaporator conditions: In this section, the model predicts the possibility of refrigeration cycle by altering the evaporator conditions. Three factors which affect the cycle are considered; no pressure drop across the evaporator, the subcooled point at the condenser exit is isenthalpic to the point at the evaporator entry, and the work done by the compressor is isentropic (see **Fig.6.1.8(b)** for the possible cycle).

Compressor isentropic efficiencies of 50%,55% and 60% are considered to predict the possible COP of the heat pump system, for freon evaporator entry temperature increasing in steps of 2.0°C. The temperatures are set to be lower than the condensing temperature for a particular Runs.

6.1.3: Results in general

It is important to mention that only the results within the operating conditions explained in chapter 1 and 4 are presented in the discussion.

As discussed in chapter 4, over 100 Runs were recorded, but 20 sets of the results (Runs) are selected which cover the working ranges. The results will be summarized in two ways; tables and graphs, which includes the experimental and predicted data.

Experimental results

The results are further subdivided to two sections; experimental results directly measured from the rig, and secondary parameters which are indirectly measured but calculated from the primary parameters (freon mass flowrate, thermal power, and heat lost across the condenser).

There are 68 sets of data (Runs) taken between May 1987 to January 1988, which were grouped according to the freon inlet pressures and temperatures, called Run 1 to Run 68 shown in Table A-6.1 to Table A-6.11. It covers the following operating conditions; 7.6-12.3 bar for the inlet pressure, 61.2-81.7°C for the freon inlet temperature, 13.5-21.7 °C for the water inlet temperature, and 6.72-21.49 g/s for the water mass flowrate.

In the tables stated above, the first part of the results concerns the temperature distribution in the heat pump condenser and the second part the parameters measured outside the condenser. In general, the temperature of freon decreases over the length of heat pump condenser (direction of freon flow) and at the same time, water temperature increases in the opposite direction. For higher freon inlet temperature, the inlet pressure becomes higher, and the water mass flowrate decreases. Room temperature ranged from 18°C to 26°C.

The minimum and maximum operating conditions recorded in Table A-6.1 to Table A-6.11 can be summarized as follows.

Items	Minimum	Maximum
Freon inlet temperature (°C)	61.2	81.7
Freon outlet temperature (°C)	15.6	40.4
Freon outlet pressure (bar)	7.6	12.3
Temperature at the evaporator entry (°C)	1.2	9.3
Temperature at the evaporator exit (°C)	13.7	21.3
Pressure at the evaporator entry (bar)	3.3	4.2
Pressure at the evaporator exit (bar)	3.1	3.9

Table 6.1: Freon operating conditions taken from Run 1 to Run 68

The above table can be approximately drawn in a p-h diagram shown in Fig.6.1.5, where there is a pressure drop from point 1 to point 2 and from point 3 to point 4. In the results, the pressure drop in the maximum cycle of the higher pressure line is 0.5 bar, and in the minimum cycle is 1.2 bar. The pressure drop in the lower pressure line for the maximum cycle is 0.2 bar and 0.1 bar for the minimum cycle.

The general shape of the temperature distribution for both the fluids is shown in Fig.6.1.6(b) where there is a sharp drop in the freon temperature over the first few meters of the condenser entry (as a result of pressure drop in the tube), and after that, the drop is moderate before continuing to drop as the freon flows towards the condenser exit. The desuperheating-region can be represented by the tremendous drop just after the freon flow in the condenser. The two-phase region can be represented by the small temperature drop which covers most of the condenser length. Finally, the moderate drop indicated by the few points towards the condenser exit can be regarded as the subcooling region.

On the other hand, the big increase in the water temperature can be clearly seen as the water flows through the condenser exit. In general, the increase in the temperature is more pronounced over the first few meters as the water flows into the condenser exit but after that, the increase becomes smaller as the water approaches the condenser entry.

At the same time, heat lost from the freon side is picked-up by the water side causing the water temperature to increase in the opposite direction. The increase in the water temperature compared to that in the freon temperature drop is quite constant except for the first few points towards the condenser exit.

As the freon inlet pressure increases where TR_1 is high, the freon and water mass flowrate are decreased. The experiment records the pressure drop across the condenser between 1.0 bar to 1.5 bar.

<u>Predicted results</u>

The results were obtained by putting input data (taken from appropriate experimental results) to the model program. The inputs are as follows; total thermal power, water inlet temperature, freon inlet temperature, freon inlet pressure, and overall percentage of thermal energy lost to the surroundings. The other input, assumed to have fixed values, are wall thickness of the tube ($7.4x10^{-4}$ m), outside diameter of the freon and water tube ($5.75x10^{-3}$ m and $7.65x10^{-3}$ m respectively), total length of the condenser (15 m), and conductivity of thermal bond between the tubes (500 W/m.°C). These inputs are separately recorded in each set of results.

Out of 68 results recorded in **Table A-6.1** to **Table A-6.11**, 29 sets have been analysed, corresponding to the sets measured in the experiment. The same numbers are used as in experimental results except a subscript m is introduced to denote the results predicted by the model. The results are classified in five sections according to the freon inlet

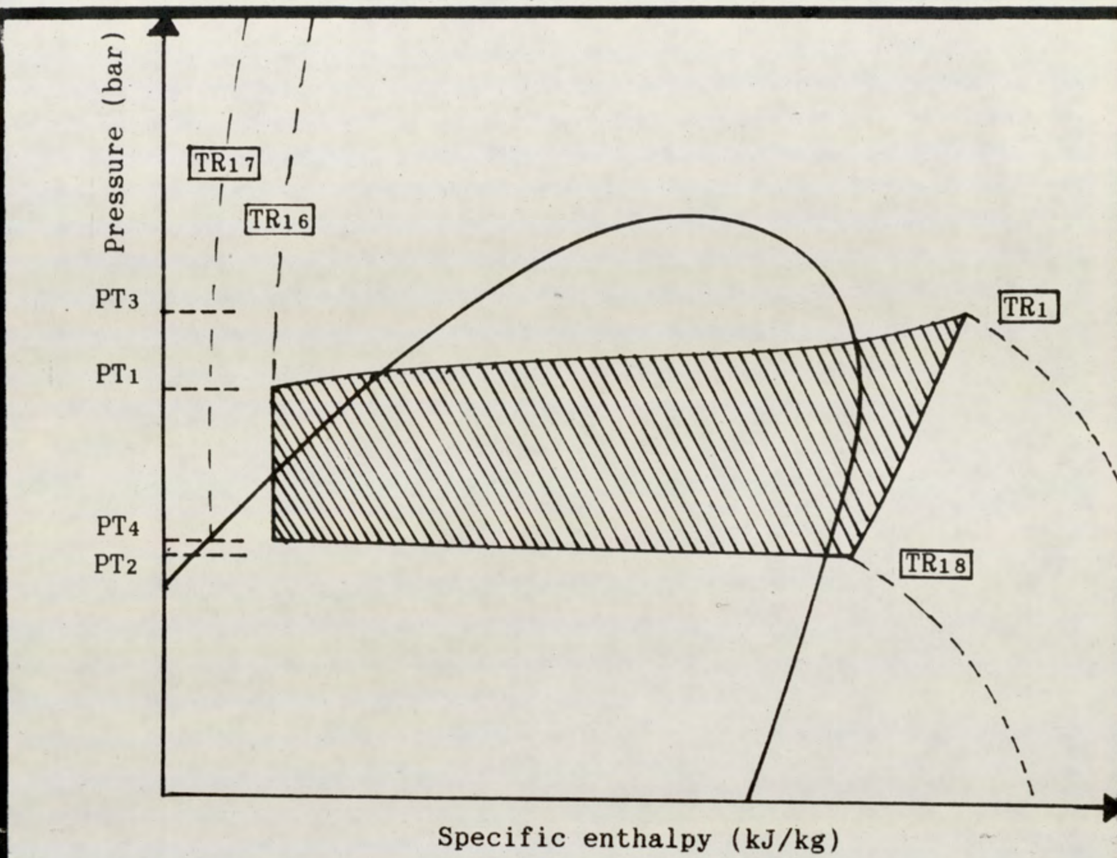

Fig.6.1.6(a): The possible refrigeration cycle showing the position of temperatures and pressures in the experiment

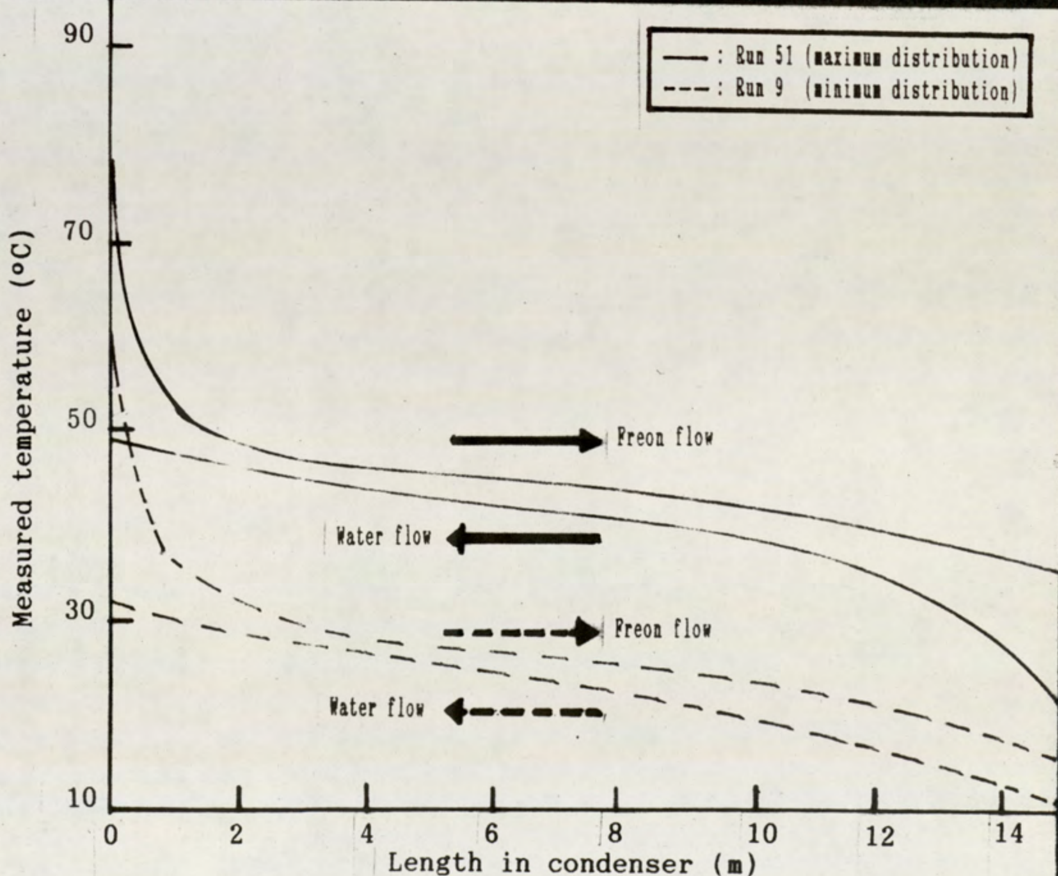

Fig.6.1.6(b): The possible temperature distribution taken from experiment (as an example)

pressures.

Section	Run■	Inlet pressure (bar)
A	9,10,11,12,5 (5)	7.65 - 10.89
B	38,40,42,44,54,56,59,61 (8)	8.82 - 12.06
C	39,41,45,47,57,58,60 (7)	9.02 - 12.11
D	1,2,43 (3)	9.23 - 9.93
E	3,46,4,53,52,55 (6)	10.20 - 10.92

Table 6.2: Classification of predicted results (29 Run■)

The results in section A, B and C which consists of 20 sets of data will be used for discussion later. Each set of results provided in this thesis is divided into three parts;thermodynamic and physical properties of the fluids at three separate regions, output of the numerical integration which includes the profiles of the fluids for various properties, and the summary of range of possible evaporator conditions by assuming certain values of compressor isentropic efficiency. Some the results (Run■ 9, 10, 40, 44, 58 and 60) are shown in **Table A-6.12** to **Table A-17** of **Appendix 6**, where the three sections described above are indicated by part **a**, **b** and **c** respectively.

a. **Part a**: The first part of the result records the input values, properties of the fluids in the three separate regions, and energy balance analysis from entropy and enthalpy point of view.

As the freon inlet temperature and pressure increases, water exit and water inlet temperature are also increased but other parameters such as freon and water mass flowrate, and thermal power are decreased. The length of the desuperheating region becomes longer, the length of subcooler becomes shorter, and the length of the two-phase region moderately decreases as the freon inlet pressure increases.

The following conclusions can be drawn for the three separate regions (part **a** of the results), if the freon inlet pressure and temperature are increased,

Properties	Superheat	Two-phase	Subcooler
R12 side heat transfer coefficient	decrease	decrease	decrease
Water side heat transfer coefficient	decrease	decrease	decrease
R12 side Reynolds number	decrease	decrease	decrease
Water side Reynolds number	decrease	decrease	decrease
Overall linear conductance	decrease	decrease	decrease
Number of transfer units	increase	decrease	decrease
Effectiveness of each segment	increase	increase	decrease
Thermal power picked-up or transferred	decrease	decrease	increase
Specific enthalpy of refrigerant	increase	increase	increase
Specific entropy of refrigerant	decrease	decrease	increase
Temperature	increase	increase	increase
Pressure	increase	increase	increase

Table 6.3: Overall summary of some properties of fluids in three-separate regions as PR_{inlet} increases

b. Part b: The second part of the results is to list out the outputs of the numerical integration where the three separate regions (desuperheating, condensing, and subcooling region) are clearly shown. In this section, the parameter distributions along the 15-meter long condenser such as freon temperature, water and wall temperature, freon and water pressure, vapour quality, freon and water heat transfer coefficient, freon and water number of transfer units, and overall linear heat transfer coefficient are listed in the results. The outputs were printed for every 0.2 meter.

A comparison with the experimental data can be directly made based on the temperature distribution of the freon and water along the condenser at every one meter apart. In general, as tha inlet pressure increases, a longer length is required for the vapour to be desuperheated before it begins to condense. At the same time, a shorter length is needed in the subcooling region, after condensation has completed (see Fig.6.1.7(a)). Other parameters described above, such as temperature, pressure, and number of transfer units of water are increased, while the heat transfer coefficients and number of transfer units of freon are decreased as the inlet pressure increases. Fig.6.1.7(b) shows the maximum and minimum possibility of temperature profiles predicted by the model taken from Runs 9 and Runs 59. Looking back to Fig.6.1.6(b), it is clearly seen that both curves show approximately the same pattern.

c. Part c: The final part of the results show the summary of range of possible evaporator conditions by assuming 50%, 55% and 60% compressor isentropic efficiencies. The value of condensing pressure, condensing temperature, specific enthalpy at the entry and exit, specific entropy at

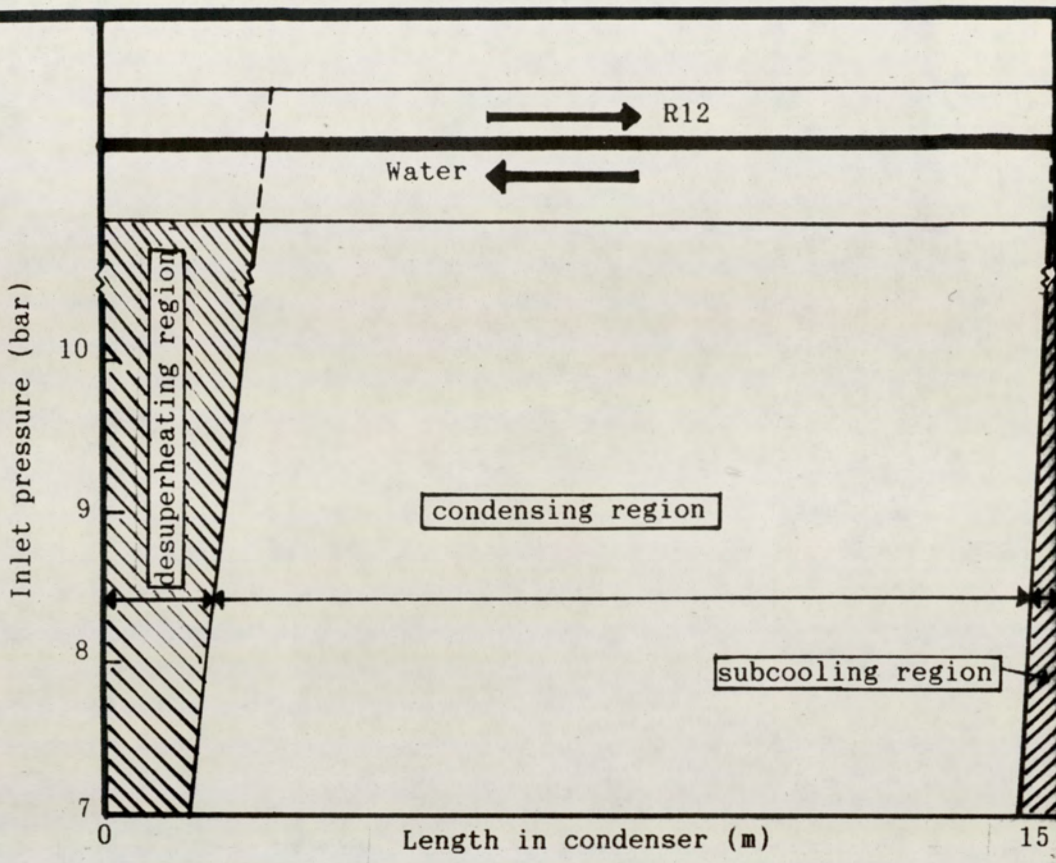

Fig.6.1.7(a): The possible length in three regions as the inlet pressure increases

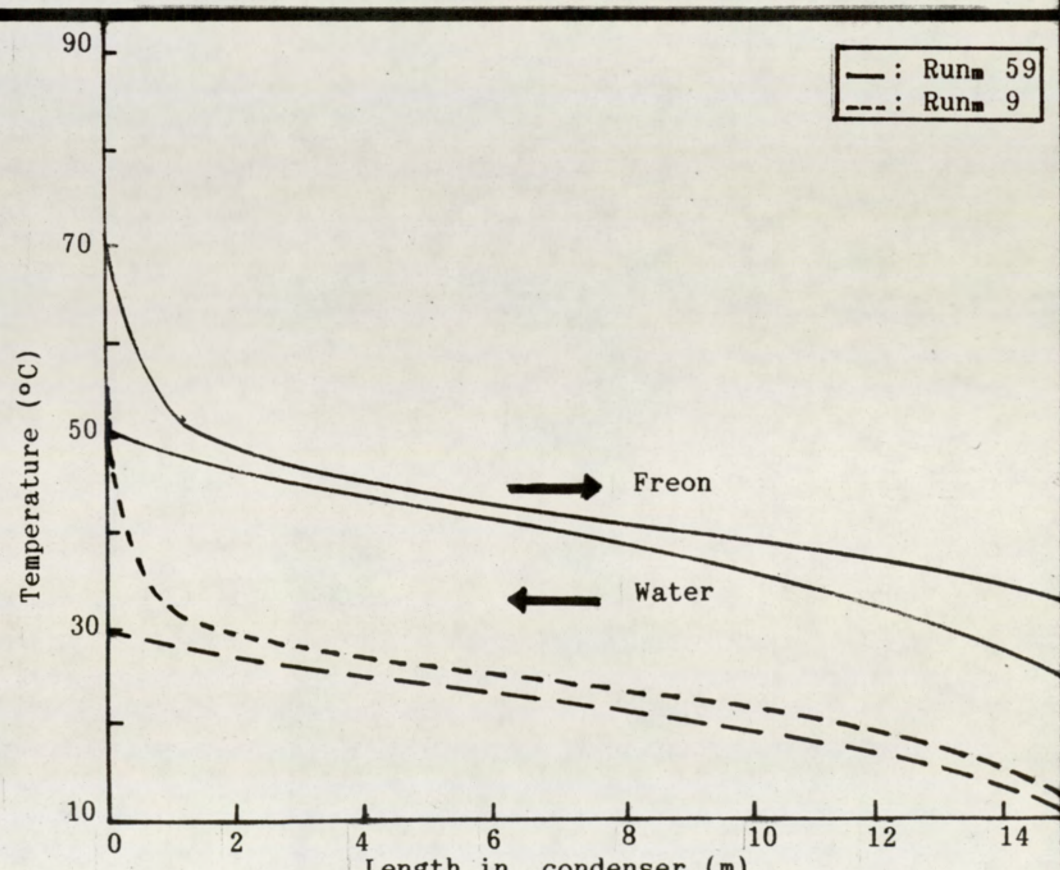

Fig.6.1.7(b): Example showing the temperature profile for Runm 9 and Runm 59 of the prediction

the entry and exit, and the exit temperature are fixed in each Run$_m$. The possible summary is shown in **Fig.6.1.8** where point 1, 2, 3 and 4 indicate the position in the refrigeration cycle (entry and exit of the four basic heat pump components).

The model also predicts the thermodynamic properties at given temperature and pressure at the evaporator entry and exit by varying the compressor efficiency. At the entry, point 3 is assumed to be in the two-phase region, while at the exit, point 4 is considered in the vapour region where its temperature is also predicted. The other parameters calculated in this part are the evaporation capacity, compression capacity, pressure ratio, and the possible coefficient of performance of the heat pump system (see also **Fig.6.1.8**).

As the temperature and pressure at point 3 increases, the specific enthalpy of saturated R12 at vapour fraction, x=0 and x=1 is also increased, and the specific entropy of saturated R12 at x=0 is increased but decreases moderately at x=1. The specific entropy and specific enthalpy at the superheated region (point 4) is increased and the possible temperature of the fluid predicted at this point is also increased ($TR_4 > TR_3$). Finally, as the temperature and pressure at point 3 increases, the evaporation capacity and coefficient of performance are also increased but compression capacity, and pressure ratio decreases. **Fig.6.1.8(b)** shows the possible situations for varying temperature and pressure at point 3. The conditions are changed when different freon inlet pressure and temperature are employed (see result in **Table A-6.12** to **Table A-6.17** of part c).

The results described in section A, B and C of **Table 6.2** are used throughout this chapter for discussion and comparison. Experimental data is denoted by Run and Run$_m$ represents the results predicted by the model. The comparison is made between the Run and Run$_m$ of the same number.

6.2: Comparison of experiment and model

In this section, the results classified in **Table 6.2**; section A, B and C which consists of 20 sets of Run are considered for comparison. It covers the working pressure from 7.65 bar to 12.11 bar, and 55.4°C to 74.2°C for the freon inlet temperature. The experimental results can be found in **Table A-6.1** to **Table A-6.11** and the predicted results are shown from **Table A-6.12** to **Table A-6.17** of part b. The results from appropriate Run number are compared.

Temperature distribution at one meter intervals along the condenser

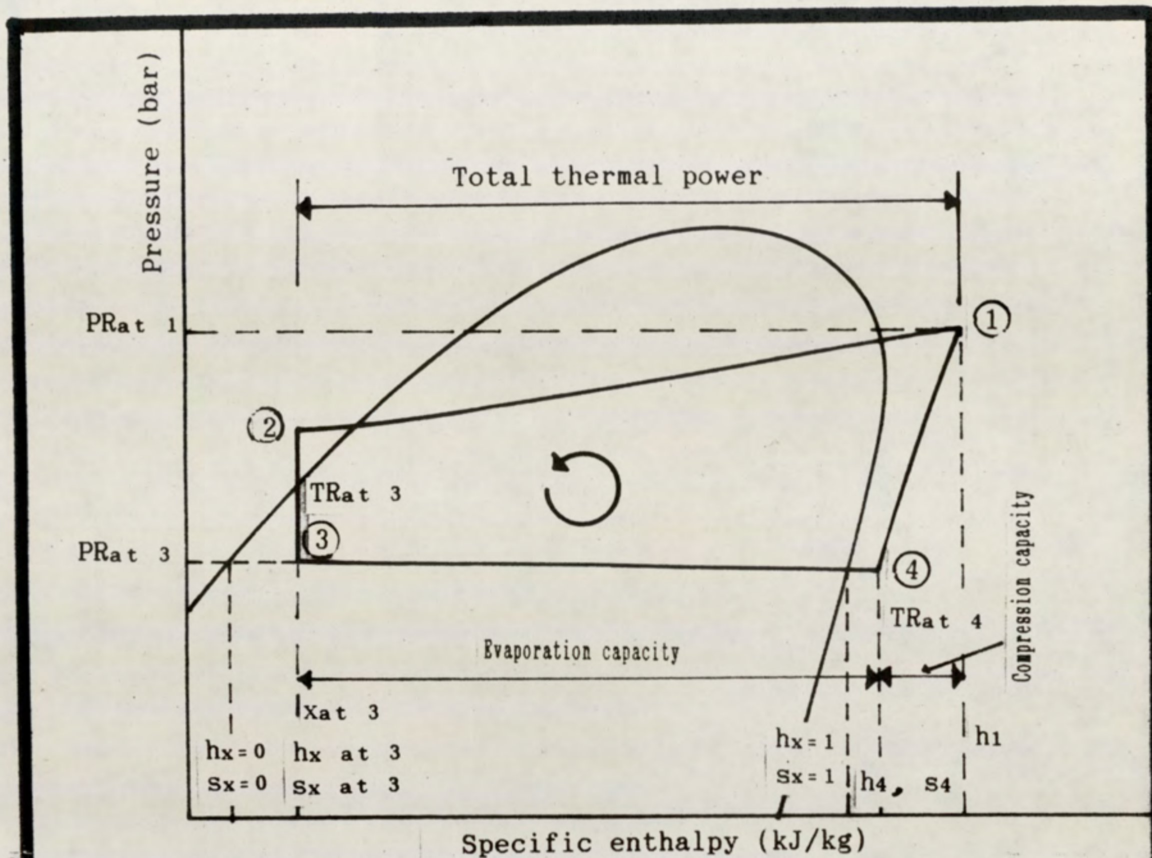

Fig.6.1.8(a): The summary of range of possible evaporator conditions at certain percentage of compressor isentropic effeciency

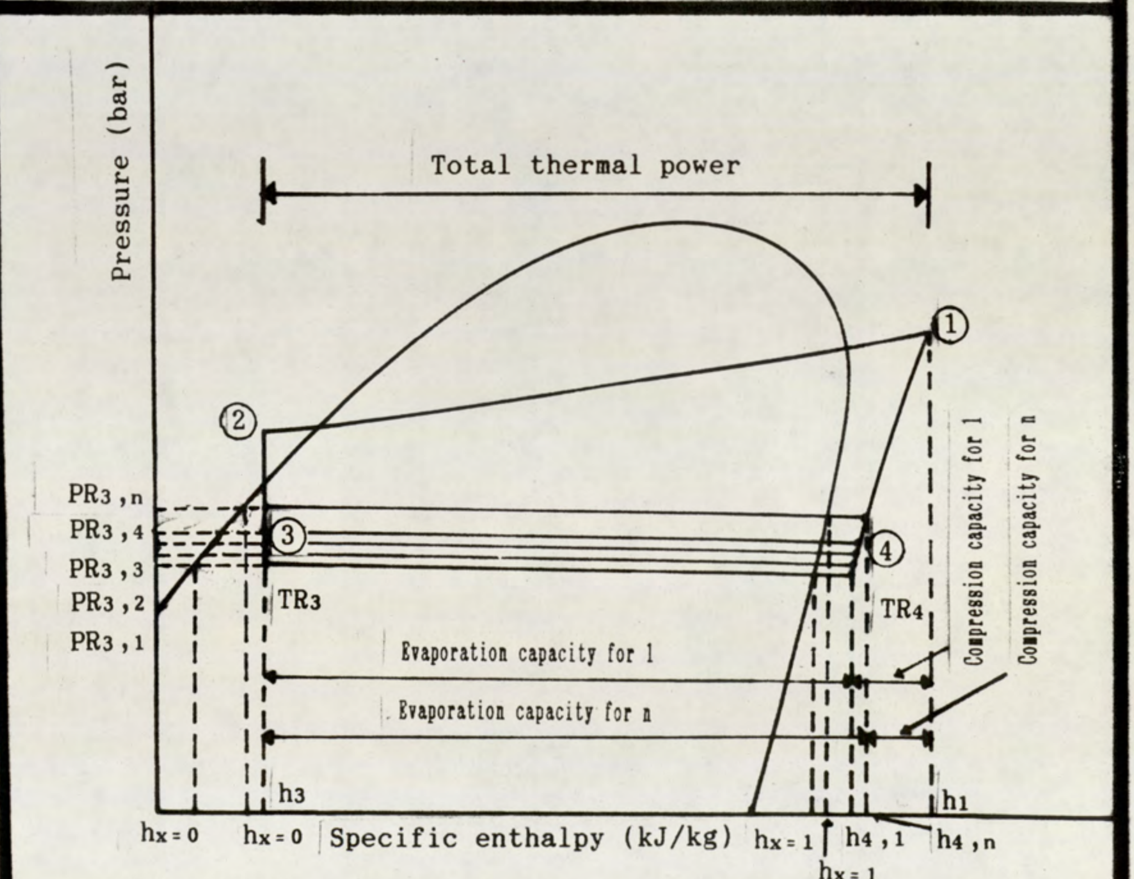

Fig.6.1.8(b): The possible refrigeration cycle by varying temperature and pressure at point 3

can be directly compared with the predicted results where the temperature profile for every 0.2 meter is shown. Other parameters measured during experiment which can be compared are freon outlet pressure, water outlet temperature, and water and freon mass flowrate.

6.2.1: Temperature profile

Section A

In this section, the results are compared for the freon inlet pressure from 7.65 bar to 10.89 bar, and 55.4°C to 68.6°C of the freon inlet temperature with the room temperature varied from 18.5°C to 19.5°C (using polystyrene insulating materials in the experiment). Fig.6.2.1 shows the overall comparison taken from section A of Table 6.2 where the points are drawn at different Runs for each meter.

For the freon side, the temperature distribution deviates from -1.7°C to 6.5°C from the experimental results. The majority of the points (a total of 76 points in Fig.6.2.1(a)) lie very close to the reference line except the predicted temperature at point 71 (equivalent to point 15 of the experimental result) which shows a higher value. As the freon inlet pressure increases, the temperature at this point came down to with 2.6°C of the measurement, which lies in the two-phase region, just before the mixture of liquid-vapour completely changed to freon liquid in the subcooler. In general, the distributions are in fairly good agreement with the experiment, except at the points just before the subcooling region.

For the water side, as shown in Fig.6.2.1(b), the distribution is much better, within the range of -1.6°C to 0.8°C from the experimental results. The water is assumed to be completely in the liquid state throughout the process.

Fig.6.2.2(a->f) show the temperature distribution for both the experimental and predicted results. The experimental results indicated by the small squares, consist of 16 points at one meter intervals. The small dots consist of 76 points, at intervals of 0.2 meter, showing the profile predicted by the model. The freon temperature is always higher than the water temperature. As the pressure increases, the distributions are in good agreement with the experiment except at the few meters before the condenser exit, where the temperature predicted by the model is slightly higher. At higher inlet pressure, the water and freon mass flowrate decrease with increasing of freon inlet temperature and water outlet temperature.

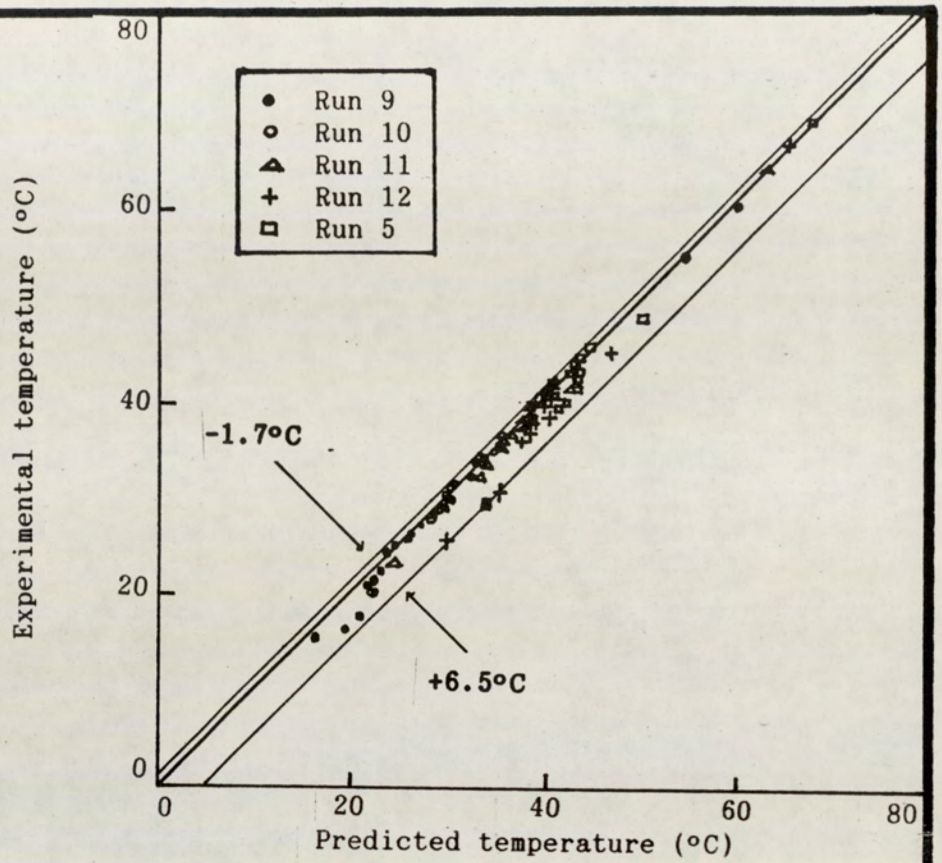

Fig.6.2.1(a): Experimental and predicted temperature profile for the freon side compared (Section A of Table 6.2)

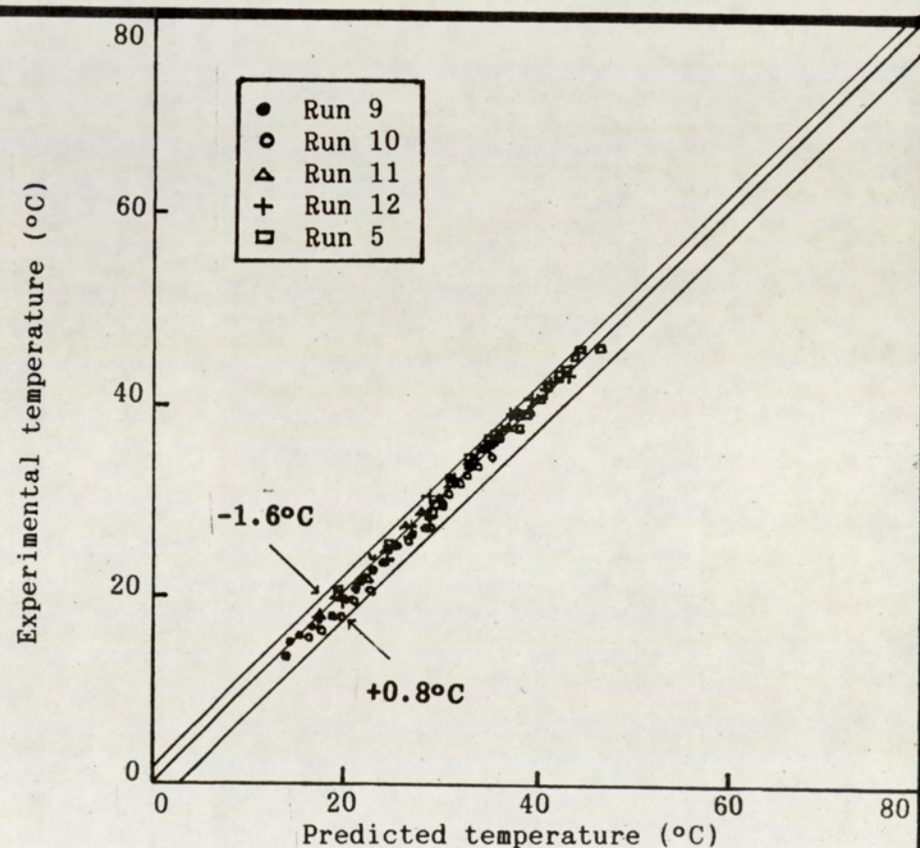

Fig.6.2.1(b): Experimental and predicted temperature profile for the water side compared (Section A of Table 6.2)

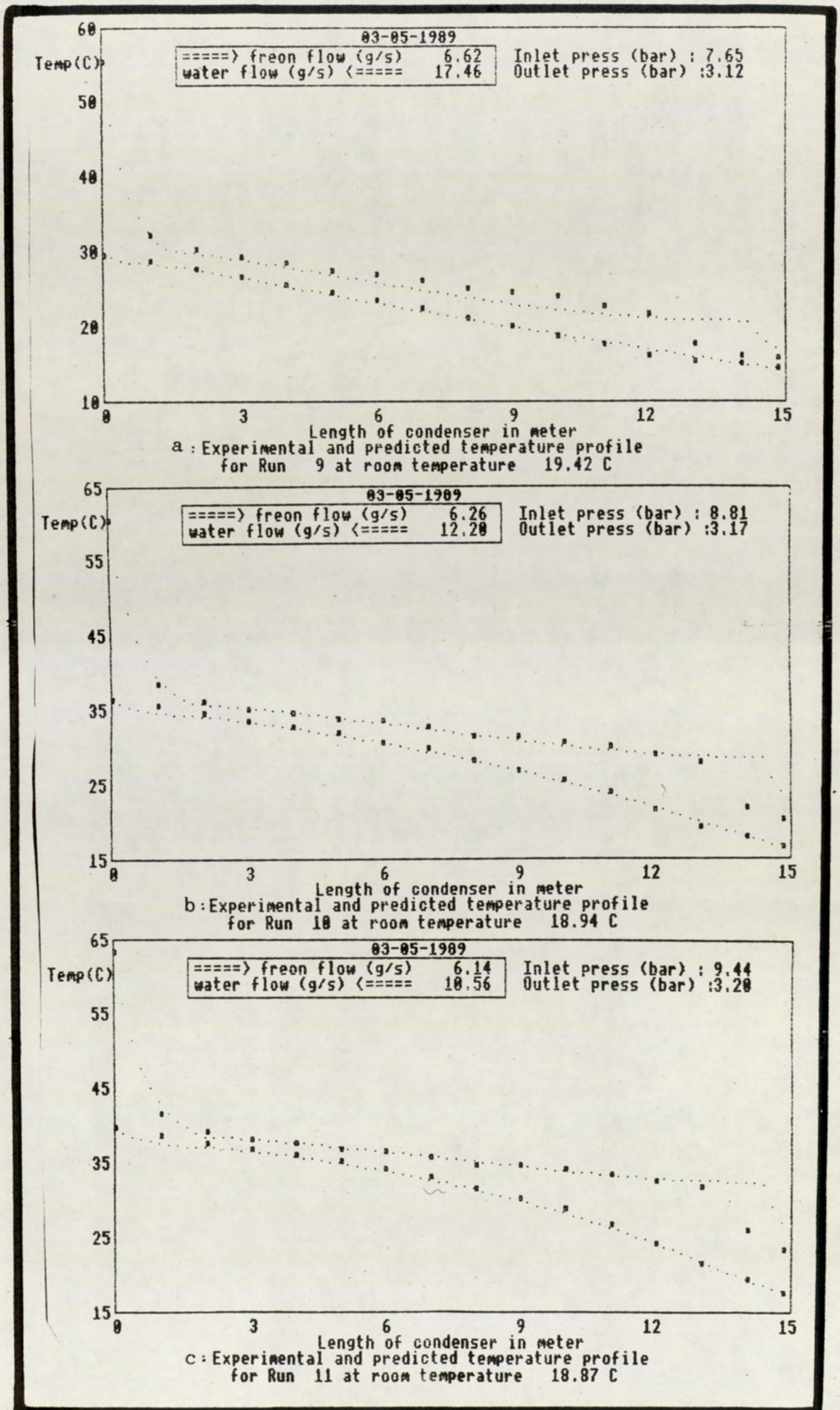

a : Experimental and predicted temperature profile for Run 9 at room temperature 19.42 C

b : Experimental and predicted temperature profile for Run 10 at room temperature 18.94 C

c : Experimental and predicted temperature profile for Run 11 at room temperature 18.87 C

Fig.6.2.2: Experimental and predicted temperature profile of Section A for freon inlet pressure 7.65-10.89 bar

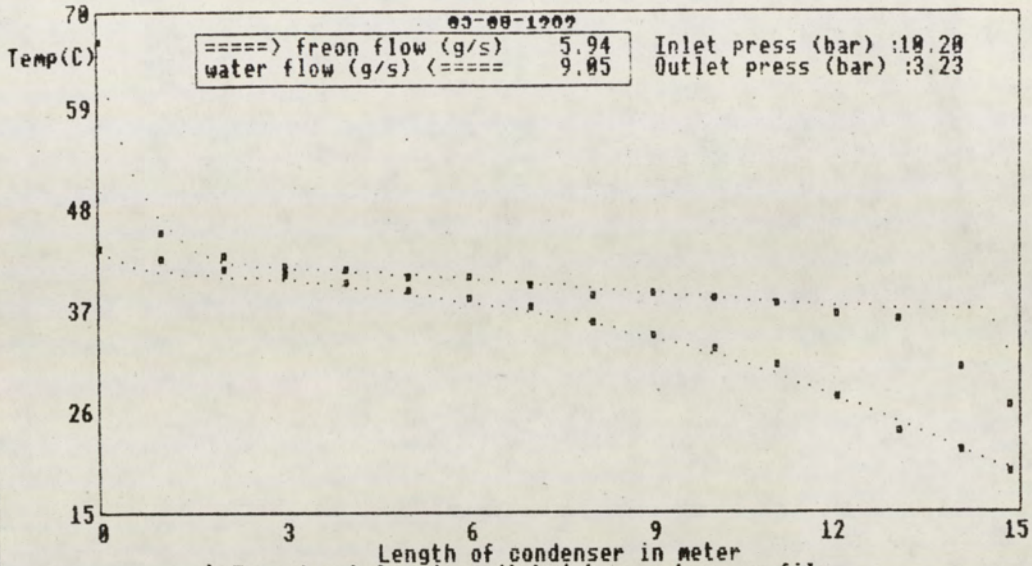

d: Experimental and predicted temperature profile
for Run 12 at room temperature 19.04 C

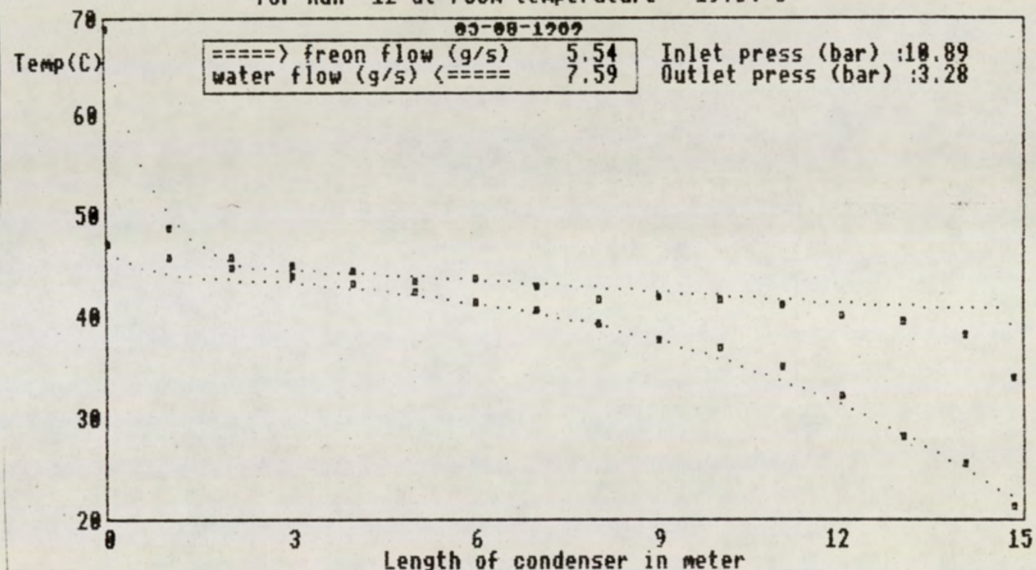

e: Experimental and predicted temperature profile
for Run 5 at room temperature 19.80 C

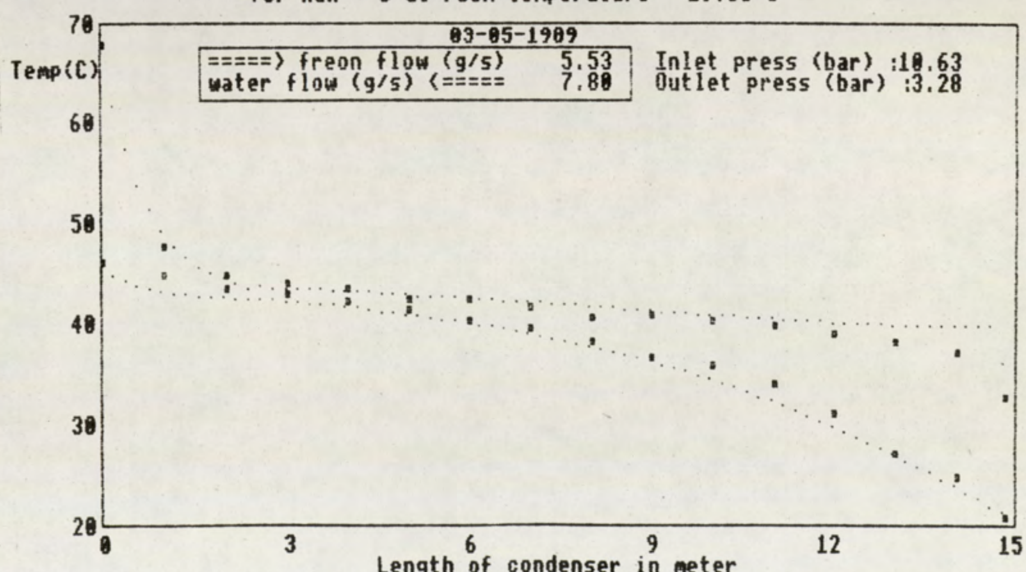

f: Experimental and predicted temperature profile
for Run 4 at room temperature 19.49 C

Section B

In this section, the working conditions are from 8.82 bar to 12.06 bar for the inlet pressure, 62.5°C to 74.1°C for the freon inlet temperature, and room temperature ranged from 23.8°C to 26.1°C (using vermiculite materials as insulation). **Fig.6.2.3(a->i)** show the graphical representation of the temperature distribution along the condenser for both experimental and predicted results. Comparison with the results in Section A shows an improvement, the predicted freon temperature at the points a few meters away from the condenser exit coming quite close to the experimental temperature. **Fig.6.2.4(a)** shows a deviation between -0.9°C to 4.0°C from the measurement. In general, the freon temperature profiles are in good agreement with experiment.

For the inlet pressure 8.82 bar, the subcooling region does not exist, there still being a mixture of freon liquid-vapour at the condenser exit, as can be seen from the vapour quality at this point where the value is still above zero (x=1.26%). As the pressure increases, the three regions can be clearly seen but the subcooling region occupies a small portion of condenser length.

The water side shows a better agreement, with almost all experimental points lying on the predicted points at the same length. The deviation is between -1.6°C to 0.5°C from the measurement (see **Fig.6.2.4(b)**). The water picks up more heat from the freon side as the freon inlet pressure increases, where the water temperarure at corresponding points is close to the freon temperature, especially in the first few meters of the mixed-region, in the direction of freon flow.

Similarly, as the freon inlet pressure increases, the freon inlet temperature and water outlet temperature also increase but the water and freon mass flowrate decreases.

Section C

The freon inlet pressure and temperature range from 9.02 bar to 12.11 bar and 62.9°C to 73.9°C respectively, at room temperature ranged from 23.9°C to 25.9°C are shown in **Fig.6.2.5(a->f)** using the same insulating materials as in Section B.

Similarly, the freon temperature distribution shows a fair agreement with the experimental temperature profile along the condenser except at the points just before the freon is completely condensed, where the predictions are slightly higher. In general, **Fig.6.2.6(a)** shows a deviation from -1.1°C to 2.5°C from the measurement. The model predicts

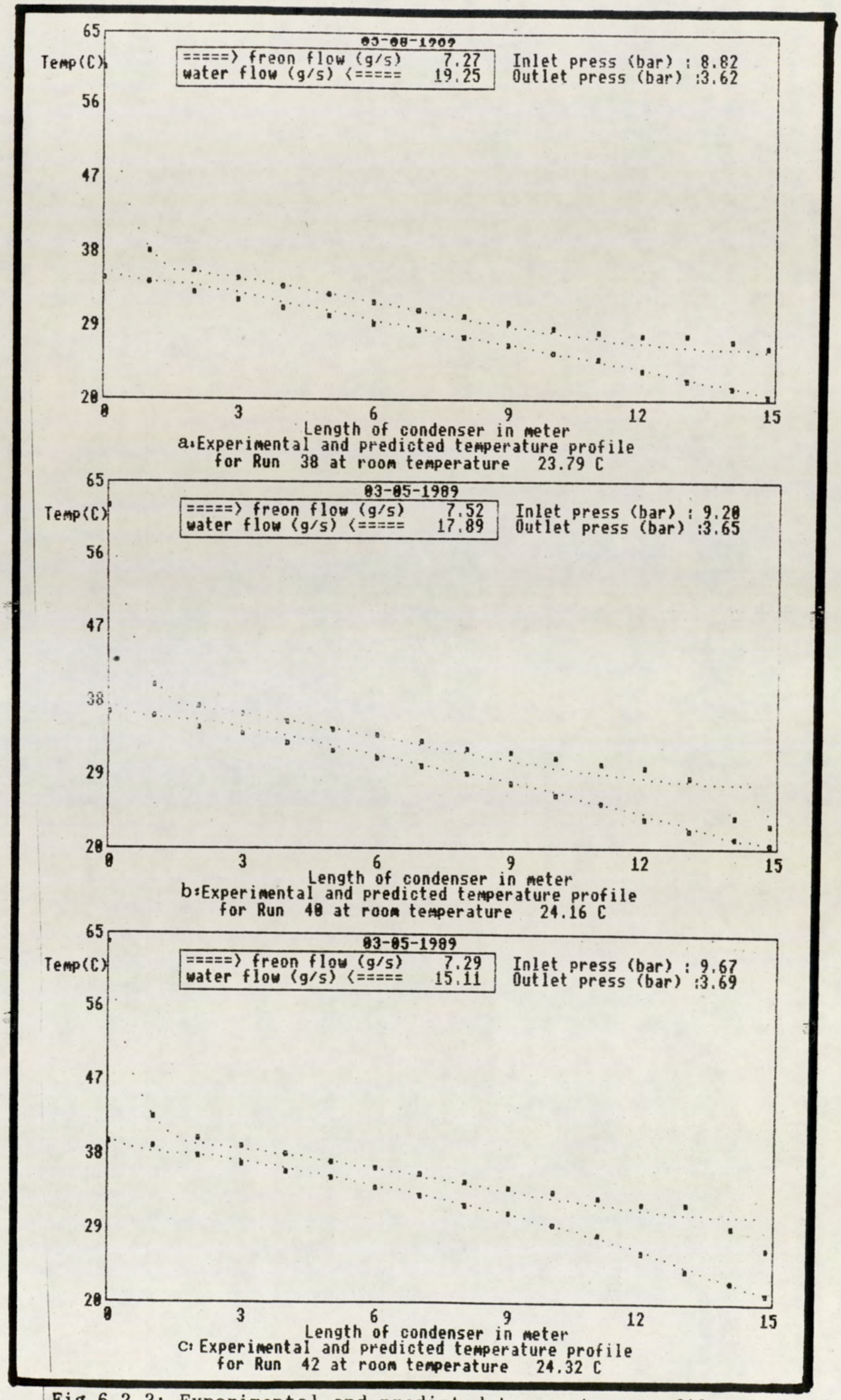

a: Experimental and predicted temperature profile for Run 38 at room temperature 23.79 C

b: Experimental and predicted temperature profile for Run 40 at room temperature 24.16 C

c: Experimental and predicted temperature profile for Run 42 at room temperature 24.32 C

Fig.6.2.3: Experimental and predicted temperature profile of Section B for freon inlet pressure 8.82-12.06 bar

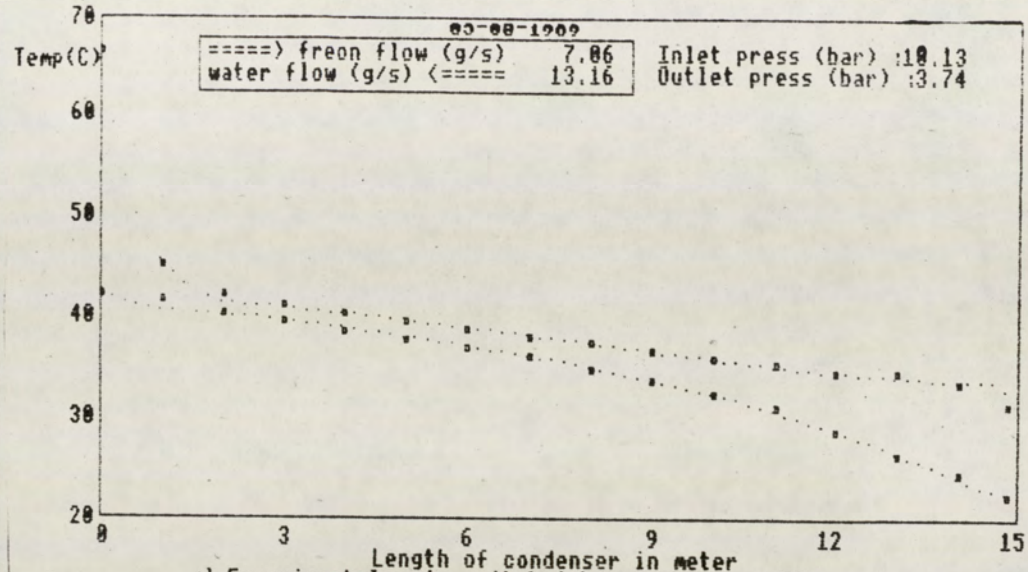

d: Experimental and predicted temperature profile for Run 44 at room temperature 24.78 C

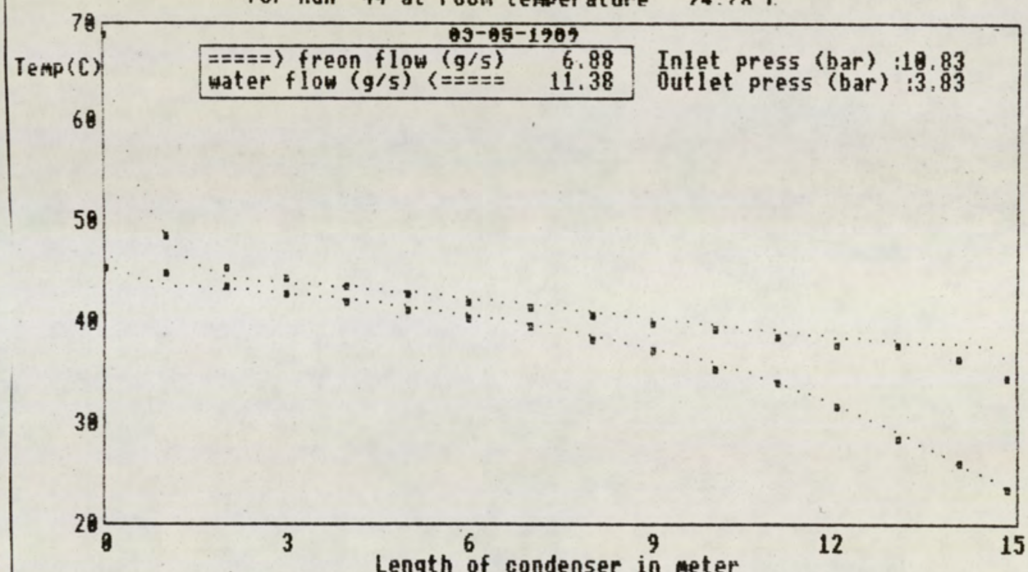

e: Experimental and predicted temperature profile for Run 54 at room temperature 24.88 C

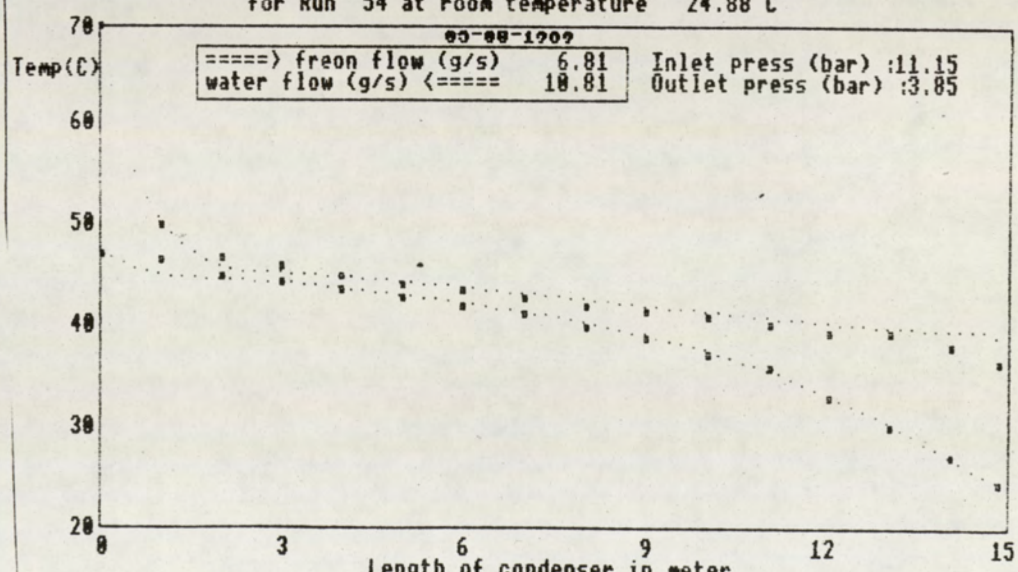

f: Experimental and predicted temperature profile for Run 56 at room temperature 25.17 C

continue

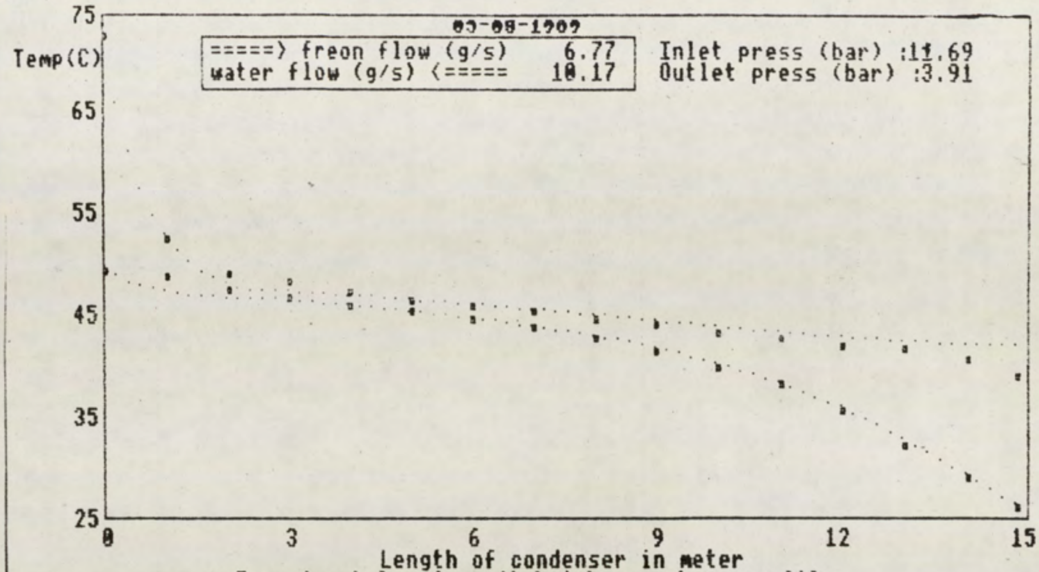

g: Experimental and predicted temperature profile
for Run 59 at room temperature 25.70 C

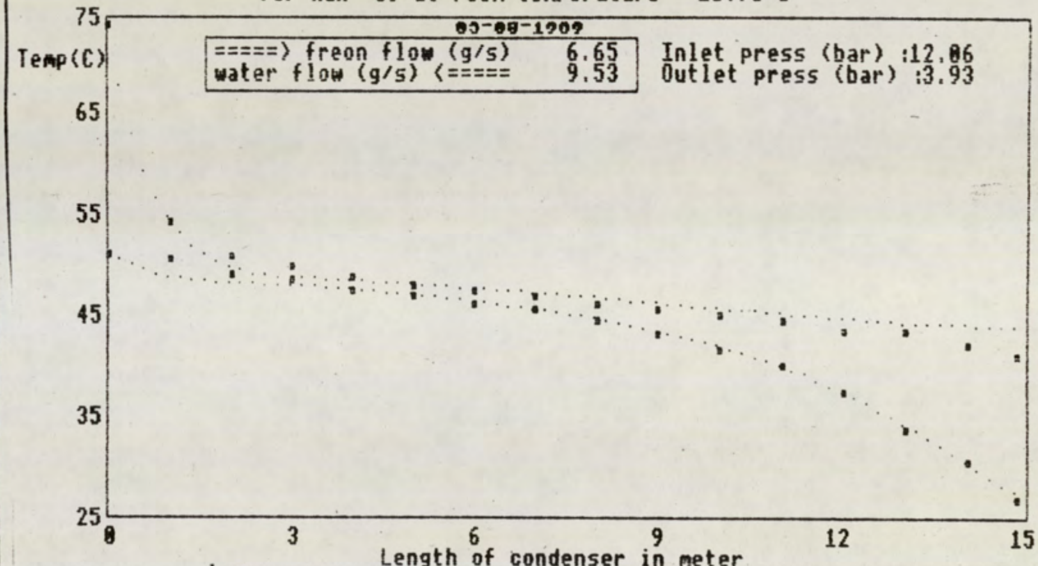

h: Experimental and predicted temperature profile
for Run 61 at room temperature 26.14 C

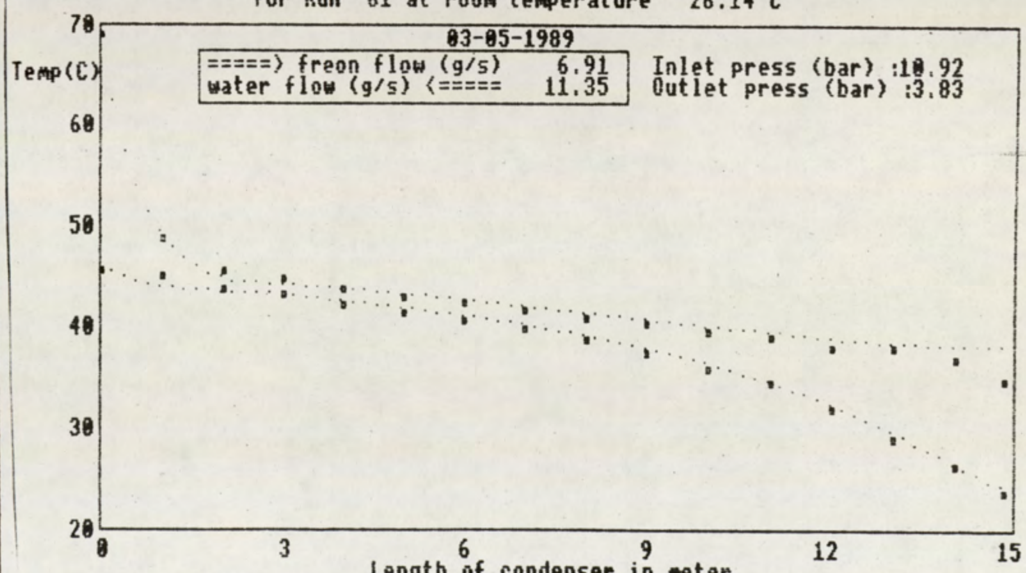

i: Experimental and predicted temperature profile
for Run 55 at room temperature 25.02 C

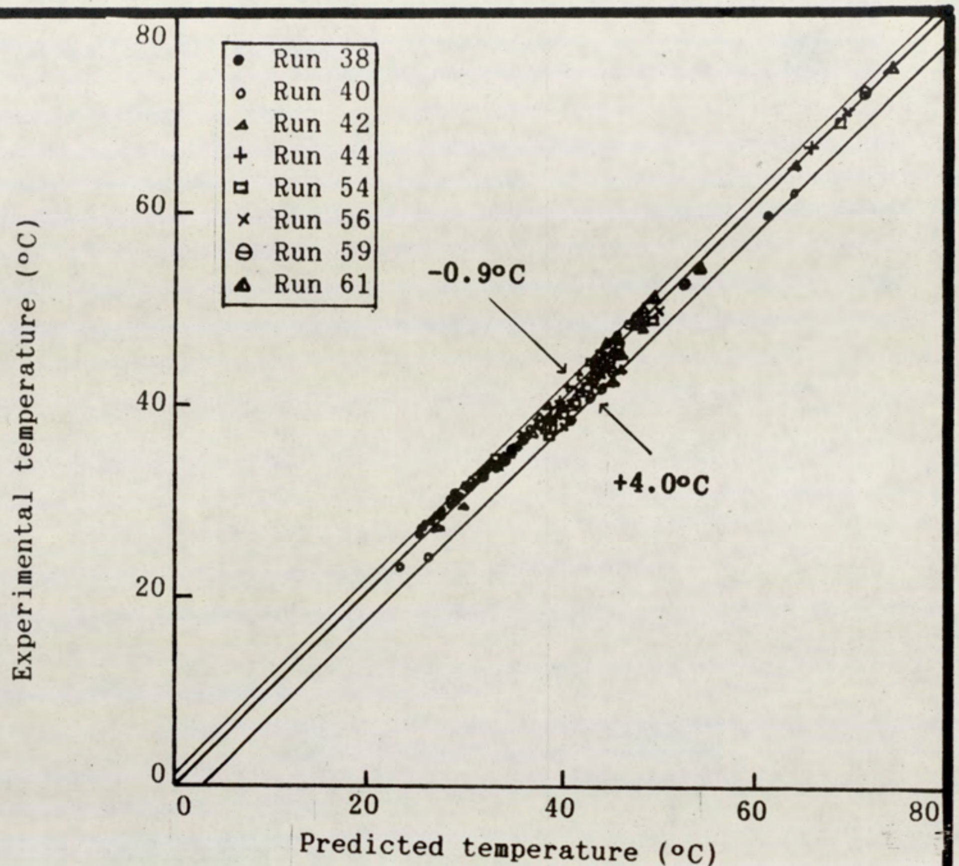

Fig.6.2.4(a): Experimental and predicted temperature profile for the freon side compared (Section B of Table 6.2)

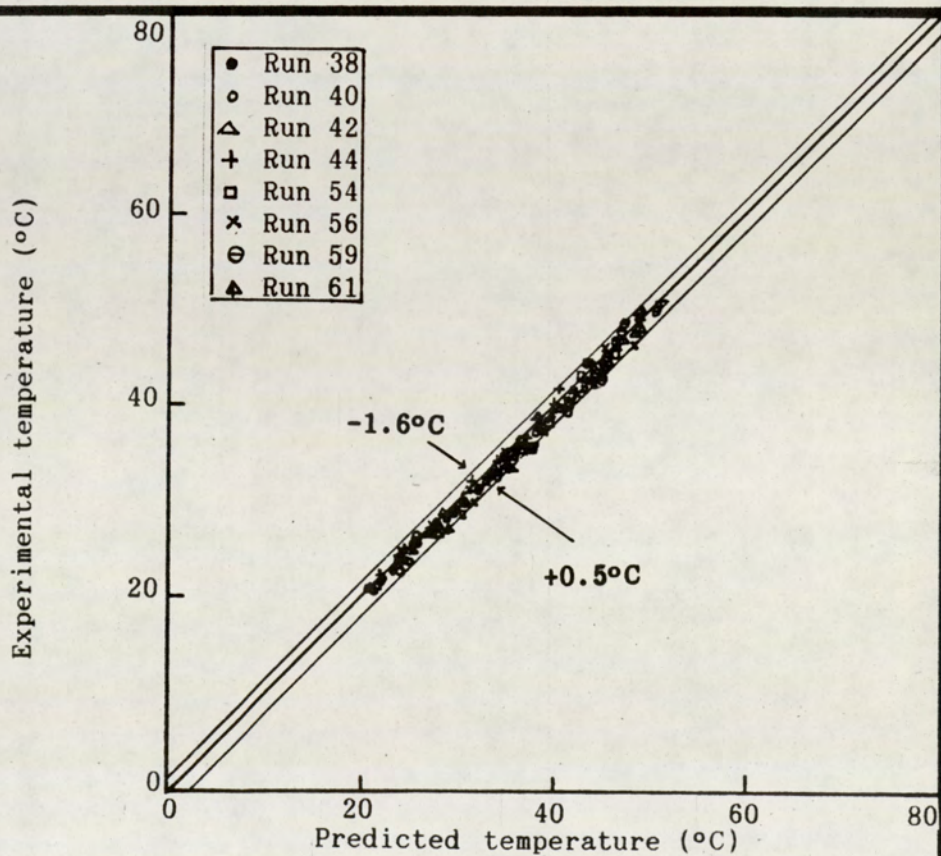

Fig.6.2.4(b): Experimental and predicted temperature profile for the water side compared (Section B of Table 6.2)

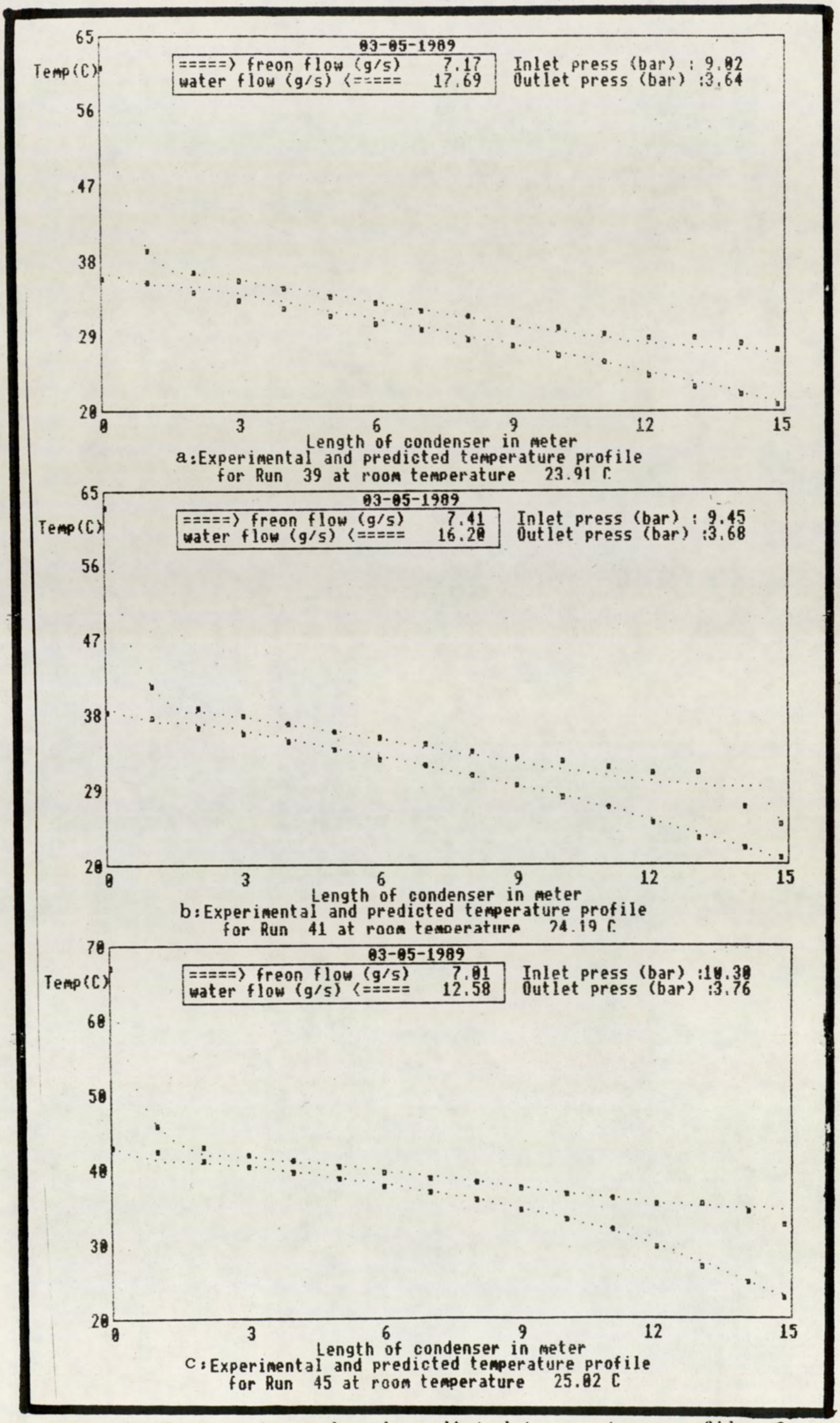

Fig.6.2.5: Experimental and predicted temperature profile of Section C for freon inlet pressure 9.02-12.11 bar

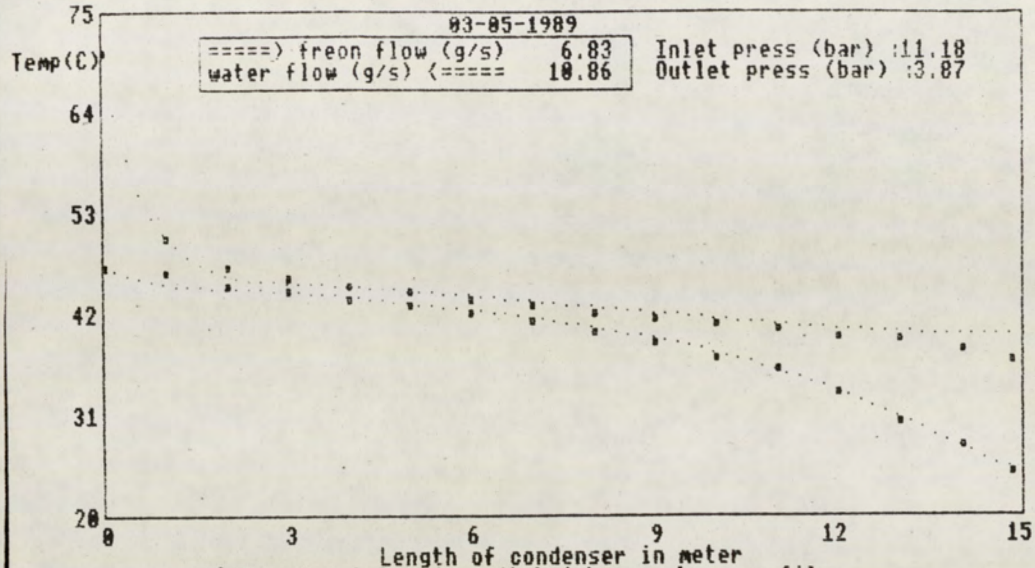

d: Experimental and predicted temperature profile
for Run 57 at room temperature 25.31 C

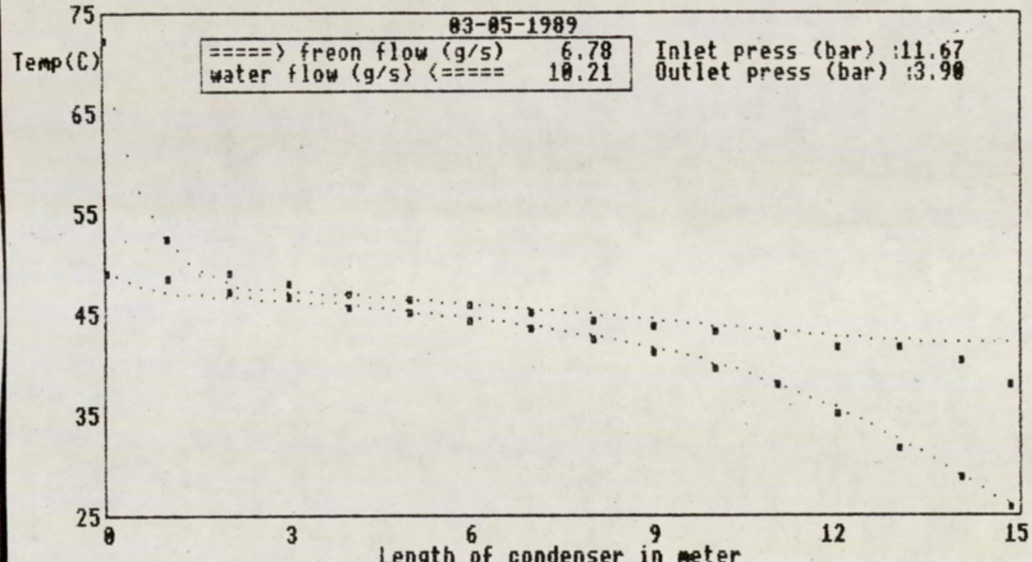

e: Experimental and predicted temperature profile
for Run 58 at room temperature 25.46 C

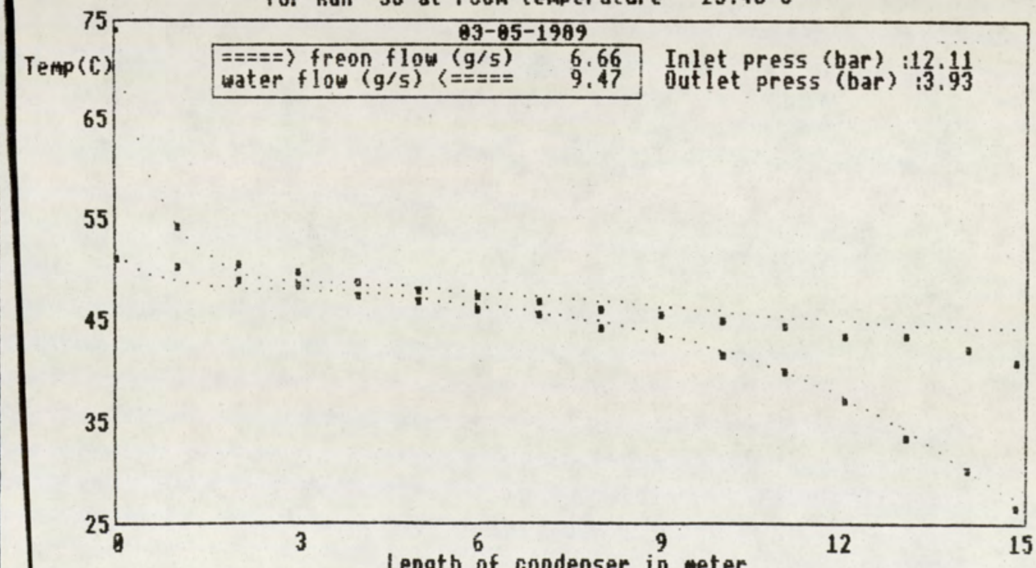

f: Experimental and predicted temperature profile
for Run 60 at room temperature 25.89 C

the distribution quite well in the single vapour region and two-phase region, but differs by a maximum of 2.5°C from the experiment at the end of the two-phase regime. Referring to Fig.6.2.5, it is clearly seen that, in the experiment, the liquid freon occupies a small portion of condenser length compared to the total length of 15 meter. The model predicts the length of the tube occupied completely by the liquid freon is between 2.5×10^{-2} m to 4.25×10^{-1}m.

For the water side, the temperature distributions are in good agreement with the temperatures measured in the experiment. The deviations from the experiment shown in Fig.6.2.6(b) are from -1.4°C to 0.9°C.

Comparison in general

The temperatures along the condenser predicted by the model for the freon side with the same freon inlet temperature (the model uses the same freon inlet temperature as in the experiment as input data) are in quite good agreement with the measurements, except at the few points just before the mixture of liquid-vapour is completely condensed, where the predictions are slightly higher. The predictions in the water side are much better than those in the freon side.

As mentioned in earlier chapters, the iteration is completed when the correct value of outlet water temperature is obtained. The important point is that the outlet water temperature predicted by the model is almost on par with the outlet water temperature measured during experiment with the deviation between -1.6°C to 0.9°C.

The maximum deviation for the freon temperature occured at point 15 of Runm 10 (6.5°C from the measurement) and the minimum deviation at this point is 2.6°C, occured in Runm 5. The overall deviation for the freon temperature along the condenser after using vermiculite insulating materials, room temperature ranged from 23.8°C to 25.9°C, is found to be within -0.9°C to 4.0°C. The overall water temperatures lie between -1.6°C to 0.9°C from the experimental measurement.

There is a sharp drop in the freon temperature between the last point in the mixed-region and the last point in the condenser exit (in subcooling region), but the drop predicted in the two-phase region is quite moderate. Another tremendous drop in the freon temperature is in the vapour region where the drop between the freon inlet temperature and the temperature at the end of the first meter (direction of freon flow) is between 19°C to 24°C. As the freon inlet pressure increases, the drop is moderately decreased.

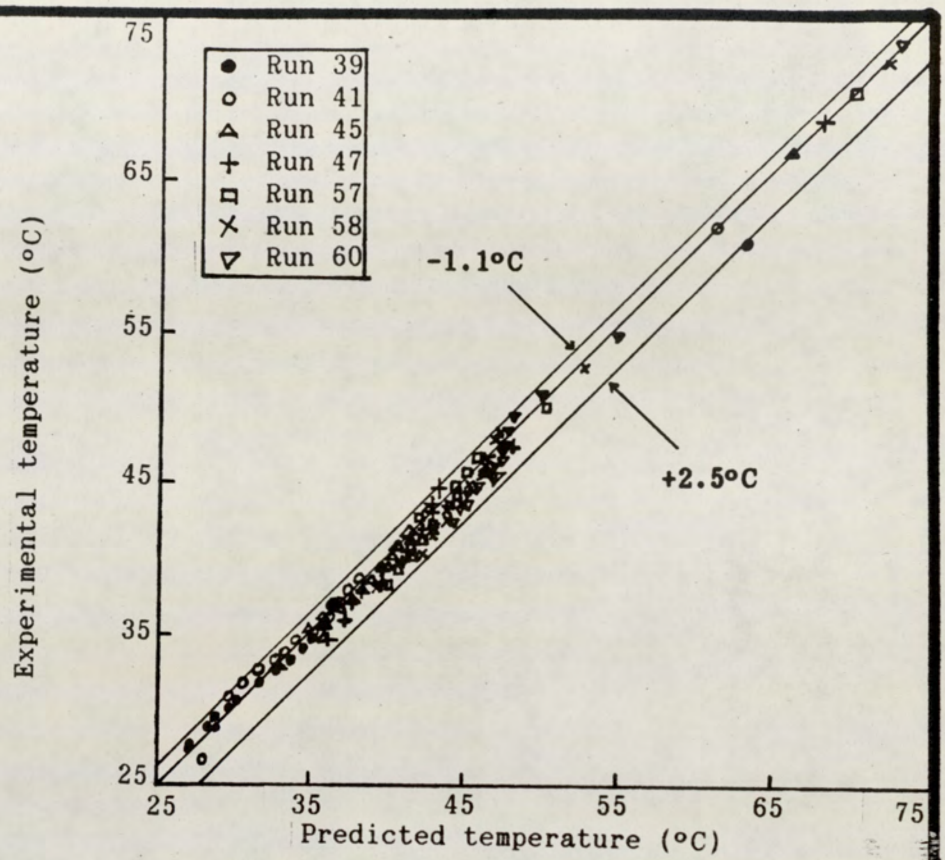

Fig.6.2.6(a): Experimental and predicted temperature profile for the freon side compared (Section C of Table 6.2)

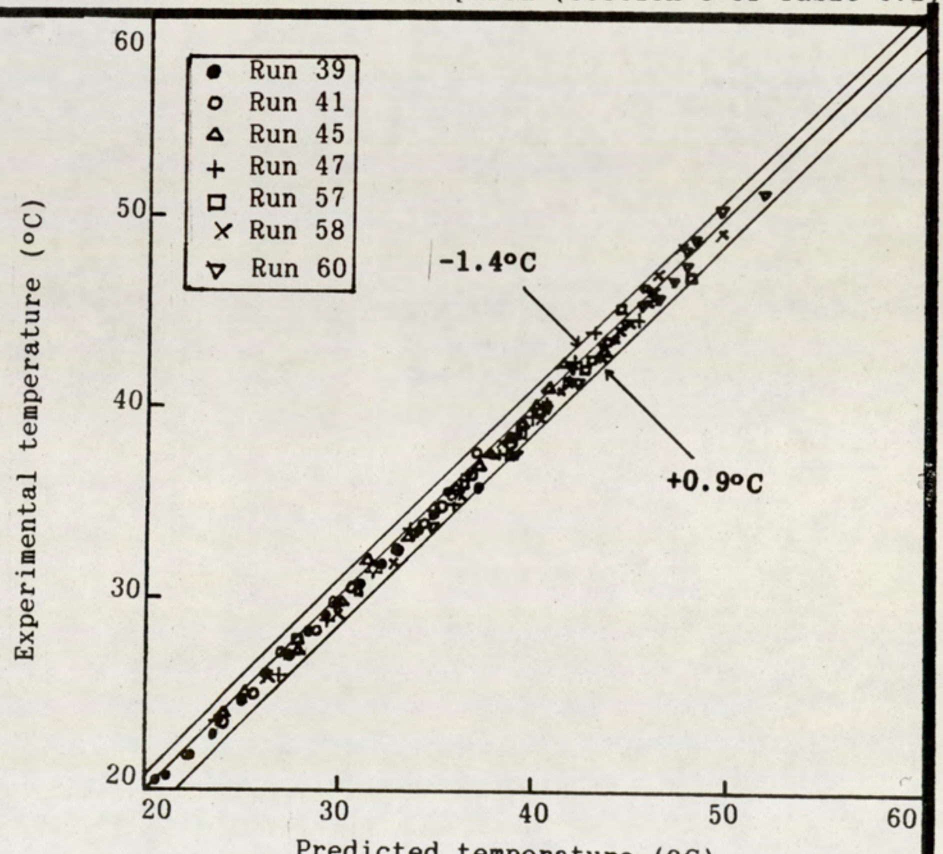

Fig.6.2.6(b): Experimental and predicted temperature profile for the water side compared (Section C of Table 6.2)

For the water side, the temperature rise can be clearly seen after the water enters the condenser exit and flows a few meters through the condenser, and after that the slope is gradually decreased until the water leaves the condenser entry. In general, as it flows, the water picks up more heat at the start of its flow and gradually less as it flows towards the water exit. This can be seen from the figures illustrated earlier where the distance between the two points (both for the freon and water side) of the same position becomes further apart.

6.2.2: Other parameters

Other parameters that can be directly compared are freon outlet pressure, water outlet and inlet temperature, freon outlet temperature, and water and freon mass flowrate. The following discussion is based on the results summarized in Table 6.2 where 29 points are drawn for the inlet pressure ranged from 7.65 bar to 12.11 bar, and 55.4°C to 74.2°C for the freon inlet temperature. These points are also taken from the respective experimental Run which is then compared with the corresponding predicted Runs.

Freon outlet pressure

In this case, the freon outlet pressure is referred to as the freon pressure at the condenser exit. In the heat pump system, it is equivalent to the freon pressure just after leaving the subcooling region. At this point, it is assumed to be in the liquid region of a p-h diagram (the pressure at point 2 in Fig.6.1.8). As the freon flows towards the condenser exit, the pressure and temperature are reduced. At the same time, the water gradually picks up the heat rejected from the freon side, causing an increase in the temperature.

Fig.6.2.7 shows a deviation between -0.63 bar to 0.01 bar from the experimental outlet pressure. Generally, the outlet pressure for various Runs predicted by the model are slightly lower. As the inlet pressure increases, there is also an increase in the outlet pressure with the points in Fig.6.2.7 slowly approaching the reference line. It seems the model predicts quite well at higher freon inlet pressure. For the inlet pressure higher than 10.3 bar, the prediction is almost on par with the experimental measurement. For inlet pressure less than 10.3 bar, the predicted outlet pressures are somewhat scattered, and predict values lower than in the experiment.

Since there is a pressure limit in the pressure transducer used in

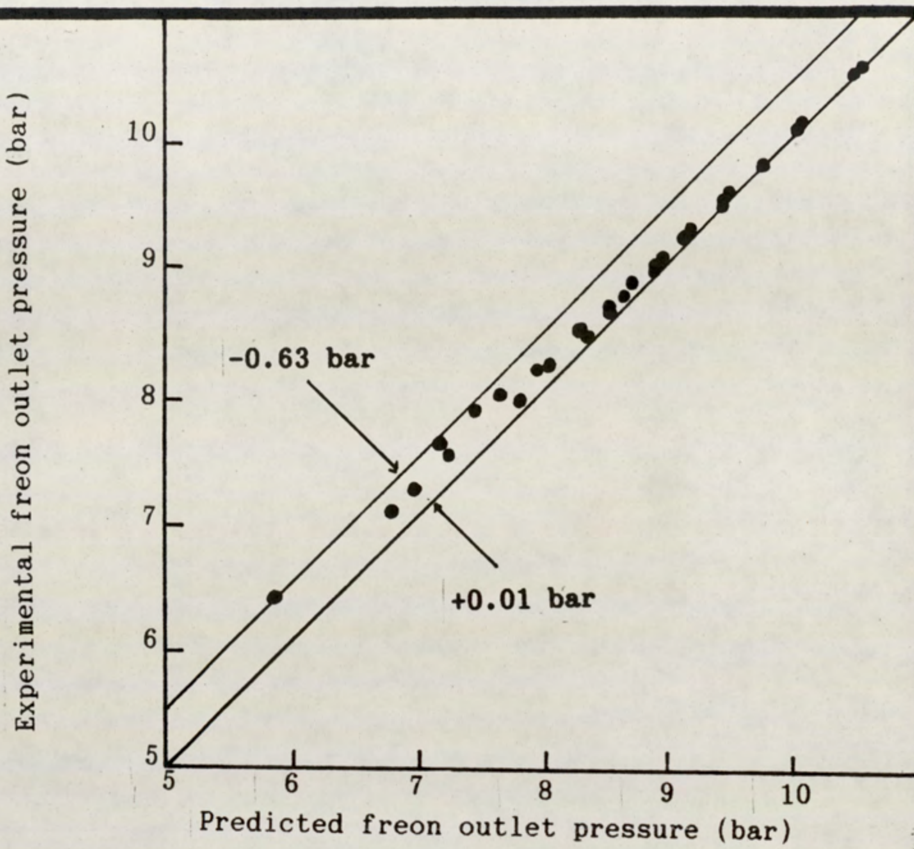

Fig.6.2.7: Experimental and predicted freon outlet pressure compared (from Table 6.2)

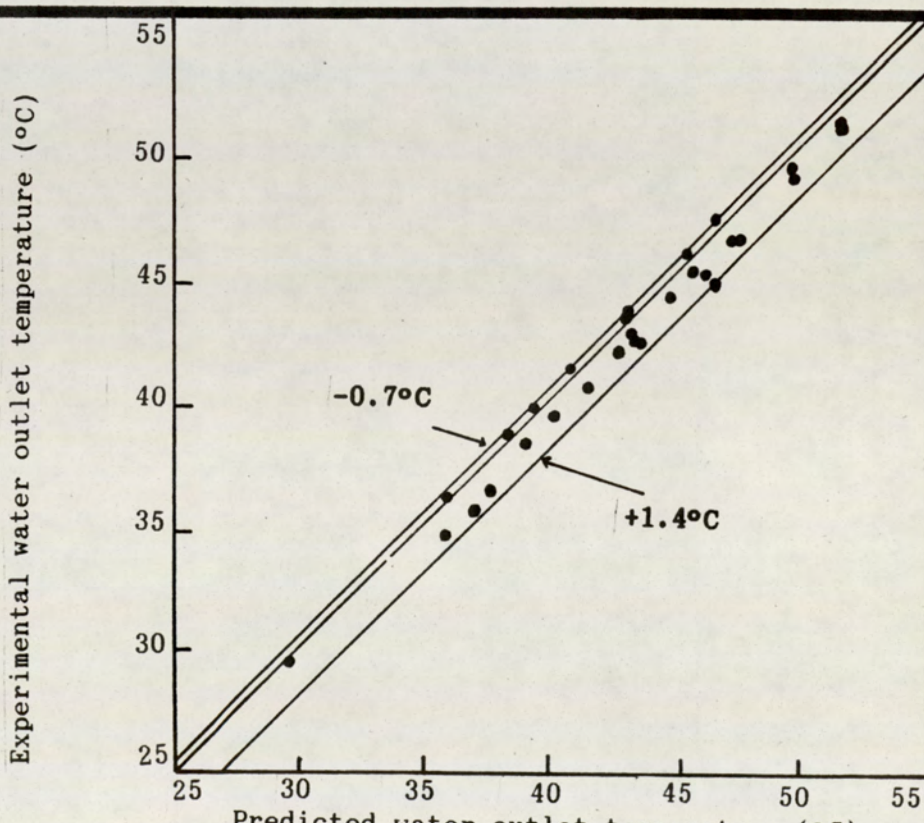

Fig.6.2.8: Experimental and predicted water outlet temperature compared (from Table 6.2)

the system (see chapter 3 and 4), it is difficult to verify the predictions at pressures higher than those operated in the present system. For the inlet pressure ranging from 10.3 bar to 12.1 bar, the prediction of the outlet pressure is in good agreement with experiment (-0.20 bar to 0.01 bar from the measurement).

Water outlet temperature

The correct value of the water outlet temperature indicates whether iteration has completed (see also chapter 5 under modelling) and satisfied all the possible conditions used in the model. The water outlet temperature predicted by the model compared with the measurement is shown in Fig.6.2.8 where the deviation is between -0.7°C to 1.4°C.

The water outlet temperature is greatly influenced by the freon inlet temperature and pressure. As the freon inlet pressure and temperature increases, the water outlet temperature is also increased with a decrease in the water mass flowrate. The ratio of the freon inlet temperature to the water outlet temperature is gradually decreased at higher inlet pressure. It means (in term of ratio), the water outlet temperature is much closer to the freon inlet temperature at lower inlet pressure. For the given operating condition, the ratio decreases from 1.85 to 1.45.

About 69% of the points which represent the water outlet temperature recorded by the model lie just above the experimental line. This means the model predicts a slightly higher value than the water outlet temperature measured in the experiment.

Freon outlet temperature

This concerns the temperature at point 2 of **Fig.6.1.8(a)** or the temperature at the condenser exit. For higher freon inlet temperature, the freon outlet temperature is relatively higher, with a decrease in the freon mass flowrate. Similarly, it is greatly dependent upon the freon inlet pressure.

Fig.6.2.9 shows a summary from 29 Runs, illustrating the deviation from the measured values within a range of -1.1°C to 3.4°C. More than 50% of the recorded points lie to the right of the reference line. It was estimated that about 62% of the freon outlet temperatures predicted by the model are higher than those measured in the experiment.

Water inlet temperature

The water inlet temperature predicted by the model is very close to that measured. Fig.6.2.10 shows a deviation from the experiment, ranging from -0.2°C to 0.3°C. For the freon inlet pressure and temperature ranging from 7.65 bar to 12.11 bar and 55.4°C to 73.9°C respectively, the output predicted by the model is slightly higher than that measured.

The increase in the water outlet temperature as the freon inlet pressure and temperature increases is small and quite constant. The difference between the two consecutive temperatures (at one meter distance) is almost constant as illustrated in **Fig.6.2.10**. In general, the increase seems to be almost linear with the increase in the freon inlet pressure and temperature at given operating conditions.

Overall freon temperature drop

In this case, the overall freon temperature drop across the condenser is regarded as the difference between the freon inlet temperature and the freon outlet temperature. Referring to **Fig.6.1.8(a)**, the temperature drop is between the temperature at point 1 and at point 2. The overall drop in the temperature and pressure is used to calculate the overall freon thermal power across the condenser by treating the difference in the specific enthalpy at these two points.

The predicted overall temperature drop as shown in **Fig.6.2.11** shows that the points are scattered within -3.4°C to 2.7°C from the central line. In general, the drop increases for higher freon inlet pressure.

Overall water temperature drop

Similarly, the drop is based on the two points corresponding to the two points discussed in the overall freon temperature drop (above) but in the opposite direction of flow. The drop in the water temperature is more orderly and the points are more closer to the reference line as shown in Fig.6.2.12.

It was found that the deviation from the expriment is from -0.9°C to 1.2°C. At given operating conditions, the prediction shows, more than 50% of the overall temperature drop are slightly higher than that measured.

The water mass flowrate can be directly calculated from the overall temperature drop by introducing the constant value of water specific heat or can be calculated from the difference in the water specific enthalpy at those two points.

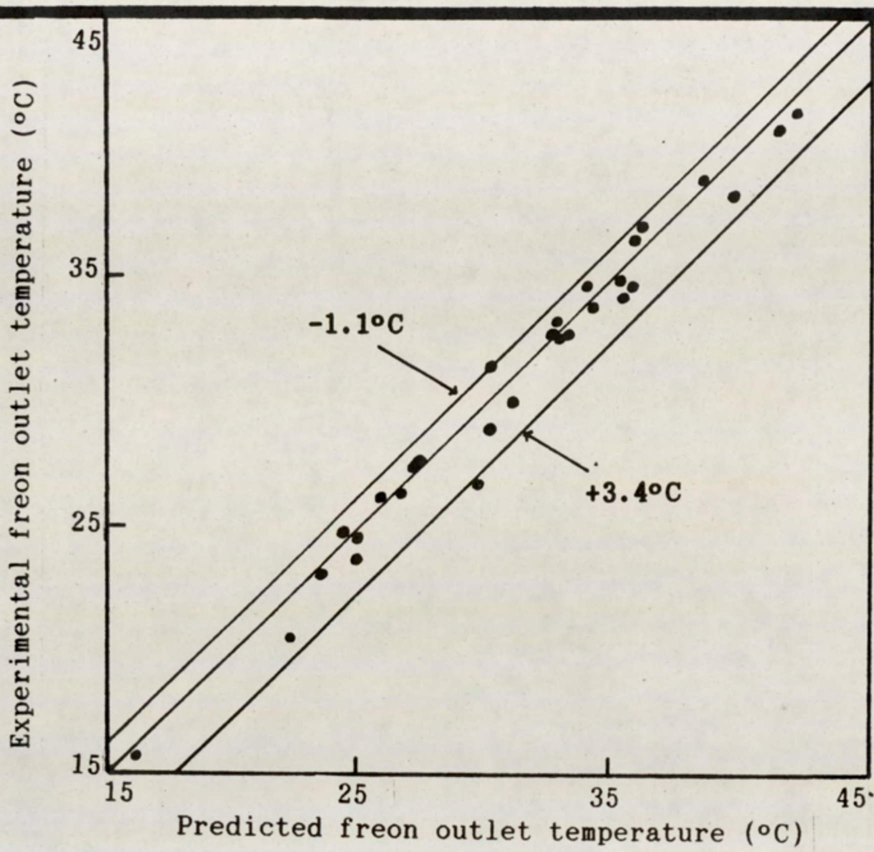

Fig.6.2.9: Experimental and predicted freon outlet temperature compared (from Table 6.2)

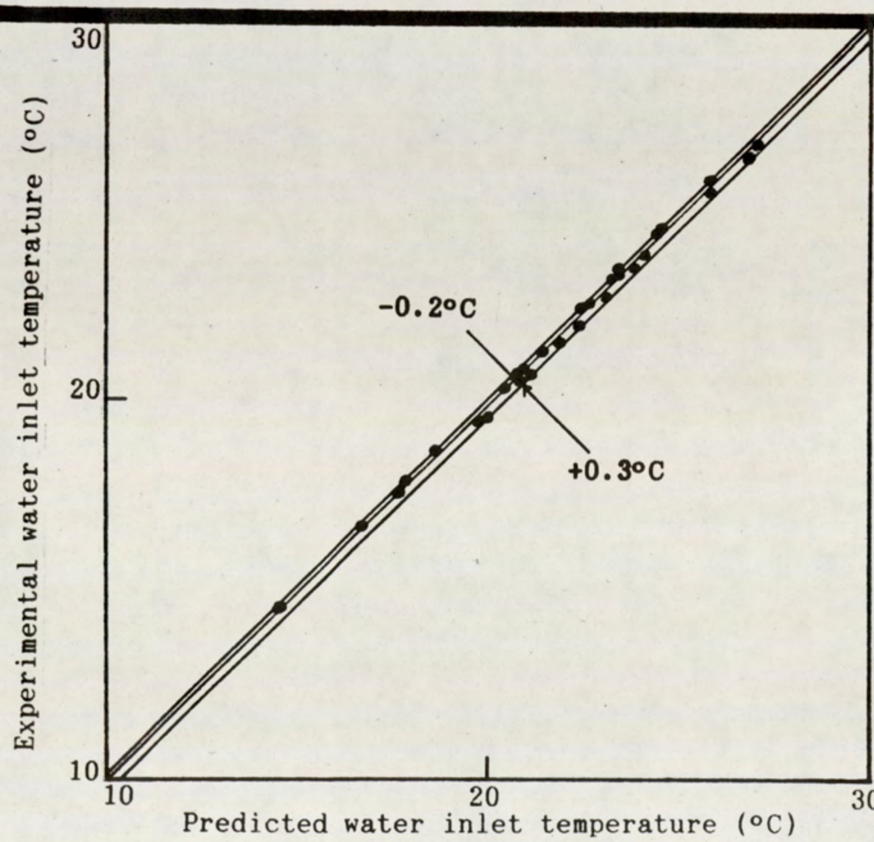

Fig.6.2.10: Experimental and predicted water inlet temperature compared (from Table 6.2)

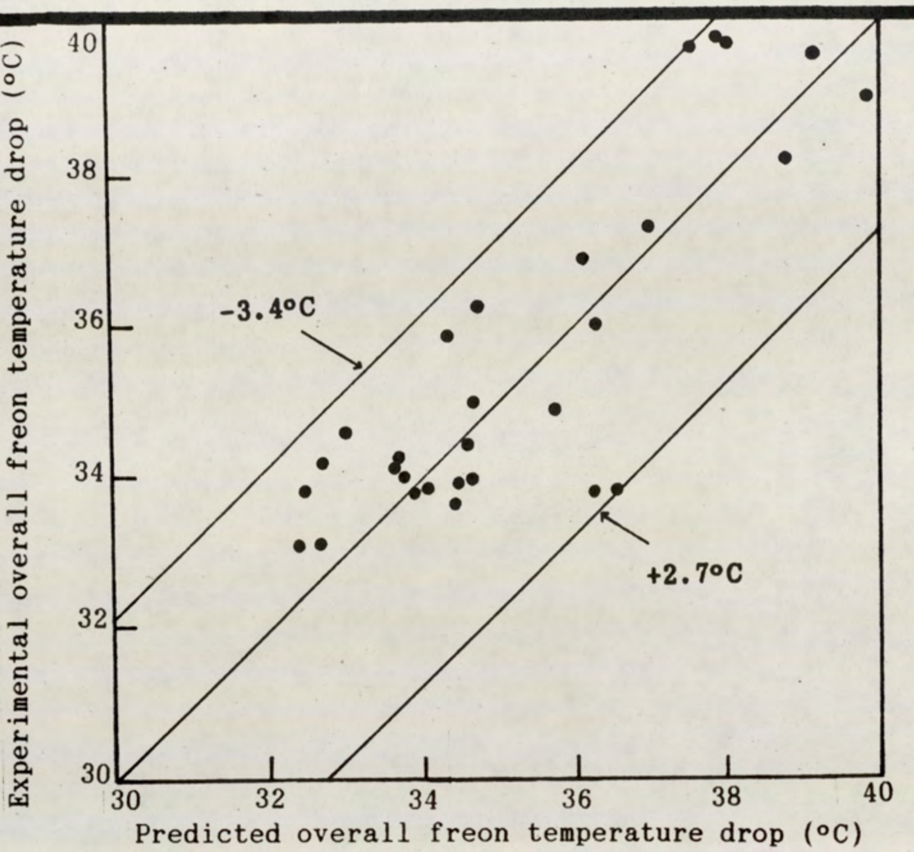

Fig.6.2.11: Experimental and predicted overall freon temperature drop compared (from Table 6.2)

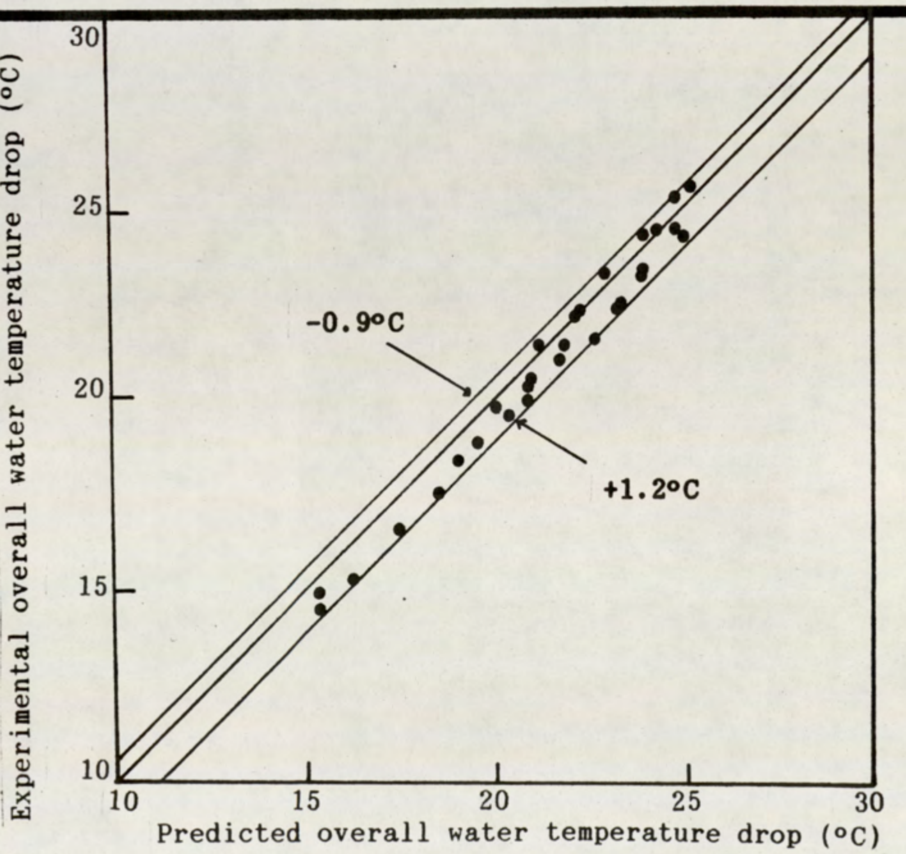

Fig.6.2.12: Experimental and predicted overall water temperature drop compared (from Table 6.2)

Freon mass flowrate

The freon mass flowrate predicted by the model is found to be slightly lower than that calculated in the experiment. As the freon inlet pressure and temperature increases, the flowrate is decreased.

Fig.6.2.13 shows a comparison where for given operating conditions, the model predicts less by between 0.2 g/s in Run■ 9 (minimum value) and 0.1 g/s in Run■ 5 (maximum value). About 72% of the recorded Runs■, indicate the freon mass flowrate is scattered between 6.5 g/s to 7.5 g/s and fairly closed to the reference line.

Water mass flowrate

The water mass flowrate is more spread within the operating conditions. As the freon inlet pressure and temperature imcreases, the amount of water flow in the condenser per second slowly decreases.

Fig.6.2.14 illustrates the comparison based on the 29 sets of data described in Table 6.2 where the minimum value was predicted less by 1.7 g/s in Run■ 38 and higher by 0.2 g/s in Run■ 5 for maximum value (from the experimental measurement). The tremendous decrease can be seen at the lower inlet pressure, but as the pressure increases, the decrease is not so great. Most of the points drawn in Fig.6.2.14 are quite close to the central line.

6.2.3: Summary

The following tables give an overall summary which compares the experimental measurements with the results of the same Run predicted by the model. The comparison is based on the following operating conditions, 7.65 bar to 12.11 bar for the freon inlet pressure, and 55.4°C to 74.2°C for the freon inlet temperature, which consist of 29 Runs.

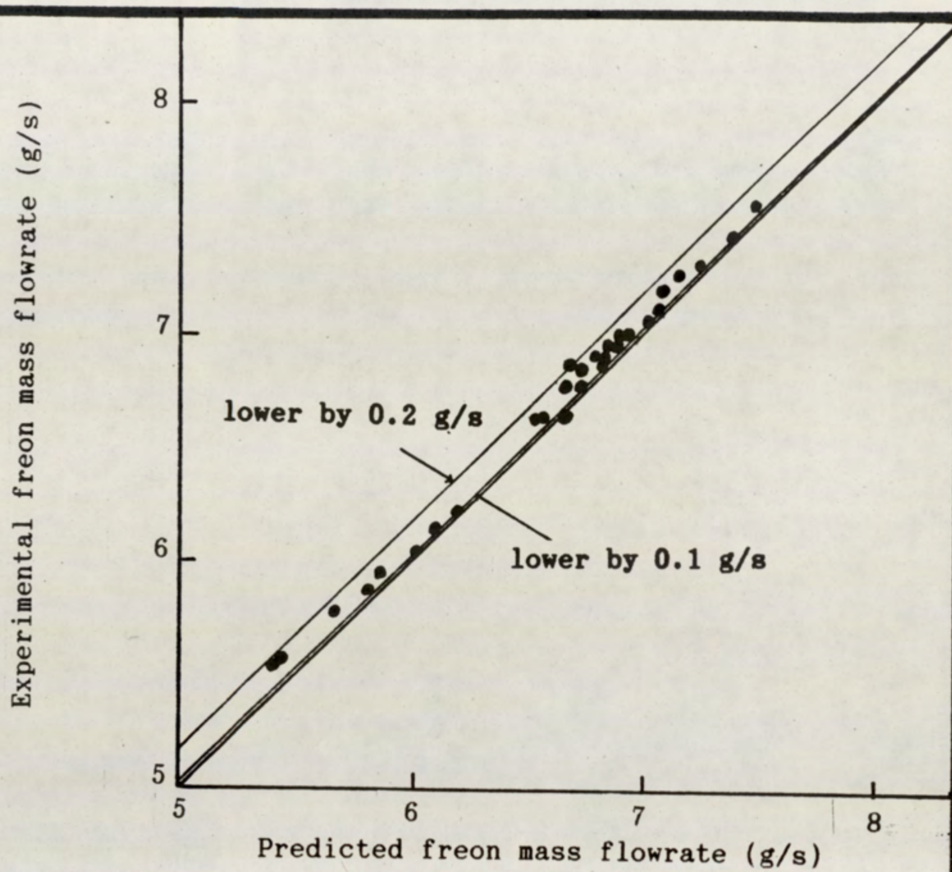

Fig.6.2.13: Experimental and predicted freon mass flowrate compared (from Table 6.2)

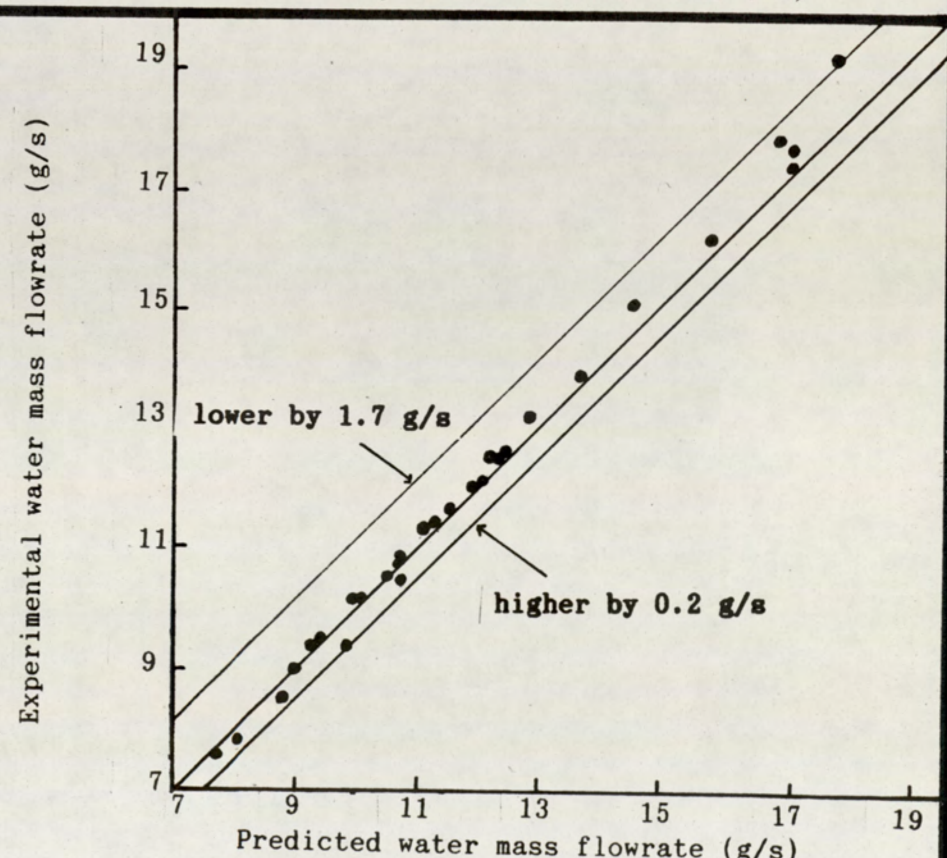

Fig.6.2.14: Experimental and predicted water mass flowrate compared (from Table 6.2)

Items	Deviation from experiment minimum	maximum	Refer to figure
Temperature profile (Section A)			
Freon side (°C)	-1.7	6.5	6.2.1(a)
Water side (°C)	-1.6	0.8	6.2.1(b)
Temperature profile (Section B)			
Freon side (°C)	-0.9	4.0	6.2.4(a)
Water side (°C)	-1.6	0.5	6.2.4(b)
Temperature profile (Section C)			
Freon side (°C)	-1.1	2.5	6.2.6(a)
Water side (°C)	-1.4	0.9	6.2.6(b)
Freon outlet pressure (bar)	-0.63	0.01	6.2.7
Water outlet temperature (°C)	-0.7	1.4	6.2.8
Freon outlet temperature (°C)	-1.1	3.4	6.2.9
Water inlet temperature (°C)	-0.2	0.3	6.2.10
Overall freon temperature drop (°C)	-3.4	2.7	6.2.11
Overall water temperature drop (°C)	-0.9	1.2	6.2.12
Freon mass flowrate (g/s)	-0.2	-0.1	6.2.13
Water mass flowrate (g/s)	-1.7	0.2	6.2.14

(negative and positive sign means the model predicts lower and higher than the experiment respectively)

Table 6.4: Summary of overall results compared

6.3: Thermodynamic and physical properties in three-separate region

In this section, the discussion focuses on the results predicted by the model by assuming the comparisons described above are within the experimental agreement. The thermodynamic and physical properties of the freon and water in three-separate region (desuperheating-, condensing-, and subcooling-regime) are discussed based on the values calculated at the entry of each region. The possible average or total values based on the fluid properties for the whole region are also outlined.

The properties of water is also divided to three sections corresponding to the three separate regions in the freon side, although it has been assumed earlier that only liquid water flows throughout the system. What is important is to predict the water properties at the positions where there exist the three regions in the freon side. The results are based on the 29 Runs■ described earlier in **Table 6.2** within the operating conditions.

6.3.1: Length in each segment

The results predicted in Section A correspond to the experiment where the system is insulated by the polystyrene materials with the freon inlet pressure ranging from 7.65 bar to 10.89 bar. As the freon inlet pressure increases, the length of desuperheater is also increased from 1.475 m to 2.375 m. At the same time, the length of condensing and subcooling region decrease from 12.7 m to 12.4 m and 0.825 m to 0.225 m respectively. In general, more length is used for the mixture of liquid-vapour freon to flow in the condenser but a small portion of the tube is used for the liquid freon to flow in the subcooling region. Comparatively, at higher freon inlet pressure more freon vapour, and liquid-vapour mixture occupy the condenser tube.

Similarly, in Section A and B, when the freon inlet pressure increases, the length of desuperheater is also increased (more freon present in vapour state at higher pressure). At the same time, the length of condensing region, where freon is in a state of liquid-vapour mixture, slowly decreases with the decrease in the length of subcooler.

For the inlet pressure range from 8.82 bar to 12.06 bar in Section B, the length of desuperheater is increased from 1.675 m to 2.475 m, and the length of condensing and subcooling region decreases from 13.3 m to 12.5 m and from 0.525 m to 0.025 m respectively. For the inlet pressure range from 9.02 bar to 12.11 (Section C), the length of desuperheater increases from 1.675 m to 2.575 m , while the length of two-phase and subcooling region decreases from 13.30 m to 12.40 m and from 0.425 m to 0.025 m respectively.

The length of subcooling segment is very small compared to the length of the two other segments, especially at higher inlet pressure. There is a possibility at a higher pressure, if the pressure transducer can measure a pressure higher than the operating pressure, that only two regions (desuperheating and condensing region) can be seen clearly and the subcooling region does not exist.

6.3.2: Refrigerant thermodynamic and physical properties

<u>Heat transfer coefficient</u>

The refrigerant heat transfer coefficient is higher in the liquid region than in the vapour region. As the pressure and temperature at the condenser entry increases, its value in all the three regions are decreased. The results show that the heat transfer coefficients in the vapour, two-phase, and liquid region are respectively as follows; 6.711×10^2-$8,523\times10^2$ W/m^2.°C, 3.975×10^3-4.900×10^3 W/m^2.°C, and 8.592×10^2-1.356×10^3 W/m^2.°C. These values are calculated at the entry of each region.

<u>Linear heat transfer coefficient</u>

For the linear heat transfer coefficient, it is found that the value predicted by the model is higher in the mixed-region than the values in two other regions. The range of linear heat transfer coefficient within the operating conditions for the desuperheating, condensing, and subcooling region is summarized in the following order; 8.965-1.138x10 W/m.°C, 5.306x10-6.540x10 W/m.°C, and 1.153x10-1.818x10 W/m.°C .

Refrigerant Reynolds number

The freon Reynolds number is higher in the vapour region (in the order of 10^5), so that the flow is characterized by the turbulent flow mechanism. The Reynolds number in the two other regions (two-phase and liquid region) is in the order of 10^3-10^4, where the flow is determined either by the turbulent or laminar or transition flow mechanism. As the freon inlet pressure increases, the Reynolds number is decreased in all the regions. The range of the Reynolds number in the three regions is as follows; 1.112×10^5-1.557×10^5 in the vapour region, 2.711×10^3-4.954×10^3 in the two-phase region, and 7.959×10^3-1.021×10^4 in the liquid region.

Refrigerant number of transfer units

The number of transfer units is higher in the vapour region, while the lowest value can be found in the two-phase region. As the freon inlet pressure increases, the value is gradually increased in the vapour region, but decreased in the two-phase and subcooling region. It was estimated that the value is in the range of 2.782 to 3.885 in the vapour regime, 0.111 to 0.162 in the condensing regime, and 0.117 to 1.207 in the liquid regime.

Freon specific enthalpy and specific entropy

These parameters are used to calculate the average freon mass flowrate from the energy equation. The specific enthalpy and specific entropy are high in the vapour but decrease in the two-phase and subcooling regions (refer to p-h diagram in Fig.6.1.5). There is a great drop in the specific enthalpy as the freon enters the subcooling region. Both of these thermodynamic parameters are greatly influenced by the pressure and temperature.

Based on the calculation in the model, the specific enthalpy is within the range of 217.8-226.0 kJ/kg in the vapour region, 199.6-206.1 kJ/kg in the mixed region, and 55.4-76.6 kJ/kg in the liquid region.

As the pressure and temperature increases, the specific entropy in the vapour and two-phase region decreases, and increases in the liquid region (refer to p-h diagram in Fig.6.1.5). It is found that the specific entropy decreases from 7.439×10^{-1} kJ/kg.°C to 7.367×10^{-1} kJ/kg.°C in the vapour region, 6.855×10^{-1} kJ/kg.°C to 6.801×10^{-1} kJ/kg.°C in the two-phase region, and increases from 2.270×10^{-1} kJ/kg.°C to 2.781×10^{-1} kJ/kg.°C in the subcooling region.

<u>Temperature and pressure</u>

Finally, the temperature and pressure predicted at the beginning of each segment shows that there is a great drop in the temperature from the vapour region to condensing region. Comparatively, the temperature drop from the two-phase region to the subcooling region is not so great.

The drop in the pressure from the two-phase region to the subcooling region is much higher than the drop from the vapour region to the two-phase region. the pressure at the beginning of the two-phase region is from 7.46-11.93 bar, and from 5.77-10.64 bar in the liquid region. By percentage, the longer the length in each region, the greater is the drop in the pressure.

6.3.3: Water thermodynamic and physical properties

As earlier mentioned, the water was assumed to flow in the liquid state throughout the process, but in this case, the properties at corresponding points in each segment of the freon side are described.

There is an increase in the water heat transfer coefficient, Reynolds number, and water temperature as the water flows from the condenser exit to the condenser entry which is equivalent to the travel from liquid region exit to the vapour region entry of the freon side. A summary of some properties of water at the equivalent entry of each region within the operating conditions is shown in the following table,

Properties	Value at corresponding length in each segment (based on freon side)					
	Vapour region		Two-phase region		Subcooling region	
	minimum	maximum	minimum	maximum	minimum	maximum
Heat transfer coefficient (W/m².°C)	9.79×10^2	4.48×10^3	7.91×10^2	3.49×10^3	7.40×10^2	2.58×10^3
Linear heat transfer coeff. (W/m².°C)	1.69×10	7.73×10	1.36×10	6.48×10	1.31×10	4.59×10
Reynolds number	2.95×10^3	5.56×10^3	2.57×10^3	4.82×10^3	1.82×10^3	3.82×10^3
Number of transfer units	0.1875	0.5240	4.3681	5.5924	0.0152	0.1054
Water temperature (°C)	29.7	51.5	28.0	48.2	14.8	27.0

Table 6.5: Summary of some properties of water

6.3.4: Properties of freon and water in general

As the freon inlet pressure increases the overall linear heat conductance in each segment decreases, the value in the two-phase region being higher than the value in the two other regions. Within the operating conditions, the model shows a variation from 10.12 W/m.°C to 5.85 W/m.°C in the vapour region, 30.45 W/m.°C to 10.56 W/m.°C in the two-phase region, and 13.02 W/m.°C to 6.14 W/m.°C in the liquid region. The overall heat conductance is evaluated from the linear heat transfer coefficient of freon and water.

The effectiveness in each segment (see **Eqn.5.49** and **Eqn.5.50**), which is calculated using ε-Ntu method, is greatly affected by the number of transfer units. The effectiveness of the condenser in the vapour and two-phase segments is higher than the effectiveness in the liquid segment. The higher the freon inlet pressure and temperature, the higher is the effectiveness of the condenser in the vapour and two-phase segments. It was calculated that the effectiveness varies from 92.99% to 96.98% in the vapour regime, and from 87.30% to 96.50% in the two-phase regime. The effectiveness in the last region decreases as the pressure increases. It is estimated that, within the working conditions, the effectiveness in the liquid segment decreases from 68.77% to 10.92% as the pressure increases. The overall effectiveness is within 67.87% to 83.02%.

Finally, with increase in the freon inlet pressure and temperature, there is a decrease in the total thermal power; 1209 W to 817 W. Based on the total energy across the condenser, more than 80% is transferred in the two-phase region as latent heat of vapourization . The remainder occurs in the two other segments, with the vapour region being greater. The energy released from the freon side is picked up by the water side as the freon flows into the condenser.

The results show that there is an imbalance between the energy being transferred by the freon and the energy gained by the water. Within the operating conditions, the energy imbalance is from -1.05% to 0.16% of the total energy being transferred from the freon side.

6.4: Other physical and thermodynamic profiles predicted by model

In this section, parameter distributions other than the freon and water temperature profiles predicted along the condenser are discussed. It is assumed that the predictions described earlier are within the experimental range. Various parameters are plotted for one meter intervals, based on the results summarized in **Table 6.2**.

In general, as the freon flows through the condenser, the pressure, wall temperature, vapour quality, freon and water heat transfer coefficient, number of transfer units of water, and overall linear heat transfer coefficient are all decreased in value. An increase in the freon inlet pressure causes an increase in the value of the parameters described above.

The parameters described above, taken from 20 Runs$_{m}$, ranging from 7.65 bar to 12.11 bar for the freon inlet pressure and 55.4°C to 74.2°C for the freon inlet temperature, are discussed.

6.4.1: Freon pressure

There is a sequence of patterns illustrated in **Fig.6.4.1 (a,b and c)** as the freon flow along the condenser. These patterns did not change very much as the freon inlet pressure increases, except at higher pressure.

Fig.6.4.1(a) shows the results taken from Section A of **Table 6.2**, where the drop between each meter becomes smaller as the freon inlet pressure increases from 7.65 bar to 10.89 bar. The distribution is almost linear at higher pressure. Similarly, **Fig.6.4.1(b and c)** show the results taken from Section B and C respectively, which illustrate a bigger drop in the pressure at lower freon inlet pressure but the drop becomes less at higher inlet pressure.

At higher freon inlet pressure, the pressure drop across the condenser decreases and the pressure distribution is almost linear.

6.4.2: Vapour quality

The vapour fractions in the vapour and liquid regions are taken to be 1 and 0 respectively. The amount of freon vapour (by weight) contained in the two-phase region is determined by the vapour quality. A greater percentage of vapour quality means more vapour present in the condensing region. As the freon flow from the two-phase entry, the amount of vapour will be slowly decreased as the flow reaches the two-phase exit. On the

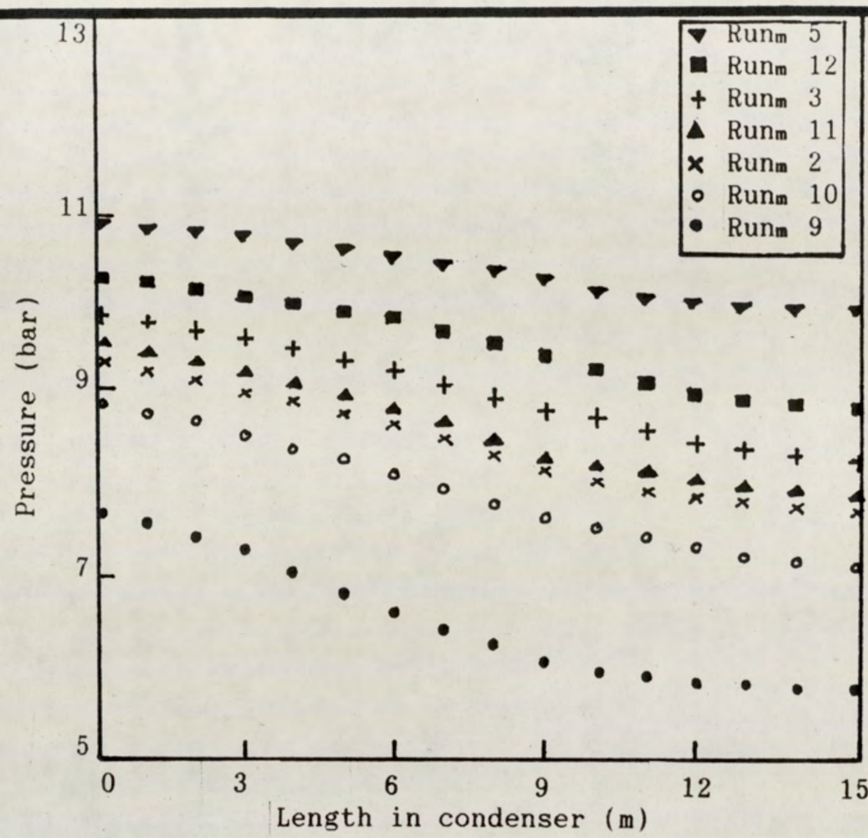

Fig.6.4.1(a): Refrigerant pressure distribution for Run$_m$ in Section A (Table 6.2)

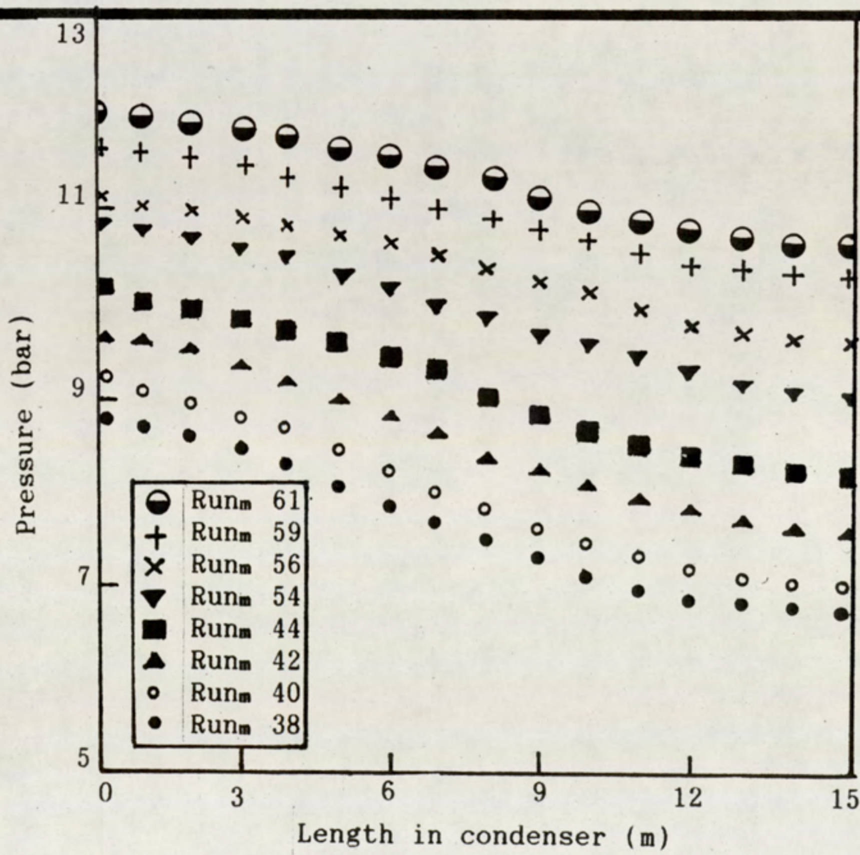

Fig.6.4.1(b): Refrigerant pressure distribution for Run$_m$ in Section B (Table 6.2)

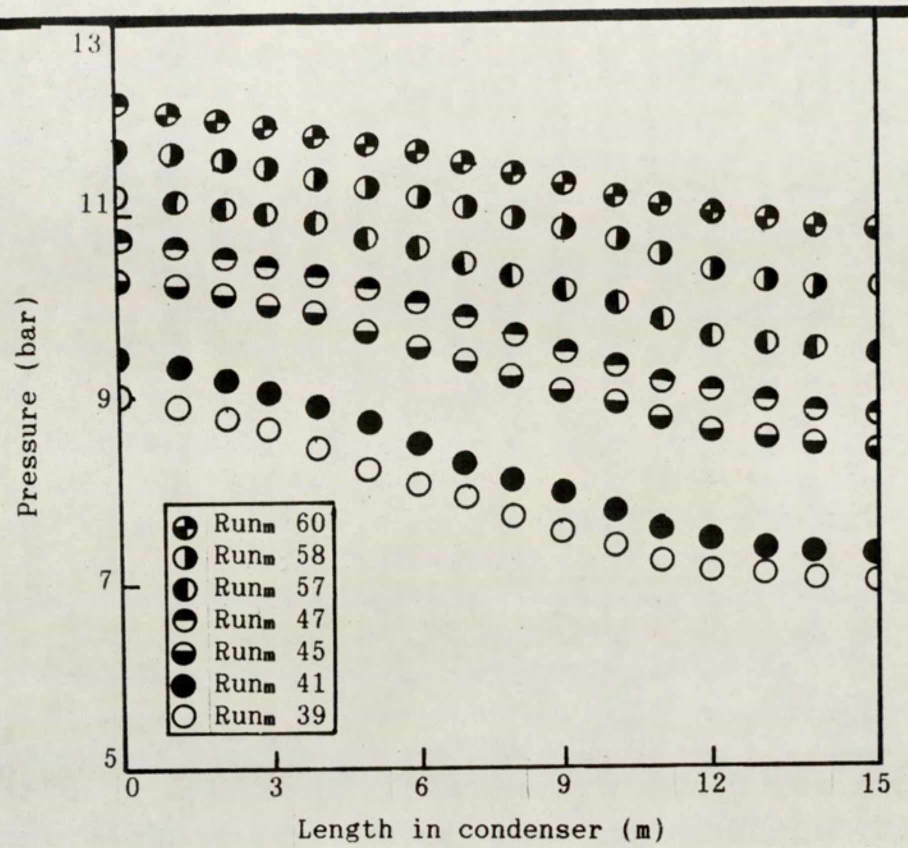

Fig.6.4.1(c): Refrigerant pressure distribution for Run■ in Section C (Table 6.2)

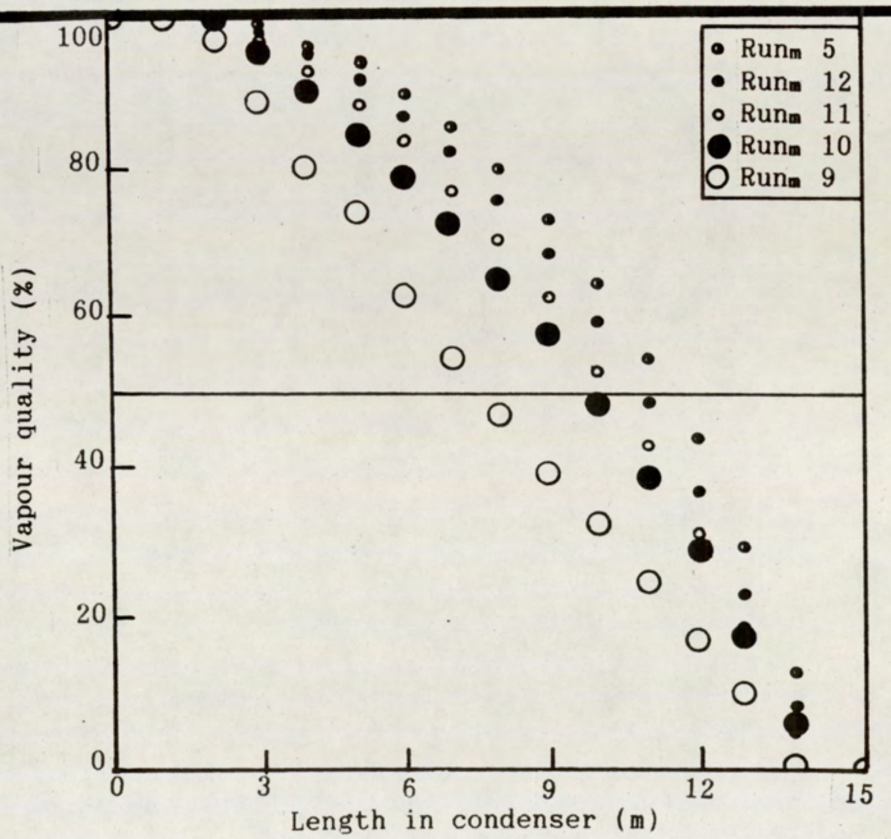

Fig.6.4.2(a): Vapour quality distribution for Run■ in Section A at inlet pressure 7.65-10.89 bar

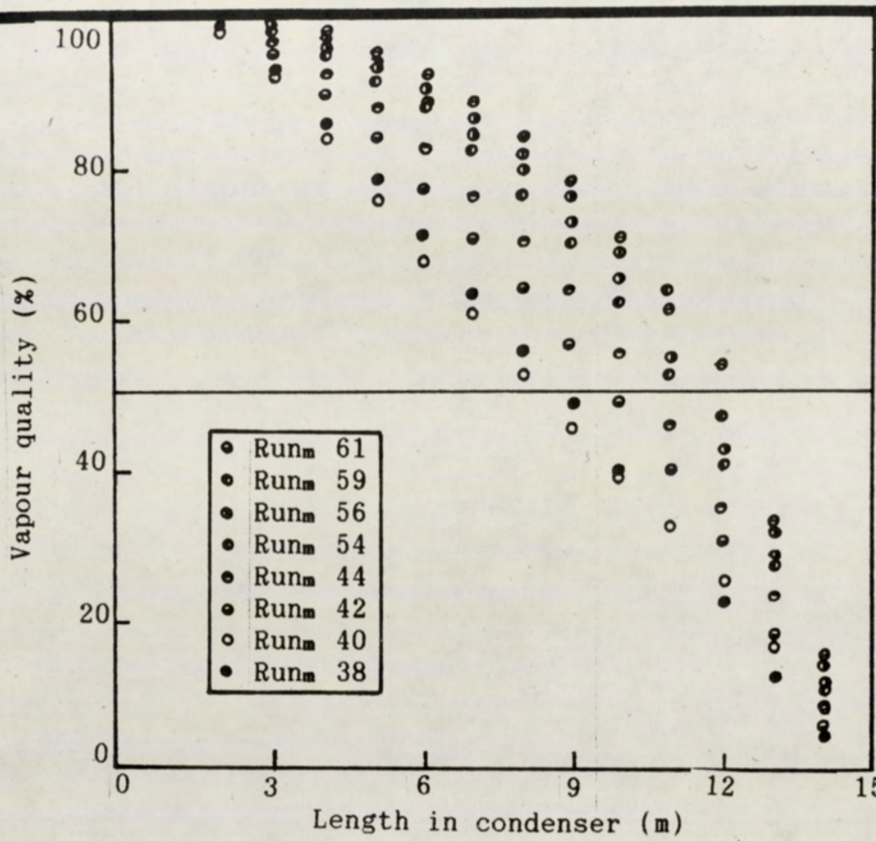

Fig.6.4.2(b): Vapour quality distribution for Runm in Section B at inlet pressure 8.82-12.06 bar

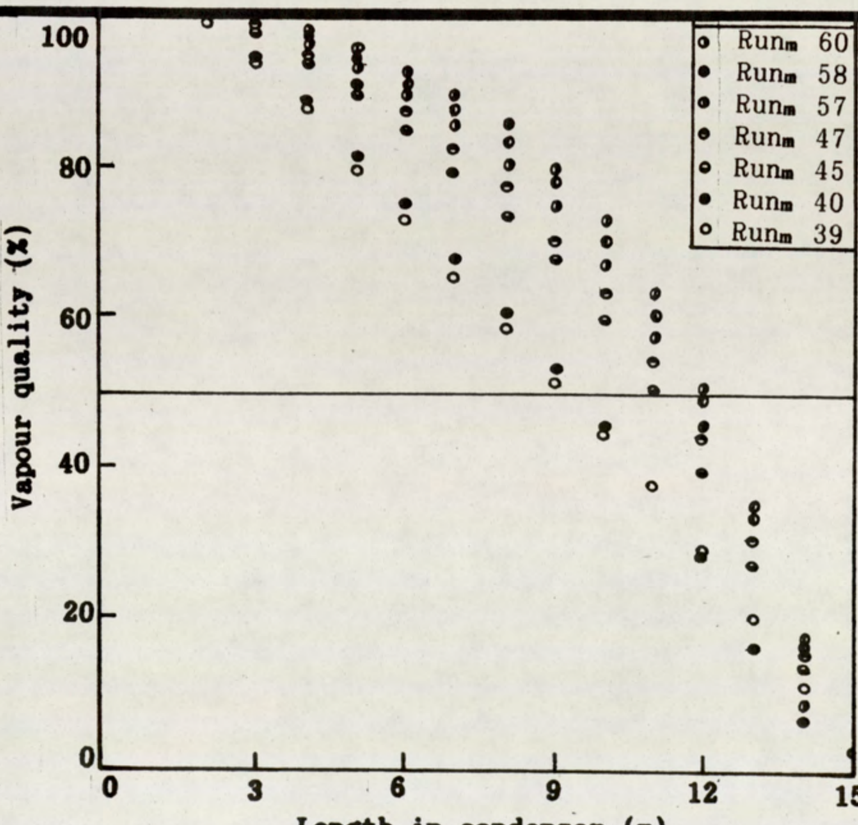

Fig.6.4.2(c): Vapour quality distribution for Runm in Section C at inlet pressure 9.02-12.11 bar

other hand, the amount of liquid freon increases as the flow reaches the condenser exit.

Fig.6.4.2(a,b and c) show examples of quality profiles at one meter intervals, taken from results in Section A, B and C of Table 6.2 respectively. At lower freon inlet pressures, the decrease in the amount of freon vapour is almost linear. As the pressure increases, the pattern shows a convex-shape, with the amount of vapour decreasing sharply as the flow reaches the two-phase exit.

The decrease in the vapour quality indicates the increase in the amount of liquid freon in the flow. It is estimated that, for inlet pressure between 7.65 bar to 12.11 bar, the two-phase region contains equal amounts of freon vapour and freon liquid roughly at a distance between 7.5 m to 12.0 m (measured from the condenser entry) and denoted by a straight line drawn parallel to the length-axis in Fig.6.4.2(a,b and c).

In general, within the operating conditions, the model predicts between 81.3% to 86.7% of the total condenser length occupied by the mixture of freon liquid-vapour in the two-phase region.

6.4.3: Heat transfer coefficient

The freon heat transfer coefficient in the liquid region is greater than that in the vapour region, but in general, smaller than that in the mixed region. The value in the two-phase region is greater at the beginning of the region and reduces as the vapour quality decreases. The decrease in the heat transfer coefficient in the vapour and liquid regions is not so great, since the freon occupies a small length of condenser compared to the length of condensing region.

As the freon inlet pressure and inlet temperature increases, the heat transfer coefficient in the vapour and liquid region is decreased. For the given conditions, the decrease is between 8.68×10^2 $W/m^2.^oC$ to 6.88×10^2 $W/m^2.^oC$ (about 21% drop) in the vapour region and from 1.11×10^3 $W/m^2.^oC$ to 8.56×10^2 $W/m^2.^oC$ (about 23% drop) in the subcooling region.

Fig.6.4.3(a) shows an example of heat transfer coefficient profile at one meter intervals along the condenser, taken from the results in Section A. There is a sequence drop in the two-phase region.

As the water flow through the condenser , the water heat transfer coefficient increases (starting from the subcooling exit of the freon side). The increase in the value is not so marked as the decrease in the freon side. The coefficients at the bends of the tube were found to be higher than those in the straight pipe. As mentioned in an earlier chapter,

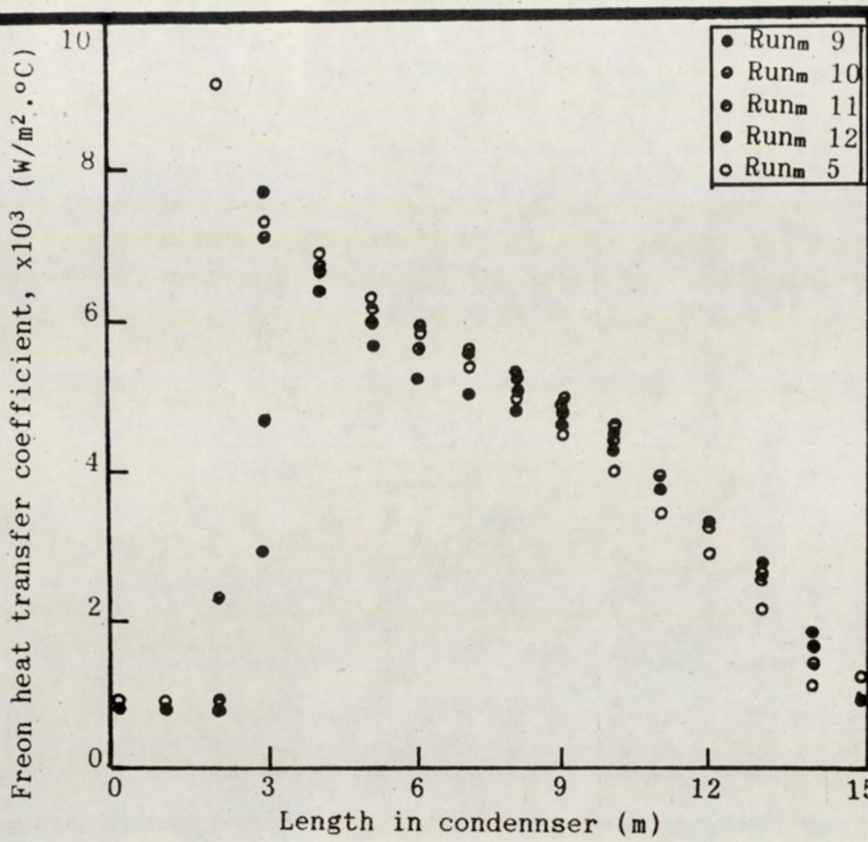

Fig.6.4.3(a): Freon heat transfer coefficient distribution of Section A at inlet pressure 7.65-10.89 bar

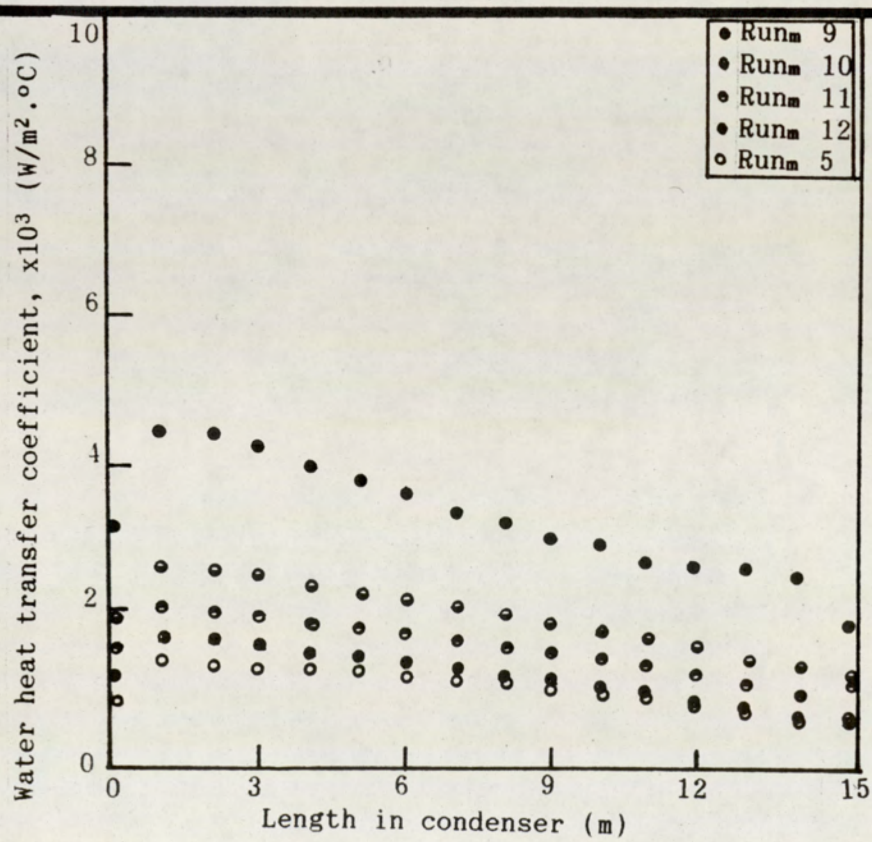

Fig.6.4.3(b): Water heat transfer coefficient distribution of Section A at inlet pressure 7.65-10.89 bar

the pipe diameter at the bend was assumed to be slightly smaller than the diameter of straight pipe. This is quite important because the heat transfer coefficient is inversely proportional to the pipe diameter; the smaller the pipe diameter, the bigger the heat transfer coefficient.

Fig.6.4.3(b) shows an example of water heat transfer coefficient taken from the results in Section A, plotted one meter intervals. As the freon inlet pressure and inlet temperature increases, the coefficients decrease, with the drop in the value between each meter becoming smaller. Within the given operating conditions, the model predicts the coefficients lie between 7.90×10^2 $W/m^2.°C$ to 5.98×10^3 $W/m^2.°C$.

6.4.4: Overall heat transfer coefficient

The inverse of the overall heat transfer conductance is the sum of the inverse of linear freon and water heat transfer coefficient. It is used to evaluate the number of transfer units, which is then employed to calculate freon and water temperature distributions along the condenser. Tha value predicted by the model is an average value which greatly depends upon the freon and water heat transfer coefficients.

The value calculated in the vapour region is lower than the value evaluated in the two-phase and subcooling region. As the freon flows, the overall heat transfer coefficients decrease with decrease in the freon inlet pressure. The sharp drop in the value can be seen in the two-phase region, with very small increase in the subcooling region, as the freon flows through the condenser.

Fig.6.4.4(a,b and c) illustrate the results taken from Section A, B and C of Table 6.2 respectively. Section A shows a drop from 8.6% to 6.7% (equivalent to a drop from 9.17 W/m.°C to 5.59 W/m.°C) in the vapour region corresponding to respective Runs. There is a small increase in the value when the freon just enters the two-phase region, but after that, the value decreases slowly. The coefficient decreases from 4.38x10 W/m.°C to 5.44 W/m.°C in the two-phase region but increases from 5.96 W/m.°C to 1.11x10 W/m.°C in the subcooler.

Fig.6.4.4(b) shows another result (Section B) which covers the pressure from 8.82 bar to 12.06 bar. The same pattern of profile can be seen in this result, the overall heat transfer coefficient dropping from 1.04x10 W/m.°C to 7.55 W/m.°C in the vapour region, 4.49x10 W/m.°C to 6.39 W/m.°C in the two-phase region, and increasing from 7.70 W/m.°C to 1.26x10 W/m.°C in the subcooling region.

Similarly, Fig.6.4.4(c), where the inlet pressure ranges from 9.02

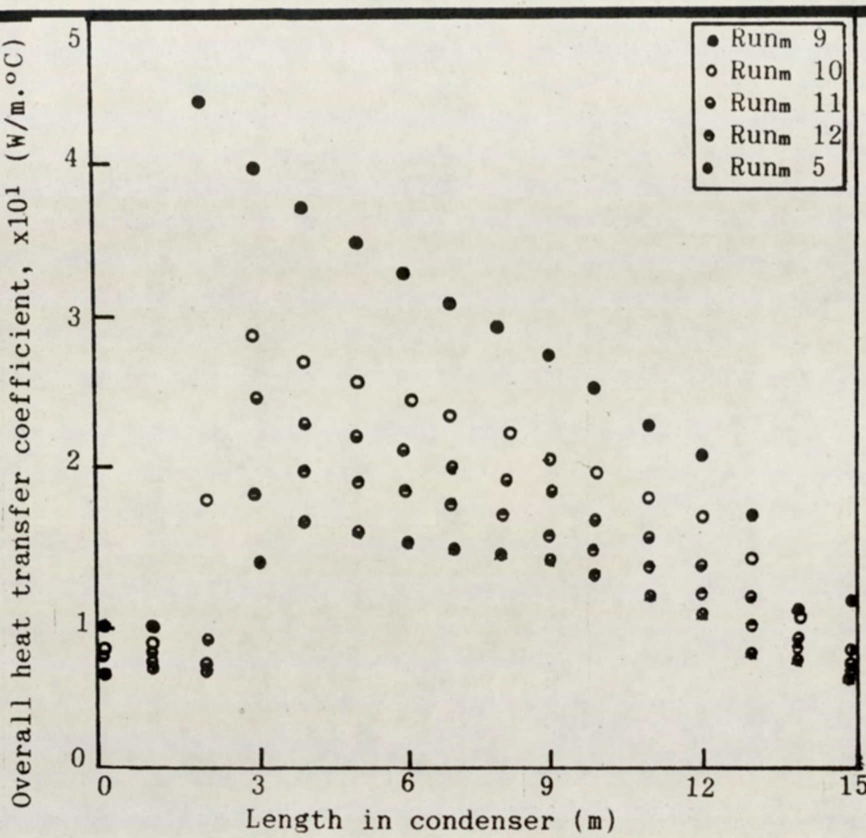

Fig.6.4.4(a): Overall heat transfer coefficient for Runm in Section A at inlet pressure 7.65-10.89 bar

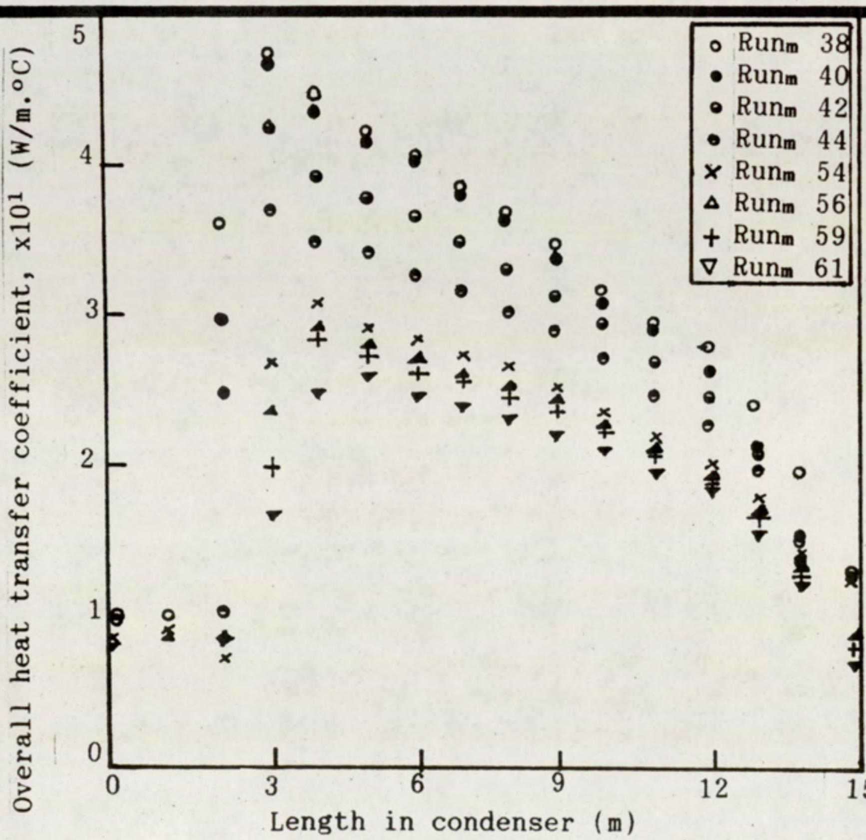

Fig.6.4.4(b): Overall heat transfer coefficient for Runm in Section B at inlet pressure 8.82-12.06 bar

bar to 12.11 bar, shows roughly the same pattern as above. The drop in the vapour region is from 1.03x10 W/m.°C to 7.96 W/m.°C, 4.49x10 W/m.°C to 6.49 W/m.°C for the two-phase region, and an increase from 7.66 W/m.°C to 1.38x10 W/m.°C in the liquid region.

6.4.5: Wall temperature distribution

In this case, the wall temperature is referred to the fluid temperature at the wall, in fact for simplicity, the wall temperature is taken to be the same as the fluid temperature at the wall. To be more precise, the wall temperature of the freon and water are assumed to be the same (by omitting the difference in the temperature between these two), and we shall refer to as 'wall temperature'. The wall temperature at the condenser entry was estimated as an average of the freon inlet and water outlet temperature. The wall temperature at other points along the condenser was evaluated from the inverse of freon linear heat transfer coefficient to the inverse of overall heat transfer coefficient by assuming the quantity of heat per unit length travel from the freon side to the wall is the same as the amount of heat travel from the freon side to the water side.

The results show that, $TR < T_{wall} < TW$. As the freon travels from the condenser entry, the wall temperature is initially close to the freon temperature, but the difference becomes quite large as the freon reaches the condenser exit. In general, the ratio of the freon temperature to the wall temperature is smaller than the ratio of the wall temperature to the water temperature. Fig.6.4.5(a->e) shows examples of wall temperature profiles taken from the results in Section A, B and C of Table 6.2 at different freon inlet pressure, and freon and water mass flowrate. The wall temperature distribution is drawn between the freon and water temperature distributions at one meter intervals.

As the freon inlet pressure and temperature increases, the wall temperature is also increased, falling in value as the freon flows from the condenser entry to condenser exit. For the given operating conditions, the wall temperature at the condenser entry varies from 42.5°C to 62.7°C, which corresponds to the variation of freon inlet temperature and water exit temperature from 55.4°C to 74.2°C and from 29.7°C to 51.3°C respectively.

At the condenser exit, the variation is from 15.0°C to 33.0°C corresponding to the variation from 16.4°C to 42.0°C for the freon exit temperature and from 14.5°C to 27.0°C for the water inlet temperature.

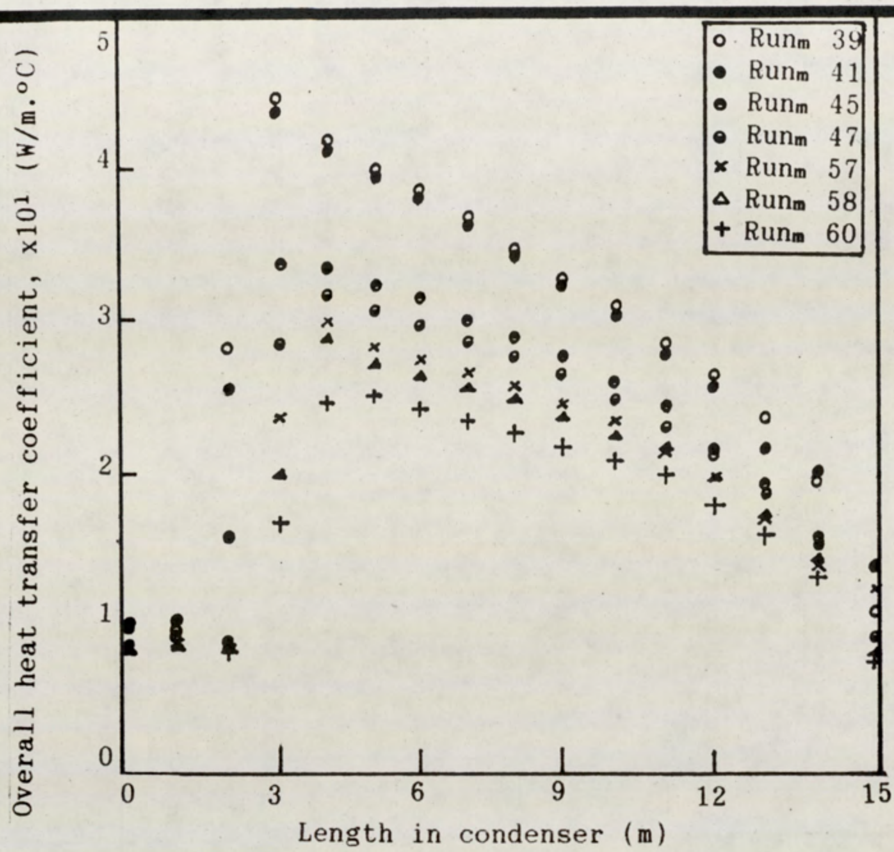

Fig.6.4.4(c): Overall heat transfer coefficient for Run$_m$ in Section C at inlet pressure 9.02-12.11 bar

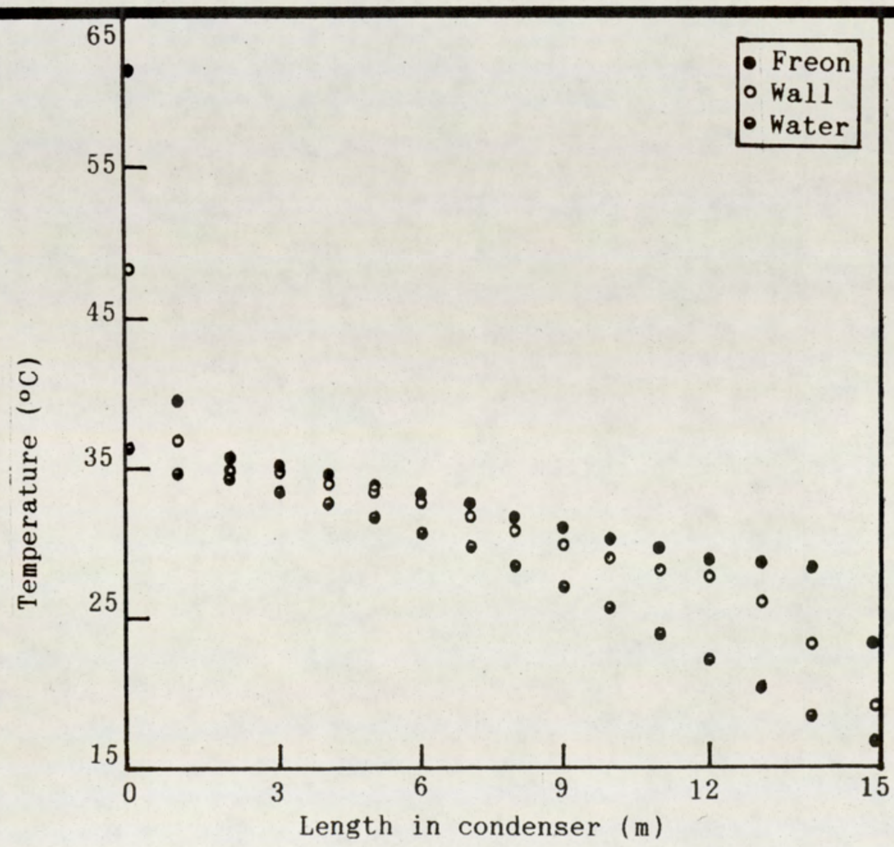

Fig.6.4.5(a): Temperature distribution for Run$_m$ 10 at inlet pressure 8.81 bar, $\dot{m}r$=6.16 g/s, and $\dot{m}w$=12.10 g/s

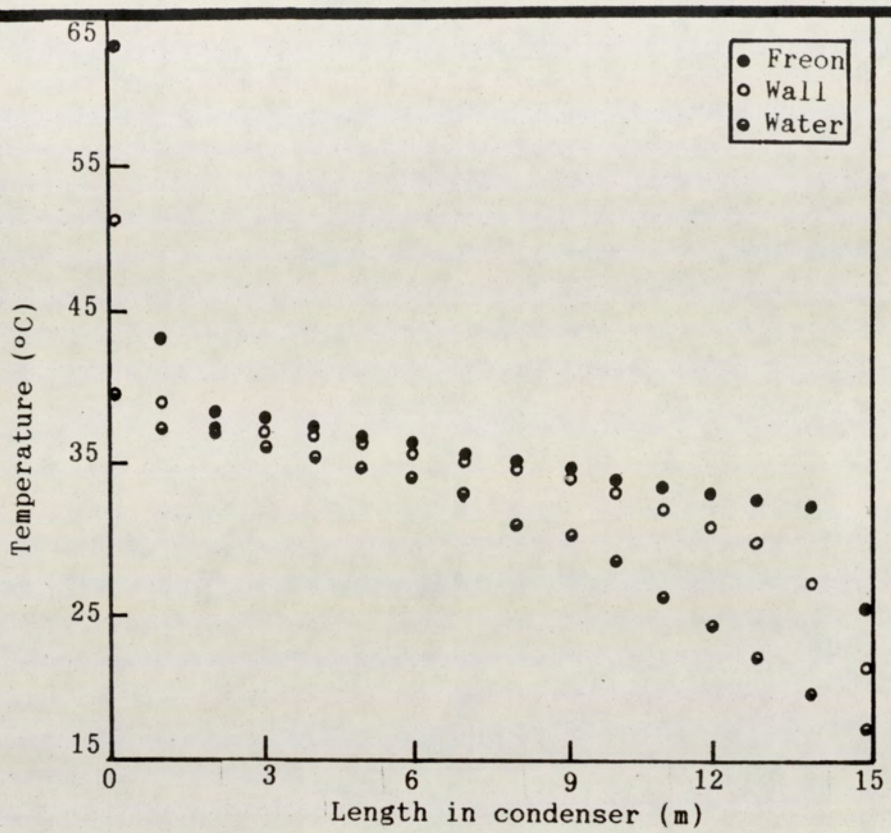

Fig.6.4.5(b): Temperature distribution for Run 11 at inlet pressure 9.44 bar, $\dot{m}r$=6.00 g/s, and $\dot{m}w$=10.54 g/s

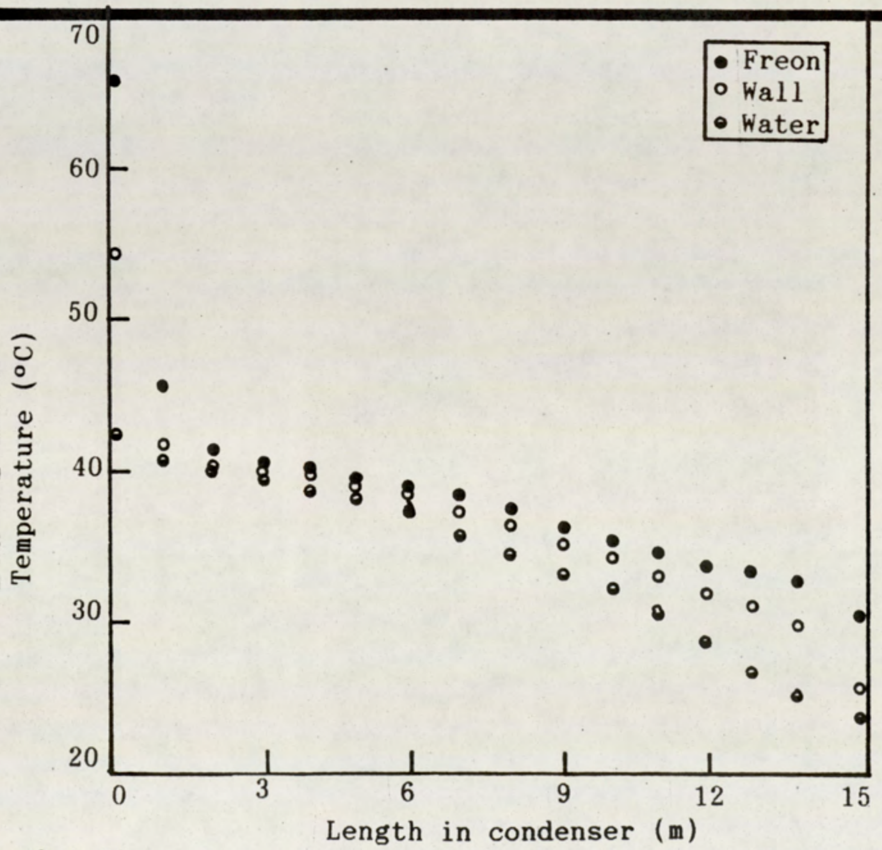

Fig.6.4.5(c): Temperature distribution for Run 44 at inlet pressure 10.13 bar, $\dot{m}r$=6.93 g/s, and $\dot{m}w$=12.84 g/s

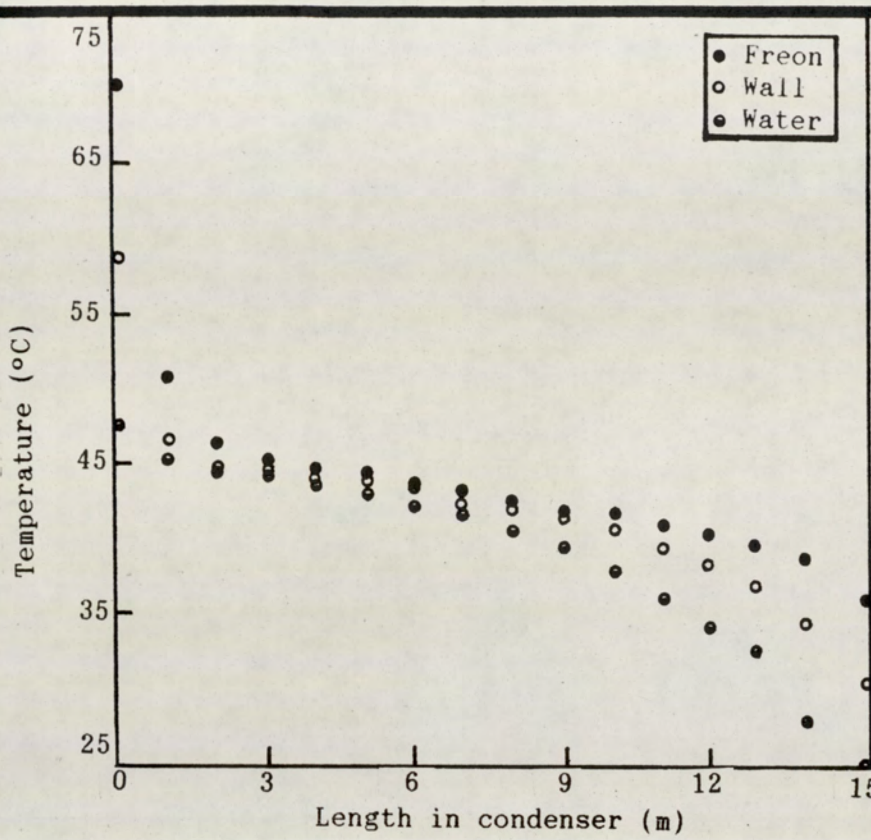

Fig.6.4.5(d): Temperature distribution for Run$_m$ 57 at inlet pressure 11.18 bar, $\dot{m}r$=6.65 g/s, and $\dot{m}w$=10.64 g/s

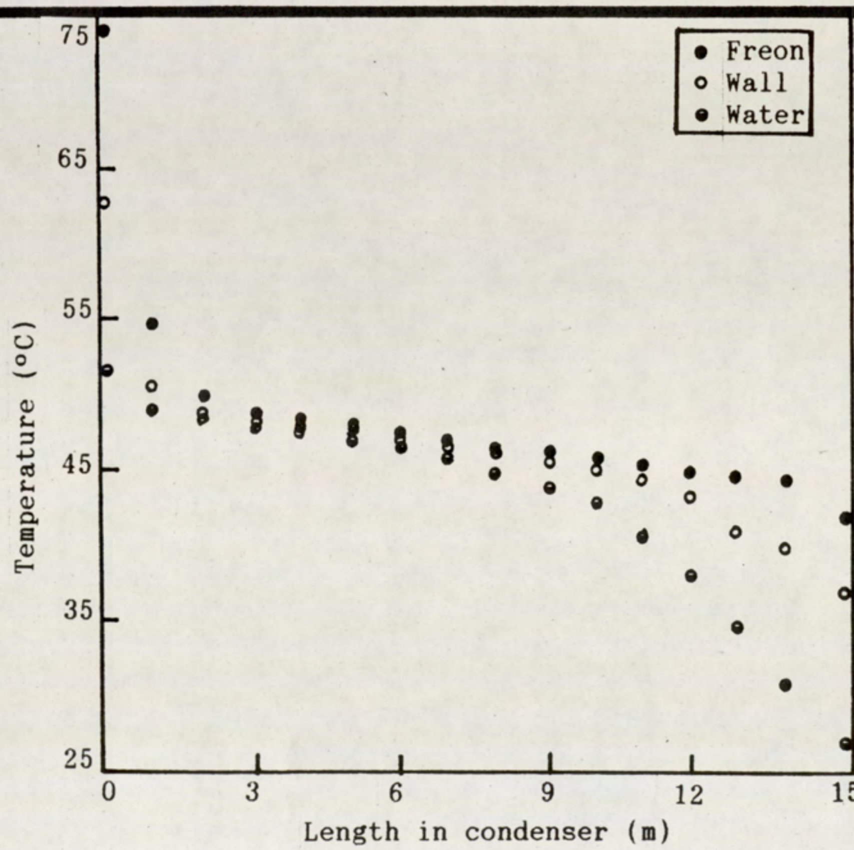

Fig.6.4.5(e): Temperature distribution for Run$_m$ 60 at inlet pressure 12.11 bar, $\dot{m}r$=6.43 g/s, and $\dot{m}w$=9.30 g/s

6.4.6: Number of transfer units (Ntu)

This is a dimensionless parameter which is used to evaluate the effectiveness of the condenser in various regimes, and to calculate the temperature of freon and water at the next points. In chapter 5, the freon Ntu in the two-phase region was assumed to be zero.

The freon Ntu, which is directly proportional to the overall heat transfer coefficient in the vapour region is higher than that in the liquid region. As the freon flows in the condenser, the value in the vapour regime decreases, but there is a small increase in the liquid regime as the flow reaches the condenser exit (see results in **Table A-6.12** to **Table A-6.17** of part b). In general, there is a drop in the value as the freon inlet pressure increases. The Ntu based on the results taken from Table 6.2 varies from 1.0×10^{-1} to 2.0×10^{-1} in both vapour and liquid regions.

The water Ntu is expected to be lower than those predicted in the freon vapour and liquid. This is simply because the Ntu is also influenced by the specific heat capacity; the higher the specific heat capacity, the lower the number of transfer units are. In general, the specific heat capacity of water is of order 10^3 compared to the order of 10^2 for the specific heat capacity of both the liquid and vapour freon.

Fig.6.4.6(a and b) show the variation of number of transfer units of water along the length of condenser at one meter intervals taken from Table 6.2. As the water flows from the condenser exit, the values are slowly increased. At the beginning of the two-phase region (corresponding to freon side), the water Ntu slowly decreases, but as the water approaches the corresponding freon vapour end regime, the drop is sharper and then continues to drop but less rapidly. As the freon inlet pressure increases, the water Ntu is increased accordingly.

6.5: Summary of range of possible evaporator conditions

In this section, the summary of possible simple refrigeration cycles predicted by the model is presented. Fig.6.1.8 shows the basic cycle with numbers 1, 2, 3 and 4 indicating the stations where the following items (in order) begin; discharge gas, subcooled liquid, evaporator entry and superheated suction gas, which is equivalent to position 1->2->3->4 in the anti-clock direction. The following discussion referrs to the same numbers used in the cycle illustrated in Fig.6.1.8. The compressor isentropic efficiencies of 50%, 55% and 60%, with different evaporator conditions, the possible COP of the system is predicted.

The dew temperature at saturated vapour line of the p-h diagram was calculated from the given freon inlet temperature. The cycle is also

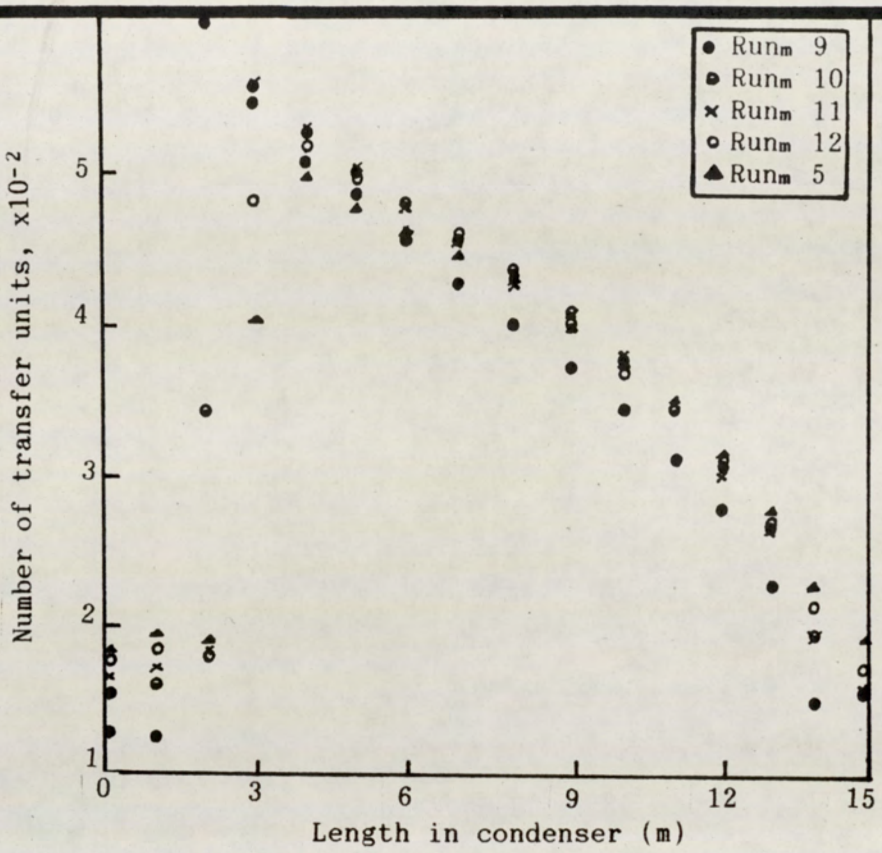

Fig.6.4.6(a): Water Ntu distribution for results in Section A at inlet pressure 7.65-10.89 bar

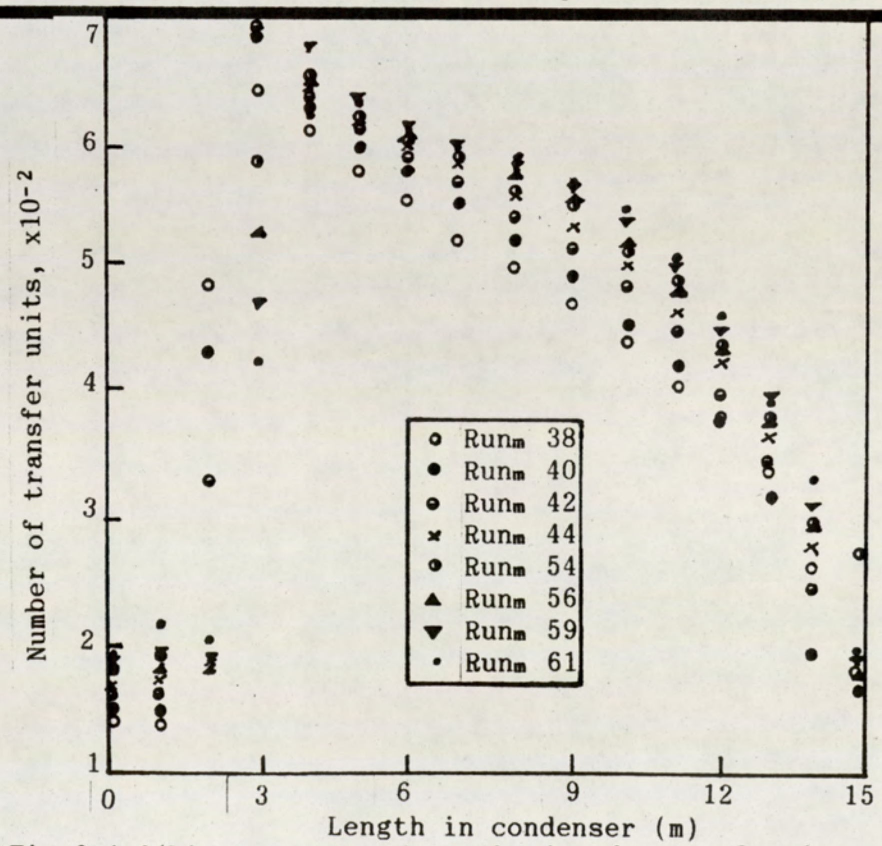

Fig.6.4.6(b): Water Ntu distribution for results in Section B at inlet pressure 8.82-12.06 bar

greatly influenced by the freon outlet temperature, and the specific enthalpy and specific entropy of the freon at point 2. These values are fixed for predicting the possible cycle at different compressor efficiencies for a particular Run$_m$. In fact, the position at point 1 and 2 have already been predicted and discussed in the previous section.

The main idea of this section is to predict the position at point 3 and 4 in terms of (PR,TR) coordinate of a p-h diagram. It involves other thermodynamic and physical properties of the freon such as enthalpy, entropy, and vapour quality at point 3. For simplicity, the pressure at point 3 is assumed to be the same as pressure at point 4 (no pressure drop between these two points). Point 3 is also assumed to be in the mixed-phase region while point 4 lies in the superheating region. Other properties stated above are used to predict the possible evaporating capacity, compression capacity (work done by the compressor), and coefficient of performance of the refrigeration cycle (or COP of the heat pump system).

For given properties at point 1 and 2 for a particular Run$_m$, the possible temperature at point 3 was chosen, always to be lower than the dew temperature. For values of vapour quality less than zero ($x<0.0$), the specific entropy at point 3, which is a function of vapour quality and temperature, is simply solved at $x=0$ and at the freon outlet temperature.

All the possibilities can be seen in the results shown in **Table A-6.12** to Table A-6.17 of part c. **Fig.6.1.8(b)** shows the possible temperatures at point 3 and the possible cycle by assuming the specific enthalpy at point 2 and at point 3 to be equal (shown by isenthalpic line drawn parallel to the pressure-axis).

6.5.1: Parameters at point 1 and 2

The parameters which are included at these points are already predicted in Section 6.2. The freon inlet pressure and temperature (at condenser entry) are the coordinates of point 1 and the freon outlet pressure and temperature (at condenser exit) are the coordinates of point 2. The specific enthalpy and specific entropy are evaluated from these coordinates using the equation of state. Dew temperature (or saturated temperature at given inlet pressure) is calculated from the inlet pressure.

From the results, at higher freon inlet pressure and inlet temperature, the dew temperature, specific enthalpy at point 1 and 2, and specific entropy at point 2 increases with small decreasing in the specific entropy at point 1. For given operating conditions, taken from the results, freon inlet pressure increasing from 7.65 bar to 12.11 bar, **Table 6.6** shows a summary of the related parameters at point 1 and 2.

Parameter	Value
Dew temperature (°C)	increase from 3.10×10 to 4.97×10
Specific entropy at 1 (kJ/kg.°C)	decrease from 7.4358×10^{-1} to 7.3665×10^{-1}
Specific enthalpy at 1 (kJ/kg)	increase from 2.17813×10^{2} to 2.25976×10^{2}
Specific entropy at 2 (kJ/kg.°C)	increase form 1.9548×10^{-1} to 2.7662×10^{-1}
Specific enthalpy at 2 (kJ/kg)	increase from 5.1237×10 to 7.61111×10

Table 6.6: Summary of parameters at point 1 and 2 for inlet pressure 7.65-12.11 bar

Fig.6.5.1 shows the possible variation of dew temperature for a given range of freon inlet pressure. **Fig.6.5.2(a)** and **Fig.6.5.2(b)** show the variation of specific entropy and specific enthalpy at points 1 and 2 respectively at given freon inlet pressures.

6.5.2: Parameters at point 3

At a given compressor isentropic efficiency, the temperature at point 3 is varied so that its value does not exceed the dew temperature. This temperature is used to calculate the pressure at its saturated temperature. Considering there is no pressure drop from point 3 to point 4 (parallel to specific enthalpy-axis of a p-h diagram), the specific enthalpy and specific entropy at saturated liquid and at saturated vapour based on (PR,TR) at point 3 are determined. The vapour quality at point 3 is predicted from the ratio difference in the specific enthalpy. The next step is to calculate the specific entropy at point 3.

As the temperature at point 3 set to increase (in steps of 2°C) the saturated pressure at point 3, specific enthalpy and specific entropy at x=0, and specific enthalpy at x=1 also increase with decreasing in the specific entropy at x=1, and vapour quality and specific entropy at point 3. As the compressor efficiency is increased to 55% and 60%, the starting temperature at point 3 can be set lower than that when it is 50% efficiency. In such cases, the value of parameters described earlier are also changed; but remain unchanged for the same evaporator entry temperature.

The details are given in **Table A-6.12** to **Table A-6.17** of part c. All other parameters calculated in this section, with negative value of the vapour quality at point 3 are negligible.

6.5.3: Parameters at point 4

Assuming the pressure at point 3 to be equal with the pressure at point 4 (no pressure drop), the position at point 4 can then be evaluated in terms of (PR_3,TR_4). Point 4 is assumed to be in the vapour region (see

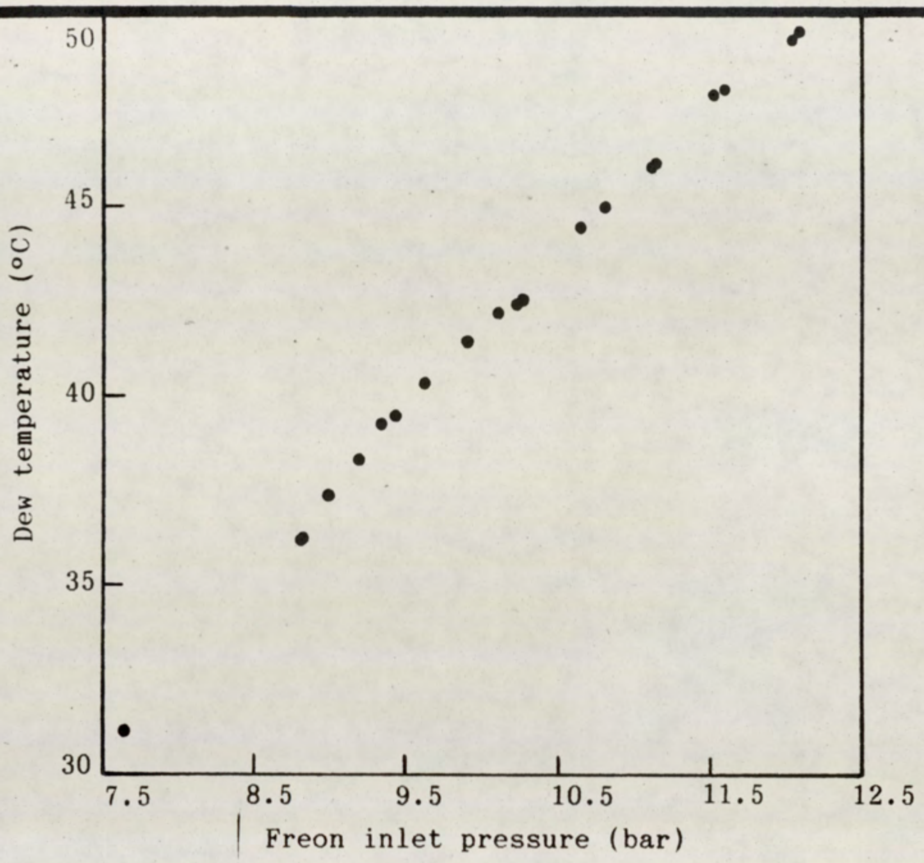

Fig.6.5.1: Freon inlet pressure versus dew temperature

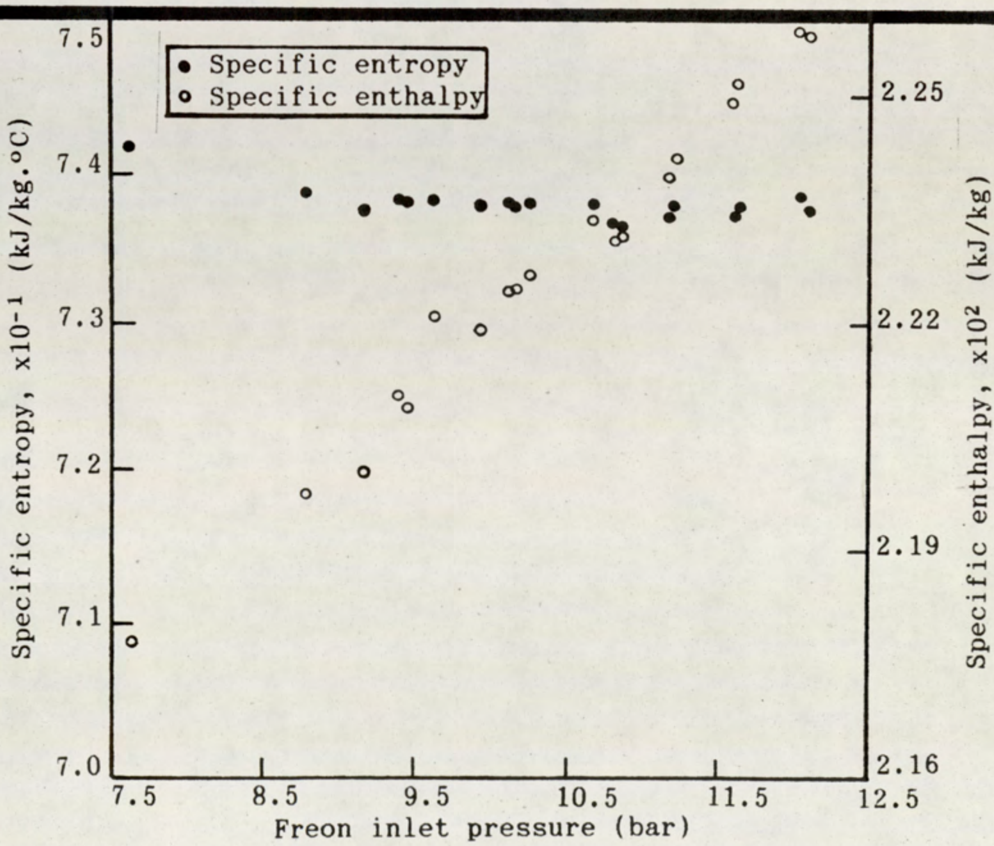

Fig.6.5.2(a): Freon inlet pressure versus specific enthalpy and specific entropy at point 1

also Fig.6.1.8(b)). With two known variables (PR_4 and TR_4), the specific enthalpy and specific entropy at this point can be predicted.

The temperature at point 4 is found to be higher than the temperature at point 3. The specific enthalpy is slightly higher than the specific enthalpy at x=1 at the same pressure, but lower than the specific enthalpy at point 1. The specific entropy at point 4 is found to be slightly higher than the specific entropy at the saturated vapour line.

In general, as the evaporator entry temperature is set to increase in steps of 2°C, the specific enthalpy and specific entropy, and the temperature at point 4 are also increased, with a decrease in the ratio of the temperature at point 3 to the temperature at point 4.

For an increase in the compressor efficiency from 50% to 55% and 60%, at the same evaporator entry pressure and temperature, the model predicts that more freon vapour is superheated. The superheated vapour has a higher temperature and therefore, the specific enthalpy and specific entropy are also estimated higher than for the lower efficiency.

Fig.6.5.3 shows the possibility of these situations at given pressure for different compressor isentropic efficiency.

6.5.4: Characteristic of possible cycle

In this part, the discussion is only based on the value of quality greater than zero where point 3 is assumed in the two-phase regime. The total evaporation capacity, in terms of thermal power can be directly predicted from the product of the average freon mass flowrate and the difference in the specific enthalpy between point 3 (or point 2) and point 4. The value is always less than the total thermal power across the condenser.

The work done by the compressor (in terms of thermal energy), if the process is assumed to be isentropic, is much less than the total power across the condenser. It is just simply the product of the average freon mass flowrate and the difference between the specific enthalpy at point 1 and at point 4.

The coefficient of performance of the heat pump system for various pressures and temperatures, and at different efficiencies is also predicted. By definition, the COP is just the ratio of the total thermal power across the condenser to the work done by the compressor.

As the pressure at point 3 increases, the evaporation capacity is also increased (see also **Fig.6.1.5(b)**) with less work produced by the compressor. The ratio of the freon inlet pressure (or pressure at point 1)

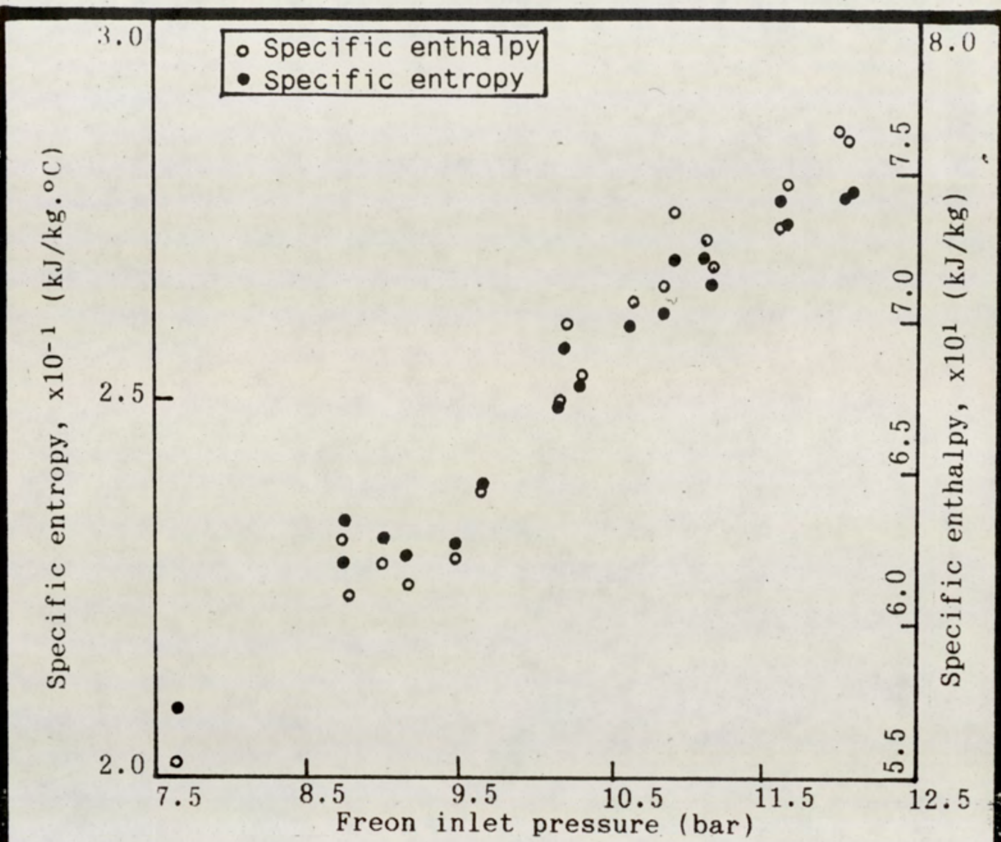

Fig.6.5.2(b): Freon inlet pressure versus specific enthalpy and specific entropy at point 2

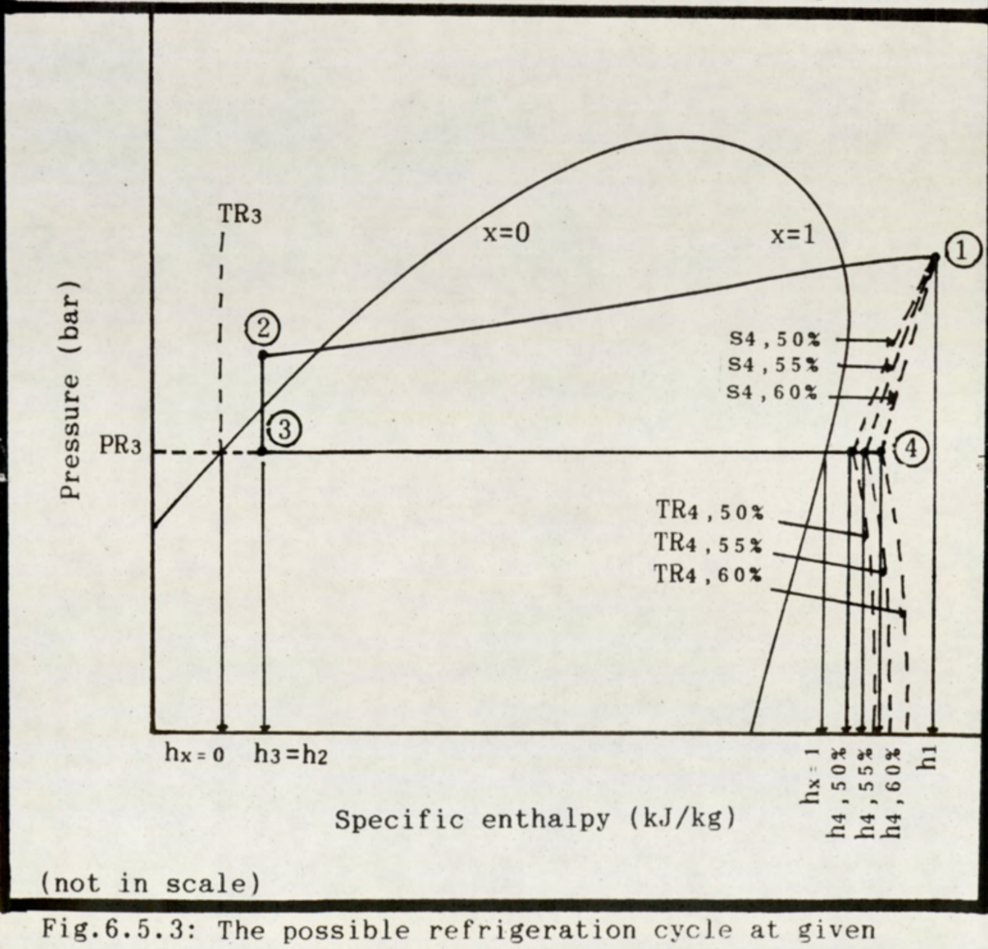

Fig.6.5.3: The possible refrigeration cycle at given pressure with different compressor efficiency

to the pressure at the evaporator entry is decreased as the temperature at point 4 increases. Less work is done as the pressure at point 3 increases, therefore the COP is also increased.

On the other hand, by increasing the compressor efficiency from 50% to 55% and 60%, at the same evaporating pressure, there is an an increase in the specific enthalpy, specific entropy, and temperature at point 4, the evaporation capacity is increased but the work done becomes less. The smaller the work done by the compressor, the bigger is the COP. Therefore, the COP at fixed evaporating pressure is larger for higher compressor efficiencies, assuming the same amount of total power across the condenser.

At a particular freon temperature and pressure at point 3, as the freon inlet pressure increases from 7.65 bar to 12.11 bar, the COP decreases. The COP is higher at higher compressor efficiency. **Fig.6.5.4** shows an example at TR_{point3}=16°C and PR_{point3}=5.06 bar in the range 7.65-12.11 bar for the freon inlet pressure. At higher pressure, the total power across the condenser becomes less and at the same time there is an increase in the work done by the compressor, therefore the COP reduces.

Fig.6.5.5 shows an example of the COP and work done versus the freon temperature at point 3 with the freon inlet pressure fixed at 7.65 bar (Run$_m$ 9). As the temperature is set to increase in steps of 2°C, the COP is also increased. The COP at higher efficiency is bigger than that at the lower efficiency. On the other hand, as the evaporating temperature increases the work done is decreased and the lower compressor efficiency produces more work (denoted by the joined lines in **Fig.6.5.5**).

Fig.6.5.6(a and b) show other examples taken from the results predicted by the model. At a given evaporator entry temperature, the COP is decreased as the freon inlet pressure increases. At TR_{point3}=18°C, the COP predicted in Run$_m$ 10 with the freon inlet pressure 8.81 bar has the highest value. The COP just mentioned above is a comparison of four different freon inlet pressures given in **Fig.6.5.6(a and b)** ; 8.81 bar, 9.66 bar, 10.83 bar and 12.11 bar.

The ratio of freon inlet pressure (pressure at point 1) to the pressure at point 3 and the work done by the compressor at the same evaporator entry temperature show an increase in value as the discharge gas pressure increases but the evaporation capacities are decreased. The prediction of temperature at point 4 (in the superheated region), at given evaporator entry pressure and temperature (at point 3) becomes less as the discharge pressure increases (pressure at point 1), but increases with increasing of compressor efficiency.

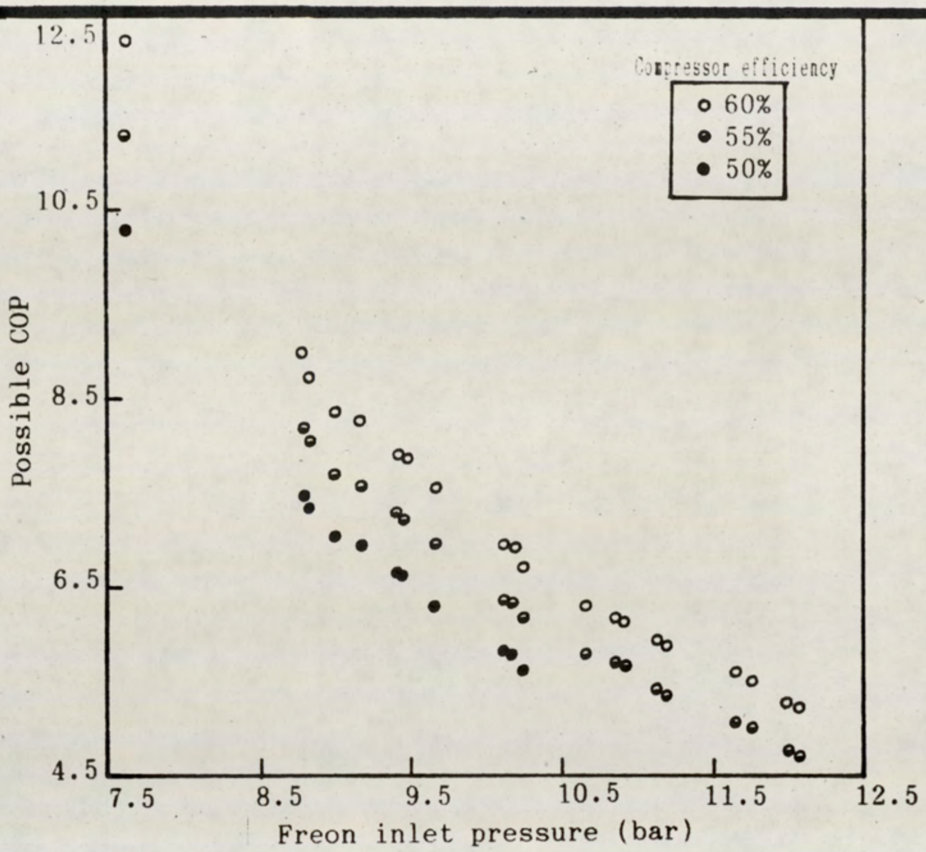

Fig.6.5.4: The possible COP at $TR_3=16^oC$, and $PR_3=5.06$ bar for freon inlet pressure from 7.65-12.11 bar

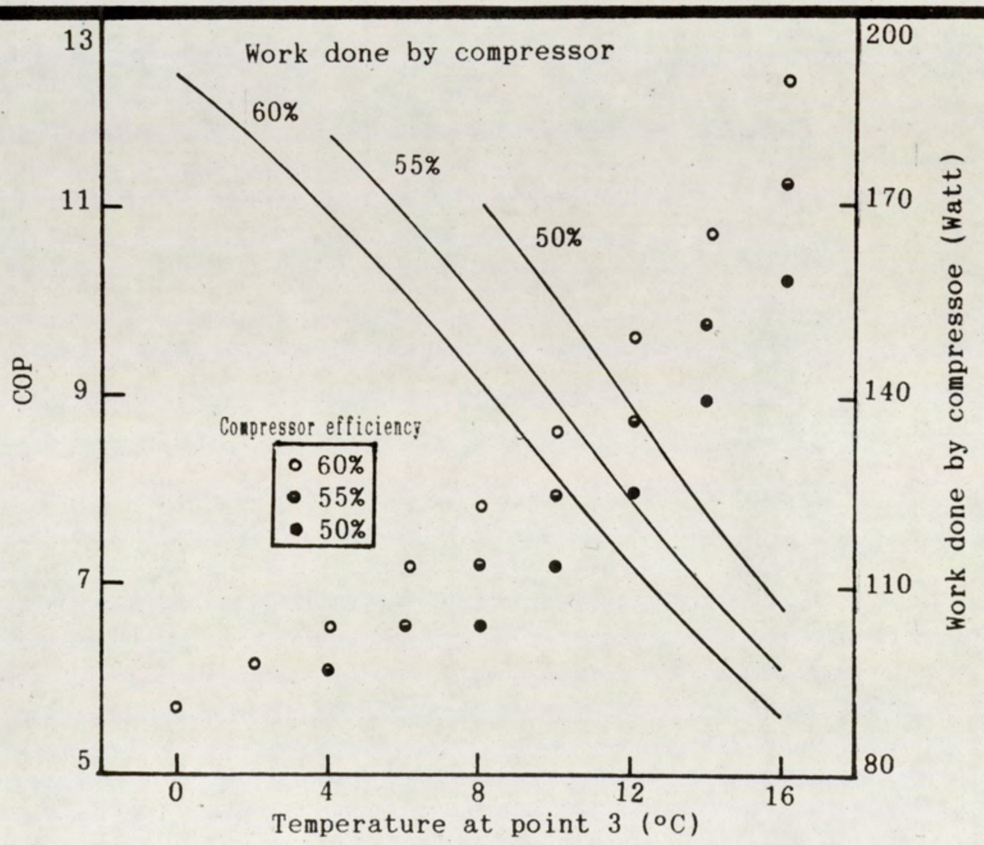

Fig.6.5.5: COP and work done by compressor at freon inlet pressure 7.65 bar and $TR_{dew}=31.02^oC$ (Run_m 9)

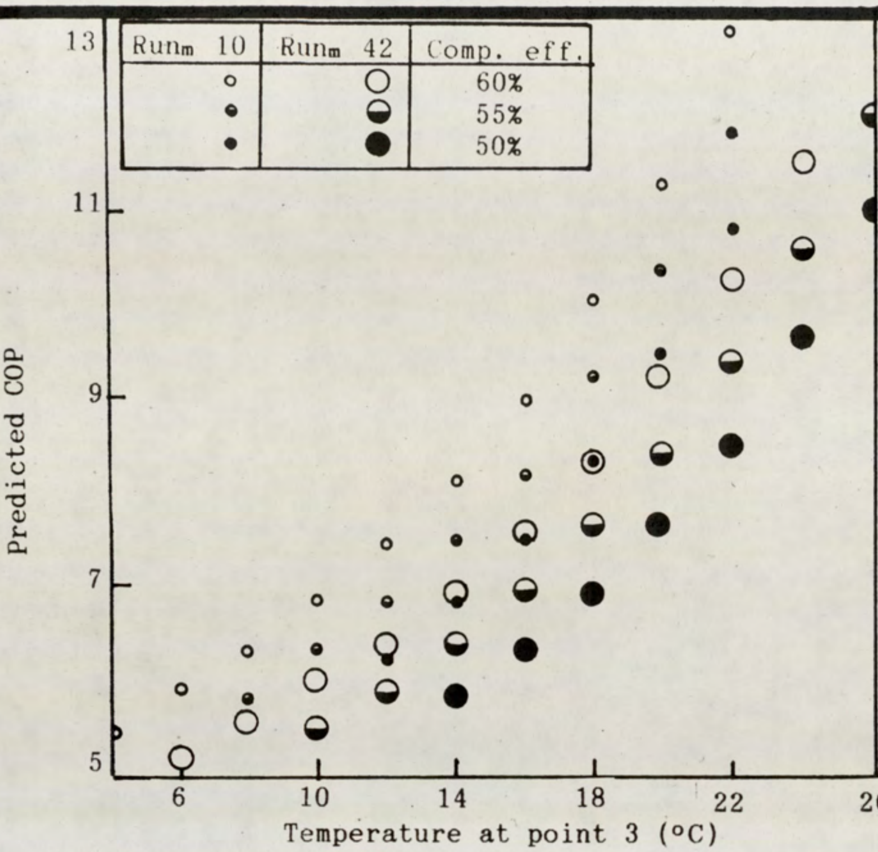

Fig.6.5.6(a): COP at different compressor efficiency for Runm 10 and Runm 42; inlet pressure 8.81 bar and 9.66 bar

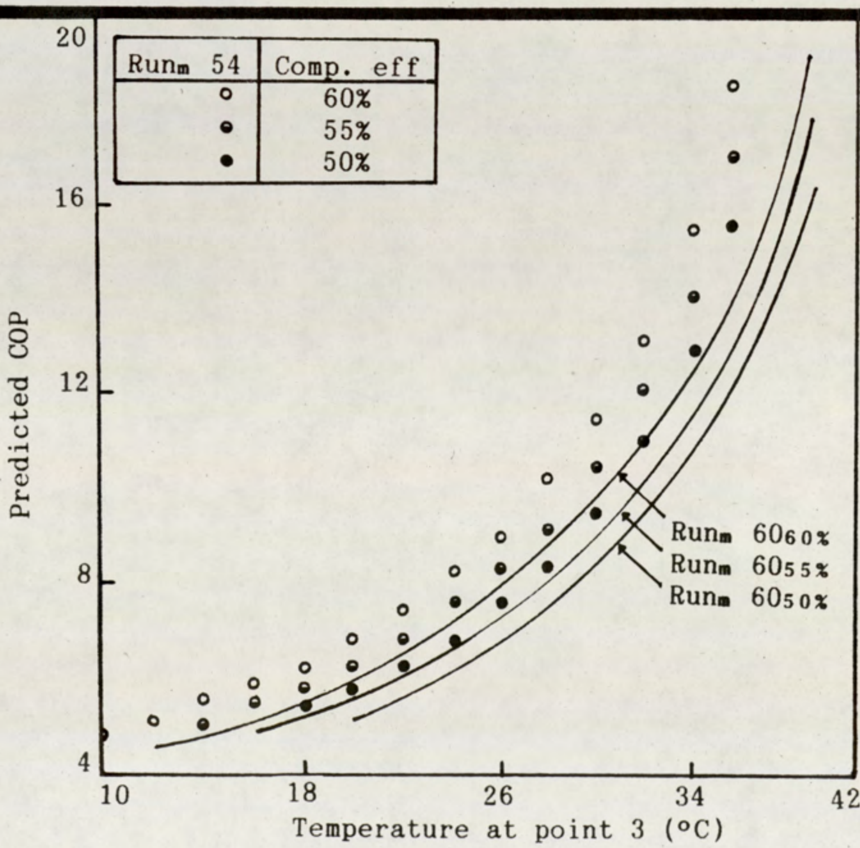

Fig.6.5.6(b): COP at different compressor efficiency for Runm 54 and Runm 60; inlet pressure 10.83 bar and 12.11 bar

CHAPTER 7

CONCLUSIONS

7.1: Introduction

In this final chapter, general conclusions concerning the predictive model of a counter-flow heat exchanger are made, and suggestions for possible future work are outlined and discussed.

7.2: General conclusions

For normal operating conditions, the model is in fair agreement with the experimental results.

7.2.1: Comparison between experiment and model

The main conclusions focus on the comparison between the experiment and prediction, based on the temperature profiles along the condenser. A summary of overall deviations from experiment is given in **Table 6.4** of chapter 6.

From the results, the temperature profiles of the freon deviated from -1.7°C to 6.5°C (see also **Fig.6.2.1(a)**, **Fig.6.2.4(a)**, and **Fig.6.2.6(a)**). The model predicts slightly higher temperature at the first few points of the condenser exit. The maximum deviations are as follows; 6.5°C in Section A, 4.0°C in section B, and 2.5°C in Section C (see also **Table A-6.1** to **Table A-17** for the experimental and predicted results). The results in section B and C predict quite fair agreement with the experiment , between -0.9°C to 4.0°C and -1.1°C to 2.5°C respectively. In section A, the experimental condenser was covered by the polystyrene insulating materials, while in Section B, it was covered by the vermiculite insulating materials. In section C, the condenser tube was lagged with pipe lagging insulation, with the whole condenser covered by vermiculite shows an improvement. More heat rejected from the freon side was lost to the surroundings in section A, but in section C, the losses were reduced.

For the water side, the predicted temperature profiles are in good agreement with the experiment. The overall deviation is from -1.6°C to 0.8°C, with the results predicted in section C showing an improvement (between -1.4°C to 0.9°C).

The freon outlet pressure predicted by the model is slightly low, deviating from 0.63 bar to 0.01 bar (see **Fig.6.2.7**). For other parameters, the comparisons are listed in Table 6.4.

7.2.2: Fluid properties in three separate regions

The thermodynamic and physical properties of the fluid are predicted at the entry of each region (desuperheating, condensing and subcooling) within the operating conditions. For the water side, the properties were calculated at the entry of equivalent region of the freon side.

As the freon inlet pressure increases from 7.65-12.11 bar, the length of desuperheater is increased, with a decrease in the condensing region and subcooling region. For the given conditions, the two-phase region occupies between 83% to 89% of the total length of condenser. Comparatively, the length of desuperheater is longer than the length of subcooler, especially at higher inlet pressure.

<u>Properties of freon</u>

The following table shows a summary of some of the properties of freon taken from the results predicted by the model, based on the 29 Runs (see also **Table A-6.12** to **Table A-6.17** of part a as examples), within the conditions mentioned earlier.

Properties	Value in each region					
	Vapour region		Condensing region		liquid region	
	minimum	maximum	minimum	maximum	minimum	maximum
Heat transfer coefficient (W/m^2.C)	6.711×10^2	8.523×10^2	3.975×10^2	4.900×10^2	8.592×10^2	1.356×10^3
Linear heat transfer coefficient (W/m.C)	8.965×10^0	1.138×10^1	5.306×10^1	6.540×10^1	1.153×10^1	1.818×10^1
Refrigerant Reynolds number	1.112×10^5	1.557×10^5	2.711×10^3	4.954×10^3	7.959×10^3	1.021×10^4
Refrigerant number of transfer units	2.782	3.885	0.111	0.162	0.117	1.207
Refrigerant specific enthalpy (kJ/kg)	217.8	226.0	199.6	206.1	55.4	76.6
Refrigerant specific entropy (kJ/kg.°C)	7.439×10^{-1}	7.367×10^{-1}	6.855×10^{-1}	6.801×10^{-1}	2.270×10^{-1}	2.781×10^{-1}
Pressure (bar)	7.65	12.11	7.46	11.93	5.77	10.64
Temperature (°C)	55.4	74.2	29.9	48.9	20.5	42.0

Table 7.1: Summary of some properties of freon

In general, as the freon inlet pressure increases, from 7.65-12.11 bar the properties tabulated in Table 7.1 also increase in the value from minimum to maximum.

<u>Properties of water</u>

The properties of water summarized in **Table 6.5** show that as the freon inlet pressure increases, the heat transfer coefficients, Reynolds number, and water outlet temperature decrease as the freon flows along the tube. The water Ntu is much higher at the entry of the equivalent two-phase region, with the value increasing as the pressure increases.

Overall properties of the fluid

Overall linear heat transfer coefficient of the fluids at the entry of each region decreases as the pressure increases, with the value calculated at the entry of the two-phase segment higher than in the other two segments.

The effectiveness in each segment shows that there is an improvement in the vapour region and two-phase region as the pressure increases. At the same time, the effectiveness in the liquid region decreases. The overall effectiveness varies from 67.9% to 83.0% as the pressure increases from 7.65 bar to 12.11 bar.

The total thermal power transferred to the water side decreases as the pressure increases.

7.2.3: Other profiles predicted by the model

The profiles which are not measured experimentally, such as freon pressure, vapour quality, freon and water heat transfer coefficient, overall linear heat transfer, freon and water number of transfer units, wall temperature are summarized in Table 7.2, showing the change as the freon inlet pressure increases from 7.65-12.11 bar. Some of the examples can be found in Table A-6.12 to Table A-17 of part b.

Parameter	Increase or decrease		Refer to figure	Remarks
	as the freon flows along the condenser	as the freon inlet pressure increases		
Freon pressure (bar)	decrease	increase	6.4.1(a,b,c)	Pressure drop across the condenser decreases at higher inlet pressure
Vapour quality (%)	decrease	increase	6.4.2(a,b,c)	As the inlet pressure increases,the drop shows a convex-shape, but drop sharply as it reaches condenser exit
R12 heat transfer coefficient ($W/m^2.C$)	decrease	decrease	6.4.3(a)	Increase in vapour and liquid region as freon flows along the condenser. $H_{two\_phase}<H_{liquid}<H_{vapour}$
H_2O heat transfer coefficient ($W/m^2.C$)	decrease	decrease	6.4.3(b)	The drop between each meter becomes smaller as the freon inlet pressure increases
Overall heat conductance (W/m.C)	decrease	decrease	6.4.4(a,b,c)	Increase in liquid region as the inlet pressure increases
Wall temperature (°C)	decrease	increase	6.4.5(a,b,c,d,e)	More close to R12 temperature.
Water number of transfer units	decrease	increase	6.4.6(a,b)	The increase is sharp as R12 flows in the vapour regime

Table 7.2: Summary of other parameter profiles

7.2.4: Possible refrigeration cycle

Based on the results predicted by the model, the following conclusions can be summarized. The points used in this section are referred to Fig.6.1.8, with the possible range of evaporator conditions given in chapter 6

1. As the freon inlet pressure increases, the dew temperature at particular given pressure is also increased. **Table 6.6** shows a summary of other freon thermodynamic properties evaluated at point 1 and 2 of Fig.6.1.8, illustrated in **Fig.6.5.2(a,b)**

2. At fixed specific entropy and specific enthalpy (point 1 and 2), constant freon mass flowrate, and fixed evaporator inlet pressure, with compressor isentropic efficiency values of 50%, 55% and 60%, the following conclusions can be made,

<u>Freon temperature at point 4</u>: At higher efficiency, the freon temperature is also increased.

<u>Work done by compressor</u>: Less work is done by the compressor.

<u>Evaporation capacity</u>: The evaporation capacity increases as the compressor efficiency increases.

<u>Coefficient of performance</u>: At fixed total thermal energy across the condenser, less work is done by the compressor, the COP increases.

3. At given freon inlet pressure (at point 1), the specific enthalpy and specific entropy at point 1 and 2 are fixed, so that freon mass flowrate and thermal energy across the condenser are also fixed. The freon evaporator inlet temperature can be set to increase, so that the pressure at point 3 is also increased. At given compressor isentropic efficiency, with all these conditions, the following can be concluded.

<u>Freon temperature at point 4</u>: There is an increase in the temperature at point 4.

<u>Work done by compressor</u>: For the isentropic work, compressor does less work.

<u>Evaporation capacity</u>: The evaporation increases as the pressure at point 3 increases.

<u>Coefficient of performance</u>: The calculated COP is increased.

4. At a particular evaporator inlet temperature and pressure, as the freon condenser inlet pressure increases, more work is done isentropically, the COP decreases. With the same condition, by increasing the efficiency from 50% to 55% and 60%, the COP is increased.

5. At given evaporator entry pressure, the temperature at point 4 becomes less as the freon inlet pressure increases, but increases with

increasing of compressor efficiency. At the same time, the pressure ratio (pressure at 1 to pressure at 3) and work done by compressor increases with decrease of evaporator capacity.

7.3: Suggestions for future work

Followings are the suggestions for future work, which can be observed in two sections as mentioned earlier in the chapter, based on the experiment and theory done in the research.

7.3.1: Experimental rig

In this section, the problems are divided to heat pump as a system, and experimental condenser as a component of the system.

Heat pump system: To achieve a better performance, more sensors and detectors must be included, especially for measuring temperature and pressure along the lower and higher pressure line of the system. The total energy across the condenser and the work done by the compressor must be carefully calculated and measured, since in practice, the work done is nonisentropic.

A study can also be carried out to measure the water and freon mass flowrate, air speed, and power comsumption directly from the sensors. It is also suggested that more flowrate sensors can be placed at strategic positions in the system.

Experimental condenser

1. The sensors for measuring temperature and pressure at the condenser entry and exit must be at the right place.

2. More pressure transducers should be placed along the condenser to measure the actual pressure distribution.

3. It is necessary to improve the measuremenet of water and freon flowrate directly from the sensor. In this case, the fluctuation and instabilities of the readings must be taken into consideration.

4. It is also possible to place the flowrate sensors for measuring water and freon flowrate at various places, especially at the condenser entry and exit.

5. A study of temperature distribution across the tube by penetrating the thermocouples into fluid at various depth can also be carried out.

7.3.2: Theory

In this section the heat transfer and pressure drop in the single-phase and two-phase flow should be carefully studied to suit the system, especially at the 180-deg pipe bends.

1. An accurate experimental measurement is important to perform an empirical correlation in the transportation processes to represent the experimental evidence.

2. The two-phase flow is so unpredictable that the research is likely to be profitable, with better understanding of the flow mechanisms and flow distribution.

3. In the single-phase flow, involving the vapour and liquid, if applicable, using different working fliuds in a wide range of Reynolds number to predict the heat transfer and pressure drop.

4. Finally, research could also be carried out to predict the heat transfer and pressure drop in the transition regime accurately for the Reynolds number ranging from $2x10^3$ to 10^4.

REFERENCES

Journals, Papers and Reports

1. C.G.Carrington, "Computer Program of A Counterflow R12 Condenser Comprised of Two Tubes Thermally Coupled," Unpublished, Aston Univ., Birmingham, 1982.

2. M.Crew, "Showing How A Heat Pump Works," The Heating & Ventilating Engineers, April/May 1984, pp.22-26.

3. Edison Electric Institute, "Final Report, Heat Pump Improvement Research Project," (RP69), Pub. No. 71-901, May 1971.

4. E.C.Hise, "Seasonal Fuel Utilization of Residential Heating System," (ORNL Report), No. ORNL-NSF-EP-82, April 1975.

5. Gordian Associates, Inc., "Evaluation of Air-Air Heat Pump for Residential Space Conditioning," Report Proposed by FEA, NTIS No. PB-255-652, April 1976.

6. Gordian Associates, Inc., "Heat Pump Technology, A Survey of Technical Development Market Prospects," Report Proposed by DOE., HCP/M 212-01, June 1978.

7. International Energy Agency, "A Technical Review, Heat Pump System," OECD., 1982.

8. P.Freund, and K.Seymour, "Heat Pumps for Use in Buildings," CP 19/76, BRE.

9. E.R.G.Eckert, "Pioneering Contributions to Our Knowledge of Convective Heat Transfer," Trans. ASME, J. Heat Transfer, Vol.103, August 1981, pp.409-414.

10. R.A.Seban, "Llewellyn M.K.Boelter, 1898-1966," Int. J. Heat Mass Transfer, Vol.11, 1968, pp.3-5.

11. W.P.Berggren, "The Brief Careers of Cherry, Martinelli and Morrin," Int. J. Heat Transfer, Vol.11, 1968, pp.7-8.

12. R.W.Lockhart, and R.C.Martinelli, "Proposed Correlation of Data for Isothermal Two-Phase, Two-Component Flows in Pipes," Chem. Engng. Progress, Vol.45, No.1, Jan. 1949, pp.39-45.

13. R.A.Gowen, and J.W.Smith, "Turbulent Heat Transfer from Smooth and Rough Surfaces," Int. J. Heat Transfer, Vol.11, 1968, pp.1657-1673.

14. A.T.Wassel, and A.F.Mills, "Calculation of Variable Property Turbulent Friction and Heat Transfer in Rough Pipes," Trans. ASME, J. Heat Transfer, Vol.101, August 1979, pp.469-474.

15. K.R.Perkins, and D.M.McEligot, "Roughness of Heat Transfer Surfaces," Int. J. Heat Mass Transfer, Vol.16, 1973, pp.679-681.

16. R.H.Norris, "Some Simple Approximate Heat Transfer Correlations for Turbulent Flow in Ducts with Rough Surfaces," Augmentation of Convective Heat and Mass Transfer, ASME, New York, Dec. 1970.

17. J.V.Vilemas, and J.E.J.Adomaitis, "Heat Transfer and Friction of A Rough Cylinder in Longitudinal Turbulent Gas Flow with Variable Properties," Int. J. Heat Mass Transfer, Vol.31, No.8, August 1988, pp.1669-1677.

18. R.D.Haberstroh, and L.V.Baldwin, "Application of A Simplified Velocity Profile to the Prediction of Pipe-Flow Heat Transfer," Trans. ASME, J. Heat Transfer, Vol.90, May 1968, pp.191-200.

19. R.W.Allen, and E.R.G.Eckert, "Friction and Heat-Transfer Measurements to Turbulent Pipe Flow of Water (Pr=7 and 8) at Uniform Wall Heat Flux,"Trans. ASME, J. Heat Transfer, Vol.80, August 1964, pp.301-310.

20. A.J.Ede, "The Heat Transfer Coefficient for Flow in A Pipe," Int. J. Heat Mass Transfer, Vol.4, 1961, pp.105-110.

21. M.Soliman, J.R.Schuster, and P.J.Berenson, "A General Heat Transfer Correlation for Annular Flow Condensation," Trans. ASME, J. Heat Transfer, Vol.90, May 1968, pp.267-276.

22. W.W.Akers, H.A.Deans, and O.K.Crosser, "Condensing Heat Transfer within Horizontal Tubes," Chem. Engng. Progress Symp. Seires, Heat Transfer, Chicago, Vol.55, No.29, pp.171-176.

23. H.R.Kunz, and S.Yerazunis, "An Analysis of Film Condensation, Film Evaporation, and Singla-Phase Heat Transfer for Liquid Prandtl Numbers from 10^{-3} to 10^{4}," Trans. ASME, J.Heat Transfer, Vol.91, August 1969, pp.413-420.

24. G.Breber, J.W.Palen, and J.Taborek, "Prediction of Horizontal Tubeside Condensation of Pure Components using Flow Regime Criteria," Trans. ASME, J. Heat Transfer, Vol.102, August 1980, pp.471-476.

25. M.Altman, R.H.Norris, and F.W.Staub, "Local and Average Heat Transfer and Pressure Drop for Refrigerants Evaporating in Horizontal Tubes," Trans. ASME, J. Heat Transfer, Vol.82, August 1960, pp.189-198.

26. S.M.Zivi, "Estimation of Steady-State Steam Void-Fraction by Means of the Principle of Minimum Entropy Productions," Trans. ASME, J. Heat Transfer, Vol.86, May 1964, pp.247-252.

27. R.C.Martinelli, L.M.Boetler, T.H.M.Taylor, E.G.Thomsen, and E.H.Morrin, "Pressure Drop for Two-Phase Two-Componenet Flow in A Horizontal Pipe," Trans. ASME, Feb. 1944, pp.139-151.

28. M.R.Hatch, and R.B.Jacobs, "Prediction of Pressure Drop in Two-Phase Single-Component Fluid Flow," A.I.Ch.E. Journal, Vol.8, No.1, March 1962, pp.18-25.

29. S.Levy, "Prediction of Two-Phase Pressure Drop and Density Distribution from Mixing Length Theory," Trans. ASME, J. Heat Transfer, Vol.85, May 1963, pp.137-152.

30. D.Chisholm, "Pressure Gradients due to Friction during the Flow of Evaporating Two-Phase Mixtures in Smooth Tubes and Channels," Int. J. Heat Mass Transfer, Vol.16, 1973, pp.347-358.

31. J.Kubie, and H.S.Oates, "Aspects of Two-Phase Frictional Pressure Drop in Tubes," Trans. I. Chem. E., Vol.56, 1978, pp.205-209.

32. T.Johannessen, "A Theoretical Solution of the Lockhart and Martinelli Flow Model for Calculating Two-Phase Flow Pressure Drop and Hold-up," Int. J. Heat Mass Transfer, Vol.15, 1972, pp.1443-1449.

33. A.Rouet, "A Note on the Lockhart-Martinelli Correlation in the Turbulent-Turbulent Case," Int. J. Heat Mass Transfer, Vol.10, No.1, 1982, pp.145-146.

34. J.J.J.Chen, "Comments on "A Note on the Lockhart-Martinelli Correlation in the Turbulent-Turbulent Case" by A.Rouet, IJHMT, 10,145-146, 1982," Int. Comm. Heat Mass Transfer, Vol.10, No.5, 1983, pp.441-444.

35. T.B.Swearingen, and D.M.McEligot, "Internal Laminar Heat Transfer with Gas-Property Variations," Trans. ASME, J. Heat Transfer, Vol.93, Nov. 1971, pp.432-440.

36. K.T.Yang, "Laminar Forced Convection of Liquids in Tubes with Variable Viscosity," Trans. ASME, J. Heat Transfer, Vol.84, Nov. 1962, pp.157-163.

37. F.L.Test, "Laminar Flow Heat Transfer and Fluid Flow for Liquids with Temperature-Dependent Viscosity," Trans. ASME, J. Heat Transfer, Vol.90, Nov. 1968, pp.385-394.

38. P.M.Worsoe-Schmidt, "Heat Transfer and Friction for Laminar Flow of Helium and Carbon Dioxide in A Circular Tube at High Heating Rate," Int. J. Heat Mass Transfer, Vol.9, 1966, pp.1291-1295.

39. O.T.Hanna, and O.C.Sandall, "Heat Transfer in Turbulent Pipe Flow for Liquids Having A Temperature-Dependent Viscosity," Trans. ASME, J. Heat Transfer, Vol.100, May 1978, pp.224-229.

40. C.A.Sleicher, and M.W.Rouse, "A Convenient Correlation for Heat Transfer to Constant and Variable Property Fluids in Turbulent Pipe Flow," Int. J. Heat Mass Transfer, Vol.18, No.5, May 1975, pp.677-683.

41. R.B.Hassan, "A Study of Thermodynamic Characteristics and Predictive Computer Modelling of An Air to Water Heat Pump System," Ph.D. Thesis, Aston Univ., Birmingham, England, 1984.

42. M.N.Khan, "Verbal Communications and Personal Discussion- Notes and First Year Report," Aston Univ., Birmingham, England, 1986.

43. I.A.Criddle, "TBT- A Counterflow Heat Exchanger Simulation Program," Undergraduate Final Year Report, Aston Univ., Birmingham, England, 1987.

44. D.C.Hickson, "R12 Thermodynamic Property- Computer Program," Aston Univ., Birmingham, England.

45. B.S.Petukhov, and V.N.Popov, "Theoretical Calculation of Heat Exchanger and Frictional Resistance in Turbulent Flow in Tubes of An Incompressible Fluid with Variable Physical Properties," High Temperature, Vol.1, No. 1, 1963, pp.69-83.

46. T.K.Serghides, "Estimate Friction Factor Accurately," Chem. Engng., 1984, pp.63-64.

47. R.H.Pletcher, and H.N.McManus, Jr., "Heat Transfer and Pressure Drop in Horizontal Annular Two-Phase, Two-Component Flow," Int. J. Heat Mass Transfer, Vol.11, No.7, 1968, pp.1087-1104.

48. T.N.Tandon, H.K.Varma, and C.P.Gupta, "A New Flow Regimes Map for Condensation Inside Horizontal Tubes," Trans. ASME, J. Heat Transfer, Vol.104, 1982, pp.763-768.

49. V.V.Klimenko, "A Generalized Correlation for Two-Phase Forced Flow Heat Transfer," Int. J. Heat Mass Transfer, Vol.31, No.3, 1988, pp.541-552.

50. D.Frederick, and R.Greif, "A Method for the Solution of Heat Transfer Problems with A Change of Phase," Trans. ASME, J. Heat Transfer, Vol.107, August 1985, pp.520-526.

51. K.Hijikata, T.Nagasaki, J.Yoshioka, and Y.Mori, "A Study on Flow Characteristics and Heat Transfer in Counter Current Water and Air Flows," JSME Int. J., Seires 11, Vol.31, No.3, Aug. 1988, pp.429-436.

52. H.P.Soumerai, "Practical Application of the Corresponding States Principle in Heat Transfer Engineering," Heat Transfer Engng., Vol.9, No.2, 1988, pp.19-28.

53. V.Yakhot, S.A.Orszag, and A.Yakhot, "Heat Transfer in Turbulent Fluids- 1. Pipe Flows," Int. J. Heat Mass Transfer, Vol.30, No.1, 1987, pp.15-22.

54. A.Cordoba, "Effects of Variable Fluid Properties and Boundary Conditions on Thermal Convection," Int. Comm. Heat Mass Transfer, Vol.10, No.2, March-April 1983, pp.147-151.

55. T.N.Tandon, H.K.Varma, and C.P.Gupta, "A Void Fraction Model for Annular Two-Phase Flow," Int. J. Heat Mass Transfer, Vol.28, No.1, Jan. 1985, pp.191-198.

56. J.J.J.Chen, "A Further Examination of Void Fraction in Annular Two-Phase Flow," Int. J. Heat Mass Transfer, Vol.29, No.11, Nov. 1986, pp.1760-1763.

57. V.M.Borishansky, et. al., "Some Problems of Heat Transfer and Hydraulics in Two-Phase Flows," Int. J. Heat Mass Transfer, Vol.16, 1973, pp.1073-1085.

58. L.B.Koppel, and J.M.Smith, "Laminar Flow Heat Transfer for Variable Physical Properties," Trans. ASME, J. Heat Transfer, Vol.84, 1962, pp.157-163.

59. L.C.Thomas, R.Rajagopal, and B.T.F.Chung, "An Analysis of Heat Transfer in Turbulent Pipe Flow with Variable Properties," Trans. ASME, J. Heat Transfer, Vol.96, 1974, pp.107-111.

<u>Handbooks, Text-Books and other Source-Books</u>

A. Text-Books

60. R.D.Heap, "Heat Pump," John Wiley & Sons, New York, Pr., in G.B., 1979, pp.1-50.

61. D.A.Reay, and D.B.A.Macmichael, "Heat Pumps," 2nd. Ed., Pergamon Press., U.K., 1988, pp.1-49.

62. E.R.Ambrose, "Heat Pump and Electric Heating," John Wiley & Sons, N.Y., 1966.

63. J.Harry, Jr., and R.H.Howell, "Heat Pump System," John Wiley & Sons, 1983, pp.1-24.

64. Cube, Steimle, and E.G.A.Goodall, "Heat Pump Technology," Butterworth & Co. (Pub.) Ltd., 1981, pp.1-2.

65. B.C.Langley, "Heat Pump Technology," Preston Pub. Co., 1983, pp.1-54.

66. R.K.Shah, and A.L.London, "Laminar Flow Forced Convection in Ducts, Supplement 1 to Advances in Heat Trabsfer," Academic, N.Y., 1978.

67. M.N.Ozisik, "Basic Heat Transfer," McGraw-Hill Inc., U.S.A., 1977, pp.247-257.

68. J.M.Kay, and R.M.Nedderman, "Fluid Mechanics and Transfer Processes," Cambridge Univ. Press., G.B., 1985, pp.217-238.

69. B.V.Karlekar, and R.M.Desmond, "Heat Transfer," West Pub. Co., 2nd. Ed., U.S.A., 1982, pp.403-592, and pp.661-752.

70. M.Becker, "Heat Transfer: A Modern Approach," Plenum Press., N.Y., 1986, pp.159-200, pp.231-260, pp.305-338, and pp.351-360.

71. W.B.Gosney, "Principles of Refrigeration," Cambridge Univ., U.S.A., 1982, pp.254-266.

72. J.P.Holman, "Heat Transfer," 6th. Ed., McGraw-Hill Int. Ed., 1986, pp.207-322.

73. J.R.Simonson, "Engineering Heat Transfer," Macmillan Pub. Ltd., H.K., 1984, pp.178-199.

74. A.J.M.Spencer, et. al., "Engineering Mathematics; Volume 1," Van Nostrand Reinhold Co. Ltd., England, 1981, pp.381-407.

75. D.Chisholm, "Two-Phase Flow in Pipelines and Heat Exchanger," George Godwin, Pitman Press. Ltd., G.B., 1983, pp.92-119.

76. H.Hausen, "Heat Transfer in Counter Flow, Parallel Flow and Cross Flow," (*Trans. ed. by A.J.Willmott*), McGraw-Hill, Inc., U.S.A., 1983, pp.115-153.

77. R.C.Reid, and T.K.Sherwood, "The Properties of Gases and Liquids," McGraw-Hill Co., 1958.

78. M.N.Ozisik, "Basic Heat Transfer," Int. Student Ed., McGraw-Hill Co., Pr.in S'pore, Fonf & Sons Pr. Ptl. Ltd., 1985.

79. W.M.Kays, and A.L.London, "Compact Heat Exchanger," McGraw-Hill Book Co., N.Y., 1986, pp.17.

80. L.M.K.Boetler, V.H.Cherry, H.A.Johnson, and R.C.Martinelli, "Heat Transfer Notes," McGraw-Hill Book Co., U.S.A., 1965.

81. W.H.McAdam, "Heat Transmission," Chem. Eneng. Series, McGraw-Hill, 3rd Ed., U.S.A., 1954.

B. Handbooks

Handbook of Single-Phase Convective Heat Transfer, (*Edited by S.Kakac, R.K.Shah, and W.Aung*), Wiley-Interscience Pub., John Wiley & Sons, U.S.A., 1987

82. M.S.Bhatti, and R.K.Shah, "Turbulent and Transition Flow Convective Heat Transfer in Ducts," Chap.4, pp.4.1-4.73.

83. R.K.Shah, and M.S.Bhatti, "Laminar Convective Heat Transfer in Ducts," Chap.3, pp.3.1-3.137.

84. S.Kakac, "The Effect of Temperature-Dependent Fluid Properties on Convective Heat Transfer," Chap.18, pp.18.1-18.56.

85. S.Kakac, and Y.Yener, "Basic of Heat Transfer," Chap.1, pp.1.1-1.35.

86. P.E.Liley, "Thermophysical Properties," Chap.22, pp.22.1-22.41.

Handbooks of Heat Transfer Fundamental (*Edited by W.M.Rohsenow, J.P.Hartnett, and E.N.Ganic*), McGraw-Hill, 2nd. Ed., U.S.A., 1985.

87. W.M.Rohsenow, "Condensation; Part 1, Film Condensation," Chap.11, pp.11.2-11.36.

88. P.Griffith, "Condensation; Part 2, Dropwise Condensation," Chap.11, pp.11.37-11.50.

89. W.M.Rohsenow, "Boiling," Chap.12, pp.12.40-12.48.

90. P.Griffith, "Two-Phase Flow," Chap.13, pp.13.1-13.41.

Handbooks of Heat Transfer Applications, (*Edited by W.M.Rohsenow, J.P.Hartnett, and E.N.Ganic*), McGraw-Hill, 2nd. Ed., U.S.A., 1985.

91. R.K.Shah, "Heat Exchanger; Compact Heat Exchanger," Chap.2, Part 3, pp.4.183-4.197.

C. Source-Books and Edited Papers

Heat Exchanger, Thermal-Hydraulic Fundamental and Design, (*Edited by S.Kakac, A.E.Bergles, and F.Mayingger*), McGraw-Hill, Hemisphere Pub. Corp., U.S.A., 1981.

92. R.K.Shah, "Classification of Heat Exchanger," pp.9-46.

93. D.Butterworth, "Condenser: Basic Heat Transfer and Fluid Flow," pp.289-313.

94. W.M.Rohsenow, "Heat Exchanger- Basic Methods," pp.429-454.

95. D.Butterworth, "Unresolved Problems in Heat Exchanger Design," pp.1087-1106.

96. E.Achenbach, et. al., "Suggestions for Further Research and Development on Heat Exchanger," pp.1107-1112.

Advances in Heat Transfer, (*Edited by J.P.Hartnett, and T.F.Irvine*), Academic, New York, 1970.

97. B.S.Petukhov, "Heat Transfer and Friction in Turbulent Pipe Flow with Variable Physical Properties," Vol.6, pp.504-564.

Heat Exchanger: Design and Theory Sourcebook, (*Edited by N.H.Afgan, and E.U.Schlunder*), McGraw-Hill, Washington D.C., 1974.

98. B.S.Petukhov, "Turbulent Heat Transfer in Tubes with Variable Fluid Properties," Chap.11, pp.239-263.

Heat Pump Fundamental, (*Edited by J.Berghmans*), Martinus Nijhoff Pub., Netherlands, 1983.
99. H.F.Sullivan, "Principles of Vapour Compression Heat Pumps," pp.14-23.
100. J.Bberhmans, "Domestic Heat Pump Applications," pp.279-301.

Two-Phase Flow and Heat Transfer in the Power and Process Industrial," Hemisphere Pub. Corp., U.S.A., 1981.
101. J.M.Delhaye, "Frictional Pressure Drops," Chap.3, pp.48-76.
102. A.E.Bergles, "Two-Phase Flow and Heat Transfer, 1756-1980," Chap.24, pp.671-690.
103. G.F.Hewitt, "Introduction to Two-Phase Heat Transfer," Chap.6, pp.172-189.

Multi-Phase Flow System, Vol.1, Symp. at Univ. Strathclyde, Glasgow; 2-4 April 1974, I. Chem. E. Symp. Seires, No.38, 1974.
104. D.Butterworth, F.C.Hazell, and D.J.Pulling, "Heat Transfer with Phase Change; A Technique for Measuring Local Heat Transfer Coefficient for Condensation in A Horizontal Tube," D1: pp.1-11.

ASHRAE Handbook, Pub. by ASHRAE, Inc..
105. 1985 Fundamental Handbook, Chap.1, Chap.2, Chap.3, Chap.4, and Chap.13.
106. 1981 Fundamental Handbook, Chap.1, Chap.2, and Chap.4.

Manual, Maintenance and Manufacturer Specifications
107. Danfoss: Compression for Heat Pump System, Hermetic Notes: Product Line: Components for Refrigeration Application, Oct. 1978.
108. Danfoss: Instructions T2/TE2 N-B, 68-2006, 1976.
109. Danfoss: Instructions WVFX-WVA, 10-40; KI.35.B1.60, 1973.

110. Acron Computer: The BBC Micro-Computer IEEE 488 Interface User Guide, 1983.
111. C.I.L.: Operating and Maintenance Manual for PCI Seires; C.I.L. Electronics Ltd., West Sussex, U.K.
112. T.C.Limited: Thermocouple and Resistance Thermometry Data, 1987.
113. Maywood Instruments Ltd.: Semiconductor Strain Gauges Technical Notes, 1980.

114. R.S.Components: Reflective and Slotted Opto Switches: Data Sheet, March 1981.
115. Computer Program: DAP2 V2.S(C), M.Shammas 1985 for BBC Micro Model B (Disc), 1985.
116. Imperial Chemical Industries Limited, Mond Division, Marketing Department, General Chemical Group, 'ARCTON' 12.

APPENDIX A-1

LISTING OF APPARATUS EMPLOYED IN LABORATORY HEAT PUMP SYSTEM

A-1.1: Introduction

As mentioned in Chapter 3, the apparatus can be classified into the basic heat pump components, piping and joining system, and sensing equipment. The equipment has been supplied by companies or appointed agents in United Kingdom . Some of the equipment is provided with calibration certificate.

A-1.2: Heat pump components and related devices

Compressor

Items	Descriptions
Compressor	Hermetic SC10H
Refrigerant	R12
Compressr cooling	Oil/or fan cooling
Displacement	10.3 cm^3/rev
Motor type	Induction motor with starting capacitor (CSIR)
Motor size	250 W
Starting current	10 A
Oil charge	650 cm^3
Weight without el. equipment	12.1 kg
Code number	104L2515
Working range (*)	< 60°C condensing temperature
Energy consumption (*)	315 W
Heat-output (*)	1120 W
Supplier	Danfoss

(*): at 0°C evaporating temperature and 45°C condensing temperature.

Thermostatic expansion valve (TEV)

Items	Descriptions
Model	T2/TE2
Maximum permissible test pressure	26.25 bar (375 psig)
Rated capacity	= capacity at +5°C/+32°C
Suction superheat	6°C at bulb temperature, 0°C
Model	T2/TE2 N-B
Supplier	Danfoss

__Evaporator__

Items	Descriptions
Model	Vm 220
Size	0.61x0.205x0.065 m
Depth	3 rows (0.065 m)
Frontal area	0.125 m^2
Total volume	0.00813 m^3
Outside diameter for freon side	0.01 m
Inside diameter for freon side	0.008 m
Surface area for freon side	0.322 m^2
Length of tube for freon side	7.32 m of two parallel tube
Air side surface area	9.66 m^2
Fin area	8.12 m^2
Fin spacing	0.002 m
Fin tube spacing	0.025 m
Fin metal thickness	0.0002 m
Free flow area	0.055 m^2
Hydraulic radius	0.002 m
Manufactured by	Verma Temp Heat Pump Co.

__Condenser__

Items	Descriptions
Material	Copper
Outside diameter for freon side	5.75×10^{-3} m
Internal diameter for freon side	4.27×10^{-3} m
Thickness of tube for freon side	0.74×10^{-3} m
Outside diameter for water side	7.65×10^{-3} m
Internal diameter for water side	5.65×10^{-3} m
Thickness of tube for water side	1.00×10^{-3} m
Soldering materials	Savbit solder, SN 554-951 supplied by RS Components Ltd.
Total Length	15 m
Allignment	Horizontal with 26 180deg-bends at every half meter length.
Sensing joints	Tee, cross, and straight joints.
Tube insulation	Logging pipe type of insulation.
Outside insulation (system)	Vermiculite materials supplied by Dupre Vermiculite Ltd.

__Fan__

Items	Descriptions
Type	Double centrifugal (backward curved blades) fan.
Supplier	Unit taken from Versa temp air-water heat pump.

Filter drier

Items	Descriptions
Type	DX : 032
Maximum test pressure	28.0 bar (400 psig)
Supplier	Danfoss

Water regulator

Items	Descriptions
Type	WVFX-WVA 10-25
Pressure range	3.5 bar - 16.0 bar
Max. permissible test pressure	26.4 bar (377 psig)
Max. permissible water pressure	9.9 bar (142 psig)
Suction valve at condensing	: Min. 3.5 bar (3.5kg/cm²)
pressure	: Max. 16.0 bar (16 kg/cm²)
Supplier	Danfoss

Sight glass

Items	Descriptions
Type	SGI
Design for refrigerant	R12,R22,R502,R40
Max. permissible pressure	28.0 bar
Max. permissible temperature	60°C
Supplier	Danfoss

Electronic thermometer

Items	Descriptions
Type	1621 Cu/Con
Serial number	26839
Scales	A: -60°C to 10°C
	B: 0°C to 60°C
	C: 0°C to 180°C
	D: 0°C to 400°C
Supplier	Comark

Water pump

Items	Descriptions
Type	130-45 (SMC)
Input	240 V,50 Hz
Horse power	1
Supplier	Comet

A-1.3: Computer and related devices informations

Data acquisition system

Computer keyboard		
	Type	BBC 64K
Disc drive		
	Type	Double drive
	Supplier	Pace Micro Technology
Monitor		
	Type	Green monitor
	Model number	ZVM-123-E
	Supplier	Zenith Radio Corp.

Modelling analysis

Computer keyboard		
	Type	BBC (Master) 128K
	Designed by	Acorn computer
Disc drive		
	Type	Double drive
	Supplier	Pace Micro Technology
Monitor		
	Type	Colour
	Model No.	1451/DS2
	Manufactured by	Microvitec Plc.
Second processor		
	Type	PN: 0831,113
	Supplier	Acorn Computer
Hard-disc		
	Type	Winchester Disc 120
	Supplier	Acorn Computer

Analogue to digital converter (ADC)

Model	PC1001	PC1001	PC1002
Serial no.	17433	18352	17369
Input	10 mV	10 mV	10 mV
Output to	IEEE interface	IEEE interface	IEEE interface
Supplier	CIL Electronic Limited		

IEEE interface

Items	Descriptions
Type	IEEE 488 Interface
Supplier	Acorn Computer

A-1.4: Sensing equipments

Thermocouples

Wire	
Type & Stock no.	BS4937 part 5 ANSI/MC96.1, typeT, NF C 42-321 J/SC, 1602 (Cu/Cu-Ni)
Insulation	Twisted teflon with 7 strands
Insulating rating(°C)	-273 to +250
EMF/°C at 0°C reference junction at 100°	46 μV
Working temp. range (°C)	-185 to 300
Supplier	TC Limited
Thermowell	
Material	Copper
Inside	Cylindrical shape with 2.0 mm outer diameter and 3.0 mm length
Outside	At the tip:2.0 mm outer diameter, 1.5 mm height Main body:1.1 cm height, 4.0 mm circumference; bell-mouth shape
PTFE insulating bush	Total length of 1.2 cm, internal diameter of 4.00 mm; bell-mouth shape
PTFE withstand fitting	Total length of 2.4 cm, 3.0 mm of internal diameter, and 6.0 mm length at the tip with 6.0 mm external diameter
Standard compression	8 mm and 6 mm

Pressure transducer

Type	P102
Supplier	Maywood Instruments Ltd.

The following table shows a calibration certificate for the P102 pressure transducers used in the present system given by the manufacturer.

Pressure transducer	PT_1	PT_2	PT_3	PT_4
Serial number	4727	4801	4707	4728
Range (psig)	0-200	0-200	0-200	0-200
Test temperature (°C)	18	20	20	18
Excitation (Volts dc)	10	10	10	10
Non-linearity (% FRO)	0.04	0.06	0.03	0.05
Hysterises & Non-repeatibility (% FRO)	<C.05	<0.05	<0.05	<0.05
Full range output (mV)	202.40	200.76	201.33	201.11
Input resistance (Ω)	1427	1316	1403	1397
Output resistance (Ω)	493	443	477	458
Compensated temperature range (°C)	-18to65	-18to65	-18to65	-18to65
Thermal zero shift (% FRO/°C)	<+0.01	<+0.01	<+0.02	<+0.02
Thermal sensitivity shift (% FRO/°C)	<+0.02	<+0.02	<+0.02	<+0.02

Table A-1.1: Calibration data for P102 pressure transducers

Frequency-voltage converter i.c

Stock number	307-070
Supplier	RS Components Ltd.

Reflective optoswitch,[114]

Stock number	307-913
Absolute maximum rating at 25°C:	
Operating temperature range	-0°C to 70°C
Storage temperature range	-20°Cto 80°C
Lead soldering temperature	260°C
Input	2V,50mW,40mA
Output sensor	
Collector-emitter voltage	15V
Emitter-collector voltage	5V
Power dissipation	5mW
Supplier	RS Components Ltd.

Miscellenous items

Pressure calibrating machine	SN 7607/279 supplied by Budenburg Co.
Standard ordinary thermometer	-5°C to 105°C, 0.1°C scale, supplied by Philip Harris
Heat shrinkable sleeving	3.2 mm blue bore size supplied by RS Components
Heat sink compound	SN 554-311 supplied by RS Components Ltd.
Weighing machine	Triple beam balance; PAT. no. 2,729,439; maximum capacity 2610g

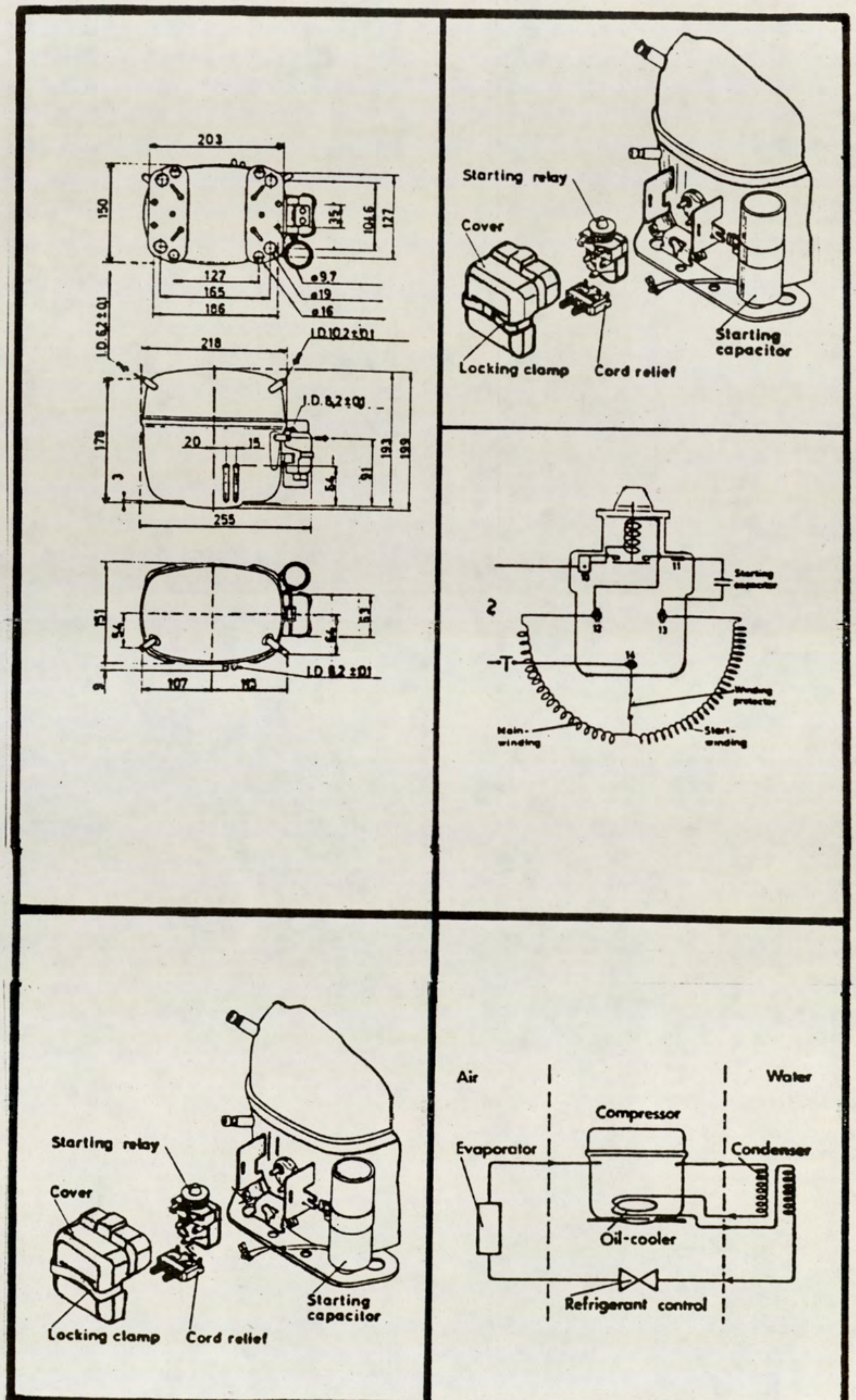

Fig.A-1.2.1: Danfoss SC10H compressor at different view given by the manufacturer

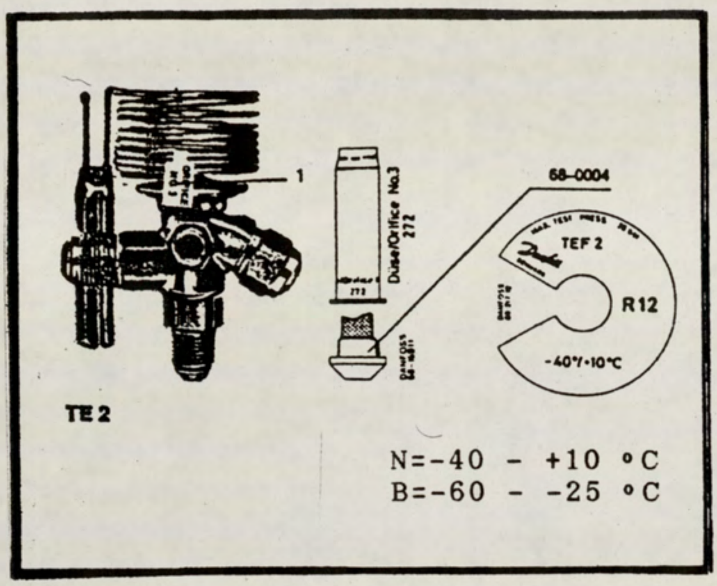

Fig.A-1.2.2: Danfoss instruction T2/TE2:N-B of TEV

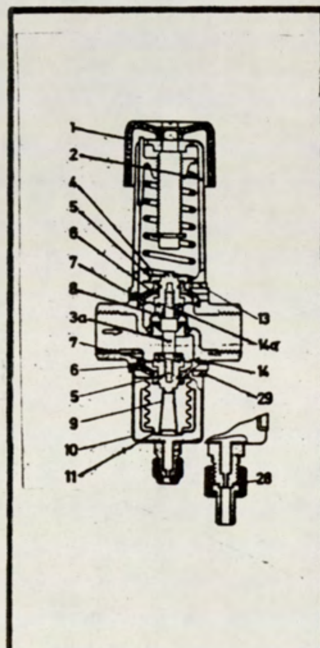

Keys:

1.hand wheel
2.top part
3a.spindle
4.spring retainer
5.o-ring
6.giude bushing
7.diaphragm/membrane
8.valve cone
9.spring holder
10.bellows unit
11.bellows stop
13.screw for spring housing
14.diaphragm plate
14a.retaining bushing
28.packing for weld nipple
29.screw for belows housing

Fig.A-1.2.3: Danfoss internal instruction WVFX-WVA, 10-40 of water regulator

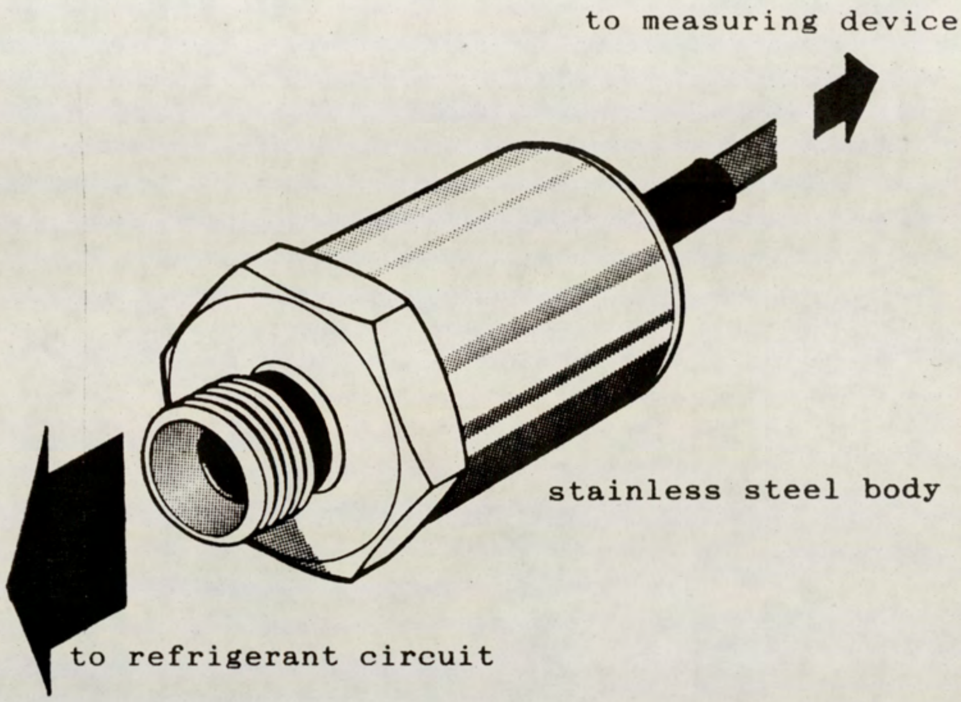

(a): The external features of a P102 transducer

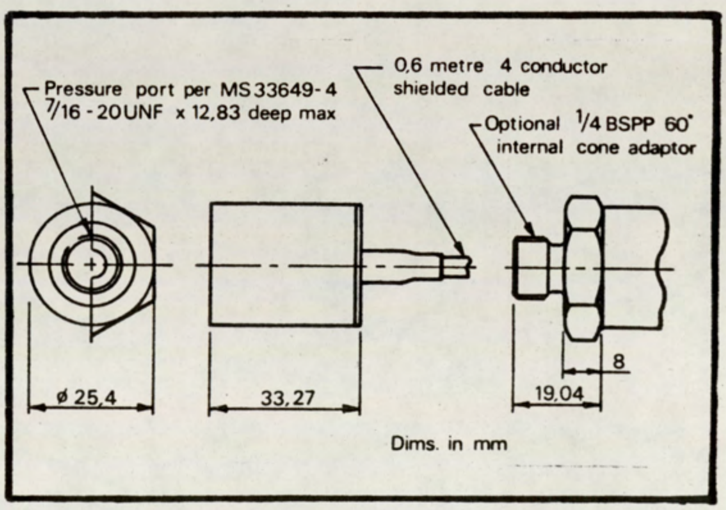

(b): The technical dimension given by manufacturer

Fig.A-1.4.1: P102 pressure transducer

CN	Calibration bits										
1	-2.00	135.00	317.00	492.40	629.00	716.00	844.50	1009.90	1143.00	1262.30	1528.80
2	7.00	145.00	327.20	503.90	641.10	728.10	856.90	1022.00	1155.80	1273.90	1539.70
3	-1.50	135.00	315.90	491.80	629.10	715.90	843.30	1007.40	1140.40	1256.70	1522.10
4	-2.90	134.80	315.90	492.80	631.00	717.70	846.00	1010.40	1144.00	1260.00	1526.90
5	-3.00	134.90	316.00	493.00	631.00	717.80	846.00	1011.00	1144.90	1262.50	1528.80
6	2.00	141.00	322.20	500.00	638.00	725.00	853.30	1019.40	1152.90	1271.30	1538.00
7	-1.00	138.00	319.70	496.70	633.90	721.00	849.00	1015.40	1147.90	1267.20	1533.00
8	-8.00	130.00	312.00	489.00	626.50	713.20	841.50	1007.40	1140.00	1258.80	1525.00
9	1.00	139.00	321.00	498.00	635.00	722.00	850.00	1015.80	1148.50	1267.30	1533.00
10	2.90	141.00	322.40	499.70	637.00	724.00	852.00	1017.70	1150.80	1268.80	1534.80
11	0.00	137.50	320.00	496.80	633.90	721.00	849.00	1015.00	1148.40	1268.30	1532.80
12	3.10	140.50	321.10	495.40	631.00	717.40	844.00	1008.00	1139.90	1258.60	1520.20
13	-5.00	132.00	313.00	487.10	622.00	709.00	835.00	1000.10	1131.30	1251.70	1512.20
14	1.90	139.00	319.90	494.80	629.00	716.00	842.30	1007.00	1137.50	1258.30	1519.40
15	-1.00	136.00	317.00	492.00	627.00	713.90	840.10	1005.10	1136.20	1256.10	1517.90
16	-1.80	134.90	314.10	488.80	623.00	709.60	835.90	1000.90	1131.80	1252.00	1513.90
17	3.00	142.00	324.70	499.30	635.90	723.00	850.10	1018.10	1150.60	1271.90	1536.00
18	4.50	144.00	326.60	502.70	639.90	727.00	854.80	1021.90	1154.70	1273.60	1538.90
19	0.00	139.00	321.80	497.60	635.00	722.00	849.90	1016.90	1149.80	1268.90	1533.90
20	-502.00	-362.40	-179.20	-3.00	134.10	222.00	351.60	519.00	652.40	772.20	1038.20
21	-503.00	-362.90	-178.90	-3.00	133.90	222.00	351.00	519.20	651.90	774.00	1038.00
22	-489.00	-350.00	-166.70	9.00	146.00	234.00	363.00	530.00	663.00	783.20	1047.00
23	-490.00	-351.00	-168.50	7.90	146.00	233.70	363.00	529.70	663.30	780.20	1047.40
24	-481.00	-341.90	-158.80	18.00	156.00	244.00	373.00	539.90	673.80	790.70	1057.80
25	-483.00	-344.00	-161.10	15.60	153.00	241.10	370.00	537.10	670.70	787.90	1054.90
26	-500.00	-360.00	-177.00	-0.20	136.80	224.00	353.30	521.00	653.70	771.70	1038.10
27	-499.00	-359.10	-176.80	0.00	138.00	225.00	355.00	522.70	654.90	773.50	1039.80
28	-496.90	-357.90	-175.30	2.00	140.00	227.70	357.00	524.00	657.10	774.30	1041.60
29	-490.90	-351.80	-169.40	8.00	146.00	233.70	362.70	529.70	662.90	780.60	1047.10
30	-496.00	-357.00	-175.00	2.00	140.00	227.80	357.00	523.10	656.90	774.40	1040.90
31	-487.00	-348.00	-165.00	11.30	149.10	237.00	366.80	533.90	667.20	786.40	1052.00
32	0.00	139.00	320.20	496.90	632.40	719.60	847.00	1013.90	1145.80	1267.00	1530.30
33	-7.10	130.70	313.00	489.00	624.30	711.90	839.40	1007.10	1139.30	1262.30	1526.20
34	-1.00	137.00	322.00	496.20	631.20	719.50	846.90	1015.70	1147.40	1272.20	1534.10
35	-2.00	136.00	320.00	494.00	629.20	717.00	844.00	1011.50	1143.20	1267.90	1528.80

Table A-1.2: Average of bits reading during thermocouple calibration (see Table 4.7(a) and 4.7(b) for corresponding temperature)

Ca28487						
Parameter (1)	CN (2)	Symbol (3)	Device (4)	a_o (5)	a_1 (6)	a_2 (7)
Temperature in °C	1	TR_1	9	-2.8960	15.206	0.018311
	2	TR_2		5.9054	15.328	0.017240
	3	TR_3		-3.0586	15.249	0.017020
	4	TR_4		-4.3080	15.329	0.016855
	5	TR_5		-4.2325	15.311	0.017317
	6	TR_6		1.0698	15.358	0.017273
	7	TR_7		-1.6477	15.333	0.017279
	8	TR_8		-9.0500	15.325	0.017274
	9	TR_9		-0.0822	15.320	0.017209
	10	TR_{10}		1.7789	15.325	0.017166
	11	TR_{11}		-1.2360	15.317	0.017450
	12	TR_{12}		2.5143	15.170	0.017060
	13	TR_{13}		-5.6295	15.148	0.017371
	14	TR_{14}		1.3969	15.148	0.017302
	15	TR_{15}		-1.7102	15.173	0.017255
	16	TR_{16}		-2.3098	15.057	0.018144
	17	TW_1	10	2.9778	15.246	0.018128
	18	TW_2		4.1185	15.351	0.017115
	19	TW_3		-0.5750	15.341	0.017211
	20	TW_4	8	12.3180	16.477	0.017791
	21	TW_5		12.1910	16.492	0.017656
	22	TW_6		24.5420	16.450	0.017394

Table A-1.3: The summary of calibrating coefficients

1	2	3	4	5	6	7
Temperature in °C	23	TW_7	8	23.8050	16.461	0.017264
	24	TW_8		33.7150	16.483	0.017034
	25	TW_9		31.0660	16.467	0.017250
	26	TW_{10}		14.7770	16.466	0.017089
	27	TW_{11}		15.6440	16.477	0.017226
	28	TW_{12}		17.5800	16.479	0.017047
	29	TW_{13}		23.5510	16.477	0.017015
	30	TW_{14}		17.7390	16.460	0.017199
	31	TW_{15}		27.1650	16.480	0.017496
	32	TR_{17}	10	-0.3052	15.264	0.017628
	33	TR_{18}		-7.5623	15.209	0.018651
	34	RT		-1.2451	15.254	0.018416
	35	TW_{16}		-2.1705	15.224	0.018207
Pressure in bar	36	PT_1		-0.8640574	0.0029317	0.000000
	37	PT_2		-0.3027839	0.0029170	0.000000
	38	PT_3		0.0454878	0.0029158	0.000000
	39	PT_4		-1.2478134	0.0029155	0.000000

APPENDIX A-2

LISTING OF COMPUTER PROGRAM FOR DATA ACQUISITION SYSTEM

A-2.1: Introduction

Followings are the listing of computer program for data acquisition system which comprises the reading of sensors through ADC and IEEE interface, bits-temperature and bits-pressure conversion, program for measuring water mass flowrate, temperature profile along the condenser, a block diagram showing four basic heat pump components (display the parameters at the entry and exit of each component), and experimental outputs storing program.

A-2.2: Computer program

The listing of the computer program for data acquisition system is given below;

```
10 REM ------------------------------------------------------------
20 REM
30 REM COMPUTER PROGRAM FOR DATA ACQUISITION SYSTEM (APPENDIX A-2)
40 REM
50 REM ------------------------------------------------------------
60 MODE128
70 ON ERROR GOTO 1190
80 DIM CH(43),DN(43),D(43),D%(43),DAV(43),T(43),A(43),B(43),C(43),Temp(40)
90 DIM N$(40),Vflow(20),Mflow(20),G(20,46),F(20,46)
100 ?&FE62=255
110 PROCSetup:@%=&404:PROCreadcoeff:VDU28,0,31,79,29
120 INPUT"Today's date (do not include year)",M$:VDU4
130 VDU4:PRINT"PRESS KEY: 1 BASIC DIAGRAM OF HEAT PUMP SYSTEM "
140 VDU4:PRINT"           : 2 DIAGRAM SHOWING TEMPERATURE PROFILE ALONG CONDENSER"
150 A$=GET$: IF A$="1" THEN GOTO 170
160 IF A$="2" THEN GOTO 190 ELSE GOTO 130
170 CLS:PRINT"THIS PROGRAM IS TO DRAW A BLOCK DIAGRAM OF HEAT PUMP SYSTEM "
180 PROCDaigram:PROCStatement:FOR III=0 TO 1000:PROCNoncond:NEXT:END
190 CLS:PRINT"THIS PROGRAM IS TO DRAW TEMPERATURE PROFILE ALONG THE CONDENSER (EVERY ONE METER)"
200 off=-2:PROCAxes:x=110:y=250:xx=1240:yy=1010:VDU24,0;100;1279;1023;:PROCBox(x,y,xx,yy)
210 FOR III= 0 TO 2:PROCconvert:NEXT:END
220 DEFPROCread: REM [***TO SELECT THE CORRECT DEVICE NUMBER FROM ADC***]
230 IF CN%=0 THEN DN=8:A$=STR$(DN)+",3":GOTO 280 ELSE IF CN%>=1 AND CN%<=16 THEN DN=9
240 CH=CN%-1 ELSE IF CN%>=20 AND CN%<=31 THEN DN=8:CH=CN%-16 ELSE DN=10
250 IF CN%>=17 AND CN%<=19 THEN CH=CN%-8 ELSE IF CN%>=32 AND CN%<=35 THEN CH=CN%-20 ELSE
260 IF CN%>=36 AND CN%<=39 THEN CH=CN%-32 ELSE IF CN%>=40 AND CN%<=43 THEN CH=CN%-40
270 A$=STR$(DN)+","+STR$(CH)
280 PROCreadADC(A$)
290 CH(CN%)=D%
300 ENDPROC
```

```
310 DEFPROCreadADC(A$): REM [***READING BITS FROM ADC***]
320  D%=0
330 *IEEE
340 adc%=OPENIN(A$)
350 H%=1
360 FORG=1TO H%
370   PRINT£cmd%,"TALK",adc%
380   PRINT£cmd%,"READ BINARY",2
390   J%=BGET£data%
400   K%=BGET£data%
410   B%=K%-224
420   IF B%<0 THEN Bi%=-1*(256*(B%+32)+J%) ELSE Bi%=256*B%+J%
430    D%=D%+Bi%
440   PRINT£cmd%,"UNTALK"
450 NEXTG
460 D%=D%/H%
470 CLOSE£adc%
480  *DISC
490 ENDPROC
500 DEFPROCSetup: REM [***COMMUNICATION BETWEEN ADC AND IEEE INTERFACE***]
510 *IEEE
520 cmd%=OPENIN("COMMAND")
530  data%=OPENIN("DATA")
540  PRINT£cmd%,"BBC DEVICE NO",21
550  PRINT£cmd%,"CLEAR"
560 PRINT£cmd%,"REMOTE ENABLE"
570   *DISC
580 ENDPROC
590 DEFPROCconvert: REM [***BITS-TEMPERATURE & PRESSURE CONVERSION AND PROFILE***]
600 CLS
610 CLS:@%=&404
620 FOR s= 1 TO 20
630 PROCErase
640 PROCSmallbox
650 PROCzero:PROCtime:SOUND 1,-15,1000,2:REPEAT UNTIL (TIME-T)>1000
660 PROCsound:PROCtime:PROCavread
670 CN%=0:G(s,0)=DAV(0):F(s,0)=T(0)
680 FOR I=1 TO 15
690 CN%=I:X=CN%
700 G(s,I)=DAV(CN%):F(s,I)=T(CN%):PROCequation
710 CN%=(I+16):X=CN%-16
720 G(s,I+16)=DAV(CN%):F(s,I+16)=T(CN%):PROCequation
730 VDU4:PRINT I," "G(s,I)," "F(s,I)
740 PLOT 69,(X-Xmin)*J+x+(35*off),(F(s,I)-Ymin)*K+y
750 VDU4:PRINT I+16," "G(s,I+16)," "F(s,I+16)
760 PLOT 69,(X-Xmin)*J+x+(35*off),(F(s,I+16)-Ymin)*K+y
770 NEXT
780 I=16:CN%=I
790 G(s,I)=DAV(CN%):F(s,I)=T(CN%):PROCequation
800 CN%=(I+19):G(s,I+19)=DAV(CN%):F(s,I+19)=T(CN%):PROCequation
810 PLOT 69,(X-Xmin)*J+x+(5*off),(F(s,I)-Ymin)*K+y
820 PLOT 69,(X-Xmin)*J+x+(5*off),(F(s,I+19)-Ymin)*K+y
830 VDU4:PRINT CN%," "G(s,CN%)," "F(s,CN%)
840 FOR CN%=32 TO 34:G(s,CN%)=DAV(CN%):F(s,CN%)=T(CN%):PROCequation
850 VDU5:MOVE (x+xx)/1.3,y-80:PROCDelete:@%=&00020205:PRINT F(s,34):VDU4
860 VDU4:PRINT CN%," "G(s,CN%)," "F(s,CN%)
870 NEXT
880 VDU5:MOVE (x+xx)/1.45,y-120:PROCDelete:@%=&00020205:PRINTF(s,35)," & "F(s,17):VDU4
```

```
890 FOR CN%=36 TO 43:G(s,CN%)=DAV(CN%):F(s,CN%)=T(CN%):PROCequat:PROCprlimit
900 REM VDU5:MOVE (x+xx)/1.35,y-120:PROCDelete:PRINTTin," & "Tout
910 VDU5:MOVE aa+450,bb+40:PROCDelete:PRINTF(s,37):VDU4
920 VDU5:MOVE aa+450,bb+70:PROCDelete:PRINTF(s,38):VDU4
930 VDU5:MOVEa+530,bb+40:PROCDelete:PRINTF(s,40)
940 VDU5:MOVEa+530,bb+70:PROCDelete:PRINTF(s,41):@%=&404
950 VDU4:PRINT CN%,"  "G(s,CN%),"  "F(s,CN%)
960 NEXT
970 PRINT:PRINT
980 PROCfilename
990 VDU5:MOVE(x+xx)/2.4,yy-10:PRINT T$:MOVE(x+xx)/1.23,yy-10:PRINT N$:VDU4
1000 VDU4:PRINTtime
1010 VDU4:PRINTG(s,44)," "G(s,45)," "G(s,46)
1020 PROCdwbits:PROCdelay(n):*SMALLDUMP
1030 PROCzero
1040 NEXT s
1050 ENDPROC
1060 DEFPROCdelay(n): REM [***SET DELAYING TIME IN MINUTE***]
1070 n=30
1080 PROCtime
1090 REPEAT UNTIL (TIME-T)>=n*6000
1100 ENDPROC
1110 DEFPROCfilename: REM [***AUTOMATIC FILENAME FOR STORING AND READING DATA***]
1120 T$=M$ +"  1987"
1130 FILENUMBER=s
1140 REM N$(s)=MID$(T$,5,2)+MID$(T$,8,3)+STR$(s)
1150 S=(20*III)+s
1160 N$=M$+STR$(S)
1170 ENDPROC
1180 DEF FN@(P%):@%=P%:=""
1190 VDU3:MODE128:PRINT"ERROR NO ";ERR; "AT LINE " ERL:END
1200 DEFPROCequat: REM [***BITS-PRESSURE CONVERSION***]
1210 F(s,CN%)=A(CN%)+B(CN%)*G(s,CN%)+C(CN%)*(G(s,CN%))^2
1220 ENDPROC
1230 REM-----------------------------------------------
1240 DEFPROCreadcoeff: REM READING CALIBRATION COEFFICIENTS
1250 REM-----------------------------------------------
1260 REM INPUT"Enter filename for calibration coefficients",F$
1270 F$="Ca28487"
1280 QQ%=OPENIN(F$)
1290 FOR CN%=1 TO 43
1300 INPUT£QQ%,A(CN%),B(CN%),C(CN%)
1310 NEXT
1320 CLOSE£QQ%
1330 ENDPROC
1340 DEFPROCsound: REM [***SET WARNING SOUND AT THE END AND BEGINNING OF EACH RUN***]
1350 SOUND 2,-15,97,10
1360 SOUND 2,-15,105,10
1370 SOUND 2,-15,89,10
1380 SOUND 2,-15,41,10
1390 SOUND 2,-15,69,20
1400 ENDPROC
1410 DEFPROCAxes: REM [***SET X,Y-AXIS FOR TEMPERATURE PROFILE***]
1420 Xmin=0:Xmax=15
1430 Xinterval=(Xmax-Xmin)/5:Xrange=(Xmax-Xmin)
1440 INPUT"Yminimum,Ymaximum (temperature in deg. celcius)",Ymin,Ymax
1450 Yinterval=(Ymax-Ymin)/5:Yrange=(Ymax-Ymin)
1460 ENDPROC
```

```
1470 DEFPROCBox(x,y,xx,yy): REM [***DRAW A BLOCK AND SCALES FOR GRAPH***]
1480 CLG
1490 VDU5:MOVEx,y:DRAWxx,y:DRAWxx,yy:DRAWx,yy:DRAWx,y
1500 J=(xx-x)/Xrange:K=(yy-y)/Yrange
1510 VDU5:FOR Y=Ymin TO Ymax STEP Yinterval:MOVE x-70,(Y-Ymin)*K+y+10:PRINT Y:NEXT
1520 MOVE x-x,yy-60:PRINT"Temp(C)"
1530 VDU5:FOR X=Xmin TO Xmax STEP Xinterval:MOVE (X-Xmin)*J+x-50+off,y-15:PRINT X:NEXT
1540 MOVE (x+xx)/3,y-50:PRINT"Length in condenser in meter"
1550 MOVE (x+xx)/3.7,y-80:PRINT"at room temperature (deg. celcius)"
1560 MOVE (x+xx)/7,y-120:PRINT"Water Inlet & Outlet temperature (C)"
1570 VDU19,0,4,0,0,0
1580 GCOL 0,1:VDU4
1590 ENDPROC
1600 DEFPROCSmallbox: REM [***DRAW SMALL BOX TO WRITE OTHER PARAMETERS OUTSIDE CONDENSER***]
1610 a=(x+xx)/5.8:b=(yy-40):aa=(xx-475):bb=(yy-120)
1620 VDU5:MOVEa,b:DRAW aa,b:DRAW aa,bb:DRAW a,bb:DRAW a,b
1630 VDU5:MOVE a+10,bb+70:PRINT"=====> freon flow (g/s) "
1640 VDU5:MOVE a+10,bb+40:PRINT"water flow (g/s) <===== "
1650  VDU5:MOVE aa+30,bb+70:PRINT"disc press (bar) :"
1660 VDU5:MOVE aa+30,bb+40:PRINT"suct press (bar) :"
1670 VDU4
1680 ENDPROC
1690 DEFPROCDaigram: REM [***DRAW SMALL BLOCK FOR HEAT PUMP DIAGRAM***]
1700 x=110:y=250:xx=1260:yy=1010
1710 VDU24,0;100;1279;1023;
1720 MOVEx,y:DRAW xx,y:DRAW xx,yy:DRAW x,yy:DRAW x,y
1730 a=(x+xx)/3.5:b=(y+100):aa=(a+600):bb=(y+200)
1740 VDU5:MOVEa,b:DRAW aa,b:DRAW aa,bb:DRAW a,bb:DRAW a,b
1750 c=a:d=(y+480):cc=aa:dd=(y+600)
1760 VDU5:MOVEc,d:DRAW cc,d:DRAW cc,dd:DRAW c,dd:DRAW c,d
1770 e=(a-150):f=(y+300):ee=a-20:ff=(y+400)
1780 VDU5:MOVEe,f:DRAW ee,f:DRAW ee,ff:DRAW e,ff:DRAW e,f
1790 g=(a+630):h=f:gg=(a+770):hh=ff
1800 VDU5:MOVEg,h:DRAW gg,h:DRAW gg,hh:DRAW g,hh:DRAW g,h
1810 i=(x+xx)/4.5:j=(b+bb)/2:ii=a+700:jj=(d+dd)/2.05
1820 VDU5:MOVEi,j:DRAW ii,j:DRAW ii,jj:DRAW i,jj:DRAW i,j
1830 VDU5:MOVEi,jj+25:DRAW ii,jj+25
1840 ENDPROC
1850 DEFPROCStatement: REM [***WRITE STATEMENTS FOR HEAT PUMP DIAGRAM***]
1860 MOVE (x+xx)/3,y-30:PRINT"A basic diagram of heat pump"
1870 MOVE i+210,jj+60:PRINT"water  ========>"
1880 MOVE i+330,jj-5:PRINT"<========  freon"
1890 MOVE i+280,jj-45:PRINT"**condenser**"
1900 MOVE i+280,j+85:PRINT"**evaporator**"
1910 MOVE i+280,j+40:PRINT"freon  ========>"
1920 FOR I= 0 TO 40 STEP 10:MOVE i+80,(j+230)-I:PRINT"¦":NEXT:MOVE i+80,(j+190):PRINT"v"
1930 VDU5:MOVE i+95,(j+230):PRINT"throttling valve"
1940 FOR I= 0 TO 40 STEP 10:MOVE ii-100,(j+230)-I:PRINT"¦":NEXT:MOVE ii-100,(j+230):PRINT"^"
1950 VDU5:MOVE ii-265,(j+200):PRINT"compressor"
1960 MOVE ii-30,jj+10:PRINT"I":MOVE i+20,jj+10:PRINT"I"
1970 MOVE ii-30,j+15:PRINT"I":MOVE i+20,j+15:PRINT"I"
1980 MOVE ii-30,jj+48:PRINT"I":MOVE i+20,jj+48:PRINT"I"
1990 VDU19,0,4,0,0,0
2000 GCOL 0,1:VDU4
2010 ENDPROC
```

```
2020 DEFPROCNoncond: REM [***READING DATA FOR BASIC HEAT PUMP DIAGRAM***]
2030 REM CLS:@%=&00020205:PROCreadcoeff
2040 CLS:@%=&00020205
2050 FOR s= 1 TO 25
2060 PROCtime:PROCfilename
2070 VDU5:MOVE(x+xx)/2.5,yy-10:PRINT T$:VDU4
2080 PROCzero:PROCavread
2090 CN%=0:G(s,0)=DAV(0):F(s,0)=T(0)
2100 CN%=1:G(s,CN%)=DAV(CN%):F(s,CN%)=T(CN%):PROCequation
2110 VDU5:MOVE (ii+135),jj+30:PROCDelete:PRINTF(s,1);"(C)":VDU4
2120 @%=&00020208:PRINT"  "G(s,CN%);"     "F(s,CN%):VDU4:@%=&00020205
2130 FOR CN%=16 TO 17:G(s,CN%)=DAV(CN%):F(s,CN%)=T(CN%):PROCequation
2140 VDU5:MOVE i-40,jj+30:PROCDelete:PRINTF(s,16);"(C)":VDU4:VDU5:MOVE (ii+135),jj+70:PROCDelete
2150 PRINTF(s,17);"(C)":VDU4:@%=&00020208:PRINT"  "G(s,CN%);"     "F(s,CN%):@%=&00020205
2160 NEXT
2170 FOR CN%=32 TO 35:G(s,CN%)=DAV(CN%):F(s,CN%)=T(CN%):PROCequation
2180 VDU5:MOVE i-40,j+35:PROCDelete:PRINTF(s,32);"(C)":VDU4:VDU5:MOVE (ii+135),j+35:PROCDelete
2190 PRINTF(s,33);"(C)":VDU4:@%=&00020208:PRINT"  "G(s,CN%);"     "F(s,CN%):@%=&00020205
2200 VDU5:MOVE (x+xx)/3,y-60:PRINT "at room temperature ":VDU4:VDU5:MOVE ii-180,y-60:PROCDelete
2210 PRINT F(s,34);"(C)":VDU4:VDU5:MOVE i-40,jj+70:PROCDelete:PRINTF(s,35);"(C)":VDU4
2220 NEXT
2230 FOR CN%=36 TO 43:G(s,CN%)=DAV(CN%):F(s,CN%)=T(CN%):PROCequat:PROCprlimit
2240 VDU5:MOVE i-40,jj-5:PROCDelete:PRINTF(s,36);"(bar)":VDU4:VDU5:MOVE (ii+135),jj-5:PROCDelete
2250 PRINTF(s,38);"(bar)":VDU4
2260 VDU5:MOVE i-40,j-5:PROCDelete:PRINTF(s,39);"(bar)":VDU4:VDU5:MOVE (ii+135),j-5:PROCDelete
2270 PRINTF(s,37);"(bar)":VDU4
2280 VDU5:MOVE ii-165,jj+60:PROCDelete:PRINTF(s,40);"(cc/s)":VDU4:VDU5:MOVE ii-550,jj-5:PROCDelete
2290 PRINTF(s,41);"(cc/s)":VDU4
2300 NEXT:NEXT
2310 ENDPROC
2320 DEFPROCDelete: REM [***TO DELETE***]
2330 FOR I=1TO8:VDU127:NEXT
2340 ENDPROC
2350 DEFPROCErase: REM [***TO ERASE TEXT WINDOW***]
2360 VDU24,x+5;y+5;xx-3;yy-3;
2370 CLG:VDU5
2380 VDU24,0;100;1279;1023;
2390 ENDPROC
2400 DEFPROCdwbits: REM [***SAVING DATA ONTO DISC***]
2410 CLS
2420 IF S>30 THEN DR$=":3." ELSE DR$=":1."
2430 F$=DR$+N$
2440 QQ%=OPENOUT (F$)
2450 PRINT#QQ%,T$
2460 FOR CN%=0 TO 46
2470 PRINT#QQ%,G(s,CN%)
2480 NEXT
2490 CLOSE#QQ%
2500 ENDPROC
2510 DEFPROCprinter: REM [***TO PRINTER***]
2520 VDU2:VDU1,27,1,33,1,4
2530 ENDPROC
```

```
2540 DEFPROCbits: REM [***DISPLAY OUTPUTS ON SCREEN***]
2550 PROCprinter
2560 PRINT"Channel   Bits  Temperature   Channel   Bits  Temperature   BW-BR12   TW-TR12"
2570 FOR CN%=1 TO 15
2580 PRINTCN%,G(s,CN%),F(s,CN%),CN%+16,G(s,CN%+16),F(s,CN%+16),G(s,CN%+16)-G(s,CN%),F(s,CN%+16)-F(s,CN%)
2590 NEXT
2600 CN%=16
2610 PRINTCN%,G(s,CN%),F(s,CN%),CN%+19,G(s,CN%+19),F(s,CN%+19),G(s,CN%+19)-G(s,CN%),F(s,CN%+19)-F(s,CN%)
2620 N=0
2630 REPEAT
2640 N=N+1
2650 G(s,CN%)=G(s,CN%)+G(s,CN%+1)
2660 UNTIL N=30
2670 PRINT:PRINT" The bits from PCI 1002:SN/17369(DN8)"," "G(s,0),"Bits"," "G(s,0)*0.025,"C"
2680 VDU3
2690 ENDPROC
2700 DEFPROCequation: REM [***BITS-TEMPERATURE CONVERSION***]
2710 IF CN%>=20 AND CN%<=31 THEN F(s,0)=G(s,0)*0.025 ELSE F(s,0)=0
2720 Z1=B(CN%)^2:Z2=(4*C(CN%)*(A(CN%)-G(s,CN%))):Z3=SQR(Z1-Z2)
2730 IF Z1>Z2 THEN F(s,CN%)=F(s,0)+((-B(CN%)+Z3)/(2*C(CN%)))ELSE
2740 IF Z1=Z2 THEN F(s,CN%)=F(s,0)+(-B(CN%)/(2*C(CN%))) ELSE F(s,CN%)=0
2750 ENDPROC
2760 REM
2770 DEFPROCavread: REM [***READING AVERAGE VALUE***]
2780 N=0
2790 REPEAT
2800 N=N+1
2810 FOR CN%= 0 TO 43
2820 PROCread
2830 D%(CN%)=D%(CN%)+D%
2840 VDU4:PRINTTAB(10)CN%,"  "D%(CN%)
2850 NEXT
2860 UNTIL N=10
2870 FOR CN%=0 TO 43:DAV(CN%)=D%(CN%)/N:NEXT
2880 PROCsound:INPUT"The time taken to fill up the container in second",time
2890 INPUT"The quantity of water in container in c.c",CC
2900 INPUT"The mass of collected water in gram",Ww
2910 INPUT"The temperature of exit water in C",Tw
2920 Vflow(s)=(CC/time):G(s,44)=Vflow(s)
2930 Mflow(s)=(Ww/time):G(s,45)=Mflow(s)
2940 Temp(s)=Tw:G(s,46)=Temp(s)
2950 VDU12:ENDPROC
2960 DEFPROCzero: REM [***TO RESET***]
2970 FORII=0 TO 43:D%(II)=0:NEXT
2980 ENDPROC
2990 DEFPROCtime: REM [***SET TIME***]
3000 TIME=0:T=TIME
3010 ENDPROC
3020 DEFPROCprlimit: REM [***LIMIT FOR PRESSURE***]
3030 IF F(s,38)>13.0 THEN FOR sound=1 TO 100 :PROCsound:NEXT:END
3040 ENDPROC
```

APPENDIX A-3

LISTING OF COMPUTER MODEL

A-3.1: Introduction

The main program comprises the following; input data from appropriate experimental run, main program divided into vapour region, two-phase region and liquid region (numerical integration and iteration process), monitoring program, and outputs.

The input data read from a separate subroutine are taken from appropriate experimental runs. The effective parameters are then calculated in subroutine 1. At this level, the program reads all the constant coefficients,[44], coil descriptions, and fluid input and output temperature. The next step is to calculate dew temperature at given freon inlet pressure, freon mass flowrate, and coil internal diameters for both side of the tube.

The second part shows the main body of the program within the iteration loop. The calculation in the numerical integration is divided to three sections; desuperheating, two-phase (or condensing) and subcooling regimes. The basic objective is to calculate the correct outlet temperature of water by considering all possible properties of the fluids within the iteration at particular condition. The properties of the fluids are as follows; heat transfer coefficients, properties of freon at various state, properties of water, linear conductivity of heat exchanger, number of transfer units of the fluids, effectiveness, and the next point parameters. The thermodynamic, physical and other properties of the fluids are evaluated in subroutine 1 and 2.

The monitoring program is to check whether the correct water outlet temperature has been obtained.

Finally, the outputs are as follows; summary of separate results for three segments, detailed profile of various fluids properties (temperature, pressure, heat transfer coefficients, and number of transfer units), summary of enthalpy balance and entropy creation rates, and the summary of possible simple refrigeration cycle.

A-3.2: Computer program

The listing of the computer program can be seen in the next page.

```
C**********************************************************************C
C                                                                      C
C       COMPUTER MODELLING FOR APPENDIX A-3 IN SECTION A-3.2           C
C                                                                      C
C      PROGRAM TBTCOND-F77 COMPILED AND LINKED WITH SUBROUTINE         C
C       TBTSUBROU-F77 AND R12-F77, AND INPUT DATA; TBTINDATA           C
C                                                                      C
C**********************************************************************C
      PROGRAM TBT
C****-----------------------------------------------------------****
C**** COUNTERFLOW HEAT EXCHANGER INTEGRATION AND ITERATION ROUTINE ****
C**** FLUIDS: R12 & WATER **** AUTHOR: C.G.CARRINGTON, OTAGO, N.Z. ****
C**** MODIFIED BY M.B.ABDUL WAHAB, ASTON UNIV.,B'HAM, ENGLAND, 1988****
C**** ------------------------------------------------------------****

C**** THIS PROGRAM MODELS THE BEHAVIOUR OF A COUNTERFLOW R12       ****
C**** CONDENSER COMPRISED OF TWO TUBES THERMALLY COUPLED.          ****
C**** WALL THERMAL GRADIENTS ARE IGNORED.  THE SINGLE PHASE AND    ****
C**** TWO PHASE REGIONS ARE TREATED SEPARATELY.  TEMPERATURE       ****
C**** DEPENDENT FLUID PROPERTIES (VISCOSITIES,CONDUCTIVITIES       ****
C**** HEAT CAPACITIES ETC.) FROM ASHRAE GUIDE & DATA BOOK ARE USED.****
C**** THIS PROGRAM USES R12 THERMODYNAMIC PROPERTY SUBROUTINES     ****
C**** WRITEN BY DEREK HICKSON, U.A.B.  THESE ARE IN AGREEMENT WITH ****
C**** ASHRAE VALUES AND DUPONT DATA.  COULD BE SUSPECT NEAR THE    ****
C**** CRITICAL POINT.                                              ****

C**** THE FOLLOWING FUNCTIONS FROM D.HICKSON'S LIBRARY ARE USED:-  ****
C**** (REDUCED VALUES ARE USED FOR ALL ARGUMENTS)                  ****

C**** PSATR12(T)      PRESSURE OF SATURATED R12                    ****
C**** TSATR12(P)      TEMPERATURE OF SATURATED R12                 ****
C**** VR12(P,T)       SPECIFIC VOLUME OF SUPERHEATED R12           ****
C**** VFR12(T)        SPECIFIC VOLUME OF LIQUID R12                ****
C**** HFGR12(T,P,VG,VF) LATENT HEAT OF R12                         ****
C**** HR12(VG,T)      SPECIFIC ENTHALPY OF SUPERHEATED R12         ****
C**** SR12(VG,T)      SPECIFIC ENTROPY OF SUPERHEATED R12          ****

C**** INPUT DATA FROM PROGRAM TBTINDATA ARE:-                      ****

C**** A:COIL DESCRIPTIONS:                                         ****
C****     TWALL  THICKNESS OF WALL OF THE TWO TUBES (M.M.)         ****
C****     DIAF   OUTSIDE DIAM OF THE R12 TUBE AT LIQUID EXIT END   ****
C****     DIAG   OUTSIDE DIAM OF THE R12 TUBE AT GAS INLET END(M.M) ****
C****     LNTH   TOTAL LENGTH OF THE CONDENSER ( METER)            ****
C****     PCNTF  PERCENTAGE OF REFRIGERANT TUBE WITH O.D. DIAF     ****
C****     DIAW   OUTSIDE DIAM OF THE WATER TUBE (M.M.)             ****

C**** B:FLUID PARAMETERS AT THE ENTRANCE/EXIT (FROM EXPERIMENT):
C****     TR1    TEMPERATURE OF R12 AT POINT 1 (C)                 ****
C****     TR2    TEMPERATURE OF R12 AT POINT 2 (C)                 ****
C****     TR15   TEMPERATURE OF R12 AT POINT 15 (C)                ****
C****     TR16   TEMPERATURE OF R12 AT POINT 16 (C)                ****
C****     TW1    TEMPERATURE OF WATER AT POINT 1 (C)               ****
C****     TW2    TEMPERATURE OF WATER AT POINT 2 (C)               ****
C****     TW15   TEMPERATURE OF WATER AT POINT 15 (C)              ****
C****     TW16   TEMPERATURE OF WATER AT POINT 16 (C)              ****
C****     PRIN   PRESSURE OF R12 AT POINT 1 (BAR)                  ****
C****     PROUT  PRESSURE OF R12 AT POINT 16 (BAR)                 ****
C****     MWATER WATER MASS FLOWRATE (GRAM/S)                      ****
```

```
C**** C:EFFECTIVE FLUID  PARAMETERS AT THE ENTRANCE/EXIT (MODEL):
C****      BONDU  CONDUCTIVITY OF THERMAL BOND BETWEEN TUBES (W/M.C) ****
C****      THPWR  THERMAL POWER TO BE TRANSFERRED TO WATER (WATT)    ****
C****      TR(1)  TEMPERATURE OF ENTERING HOT REFRIGERANT GAS (C)    ****
C****      PRES   PRESSUREE OF ENTERING HOT REFRIGERANT GAS (BAR)    ****
C****      TSUB   EXIT TEMPERATURE OF CONDENSED LIQUID REFRIG. (C)   ****
C****      TWIN   TEMPERATURE OF WATER ENTERING CONDENSER (C)        ****
C
C**** THE PRIMARY OUTPUT DATA IS:-                                   ****
C****      (A)    THE EXIT WATER TEMPERATURE                         ****
C****      (B)    THE CORRESPONDING WATER FLOW RATE                  ****
C****      (C)    PRESSURE AND TEMPERATURE PROFILES, MASS OF         ****
C****             R12, HEAT TRANSFER COEFFICIENTS ETC                ****

C     DECLARATION

      REAL LNTH,MRDOT,MWDOT,NTUR(155),NTUW(155),IDR(155),IDW(155),MEWR
      REAL MEWW,NUS,MEWF,MEWG,ODW(155),ODR(155)
      COMMON/BLK1/HC,TC,VC,PC
      DIMENSION TR(155),TW(155),PR(155),PW(155),X(155),UL(155),ER(155)
      DIMENSION EW(155),HR(155),HW(155),AL(155),HHR(155),TWL(155)
      DIMENSION S(1000),ISN(1000)
      LOGICAL FOOLED,HALVE
      CHARACTER File*14

      OPEN (3,FILE='kb:')
      OPEN (4,FILE='vdu:')
      OPEN (5,FILE='TBTindata')

C     READ IN PRINT VARIABLE:  KPRINT=1 FOR BRIEF SUMMARY; 2 FOR SUMMARY
C     AND SECOND LAW ANALYSIS; 3 FOR COMPLETE PRINT OUT WITH TEMPERATURE
C     AND PRESSURE PROFILE; 4 FOR PRINTOUT AFTER FIRST INTEGRATION.
C
      WRITE (4,601)
      READ (3,602) KPRINT

C     READ IN COIL DESCRIPTION, FLUID INPUT & OUTPUT TEMPERATURES.

      READ (5,600,END=2) TWALL,DIAF,DIAG,LNTH,PCNTF,DIAW
      IF(TWALL.EQ.0.0) GOTO 2
      READ (5,600,END=2) BONDU,TR1,TR2,TR14,TR15,TW1
      READ (5,600,END=2) TW2,TW14,TW15,PRIN,PROUT,WATER
      READ (5,600,END=2) Qlost

      CLOSE (5)
      CLOSE (4)

      CALL AIMPUT(TR1,TR2,TR14,TR15,TW1,TW2,TW14,TW15,PRIN,
     1PROUT,WATER,TSUB,TR(1),TWOUT,TWIN,PRES,Qwater)

      D1=PCNTF*LNTH/100.0
      D2=LNTH-D1

C     DEFINE CRITICAL POINT VALUES FOR R12.
      HC=7.37412E3
      TC=385.17
      VC=1.7918E-3
      PC=41.155E5
```

```
C     THESE CONSTANTS ARE IN S.I. UNITS: J, DEG K, M**3, KG.
C     THESE VALUES AND THERMODYNAMIC FUNCTIONS KINDLY PROVIDED BY
C     DEREK HICKSON, U.A.B.

C     CALCULATE DEW TEMPERATURE , ETC OF WATER AND REFRIGERANT.

      PR(1)=(PRES*100000.0)
      TDEW=(TC*TSATR12(PR(1)/PC))-273.15
      PW(1)=0.00

C     FIND MASS FLOW RATE OF REFRIGERANT

      THPWR=(Qwater+Qlost)
      Flost=(Qlost/THPWR)
      MRDOT=THPWR/(HG(PR(1),TR(1))-HSAT(0.0,TSUB))

C  FIND COIL INTERNAL DIAMETERS AND INTEGRATION INCREMENT, DLNTH.
C  f=1.0 FOR STRAIGHT PIPE & fr12=0.976 & fwat=0.886 FOR PIPE AT THE BEND.

       DO I=1,155
        IF((I .GT. 1) .AND.(I .LT. 151)) THEN
        IF(MOD(I,5).EQ.1) THEN
         fr12=0.97584
         fwater=0.88620
        ELSE
         fr12=1.00
         fwater=1.00
        END IF
        ELSE
         fr12=1.00
         fwater=1.00
        END IF
         ODW(I)=(DIAW*fwater)/1000
         IDW(I)=(DIAW-2*(TWALL*1.3513514))*fwater/1000
         IF (I .GT. (100-PCNTF)) THEN
          ODR(I)=(DIAF*fr12)/1000
          IDR(I)=(DIAF-(2*TWALL))*fr12/1000
         ELSE
          ODR(I)=(DIAG*fr12)/1000
          IDR(I)=(DIAG-(2*TWALL))*fr12/1000
         END IF

        END DO

       DLNTH=LNTH/150

C      CHOOSE TDEW AS A TRIAL WATER EXIT TEMPERATURE.

       S(1)=TDEW
       STEP=2

C**********************************************************************
C
C       COMMENCE ITERATION TO CALCULATE CORRECT WATER EXIT TEMPERATURE
C
C**********************************************************************
```

```
      K=0
1001  K=K+1
      WRITE(4,'('' Iteration number ='',I3)')K

C     SET REYNOLDS NUMBER ACCUMULATORS TO ZERO.
      RR1=0.0
      RW1=0.0
      RR2=0.0
      RW2=0.0
      RR3=0.0
      RW3=0.0

C     SET REFRIGERANT MASS ACCUMULATORS TO ZERO.

      AMSUP=0.0
      AM2PS=0.0
      AMSUB=0.0
      TW(1)=S(K)

C     CALCULATE CORRESPONDING WATER MASS FLOW RATE.

      MWDOT=Qwater/(FP(9,TW(1)) - FP(9,TWIN))

C************************************************************************
C
C  MOVE INTO LENGTH INTEGRATION SEGMENT;  MAKE DECISIONS ON WHAT TO DO
C  WITH S(K).
C
C  INTEGRATE THROUGH THE HEAT EXCHANGER.  I  INCREASES IN THE DIRECTION
C  OF REFRIGERANT FLOW.  THE POSITION I IS AT THE START OF THE
C  SEGMENT I, NUMBER 1 BEING AT THE START OF THE REFRIGERANT ENTRY END.
C
C************************************************************************

C************************************************************************
C            **** FIRSTLY : THE DESUPERHEATING REGION ****
C************************************************************************

C     ASSUME A STARTING VALUE FOR WALL TEMPERATURE,TWL(1).

      TWL(1)=(TR(1)+TW(1))/2.0

      FOOLED=.FALSE.

      DO I=1,150
        AL(I)=1.0
        X(I)=1.0
        JSUP=I
        TSAT=TC*TSATR12(PR(I)/PC) - 273.15

C       IF TW(I).GT.TR(I) IN SUPERHEAT REGION ABANDON INTEGRATION AND
C       RETURN TO STATEMENT 1500 IN ITERATION SEGMENT TO ADJUST TW(1) (=S(K))

        FOOLED=TW(I).GT.TR(I)
        IF (FOOLED) GOTO 1500

C       LEAVE THE DESUPERHEATING REGION WHEN TR DROPS BELOW TSAT.
```

```
      IF (TR(I) .LT. TSAT) GOTO 4200

      HHR(I)=HG(PR(I),TR(I))

C     CALCULATE HEAT TRANSFER COEFFICIENTS OF REFRIGERANT AND WATER.
C     FIRST DEFINE FLUID PROPERTIES OF THE REFRIGERANT VAPOUR.

      GR=1.273*MRDOT/(IDR(I)*IDR(I))
      PRED=PR(I)/PC
      TRED=(TR(I)+273.15)/TC
      RTTR=TR(I)/TWL(I)
      RHOR=1/(VC*VR12(PRED,TRED))
      MEWR=FP(1,TR(I))
      RMUR=MEWR/FP(1,TWL(I))
      CONR=FP(2,TR(I))
      CPR=HG(PR(I),TR(I)+0.5) -HG(PR(I),TR(I)-0.5)
      PRAR=MEWR*CPR/CONR
      REYR=GR*IDR(I)/MEWR
      RR1=RR1+REYR
      CALL AICHG(GR,REYR,PRAR,IDR(I),I*DLNTH,CONR,RHOR,RMUR,RTTR,
C    1 HR(I),PGRADR)
C
C     NOW DEFINE FLUID PROPERTIES OF WATER

      GW=1.273*MWDOT/(IDW(I)*IDW(I))
      MEWW=FP(3,TW(I))
      RMUW=MEWW/FP(3,TWL(I))
      RHOW=FP(5,TW(I))
      CNW=FP(4,TW(I))
      CPW=FP(8,TW(I))
      PRAW=MEWW*CPW/CNW
      REYW=GW*IDW(I)/MEWW
      RW1=RW1+REYW
      CALL AICH(GW,REYW,PRAW,IDW(I),(152-I)*DLNTH,CNW,RHOW,
     1 RMUW,HW(I),PGRADW)

C     CALCULATE LINEAR CONDUCTIVITY OF HEAT EXCHANGER

      a1=1/(HR(I)*3.1416*IDR(I))
      a2=(ALOG(ODR(I)/IDR(I)))/(2*3.1416*BONDU)
      a3=(ALOG(IDW(I)/ODW(I)))/(2*3.1416*BONDU)
      a4=1/(HW(I)*3.1416*IDW(I))
      UL(I)=1/(a1+a2+a3+a4)

C     ADD MASS OF REFRIGERANT IN THE I TH  SEGMENT.

      AMSUP=AMSUP + 0.7854*RHOR*DLNTH*IDR(I)**2

C     CALCULATE NUMBER OF TRANSFER  UNITS AND EFFECTIVENESS.
C     FIND TEMPS. AND PRESS. AT POINT (I+1). REFERENCE: ALFA LAVAL HNDBK.

      CAPW=MWDOT*CPW
      CAPR=MRDOT*CPR
      NTUW(I)=DLNTH*UL(I)/CAPW
      NTUR(I)=DLNTH*UL(I)/CAPR
      A=NTUW(I)/NTUR(I)
```

```
          B=EXP(-NTUR(I)+NTUW(I))
          ER(I)=(1-B)/(1-(B*A))
          EW(I)=(1.0-Flost)*ER(I)*A
          TW(I+1)=(TW(I)-EW(I)*TR(I))/(1-EW(I))
          TR(I+1)=TR(I)+ER(I)*(TW(I+1)-TR(I))
          Qf=CAPR*(TR(I)-TR(I+1))
          Qh=CAPW*(TW(I)-TW(I+1))

          PR(I+1)=PR(I)-DLNTH*PGRADR
          PW(I+1)=PW(I)+DLNTH*PGRADW

          IF (PR(I+1) .LT. 0.0) GOTO 3

C         CALCULATE NEW WALL TEMPERATURE. NOTE: THIS IS AN APPROXIMATION
C         FOR CALCULATING HEAT TRANSFER COEFFICIENTS ONLY.  IT NEGLECTS
C         DIFFERENCE BETWEEN WALL TEMPERATURES OF REFRIGERANT AND WATER TUBES.

          TWL(I+1)=TR(I+1)-(TR(I+1)-TW(I+1))*UL(I)/(3.1416*IDR(I+1)*HR(I))

         END DO

C-----------------------------------------------------------------------
C
C        PROGRAM MONITOR
C        ---------------
C
C        CONDITION:-
C        IF CONTROL GETS TO THIS POINT THE STARTING WATER TEMP NEEDS CHANGING
C        BECAUSE 150 SEGMENTS HAVE BEEN USED IN DESUPERHEATING ALONE
C        SO RETURN TO S(K) ITERATING SEGMENT.
C
C
1500     CONTINUE

         I1=I-1
         IF (KPRINT .EQ. 4) GOTO 3000

         IF (I .LT. 151) THEN

C        CONDITION:-
C        AT THIS POINT CONDENSATION IS EITHER PREMATURELY COMPLETE (INCREASE
C        S(K))  OR TW HAS EXCEEDED TR IN DESUPERHEATING OR TWO-PHASE
C        REGIONS.  I.E. FOOLED=.TRUE.   IN THIS CASE REDUCE S(K).

         IF (FOOLED) THEN
          ISN(K)=-1
         ELSE
          ISN(K)=1
         END IF

        ELSE

C        CONDITION:-
C        AT THIS POINT CONDENSATION IS EITHER COMPLETE (EXIT FROM ITERATION)
C        OR PREMATURELY COMPLETE WITHIN THE ALLOWED "I" EXIT WINDOW
C        (TW(I).LT.TWIN) IN WHICH CASE INCREASE S(K),  OR NOT COMPLETE
C        (TW(I).GT.TWIN) IN WHICH CASE REDUCE S(K).
```

```
      IF (ABS(TW(I)-TWIN) .LT. 0.2) GOTO 3000

      IF (TW(I) .GT. TWIN) THEN
       ISN(K)=-1
      ELSE
       ISN(K)=1
      END IF

     END IF

C    NOW ARRANGE CHANGES IN STEP SIZE FOR RAPID CONVERGENCE

     S(K+1)=S(K) + ISN(K)*STEP

     IF (K.EQ.1) GOTO 1000

     IF (ISN(K).NE.ISN(K-1)) STEP=STEP/2.0

     IF (K.EQ.2) GOTO 1000

     HALVE=.FALSE.

     KSTEP=2

     DO WHILE ((KSTEP .LE. 20) .AND. (.NOT.(HALVE)))
      HALVE=(ABS(S(K+1) - S(K-KSTEP)).LT.1.0E-7)
      KSTEP=KSTEP+1
     END DO

     IF (HALVE) THEN
      STEP=STEP/2.0
      S(K+1)=S(K) + ISN(K)*STEP
     END IF

C    END OF MONITORING PROGRAM

C-----------------------------------------------------------------------------

1000 IF (K .LT. 500) GOTO 1001

C************************************************************************
C
C AT THIS POINT A CONSISTENT SET OF TEMPERATURES HAS BEEN FOUND.
C NOW, PROCEED TO THE PRINT OUT AND SUMMARIZING SEGMENT
C
C************************************************************************

      GOTO 3000

C************************************************************************
C          **** SECONDLY : THE TWO-PHASE CONDENSING REGION ****
C************************************************************************
C
C    FIRST CALCULATE STARTING VAPOUR QUALITY FROM FICTITIOUS DEPRESSION
C    OF TR(JSUP) BELOW TSAT.  FIND STARTING VALUES OF OTHER PARAMETERS.
C
4200 HFG=HSAT(1.0,TSAT) - HSAT(0.0,TSAT)
```

```
      X(JSUP)=1.0 - CPR*(TSAT-TR(JSUP))/HFG
      HHR(JSUP)=HSAT(X(JSUP),TSAT)
      PRED=PR(JSUP)/PC
      TRED=(TSAT+273.15)/TC
      VGRED=VR12(PRED,TRED)
      VFRED=VFR12(TRED)

      DO I=JSUP,151
        J2PSE=I
        IF( X(I).LT.0.00) GOTO4400
C
C       CONDITION:-
C       IF PRESSURE GRADIENT IS HIGH TW MAY EXCEED TR.  IN THAT CASE SET
C       FOOLED = .TRUE. AND RETURN TO STARTING TEMPERATURE ADJUST SEGMENT.
C
        FOOLED=TW(I).GT.TR(I)
        IF (FOOLED) GOTO 1500
C
C       ADOPT 0.97 AS THE MAX VALUE OF X(I) WHEN CALCULATING HR(I), BUT USE
C       ACTUAL VALUE FOR ENERGETIC CALCULATIONS.
C
        XTEMP=X(I)

        IF (XTEMP .GE. 0.97) X(I)=0.97
C
C       NOW PERFORM HEAT TRANSFER COEFFICIENT AND PRESSURE GRADIENT CALCNS
C       THESE CORRELATIONS COME FROM ROHSENOW AND HARTNETT: HDBK OF HT TRANS.
C       EQUATION 56, P12-23 OF R & H SEEMS TO BE WRONG. CARRINGTON,[1] USE
C       REL**0.9 (C.J.BLUNDELL DOES TOO).
C
        GR=1.273*MRDOT/(IDR(I)*IDR(I))
C
C       DEFINE FLUID PROPERTIES:  F: FOR LIQUID & G: FOR VAPOUR.
C
        RHOG=1/(VC*VR12(PRED,TRED))
        RHOF=1/(VC*VFR12(TRED))
        MEWG=FP(1,TR(I))
        MEWF=FP(6,TR(I))
        RMUF=MEWF/FP(6,TWL(I))
        RMUG=MEWG/FP(6,TWL(I))
        CONF=FP(7,TR(I))
        CONG=FP(2,TR(I))
        CPRF=HSAT(0.0,TR(I)+0.5) - HSAT(0.0,TR(I)-0.5)
        CPRG=HSAT(1.0,TR(I)+0.5) - HSAT(1.0,TR(I)-0.5)
        caprf=MRDOT*CPRF
        caprg=MRDOT*CPRG
        HFG=HC*HFGR12(TRED,PRED,VGRED,VFRED)
        PRAF=MEWF*CPRF/CONF
        PRAG=MEWG*CPRG/CONG
        REYF=(1-XTEMP)*GR*IDR(I)/MEWF
        REYG=XTEMP*GR*IDR(I)/MEWG
        RR2=RR2+REYF
C
C       TAKE THE LOWER LIMIT FOR REYF TO BE 1 AT START OF 2-PHASE REGION.
C
        IF(REYF.LT.1.0) REYF=1.0
C
C       ADD MASS OF REFRIGERANT IN THE I TH SEGMENT.
```

```
C
      AM2PS=AM2PS+0.7854*IDR(I)**2*(AL(I)*RHOG+(1-AL(I))*RHOF)*DLNTH
C
C     CALCULATE HEAT TRANSFER  COEFFICIENT. NOTE: XTT IS THE MARTINELLI
C     PARAMETER. WHEN X(I).LT.0.015 XTT WILL GO OUT OF RANGE, ADAPT THE
C     SINGLE PHASE HEAT TRANSFER COEFF IN THIS SITUATION. THE ANNULAR
C     FLOW MODEL IN LONG CONDENSING HORIZONTAL TUBE IS ADAPTED.
C
      IF( X(I) .GT. 0.015) THEN

       IF (REYF .GT. 1125) F2=5*PRAF +
     1  5*ALOG(1 + 5*PRAF) + 2.5*ALOG(0.0031*REYF**0.812)

       IF ((REYF .GT. 50) .AND. (REYF .LE. 1125)) F2=
     1  5*PRAF + 5*ALOG(1 + PRAF*(0.09636*REYF**0.585 - 1))

       IF (REYF .LE. 50) F2=0.707*PRAF*REYF**0.5

       B1=MEWF/MEWG
       B2=RHOG/RHOF

       XTT=B1**0.1*B2**0.5*((1-X(I))/X(I))**0.9
       FXTT=0.15*(1/XTT + 2.85/(XTT**0.476))

       IF (FXTT .LE. 0.1) WRITE (4,605) FXTT

       IF (FXTT .LE. 1.0) NUS=PRAF*REYF**0.9*FXTT/F2

       IF (FXTT .GT. 1.0) THEN
        IF (FXTT .GE. 20.0) WRITE (4,605) FXTT
        NUS=PRAF*REYF**0.9*FXTT**1.15/F2
       END IF

       HR(I)=NUS*CONF/IDR(I)
      END IF
C
C     PROCEED WITH WATER SIDE HEAT TRANSFER  CALCULATION AND
C     PREDICTION OF TEMPERATURES  AND PRESSURES AT THE (I+1) POINT.
C     THIS IS THE ENTRY POINT WHEN X(I).LT.0.015.
C
      GW=1.273*MWDOT/(IDW(I)*IDW(I))
      RHOW=FP(5,TW(I))
      MEWW=FP(3,TW(I))
      RMUW=MEWW/FP(3,TWL(I))
      CNW=FP(4,TW(I))
      CPW=FP(8,TW(I))
      PRAW=MEWW*CPW/CNW
      REYW=GW*IDW(I)/MEWW
      RW2=RW2+REYW
      CALL AICH(GW,REYW,PRAW,IDW(I),(152-I)*DLNTH,CNW,RHOW,RMUW,
     1 HW(I),PGRADW)

      a1=1/(HR(I)*3.1416*IDR(I))
      a2=(ALOG(ODR(I)/IDR(I)))/(2*3.1416*BONDU)
      a3=(ALOG(IDW(I)/ODW(I)))/(2*3.1416*BONDU)
      a4=1/(HW(I)*3.1416*IDW(I))
      UL(I)=1/(a1+a2+a3+a4)
```

```
      CAPW=MWDOT*CPW
      NTUR(I)=0.0
      ER(I)=0.0
      NTUW(I)=DLNTH*UL(I)/CAPW
      EW(I)=(1 - EXP(-NTUW(I)))
      TW(I+1)=(TW(I) - EW(I)*TR(I))/(1-EW(I))
C
C     FIND PROVISIONAL VALUE OF X(I+1) NEGLECTING PRESSURE GRADIENT.
C
      X(I+1)=XTEMP-CAPW*EW(I)*(TR(I)-TW(I))/((1-EW(I))*MRDOT*HFG)


C
C     NOW CALCULATE TWO PHASE PRESSURE DROP USING LOCKART-MARTINELLI METHOD

C     **** FIRSTLY: THE FRICTIONAL TERMS ****
C
      A1=X(I)**1.8
      A2=5.7*B1**0.0523*(1 - X(I))**0.47*X(I)**1.33*B2**0.261
      A3=8.11*B1**0.105*(1 - X(I))**0.94*X(I)**0.86*B2**0.522
      A4=GR*GR/(RHOG*IDR(I))
      A5=.09*(MEWG/(GR*IDR(I)))**0.2
C
C     **** SECONDLY: THE MOMENTUM TERMS ****
C
      A6=2*X(I) + (1 - 2*X(I))*B2**0.333 + (1 - 2*X(I))*B2**0.667
     1 - 2*( 1 - X(I))*B2
C
C     BEFORE PROCEDING REPLACE X(I) WITH CORRECT VALUE IN THE CASE
C     WHERE X(I).GT.0.97.
C
      X(I)=XTEMP
      A7=IDR(I)*(X(I+1) - X(I))/DLNTH
      PGRADR=A4*(A5*(A1 + A2 + A3) + A6*A7)
      RAD=PGRADR
      PR(I+1)=PR(I) - DLNTH*PGRADR
      PW(I+1)=PW(I) + DLNTH*PGRADW
      IF (PR(I+1) .LT. 0.0) GOTO 3


C
C     REPEAT CALCULATION OF X(I+1) TO ACCOUNT FOR PRESSURE DROPS.
C
      Water=CAPW*(TW(I)-TW(I+1))/MRDOT
      HHR(I+1)=HHR(I) - Water
      PRED=PR(I+1)/PC
      TRED=TSATR12(PRED)
      VGRED=VR12(PRED,TRED)
      VFRED=VFR12(TRED)
      HFG=HC*HFGR12(TRED,PRED,VGRED,VFRED)
      TR(I+1)=(TC*TRED)-273.15
      X(I+1)=(HHR(I+1)-HSAT(0.0,TR(I+1)))/HFG

      delH=HHR(I)-HHR(I+1)
C
C     CALCULATE NEW WALL TEMPERATURE
C
      TWL(I+1)=TR(I+1)-(TR(I+1)-TW(I+1))*UL(I)/(3.1416*IDR(I+1)*HR(I))
C
```

```
C       CALCULATE VOID FRACTION. ROHSENOW & HARTNETT REFER TO ZIVI.
C
        AL(I+1)= 1/(1 + ((1-X(I+1))*B2**0.667/X(I+1)))
       END DO
C
C      CONDITION:-
C      IF CONTROL GETS TO THIS POINT , CHECK TO SEE IF CONDENSATION
C      IS COMPLETE.  IF NOT RETURN TO S(K) ITERATING SEGMENT.
C
       IF (X(I).GT.0.005) GOTO 1500
C
C***********************************************************************
C             **** THIRDLY : THE SUBCOOLING REGION ****
C***********************************************************************

C***********************************************************************
C
C  NOTE: X(I) IS NEGATIVE AT THIS  POINT, USE THIS VALUE TO FIND T(I)
C
C***********************************************************************
C
4400  AL(J2PSE)=0
      TR(J2PSE)=TR(J2PSE - 1) + X(J2PSE)*HFG/CPR

      DO I=J2PSE,152
        AL(I)=0.0
        X(I)=0.0
        HHR(I)=HSAT(0.0,TR(I))

        IF(TW(I).LT.TWIN) GOTO 1500
        IF( TW(I).GT.TR(I) )GOTO 1500

        GR=1.273*MRDOT/(IDR(I)*IDR(I))
C
C       DEFINE FLUID PROPERTIES OF SUBCOOLED R12 AND CALCULATE HR(I).
C
        TRED=(TR(I)+273.16)/TC
        RHOF=1/(VC*VFR12(TRED))
        MEWF=FP(6,TR(I))
        RMUF=MEWF/FP(6,TWL(I))
        CON=FP(7,TR(I))
        CPR=HSAT(0.0,TR(I)+0.5) - HSAT(0.0,TR(I)-0.5)
        PRAF=MEWF*CPR/CON
        REYF=GR*IDR(I)/MEWF
        RR3=RR3+REYF
        CALL AICH(GR,REYF,PRAF,IDR(I),I*DLNTH,CON,RHOF,RMUF,
     1  HR(I),PGRADR)
C
C       ADD MASS OF REFRIGERANT IN THE  I TH  SEGMENT.
C
        AMSUB=AMSUB + 0.7854*IDR(I)**2*DLNTH*RHOF
C
C       DEFINE FLUID PROPERTIES OF WATER AND CALCULATE HW(I).
C
        GW=1.273*MWDOT/(IDW(I)*IDW(I))
        RHOW=FP(5,TW(I))
        MEWW=FP(3,TW(I))
        RMUW=MEWW/FP(3,TWL(I))
```

```
      CNW=FP(4,TW(I))
      CPW=FP(8,TW(I))
      PRAW=MEWW*CPW/CNW
      REYW=GW*IDW(I)/MEWW
      RW3=RW3+REYW
      CALL AICH(GW,REYW,PRAW,IDW(I),(153-I)*DLNTH,CNW,RHOW,RMUW,
     1 HW(I),PGRADW)

      a1=1/(HR(I)*3.1416*IDR(I))
      a2=(ALOG(ODR(I)/IDR(I)))/(2*3.1416*BONDU)
      a3=(ALOG(IDW(I)/ODW(I)))/(2*3.1416*BONDU)
      a4=1/(HW(I)*3.1416*IDW(I))
      UL(I)=1/(a1+a2+a3+a4)

      CAPW=MWDOT*CPW
      NTUW(I)=DLNTH*UL(I)/CAPW
      CAPR=MRDOT*CPR
      NTUR(I)=DLNTH*UL(I)/CAPR
C
C     DEFINE TEMPORARY CONSTANTS
C
      A=NTUW(I)/NTUR(I)
      B=EXP(-NTUR(I) + NTUW(I))
      ER(I)=(1 - B)/(1 - (A*B))
      EW(I)=(1.0-Flost)*ER(I)*A
      TW(I+1)=(TW(I) - EW(I)*TR(I))/(1 - EW(I))
      TR(I+1)=TR(I) + ER(I)*(TW(I+1) - TR(I))
      Qf=CAPR*(TR(I)-TR(I+1))
      Qh=CAPW*(TW(I)-TW(I+1))

      PR(I+1)=PR(I) - DLNTH*PGRADR
      PW(I+1)=PW(I) + DLNTH*PGRADW
C
C     CALCULATE NEW WALL TEMPERATURE.
C
      TWL(I+1)=TR(I+1)-(TR(I+1)-TW(I+1))*UL(I)/(3.1416*IDR(I+1)*HR(I))
     END DO
C
C    RESTORE VALUE OF I TO 152.
C
     I=152
     GOTO 1500
C
C*************************************************************************
C
C  THIS IS THE END OF THE SEGMENT INTEGRATING THROUGH THE HEAT EXCHANGER
C
C*************************************************************************
C
C       *****SUMMARY AND PRINT OUT SEGMENT AS FOLLOWS*****
C
C*************************************************************************
C
3000 CONTINUE
C
C    SUMMARY OF BASIC RESULTS
C
C    DETERMINE WHETHER DATA IS TO BE OUTPUT TO PRINTER, FILE, OR BOTH
```

```
C
      WRITE (4,650)
      READ (3,602) LPRINT
C
C     LPRINT=1 FOR PRINTER ONLY, 2 FOR DISC ONLY, 3 FOR BOTH
C

      IF (LPRINT .EQ. 3) THEN
       LCOUNT=2
      ELSE
       LCOUNT=1
      END IF

      IF (LPRINT .GE. 2) THEN
       WRITE (4,654)
       READ (3,656) File
      END IF

      II=1

 3050 CONTINUE

      IF ((LPRINT .EQ. 1) .OR. ((LPRINT .EQ. 3)
     1   .AND. (II .EQ. 1))) THEN
       OPEN (6,FILE='lp:')
      ELSE
       OPEN (6,FILE=File)
      END IF

      WRITE(6,610)D1,DIAF,D2,DIAG,DIAW,TWALL
      WRITE(6,611)BONDU,THPWR,TWIN,TR(1),TDEW,TSUB
      WRITE(6,604) K,I1,S(K),TW(I),TR(I)
      WRITE(6,626)
      D1=MWDOT*1000
      D2=PW(I)/100000
      D3=PW(I)*MWDOT/1000
      D4=100.0*D3/THPWR
      WRITE(6,609) TW(1),D1,D2,D3,D4
      WRITE(6,627) MRDOT*1000
      WRITE(6,626)
C
C     SECTION A OF TABLE A-6.12 TO TABLE A-6.31:-
C
C     SUMMARY OF SEPARATE RESULTS FOR SUPERHEAT, TWO-PHASE AND
C     SUBCOOLING SEGMENTS.
C
      WRITE(6,612)
      D1=DLNTH*(JSUP-1.25)
      D2=DLNTH*(J2PSE-JSUP)
      D3=DLNTH*(151.25-J2PSE)
      D4=DLNTH*150
      WRITE(6,613)D1,D2,D3,D4
      D1=AMSUP + AM2PS + AMSUB
      WRITE(6,614)AMSUP,AM2PS,AMSUB,D1
      WRITE(6,637)
      H1=0.0
      H2=0.0
      H3=0.0
```

```
H5=0.0
H6=0.0
H7=0.0
U1=0.0
U2=0.0
U3=0.0
C1=0.0
C2=0.0
C3=0.0
C5=0.0
C6=0.0
C7=0.0
UR1=0.0
UR2=0.0
UR3=0.0
UW1=0.0
UW2=0.0
UW3=0.0

 DO I1=1,(JSUP-1)
  H1=H1+HR(I1)
  H5=H5+HW(I1)
  U1=U1+UL(I1)
  C1=C1+NTUR(I1)
  C5=C5+NTUW(I1)
  UR1=UR1+3.1416*IDR(I1)*HR(I1)
  UW1=UW1+3.1416*IDW(I1)*HW(I1)
 END DO

H11=H1/(JSUP-1)
H55=H5/(JSUP-1)
U11=U1/(JSUP-1)
UR11=UR1/(JSUP-1)
UW55=UW1/(JSUP-1)
 DO I1=JSUP,J2PSE
  H2=H2+HR(I1)
  H6=H6+HW(I1)
  U2=U2+UL(I1)
  C2=C2+NTUR(I1)
  C6=C6+NTUW(I1)
  UR2=UR2+3.1416*IDR(I1)*HR(I1)
  UW2=UW2+3.1416*IDW(I1)*HW(I1)
 END DO

H22=H2/(J2PSE-JSUP)
H66=H6/(J2PSE-JSUP)
U22=U2/(J2PSE-JSUP)
UR22=UR2/(J2PSE-JSUP)
UW66=UW2/(J2PSE-JSUP)
 DO I1=J2PSE,(I-1)
  IF( J2PSE.EQ.I ) GOTO 3600
  H3=H3+HR(I1)
  H7=H7+HW(I1)
  U3=U3+UL(I1)
  C3=C3+NTUR(I1)
  C7=C7+NTUW(I1)
  UR3=UR3+3.1416*IDR(I1)*HR(I1)
  UW3=UW3+3.1416*IDW(I1)*HW(I1)
```

```
      END DO

      H33=H3/(I-J2PSE)
      H77=H7/(I-J2PSE)
      U33=U3/(I-J2PSE)
      UR33=UR3/(I-J2PSE)
      UW77=UW3/(I-J2PSE)
3600  CONTINUE

      D1=(H1+H2+H3)/(I-1)
      WRITE(6,615)H11,H22,H33,D1
      D1=(UR1+UR2+UR3)/(I-1)
      WRITE(6,636)UR11,UR22,UR33,D1
      D1=RR1/(JSUP-1)
      D2=RR2/(J2PSE-JSUP)
      D3=RR3/(I-J2PSE)
      D4=(RR1+RR2+RR3)/(I-1)
      WRITE(6,633)D1,D2,D3,D4
      WRITE(6,637)
      D1=(H5+H6+H7)/(I-1)
      WRITE(6,616)H55,H66,H77,D1
      D1=RW1/(JSUP-1)
      D2=RW2/(J2PSE-JSUP)
      D3=RW3/(I-J2PSE)
      D4=(RW1+RW2+RW3)/(I-1)
      UW88=(UW1+UW2+UW3)/(I-1)
      WRITE(6,638)UW55,UW66,UW77,UW88
      WRITE(6,634)D1,D2,D3,D4
      WRITE(6,637)
      D1=(U1+U2+U3)/(I-1)
      WRITE(6,617)U11,U22,U33,D1
      D1=C1 + C2 + C3
      WRITE(6,618)C1,C2,C3,D1
      D12=C5 + C6 + C7
      WRITE(6,619)C5,C6,C7,D12
      E1=100*(TR(1)-TR(JSUP))/(TR(1)-TW(JSUP))
      E2=100*(TW(JSUP)-TW(J2PSE))/(TR(JSUP)-TW(J2PSE))
      E3=100*(TR(J2PSE)-TR(I))/(TR(J2PSE)-TW(I))
      Eav=(E1+E2+E3)/3
      WRITE(6,620) E1,E2,E3,Eav
      D1=(PR(1) - PR(JSUP))/100000
      D2=(PR(JSUP) -PR(J2PSE))/100000
      D3=(PR(J2PSE) - PR(I))/100000
      D4=(PR(1) - PR(I))/100000
      WRITE(6,621) D1,D2,D3,D4
      WRITE(6,637)
C
C     CALCULATION OF THERMAL POWER IN EACH SEGMENT.
C
      TPRSUP=MWDOT*(FP(9,TW(1))-FP(9,TW(JSUP)))
      TPR2PS=MWDOT*(FP(9,TW(JSUP)) - FP(9,TW(J2PSE)))
      TPRSUB=MWDOT*(FP(9,TW(J2PSE)) - FP(9,TW(I)))
      TPR=TPRSUP + TPR2PS + TPRSUB
      PSUP=100*TPRSUP/TPR
      P2PS=100*TPR2PS/TPR
      PSUB=100*TPRSUB/TPR
      WRITE(6,625) TPRSUP,PSUP,TPR2PS,P2PS,TPRSUB,PSUB,TPR
      D1=HG(PR(1),TR(1))
```

```
      D2=HSAT(1.0,TR(JSUP))
      D3=HSAT(0.0,TR(J2PSE))
      D4=HSAT(0.0,TR(I))
      TPFSUP=MRDOT*(D1-D2)
      TPF2PS=MRDOT*(D2-D3)
      TPFSUB=MRDOT*(D3-D4)
      TPF=TPFSUP + TPF2PS + TPFSUB
      FSUP=100*TPFSUP/TPF
      F2PS=100*TPF2PS/TPF
      FSUB=100*TPFSUB/TPF
      QALL1=TPFSUP*(1.0+Flost)
      QALL2=TPF2PS*(1.0+Flost)
      QALL3=TPFSUB*(1.0+Flost)
      QLOST1=(QALL1-TPFSUP)
      QLOST2=(QALL2-TPF2PS)
      QLOST3=(QALL3-TPFSUB)
      QLOST=(QLOST1+QLOST2+QLOST3)
      PER=(QLOST*100.00)/THPWR
      QALL=(QALL1+QALL2+QALL3)
      WRITE(6,660) TPFSUP,FSUP,TPF2PS,F2PS,TPFSUB,FSUB,TPF
      WRITE(6,670) QALL1,QALL2,QALL3,QALL
      WRITE(6,665) QLOST1,QLOST2,QLOST3,QLOST,PER
      WRITE(6,628) D1,D2,D3,D4
      WRITE(6,637)
      D1=SG(PR(1),TR(1))
      D2=SSAT(1.0,TR(JSUP))
      D3=SSAT(0.0,TR(J2PSE))
      D4=SSAT(0.0,TR(I))
      WRITE(6,631) D1,D2,D3,D4
      WRITE(6,644)TR(1),TR(JSUP),TR(J2PSE),TR(I)
      D1=(PR(1)/100000.0)
      D2=(PR(JSUP)/100000.0)
      D3=(PR(J2PSE)/100000.0)
      D4=(PR(I)/100000.0)
      WRITE(6,645) D1,D2,D3,D4
      WRITE(6,646) TW(1),TW(JSUP),TW(J2PSE),TW(I)
      WRITE(6,626)
      IF(KPRINT.EQ.1) GOTO 2

       IF(KPRINT.NE.2) THEN
C
C       SECTION B OF TABLE A-6.12 TO TABLE A-6.31:-
C
C       DETAILED TEMPERATURE, PRESSURE AND HEAT TRANSFER COEFFNT PROFILE.
C
        WRITE(6,622)

         DO I1=1,76
          M=2*I1-1
          IF (M.GT.I) M=I
          FOOLED=(M .GE. JSUP .AND. (M-2) .LT. JSUP) .OR.
     1    (M .GE. J2PSE .AND. (M-2) .LT. J2PSE)
          IF(FOOLED) WRITE(6,622)
          D1=(M-1)*DLNTH
          D2=(PR(M)/100000)
          D3=PW(M)/100000
          D4=TWL(M)
          D5=X(M)*100
```

```
        D6=3.1416*IDR(M)*HR(M)
        D7=3.1416*IDW(M)*HW(M)
        WRITE(6,623) D1,TR(M),D2,TW(M),D3,D4,D5,
     1  HR(M),NTUR(M),D6,HW(M),NTUW(M),D7,UL(M)
       END DO

      WRITE(6,626)
     END IF
C
C     SUMMARY OF ENTHALPY BALANCE AND ENTROPY CREATION RATES.
C
      D1=MRDOT*(HHR(1) - HHR(I))
      D2=MWDOT*(FP(9,TW(1)) - FP(9,TW(I)))
      D3=D2 - D1
      D4=100.0*D3/THPWR
      D5=THPWR-D1
      D6=100.0*D5/THPWR
      D7=THPWR-D2
      D8=100.0*D7/THPWR
      WRITE(6,629)D1,D2,D3,D4
      WRITE(6,662)D5,D6,D7,D8
      D1=MRDOT*(SG(PR(1),TR(1)) - SSAT(0.0,TR(I)))
      D2=MWDOT*(FP(10,TW(1)) - FP(10,TW(I)))
      D3=D2-D1
      D4=0

      DO I1=1,(I-1)
       A=2.0/(TW(I1)+TW(I1+1)+546.3) - 2.0/(TR(I1)+TR(I1+1)+546.3)
       D4=D4 - MRDOT*A*(HHR(I1+1) - HHR(I1))
      END DO

      D5=D3-D4
      D6=D3*(TDEW+273.15)
      WRITE(6,632) D1,D2,D3,D4,D5,D6,TDEW
      D7=MWDOT*(FP(10,(TW(1)+10.0)) - FP(10,(TW(I)+10.0)))
      D8=10.0*D3/(D2-D7)
      A=TW(1) - TW(I)
      D9=100.0*A/(D8+A)
      D10=1.0/(100.0/D9 - 1.0)
      D11=100.0*D10/D12
      WRITE(6,637)
      WRITE(6,639) D7,D8,D9,D10,D11
      IF (KPRINT .EQ. 2) GOTO 3980
C
C     SECTION C OF TABLE A-6.12 TO TABLE A-6.31:-
C
C     SUMMARY OF POSSIBLE SIMPLE CYCLES.    LABELS 1,2,3 & 4 REFER TO THE
C     FOLLOWING POINTS IN THE CYCLE: DISCHARGE GAS 1; SUBCOOLED LIQUID 2;
C     EVAPORATOR ENTRY 3; SUPERHEATED SUCTION GAS 4.
C

      DO IE=1,3
       EFNCY=0.45 + IE/20.0
       I1=100*EFNCY
       T1=TDEW
       H1=HHR(1)
       S1=SG(PR(1),TR(1))
       P1=(PR(1)/100000.0)
```

```
      T2=TSUB
      H2=HSAT(0.0,TSUB)
      S2=SSAT(0.0,TSUB)
      WRITE(6,642) I1,P1,T1,H1,S1,T2,H2,S2
      WRITE(6,641)

      DO M=1,31
       T3=2.0*M - 12.0
       S6=SSAT(0.0,T3)
       S7=SSAT(1.0,T3)
       IF (S1 .LT. S7) GOTO 3940
       IF (ANINT(T3) .GE. ANINT(TDEW)) GOTO 3960
       H6=HSAT(0.0,T3)
       H7=HSAT(1.0,T3)
       X3=(H2-H6)/(H7-H6)

       IF (X3 .GT. 0.0) THEN
        S3=SSAT(X3,T3)
       ELSE
        S3=SSAT(0.0,TSUB)
       END IF

       TRED=(T3 + 273.15)/TC
       P3=(PC*PSATR12(TRED))
       CALL VTHFPS(P3,S1,V5,T5,H5)
       H4=H1 - (H1-H5)/EFNCY
       IF(H4.LT.HSAT(1.0,T3)) GOTO 3940
       CP5=HG(P3,(T5+0.5)) - HG(P3,(T5-0.5))
       T4=T5 - (H5-H4)/CP5
       S4=SG(P3,T4)
       D1=MRDOT*(H4-H2)
       D2=MRDOT*(H1-H4)
       D3=PR(1)/P3
       T4RED=(T4 + 273.15)/TC
       D4=3600.0*MRDOT*VC*VR12((P3/PC),T4RED)
       D5=THPWR/D2
       D6=(P3/100000.0)
       WRITE(6,640) T3,D6,H6,H7,S6,S7,S3,X3,S4,H4,T4,D1,D2,D3,D4,D5
3940   CONTINUE
      END DO
3960  CONTINUE
     END DO
3980 CONTINUE
     WRITE(6,635)
     GOTO 2
3    WRITE(6,630)
2    CONTINUE
     WRITE(6,635)

     CLOSE (6)

     IF (LCOUNT .EQ. 2) THEN
      LCOUNT=99
      II=2
      GOTO 3050
     END IF

     CLOSE (3)
```

```
      CLOSE (4)
C
C***************************************************************************
C
C                         FORMAT STATEMENTS
C
C***************************************************************************
C
600   FORMAT (6F10.5)
601   FORMAT (1X,'INPUT PRINT VARIABLE:',
     1/,5X,'1      BRIEF SUMMARY',
     2/,5X,'2      SUMMARY AND SECOND LAW ANALYSIS',
     3/,5X,'3      COMPLETE PRINT OUT WITH TEMPERATURE '
     4'AND PRESSURE PROFILES',
     5/,5X,'4      PRINT OUT AFTER FIRST INTEGRATION',/)
602   FORMAT(I1)
604   FORMAT(1X,'ITERATION NUMBER:',I3,' USED I=',I4,' SEGMENTS.',
     1'       TRIAL WATER EXIT TEMP:',F8.4,'    CORRESPONDING TO ',
     2'TW(I)=',F8.4,'  & TR(I)=',F8.4)
605   FORMAT(1X, ' MARTINELLI PARAMETER OUT OF VALID RANGE BUT USED ANY
     1WAY.   F(XTT) = ', F7.3)
609   FORMAT(1X,'EXIT WATER TEMP',F8.2,'C.    FLOW RATE',F8.4,
     1' GRAM/SEC.    WATER PRESS DROP',F9.4,' BAR.    PUMP PWR',
     2F8.4,' WATT (OR',F8.4,'%)')
610   FORMAT(1X,//,13X,'****** TUBE-BESIDE-TUBE CONDENSER ',
     1'SIMULATION ****** ASSUME TUBE WALLS HAVE INFINITE CONDUCTIVITY',
     2' ******',/,' GEOMETRY:  SUBCOOLER',F6.2,'M OF',F5.2,
     3'MM OD.   CONDENSER:',F6.2,'M OF',F5.2,'MM OD.   WATER SIDE',
     4F5.2,'MM OD.   ALL WALLS',F5.2,'MM THICK.')
611   FORMAT(1X,'BOND CNDCTNCE',F6.1,'W/M.C   THML PWR',F8.1,
     1'W.    WATER IN',F5.1,'C.    HOT GAS',F6.1,'C.    DEW POINT',
     2F5.1,'C.    SUBCLD LIQD',F5.1,'C.',///)
612   FORMAT(1X,'SEPARATE RESULTS FOR THE THREE SEGMENTS          SUPE
     1RHEAT           TWO-PHASE           SUBCOOLER           TOTAL/AVERAGE
     2  ',/)
613   FORMAT(1X,'LENGTH OF EACH SEGMENT IN METRES           ',4(1PE19.4))
614   FORMAT(1X,'MASS OF REFRIGERANT IN KG.                 ',4(1PE19.4))
615   FORMAT(1X,'REFRIG SIDE HEAT TRANS COEFNT: W/SQ M C. ',4(1PE19.4))
616   FORMAT(1X,'WATER SIDE HEAT TRANS COEFNT: W/SQ M C.  ',4(1PE19.4))
617   FORMAT(1X,'OVERALL LINEAR CONDUCTANCE: W/M C        ',4(1PE19.4))
618   FORMAT(1X,'NO. OF HEAT TRANSFER UNITS REFRIG. SIDE  ',4F19.4)
619   FORMAT(1X,'NO. OF HEAT TRANSFER UNITS WATER SIDE    ',4F19.4)
620   FORMAT(1X,'EFFECTIVENESS OF EACH SEGMENT (PERCENT)  ',4F19.4)
621   FORMAT(1X,'REFRIGERANT SIDE PRESSURE DROP IN BAR    ',4(1PE19.4))
622   FORMAT(1X,//,' LNTH   TR(I)    PR(I)     TW(I)   PW(I)      TWL(I
     1)  X(I)    HR(I)     NTUR(I)  UR(I)     HW(I)      NTUW(I)  UW(I)
     2     UL(I)')
623   FORMAT(1X,F5.2,F8.2,F11.2,F8.2,1PE11.2,0P
     1F8.2,F8.2,7(1PE10.2))
624   FORMAT(1X,'NUMBER OF ITERATIONS REQUIRED FOR SELF CONSISTENT SOLU
     1TION ',I3,'   ACTUAL NO. OF SEGMENTS USED',I4,/)
625   FORMAT(1X,'THERMAL POWER PICK-UP BY WATER  (W & %) ',F14.1,'(',F4
     1.1,')',F13.1,'(',F4.1,')',F13.1,'(',F4.1,')',F19.1)
660   FORMAT(1X,'THERMAL POWER TRANSFERRED BY R12 (W & %)',F14.1,'(',F4
     1.1,')',F13.1,'(',F4.1,')',F13.1,'(',F4.1,')',F19.1)
670   FORMAT(1X,'TOTAL MAX THERMAL POWER WITHOUT LOSS (W)',F19.2,F19.2,
     1F19.2,F19.2)
665   FORMAT(1X,'THERMAL POWER LOSS FROM FREON   (W & %) ',F19.4,F19.4,
```

```
     1F19.4,F18.2,'(',F4.1,')')
626   FORMAT(1X, ///)
627   FORMAT(1X,'REFRIGERANT MASS FLOW RATE ',1PE10.3,' GRAM/SEC')
628   FORMAT(1X,'SPECIFIC ENTHALPY OF REFRIG (J/KG)       ',1PE17.4,
     13(E19.4))
629   FORMAT(1X,'RATE OF LOSS OF ENTHALPY BY R12 ',1PE11.4,' WATTS',
     1'     RATE OF GAIN OF ENTHALPY BY WATER ',1PE11.4,' WATTS',/,
     2' CORRESPONDING TO AN ENERGY IMBALANCE OF ',1PE11.4,' WATTS',
     3'     OR ',0PF8.4,' % OF SPECIFIED POWER',/)
662   FORMAT(1X,'THE POWER LOSS BY R12 TO OUTSIDE ',1PE11.4,'WATTS',
     1' BY ',0PF8.4,' % OF THE SPECIFIED POWER ',/,
     2' THE POWER LOSS BY WATER TO OUTSIDE  ',1PE11.4,' WATTS ',
     3' BY ',0PF8.4,' % OF THE SPECIFIED POWER ',/)
630   FORMAT(1X,' **** INTEGRATION ABANDONED WHEN REFRIGERANT ',
     1'PRESSURE BECAME NEGATIVE ****')
631   FORMAT(1X,'SPECIFIC ENTROPY OF R12 (J/KG.C)          ',1PE17.4,
     13(E19.4))
632   FORMAT(1X,'RATE OF LOSS OF ENTROPY BY R12 ',1PE11.4,' WATTS/C',
     1'     RATE OF INCREASE OF ENTROPY BY WATER ',E11.4,' WATTS/C',/,
     2' NET RATE OF ENTROPY FLOW THRU SYSTEM BOUNDARY',E11.4,
     3' WATT/C      THERMAL ENTROPY CREATION RATE',E11.4,
     4' WATT/C ',/,' R12 P.D. ENTROPY CREATION RATE ',E11.4,
     5' WATT/C       RATE OF LOSS OF GROSS WORK ',E11.4,
     6' WATTS AT ',0PF6.2,' C')
633   FORMAT(1X,'REFRIGERANT SIDE REYNOLDS NUMBER        ',4(1PE19.4))
634   FORMAT(1X,'WATER SIDE REYNOLDS NUMBER              ',4(1PE19.4))
635   FORMAT(1X,////,'                          ********************',
     1'******************** END ********************',
     2'********************')
636   FORMAT(1X,'REFRIG SIDE LINEAR H.T.C.: W/M C.       ',4(1PE19.4))
637   FORMAT(1X)
638   FORMAT(1X,'WATER SIDE LINEAR H.T.C.  W/M C.        ',4(1PE19.4))
639   FORMAT(1X,'RATE OF ENTROPY GAIN OF WATER HAD IT BEEN 10C',
     1' HOTTER ',1PE11.4,' WATTS/C.   FOR SAME GROSS RATE OF ENTROPY',
     2' INCREASE,',/,' A COUNTER-FLOW WATER-WATER HEAT EXCHANGER ',
     3'WOULD HAVE DELTA-T OF ', 0PF8.4,' DEG C    CORRESPONDING TO',
     4' AN EFFECTIVENESS OF ',F6.2,'%',/,' OR ',F6.3,' HEAT TRANSFER',
     5' UNITS, WHICH IS ',F6.2,' % OF THAT FOR THE WATER SIDE OF THE',
     6' PRESENT HT.XR.')
640   FORMAT(1X,F6.2,F6.2,F8.0,F8.0,F8.2,F8.2,' * ',F8.2,F8.4,F8.2,
     1F8.0,F6.2,' * ',F8.0,F8.0,F6.3,F7.2,F8.3)
641   FORMAT(1X,'                    EVAPORATOR                  *',
     1'     ENTRY               EXIT           *    EVAP    COMP ',
     2' PRESS  VDOT    COPH',/' TEMP  PRESS    H(X=0) H(X=1)  S(X=0)'
     3,' S(X=1)  *    S       X      S      H      T      *',
     4'    CAP     CAP   RATIO  CUM/H')
642   FORMAT(1X,////,' SUMMARY OF RANGE OF POSSIBLE EVAPORATOR',
     1' CONDITIONS ASSUMING ',I2,'% COMPRESSOR ISENTROPIC EFFICIENCY',
     2/,' COND. PRESS=',F8.1,'  COND. TEMP=',F7.2,'  ENT. H=',F9.0,
     3'  ENT. S=',F8.2,'  LEAV. TEMP=',F6.2,'  LEAV. H=',F8.0,
     4'  LEAV. S=',F8.2,//)
644   FORMAT(1X,'REFRIGERANT TEMPERATURE (DEG.C)         ',4(1PE19.4))
645   FORMAT(1X,'REFRIGERANT PRESSURE (BAR)              ',4(1PE19.4))
646   FORMAT(1X,'WATER TEMPERATURE (DEG.C)               ',4(1PE19.4))
650   FORMAT(1X,'DESTINATION OF RESULTS ?',
     1/,'     1      PRINTER ONLY',/,'     2      DISC ONLY',
     2/,'     3      PRINTER AND DISC',/)
654   FORMAT(1X,'DESTINATION FILENAME ?')
656   FORMAT(A14)
```

APPENDIX A-4

THERMODYNAMIC AND PHYSICAL PROPERTIES OF R12 AND WATER (SUBROUTINE 1)

A-4.1: Introduction

The derivation of thermal and physical properties of the fluids provided by Hickson,[44] is found in subroutine 1. In this subroutine, the program can be divided as follows; estimation of effective parameters taken from experimental parameters at the condenser entry and exit, calculation of heat transfer coefficients and pressure drop in a single-phase flow (freon vapour and liquid, and liquid water), and thermodynamic and physical properties of the fluids.

For the water side, the properties are solved in term of function of temperature only. Similarly, the physical properties of the freon (conductivity and viscosity of saturated freon liquid and vapour) are also a function of temperature, but other thermal properties (specific enthalpy and specific entropy) in the vapour,liquid, and mixed-phase are the function of two variables (either pressure and temperature or vapour quality and temperature).

The heat transfer coefficients and pressure drop calculation in the single-phase flow are further classified to vapour and liquid side. For the vapour flowing alone, the calculation is only focused on the turbulent flow (based on the Reynolds number of the freon side). For the liquid (either freon or water), the calculation is further classified according to the flow mechanisms; turbulent, laminar and transition flow. This was done by considering the Reynolds numbers of the fluids.

In general, for the freon side, the thermal and physical properties are greatly influenced by the state of the freon itself; vapour only, saturated vapour, mixture of liquid-vapour, saturated liquid and liquid only (see Fig.6.1.5). The heat transfer coefficients and pressure drop calculation in two-phase flow can be found in the main program.

The mathematical derivation for various thermal and physical properties of freon and water is shown in the computer program listed in section A-4.2.

A-4.2: Computer program

The listing of the computer program for subroutine 1 can be seen in the next page.

```
C***********************************************************************C
C                                                                       C
C         THERMODYNAMIC AND PHYSICAL PROPERTIES OF R12 AND WATER        C
C            (SUBROUTINE 1) FOR APPENDIX A-4 IN SECTION A-4.2           C
C                                                                       C
C    SUBROUTINE AND FUNCTION FROM PROGRAM TBT-SUBROU-F77 TO BE LINKED   C
C              WITH MAIN PROGRAM AND SUBROUTINE R12-F77                 C
C                                                                       C
C                                                                       C
C***********************************************************************C

      SUBROUTINE AINPUT(A,B,C,D,E,F,G,H,AI,AJ,AP,AK,AL,AM,AN,AO,AQ)
      REAL DTRVAP,DTRSUB,DTWVAP,DTWSUB,DPR

C  ESTIMATION OF EFFECTIVE FLUID PARAMETERS FROM EXPERIMENT TO BE USED IN
C  THE MODEL USING EXTRAPOLATION METHOD. THE EFFECTIVE VALUES ARE TR(1),
C  TSUB, TWIN, PRES AND THPWR (CALCULATED FROM MWDOT, (TWOUT-TWIN) & CPW),
C  WHERE A1, A2, A3 AND A4 THE DISTANCE AWAY FROM/TO THE FINAL/INITIAL
C  POINT OF THE CONDENSER IN CM

        A1=25.00
        A2=68.00
        A3=82.00
        A4=148.00
        DTRVAP=(A-B)
        AL=A - (A1*DTRVAP/(A1+100.00))
        DTRSUB=(C-D)
        AK=D + (A2*DTRSUB/(A2+100.00))
        DTWVAP=(E-F)
        AM=E - (A3*DTWVAP/(A3+100.00))
        DTWSUB=(G-H)
        AN=H + (A4*DTWSUB/(A4+100.00))
        DPR=(AI-AJ)
        AO=AI - (A1*DPR/(1500.00+(2*A1)))
        AR=AJ + (A2*DPR/(1500.00+(2*A2)))
        AQ=AP*(AM-AN)*4.1833333
        RETURN
        END

      SUBROUTINE AICHG(G,R,P,D,L,C,RH,RM,TM,H,PG)
      REAL L,N,NTCP,FRAC,NT,FT,F

C  HEAT TRANSFER COEFFICIENT FOR SUPERHEATED VAPOUR AND PRESSURE GRADIENT.

C  ASSUME ROUGH LONG TUBE, FULLY DEVELOPED TURBULENT FLOW REGION ONLY,
C  NEGLECT THE EFFECT OF DEW FORMATION ON WALLS.   THESE CORRELATIONS
C  RECOMMENDED FOR GAS FLOW IN HANDBOOK OF SINGLE-PHASE CONVECTIVE
C  HEAT TRANSFER BY KAKAC et. al.,[82,83,84]  REFER SECTIONS 3, 4 AND 18.
C  THE L DEPENDENCE HAS BEEN FITTED TO G.E. DATA BOOKS. IT IS ASSUMED
C  THAT THE DE-SUPERHEATING IS PRECEEDED BY A LONG LENGTH OF UNCOILED
C  TUBE. NOTE :(i)RM = MU(BULK)/MU(WALL) & (ii)TM = T(BULK)/T(WALL).
C  ALSO F IS FANNING FRICTION FACTOR CORRECTED FOR WALL TEMPERATURE
C  IN COOLING FREON VAPOUR FOR Re>1E4 AND 0.5<Pr<2000 .

C      ----------------------------------------------------------
C              ***TURBULENT VAPOUR CALCULATION (Re>1E4)***
C      ----------------------------------------------------------
        FT=(1.82*ALOG10(R)-1.64)**(-2)
```

```
      K1=1.0+(3.4*FT)
      K2=11.70+1.8*(P**(-0.33333))
      EE=(FT/8)
      NTCP=(EE*R*P)/(K1+(K2*(EE**0.5)*((P**0.667)-1.0)))
      A=(TM**0.5)
      B=(2/(1+(1/A)))**2.0
      NT=NTCP*B
      Rough=1.524E-6/D
      ruf=2*Rough
      A1=ruf/7.4
      A2=-0.8686*ALOG(A1+(12/R))
      A3=-0.8686*ALOG(A1+(2.51*A2/R))
      A4=((A2-4.781)**2.0)/(4.781-(2.0*A2)+A3)
      FR=(1/(4.781-A4))**2.0
10    FRR=SQRT(FR)
      A5=ALOG(ruf+(9.35/(R*FRR)))
      FRAC=1/((3.48-(1.7372*A5))**2.0)
        IF ((ABS(FRAC-FR)/FR).LT.1E-6)GOTO 20
        FR=FRAC
        GOTO 10
20      N=NT
        FTCP=FRAC
        F=FTCP*B

C    -----------------------------------------------------------------
C    ***CALCULATION OF HEAT TRANSFER COEFFICIENT AND PRESSURE DROP***
C    -----------------------------------------------------------------
       H=N*C/D
       PG=2.0*F*G**2.0/(D*RH)
       RETURN
       END

      SUBROUTINE AICH(G,R,P,D,L,C,RH,RM,H,PG)
      REAL N,L,NL,NT,NLCP,NTCP,FL,FT,FTT

C  HEAT TRANSFER COEFFICIENT FOR LIQUIDS IN A LONG SMOOTH & ROUGH TUBE.

C  FOR LAMINAR FLOW, CONSIDER A LONG SMOOTH TUBE WHILE FOR TURBULENT FLOW
C  A LONG ROUGH TUBE IS CONSIDERED.
C  FOR TURBULENT AND LAMINAR FLOW THESE CORRELATIONS ARE RECOMMENDED
C  IN SECTIONS 4 ,7 AND 18 OF HANDBOOK OF SINGLE-PHASE CONVECTIVE
C  HEAT TRANSFER BY KAKAC et. al.,[82,83,84] .IN THE TRANSITION REGION,
C  THE RANGE OF REYNOLDS NUMBER (2100 - 7100), THE HEAT TRANS. COEFF. IS
C  IS UNPREDICTABLE BUT HERE A PRO-RATA MIXTURE OF THE LAMINAR AND
C  TURBULENT VALUES IS ADOPTED. NOTE:  RM= MU(BULK)/MU(WALL).
C  THE TEMPERATURE-DEPENDENCE ON THE FLUID PROPERTIES IS CONSIDERED .

C    -----------------------------------------------------------------
C              ***LAMINAR LIQUID CALCULATION (Re<2.1E3)***
C    -----------------------------------------------------------------
      Remin=2100.00
      Remax=7100.00
      Rediff=(Remax-Remin)
      X=R*P*D/L
      IF (RM.LT.1.0)GOTO 10
      AN=-0.58
      GOTO 20
10    AN=-0.50
```

```
20    CONTINUE
      FL=(16/R)*(RM**AN)
      F=FL
      NLCP=(3.66 + 0.057*X/(1.0+0.04*X**0.8))
      NL=NLCP
      N=NL
      IF(R.LT.Remin)GOTO 100

C     ----------------------------------------------------------------
C             ***TURBULENT LIQUID CALCULATION (Re>7.1E3)***
C     ----------------------------------------------------------------
        FT2=1.0/(1.581*ALOG(R) - 3.28)**2.0
        B1=1+(13.6*FT2)
        B2=9.0*((FT2/2)**0.5)
        B3=(P**0.6667)-1.0
        IF(RM.GT.1.0) GOTO 50
         CN=0.25
         GOTO 60
50       CN=0.08
60       CONTINUE
         NTCP2=((FT2/2)*R*P)/(B1+(B2*B3))
         NT2=NTCP2*(RM**CN)
         N=NT2
65     IF(R.GT.4000.0)THEN
       Rough=1.524E-6/D
       ruf=2*Rough
       A1=ruf/7.4
       A2=-0.8686*ALOG(A1+(12/R))
       A3=-0.8686*ALOG(A1+(2.51*A2/R))
       A4=-0.8686*ALOG(A1+(2.51*A3/R))
       A5=((A2-A3)**2.0)
       A6=A2-(2.0*A3)+A4
       FR=(1/(A2-(A5/A6)))**2.0
       FTCP=FR
       ELSE
       FRR=0.0054+(2.3E-8/(R**(-1.5)))
       FTCP=FRR
       END IF
       IF (RM.GT.1.0) GOTO 90
       FTT=FTCP/(RM**0.24)
       GOTO 95
90     FTT=(FTCP/6)*(7.0-RM)
95     CONTINUE
       F=FTT
       IF(R.GT.Remax) GOTO 100

C     ----------------------------------------------------------------
C       ***TRANSITION REGIME LIQUID CALCULATION (2.1E3<=Re<=7.1E3)***
C     ----------------------------------------------------------------
      N=((Remax-R)*NL/Rediff)  +  ((R-Remin)*NT2/Rediff)
      F=((Remax-R)*FL/Rediff)  +  ((R-Remin)*FTT/Rediff)

C     ----------------------------------------------------------------
C     ***CALCULATION OF HEAT TRANSFER  COEFFICIENT AND PRESSURE DROP***
C     ----------------------------------------------------------------
100   H=N*C/D
      PG=2.0*F*G**2.0/(D*RH)
      RETURN
      END
```

```
      SUBROUTINE VTHFPS(P,S,V,T,H)

C     ------------------------------------------------------------------
C     *CALCULATES VOLUME, TEMP., AND ENTHALPY FROM PRESSURE AND ENTROPY*
C     ------------------------------------------------------------------
      COMMON/BLK1/HC,TC,VC,PC
      SC=19.15
      PRED=P/PC
      SRED=S/SC
      CALL VTFPSR12(PRED,SRED,VRED,TRED)
      V=VC*VRED
      T=TC*TRED - 273.15
      H=HC*HR12(VRED,TRED)
      RETURN
      END

      FUNCTION FP(M,T)

C  A SINGLE FUNCTION FOR VISCOSITY & CONDUCTIVITY OF SATURATED
C  R12 LIQUID AND VAPOUR AND OF LIQUID WATER.  ALSO INCLUDED
C  ARE WATER DENSITY, SPECIFIC HEAT CAPACITY, SPECIFIC ENTHALPY
C  AND SPECIFIC ENTROPY.  THE LAST TWO FUNCTIONS HAVE BEEN SIMPLY
C  CALCULATED BY C.G.C. FROM THE SPECIFIC HEAT CAPACITY.
C  T IS IN DEG C AND ALL VALUES OF FP ARE IN S.I. UNITS.

      S=32 + 9*T/5
      SA=(273.15 + T)
      GOTO (10,20,30,40,50,60,70,80,90,100),M
10    FP=4.134E-4*(0.02906 - 2.623778E-5*S + 5.54779E-7*S*S)
C  VISCOSITY OF SAT R12 VAPOUR.
      RETURN

20    FP=1.731*(3.755E-3 + 4.26982E-5*S - 3.11736E-7*S*S +
     11.084798E-9*S**3)
C  CONDUCTIVITY OF SAT R12 VAPOUR.
      RETURN

30    FP=1E-10*(1.0478E9 - 8.0753E6*SA + 1.7053E4*(SA**2) +
     13.7263*(SA**3) - 3.1108E-2*(SA**4))
C  VISCOSITY OF WATER.
      RETURN

40    FP=1.731*(0.3050 + 7.3961E-4*S - 1.534988E-6*S*S)
C  CONDUCTIVITY OF WATER.
      RETURN

50    FP=16.019*(62.464 + 1.605602E-3*S - 6.646718E-5*S*S)
C  DENSITY OF WATER.
      RETURN

70    FP=1.731*(0.05051 - 1.910131E-4*S + 9.009009E-7*S*S -
     13.0536407E-9*S**3)
C  CONDUCTIVITY OF SAT R12 LIQUID.
      RETURN
```

```
60    FP=4.134E-4*(0.7640 - 4.56620E-3*S + 2.387539E-5*S*S -
     16.689518E-8*S**3)
C  VISCOSITY OF SAT R12 LIQUID.
      RETURN

80    FP=4.1868E3*(1.0144 - 2.85919E-4*S + 1.174337E-6*S*S)
C  SPECIFIC HEAT CAPACITY OF WATER.
      RETURN

90    FP=2.326E3*S*(1.0144 - 1.42959E-4*S + 3.914457E-7*S*S)
C  SPECIFIC ENTHALPY OF WATER REFERRED TO 0 DEG F.
      RETURN

100   FP=5836.2*ALOG((T+273.15)/273.15) - 10.2910*T +
     1 0.007965*(T*T + 2.0*273.15*T)
C  SPECIFIC ENTROPY OF WATER REFERRED TO 0 DEG C.
      RETURN
      END

      FUNCTION HSAT(X,T)

C  HSAT IS SPECIFIC ENTHALPY OF SAT R12 AS FUNCTN OF QUALITY & TEMP.
C  PRESS IS IN PA ABSOLUTE; T IS IN DEG C; H IN J/KG; X IS GAS FRACTION.
C  REDUCED VARIABLES END IN "RED".

      COMMON/BLK1/HC,TC,VC,PC
      TRED=(T+273.15)/TC
      PRED=PSATR12(TRED)
      VGRED=VR12(PRED,TRED)
      VFRED=VFR12(TRED)
      HGSAT=HC*HR12(VGRED,TRED)
      HFG=HC*HFGR12(TRED,PRED,VGRED,VFRED)
      HSAT=HGSAT - (1-X)*HFG
600   FORMAT(1H ,'IN HSAT', 8(1PE13.4))
      RETURN
      END

      FUNCTION HG(P,T)

C  HG(P,T) IS SPECIFIC ENTHALPY OF SUPERHEATED R12 AS A FNCTN OF P & T.
C  UNITS ARE-  PRESSURE IN PA ABSOLUTE; T IN DEG C; H IN J/KG.
      COMMON/BLK1/HC,TC,VC,PC
      TRED=(T+273.15)/TC
      PRED=P/PC
      VRED=VR12(PRED,TRED)
      HG=HC*HR12(VRED,TRED)
      RETURN
      END

      FUNCTION SSAT(X,T)

C  SSAT IS SPECIFIC ENTROPY OF SAT R12 AS FUNCTION OF QUALITY AND TEMP
C  PRESS IS IN PA ABSOLUTE; T IN DEG. C; S IN J/KG.C; X IS GAS FRACTION
C  REDUCED VARIABLES END IN RED.
      COMMON/BLK1/HC,TC,VC,PC
      SC=19.15
```

```
      TRED=(T + 273.15)/TC
      PRED=PSATR12(TRED)
      VGRED=VR12(PRED,TRED)
      VFRED=VFR12(TRED)
      SGSAT=SC*SR12(VGRED,TRED)
      SFG=SC*HFGR12(TRED,PRED,VGRED,VFRED)/TRED
      SSAT=SGSAT - (1.0 - X)*SFG
      RETURN
      END

      FUNCTION SG(P,T)

C  SG IS SPECIFIC ENTROPY OF SUPERHEATED R12 AS FUNCTION OF P & T.
C  UNITS ARE PRESSURE IN PA ABSOLUTE; T IN DEG C.; S IN J/KG.C.
C  REDUCED VARIABLES END IN RED.
      COMMON/BLK1/HC,TC,VC,PC
      TRED=(T + 273.15)/TC
      PRED=P/PC
      SC=19.15
      VRED=VR12(PRED,TRED)
      SG=SC*SR12(VRED,TRED)
      RETURN
      END
```

APPENDIX A-5

FREON PROPERTIES AT GIVEN PARAMETERS (SUBROUTINE 2)

A-5.1: Introduction

Subroutine 2 consists of two major programs; calculation of pressure, temperature, specific enthalpy, and specific entropy at point 1, 2, 3 and 4 (see Fig.6.1.5 and Fig.6.1.8), and the derivation of thermal and physical properties of freon at various state using equation of state. All symbols used are explained in the computer program.

The first part of the program calculates the possible properties of freon; specific volume, specific entropy, specific enthalpy, pressure, and temperature at different state (vapour, saturated vapour, two-phase, saturated liquid and liquid). These properties are used to predict the possible simple refrigeration cycle. Other related properties which are not calculated in this subroutine are evaluated in the main program (such as vapour quality at point 3).

The second part is to derive the calculation of those properties (mentioned above) from equation of state. The mathematical derivation is shown in the program listed in section A-5.2.

APPENDIX A-6

RESULTS

A-6.1: Introduction

The results are classified to two groups; experimental and predicted results. They are presented in the form of tables.

The experimental results are tabulated from Table A-6.1 to Table A-6.11 which consist of 68 Runs starting from Run 1 to Run 68.

The predicted results are presented in Table A-6.12 to Table A-6.17 (6 Runs). The results are divided to three sections; A, B and C (see Table 6.2) according to the operating conditions and insulating materials used in the system. Each Runs consists of three separate results; results in three segments, numerical integration outputs, and summary of possible simple refrigeration cycle.

The same number used in both the experimental and predicted results to represents the same inputs had been introduced. The outputs from the same number can be compared. The results are tabulated in section A-6.2.

```
C***********************************************************************C
C                                                                       C
C                 FREON PROPERTIES AT GIVEN PARAMETERS                  C
C           (SUBROUTINE 2) FOR APPENDIX A-5 IN SECTION A-5.2            C
C                                                                       C
C     SUBROUTINE & FUNCTION FROM PROGRAM R12-F77 TO BE LINKED WITH      C
C              MAIN PROGRAM AND SUBROUTINE TBT-SUBROU                   C
C                                                                       C
C***********************************************************************C

      SUBROUTINE RANK12(PR1,TR2,TR4,PR,VR,TR,HR,IX)

C   TO CALCULATE THERMODYNAMIC PROPERTIES OF R12 AT CONDENSER AND BOILER
C                              INLET AND OUTLET

C STATE 1 - BOILER INLET
C   "   2 -   "    OUTLET
C   "   3 - CONDENSER INLET
C   "   4 -      "     OUTLET (SAT)
C PR1 - REDUCED BOILER PRESSURE
C TR2 -    "    TEMPERATURE AT STATE 2
C TR4 -    " CONDENSER TEMPERATURE
C IX = 0 - STURATED TURBINE OUTLET
C IX = 1 - SUPERHEATED "      "
      DIMENSION PR(4),VR(4),TR(4),HR(4),SR(4)
      PR(1)=PR1
      PR(2)=PR(1)
      TR(2)=TR2
      TR(4)=TR4
      PR(4)=PSATR12(TR(4))
      PR(3)=PR(4)
      VR(2)=VR12(PR(1),TR(2))
      VR(3)=VR12(PR(4),TR(4))
      VR(4)=VFR12(TR(4))
      HR(2)=HR12(VR(2),TR(2))
      SR(2)=SR12(VR(2),TR(2))
      HFGR=HFGR12(TR(4),PR(4),VR(3),VR(4))
      HR(3)=HR12(VR(3),TR(4))
      HR(4)=HR(3)-HFGR
      HR(1)=HR(4)+VR(4)*(PR(1)-PR(4))
      CALL VTPPSR12(PR(4),SR(2),VR(3),TR(3))
      IF(TR(3).GT.TR(4))GOTO 10
      IX=0
      SR(3)=SR12(VR(3),TR(4))
      TR(3)=(SR(2)-SR(3))*TR(4)/HFGR+1
      HR(3)=HR(3)-(1-TR(3))*HFGR
      RETURN
   10 HR(3)=HR12(VR(3),TR(3))
      IX=1
      RETURN
      END

      FUNCTION P12FPRWAT(PR)

      DIMENSION C(9)
      DATA C/0.731431, 0.3668035, -0.6783723,
     1 .174895, 2.635912, -15.82026,
     2 28.96178, -23.81524, 7.443050/
```

```
      P12FPRWAT=0
      DO 10 I=1,9
   10 P12FPRWAT=(P12FPRWAT+C(10-I))*PR
      RETURN
      END

      FUNCTION PFRV12(R)

      DATA VGRM/720.E3/
      VGR=R
   10 CALL PTFVGR12(VGR,PR,TR)
      IF(ABS(1-PFRV12/PR).LT.5.E-6)RETURN
      VGR=R*VFR12(TR)
      IF(VGR.GT.VGRM)VGR=VGRM
      PFRV12=PR
      GOTO 10
      END

      SUBROUTINE PVTFSFR12(SR,PR,VR,TR)

C     TO CALCULATE REDUCED SPECIFIC VOLUME AND TEMPERATURE FROM REDUCED
C                 PRESSURE AND SPECIFIC ENTROPY IN LIQUID STATE

      DIMENSION TTR(3),DSR(3)
      VR=1.2
      DO 10 I=1,2
      J=4-I
      VR=VR-0.2
      CALL PTFVFR12(VR,PR,TTR(J))
      VGR=VR12(PR,TTR(J))
   10 DSR(J)=SR12(VGR,TTR(J))-HFGR12(TTR(J),PR,VGR,VR)/TTR(J)-SR
   20 RDSR=DSR(3)/DSR(2)
      TTR(1)=(TTR(2)*RDSR-TTR(3))/(RDSR-1)
      IF(TTR(1)-1.GT.1.E-8)TTR(1)=1-1.E-8
      IF(TTR(1).LT.0.)TTR(1)=0.44
      PR=PSATR12(TTR(1))
      VGR=VR12(PR,TTR(1))
      VR=VFR12(TTR(1))
      DSR(1)=SR12(VGR,TTR(1))-HFGR12(TTR(1),PR,VGR,VR)/TTR(1)-SR
      IF(ABS(DSR(1)/SR).GT.5.E-6)GOTO 30
      TR=TTR(1)
      RETURN
   30 DO 40 I=1,2
      J=4-I
      JJ=3-I
      TTR(J)=TTR(JJ)
   40 DSR(J)=DSR(JJ)
      GOTO 20
      END

      SUBROUTINE PVTFSGR12(SR,PR,VR,TR)

C     TO CALCULATE REDUCED SPECIFIC VOLUME AND TEMPERATURE FROM REDUCED
C                 PRESSURE AND SPECIFIC ENTROPY IN VAPOUR STATE

      DIMENSION TTR(3),DSR(3)
      PR=1
      IF(ABS(SR12(1., 1.)-SR).GT.1.E-8)GOTO 5
```

```
      VR=1
      TR=1
      RETURN
    5 DO 10 I=1,2
      J=4-I
      CALL VTFPSR12(PR,SR,VR,TR)
      CALL PTFVGR12(VR,PR,TTR(J))
   10 DSR(J)=SR12(VR,TTR(J))-SR
   20 RDSR=DSR(3)/DSR(2)
      TTR(1)=(TTR(2)*RDSR-TTR(3))/(RDSR-1)
      IF(TTR(1).LT.0.44)TTR(1)=0.44
      PR=PSATR12(TTR(1))
      VR=VR12(PR,TTR(1))
      DSR(1)=SR12(VR,TTR(1))-SR
      IF(ABS(DSR(1)/SR).GT.5.E-6)GOTO 30
      TR=TTR(1)
      RETURN
   30 DO 40 I=1,2
      J=4-I
      JJ=3-I
      TTR(J)=TTR(JJ)
   40 DSR(J)=DSR(JJ)
      GOTO 20
      END

      SUBROUTINE PVFTSR12(TR,SR,PR,VR)

C      TO CALCULATE REDUCED PRESSURE AND SPECIFIC VOLUME FROM REDUCED
C                     TEMPERATURE AND SPECIFIC ENTROPY
      PR=PSATR12(TR)
      VR=VR12(PR,TR)
      F=1.1
   10 SRE=SR12(VR,TR)
      IF(ABS(1-SRE/SR).GT.5.E-6)GOTO 20
      PR=PR12(VR,TR)
      RETURN
   20 IF(F.LT.1..OR.SR.LT.SRE)F=1/F
      VVR=F*VR
      SSRE=SR12(VVR,TR)
      F=EXP(ALOG(F)*(SR-SRE)/(SSRE-SRE))
      VR=F*VR
      GOTO 10
      END

      SUBROUTINE PTFVSR12(VR,SR,PR,TR)

C         TO CALCULATE REDUCED PRESSURE AND TEMPERATURE FROM REDUCED
C                    SPECIIC VOLUME AND SPECIFIC ENTROPY

      CALL PTFVGR12(VR,PR,TR)
      F=1.1
   10 SRE=SR12(VR,TR)
      IF(ABS(1-SRE/SR).GT.5.E-6)GOTO 20
      PR=PR12(VR,TR)
      RETURN
   20 IF(F.LT.1..OR.SR.LT.SRE)F=1/F
      TTR=F*TR
      SSRE=SR12(VR,TTR)
```

```
      F=EXP(ALOG(F)*(SR-SRE)/(SSRE-SRE))
      TR=F*TR
      GOTO 10
      END

      SUBROUTINE VTFPSR12(PR,SR,VR,TR)

C     TO CALCULATE REDUCED SPECIFIC VOLUME AND TEMPERATURE FROM REDUCED
C                          PRESSURE AND SPECIFIC ENTROPY
      TR=TSATR12(PR)
      F=1.1
   10 VR=VR12(PR,TR)
      SRE=SR12(VR,TR)
      IF(ABS(1-SRE/SR).LT.5.E-6)RETURN
      IF(F.LT.1.)F=1/F
      IF(SR.LT.SRE)F=1/F
      TTR=F*TR
      VVR=VR12(PR,TTR)
      SSRE=SR12(VVR,TTR)
      F=EXP(ALOG(F)*(SR-SRE)/(SSRE-SRE))
      TR=F*TR
      GOTO 10
      END

      SUBROUTINE PTFVFR12(VR,PR,TR)

C  TO CALCULATE REDUCED TEMPERATURE FORM REDUCED PRESSURE AND SPECIFIC VOLUME
C                             OF SATURATED LIQUID
      DIMENSION C(4)
      DATA C/0.536468, 0.630984, 1.53101, -0.0904340/
      IF(ABS(VR-1).GT.1.E-8)GOTO 5
      PR=1
      TR=1
      RETURN
    5 RHOR=1/VR
      TR=0.9999
   10 RHORE=1/VFR12(TR)
      DRHORE=RHORE-RHOR
      IF(ABS(DRHORE/RHOR).GT.5.E-6)GOTO 20
      PR=PSATR12(TR)
      RETURN
   20 TRC=1-TR
      DRHOR=-C(1)-0.5*C(2)/SQRT(TRC)-C(3)/(3*TRC**(2./3))-2*C(4)*TRC
      TR=TR-DRHORE/DRHOR
      GOTO 10
      END

      SUBROUTINE PTFVGR12(VR,PR,TR)

C  TO CALCULATE REDUCED TEMPERATURE FOR REDUCED PRESSURE AND SPECIFIC VOLUME
                              OF SATURATED VAPOUR
      DIMENSION PPR(3),DVR(3)
      IF(ABS(VR-1.1).GT.0.1+1.E-8)GOTO 5
      TR=1.024259-0.027233*VR+0.012727*SQRT(VR-0.9454)
      PR=PSATR12(TR)
      RETURN
    5 TR=0.998
      DO 10 I=1,2
```

```
      J=4-I
      PPR(J)=PR12(VR,TR)
      TR=TSATR12(PPR(J))
   10 DVR(J)=VR12(PPR(J),TR)-VR
   20 RDVR=DVR(3)/DVR(2)
      PPR(1)=(PPR(2)*RDVR-PPR(3))/(RDVR-1)
      TR=TSATR12(PPR(1))
      DVR(1)=VR12(PPR(1),TR)-VR
      IF(ABS(DVR(1)/VR).GT.5.E-6)GOTO 30
      PR=PPR(1)
      RETURN
   30 DO 40 I=1,2
      J=4-I
      JJ=3-I
      PPR(J)=PPR(JJ)
   40 DVR(J)=DVR(JJ)
      GOTO 20
      END

      FUNCTION HR12(VR,TR)

C             TO CALCULATE SPECIFIC ENTHALPY OF SUPERHEATED R12
      REAL K,KTR
      DIMENSION A(5),C(5),E(4)
      DATA A/0., -6.934977529, 4.267936535, -1.354488423, 0./,
     1 C/0., -115.1596917, 92.90090309, 0., -2.187472214/,
     2 BR,K/0.22678710, -5.475/,
     3 E/1.772181, 50.42774, -25.36853, 4.898847/,
     4 HDR/12.474812015/
      KTR=K*TR
      FKTR=(KTR-1)*EXP(KTR)
      VB=VR-BR
      VBEX=1
      FHR=0
      DO 10 I=2,5
      VBEX=VBEX*VB
   10 FHR=FHR+(A(I)-C(I)*FKTR)/((I-1)*VBEX)
      SCVZR=(E(1)+(E(2)*0.5+(E(3)/3+E(4)*0.25*TR)*TR)*TR)*TR
      HR12=HDR+SCVZR+FHR+PR12(VR,TR)*VR
      RETURN
      END

      FUNCTION SR12(VR,TR)

C             TO CALCULATE SPECIFIC ENTROPY OF SUPERHEATED R12
      REAL K
      DIMENSION B(5),C(5),E(4)
      DATA B/3.590772057, 2.24780781, -0.9232594576, 0.,0.2068197136/,
     1 C/0., -115.1596917, 92.90090309, 0., -2.187472214/,
     2 BR,K/0.22678710, -5.475/,
     3 E/1.772181, 50.42774, -25.36853, 4.898847/,
     4 SDR/-4.78453976/
      FKTR=K*EXP(K*TR)
      VB=VR-BR
      VBEX=1
      FSR=B(1)*ALOG(VB)
      DO 10 I=2,5
      VBEX=VBEX*VB
```

```
10  FSR=FSR-(B(I)+C(I)*FKTR)/((I-1)*VBEX)
    SCVZBTR=B(1)*ALOG(TR)+(B(2)+(B(3)*0.5+B(4)/3*TR)*TR)*TR
    SR12=SDR+SCVZBTR+FSR
    RETURN
    END

    FUNCTION VR12(PR,TR)

C             TO CALCULATE SPECIFIC VOLUME OF SUPERHEATED R12
    REAL K
    DIMENSION A(5),B(5),C(5),F(5),FD(5),XEX(6)
    DATA A/0., -6.934977529, 4.267936535, -1.354488423, 0./,
   1 B/3.590772057, 2.24780781, -0.9232594576, 0., 0.2068197136/,
   2 C/0., -115.1596917, 92.90090309, 0., -2.187472214/,
   3 BR,K/0.22678710, -5.475/
    IF(ABS(PR-1).GT.1.E-8.OR.ABS(TR-1).GT.1.E-8)GOTO 5
    VR12=1
    RETURN
 5  EKT=EXP(K*TR)
    DO 10 I=1,5
    F(I)=A(I)+B(I)*TR+C(I)*EKT
10  FD(I)=I*F(I)
    IF(ABS(TR-0.999).GT.0.001.OR.PR.LT.0.9875)GOTO 15
    VR12=1+2.832*SQRT(1-TR)+36.72*(1-TR)
    RETURN
15  X=PR/F(1)
    X=(PR-(F(2)+(F(3)+(F(4)+F(5)*X)*X)*X)*X*X)/F(1)
20  VRE=BR+1/X
    Y=-PR
    DY=0
    XEX(1)=1
    DO 30 I=2,6
30  XEX(I)=XEX(I-1)*X
    DO 40 I=1,5
    Y=Y+F(I)*XEX(I+1)
40  DY=DY+FD(I)*XEX(I)
    X=X-Y/DY
    VR12=BR+1/X
    IF(ABS(1-VRE/VR12).LT.5.E-6)RETURN
    GOTO 20
    END

    FUNCTION TSATR12(PR)

C             TO CALCULATE TEMPERATURE OF SATURATED R12
    DIMENSION C(4)
    DATA C/3.862336922, -11.41020509, -12.46463173, 7.547868173/
    TSATR12=1
    IF(ABS(PR-1).LT.1.E-8)RETURN
10  PRE=PSATR12(TSATR12)
    IF(ABS(1-PRE/PR).LT.5.E-6)RETURN
    DPR=PRE*((-C(2)/TSATR12+C(3))/TSATR12+C(4))
    TSATR12=TSATR12-(PRE-PR)/DPR
    GOTO 10
    END

    FUNCTION HFGR12(TR,PR,VR,VFR)
```

```
C                   TO CALCULATE LATENT HEAT OF R12
      DIMENSION C(4)
      DATA C/3.862336922, -11.41020509, -12.46463173, 7.547868173/
      DPR=PR*((-C(2)/TR+C(3))/TR+C(4))
      HFGR12=TR*(VR-VFR)*DPR
      RETURN
      END

      FUNCTION VFR12(TR)

C             TO CALCULATE REDUCED SPECIFIC VOLUME OF LIQUID R12
      DIMENSION C(4)
      DATA C/0.536468, 0.630984, 1.53101, -0.0904340/
      TRC=1-TR
      RHOFR=1+C(1)*TRC+C(2)*SQRT(TRC)+C(3)*TRC**(1./3)+C(4)*TRC*TRC
      VFR12=1/RHOFR
      RETURN
      END

      FUNCTION PR12(VR,TR)

C             TO CALCULATE REDUCED PRESSURE OF SUPERHEATED R12
      REAL K
      DIMENSION A(5),B(5),C(5)
      DATA A/0., -6.934977529, 4.267936535, -1.354488423, 0./,
     1 B/3.590772057, 2.24780781, -0.9232594576, 0., 0.2068197136/,
     2 C/0., -115.1596917, 92.90090309, 0., -2.187472214/,
     3 BR,K/0.22678710, -5.475/
      VB=VR-BR
      VBEX=VB
      PR12=B(1)*TR/VB
      DO 10 I=2,5
      VBEX=VBEX*VB
   10 PR12=PR12+(A(I)+B(I)*TR+C(I)*EXP(K*TR))/VBEX
      RETURN
      END

      FUNCTION PSATR12(TR)

C                TO CALCULATE PRESSURE OF SATURATED R12
      DIMENSION C(4)
      DATA C/3.862336922, -11.41020509, -12.46463173, 7.547868173/
      PSATR12=EXP(C(1)+C(2)/TR+C(3)*ALOG(TR)+C(4)*TR)
      RETURN
      END
```

Run	1	2	3	4	5	6
TEMPERATURE DISTRIBUTION IN HEAT PUMP CONDENSER (in Degree Celcius)						
freon inlet temp. =	66.43	68.63	70.69	72.59	73.54	74.38
freon temp. at 2 =	40.50	43.07	45.44	47.51	48.62	49.75
freon temp. at 3 =	38.22	40.61	42.81	44.80	45.84	46.92
freon temp. at 4 =	37.21	39.60	41.84	43.84	44.88	45.96
freon temp. at 5 =	36.61	39.05	41.30	43.32	44.39	45.45
freon temp. at 6 =	35.72	38.17	40.45	42.47	43.54	44.59
freon temp. at 7 =	35.59	38.11	40.40	42.49	43.58	44.63
freon temp. at 8 =	34.76	37.29	39.59	41.70	42.77	43.83
freon temp. at 9 =	33.68	36.19	38.47	40.56	41.59	42.66
freon temp. at 10 =	33.60	36.23	38.65	40.83	41.94	43.04
freon temp. at 11 =	32.99	35.65	38.11	40.34	41.48	42.60
freon temp. at 12 =	32.39	35.07	37.54	39.84	41.00	42.14
freon temp. at 13 =	31.47	34.12	36.56	38.86	40.03	41.15
freon temp. at 14 =	30.89	33.59	36.00	38.27	39.44	40.54
freon temp. at 15 =	27.85	31.66	34.37	37.01	38.25	39.45
freon outlet temp. =	22.06	24.72	26.67	29.57	31.10	32.51
OTHER PARAMETERS MEASURED IN THE EXPERIMENT						
freon temp. at 17 =	2.17	2.40	2.54	2.80	2.93	3.09
pressure(bar) at 1 =	7.91	8.43	8.96	9.46	9.74	9.99
pressure(bar) at 2 =	3.22	3.24	3.25	3.28	3.28	3.30
mass waterflow(g/s) =	10.58	9.40	8.58	7.80	7.59	7.07
eff. R12 inlet temp. =	61.24	63.52	65.64	67.57	68.55	69.45
eff. WAT inlet temp. =	17.49	18.65	19.50	20.82	21.45	21.56
eff.outlet press(bar)=	7.97	8.48	9.01	9.51	9.79	10.04
room temperature =	18.45	18.73	19.24	19.49	19.80	20.17

Run	1	2	3	4	5	6
water outlet temp. =	39.86	42.54	44.97	47.17	48.30	49.42
water temp. at 2 =	37.70	40.29	42.66	44.73	45.82	46.95
water temp. at 3 =	36.77	39.30	41.54	43.55	44.63	45.69
water temp. at 4 =	35.83	38.39	40.72	42.80	43.91	44.99
water temp. at 5 =	35.01	37.67	40.01	42.14	43.22	44.33
water temp. at 6 =	34.12	36.85	39.15	41.28	42.36	43.46
water temp. at 7 =	33.03	35.75	38.11	40.29	41.42	42.53
water temp. at 8 =	32.17	34.91	37.27	39.52	40.62	41.71
water temp. at 9 =	30.82	33.52	35.82	38.03	39.10	40.18
water temp. at 10 =	29.40	32.10	34.30	36.58	37.56	38.64
water temp. at 11 =	28.14	30.91	33.33	35.76	36.95	38.17
water temp. at 12 =	26.51	29.23	31.33	34.04	34.94	36.38
water temp. at 13 =	23.94	26.38	28.67	31.14	32.20	33.35
water temp. at 14 =	21.32	23.02	25.02	27.11	28.22	29.11
water temp. at 15 =	19.49	21.39	22.86	24.78	25.64	26.27
water inlet temp. =	14.54	14.59	14.54	14.97	15.24	14.58
freon temp. at 18 =	14.34	14.60	14.77	15.02	15.10	15.30
pressure (bar) at 3 =	9.25	9.72	10.22	10.65	10.91	11.13
pressure (bar) at 4 =	3.36	3.38	3.39	3.42	3.43	3.44
exit Wtem at sink(C) =	37.30	40.50	43.10	44.90	46.00	46.70
eff.R12 outlet temp. =	24.40	27.53	29.78	32.58	33.99	35.32
eff.WAT outlet temp. =	38.89	41.53	43.93	46.07	47.19	48.31
eff.inlet press(bar) =	9.23	9.70	10.20	10.63	10.89	11.11
FREON mass flowrate =	6.05	5.85	5.78	5.53	5.54	5.41

Table A-6.1: Experimental results for Run 1 to Run 6

Run		7	8	9	10	11	12
TEMPERATURE DISTRIBUTION IN HEAT PUMP CONDENSER (in Degree Celcius)							
freon inlet temp.	=	75.26	75.92	61.17	65.63	68.48	71.62
freon temp. at 2	=	50.81	51.26	32.12	38.30	41.57	45.33
freon temp. at 3	=	47.94	48.40	30.20	36.08	39.17	42.69
freon temp. at 4	=	46.96	47.39	29.10	35.03	38.15	41.73
freon temp. at 5	=	46.44	46.88	28.33	34.45	37.63	41.27
freon temp. at 6	=	45.59	46.05	27.47	33.69	36.89	40.53
freon temp. at 7	=	45.65	46.10	26.76	33.31	36.65	40.40
freon temp. at 8	=	44.83	45.26	26.03	32.51	35.83	39.61
freon temp. at 9	=	43.63	44.09	24.94	31.41	34.75	38.48
freon temp. at 10	=	44.07	44.53	24.59	31.23	34.71	38.62
freon temp. at 11	=	43.64	44.11	23.86	30.65	34.15	38.11
freon temp. at 12	=	43.19	43.66	22.74	29.93	33.53	37.54
freon temp. at 13	=	42.23	42.71	21.56	29.07	32.54	36.44
freon temp. at 14	=	41.56	42.04	17.70	28.01	31.80	35.82
freon temp. at 15	=	40.57	41.05	16.03	21.93	25.97	30.75
freon outlet temp.	=	34.54	35.76	15.60	19.28	21.50	23.82
water outlet temp.	=	50.53	51.07	30.11	37.17	40.67	44.61
water temp. at 2	=	48.02	48.44	28.61	35.42	38.79	42.56
water temp. at 3	=	46.65	47.12	27.60	34.37	37.70	41.42
water temp. at 4	=	46.01	46.48	26.70	33.53	36.88	40.68
water temp. at 5	=	45.36	45.81	25.62	32.64	36.07	39.95
water temp. at 6	=	44.50	44.96	24.56	31.74	35.23	39.12
water temp. at 7	=	43.58	44.05	23.43	30.52	34.08	38.03
water temp. at 8	=	42.72	43.22	22.42	29.65	33.21	37.15
water temp. at 9	=	41.21	41.62	21.16	28.19	31.65	35.60
water temp. at 10	=	39.75	40.22	20.07	26.80	30.23	34.10
water temp. at 11	=	39.36	39.88	18.72	25.53	28.83	32.75
water temp. at 12	=	37.47	37.92	17.59	23.92	26.88	30.93
water temp. at 13	=	34.58	35.19	16.07	21.56	24.19	27.49
water temp. at 14	=	30.20	30.61	15.33	19.31	21.52	23.77
water temp. at 15	=	27.28	27.81	15.09	17.83	19.53	21.77
water inlet temp.	=	14.98	15.24	13.54	14.77	15.11	15.51
OTHER PARAMETERS MEASURED IN THE EXPERIMENT							
freon temp. at 17	=	3.36	3.43	1.24	1.68	1.95	2.27
pressure(bar) at 1	=	10.25	10.36	6.39	7.50	8.21	9.04
pressure(bar) at 2	=	3.33	3.33	3.12	3.17	3.20	3.23
mass waterflow(g/s)	=	6.86	6.72	17.46	12.20	10.56	9.05
eff. R12 inlet temp.	=	70.37	70.99	55.36	60.17	63.10	66.36
eff. WAT inlet temp.	=	22.32	22.74	14.47	16.60	17.75	19.25
eff.outlet press(bar)	=	10.30	10.41	6.44	7.55	8.26	9.09
room temperature	=	20.42	20.78	19.42	18.94	18.87	19.04
freon temp. at 18	=	15.52	15.70	13.94	14.13	14.28	14.70
pressure (bar) at 3	=	11.38	11.47	7.68	8.83	9.46	10.22
pressure (bar) at 4	=	3.47	3.47	3.26	3.31	3.33	3.36
exit Wtem at sink(C)	=	47.60	48.10	29.90	36.50	39.60	43.20
eff.R12 outlet temp.	=	36.98	37.90	15.78	20.35	23.31	26.62
eff.WAT outlet temp.	=	49.40	49.88	29.43	36.38	39.83	43.68
eff.inlet press(bar)	=	11.36	11.45	7.65	8.81	9.44	10.20
FREON mass flowrate	=	5.38	5.31	6.62	6.26	6.14	5.94

Table A-6.2: Experimental results for Run 7 to Run 12

Run		13	14	15	16	17	18	19
TEMPERATURE DISTRIBUTION IN HEAT PUMP CONDENSER (in Degree Celcius)								
freon inlet temp.	=	62.69	63.36	65.10	65.58	66.65	67.84	69.37
freon temp. at 2	=	33.48	33.83	35.09	35.89	37.32	38.48	40.16
freon temp. at 3	=	31.39	31.75	32.99	33.70	35.05	36.12	37.66
freon temp. at 4	=	30.30	30.66	31.96	32.64	33.98	35.07	36.59
freon temp. at 5	=	29.32	29.73	31.05	31.73	33.13	34.22	35.75
freon temp. at 6	=	28.49	28.92	30.26	30.95	32.41	33.54	35.07
freon temp. at 7	=	27.62	28.07	29.47	30.17	31.65	32.81	34.42
freon temp. at 8	=	26.87	27.32	28.73	29.43	30.96	32.12	33.74
freon temp. at 9	=	26.04	26.47	27.88	28.58	30.11	31.29	32.92
freon temp. at 10	=	25.44	25.86	27.15	27.98	29.48	30.67	32.32
freon temp. at 11	=	24.80	25.27	25.98	27.29	28.90	30.06	31.71
freon temp. at 12	=	23.94	24.62	24.01	26.21	28.15	29.44	31.07
freon temp. at 13	=	23.49	24.15	20.08	25.47	27.43	28.67	30.28
freon temp. at 14	=	20.59	23.83	18.95	22.13	26.98	28.49	30.14
freon temp. at 15	=	18.06	21.51	18.39	19.10	23.04	26.78	28.96
freon outlet temp.	=	17.62	19.61	18.34	18.48	20.44	23.38	26.30
water outlet temp.	=	30.71	31.21	32.36	33.53	35.21	36.50	38.32
water temp. at 2	=	29.42	29.96	31.08	32.15	33.77	34.98	36.62
water temp. at 3	=	28.35	28.90	29.97	31.09	32.71	33.94	35.60
water temp. at 4	=	27.47	28.13	29.05	30.16	31.83	33.08	34.76
water temp. at 5	=	26.41	27.10	27.92	29.11	30.84	32.12	33.84
water temp. at 6	=	25.38	26.18	26.79	28.11	30.00	31.32	33.02
water temp. at 7	=	24.45	25.33	25.68	27.12	28.98	30.37	32.15
water temp. at 8	=	23.58	24.53	24.59	26.19	28.17	29.62	31.42
water temp. at 9	=	22.51	23.56	23.20	24.95	27.00	28.51	30.32
water temp. at 10	=	21.60	22.77	22.06	23.88	26.05	27.60	29.33
water temp. at 11	=	20.37	21.69	20.47	22.31	24.58	26.21	27.98
water temp. at 12	=	19.46	20.84	19.40	21.10	23.41	25.06	26.82
water temp. at 13	=	18.29	19.73	18.41	19.53	21.69	23.32	24.98
water temp. at 14	=	17.39	18.76	18.16	18.31	20.09	21.61	23.02
water temp. at 15	=	16.92	17.97	18.05	17.75	18.88	20.23	21.41
water inlet temp.	=	15.70	16.19	16.87	16.19	16.50	16.89	17.20
OTHER PARAMETERS MEASURED IN THE EXPRIMENT								
freon temp. at 17	=	3.19	3.13	2.67	2.80	3.00	3.16	3.41
pressure(bar) at 1	=	6.52	6.49	7.08	6.99	7.15	7.30	7.58
pressure(bar) at 2	=	3.32	3.31	3.31	3.31	3.31	3.32	3.33
mass waterflow(g/s)	=	19.76	19.19	17.98	16.73	15.18	14.10	12.97
eff. R12 inlet temp.	=	56.85	57.45	59.10	59.64	60.78	61.97	63.52
eff. WAT inlet temp.	=	16.43	17.25	17.57	17.12	17.92	18.88	19.71
eff.outlet press(bar)	=	6.58	6.55	7.13	7.05	7.21	7.36	7.64
room temperature	=	19.62	19.71	19.74	19.79	19.74	19.89	20.17
freon temp. at 18	=	14.32	14.28	14.08	14.18	14.13	14.27	14.63
pressure (bar) at 3	=	7.97	8.03	8.28	8.37	8.64	8.82	9.09
pressure (bar) at 4	=	3.47	3.46	3.46	3.47	3.46	3.47	3.49
exit Wtem at sink(C)	=	30.70	31.10	32.20	33.40	34.90	36.10	37.60
eff.R12 outlet temp.	=	17.80	20.38	18.36	18.73	21.50	24.75	27.38
eff.WAT outlet temp.	=	30.13	30.64	31.78	32.91	34.56	35.81	37.55
eff.inlet press(bar)	=	7.94	8.00	8.26	8.35	8.61	8.79	9.06
FREON mass flowrate	=	6.92	6.67	6.52	6.74	6.55	6.31	6.21

Table A-6.3: Experimental results for Run 13 to Run 19

Run		20	21	22	23	24	25
TEMPERATURE DISTRIBUTION IN HEAT PUMP CONDENSER (in Degree Celcius)							
freon inlet temp.	=	69.93	70.62	71.56	72.02	72.70	73.55
freon temp. at 2	=	41.18	42.20	43.16	44.03	44.49	45.95
freon temp. at 3	=	38.65	39.61	40.46	41.27	41.68	42.99
freon temp. at 4	=	37.65	38.62	39.44	40.26	40.63	41.98
freon temp. at 5	=	36.80	37.78	38.64	39.41	39.82	41.15
freon temp. at 6	=	36.19	37.18	38.03	38.81	39.23	40.56
freon temp. at 7	=	35.58	36.59	37.41	38.24	38.64	39.99
freon temp. at 8	=	34.95	36.00	36.82	37.62	38.05	39.43
freon temp. at 9	=	34.18	35.23	36.10	36.92	37.31	38.72
freon temp. at 10	=	33.60	34.69	35.57	36.38	36.79	38.19
freon temp. at 11	=	33.03	34.13	34.98	35.80	36.23	37.64
freon temp. at 12	=	32.42	33.54	34.37	35.20	35.63	37.05
freon temp. at 13	=	31.67	32.77	33.58	34.40	34.80	36.17
freon temp. at 14	=	31.57	32.68	33.50	34.29	34.71	36.09
freon temp. at 15	=	30.70	31.80	32.57	33.44	33.86	35.21
freon outlet temp.	=	28.05	29.27	28.79	31.01	31.51	32.88
water outlet temp.	=	39.48	40.52	41.40	42.27	42.69	44.15
water temp. at 2	=	37.80	38.91	39.82	40.57	41.11	42.51
water temp. at 3	=	36.72	37.75	38.62	39.44	39.86	41.24
water temp. at 4	=	35.86	36.91	37.83	38.62	39.04	40.41
water temp. at 5	=	34.99	36.05	36.97	37.73	38.20	39.58
water temp. at 6	=	34.23	35.32	36.24	37.08	37.50	38.93
water temp. at 7	=	33.43	34.51	35.37	36.24	36.69	38.13
water temp. at 8	=	32.73	33.88	34.74	35.59	36.05	37.53
water temp. at 9	=	31.67	32.79	33.58	34.47	34.95	36.39
water temp. at 10	=	30.77	31.92	32.77	33.59	34.07	35.47
water temp. at 11	=	29.30	30.40	31.12	32.03	32.51	33.83
water temp. at 12	=	28.11	29.20	29.85	30.77	31.25	32.57
water temp. at 13	=	26.08	27.03	27.53	28.47	28.90	30.02
water temp. at 14	=	23.72	24.56	24.87	25.77	26.15	27.10
water temp. at 15	=	21.89	22.58	22.74	23.56	23.91	24.60
water inlet temp.	=	16.75	16.98	16.99	17.22	17.45	17.17
OTHER PARAMETERS MEASURED IN THE EXPERIMENT							
freon temp. at 17	=	3.26	3.28	3.56	3.89	4.10	4.26
pressure(bar) at 1	=	7.81	8.03	8.19	8.37	8.46	8.76
pressure(bar) at 2	=	3.30	3.30	3.32	3.36	3.38	3.40
mass waterflow(g/s)	=	11.64	11.11	11.22	10.54	10.40	9.68
eff. R12 inlet temp.	=	64.18	64.93	65.88	66.43	67.06	68.03
eff. WAT inlet temp.	=	19.82	20.32	20.42	21.00	21.30	21.60
eff.outlet press(bar)	=	7.87	8.09	8.25	8.43	8.52	8.82
room temperature	=	20.11	20.26	20.55	20.92	21.17	21.36
freon temp. at 18	=	13.72	13.71	14.06	14.38	14.56	14.64
pressure (bar) at 3	=	9.27	9.46	9.61	9.80	9.92	10.17
pressure (bar) at 4	=	3.45	3.45	3.47	3.51	3.54	3.56
exit Wtem at sink(C)	=	38.80	39.60	40.30	41.40	41.90	43.20
eff.R12 outlet temp.	=	29.12	30.29	30.32	31.99	32.46	33.82
eff.WAT outlet temp.	=	38.72	39.79	40.69	41.50	41.98	43.41
eff.inlet press(bar)	=	9.24	9.44	9.59	9.78	9.89	10.15
FREON mass flowrate	=	5.98	5.92	6.20	5.96	5.94	5.88

Table A-6.4: Experimental results for Run 20 to Run 25

Run	26	27	28	29	30
TEMPERATURE DISTRIBUTION IN HEAT PUMP CONDENSER (in Degree Celcius)					
freon inlet temp.	= 74.33	74.58	75.47	76.91	77.55
freon temp. at 2	= 46.89	46.99	47.80	49.67	50.57
freon temp. at 3	= 43.89	43.96	44.71	46.42	47.22
freon temp. at 4	= 42.88	42.96	43.71	45.41	46.22
freon temp. at 5	= 42.04	42.15	42.87	44.56	45.37
freon temp. at 6	= 41.49	41.56	42.32	44.00	44.81
freon temp. at 7	= 40.94	41.03	41.78	43.49	44.33
freon temp. at 8	= 40.38	40.47	41.25	42.96	43.78
freon temp. at 9	= 39.68	39.77	40.57	42.29	43.14
freon temp. at 10	= 39.18	39.30	40.11	41.87	42.70
freon temp. at 11	= 38.62	38.76	39.56	41.35	42.20
freon temp. at 12	= 38.02	38.15	38.99	40.78	41.65
freon temp. at 13	= 37.20	37.33	38.17	39.90	40.78
freon temp. at 14	= 37.10	37.20	38.05	39.81	40.63
freon temp. at 15	= 36.24	36.35	37.17	38.92	39.75
freon outlet temp.	= 33.26	34.27	34.95	36.11	37.78
water outlet temp.	= 45.08	45.20	46.03	47.89	48.78
water temp. at 2	= 43.44	43.50	44.19	46.11	46.93
water temp. at 3	= 42.17	42.24	42.99	44.71	45.55
water temp. at 4	= 41.33	41.46	42.20	43.93	44.76
water temp. at 5	= 40.53	40.63	41.40	43.09	43.94
water temp. at 6	= 39.87	39.99	40.75	42.48	43.37
water temp. at 7	= 39.14	39.28	40.06	41.80	42.70
water temp. at 8	= 38.50	38.67	39.46	41.24	42.15
water temp. at 9	= 37.41	37.61	38.38	40.18	41.07
water temp. at 10	= 36.47	36.71	37.52	39.31	40.20
water temp. at 11	= 34.83	35.10	35.88	37.65	38.61
water temp. at 12	= 33.55	33.80	34.54	36.21	37.20
water temp. at 13	= 30.84	31.16	31.85	33.28	34.25
water temp. at 14	= 27.78	28.17	28.84	30.24	31.08
water temp. at 15	= 25.21	25.62	26.23	27.19	28.05
water inlet temp.	= 17.33	17.57	17.57	17.20	17.46
OTHER PARAMETERS MEASURED IN THE EXPERIMENT					
freon temp. at 17	= 4.39	4.26	4.21	4.63	4.84
pressure(bar) at 1	= 8.99	9.01	9.20	9.61	9.81
pressure(bar) at 2	= 3.41	3.40	3.39	3.43	3.46
mass waterflow(g/s)	= 9.61	9.35	9.03	8.41	8.15
eff. R12 inlet temp.	= 68.84	69.07	69.94	71.46	72.15
eff. WAT inlet temp.	= 22.03	22.37	22.74	23.16	23.78
eff.outlet press(bar)	= 9.05	9.07	9.25	9.67	9.86
room temperature	= 21.55	21.67	21.73	21.92	22.17
freon temp. at 18	= 14.70	14.63	14.53	14.82	15.01
pressure (bar) at 3	= 10.37	10.39	10.54	10.94	11.12
pressure (bar) at 4	= 3.57	3.56	3.55	3.60	3.63
exit Wtem at sink(C)	= 44.00	44.00	44.80	46.50	47.10
eff.R12 outlet temp.	= 34.47	35.11	35.85	37.24	38.58
eff.WAT outlet temp.	= 44.34	44.43	45.20	47.09	47.95
eff.inlet press(bar)	= 10.35	10.36	10.52	10.92	11.10
FREON mass flowrate	= 5.99	5.79	5.72	5.72	5.65

Table A-6.5: Experimental results for Run 26 to Run 30

TEMPERATURE DISTRIBUTION IN HEAT PUMP CONDENSER (in Degree Celcius)

Run		31	32	33	34	35	36	37
freon inlet temp.	=	66.51	68.46	69.76	71.45	73.63	80.30	81.45
freon temp. at 2	=	31.31	33.28	35.16	37.34	41.16	52.37	52.64
freon temp. at 3	=	29.41	31.21	33.01	35.08	38.58	49.07	49.28
freon temp. at 4	=	28.36	30.18	32.00	34.08	37.61	48.38	48.60
freon temp. at 5	=	27.55	29.36	31.17	33.26	36.76	47.39	47.66
freon temp. at 6	=	26.69	28.54	30.34	32.47	36.06	46.83	47.16
freon temp. at 7	=	25.89	27.74	29.57	31.76	35.41	46.39	46.78
freon temp. at 8	=	25.25	27.06	28.86	31.02	34.73	45.51	46.09
freon temp. at 9	=	24.71	26.37	28.14	30.28	34.01	43.85	45.05
freon temp. at 10	=	24.24	25.85	27.55	29.68	33.39	41.12	43.88
freon temp. at 11	=	23.79	25.33	26.99	29.08	32.74	34.15	41.17
freon temp. at 12	=	23.44	24.91	26.50	28.56	32.22	25.29	33.93
freon temp. at 13	=	23.21	24.57	26.05	27.99	31.51	22.42	25.97
freon temp. at 14	=	23.15	24.50	26.00	27.93	31.38	21.44	23.67
freon temp. at 15	=	22.64	24.06	25.53	27.43	30.75	20.85	22.37
freon outlet temp.	=	22.42	23.78	25.34	27.28	30.72	20.70	22.02

Run		31	32	33	34	35	36	37
water outlet temp.	=	27.66	30.20	32.42	34.90	39.09	50.66	51.02
water temp. at 2	=	26.75	29.17	31.21	33.69	37.62	48.71	49.03
water temp. at 3	=	25.90	28.22	30.32	32.67	36.60	47.27	47.67
water temp. at 4	=	25.30	27.51	29.51	31.93	35.91	46.25	46.79
water temp. at 5	=	24.55	26.68	28.66	31.04	35.07	44.82	45.64
water temp. at 6	=	23.95	25.96	27.89	30.27	34.33	43.31	44.62
water temp. at 7	=	23.37	25.28	27.14	29.47	33.53	41.24	43.07
water temp. at 8	=	22.82	24.68	26.48	28.80	32.81	38.88	41.53
water temp. at 9	=	22.37	24.08	25.81	28.01	31.93	34.39	38.50
water temp. at 10	=	21.92	23.45	25.09	27.20	31.09	30.53	35.14
water temp. at 11	=	21.50	22.82	24.31	26.29	29.94	24.59	29.29
water temp. at 12	=	21.21	22.35	23.72	25.56	29.00	22.38	26.34
water temp. at 13	=	20.71	21.62	22.80	24.40	27.42	20.95	22.89
water temp. at 14	=	20.47	21.14	22.09	23.41	25.76	20.66	22.02
water temp. at 15	=	20.29	20.75	21.52	22.60	24.39	20.56	21.73
water inlet temp.	=	19.15	19.16	19.52	19.97	20.15	17.84	18.76

OTHER PARAMETERS MEASURED IN THE EXPERIMENT

Run		31	32	33	34	35	36	37
freon temp. at 17	=	3.69	3.60	4.06	4.36	4.85	1.52	1.55
pressure(bar) at 1	=	6.17	6.41	6.66	7.02	7.66	11.36	11.31
pressure(bar) at 2	=	3.25	3.24	3.29	3.32	3.37	3.33	3.33
mass waterflow(g/s)	=	32.86	25.46	21.49	18.19	13.74	7.85	8.11
eff. R12 inlet temp.	=	59.47	61.43	62.84	64.63	67.14	74.72	75.69
eff. WAT inlet temp.	=	19.83	20.11	20.71	21.54	22.68	19.47	20.53
eff.outlet press(bar)	=	6.23	6.47	6.73	7.08	7.73	11.38	11.34
room temperature	=	24.66	24.41	24.41	24.45	24.63	19.99	20.12

Run		31	32	33	34	35	36	37
freon temp. at 18	=	20.93	21.31	21.23	21.08	20.43	14.38	14.44
pressure (bar) at 3	=	7.63	7.91	8.24	8.64	9.28	11.87	11.92
pressure (bar) at 4	=	3.44	3.43	3.47	3.51	3.56	3.56	3.56
exit Wtem at sink(C)	=	27.80	30.40	32.60	35.10	39.10	48.70	49.20
eff.R12 outlet temp.	=	22.51	23.89	25.42	27.34	30.73	20.76	22.16
eff.WAT outlet temp.	=	27.25	29.74	31.87	34.36	38.43	49.78	50.13
eff.inlet press(bar)	=	7.60	7.89	8.22	8.61	9.25	11.86	11.91
FREON mass flowrate	=	6.27	6.33	6.24	6.13	5.81	6.01	6.09

Table A-6.6: Experimental results for Run 31 to Run 37

Run		38	39	40	41	42	43	44
TEMPERATURE DISTRIBUTION IN HEAT PUMP CONDENSER (in Degree Celcius)								
freon inlet temp.	=	65.69	66.49	67.31	68.36	69.30	70.39	71.45
freon temp. at 2	=	38.02	39.14	39.86	41.34	42.47	43.80	45.03
freon temp. at 3	=	35.61	36.67	37.38	38.74	39.82	41.04	42.17
freon temp. at 4	=	34.62	35.68	36.35	37.75	38.83	40.05	41.17
freon temp. at 5	=	33.63	34.70	35.44	36.84	37.92	39.14	40.28
freon temp. at 6	=	32.70	33.80	34.55	35.98	37.09	38.34	39.48
freon temp. at 7	=	31.85	32.96	33.74	35.19	36.33	37.60	38.78
freon temp. at 8	=	31.00	32.13	32.93	34.38	35.53	36.81	38.00
freon temp. at 9	=	30.17	31.28	32.14	33.57	34.74	36.03	37.24
freon temp. at 10	=	29.49	30.59	31.49	32.90	34.05	35.36	36.58
freon temp. at 11	=	28.84	29.91	30.88	32.27	33.40	34.69	35.90
freon temp. at 12	=	28.31	29.35	30.22	31.67	32.79	34.08	35.30
freon temp. at 13	=	27.72	28.70	29.70	30.97	32.02	33.25	34.45
freon temp. at 14	=	27.70	28.69	28.60	30.93	32.06	33.29	34.46
freon temp. at 15	=	27.00	28.00	23.81	26.78	29.15	31.74	33.35
freon outlet temp.	=	25.90	26.93	22.15	23.50	24.93	26.83	29.82
OTHER PARAMETERS MEASURED IN THE EXPERIMENT								
freon temp. at 17	=	6.85	7.01	6.94	7.12	7.26	7.36	7.67
pressure(bar) at 1	=	7.02	7.22	7.58	7.80	7.98	8.20	8.44
pressure(bar) at 2	=	3.62	3.64	3.65	3.68	3.69	3.70	3.74
mass waterflow(g/s)	=	19.25	17.69	17.89	16.20	15.11	13.98	13.16
eff. R12 inlet temp.	=	60.16	61.02	61.82	62.95	63.93	65.07	66.17
eff. WAT inlet temp.	=	20.48	20.78	20.39	20.78	21.28	21.91	22.41
eff.outlet press(bar)	=	7.10	7.29	7.65	7.87	8.05	8.28	8.51
room temperature	=	23.79	23.91	24.16	24.19	24.32	24.47	24.78

		38	39	40	41	42	43	44
water outlet temp.	=	35.05	36.32	36.98	38.63	39.91	41.34	42.61
water temp. at 2	=	34.12	35.34	36.06	37.64	38.87	40.25	41.48
water temp. at 3	=	32.91	34.15	34.80	36.39	37.66	39.02	40.21
water temp. at 4	=	32.12	33.34	34.01	35.65	36.89	38.27	39.49
water temp. at 5	=	31.04	32.28	32.89	34.60	35.90	37.28	38.55
water temp. at 6	=	30.16	31.37	31.95	33.70	35.07	36.46	37.75
water temp. at 7	=	29.25	30.49	30.99	32.66	34.01	35.48	36.79
water temp. at 8	=	28.41	29.62	30.01	31.73	33.11	34.59	35.96
water temp. at 9	=	27.48	28.63	28.90	30.60	31.95	33.46	34.86
water temp. at 10	=	26.62	27.71	27.82	29.51	30.90	32.37	33.74
water temp. at 11	=	25.58	26.58	26.38	28.02	29.38	30.83	32.27
water temp. at 12	=	24.96	25.85	25.44	26.98	28.29	29.71	31.13
water temp. at 13	=	23.49	24.26	23.50	24.87	26.10	27.43	28.74
water temp. at 14	=	22.36	22.96	22.09	23.13	24.11	25.23	26.33
water temp. at 15	=	21.46	21.92	21.15	21.80	22.56	23.50	24.36
water inlet temp.	=	19.03	19.11	19.28	19.27	19.39	19.57	19.52
freon temp. at 18	=	17.33	17.40	17.34	17.41	17.48	17.52	17.75
pressure (bar) at 3	=	8.85	9.05	9.23	9.48	9.69	9.96	10.16
pressure (bar) at 4	=	3.82	3.83	3.84	3.87	3.89	3.90	3.94
exit Wtem at sink(C)	=	35.20	36.50	37.10	38.80	40.00	41.30	42.60
eff.R12 outlet temp.	=	26.35	27.36	22.82	24.83	26.64	28.82	31.25
eff.WAT outlet temp.	=	34.63	35.88	36.57	38.18	39.44	40.85	42.10
eff.inlet press(bar)	=	8.82	9.02	9.20	9.45	9.67	9.93	10.13
FREON mass flowrate	=	7.27	7.17	7.52	7.41	7.29	7.12	7.06

Table A-6.7: Experimental results for Run 38 to Run 44

TEMPERATURE DISTRIBUTION IN HEAT PUMP CONDENSER (in Degree Celcius)

Run	45	46	47	48	49	50	51
freon inlet temp.	72.02	73.02	73.57	74.63	75.97	76.64	77.29
freon temp. at 2	45.87	47.09	47.75	48.65	50.21	50.80	51.67
freon temp. at 3	42.96	44.08	44.70	45.53	46.98	47.51	48.24
freon temp. at 4	41.94	43.05	43.66	44.52	45.98	46.51	47.21
freon temp. at 5	41.03	42.14	42.75	43.62	45.08	45.60	46.31
freon temp. at 6	40.25	41.38	41.97	42.88	44.38	44.88	45.58
freon temp. at 7	39.56	40.70	41.30	42.22	43.79	44.29	44.97
freon temp. at 8	38.78	39.94	40.56	41.49	43.07	43.60	44.27
freon temp. at 9	38.04	39.20	39.80	40.78	42.38	42.91	43.62
freon temp. at 10	37.36	38.55	39.15	40.15	41.80	42.33	43.04
freon temp. at 11	36.68	37.88	38.48	39.50	41.17	41.71	42.40
freon temp. at 12	36.08	37.26	37.86	38.92	40.61	41.12	41.79
freon temp. at 13	35.19	36.37	36.97	38.04	39.71	40.24	40.92
freon temp. at 14	35.16	36.31	36.90	37.96	39.64	40.12	40.76
freon temp. at 15	34.15	35.32	35.91	36.99	38.60	39.08	39.68
freon outlet temp.	31.18	32.80	33.78	35.11	36.14	37.05	37.97

Run	45	46	47	48	49	50	51
water outlet temp.	43.51	44.75	45.39	46.28	47.85	48.49	49.31
water temp. at 2	42.30	43.46	44.09	44.99	46.52	47.06	47.85
water temp. at 3	41.05	42.22	42.82	43.69	45.22	45.77	46.52
water temp. at 4	40.32	41.49	42.10	43.02	44.58	45.14	45.89
water temp. at 5	39.35	40.57	41.17	42.11	43.69	44.26	45.03
water temp. at 6	38.57	39.80	40.42	41.42	42.99	43.60	44.34
water temp. at 7	37.64	38.89	39.53	40.47	42.19	42.76	43.52
water temp. at 8	36.81	38.09	38.72	39.75	41.47	42.04	42.80
water temp. at 9	35.70	36.94	37.60	38.63	40.37	40.89	41.66
water temp. at 10	34.56	35.80	36.43	37.52	39.25	39.77	40.57
water temp. at 11	33.05	34.23	34.90	35.97	37.69	38.21	38.93
water temp. at 12	31.90	33.02	33.64	34.76	36.37	36.90	37.65
water temp. at 13	29.46	30.53	31.11	32.27	33.71	34.19	34.83
water temp. at 14	26.89	27.79	28.32	29.51	30.69	31.12	31.61
water temp. at 15	24.79	25.52	25.96	27.14	28.06	28.40	28.76
water inlet temp.	19.52	19.66	19.84	21.15	21.43	21.46	21.41

OTHER PARAMETERS MEASURED IN THE EXPERIMENT

Run	45	46	47	48	49	50	51
freon temp. at 17	7.91	8.13	8.42	8.50	8.47	8.63	8.73
pressure(bar) at 1	8.58	8.83	8.95	9.19	9.60	9.71	9.84
pressure(bar) at 2	3.76	3.78	3.82	3.82	3.83	3.84	3.85
mass waterflow(g/s)	12.58	12.06	11.75	11.73	11.02	10.88	10.65
eff. R12 inlet temp.	66.79	67.83	68.41	69.44	70.82	71.47	72.16
eff. WAT inlet temp.	22.67	23.15	23.49	24.72	25.39	25.60	25.79
eff.outlet press(bar)	8.65	8.90	9.02	9.26	9.67	9.78	9.91
room temperature	25.02	25.21	25.39	25.67	25.89	26.07	26.21

Run	45	46	47	48	49	50	51
freon temp. at 18	17.96	18.09	18.36	18.36	18.35	18.46	18.60
pressure (bar) at 3	10.32	10.55	10.71	10.91	11.24	11.36	11.49
pressure (bar) at 4	3.97	3.99	4.03	4.04	4.04	4.06	4.07
exit Wtem at sink(C)	43.30	44.40	45.10	46.00	47.30	48.00	48.60
eff.R12 outlet temp.	32.38	33.82	34.64	35.87	37.14	37.87	38.67
eff.WAT outlet temp.	42.97	44.17	44.80	45.70	47.25	47.84	48.65
eff.inlet press(bar)	10.30	10.52	10.68	10.88	11.22	11.33	11.47
FREON mass flowrate	7.01	7.01	6.96	6.89	6.79	6.84	6.91

Table A-6.8: Experimental results for Run 45 to Run 51

Run	52	53	54	55	56
TEMPERATURE DISTRIBUTION IN HEAT PUMP CONDENSER (in Degree Celcius)					
freon inlet temp.	72.06	71.89	73.36	74.08	74.98
freon temp. at 2	46.29	46.00	48.30	48.73	49.85
freon temp. at 3	43.36	43.08	45.23	45.61	46.63
freon temp. at 4	42.37	42.08	44.25	44.61	45.67
freon temp. at 5	41.44	41.17	43.31	43.69	44.73
freon temp. at 6	40.66	40.39	42.56	42.93	44.00
freon temp. at 7	39.99	39.70	41.94	42.31	43.39
freon temp. at 8	39.23	38.93	41.18	41.58	42.70
freon temp. at 9	38.46	38.16	40.46	40.84	41.96
freon temp. at 10	37.79	37.49	39.81	40.22	41.36
freon temp. at 11	37.14	36.81	39.15	39.56	40.70
freon temp. at 12	36.53	36.17	38.53	38.93	40.10
freon temp. at 13	35.68	35.32	37.63	38.02	39.21
freon temp. at 14	35.59	35.20	37.55	37.94	39.08
freon temp. at 15	34.60	34.14	36.37	36.75	37.94
freon outlet temp.	32.03	31.60	33.12	33.45	35.15
water outlet temp.	43.61	43.39	45.65	46.11	47.23
water temp. at 2	42.65	42.46	44.72	45.08	46.20
water temp. at 3	41.42	41.15	43.40	43.75	44.85
water temp. at 4	40.71	40.44	42.71	43.09	44.19
water temp. at 5	39.76	39.49	41.76	42.18	43.31
water temp. at 6	38.98	38.70	41.04	41.43	42.59
water temp. at 7	38.06	37.78	40.15	40.56	41.72
water temp. at 8	37.28	36.96	39.35	39.74	40.97
water temp. at 9	36.17	35.79	38.20	38.58	39.83
water temp. at 10	35.03	34.67	37.02	37.43	38.67
water temp. at 11	33.48	33.10	35.38	35.76	37.00
water temp. at 12	32.23	31.87	34.06	34.44	35.66
water temp. at 13	29.99	29.60	31.52	31.84	33.01
water temp. at 14	27.45	27.04	28.54	28.88	29.87
water temp. at 15	25.33	24.93	26.05	26.37	27.17
water inlet temp.	20.02	19.50	19.77	19.99	20.21
OTHER PARAMETERS MEASURED IN THE EXPERIMENT					
freon temp. at 17	8.07	8.01	8.33	8.38	8.51
pressure(bar) at 1	8.68	8.60	9.14	9.23	9.49
pressure(bar) at 2	3.78	3.79	3.83	3.83	3.85
mass waterflow(g/s)	12.50	12.52	11.38	11.35	10.81
eff. R12 inlet temp.	66.91	66.71	68.34	69.01	69.95
eff. WAT inlet temp.	23.19	22.74	23.52	23.80	24.36
eff.outlet press(bar)	8.76	8.68	9.21	9.30	9.56
room temperature	24.54	24.71	24.88	25.02	25.17
freon temp. at 18	17.68	17.80	17.95	17.98	18.09
pressure (bar) at 3	10.42	10.37	10.86	10.95	11.17
pressure (bar) at 4	3.98	3.99	4.03	4.03	4.05
exit Wtem at sink(C)	43.60	43.50	45.60	46.00	47.00
eff.R12 outlet temp.	33.07	32.63	34.43	34.78	36.28
eff.WAT outlet temp.	43.18	42.97	45.23	45.65	46.76
eff.inlet press(bar)	10.39	10.34	10.83	10.92	11.15
FREON mass flowrate	6.91	6.98	6.88	6.91	6.81

Table A-6.9: Experimental results for Run 52 to Run 56

Run		57	58	59	60	61
TEMPERATURE DISTRIBUTION IN HEAT PUMP CONDENSER (in Degree Celcius)						
freon inlet temp.	=	75.35	77.06	77.47	78.85	79.16
freon temp. at 2	=	50.11	52.25	52.43	54.19	54.23
freon temp. at 3	=	46.87	48.88	49.04	50.66	50.68
freon temp. at 4	=	45.85	47.89	48.03	49.64	49.65
freon temp. at 5	=	44.94	46.96	47.10	48.72	48.72
freon temp. at 6	=	44.19	46.25	46.41	48.01	48.01
freon temp. at 7	=	43.56	45.69	45.81	47.46	47.46
freon temp. at 8	=	42.85	45.00	45.14	46.81	46.80
freon temp. at 9	=	42.13	44.33	44.45	46.17	46.17
freon temp. at 10	=	41.53	43.74	43.90	45.62	45.62
freon temp. at 11	=	40.87	43.14	43.27	45.04	45.04
freon temp. at 12	=	40.27	42.55	42.68	44.45	44.42
freon temp. at 13	=	39.34	41.60	41.78	43.54	43.53
freon temp. at 14	=	39.21	41.51	41.67	43.40	43.37
freon temp. at 15	=	38.06	40.25	40.48	42.19	42.14
freon outlet temp.	=	35.79	36.49	37.74	39.99	40.42
OTHER PARAMETERS MEASURED IN THE EXPERIMENT						
freon temp. at 17	=	8.72	8.94	9.04	9.28	9.26
pressure(bar) at 1	=	9.52	10.09	10.11	10.54	10.53
pressure(bar) at 2	=	3.87	3.90	3.91	3.93	3.93
mass waterflow(g/s)	=	10.86	10.21	10.17	9.47	9.53
eff. R12 inlet temp.	=	70.30	72.10	72.46	73.92	74.17
eff. WAT inlet temp.	=	24.66	25.68	25.95	26.69	26.90
eff.outlet press(bar)	=	9.59	10.16	10.18	10.61	10.59
room temperature	=	25.31	25.46	25.70	25.89	26.14

Run		57	58	59	60	61
water outlet temp.	=	47.47	49.53	49.78	51.53	51.60
water temp. at 2	=	46.40	48.46	48.71	50.38	50.40
water temp. at 3	=	45.03	47.13	47.27	48.90	48.91
water temp. at 4	=	44.40	46.49	46.68	48.32	48.36
water temp. at 5	=	43.51	45.62	45.81	47.49	47.50
water temp. at 6	=	42.80	44.95	45.15	46.85	46.89
water temp. at 7	=	41.95	44.16	44.36	46.08	46.13
water temp. at 8	=	41.17	43.41	43.64	45.40	45.44
water temp. at 9	=	40.01	42.29	42.55	44.32	44.36
water temp. at 10	=	38.85	41.07	41.32	43.15	43.19
water temp. at 11	=	37.21	39.38	39.65	41.48	41.58
water temp. at 12	=	35.83	37.90	38.21	39.99	40.08
water temp. at 13	=	33.27	35.13	35.50	37.24	37.34
water temp. at 14	=	30.17	31.67	32.03	33.44	33.62
water temp. at 15	=	27.48	28.70	29.06	30.22	30.44
water inlet temp.	=	20.47	21.21	21.34	21.46	21.65
freon temp. at 18	=	18.31	18.40	18.49	18.67	18.72
pressure (bar) at 3	=	11.21	11.69	11.71	12.14	12.09
pressure (bar) at 4	=	4.08	4.11	4.12	4.15	4.15
exit Wtem at sink(C)	=	47.20	49.10	49.30	50.90	51.00
eff.R12 outlet temp.	=	36.71	38.01	38.85	40.88	41.12
eff.WAT outlet temp.	=	46.99	49.05	49.30	51.01	51.06
eff.inlet press(bar)	=	11.18	11.67	11.69	12.11	12.06
FREON mass flowrate	=	6.83	6.78	6.77	6.66	6.65

Table A-6.10: Experimental results for Run 57 to Run 61

Run	62	63	64	65	66	67	68
TEMPERATURE DISTRIBUTION IN HEAT PUMP CONDENSER (in Degree Celcius)							
freon inlet temp.	= 79.50	79.68	76.64	76.42	72.79	72.78	81.72
freon temp. at 2	= 51.13	51.33	47.31	47.76	43.08	43.49	54.31
freon temp. at 3	= 47.93	48.17	44.50	44.73	40.62	40.91	50.82
freon temp. at 4	= 47.20	47.33	43.79	43.98	39.89	40.19	50.14
freon temp. at 5	= 46.25	46.42	42.88	43.05	38.86	39.23	49.14
freon temp. at 6	= 45.66	45.87	42.10	42.39	37.04	38.12	48.48
freon temp. at 7	= 45.21	45.46	41.29	41.86	35.15	36.78	47.94
freon temp. at 8	= 44.39	44.82	40.04	40.92	30.50	34.46	46.88
freon temp. at 9	= 42.94	43.86	36.42	39.24	21.96	28.04	44.39
freon temp. at 10	= 40.63	42.90	29.16	36.20	18.98	21.05	39.57
freon temp. at 11	= 34.91	40.68	23.16	29.39	17.64	18.50	28.73
freon temp. at 12	= 25.64	35.40	20.65	21.95	17.11	17.42	22.48
freon temp. at 13	= 22.22	25.80	19.79	19.48	16.88	17.07	20.38
freon temp. at 14	= 21.05	22.63	19.42	18.65	16.75	16.94	19.57
freon temp. at 15	= 20.37	20.89	19.20	18.13	16.67	16.80	19.06
freon outlet temp.	= 20.18	20.44	19.17	18.03	16.69	16.81	18.92
water outlet temp.	= 49.40	49.68	45.39	45.96	40.45	41.17	[illegible]
water temp. at 2	= 47.50	47.77	43.67	44.16	38.83	39.58	50.45
water temp. at 3	= 46.10	46.42	42.16	42.74	36.88	37.87	48.94
water temp. at 4	= 45.08	45.53	40.77	41.61	34.94	36.22	47.65
water temp. at 5	= 43.72	44.43	38.98	40.13	32.24	33.92	46.27
water temp. at 6	= 42.34	43.47	36.85	38.60	28.32	31.09	44.22
water temp. at 7	= 40.30	42.01	33.66	36.24	24.85	27.47	[illegible]
water temp. at 8	= 38.21	40.62	30.98	34.13	21.52	24.46	[illegible]
water temp. at 9	= 34.14	37.82	26.35	29.96	18.42	20.39	32.79
water temp. at 10	= 30.09	34.81	22.85	26.13	17.40	18.25	[illegible]
water temp. at 11	= 24.51	29.04	20.14	21.08	16.85	17.14	21.94
water temp. at 12	= 22.13	26.03	19.55	19.36	16.67	16.85	[illegible]
water temp. at 13	= 20.52	21.75	19.01	18.09	16.42	16.58	19.12
water temp. at 14	= 20.13	20.47	18.98	17.85	16.51	16.62	[illegible]
water temp. at 15	= 19.97	20.02	18.97	17.77	16.51	16.66	18.81
water inlet temp.	= 17.01	16.82	16.56	14.82	14.09	14.03	[illegible]
OTHER PARAMETERS MEASURED IN THE EXPERIMENT							
freon temp. at 17	= 1.66	1.64	1.58	1.41	1.28	1.26	2.07
pressure(bar) at 1	= 10.97	10.89	10.26	10.15	9.53	9.49	11.83
pressure(bar) at 2	= 3.34	3.34	3.32	3.32	3.29	3.30	3.40
mass waterflow(g/s)	= 8.37	8.22	9.71	9.21	11.13	10.79	7.50
eff. R12 inlet temp.	= 73.83	74.01	70.77	70.68	66.85	66.92	76.24
eff. WAT inlet temp.	= 18.77	18.73	18.00	16.58	15.53	15.63	17.27
eff.outlet press(bar)	= 11.00	10.92	10.28	10.17	9.55	9.51	11.85
room temperature	= 20.21	20.25	20.24	20.17	20.11	19.99	20.11
freon temp. at 18	= 14.56	14.62	14.51	14.49	14.42	14.41	[illegible]
pressure (bar) at 3	= 11.56	11.54	10.79	10.79	9.99	10.01	12.34
pressure (bar) at 4	= 3.57	3.57	3.55	3.55	3.53	3.55	3.62
exit Wtem at sink(C)	= 47.80	48.00	44.30	44.60	39.70	40.40	[illegible]
eff.R12 outlet temp.	= 20.26	20.62	19.18	18.07	16.68	16.81	[illegible]
eff.WAT outlet temp.	= 48.54	48.82	44.62	45.15	39.72	40.46	[illegible]
eff.inlet press(bar)	= 11.55	11.53	10.78	10.78	9.99	10.00	[illegible]
FREON mass flowrate	= 6.26	6.23	6.47	6.54	6.68	6.66	6.18

Table A-6.11: Experimental results for Run 62 to Run 68

****** TUBE-BESIDE-TUBE CONDENSER SIMULATION ****** ASSUME TUBE WALLS HAVE INFINITE CONDUCTIVITY ******
GEOMETRY: SUBCOOLER 7.50M OF 5.75MM OD. CONDENSER: 7.50M OF 5.75MM OD. WATER SIDE 7.65MM OD. ALL WALLS .74MM THICK.
BOND CNDCTNCE 500.0W/M.C THML PWR 1093.4W. WATER IN 14.5C. HOT GAS 55.4C. DEW POINT 31.0C. SUBCLD LIQD 16.2C.

ITERATION NUMBER: 15 USED I= 150 SEGMENTS. TRIAL WATER EXIT TEMP: 29.6936 CORRESPONDING TO TW(I)= 14.4512 & TR(I)= 16.3480

EXIT WATER TEMP 29.69C. FLOW RATE 17.1483 GRAM/SEC. WATER PRESS DROP .4115 BAR. PUMP PWR .7057 WATT (OR .0645%)
REFRIGERANT MASS FLOW RATE 6.564E+00 GRAM/SEC

SEPARATE RESULTS FOR THE THREE SEGMENTS	SUPE RHEAT	TWO-PHASE	SUBCOOLER	TOTAL/AVERAGE
LENGTH OF EACH SEGMENT IN METRES	1.4750E+00	1.2700E+01	8.2500E-01	1.5000E+01
MASS OF REFRIGERANT IN KG.	8.8312E-04	4.6044E-02	1.5202E-02	6.2129E-02
REFRIG SIDE HEAT TRANS COEFNT: W/SQ M C.	7.9732E+02	4.6502E+03	1.0081E+03	4.0707E+03
REFRIG SIDE LINEAR H.T.C.: W/M C.	1.0660E+01	6.2066E+01	1.3461E+01	5.4334E+01
REFRIGERANT SIDE REYNOLDS NUMBER	1.4793E+05	4.5827E+03	8.6378E+03	1.9134E+04
WATER SIDE HEAT TRANS COEFNT: W/SQ M C.	3.2674E+03	2.4958E+03	1.8396E+03	2.5380E+03
WATER SIDE LINEAR H.T.C. W/M C.	5.6780E+01	4.2904E+01	3.2012E+01	4.3711E+01
WATER SIDE REYNOLDS NUMBER	4.7399E+03	4.0439E+03	3.3771E+03	4.0779E+03
OVERALL LINEAR CONDUCTANCE: W/M C	8.9645E+00	2.4693E+01	9.4722E+00	2.2308E+01
NO. OF HEAT TRANSFER UNITS REFRIG. SIDE	2.7821	.1477	1.2071	4.1369
NO. OF HEAT TRANSFER UNITS WATER SIDE	.1875	4.3681	.1054	4.6610
EFFECTIVENESS OF EACH SEGMENT (PERCENT)	92.9966	87.2991	68.7684	83.0214
REFRIGERANT SIDE PRESSURE DROP IN BAR	1.8825E-01	1.6850E+00	1.9638E-02	1.8929E+00
THERMAL POWER PICK-UP BY WATER (W & %)	122.1(11.2)	946.0(86.4)	26.2(2.4)	1094.4
THERMAL POWER TRANSFERRED BY R12 (W & %)	119.7(11.0)	946.6(86.6)	26.2(2.4)	1092.6
TOTAL MAX THERMAL POWER WITHOUT LOSS (W)	119.75	946.59	26.22	1092.56
THERMAL POWER LOSS FROM FREON (W & %)	.0000	.0000	.0000	.00(.0)
SPECIFIC ENTHALPY OF REFRIG (J/KG)	2.1781E+05	1.9957E+05	5.5354E+04	5.1359E+04
SPECIFIC ENTROPY OF R12 (J/KG.C)	7.4157E+02	6.8547E+02	2.0944E+02	1.9590E+02
REFRIGERANT TEMPERATURE (DEG.C)	5.5360E+01	2.9908E+01	2.0524E+01	1.6348E+01
REFRIGERANT PRESSURE (BAR)	7.6481E+00	7.4598E+00	5.7748E+00	5.7552E+00
WATER TEMPERATURE (DEG.C)	2.9694E+01	2.7991E+01	1.4816E+01	1.4451E+01

RATE OF LOSS OF ENTHALPY BY R12 1.0926E+03 WATTS RATE OF GAIN OF ENTHALPY BY WATER 1.0944E+03 WATTS
CORRESPONDING TO AN ENERGY IMBALANCE OF 1.7964E+00 WATTS OR .1643 % OF SPECIFIED POWER

THE POWER LOSS BY R12 TO OUTSIDE 8.0383E-01WATTS BY .0735 % OF THE SPECIFIED POWER
THE POWER LOSS BY WATER TO OUTSIDE -9.9255E-01 WATTS BY -.0908 % OF THE SPECIFIED POWER

RATE OF LOSS OF ENTROPY BY R12 3.5816E+00 WATTS/C RATE OF INCREASE OF ENTROPY BY WATER 3.7077E+00 WATTS/C
NET RATE OF ENTROPY FLOW THRU SYSTEM BOUNDARY 1.2607E-01 WATT/C THERMAL ENTROPY CREATION RATE 5.2889E-02 WATT/C
R12 F.D. ENTROPY CREATION RATE 7.3180E-02 WATT/C RATE OF LOSS OF GROSS WORK 3.8347E+01 WATTS AT 31.02 C

RATE OF ENTROPY GAIN OF WATER HAD IT BEEN 10C HOTTER 3.5799E+00 WATTS/C. FOR SAME GROSS RATE OF ENTROPY INCREASE,
A COUNTER-FLOW WATER-WATER HEAT EXCHANGER WOULD HAVE DELTA-T OF 9.8679 DEG C CORRESPONDING TO AN EFFECTIVENESS OF 60.70%
OR 1.545 HEAT TRANSFER UNITS, WHICH IS 33.14 % OF THAT FOR THE WATER SIDE OF THE PRESENT HT.XR.

Table A-6.12(a): Results in three segments for Run 9

LNTH	TR(I)	PR(I)	TW(I)	PW(I)	TWL(I)	X(I)	HR(I)	NTUR(I)	UR(I)	HW(I)	NTUW(I)	UW(I)	UL(I)
.00	55.36	7.65	29.69	0.00E+00	42.53	100.00	8.12E+02	1.94E-01	1.09E+01	3.26E+03	1.28E-02	5.78E+01	9.17E+00
.20	46.82	7.62	29.13	7.04E-03	32.20	100.00	8.54E+02	1.99E-01	1.15E+01	3.13E+03	1.33E-02	5.56E+01	9.50E+00
.40	40.99	7.59	28.74	1.42E-02	30.81	100.00	8.21E+02	1.91E-01	1.10E+01	3.09E+03	1.28E-02	5.48E+01	9.17E+00
.60	36.99	7.57	28.47	2.51E-02	29.79	100.00	7.96E+02	1.84E-01	1.07E+01	3.06E+03	1.24E-02	5.43E+01	8.92E+00
.80	34.35	7.54	28.29	3.22E-02	29.28	100.00	7.75E+02	1.79E-01	1.04E+01	3.04E+03	1.22E-02	5.39E+01	8.72E+00
1.00	32.51	7.52	28.17	3.92E-02	28.78	100.00	7.96E+02	1.86E-01	1.04E+01	4.48E+03	1.27E-02	7.05E+01	9.08E+00
1.20	31.18	7.49	28.08	5.01E-02	28.57	100.00	7.50E+02	1.73E-01	1.01E+01	3.02E+03	1.18E-02	5.35E+01	8.46E+00
1.40	30.26	7.47	28.02	5.71E-02	28.37	100.00	7.41E+02	1.71E-01	9.94E+00	3.01E+03	1.17E-02	5.34E+01	8.38E+00
LNTH	TR(I)	PR(I)	TW(I)	PW(I)	TWL(I)	X(I)	HR(I)	NTUR(I)	UR(I)	HW(I)	NTUW(I)	UW(I	UL(I)
1.60	29.99	7.44	27.95	6.80E-02	28.43	99.60	2.64E+03	0.00E+00	3.55E+01	3.00E+03	2.97E-02	5.33E+01	2.13E+01
1.80	29.85	7.42	27.81	7.49E-02	28.82	98.53	5.35E+03	0.00E+00	7.18E+01	2.99E+03	4.25E-02	5.30E+01	3.05E+01
2.00	29.70	7.39	27.62	8.19E-02	28.94	97.05	9.15E+03	0.00E+00	1.20E+02	4.39E+03	6.11E-02	6.91E+01	4.38E+01
2.20	29.55	7.36	27.39	9.26E-02	28.86	95.16	8.09E+03	0.00E+00	1.09E+02	2.94E+03	4.91E-02	5.22E+01	3.52E+01
2.40	29.39	7.33	27.17	9.94E-02	28.66	93.45	7.68E+03	0.00E+00	1.03E+02	2.91E+03	4.80E-02	5.17E+01	3.44E+01
2.60	29.21	7.29	26.93	1.10E-01	28.33	91.56	7.36E+03	0.00E+00	9.88E+01	2.89E+03	4.71E-02	5.13E+01	3.38E+01
2.80	29.04	7.26	26.71	1.17E-01	28.24	89.83	7.15E+03	0.00E+00	9.59E+01	2.86E+03	4.63E-02	5.08E+01	3.32E+01
3.00	28.86	7.23	26.48	1.23E-01	28.01	88.11	7.29E+03	0.00E+00	9.55E+01	4.22E+03	5.46E-02	6.63E+01	3.91E+01
3.20	28.67	7.19	26.24	1.34E-01	27.82	86.21	6.85E+03	0.00E+00	9.19E+01	2.76E+03	4.46E-02	4.90E+01	3.20E+01
3.40	28.48	7.15	26.02	1.40E-01	27.62	84.49	6.75E+03	0.00E+00	9.05E+01	2.74E+03	4.41E-02	4.86E+01	3.16E+01
3.60	28.27	7.11	25.77	1.51E-01	27.27	82.60	6.64E+03	0.00E+00	8.91E+01	2.71E+03	4.36E-02	4.82E+01	3.13E+01
3.80	28.08	7.08	25.55	1.57E-01	27.19	80.89	6.55E+03	0.00E+00	8.78E+01	2.69E+03	4.31E-02	4.77E+01	3.09E+01
4.00	27.88	7.04	25.33	1.64E-01	26.96	79.17	6.76E+03	0.00E+00	8.84E+01	3.97E+03	5.10E-02	6.25E+01	3.66E+01
4.20	27.67	7.00	25.08	1.74E-01	26.75	77.29	6.36E+03	0.00E+00	8.54E+01	2.64E+03	4.22E-02	4.69E+01	3.03E+01
4.40	27.46	6.96	24.86	1.80E-01	26.54	75.59	6.28E+03	0.00E+00	8.43E+01	2.62E+03	4.17E-02	4.65E+01	3.00E+01
4.60	27.25	6.92	24.62	1.90E-01	26.18	73.72	6.19E+03	0.00E+00	8.30E+01	2.59E+03	4.13E-02	4.60E+01	2.96E+01
4.80	27.04	6.88	24.40	1.96E-01	26.10	72.03	6.11E+03	0.00E+00	8.19E+01	2.57E+03	4.08E-02	4.56E+01	2.93E+01
5.00	26.84	6.85	24.18	2.02E-01	25.86	70.36	6.30E+03	0.00E+00	8.25E+01	3.80E+03	4.83E-02	5.98E+01	3.47E+01
5.20	26.62	6.81	23.93	2.12E-01	25.65	68.52	5.94E+03	0.00E+00	7.96E+01	2.52E+03	3.99E-02	4.48E+01	2.87E+01
5.40	26.41	6.77	23.72	2.18E-01	25.44	66.87	5.86E+03	0.00E+00	7.86E+01	2.50E+03	3.95E-02	4.44E+01	2.84E+01
5.60	26.20	6.73	23.48	2.28E-01	25.07	65.06	5.77E+03	0.00E+00	7.74E+01	2.48E+03	3.91E-02	4.40E+01	2.80E+01
5.80	25.99	6.69	23.26	2.34E-01	25.01	63.44	5.69E+03	0.00E+00	7.63E+01	2.41E+03	3.82E-02	4.28E+01	2.74E+01
6.00	25.79	6.65	23.05	2.40E-01	24.78	61.84	5.87E+03	0.00E+00	7.68E+01	3.58E+03	4.52E-02	5.62E+01	3.25E+01
6.20	25.57	6.62	22.82	2.49E-01	24.58	60.09	5.52E+03	0.00E+00	7.41E+01	2.37E+03	3.74E-02	4.20E+01	2.68E+01
6.40	25.37	6.58	22.61	2.55E-01	24.37	58.52	5.44E+03	0.00E+00	7.30E+01	2.35E+03	3.70E-02	4.17E+01	2.65E+01
6.60	25.16	6.54	22.38	2.65E-01	24.00	56.81	5.35E+03	0.00E+00	7.18E+01	2.33E+03	3.65E-02	4.13E+01	2.62E+01
6.80	24.96	6.51	22.18	2.71E-01	23.94	55.27	5.27E+03	0.00E+00	7.07E+01	2.31E+03	3.61E-02	4.09E+01	2.59E+01
7.00	24.77	6.47	21.97	2.76E-01	23.71	53.74	5.43E+03	0.00E+00	7.10E+01	3.43E+03	4.27E-02	5.39E+01	3.07E+01
7.20	24.56	6.44	21.75	2.84E-01	23.52	52.07	5.10E+03	0.00E+00	6.84E+01	2.27E+03	3.53E-02	4.02E+01	2.53E+01
7.40	24.37	6.40	21.55	2.86E-01	23.32	50.57	5.02E+03	0.00E+00	6.73E+01	2.25E+03	3.49E-02	3.99E+01	2.50E+01
7.60	24.17	6.37	21.33	2.93E-01	22.96	48.93	4.92E+03	0.00E+00	6.61E+01	2.23E+03	3.44E-02	3.95E+01	2.47E+01
7.80	23.99	6.34	21.13	2.95E-01	22.91	47.45	4.84E+03	0.00E+00	6.49E+01	2.21E+03	3.40E-02	3.92E+01	2.44E+01
8.00	23.81	6.30	20.93	2.97E-01	22.69	45.98	4.97E+03	0.00E+00	6.51E+01	3.29E+03	4.01E-02	5.17E+01	2.88E+01
8.20	23.62	6.27	20.71	3.05E-01	22.51	44.37	4.66E+03	0.00E+00	6.25E+01	2.17E+03	3.32E-02	3.85E+01	2.38E+01
8.40	23.44	6.24	20.52	3.07E-01	22.32	42.92	4.57E+03	0.00E+00	6.13E+01	2.15E+03	3.28E-02	3.82E+01	2.36E+01
8.60	23.26	6.21	20.30	3.14E-01	21.98	41.34	4.48E+03	0.00E+00	6.00E+01	2.10E+03	3.20E-02	3.72E+01	2.30E+01
8.80	23.09	6.18	20.11	3.16E-01	21.95	39.91	4.39E+03	0.00E+00	5.89E+01	2.08E+03	3.16E-02	3.69E+01	2.27E+01
9.00	22.93	6.15	19.92	3.18E-01	21.74	38.50	4.49E+03	0.00E+00	5.88E+01	3.10E+03	3.71E-02	4.88E+01	2.67E+01
9.20	22.76	6.13	19.71	3.25E-01	21.57	36.94	4.20E+03	0.00E+00	5.63E+01	2.05E+03	3.07E-02	3.63E+01	2.21E+01
9.40	22.61	6.10	19.52	3.27E-01	21.39	35.53	4.10E+03	0.00E+00	5.50E+01	2.03E+03	3.03E-02	3.60E+01	2.18E+01
9.60	22.45	6.07	19.31	3.34E-01	21.03	33.99	4.00E+03	0.00E+00	5.36E+01	2.01E+03	2.99E-02	3.57E+01	2.14E+01
9.80	22.31	6.05	19.12	3.36E-01	21.03	32.58	3.90E+03	0.00E+00	5.23E+01	2.00E+03	2.94E-02	3.55E+01	2.11E+01
10.00	22.17	6.02	18.93	3.38E-01	20.82	31.16	3.99E+03	0.00E+00	5.23E+01	2.98E+03	3.44E-02	4.69E+01	2.47E+01
10.20	22.02	6.00	18.72	3.45E-01	20.67	29.61	3.73E+03	0.00E+00	5.00E+01	1.97E+03	2.86E-02	3.49E+01	2.06E+01
10.40	21.89	5.98	18.53	3.47E-01	20.51	28.18	3.64E+03	0.00E+00	4.89E+01	1.95E+03	2.82E-02	3.46E+01	2.03E+01
10.60	21.76	5.96	18.32	3.53E-01	20.14	26.61	3.55E+03	0.00E+00	4.76E+01	1.93E+03	2.78E-02	3.43E+01	1.99E+01
10.80	21.64	5.94	18.13	3.55E-01	20.16	25.16	3.45E+03	0.00E+00	4.63E+01	1.92E+03	2.73E-02	3.41E+01	1.96E+01
11.00	21.53	5.92	17.93	3.57E-01	19.96	23.70	3.51E+03	0.00E+00	4.59E+01	2.82E+03	3.14E-02	4.43E+01	2.26E+01
11.20	21.42	5.90	17.72	3.64E-01	19.82	22.10	3.24E+03	0.00E+00	4.35E+01	1.89E+03	2.64E-02	3.35E+01	1.89E+01
11.40	21.32	5.88	17.52	3.66E-01	19.67	20.62	3.14E+03	0.00E+00	4.21E+01	1.84E+03	2.56E-02	3.27E+01	1.84E+01
11.60	21.22	5.87	17.31	3.72E-01	19.28	19.00	3.01E+03	0.00E+00	4.04E+01	1.83E+03	2.51E-02	3.25E+01	1.80E+01
11.80	21.14	5.85	17.11	3.74E-01	19.33	17.50	2.89E+03	0.00E+00	3.88E+01	1.82E+03	2.45E-02	3.23E+01	1.76E+01
12.00	21.06	5.84	16.91	3.76E-01	19.11	15.99	2.90E+03	0.00E+00	3.79E+01	2.71E+03	2.79E-02	4.27E+01	2.01E+01
12.20	20.98	5.83	16.69	3.79E-01	18.97	14.34	2.62E+03	0.00E+00	3.52E+01	1.79E+03	2.32E-02	3.18E+01	1.67E+01
12.40	20.92	5.82	16.49	3.81E-01	18.79	12.80	2.48E+03	0.00E+00	3.33E+01	1.78E+03	2.25E-02	3.16E+01	1.62E+01
12.60	20.85	5.81	16.27	3.84E-01	18.35	11.14	2.31E+03	0.00E+00	3.11E+01	1.77E+03	2.17E-02	3.14E+01	1.56E+01
12.80	20.80	5.80	16.07	3.86E-01	18.39	9.61	2.15E+03	0.00E+00	2.89E+01	1.76E+03	2.08E-02	3.12E+01	1.50E+01
13.00	20.76	5.79	15.87	3.88E-01	19.11	8.09	2.07E+03	0.00E+00	2.70E+01	2.62E+03	2.27E-02	4.12E+01	1.63E+01
13.20	20.72	5.79	15.66	3.91E-01	17.93	6.48	1.77E+03	0.00E+00	2.38E+01	1.74E+03	1.87E-02	3.09E+01	1.34E+01
13.40	20.70	5.78	15.47	3.93E-01	17.67	5.03	1.56E+03	0.00E+00	2.10E+01	1.73E+03	1.73E-02	3.08E+01	1.25E+01
13.60	20.67	5.78	15.29	3.96E-01	17.16	3.56	1.32E+03	0.00E+00	1.77E+01	1.73E+03	1.56E-02	3.07E+01	1.12E+01
13.80	20.66	5.79	15.12	3.98E-01	17.02	2.28	1.07E+03	0.00E+00	1.43E+01	1.73E+03	1.36E-02	3.07E+01	9.76E-00
14.00	20.65	5.78	14.97	4.00E-01	16.51	1.15	1.05E+03	0.00E+00	1.37E+01	2.53E+03	1.42E-02	3.98E+01	1.02E+01
LNTH	TR(I)	PR(I	TW(I)	PW(I)	TWL(I	X(I)	HR(I)	NTUR(I)	UR(I)	HW(I)	NTUW(I	UW(I	UL(I
14.20	20.52	5.77	14.82	4.03E-01	16.61	.00	1.00E+03	1.48E-01	1.35E+01	1.70E+03	1.30E-02	3.02E+01	9.32E+00
14.40	19.04	5.77	14.69	4.05E-01	16.03	.00	9.95E+02	1.43E-01	1.34E+01	1.71E+03	1.29E-02	3.04E+01	9.28E+00
14.60	17.87	5.76	14.58	4.08E-01	15.48	.00	1.00E+03	1.49E-01	1.34E+01	1.74E+03	1.30E-02	3.08E+01	9.35E+00
14.80	17.01	5.76	14.51	4.10E-01	15.26	.00	1.01E+03	1.51E-01	1.35E-01	1.77E+03	1.31E-02	3.14E+01	9.44E+00
15.00	16.35	5.76	14.45	4.12E-01	15.01	.00	1.20E+03	0.00E+00	1.61E+01	1.99E+03	1.54E-02	3.53E+01	1.11E+01

Table A-6.12(b): The profiles of parameters for Run 9

SUMMARY OF RANGE OF POSSIBLE EVAPORATOR CONDITIONS ASSUMIMG 50% COMPRESSOR ISENTROPIC EFFICIENCY
COND. PRESS= 7.6 COND. TEMP= 31.02 ENT. H= 217813. ENT. S= 741.57 LEAV. TEMP= 16.22 LEAV. H= 51237. LEAV. S= 195.48

		EVAPORATOR				*	ENTRY		EXIT			*	EVAP	COMP	PRESS	VDOT	COPH
TEMP	PRESS	H(X=0)	H(X=1)	S(X=0)	S(X=1)	*	S	X	S	H	T	*	CAP	CAP	RATIO	CUM/H	
8.00	3.98	43476.	190890.	168.55	693.01	*	196.16	.0526	697.86	192278.	10.04	*	926.	168.	1.922	1.04	6.524
10.00	4.23	45353.	191720.	175.14	692.20	*	195.93	.0402	702.31	194627.	14.27	*	941.	152.	1.808	.99	7.184
12.00	4.49	47237.	192543.	181.71	691.41	*	195.73	.0275	706.62	196950.	18.44	*	956.	137.	1.702	.94	7.984
14.00	4.77	49129.	193359.	188.25	690.66	*	195.59	.0146	710.80	199248.	22.55	*	972.	122.	1.604	.90	8.973
16.00	5.06	51028.	194168.	194.77	689.93	*	195.49	.0015	714.85	201521.	26.60	*	986.	107.	1.512	.86	10.225
18.00	5.36	52935.	194970.	201.26	689.23	*	195.48	-.0120	718.77	203770.	30.60	*	1001.	92.	1.428	.82	11.862
20.00	5.67	54851.	195764.	207.74	688.55	*	195.48	-.0256	722.58	205994.	34.54	*	1016.	78.	1.349	.78	14.093
22.00	6.00	56775.	196550.	214.20	687.89	*	195.48	-.0396	726.26	208193.	38.43	*	1030.	63.	1.275	.75	17:315
24.00	6.34	58708.	197327.	220.64	687.26	*	195.48	-.0539	729.84	210368.	42.27	*	1044.	49.	1.207	.72	22.374
26.00	6.69	60651.	198095.	227.07	686.64	*	195.48	-.0685	733.31	212519.	46.06	*	1059.	35.	1.143	.69	31.464
28.00	7.06	62604.	198854.	233.48	686.03	*	195.48	-.0834	736.68	214646.	49.80	*	1073.	21.	1.083	.66	52.598
30.00	7.45	64568.	199604.	239.89	685.44	*	195.48	-.0987	739.94	216749.	53.49	*	1086.	7.	1.027	.63	156.635

SUMMARY OF RANGE OF POSSIBLE EVAPORATOR CONDITIONS ASSUMIMG 55% COMPRESSOR ISENTROPIC EFFICIENCY
COND. PRESS= 7.6 COND. TEMP= 31.02 ENT. H= 217813. ENT. S= 741.57 LEAV. TEMP= 16.22 LEAV. H= 51237. LEAV. S= 195.48

		EVAPORATOR				*	ENTRY		EXIT			*	EVAP	COMP	PRESS	VDOT	COPH
TEMP	PRESS	H(X=0)	H(X=1)	S(X=0)	S(X=1)	*	S	X	S	H	T	*	CAP	CAP	RATIO	CUM/H	
4.00	3.51	39742.	189211.	155.29	694.74	*	196.78	.0769	698.51	190260.	5.59	*	913.	181.	2.178	1.17	6.046
6.00	3.74	41606.	190054.	161.94	693.86	*	196.45	.0649	702.33	192441.	9.58	*	927.	167.	2.045	1.11	6.565
8.00	3.98	43476.	190890.	168.55	693.01	*	196.16	.0526	706.04	194600.	13.52	*	941.	152.	1.922	1.06	7.176
10.00	4.23	45353.	191720.	175.14	692.20	*	195.93	.0402	709.64	196735.	17.41	*	955.	138.	1.808	1.00	7.903
12.00	4.49	47237.	192543.	181.71	691.41	*	195.73	.0275	713.13	198847.	21.24	*	969.	124.	1.702	.96	8.783
14.00	4.77	49129.	193359.	188.25	690.66	*	195.59	.0146	716.51	200936.	25.03	*	983.	111.	1.604	.91	9.870
16.00	5.06	51028.	194168.	194.77	689.93	*	195.49	.0015	719.80	203002.	28.76	*	996.	97.	1.512	.87	11.247
18.00	5.36	52935.	194970.	201.26	689.23	*	195.48	-.0120	722.98	205046.	32.45	*	1010.	84.	1.428	.83	13.048
20.00	5.67	54851.	195764.	207.74	688.55	*	195.48	-.0256	726.07	207068.	36.09	*	1023.	71.	1.349	.79	15.503
22.00	6.00	56775.	196550.	214.20	687.89	*	195.48	-.0396	729.08	209067.	39.68	*	1036.	57.	1.275	.75	19.047
24.00	6.34	58708.	197327.	220.64	687.26	*	195.48	-.0539	731.99	211045.	43.23	*	1049.	44.	1.207	.72	24.611
26.00	6.69	60651.	198095.	227.07	686.64	*	195.48	-.0685	734.82	213000.	46.74	*	1062.	32.	1.143	.69	34.611
28.00	7.06	62604.	198854.	233.48	686.03	*	195.48	-.0834	737.57	214934.	50.21	*	1074.	19.	1.083	.66	57.857
30.00	7.45	64568.	199604.	239.89	685.44	*	195.48	-.0987	740.24	216846.	53.63	*	1087.	6.	1.027	.63	172.297

SUMMARY OF RANGE OF POSSIBLE EVAPORATOR CONDITIONS ASSUMIMG 60% COMPRESSOR ISENTROPIC EFFICIENCY
COND. PRESS= 7.6 COND. TEMP= 31.02 ENT. H= 217813. ENT. S= 741.57 LEAV. TEMP= 16.22 LEAV. H= 51237. LEAV. S= 195.48

		EVAPORATOR				*	ENTRY		EXIT			*	EVAP	COMP	PRESS	VDOT	COPH
TEMP	PRESS	H(X=0)	H(X=1)	S(X=0)	S(X=1)	*	S	X	S	H	T	*	CAP	CAP	RATIO	CUM/H	
.00	3.08	36032.	187510.	141.92	696.62	*	197.60	.1004	700.26	188491.	1.54	*	901.	192.	2.479	1.32	5.681
2.00	3.29	37884.	188363.	148.62	695.66	*	197.16	.0887	703.53	190534.	5.33	*	914.	179.	2.323	1.25	6.106
4.00	3.51	39742.	189211.	155.29	694.74	*	196.78	.0769	706.71	192556.	9.08	*	928.	166.	2.178	1.19	6.595
6.00	3.74	41606.	190054.	161.94	693.86	*	196.45	.0649	709.79	194556.	12.78	*	941.	153.	2.045	1.13	7.162
8.00	3.98	43476.	190890.	168.55	693.01	*	196.16	.0526	712.78	196534.	16.42	*	954.	140.	1.922	1.07	7.828
10.00	4.23	45353.	191720.	175.14	692.20	*	195.93	.0402	715.68	198491.	20.03	*	967.	127.	1.808	1.02	8.621
12.00	4.49	47237.	192543.	181.71	691.41	*	195.73	.0275	718.50	200427.	23.58	*	979.	114.	1.702	.97	9.581
14.00	4.77	49129.	193359.	188.25	690.66	*	195.59	.0146	721.23	202342.	27.09	*	992.	102.	1.604	.92	10.767
16.00	5.06	51028.	194168.	194.77	689.93	*	195.49	.0015	723.89	204237.	30.56	*	1004.	89.	1.512	.88	12.270
18.00	5.36	52935.	194970.	201.26	689.23	*	195.48	-.0120	726.47	206110.	33.99	*	1017.	77.	1.428	.83	14.234
20.00	5.67	54851.	195764.	207.74	688.55	*	195.48	-.0256	728.97	207963.	37.38	*	1029.	65.	1.349	.80	16.912
22.00	6.00	56775.	196550.	214.20	687.89	*	195.48	-.0396	731.41	209796.	40.73	*	1041.	53.	1.275	.76	20.779
24.00	6.34	58708.	197327.	220.64	687.26	*	195.48	-.0539	733.78	211609.	44.03	*	1053.	41.	1.207	.72	26.849
26.00	6.69	60651.	198095.	227.07	686.64	*	195.48	-.0685	736.08	213401.	47.31	*	1064.	29.	1.143	.69	37.757
28.00	7.06	62604.	198854.	233.48	686.03	*	195.48	-.0834	738.31	215174.	50.54	*	1076.	17.	1.083	.66	63.117
30.00	7.45	64568.	199604.	239.89	685.44	*	195.48	-.0987	740.49	216927.	53.74	*	1088.	6.	1.027	.63	187.963

Table A-6.12(c): Summary of range of possible evaporator conditions for Run 9

****** TUBE-BESIDE-TUBE CONDENSER SIMULATION ****** ASSUME TUBE WALLS HAVE INFINITE CONDUCTIVITY ******

GEOMETRY: SUBCOOLER 7.50M OF 5.75MM OD. CONDENSER: 7.50M OF 5.75MM OD. WATER SIDE 7.65MM OD. ALL WALLS .74MM THICK.
BOND CNDCTNCE 500.0W/M.C THML PWR 1000.6W. WATER IN 16.6C. HOT GAS 60.2C. DEW POINT 36.5C. SUBCLD LIQD 22.4C.

ITERATION NUMBER: 13 USED I= 150 SEGMENTS. TRIAL WATER EXIT TEMP: 36.3595 CORRESPONDING TO TW(I)= 16.5523 & TR(I)= 22.3301

EXIT WATER TEMP 36.36C. FLOW RATE 12.1020 GRAM/SEC. WATER PRESS DROP .1019 BAR. PUMP PWR .1233 WATT (OR .0123%)
REFRIGERANT MASS FLOW RATE 6.156E+00 GRAM/SEC

SEPARATE RESULTS FOR THE THREE SEGMENTS	SUPE RHEAT	TWO-PHASE	SUBCOOLER	TOTAL/AVERAGE
LENGTH OF EACH SEGMENT IN METRES	1.7750E+00	1.2600E+01	6.2500E-01	1.5000E+01
MASS OF REFRIGERANT IN KG.	1.2234E-03	3.6697E-02	1.1156E-02	4.9077E-02
REFRIG SIDE HEAT TRANS COEFNT: W/SQ M C.	7.5181E+02	4.6616E+03	9.6547E+02	4.0445E+03
REFRIG SIDE LINEAR H.T.C.: W/M C.	1.0044E+01	6.2221E+01	1.2898E+01	5.3987E+01
REFRIGERANT SIDE REYNOLDS NUMBER	1.3530E+05	3.5929E+03	8.5512E+03	1.9596E+04
WATER SIDE HEAT TRANS COEFNT: W/SQ M C.	1.9101E+03	1.4557E+03	1.0191E+03	1.4927E+03
WATER SIDE LINEAR H.T.C. W/M C.	3.3024E+01	2.5043E+01	1.7643E+01	2.5705E+01
WATER SIDE REYNOLDS NUMBER	3.8392E+03	3.2851E+03	2.5421E+03	3.3219E+03
OVERALL LINEAR CONDUCTANCE: W/M C	7.6869E+00	1.7474E+01	7.4395E+00	1.5898E+01
NO. OF HEAT TRANSFER UNITS REFRIG. SIDE	2.9704	.1195	.7453	3.8351
NO. OF HEAT TRANSFER UNITS WATER SIDE	.2737	4.3504	.0880	4.7120
EFFECTIVENESS OF EACH SEGMENT (PERCENT)	93.8344	91.3069	51.3159	78.8190
REFRIGERANT SIDE PRESSURE DROP IN BAR	1.6947E-01	1.4949E+00	1.3366E-02	1.6778E+00
THERMAL POWER PICK-UP BY WATER (W & %)	112.7(11.2)	853.6(85.1)	36.5(3.6)	1002.8
THERMAL POWER TRANSFERRED BY R12 (W & %)	111.0(11.1)	853.7(85.3)	36.5(3.6)	1001.2
TOTAL MAX THERMAL POWER WITHOUT LOSS (W)	111.02	853.70	36.46	1001.17
THERMAL POWER LOSS FROM FREON (W & %)	.0000	.0000	.0000	.00(.0)
SPECIFIC ENTHALPY OF REFRIG (J/KG)	2.1973E+05	2.0169E+05	6.3016E+04	5.7093E+04
SPECIFIC ENTROPY OF R12 (J/KG.C)	7.3886E+02	6.8381E+02	2.3483E+02	2.1526E+02
REFRIGERANT TEMPERATURE (DEG.C)	6.0164E+01	3.5736E+01	2.8420E+01	2.2330E+01
REFRIGERANT PRESSURE (BAR)	8.8085E+00	8.6391E+00	7.1442E+00	7.1308E+00
WATER TEMPERATURE (DEG.C)	3.6359E+01	3.4131E+01	1.7272E+01	1.6552E+01

RATE OF LOSS OF EHTHALPY BY R12 1.0012E+03 WATTS RATE OF GAIN OF ENTHALPY BY WATER 1.0028E+03 WATTS
CORRESPONDING TO AN ENERGY IMBALANCE OF 1.6370E+00 WATTS OR .1636 % OF SPECIFIED POWER

THE POWER LOSS BY R12 TO OUTSIDE -5.8807E-01WATTS BY -.0588 % OF THE SPECIFIED POWER
THE POWER LOSS BY WATER TO OUTSIDE -2.2251E+00 WATTS BY -.2224 % OF THE SPECIFIED POWER

RATE OF LOSS OF ENTROPY BY R12 3.2232E+00 WATTS/C RATE OF INCREASE OF ENTROPY BY WATER 3.3483E+00 WATTS/C
NET RATE OF ENTROPY FLOW THRU SYSTEM BOUNDARY 1.2512E-01 WATT/C THERMAL ENTROPY CREATION RATE 6.7307E-02 WATT/C
R12 P.D. ENTROPY CREATION RATE 5.7813E-02 WATT/C RATE OF LOSS OF GROSS WORK 3.8747E+01 WATTS AT 36.53 C

RATE OF ENTROPY GAIN OF WATER HAD IT BEEN 10C HOTTER 3.2355E+00 WATTS/C. FOR SAME GROSS RATE OF ENTROPY INCREASE,
A COUNTER-FLOW WATER-WATER HEAT EXCHANGER WOULD HAVE DELTA-T OF 11.0930 DEG C CORRESPONDING TO AN EFFECTIVENESS OF 64.10%
OR 1.786 HEAT TRANSFER UNITS, WHICH IS 37.89 % OF THAT FOR THE WATER SIDE OF THE PRESENT HT.XR.

Table A-6.13(a): Results in three segments for Run 10

LNTH	TR(I)	PR(I)	TW(I)	PW(I)	TWL(I)	X(I)	HR(I)	NTUR(I)	UR(I)	HW(I)	NTUW(I)	UW(I)	UL(I)
.00	60.16	8.81	36.36	0.00E+00	48.26	100.00	7.69E+02	1.73E-01	1.03E+01	1.86E+03	1.56E-02	3.30E+01	7.86E+00
.20	53.00	8.79	35.72	1.03E-03	40.01	100.00	7.91E+02	1.75E-01	1.06E+01	1.82E+03	1.58E-02	3.23E+01	7.99E+00
.40	47.86	8.77	35.25	2.08E-03	38.36	100.00	7.71E+02	1.69E-01	1.03E+01	1.79E+03	1.54E-02	3.18E+01	7.80E+00
.60	44.08	8.75	34.90	5.48E-03	36.92	100.00	7.57E+02	1.65E-01	1.01E+01	1.77E+03	1.52E-02	3.14E+01	7.67E+00
.80	41.48	8.73	34.67	6.53E-03	36.32	100.00	7.42E+02	1.61E-01	9.95E+00	1.75E+03	1.49E-02	3.11E+01	7.54E+00
1.00	39.58	8.71	34.49	7.58E-03	35.62	100.00	7.66E+02	1.72E-01	1.00E+01	2.61E+03	1.59E-02	4.10E+01	8.06E+00
1.20	38.13	8.69	34.35	1.10E-02	35.26	100.00	7.24E+02	1.57E-01	9.72E+00	1.73E+03	1.46E-02	3.08E+01	7.39E+00
1.40	37.10	8.67	34.26	1.20E-02	34.94	100.00	7.18E+02	1.55E-01	9.64E+00	1.73E+03	1.45E-02	3.07E+01	7.33E+00
1.60	36.31	8.66	34.18	1.54E-02	34.64	100.00	7.14E+02	1.54E-01	9.58E+00	1.72E+03	1.44E-02	3.06E+01	7.30E+00

LNTH	TR(I)	PR(I)	TW(I)	PW(I)	TWL(I)	X(I)	HR(I)	NTUR(I)	UR(I)	HW(I)	NTUW(I)	UW(I)	UL(I)
1.80	35.74	8.64	34.13	1.64E-02	34.51	99.99	6.29E+02	0.00E+00	8.44E+00	1.72E+03	1.31E-02	3.06E+01	6.61E+00
2.00	35.66	8.62	34.07	1.75E-02	34.68	99.64	2.34E+03	0.00E+00	3.06E+01	2.57E+03	3.45E-02	4.05E+01	1.74E+01
2.20	35.55	8.59	33.96	2.08E-02	34.87	98.97	3.77E+03	0.00E+00	5.05E+01	1.71E+03	3.75E-02	3.04E+01	1.90E+01
2.40	35.45	8.57	33.83	2.19E-02	34.91	98.21	5.42E+03	0.00E+00	7.27E+01	1.70E+03	4.22E-02	3.02E+01	2.14E+01
2.60	35.34	8.55	33.67	2.52E-02	34.82	97.24	7.39E+03	0.00E+00	9.91E+01	1.69E+03	4.56E-02	3.01E+01	2.31E+01
2.80	35.23	8.52	33.52	2.62E-02	34.85	96.29	7.54E+03	0.00E+00	1.01E+02	1.68E+03	4.56E-02	2.99E+01	2.31E+01
3.00	35.13	8.50	33.35	2.73E-02	34.71	95.32	7.54E+03	0.00E+00	9.87E+01	2.51E+03	5.58E-02	3.95E+01	2.82E+01
3.20	35.01	8.48	33.17	3.06E-02	34.57	94.21	6.96E+03	0.00E+00	9.34E+01	1.66E+03	4.44E-02	2.95E+01	2.24E+01
3.40	34.89	9.45	33.00	3.16E-02	34.43	93.20	6.78E+03	0.00E+00	9.10E+01	1.65E+03	4.39E-02	2.93E+01	2.22E+01
3.60	34.76	8.42	32.81	3.48E-02	34.20	92.06	6.61E+03	0.00E+00	8.87E+01	1.64E+03	4.34E-02	2.91E+01	2.19E+01
3.80	34.64	8.40	32.64	3.59E-02	34.14	91.02	6.49E+03	0.00E+00	8.70E+01	1.63E+03	4.30E-02	2.89E+01	2.17E+01
4.00	34.51	8.37	32.46	3.69E-02	33.98	89.96	6.66E+03	0.00E+00	8.72E+01	2.43E+03	5.26E-02	3.82E+01	2.66E+01
4.20	34.37	8.34	32.26	4.01E-02	33.84	88.76	6.27E+03	0.00E+00	8.41E+01	1.61E+03	4.21E-02	2.85E+01	2.13E+01
4.40	34.24	8.31	32.08	4.11E-02	33.69	87.67	6.18E+03	0.00E+00	8.29E+01	1.60E+03	4.18E-02	2.83E+01	2.11E+01
4.60	34.10	8.28	31.87	4.26E-02	33.43	86.44	6.12E+03	0.00E+00	8.21E+01	1.58E+03	4.14E-02	2.81E+01	2.10E+01
4.80	33.96	8.25	31.68	4.36E-02	33.38	85.31	6.06E+03	0.00E+00	8.13E+01	1.57E+03	4.11E-02	2.79E+01	2.08E+01
5.00	33.82	8.22	31.49	4.46E-02	33.22	84.13	6.28E+03	0.00E+00	8.22E+01	2.30E+03	4.97E-02	3.62E+01	2.51E+01
5.20	33.67	8.19	31.28	4.61E-02	33.07	82.90	5.94E+03	0.00E+00	7.97E+01	1.52E+03	3.98E-02	2.70E+01	2.01E+01
5.40	33.53	8.16	31.08	4.71E-02	32.91	81.75	5.89E+03	0.00E+00	7.90E+01	1.51E+03	3.95E-02	2.68E+01	2.00E+01
5.60	33.37	8.13	30.86	4.86E-02	32.62	80.43	5.83E+03	0.00E+00	7.82E+01	1.49E+03	3.92E-02	2.65E+01	1.98E+01
5.80	33.23	8.10	30.66	4.96E-02	32.58	79.24	5.78E+03	0.00E+00	7.75E+01	1.48E+03	3.89E-02	2.63E+01	1.97E+01
6.00	33.08	8.07	30.46	5.06E-02	32.40	78.04	5.99E+03	0.00E+00	7.84E+01	2.22E+03	4.77E-02	3.48E+01	2.41E+01
6.20	32.92	8.04	30.22	5.21E-02	32.24	76.66	5.67E+03	0.00E+00	7.60E+01	1.46E+03	3.82E-02	2.59E+01	1.93E+01
6.40	32.78	8.00	30.01	5.31E-02	32.07	75.42	5.62E+03	0.00E+00	7.53E+01	1.45E+03	3.79E-02	2.57E+01	1.92E+01
6.60	32.62	7.97	29.77	5.45E-02	31.76	74.00	5.55E+03	0.00E+00	7.45E+01	1.43E+03	3.75E-02	2.54E+01	1.90E+01
6.80	32.47	7.94	29.56	5.55E-02	31.73	72.72	5.50E+03	0.00E+00	7.38E+01	1.42E+03	3.72E-02	2.52E+01	1.88E+01
7.00	32.32	7.91	29.33	5.65E-02	31.54	71.42	5.69E+03	0.00E+00	7.45E+01	2.12E+03	4.56E-02	3.34E+01	2.31E+01
7.20	32.16	7.88	29.08	5.80E-02	31.37	69.93	5.38E+03	0.00E+00	7.22E+01	1.39E+03	3.64E-02	2.48E+01	1.84E+01
7.40	32.01	7.85	28.85	5.89E-02	31.20	68.59	5.32E+03	0.00E+00	7.14E+01	1.38E+03	3.61E-02	2.45E+01	1.83E+01
7.60	31.85	7.81	28.59	6.04E-02	30.86	67.05	5.26E+03	0.00E+00	7.05E+01	1.37E+03	3.57E-02	2.43E+01	1.81E+01
7.80	31.70	7.78	28.35	6.13E-02	30.84	65.65	5.19E+03	0.00E+00	6.97E+01	1.35E+03	3.53E-02	2.41E+01	1.79E+01
8.00	31.55	7.75	28.11	6.23E-02	30.65	64.24	5.37E+03	0.00E+00	7.03E+01	2.03E+03	4.33E-02	3.19E+01	2.19E+01
8.20	31.39	7.72	27.84	6.37E-02	30.48	62.61	5.06E+03	0.00E+00	6.79E+01	1.33E+03	3.46E-02	2.36E+01	1.75E+01
8.40	31.25	7.69	27.58	6.47E-02	30.30	61.14	4.99E+03	0.00E+00	6.70E+01	1.31E+03	3.42E-02	2.33E+01	1.73E+01
8.60	31.09	7.66	27.30	6.61E-02	29.94	59.47	4.92E+03	0.00E+00	6.59E+01	1.27E+03	3.33E-02	2.26E+01	1.68E+01
8.80	30.95	7.63	27.04	6.71E-02	29.95	57.96	4.85E+03	0.00E+00	6.50E+01	1.26E+03	3.29E-02	2.24E+01	1.67E+01
9.00	30.80	7.60	26.78	6.81E-02	29.74	56.42	4.99E+03	0.00E+00	6.53E+01	1.89E+03	4.03E-02	2.97E+01	2.04E+01
9.20	30.65	7.57	26.48	6.95E-02	29.58	54.66	4.69E+03	0.00E+00	6.29E+01	1.23E+03	3.21E-02	2.19E+01	1.62E+01
9.40	30.51	7.55	26.21	7.04E-02	29.40	53.06	4.61E+03	0.00E+00	6.18E+01	1.22E+03	3.17E-02	2.16E+01	1.60E+01
9.60	30.37	7.52	25.89	7.18E-02	28.99	51.22	4.52E+03	0.00E+00	6.06E+01	1.20E+03	3.12E-02	2.14E+01	1.58E+01
9.80	30.23	7.49	25.61	7.28E-02	29.02	49.55	4.43E+03	0.00E+00	5.95E+01	1.19E+03	3.08E-02	2.11E+01	1.56E+01
10.00	30.10	7.47	25.32	7.37E-02	28.81	47.84	4.54E+03	0.00E+00	5.95E+01	1.78E+03	3.76E-02	2.80E+01	1.90E+01
10.20	29.97	7.44	24.98	7.51E-02	28.65	45.89	4.24E+03	0.00E+00	5.69E+01	1.16E+03	2.99E-02	2.06E+01	1.51E+01
10.40	29.84	7.41	24.68	7.61E-02	28.46	44.10	4.14E+03	0.00E+00	5.56E+01	1.15E+03	2.94E-02	2.03E+01	1.49E+01
10.60	29.71	7.39	24.33	7.74E-02	28.00	42.06	4.03E+03	0.00E+00	5.41E+01	1.13E+03	2.89E-02	2.01E+01	1.46E+01
10.80	29.59	7.37	24.02	7.84E-02	28.08	40.19	3.93E+03	0.00E+00	5.27E+01	1.12E+03	2.84E-02	1.98E+01	1.44E+01
11.00	29.48	7.34	23.69	7.93E-02	27.85	38.29	3.99E+03	0.00E+00	5.23E+01	1.64E+03	3.41E-02	2.58E+01	1.73E+01
11.20	29.36	7.32	23.33	8.07E-02	27.68	36.13	3.69E+03	0.00E+00	4.95E+01	1.09E+03	2.74E-02	1.93E+01	1.39E+01
11.40	29.26	7.30	22.99	8.16E-02	27.51	34.15	3.57E+03	0.00E+00	4.79E+01	1.05E+03	2.66E-02	1.87E+01	1.35E+01
11.60	29.15	7.28	22.61	8.30E-02	26.98	31.91	3.46E+03	0.00E+00	4.65E+01	1.04E+03	2.61E-02	1.84E+01	1.32E+01
11.80	29.06	7.26	22.27	8.39E-02	27.12	29.86	3.36E+03	0.00E+00	4.51E+01	1.03E+03	2.56E-02	1.82E+01	1.30E+01
12.00	28.97	7.25	21.91	8.49E-02	26.88	27.77	3.39E+03	0.00E+00	4.44E+01	1.53E+03	3.08E-02	2.40E+01	1.56E+01
12.20	28.89	7.23	21.51	8.62E-02	26.71	25.39	3.11E+03	0.00E+00	4.17E+01	9.97E+02	2.45E-02	1.77E+01	1.24E+01
12.40	28.81	7.22	21.14	8.72E-02	26.50	23.19	2.98E+03	0.00E+00	3.99E+01	9.85E+02	2.40E-02	1.75E+01	1.22E+01
12.60	28.74	7.20	20.73	8.85E-02	25.86	20.72	2.82E+03	0.00E+00	3.78E+01	9.70E+02	2.34E-02	1.72E+01	1.18E+01
12.80	28.67	7.19	20.35	8.95E-02	26.03	18.46	2.66E+03	0.00E+00	3.57E+01	9.59E+02	2.28E-02	1.70E+01	1.15E+01
13.00	28.62	7.18	19.96	9.05E-02	25.71	16.16	2.61E+03	0.00E+00	3.42E+01	1.40E+03	2.64E-02	2.20E+01	1.34E+01
13.20	28.57	7.17	19.54	9.18E-02	25.47	13.61	2.29E+03	0.00E+00	3.08E+01	9.37E+02	2.13E-02	1.66E+01	1.08E+01
13.40	28.53	7.16	19.15	9.28E-02	25.18	11.29	2.09E+03	0.00E+00	2.81E+01	9.18E+02	2.03E-02	1.63E+01	1.03E+01
13.60	28.49	7.16	18.73	9.41E-02	24.29	8.77	1.85E+03	0.00E+00	2.48E+01	9.11E+02	1.93E-02	1.62E+01	9.79E+00
13.80	28.47	7.15	18.35	9.51E-02	24.31	6.49	1.59E+03	0.00E+00	2.14E+01	9.09E+02	1.81E-02	1.61E+01	9.20E+00
14.00	28.45	7.15	17.98	9.61E-02	23.59	4.28	1.36E+03	0.00E+00	1.78E+01	1.34E+03	1.91E-02	2.11E+01	9.66E+00
14.20	28.44	7.14	17.62	9.74E-02	22.80	2.07	9.22E+02	0.00E+00	1.24E+01	9.17E+02	1.39E-02	1.63E+01	7.03E+00

LNTH	TR(I)	PR(I)	TW(I)	PW(I)	TWL(I)	X(I)	HR(I)	NTUR(I)	UR(I)	HW(I)	NTUW(I)	UW(I)	UL(I)
14.40	28.42	7.14	17.27	9.84E-02	23.31	.00	9.67E+02	1.20E-01	1.30E+01	9.15E+02	1.42E-02	1.62E+01	7.21E+00
14.60	25.89	7.14	16.97	9.98E-02	20.54	.00	9.63E+02	1.21E-01	1.29E+01	9.37E+02	1.43E-02	1.66E+01	7.27E+00
14.80	23.94	7.14	16.74	1.01E-01	19.84	.00	9.56E+02	1.24E-01	1.28E+01	9.77E+02	1.45E-02	1.73E+01	7.37E+00
15.00	22.33	7.13	16.55	1.02E-01	18.97	.00	9.65E+02	1.29E-01	1.29E+01	1.07E+03	1.52E-02	1.90E+01	7.70E+00

Table A-6.13(b): The profiles of parameters for Run 10

SUMMARY OF RANGE OF POSSIBLE EVAPORATOR CONDITIONS ASSUMIMG 50% COMPRESSOR ISENTROPIC EFFICIENCY
COND. PRESS= 8.8 COND. TEMP= 36.53 ENT. H= 219728. ENT. S= 738.86 LEAV. TEMP= 22.43 LEAV. H= 57189. LEAV. S= 215.58

		EVAPORATOR				*	ENTRY			EXIT		*	EVAP	COMP	PRESS	VDOT	COPH
TEMP	PRESS	H(X=0)	H(X=1)	S(X=0)	S(X=1)	*	S	X	S	H	T	*	CAP	CAP	RATIO	CUM/H	
12.00	4.49	47237.	192543.	181.71	691.41	*	216.61	.0685	694.15	193374.	13.14	*	838.	162.	1.960	.86	6.168
14.00	4.77	49129.	193359.	188.25	690.66	*	216.32	.0559	698.46	195660.	17.27	*	852.	148.	1.847	.82	6.753
16.00	5.06	51028.	194168.	194.77	689.93	*	216.08	.0430	702.64	197920.	21.34	*	866.	134.	1.742	.79	7.453
18.00	5.36	52935.	194970.	201.26	689.23	*	215.88	.0299	706.69	200156.	25.36	*	880.	120.	1.644	.75	8.305
20.00	5.67	54851.	195764.	207.74	688.55	*	215.72	.0166	710.62	202368.	29.32	*	894.	107.	1.553	.72	9.363
22.00	6.00	56775.	196550.	214.20	687.89	*	215.60	.0030	714.43	204555.	33.23	*	907.	93.	1.469	.69	10.712
24.00	6.34	58708.	197327.	220.64	687.26	*	215.58	-.0110	718.12	206719.	37.09	*	920.	80.	1.390	.66	12.493
26.00	6.69	60651.	198095.	227.07	686.64	*	215.58	-.0252	721.70	208856.	40.90	*	934.	67.	1.316	.63	14.951
28.00	7.06	62604.	198854.	233.48	686.03	*	215.58	-.0397	725.17	210972.	44.66	*	947.	54.	1.247	.60	18.563
30.00	7.45	64568.	199604.	239.89	685.44	*	215.58	-.0546	728.54	213063.	48.37	*	960.	41.	1.183	.58	24.389
32.00	7.85	66542.	200343.	246.28	684.86	*	215.58	-.0699	731.80	215129.	52.03	*	972.	28.	1.123	.55	35.343
34.00	8.26	68528.	201071.	252.66	684.30	*	215.58	-.0856	734.98	217173.	55.65	*	985.	16.	1.066	.53	63.630
36.00	8.69	70526.	201788.	259.04	683.73	*	215.58	-.1016	738.05	219194.	59.22	*	997.	3.	1.013	.51	304.862

SUMMARY OF RANGE OF POSSIBLE EVAPORATOR CONDITIONS ASSUMIMG 55% COMPRESSOR ISENTROPIC EFFICIENCY
COND. PRESS= 8.8 COND. TEMP= 36.53 ENT. H= 219728. ENT. S= 738.86 LEAV. TEMP= 22.43 LEAV. H= 57189. LEAV. S= 215.58

		EVAPORATOR				*	ENTRY			EXIT		*	EVAP	COMP	PRESS	VDOT	COPH
TEMP	PRESS	H(X=0)	H(X=1)	S(X=0)	S(X=1)	*	S	X	S	H	T	*	CAP	CAP	RATIO	CUM/H	
8.00	3.98	43476.	190890.	168.55	693.01	*	217.34	.0930	695.25	191546.	8.94	*	827.	173.	2.213	.97	5.768
10.00	4.23	45353.	191720.	175.14	692.20	*	216.95	.0809	698.95	193669.	12.84	*	840.	160.	2.082	.92	6.238
12.00	4.49	47237.	192543.	181.71	691.41	*	216.61	.0685	702.54	195770.	16.69	*	853.	147.	1.960	.88	6.784
14.00	4.77	49129.	193359.	188.25	690.66	*	216.32	.0559	706.02	197848.	20.49	*	866.	135.	1.847	.84	7.429
16.00	5.06	51028.	194168.	194.77	689.93	*	216.08	.0430	709.40	199903.	24.24	*	879.	122.	1.742	.80	8.199
18.00	5.36	52935.	194970.	201.26	689.23	*	215.88	.0299	712.68	201935.	27.94	*	891.	110.	1.644	.76	9.135
20.00	5.67	54851.	195764.	207.74	688.55	*	215.72	.0166	715.86	203946.	31.60	*	903.	97.	1.553	.73	10.299
22.00	6.00	56775.	196550.	214.20	687.89	*	215.60	.0030	718.95	205934.	35.21	*	916.	85.	1.469	.69	11.784
24.00	6.34	58708.	197327.	220.64	687.26	*	215.58	-.0110	721.95	207900.	38.77	*	928.	73.	1.390	.66	13.743
26.00	6.69	60651.	198095.	227.07	686.64	*	215.58	-.0252	724.86	209845.	42.29	*	940.	61.	1.316	.63	16.447
28.00	7.06	62604.	198854.	233.48	686.03	*	215.58	-.0397	727.69	211768.	45.77	*	952.	49.	1.247	.60	20.420
30.00	7.45	64568.	199604.	239.89	685.44	*	215.58	-.0546	730.43	213669.	49.21	*	963.	37.	1.183	.58	26.828
32.00	7.85	66542.	200343.	246.28	684.86	*	215.58	-.0699	733.09	215547.	52.61	*	975.	26.	1.123	.55	38.878
34.00	8.26	68528.	201071.	252.66	684.30	*	215.58	-.0856	735.68	217405.	55.97	*	986.	14.	1.066	.53	69.993
36.00	8.69	70526.	201788.	259.04	683.73	*	215.58	-.1016	738.20	219243.	59.29	*	998.	3.	1.013	.51	335.348

SUMMARY OF RANGE OF POSSIBLE EVAPORATOR CONDITIONS ASSUMIMG 60% COMPRESSOR ISENTROPIC EFFICIENCY
COND. PRESS= 8.8 COND. TEMP= 36.53 ENT. H= 219728. ENT. S= 738.86 LEAV. TEMP= 22.43 LEAV. H= 57189. LEAV. S= 215.58

		EVAPORATOR				*	ENTRY			EXIT		*	EVAP	COMP	PRESS	VDOT	COPH
TEMP	PRESS	H(X=0)	H(X=1)	S(X=0)	S(X=1)	*	S	X	S	H	T	*	CAP	CAP	RATIO	CUM/H	
4.00	3.51	39742.	189211.	155.29	694.74	*	218.26	.1167	697.33	189936.	5.09	*	817.	183.	2.509	1.09	5.456
6.00	3.74	41606.	190054.	161.94	693.86	*	217.77	.1050	700.50	191926.	8.80	*	829.	171.	2.355	1.04	5.846
8.00	3.98	43476.	190890.	168.55	693.01	*	217.34	.0930	703.57	193894.	12.46	*	842.	159.	2.213	.98	6.292
10.00	4.23	45353.	191720.	175.14	692.20	*	216.95	.0809	706.54	195841.	16.08	*	854.	147.	2.082	.94	6.805
12.00	4.49	47237.	192543.	181.71	691.41	*	216.61	.0685	709.43	197766.	19.65	*	865.	135.	1.960	.89	7.401
14.00	4.77	49129.	193359.	188.25	690.66	*	216.32	.0559	712.24	199671.	23.17	*	877.	123.	1.847	.85	8.104
16.00	5.06	51028.	194168.	194.77	689.93	*	216.08	.0430	714.97	201555.	26.65	*	889.	112.	1.742	.81	8.944
18.00	5.36	52935.	194970.	201.26	689.23	*	215.88	.0299	717.62	203418.	30.09	*	900.	100.	1.644	.77	9.966
20.00	5.67	54851.	195764.	207.74	688.55	*	215.72	.0166	720.19	205261.	33.49	*	912.	89.	1.553	.73	11.235
22.00	6.00	56775.	196550.	214.20	687.89	*	215.60	.0030	722.69	207084.	36.85	*	923.	78.	1.469	.70	12.855
24.00	6.34	58708.	197327.	220.64	687.26	*	215.58	-.0110	725.12	208886.	40.17	*	934.	67.	1.390	.67	14.992
26.00	6.69	60651.	198095.	227.07	686.64	*	215.58	-.0252	727.48	210668.	43.45	*	945.	56.	1.316	.64	17.942
28.00	7.06	62604.	198854.	233.48	686.03	*	215.58	-.0397	729.77	212431.	46.70	*	956.	45.	1.247	.61	22.276
30.00	7.45	64568.	199604.	239.89	685.44	*	215.58	-.0546	732.00	214174.	49.91	*	966.	34.	1.183	.58	29.267
32.00	7.85	66542.	200343.	246.28	684.86	*	215.58	-.0699	734.17	215895.	53.09	*	977.	24.	1.123	.55	42.412
34.00	8.26	68528.	201071.	252.66	684.30	*	215.58	-.0856	736.27	217599.	56.23	*	987.	13.	1.066	.53	76.356
36.00	8.69	70526.	201788.	259.04	683.73	*	215.58	-.1016	738.32	219283.	59.34	*	998.	3.	1.013	.51	365.834

Table A-6.13(c): Summary of range of possible evaporator conditions for Runs 10

```
****** TUBE-BESIDE-TUBE CONDENSER SIMULATION ****** ASSUME TUBE WALLS HAVE INFINITE CONDUCTIVITY ******
GEOMETRY:  SUBCOOLER  7.50M OF 5.75MM OD.   CONDENSER:  7.50M OF 5.75MM OD.   WATER SIDE 7.65MM OD.   ALL WALLS  .74MM THICK.
BOND CNDCTNCE 500.0W/M.C   THML PWR  1209.0W.    WATER IN 20.4C.    HOT GAS  64.2C.    DEW POINT 38.3C.    SUBCLD LIQD 23.6C.

ITERATION NUMBER: 17 USED I= 150 SEGMENTS.      TRIAL WATER EXIT TEMP: 37.8732    CORRESPONDING TO TW(I)= 20.3641  & TR(I)= 23.2059

EXIT WATER TEMP   37.87C.    FLOW RATE 16.5577 GRAM/SEC.    WATER PRESS DROP    .5577 BAR.    PUMP PWR   .9234 WATT (OR   .0764%)
REFRIGERANT MASS FLOW RATE  7.381E+00 GRAM/SEC
```

SEPARATE RESULTS FOR THE THREE SEGMENTS	SUPE RHEAT	TWO-PHASE	SUBCOOLER	TOTAL/AVERAGE
LENGTH OF EACH SEGMENT IN METRES	1.6750E+00	1.2800E+01	5.2500E-01	1.5000E+01
MASS OF REFRIGERANT IN KG.	1.2011E-03	4.4369E-02	9.3002E-03	5.4871E-02
REFRIG SIDE HEAT TRANS COEFNT: W/SQ M C.	8.8255E+02	5.0125E+03	1.1181E+03	4.4147E+03
REFRIG SIDE LINEAR H.T.C.: W/M C.	1.1788E+01	6.6903E+01	1.4923E+01	5.8924E+01
REFRIGERANT SIDE REYNOLDS NUMBER	1.6041E+05	4.8935E+03	1.0212E+04	2.2696E+04
WATER SIDE HEAT TRANS COEFNT: W/SQ M C.	4.1795E+03	3.2317E+03	2.3531E+03	3.3098E+03
WATER SIDE LINEAR H.T.C. W/M C.	7.2184E+01	5.5598E+01	4.0504E+01	5.6975E+01
WATER SIDE REYNOLDS NUMBER	5.4229E+03	4.6505E+03	3.8223E+03	4.7105E+03
OVERALL LINEAR CONDUCTANCE: W/M C	1.0121E+01	2.9565E+01	1.0888E+01	2.6739E+01
NO. OF HEAT TRANSFER UNITS REFRIG. SIDE	3.0583	.1618	.7593	3.9794
NO. OF HEAT TRANSFER UNITS WATER SIDE	.2488	5.4666	.0785	5.7939
EFFECTIVENESS OF EACH SEGMENT (PERCENT)	94.4339	90.4717	52.1084	79.0046
REFRIGERANT SIDE PRESSURE DROP IN BAR	2.1903E-01	1.9572E+00	1.5292E-02	2.1915E+00
THERMAL POWER PICK-UP BY WATER (W & %)	149.4(12.3)	1040.7(85.9)	22.2(1.8)	1212.2
THERMAL POWER TRANSFERRED BY R12 (W & %)	146.9(12.1)	1043.0(86.1)	22.2(1.8)	1212.0
TOTAL MAX THERMAL POWER WITHOUT LOSS (W)	146.85	1043.04	22.16	1212.05
THERMAL POWER LOSS FROM FREON (W & %)	.0000	.0000	.0000	.00(.0)
SPECIFIC ENTHALPY OF REFRIG (J/KG)	2.2214E+05	2.0225E+05	6.0941E+04	5.7939E+04
SPECIFIC ENTROPY OF R12 (J/KG.C)	7.4344E+02	6.8337E+02	2.2803E+02	2.1809E+02
REFRIGERANT TEMPERATURE (DEG.C)	6.4152E+01	3.7297E+01	2.6298E+01	2.3206E+01
REFRIGERANT PRESSURE (BAR)	9.2034E+00	8.9844E+00	7.0272E+00	7.0119E+00
WATER TEMPERATURE (DEG.C)	3.7873E+01	3.5714E+01	2.0684E+01	2.0364E+01

```
RATE OF LOSS OF EHTHALPY BY R12  1.2120E+03 WATTS      RATE OF GAIN OF ENTHALPY BY WATER  1.2123E+03 WATTS
CORRESPONDING TO AN ENERGY IMBALANCE OF  2.0056E-01 WATTS     OR    .0166 % OF SPECIFIED POWER

THE POWER LOSS BY R12 TO OUTSIDE -3.0399E+00WATTS  BY   -.2514 % OF THE SPECIFIED POWER
THE POWER LOSS BY WATER TO OUTSIDE  -3.2405E+00 WATTS   BY   -.2680 % OF THE SPECIFIED POWER

RATE OF LOSS OF ENTROPY BY R12  3.8779E+00 WATTS/C      RATE OF INCREASE OF ENTROPY BY WATER  4.0116E+00 WATTS/C
NET RATE OF ENTROPY FLOW THRU SYSTEM BOUNDARY 1.3378E-01 WATT/C      THERMAL ENTROPY CREATION RATE 5.8301E-02 WATT/C
R12 P.D. ENTROPY CREATION RATE  7.5479E-02 WATT/C       RATE OF LOSS OF GROSS WORK  4.1664E+01 WATTS AT  38.28 C

RATE OF ENTROPY GAIN OF WATER HAD IT BEEN 10C HOTTER  3.8784E+00 WATTS/C.   FOR SAME GROSS RATE OF ENTROPY INCREASE,
A COUNTER-FLOW WATER-WATER HEAT EXCHANGER WOULD HAVE DELTA-T OF  10.0414 DEG C     CORRESPONDING TO AN EFFECTIVENESS OF  63.55%
OR  1.744 HEAT TRANSFER UNITS, WHICH IS  30.10 % OF THAT FOR THE WATER SIDE OF THE PRESENT HT.XR.
```

Table A-6.14(a): Results in three segments for Run. 40

LNTH	TR(I)	PR(I)	TW(I)	PW(I)	TWL(I)	X(I)	HR(I)	NTUR(I)	UR(I)	HW(I)	NTUW(I)	UW(I	UL(I)
.00	64.15	9.20	37.87	0.00E+00	51.01	100.00	8.97E+02	1.89E-01	1.20E+01	4.04E+03	1.49E-02	7.17E+01	1.03E+01
.20	55.58	9.17	37.20	7.73E-03	40.02	100.00	9.39E+02	1.94E-01	1.26E+01	3.96E+03	1.54E-02	7.03E+01	1.07E+01
.40	49.65	9.15	36.72	1.55E-02	38.67	100.00	9.08E+02	1.86E-01	1.22E+01	3.90E+03	1.50E-02	6.93E+01	1.04E+01
.60	45.51	9.12	36.39	2.74E-02	37.68	100.00	8.84E+02	1.80E-01	1.19E+01	3.86E+03	1.46E-02	6.86E+01	1.01E+01
.80	42.73	9.09	36.16	3.51E-02	37.12	100.00	8.66E+02	1.75E-01	1.16E+01	3.84E+03	1.43E-02	6.81E+01	9.92E+00
1.00	40.77	9.07	36.00	4.28E-02	36.59	100.00	8.92E+02	1.81E-01	1.17E+01	5.60E+03	1.49E-02	8.81E+01	1.03E+01
1.20	39.33	9.04	35.88	5.46E-02	36.38	100.00	8.43E+02	1.70E-01	1.13E+01	3.80E+03	1.40E-02	6.75E+01	9.68E+00
1.40	38.33	9.02	35.80	6.22E-02	36.16	100.00	8.35E+02	1.68E-01	1.12E+01	3.79E+03	1.39E-02	6.74E+01	9.60E+00
1.60	37.58	9.00	35.74	7.40E-02	35.99	100.00	8.29E+02	1.67E-01	1.11E+01	3.79E+03	1.38E-02	6.72E+01	9.54E+00

LNTH	TR(I)	PR(I)	TW(I)	PW(I)	TWL(I)	X(I)	HR(I)	NTUR(I)	UR(I)	HW(I)	NTUW(I)	UW(I	UL(I)
1.80	37.25	8.97	35.70	8.16E-02	35.87	99.88	1.51E+03	0.00E+00	2.03E+01	3.78E+03	2.25E-02	6.71E+01	1.56E+01
2.00	37.12	8.94	35.61	8.92E-02	36.07	99.32	3.35E+03	0.00E+00	4.39E+01	5.54E+03	4.22E-02	8.71E+01	2.92E+01
2.20	36.98	8.91	35.48	1.01E-01	36.18	98.40	5.58E+03	0.00E+00	7.49E+01	3.76E+03	5.10E-02	6.67E+01	3.53E+01
2.40	36.84	8.88	35.31	1.08E-01	36.20	97.25	8.26E+03	0.00E+00	1.11E+02	3.74E+03	6.00E-02	6.64E+01	4.15E+01
2.60	36.70	8.85	35.10	1.20E-01	36.04	95.78	8.28E+03	0.00E+00	1.11E+02	3.71E+03	5.98E-02	6.59E+01	4.14E+01
2.80	36.56	8.81	34.91	1.28E-01	35.93	94.41	7.90E+03	0.00E+00	1.06E+02	3.69E+03	5.85E-02	6.55E+01	4.05E+01
3.00	36.41	8.78	34.71	1.35E-01	35.74	93.04	7.97E+03	0.00E+00	1.04E+02	5.39E+03	6.76E-02	8.47E+01	4.68E+01
3.20	36.24	8.74	34.49	1.46E-01	35.56	91.52	7.41E+03	0.00E+00	9.94E+01	3.58E+03	5.60E-02	6.35E+01	3.87E+01
3.40	36.08	8.71	34.29	1.54E-01	35.37	90.13	7.24E+03	0.00E+00	9.71E+01	3.55E+03	5.53E-02	6.31E+01	3.82E+01
3.60	35.90	8.67	34.06	1.65E-01	35.08	88.59	7.13E+03	0.00E+00	9.57E+01	3.53E+03	5.47E-02	6.26E+01	3.78E+01
3.80	35.73	8.63	33.86	1.72E-01	34.98	87.17	7.04E+03	0.00E+00	9.44E+01	3.50E+03	5.42E-02	6.22E+01	3.75E+01
4.00	35.55	8.59	33.65	1.80E-01	34.77	85.74	7.27E+03	0.00E+00	9.52E+01	5.12E+03	6.31E-02	8.06E+01	4.36E+01
4.20	35.36	8.55	33.42	1.91E-01	34.58	84.17	6.87E+03	0.00E+00	9.21E+01	3.46E+03	5.32E-02	6.13E+01	3.68E+01
4.40	35.17	8.51	33.21	1.98E-01	34.39	82.73	6.79E+03	0.00E+00	9.11E+01	3.43E+03	5.28E-02	6.09E+01	3.65E+01
4.60	34.98	8.47	32.97	2.09E-01	34.07	81.14	6.71E+03	0.00E+00	9.00E+01	3.41E+03	5.23E-02	6.04E+01	3.62E+01
4.80	34.79	8.43	32.76	2.16E-01	33.97	79.69	6.64E+03	0.00E+00	8.90E+01	3.38E+03	5.18E-02	6.00E+01	3.59E+01
5.00	34.60	8.39	32.54	2.23E-01	33.75	78.22	6.87E+03	0.00E+00	8.99E+01	4.95E+03	6.03E-02	7.78E+01	4.17E+01
5.20	34.39	8.34	32.30	2.34E-01	33.55	76.62	6.49E+03	0.00E+00	8.71E+01	3.33E+03	5.09E-02	5.91E+01	3.52E+01
5.40	34.20	8.30	32.09	2.41E-01	33.34	75.15	6.42E+03	0.00E+00	8.61E+01	3.31E+03	5.04E-02	5.87E+01	3.49E+01
5.60	33.99	8.26	31.85	2.52E-01	33.02	73.55	6.34E+03	0.00E+00	8.51E+01	3.28E+03	5.00E-02	5.82E+01	3.46E+01
5.80	33.80	8.22	31.63	2.59E-01	32.91	72.08	6.28E+03	0.00E+00	8.42E+01	3.26E+03	4.95E-02	5.78E+01	3.43E+01
6.00	33.60	8.18	31.41	2.65E-01	32.68	70.60	6.49E+03	0.00E+00	8.50E+01	4.77E+03	5.76E-02	7.50E+01	3.98E+01
6.20	33.39	8.13	31.17	2.76E-01	32.48	68.99	6.13E+03	0.00E+00	8.22E+01	3.21E+03	4.86E-02	5.69E+01	3.36E+01
6.40	33.19	8.09	30.95	2.83E-01	32.28	67.53	6.06E+03	0.00E+00	8.13E+01	3.12E+03	4.76E-02	5.54E+01	3.30E+01
6.60	32.98	8.05	30.71	2.93E-01	31.94	65.93	5.98E+03	0.00E+00	8.03E+01	3.10E+03	4.71E-02	5.50E+01	3.26E+01
6.80	32.78	8.01	30.49	3.00E-01	31.85	64.47	5.91E+03	0.00E+00	7.93E+01	3.07E+03	4.67E-02	5.46E+01	3.23E+01
7.00	32.59	7.97	30.27	3.06E-01	31.62	63.02	6.11E+03	0.00E+00	8.00E+01	4.51E+03	5.43E-02	7.10E+01	3.76E+01
7.20	32.38	7.92	30.03	3.17E-01	31.42	61.43	5.76E+03	0.00E+00	7.73E+01	3.03E+03	4.58E-02	5.37E+01	3.17E+01
7.40	32.18	7.88	29.81	3.23E-01	31.21	59.97	5.69E+03	0.00E+00	7.63E+01	3.00E+03	4.53E-02	5.33E+01	3.14E+01
7.60	31.98	7.84	29.57	3.33E-01	30.87	58.39	5.61E+03	0.00E+00	7.52E+01	2.98E+03	4.48E-02	5.29E+01	3.10E+01
7.80	31.79	7.80	29.35	3.40E-01	30.78	56.93	5.53E+03	0.00E+00	7.42E+01	2.95E+03	4.44E-02	5.24E+01	3.07E+01
8.00	31.60	7.76	29.13	3.46E-01	30.55	55.47	5.71E+03	0.00E+00	7.47E+01	4.34E+03	5.15E-02	6.83E+01	3.57E+01
8.20	31.40	7.72	28.89	3.56E-01	30.35	53.88	5.37E+03	0.00E+00	7.20E+01	2.91E+03	4.34E-02	5.16E+01	3.01E+01
8.40	31.21	7.69	28.66	3.63E-01	30.14	52.41	5.29E+03	0.00E+00	7.10E+01	2.88E+03	4.30E-02	5.12E+01	2.97E+01
8.60	31.01	7.65	28.42	3.73E-01	29.79	50.81	5.20E+03	0.00E+00	6.98E+01	2.86E+03	4.24E-02	5.08E+01	2.94E+01
8.80	30.83	7.61	28.19	3.79E-01	29.72	49.33	5.12E+03	0.00E+00	6.86E+01	2.84E+03	4.19E-02	5.03E+01	2.90E+01
9.00	30.65	7.57	27.97	3.85E-01	29.49	47.84	5.26E+03	0.00E+00	6.89E+01	4.17E+03	4.85E-02	6.56E+01	3.36E+01
9.20	30.47	7.54	27.72	3.95E-01	29.29	46.22	4.93E+03	0.00E+00	6.62E+01	2.74E+03	4.05E-02	4.86E+01	2.80E+01
9.40	30.29	7.50	27.49	4.01E-01	29.10	44.73	4.85E+03	0.00E+00	6.50E+01	2.72E+03	4.00E-02	4.82E+01	2.77E+01
9.60	30.11	7.47	27.24	4.10E-01	28.74	43.09	4.74E+03	0.00E+00	6.36E+01	2.69E+03	3.94E-02	4.78E+01	2.73E+01
9.80	29.95	7.44	27.01	4.16E-01	28.69	41.57	4.65E+03	0.00E+00	6.24E+01	2.67E+03	3.89E-02	4.74E+01	2.69E+01
10.00	29.79	7.40	26.78	4.22E-01	28.45	40.04	4.76E+03	0.00E+00	6.23E+01	3.93E+03	4.48E-02	6.18E+01	3.10E+01
10.20	29.62	7.37	26.52	4.32E-01	28.27	38.35	4.44E+03	0.00E+00	5.96E+01	2.62E+03	3.77E-02	4.66E+01	2.61E+01
10.40	29.47	7.34	26.28	4.38E-01	28.07	36.78	4.34E+03	0.00E+00	5.82E+01	2.60E+03	3.72E-02	4.62E+01	2.57E+01
10.60	29.31	7.31	26.02	4.47E-01	27.68	35.05	4.22E+03	0.00E+00	5.66E+01	2.58E+03	3.65E-02	4.57E+01	2.53E+01
10.80	29.17	7.28	25.78	4.53E-01	27.65	33.43	4.12E+03	0.00E+00	5.53E+01	2.55E+03	3.60E-02	4.53E+01	2.49E+01
11.00	29.03	7.26	25.53	4.59E-01	27.41	31.78	4.21E+03	0.00E+00	5.52E+01	3.76E+03	4.12E-02	5.92E+01	2.85E+01
11.20	28.90	7.23	25.25	4.68E-01	27.23	29.95	3.92E+03	0.00E+00	5.26E+01	2.51E+03	3.48E-02	4.45E+01	2.41E+01
11.40	28.77	7.21	24.99	4.73E-01	27.03	28.24	3.81E+03	0.00E+00	5.12E+01	2.48E+03	3.42E-02	4.41E+01	2.37E+01
11.60	28.65	7.18	24.71	4.82E-01	26.61	26.34	3.69E+03	0.00E+00	4.95E+01	2.46E+03	3.35E-02	4.36E+01	2.32E+01
11.80	28.53	7.16	24.44	4.88E-01	26.60	24.54	3.57E+03	0.00E+00	4.79E+01	2.39E+03	3.25E-02	4.25E+01	2.25E+01
12.00	28.43	7.14	24.16	4.93E-01	26.36	22.73	3.60E+03	0.00E+00	4.71E+01	3.52E+03	3.68E-02	5.54E+01	2.55E+01
12.20	28.33	7.12	23.87	5.02E-01	26.18	20.73	3.29E+03	0.00E+00	4.42E+01	2.35E+03	3.09E-02	4.16E+01	2.14E+01
12.40	28.24	7.11	23.58	5.08E-01	25.96	18.84	3.14E+03	0.00E+00	4.22E+01	2.32E+03	3.01E-02	4.13E+01	2.09E+01
12.60	28.16	7.09	23.28	5.16E-01	25.48	16.78	2.97E+03	0.00E+00	3.99E+01	2.30E+03	2.91E-02	4.08E+01	2.02E+01
12.80	28.08	7.08	22.99	5.18E-01	25.47	14.84	2.80E+03	0.00E+00	3.75E+01	2.28E+03	2.81E-02	4.04E+01	1.95E+01
13.00	28.02	7.07	22.70	5.20E-01	25.15	12.87	2.73E+03	0.00E+00	3.57E+01	3.35E+03	3.07E-02	5.27E+01	2.13E+01
13.20	27.96	7.05	22.39	5.27E-01	24.93	10.77	2.39E+03	0.00E+00	3.21E+01	2.24E+03	2.56E-02	3.97E+01	1.77E+01
13.40	27.92	7.05	22.10	5.29E-01	24.64	8.81	2.17E+03	0.00E+00	2.91E+01	2.22E+03	2.41E-02	3.94E+01	1.67E+01
13.60	27.88	7.04	21.80	5.35E-01	24.06	6.78	1.91E+03	0.00E+00	2.56E+01	2.20E+03	2.23E-02	3.91E+01	1.54E+01
13.80	27.85	7.03	21.53	5.37E-01	23.93	4.94	1.63E+03	0.00E+00	2.19E+01	2.19E+03	2.02E-02	3.88E+01	1.40E+01
14.00	27.83	7.03	21.28	5.39E-01	23.42	3.22	1.39E+03	0.00E+00	1.82E+01	3.16E+03	1.92E-02	4.97E+01	1.33E+01
14.20	27.82	7.03	21.05	5.46E-01	22.99	1.62	9.60E+02	0.00E+00	1.29E+01	2.14E+03	1.39E-02	3.80E+01	9.62E+00
14.40	27.81	7.03	20.84	5.48E-01	22.80	.24	2.00E+03	0.00E+00	2.69E+01	2.14E+03	2.27E-02	3.81E+01	1.58E+01

LNTH	TR(I)	PR(I)	TW(I)	PW(I)	TWL(I)	X(I)	HR(I)	NTUR(I)	UR(I)	HW(I)	NTUW(I)	UW(I	UL(I)
14.60	25.45	7.02	20.60	5.54E-01	21.84	.00	1.11E+03	1.49E-01	1.49E+01	2.14E+03	1.54E-02	3.79E+01	1.07E+01
14.80	24.18	7.02	20.46	5.56E-01	21.51	.00	1.10E+03	1.49E-01	1.48E+01	2.16E+03	1.54E-02	3.84E+01	1.07E+01
15.00	23.21	7.01	20.36	5.58E-01	21.15	.00	1.19E+03	0.00E+00	1.60E+01	2.35E+03	1.67E-02	4.18E+01	1.16E+01

Table A-6.14(b): The profiles of parameters for Run 40

SUMMARY OF RANGE OF POSSIBLE EVAPORATOR CONDITIONS ASSUMING 50% COMPRESSOR ISENTROPIC EFFICIENCY
COND. PRESS= 9.2 COND. TEMP= 38.28 ENT. H= 222141. ENT. S= 743.44 LEAV. TEMP= 23.63 LEAV. H= 58351. LEAV. S= 219.46

		EVAPORATOR				*	ENTRY		EXIT			*	EVAP	COMP	PRESS	VDOT	COPH
TEMP	PRESS	H(X=0)	H(X=1)	S(X=0)	S(X=1)	*	S	X	S	H	T	*	CAP	CAP	RATIO	CUM/H	
12.00	4.49	47237.	192543.	181.71	691.41	*	220.69	.0765	695.54	193772.	13.73	*	1000.	209.	2.048	1.04	5.773
14.00	4.77	49129.	193359.	188.25	690.66	*	220.37	.0639	699.90	196078.	17.88	*	1017.	192.	1.930	.99	6.284
16.00	5.06	51028.	194168.	194.77	689.93	*	220.10	.0512	704.13	198360.	21.98	*	1033.	176.	1.820	.94	6.887
18.00	5.36	52935.	194970.	201.26	689.23	*	219.87	.0381	708.22	200617.	26.02	*	1050.	159.	1.718	.90	7.609
20.00	5.67	54851.	195764.	207.74	688.55	*	219.68	.0248	712.20	202849.	30.01	*	1067.	142.	1.623	.86	8.490
22.00	6.00	56775.	196550.	214.20	687.89	*	219.54	.0113	716.05	205057.	33.94	*	1083.	126.	1.535	.83	9.587
24.00	6.34	58708.	197327.	220.64	687.26	*	219.46	-.0026	719.79	207240.	37.82	*	1099.	110.	1.452	.79	10.992
26.00	6.69	60651.	198095.	227.07	686.64	*	219.46	-.0167	723.41	209399.	41.65	*	1115.	94.	1.375	.76	12.855
28.00	7.06	62604.	198854.	233.48	686.03	*	219.46	-.0312	726.93	211535.	45.44	*	1131.	78.	1.303	.72	15.443
30.00	7.45	64568.	199604.	239.89	685.44	*	219.46	-.0460	730.35	213647.	49.17	*	1146.	63.	1.236	.69	19.282
32.00	7.85	66542.	200343.	246.28	684.86	*	219.46	-.0612	733.66	215735.	52.86	*	1162.	47.	1.173	.66	25.567
34.00	8.26	68528.	201071.	252.66	684.30	*	219.46	-.0768	736.87	217800.	56.50	*	1177.	32.	1.114	.64	37.727
36.00	8.69	70526.	201788.	259.04	683.73	*	219.46	-.0928	739.99	219839.	60.10	*	1192.	17.	1.059	.61	71.131

SUMMARY OF RANGE OF POSSIBLE EVAPORATOR CONDITIONS ASSUMING 55% COMPRESSOR ISENTROPIC EFFICIENCY
COND. PRESS= 9.2 COND. TEMP= 38.28 ENT. H= 222141. ENT. S= 743.44 LEAV. TEMP= 23.63 LEAV. H= 58351. LEAV. S= 219.46

		EVAPORATOR				*	ENTRY		EXIT			*	EVAP	COMP	PRESS	VDOT	COPH
TEMP	PRESS	H(X=0)	H(X=1)	S(X=0)	S(X=1)	*	S	X	S	H	T	*	CAP	CAP	RATIO	CUM/H	
8.00	3.98	43476.	190890.	168.55	693.01	*	221.47	.1009	697.18	192087.	9.75	*	987.	222.	2.313	1.16	5.450
10.00	4.23	45353.	191720.	175.14	692.20	*	221.06	.0888	700.92	194231.	13.67	*	1003.	206.	2.175	1.11	5.868
12.00	4.49	47237.	192543.	181.71	691.41	*	220.69	.0765	704.54	196351.	17.55	*	1019.	190.	2.048	1.06	6.351
14.00	4.77	49129.	193359.	188.25	690.66	*	220.37	.0639	708.06	198448.	21.37	*	1034.	175.	1.930	1.01	6.913
16.00	5.06	51028.	194168.	194.77	689.93	*	220.10	.0512	711.48	200522.	25.14	*	1049.	160.	1.820	.96	7.576
18.00	5.36	52935.	194970.	201.26	689.23	*	219.87	.0381	714.79	202574.	28.86	*	1065.	144.	1.718	.92	8.370
20.00	5.67	54851.	195764.	207.74	688.55	*	219.68	.0248	718.01	204603.	32.53	*	1080.	129.	1.623	.87	9.339
22.00	6.00	56775.	196550.	214.20	687.89	*	219.54	.0113	721.13	206610.	36.16	*	1094.	115.	1.535	.83	10.546
24.00	6.34	58708.	197327.	220.64	687.26	*	219.46	-.0026	724.16	208595.	39.75	*	1109.	100.	1.452	.80	12.091
26.00	6.69	60651.	198095.	227.07	686.64	*	219.46	-.0167	727.11	210558.	43.29	*	1124.	86.	1.375	.76	14.140
28.00	7.06	62604.	198854.	233.48	686.03	*	219.46	-.0312	729.97	212499.	46.79	*	1138.	71.	1.303	.73	16.987
30.00	7.45	64568.	199604.	239.89	685.44	*	219.46	-.0460	732.75	214419.	50.25	*	1152.	57.	1.236	.70	21.210
32.00	7.85	66542.	200343.	246.28	684.86	*	219.46	-.0612	735.45	216317.	53.67	*	1166.	43.	1.173	.67	28.123
34.00	8.26	68528.	201071.	252.66	684.30	*	219.46	-.0768	738.07	218194.	57.05	*	1180.	29.	1.114	.64	41.499
36.00	8.69	70526.	201788.	259.04	683.73	*	219.46	-.0928	740.62	220048.	60.38	*	1194.	15.	1.059	.61	78.244

SUMMARY OF RANGE OF POSSIBLE EVAPORATOR CONDITIONS ASSUMING 60% COMPRESSOR ISENTROPIC EFFICIENCY
COND. PRESS= 9.2 COND. TEMP= 38.28 ENT. H= 222141. ENT. S= 743.44 LEAV. TEMP= 23.63 LEAV. H= 58351. LEAV. S= 219.46

		EVAPORATOR				*	ENTRY		EXIT			*	EVAP	COMP	PRESS	VDOT	COPH
TEMP	PRESS	H(X=0)	H(X=1)	S(X=0)	S(X=1)	*	S	X	S	H	T	*	CAP	CAP	RATIO	CUM/H	
2.00	3.29	37884.	188363.	148.62	695.66	*	223.03	.1360	696.44	188570.	2.33	*	961.	248.	2.795	1.39	4.879
4.00	3.51	39742.	189211.	155.29	694.74	*	222.46	.1245	699.73	190599.	6.11	*	976.	233.	2.621	1.32	5.193
6.00	3.74	41606.	190054.	161.94	693.86	*	221.94	.1128	702.92	192606.	9.83	*	991.	218.	2.461	1.25	5.546
8.00	3.98	43476.	190890.	168.55	693.01	*	221.47	.1009	706.02	194592.	13.51	*	1006.	203.	2.313	1.19	5.945
10.00	4.23	45353.	191720.	175.14	692.20	*	221.06	.0888	709.02	196556.	17.14	*	1020.	189.	2.175	1.13	6.402
12.00	4.49	47237.	192543.	181.71	691.41	*	220.69	.0765	711.94	198500.	20.73	*	1035.	175.	2.048	1.07	6.928
14.00	4.77	49129.	193359.	188.25	690.66	*	220.37	.0639	714.77	200422.	24.27	*	1049.	160.	1.930	1.02	7.541
16.00	5.06	51028.	194168.	194.77	689.93	*	220.10	.0512	717.53	202323.	27.77	*	1063.	146.	1.820	.97	8.265
18.00	5.36	52935.	194970.	201.26	689.23	*	219.87	.0381	720.20	204204.	31.22	*	1077.	132.	1.718	.93	9.131
20.00	5.67	54851.	195764.	207.74	688.55	*	219.68	.0248	722.80	206064.	34.64	*	1090.	119.	1.623	.88	10.188
22.00	6.00	56775.	196550.	214.20	687.89	*	219.54	.0113	725.33	207904.	38.02	*	1104.	105.	1.535	.84	11.505
24.00	6.34	58708.	197327.	220.64	687.26	*	219.46	-.0026	727.78	209724.	41.35	*	1117.	92.	1.452	.80	13.190
26.00	6.69	60651.	198095.	227.07	686.64	*	219.46	-.0167	730.17	211523.	44.65	*	1131.	78.	1.375	.77	15.425
28.00	7.06	62604.	198854.	233.48	686.03	*	219.46	-.0312	732.49	213303.	47.92	*	1144.	65.	1.303	.73	18.531
30.00	7.45	64568.	199604.	239.89	685.44	*	219.46	-.0460	734.74	215062.	51.14	*	1157.	52.	1.236	.70	23.138
32.00	7.85	66542.	200343.	246.28	684.86	*	219.46	-.0612	736.94	216803.	54.34	*	1170.	39.	1.173	.67	30.680
34.00	8.26	68528.	201071.	252.66	684.30	*	219.46	-.0768	739.07	218523.	57.50	*	1182.	27.	1.114	.64	45.272
36.00	8.69	70526.	201788.	259.04	683.73	*	219.46	-.0928	741.14	220222.	60.62	*	1195.	14.	1.059	.61	85.357

Table A-6.14(c): Summary of range of possible evaporator conditions for Run 40

****** TUBE-BESIDE-TUBE CONDENSER SIMULATION ****** ASSUME TUBE WALLS HAVE INFINITE CONDUCTIVITY ******
GEOMETRY: SUBCOOLER 7.50M OF 5.75MM OD. CONDENSER: 7.50M OF 5.75MM OD. WATER SIDE 7.65MM OD. ALL WALLS .74MM THICK.
BOND CNDCTNCE 500.0W/M.C THML PWR 1084.1W. WATER IN 22.4C. HOT GAS 66.2C. DEW POINT 42.2C. SUBCLD LIQD 31.3C.

ITERATION NUMBER: 12 USED I= 150 SEGMENTS. TRIAL WATER EXIT TEMP: 42.6027 CORRESPONDING TO TW(I)= 22.2758 & TR(I)= 30.4527

EXIT WATER TEMP 42.60C. FLOW RATE 12.8446 GRAM/SEC. WATER PRESS DROP .2391 BAR. PUMP PWR .3071 WATT (OR .0283%)
REFRIGERANT MASS FLOW RATE 6.926E+00 GRAM/SEC

SEPARATE RESULTS FOR THE THREE SEGMENTS	SUPE RHEAT	TWO-PHASE	SUBCOOLER	TOTAL/AVERAGE
LENGTH OF EACH SEGMENT IN METRES	1.9750E+00	1.2800E+01	2.2500E-01	1.5000E+01
MASS OF REFRIGERANT IN KG.	1.5707E-03	3.7767E-02	3.6766E-03	4.3014E-02
REFRIG SIDE HEAT TRANS COEFNT: W/SQ M C.	8.3326E+02	4.9666E+03	1.0581E+03	4.3634E+03
REFRIG SIDE LINEAR H.T.C.: W/M C.	1.1136E+01	6.6291E+01	1.4195E+01	5.8242E+01
REFRIGERANT SIDE REYNOLDS NUMBER	1.4797E+05	3.9131E+03	1.0039E+04	2.3202E+04
WATER SIDE HEAT TRANS COEFNT: W/SQ M C.	2.7235E+03	2.1965E+03	1.4195E+03	2.2564E+03
WATER SIDE LINEAR H.T.C. W/M C.	4.7200E+01	3.7772E+01	2.5197E+01	3.8862E+01
WATER SIDE REYNOLDS NUMBER	4.5603E+03	3.9976E+03	3.0327E+03	4.0512E+03
OVERALL LINEAR CONDUCTANCE: W/M C	8.9974E+00	2.3464E+01	9.0797E+00	2.1343E+01
NO. OF HEAT TRANSFER UNITS REFRIG. SIDE	3.3332	.1314	.2646	3.7292
NO. OF HEAT TRANSFER UNITS WATER SIDE	.3355	5.5961	.0338	5.9654
EFFECTIVENESS OF EACH SEGMENT (PERCENT)	95.4828	93.7198	22.9376	70.7134
REFRIGERANT SIDE PRESSURE DROP IN BAR	2.0144E-01	1.7388E+00	5.4163E-03	1.9457E+00
THERMAL POWER PICK-UP BY WATER (W & %)	132.4(12.1)	942.2(86.3)	16.7(1.5)	1091.3
THERMAL POWER TRANSFERRED BY R12 (W & %)	130.1(11.9)	943.5(86.5)	16.7(1.5)	1090.2
TOTAL MAX THERMAL POWER WITHOUT LOSS (W)	130.08	943.45	16.68	1090.20
THERMAL POWER LOSS FROM FREON (W & %)	.0000	.0000	.0000	.00(.0)
SPECIFIC ENTHALPY OF REFRIG (J/KG)	2.2241E+05	2.0363E+05	6.7421E+04	6.5014E+04
SPECIFIC ENTROPY OF R12 (J/KG.C)	7.3854E+02	6.8226E+02	2.4911E+02	2.4133E+02
REFRIGERANT TEMPERATURE (DEG.C)	6.6166E+01	4.1310E+01	3.2887E+01	3.0453E+01
REFRIGERANT PRESSURE (BAR)	1.0132E+01	9.9308E+00	8.1920E+00	8.1866E+00
WATER TEMPERATURE (DEG.C)	4.2603E+01	4.0135E+01	2.2586E+01	2.2276E+01

RATE OF LOSS OF ENTHALPY BY R12 1.0902E+03 WATTS RATE OF GAIN OF ENTHALPY BY WATER 1.0913E+03 WATTS
CORRESPONDING TO AN ENERGY IMBALANCE OF 1.0499E+00 WATTS OR .0968 % OF SPECIFIED POWER

THE POWER LOSS BY R12 TO OUTSIDE -6.0786E+00WATTS BY -.5607 % OF THE SPECIFIED POWER
THE POWER LOSS BY WATER TO OUTSIDE -7.1285E+00 WATTS BY -.6575 % OF THE SPECIFIED POWER

RATE OF LOSS OF ENTROPY BY R12 3.4438E+00 WATTS/C RATE OF INCREASE OF ENTROPY BY WATER 3.5723E+00 WATTS/C
NET RATE OF ENTROPY FLOW THRU SYSTEM BOUNDARY 1.2848E-01 WATT/C THERMAL ENTROPY CREATION RATE 6.5582E-02 WATT/C
R12 P.D. ENTROPY CREATION RATE 6.2902E-02 WATT/C RATE OF LOSS OF GROSS WORK 4.0517E+01 WATTS AT 42.20 C

RATE OF ENTROPY GAIN OF WATER HAD IT BEEN 10C HOTTER 3.4557E+00 WATTS/C. FOR SAME GROSS RATE OF ENTROPY INCREASE,
A COUNTER-FLOW WATER-WATER HEAT EXCHANGER WOULD HAVE DELTA-T OF 11.0207 DEG C CORRESPONDING TO AN EFFECTIVENESS OF 64.84%
OR 1.844 HEAT TRANSFER UNITS, WHICH IS 30.92 % OF THAT FOR THE WATER SIDE OF THE PRESENT HT.XR.

Table A-6.15(a): Results in three segments for Run 44

LNTH	TR(I)	PR(I)	TW(I)	PW(I)	TWL(I)	X(I)	HR(I)	NTUR(I)	UR(I)	HW(I)	NTUW(I)	UW(I	UL(I)
.00	66.17	10.13	42.60	0.00E+00	54.38	100.00	8.50E+02	1.77E-01	1.14E+01	2.71E+03	1.72E-02	4.81E+01	9.22E+00
.20	58.93	10.11	41.90	3.84E-03	45.32	100.00	8.77E+02	1.79E-01	1.18E+01	2.66E+03	1.76E-02	4.72E+01	9.42E+00
.40	53.77	10.09	41.39	7.68E-03	43.89	100.00	8.55E+02	1.72E-01	1.15E+01	2.56E+03	1.71E-02	4.55E+01	9.17E+00
.60	50.02	10.07	41.02	1.36E-02	42.65	100.00	8.40E+02	1.68E-01	1.13E+01	2.54E+03	1.68E-02	4.50E+01	9.02E+00
.80	47.42	10.05	40.76	1.74E-02	42.08	100.00	8.26E+02	1.64E-01	1.11E+01	2.52E+03	1.66E-02	4.47E+01	8.88E+00
1.00	45.53	10.03	40.57	2.12E-02	41.45	100.00	8.55E+02	1.73E-01	1.12E+01	3.76E+03	1.75E-02	5.91E+01	9.41E+00
1.20	44.10	10.01	40.42	2.71E-02	41.15	100.00	8.10E+02	1.60E-01	1.09E+01	2.49E+03	1.63E-02	4.42E+01	8.72E+00
1.40	43.08	9.99	40.32	3.08E-02	40.86	100.00	8.04E+02	1.58E-01	1.08E+01	2.49E+03	1.62E-02	4.41E+01	8.67E+00
1.60	42.30	9.97	40.24	3.67E-02	40.60	100.00	8.00E+02	1.57E-01	1.07E+01	2.48E+03	1.61E-02	4.40E+01	8.63E+00
1.80	41.73	9.95	40.18	4.04E-02	40.48	100.00	7.96E+02	1.56E-01	1.07E+01	2.48E+03	1.60E-02	4.39E+01	8.59E+00

LNTH	TR(I)	PR(I)	TW(I)	PW(I)	TWL(I)	X(I)	HR(I)	NTUR(I)	UR(I)	HW(I)	NTUW(I)	UW(I	UL(I)
2.00	41.31	9.93	40.13	4.42E-02	40.34	99.96	9.06E+02	0.00E+00	1.19E+01	3.71E+03	1.84E-02	5.84E+01	9.86E+00
2.20	41.26	9.90	40.08	5.00E-02	40.46	99.67	2.10E+03	0.00E+00	2.82E+01	2.47E+03	3.20E-02	4.38E+01	1.71E+01
2.40	41.16	9.88	40.00	5.38E-02	40.52	99.20	3.23E+03	0.00E+00	4.33E+01	2.46E+03	4.05E-02	4.37E+01	2.17E+01
2.60	41.05	9.85	39.89	5.96E-02	40.46	98.57	4.68E+03	0.00E+00	6.28E+01	2.45E+03	4.80E-02	4.36E+01	2.57E+01
2.80	40.95	9.83	39.77	6.33E-02	40.51	97.88	6.18E+03	0.00E+00	8.29E+01	2.45E+03	5.31E-02	4.34E+01	2.85E+01
3.00	40.85	9.80	39.64	6.70E-02	40.46	97.11	8.10E+03	0.00E+00	1.06E+02	3.59E+03	6.87E-02	5.64E+01	3.68E+01
3.20	40.74	9.78	39.48	7.27E-02	40.37	96.19	7.64E+03	0.00E+00	1.02E+02	2.43E+03	5.65E-02	4.31E+01	3.03E+01
3.40	40.63	9.75	39.34	7.64E-02	40.24	95.33	7.38E+03	0.00E+00	9.90E+01	2.41E+03	5.58E-02	4.29E+01	2.99E+01
3.60	40.51	9.72	39.17	8.21E-02	40.04	94.37	7.16E+03	0.00E+00	9.60E+01	2.40E+03	5.51E-02	4.27E+01	2.95E+01
3.80	40.39	9.70	39.02	8.58E-02	39.97	93.49	7.00E+03	0.00E+00	9.39E+01	2.39E+03	5.45E-02	4.25E+01	2.92E+01
4.00	40.27	9.67	38.86	8.94E-02	39.82	92.59	7.17E+03	0.00E+00	9.39E+01	3.51E+03	6.48E-02	5.52E+01	3.48E+01
4.20	40.14	9.64	38.69	9.51E-02	39.68	91.58	6.74E+03	0.00E+00	9.04E+01	2.37E+03	5.35E-02	4.20E+01	2.87E+01
4.40	40.02	9.61	38.53	9.87E-02	39.54	90.66	6.64E+03	0.00E+00	8.90E+01	2.36E+03	5.31E-02	4.18E+01	2.85E+01
4.60	39.88	9.57	38.35	1.04E-01	39.32	89.62	6.54E+03	0.00E+00	8.77E+01	2.34E+03	5.26E-02	4.16E+01	2.82E+01
4.80	39.75	9.54	38.18	1.08E-01	39.24	88.67	6.48E+03	0.00E+00	8.70E+01	2.33E+03	5.23E-02	4.14E+01	2.80E+01
5.00	39.61	9.51	38.02	1.11E-01	39.09	87.70	6.72E+03	0.00E+00	8.80E+01	3.42E+03	6.23E-02	5.38E+01	3.34E+01
5.20	39.47	9.48	37.83	1.17E-01	38.94	86.61	6.37E+03	0.00E+00	8.55E+01	2.31E+03	5.16E-02	4.09E+01	2.77E+01
5.40	39.33	9.45	37.65	1.21E-01	38.79	85.61	6.32E+03	0.00E+00	8.48E+01	2.29E+03	5.13E-02	4.07E+01	2.75E+01
5.60	39.18	9.41	37.46	1.26E-01	38.54	84.49	6.27E+03	0.00E+00	8.40E+01	2.28E+03	5.09E-02	4.05E+01	2.73E+01
5.80	39.04	9.38	37.28	1.30E-01	38.47	83.45	6.22E+03	0.00E+00	8.34E+01	2.27E+03	5.06E-02	4.02E+01	2.71E+01
6.00	38.90	9.34	37.09	1.33E-01	38.29	82.40	6.45E+03	0.00E+00	8.45E+01	3.33E+03	6.02E-02	5.23E+01	3.23E+01
6.20	38.74	9.31	36.89	1.38E-01	38.14	81.23	6.12E+03	0.00E+00	8.21E+01	2.24E+03	4.99E-02	3.97E+01	2.68E+01
6.40	38.59	9.27	36.70	1.42E-01	37.97	80.14	6.07E+03	0.00E+00	8.14E+01	2.23E+03	4.96E-02	3.95E+01	2.66E+01
6.60	38.44	9.24	36.48	1.47E-01	37.70	78.92	6.02E+03	0.00E+00	8.07E+01	2.17E+03	4.85E-02	3.84E+01	2.60E+01
6.80	38.29	9.20	36.29	1.51E-01	37.64	77.81	5.97E+03	0.00E+00	8.01E+01	2.15E+03	4.82E-02	3.82E+01	2.59E+01
7.00	38.14	9.17	36.09	1.54E-01	37.46	76.69	6.19E+03	0.00E+00	8.11E+01	3.22E+03	5.82E-02	5.07E+01	3.12E+01
7.20	37.97	9.13	35.86	1.59E-01	37.29	75.41	5.87E+03	0.00E+00	7.87E+01	2.12E+03	4.75E-02	3.77E+01	2.55E+01
7.40	37.82	9.10	35.66	1.63E-01	37.12	74.25	5.82E+03	0.00E+00	7.81E+01	2.11E+03	4.72E-02	3.74E+01	2.53E+01
7.60	37.66	9.06	35.42	1.68E-01	36.82	72.92	5.76E+03	0.00E+00	7.73E+01	2.09E+03	4.68E-02	3.72E+01	2.51E+01
7.80	37.51	9.03	35.21	1.71E-01	36.76	71.70	5.71E+03	0.00E+00	7.66E+01	2.08E+03	4.64E-02	3.69E+01	2.49E+01
8.00	37.35	8.99	34.99	1.75E-01	36.57	70.46	5.92E+03	0.00E+00	7.75E+01	3.05E+03	5.53E-02	4.80E+01	2.97E+01
8.20	37.19	8.96	34.74	1.79E-01	36.39	69.06	5.60E+03	0.00E+00	7.51E+01	2.05E+03	4.56E-02	3.63E+01	2.45E+01
8.40	37.04	8.92	34.51	1.80E-01	36.21	67.77	5.54E+03	0.00E+00	7.43E+01	2.03E+03	4.53E-02	3.61E+01	2.43E+01
8.60	36.87	8.88	34.25	1.84E-01	35.89	66.30	5.48E+03	0.00E+00	7.35E+01	2.01E+03	4.48E-02	3.58E+01	2.41E+01
8.80	36.72	8.85	34.01	1.85E-01	35.83	64.94	5.41E+03	0.00E+00	7.26E+01	2.00E+03	4.44E-02	3.55E+01	2.38E+01
9.00	36.57	8.82	33.76	1.86E-01	35.62	63.54	5.60E+03	0.00E+00	7.33E+01	2.94E+03	5.28E-02	4.62E+01	2.83E+01
9.20	36.41	8.78	33.48	1.90E-01	35.44	61.95	5.28E+03	0.00E+00	7.08E+01	1.96E+03	4.35E-02	3.49E+01	2.34E+01
9.40	36.25	8.75	33.22	1.92E-01	35.25	60.48	5.21E+03	0.00E+00	6.99E+01	1.95E+03	4.31E-02	3.46E+01	2.31E+01
9.60	36.10	8.71	32.93	1.96E-01	34.89	58.80	5.13E+03	0.00E+00	6.88E+01	1.93E+03	4.26E-02	3.42E+01	2.29E+01
9.80	35.95	8.68	32.65	1.97E-01	34.85	57.23	5.05E+03	0.00E+00	6.78E+01	1.91E+03	4.21E-02	3.39E+01	2.26E+01
10.00	35.80	8.65	32.36	1.98E-01	34.62	55.62	5.20E+03	0.00E+00	6.81E+01	2.80E+03	4.99E-02	4.41E+01	2.68E+01
10.20	35.65	8.61	32.04	2.02E-01	34.44	53.78	4.88E+03	0.00E+00	6.55E+01	1.87E+03	4.10E-02	3.32E+01	2.20E+01
10.40	35.51	8.58	31.73	2.03E-01	34.25	52.06	4.79E+03	0.00E+00	6.43E+01	1.82E+03	4.00E-02	3.22E+01	2.15E+01
10.60	35.36	8.55	31.39	2.07E-01	33.82	50.11	4.69E+03	0.00E+00	6.29E+01	1.79E+03	3.94E-02	3.18E+01	2.11E+01
10.80	35.22	8.52	31.07	2.08E-01	33.82	48.29	4.60E+03	0.00E+00	6.16E+01	1.77E+03	3.88E-02	3.15E+01	2.08E+01
11.00	35.09	8.49	30.74	2.09E-01	33.58	46.41	4.70E+03	0.00E+00	6.15E+01	2.60E+03	4.58E-02	4.10E+01	2.46E+01
11.20	34.95	8.46	30.36	2.13E-01	33.38	44.27	4.37E+03	0.00E+00	5.87E+01	1.73E+03	3.76E-02	3.08E+01	2.02E+01
11.40	34.83	8.44	30.01	2.14E-01	33.16	42.26	4.26E+03	0.00E+00	5.71E+01	1.71E+03	3.69E-02	3.04E+01	1.98E+01
11.60	34.70	8.41	29.60	2.18E-01	32.67	39.97	4.12E+03	0.00E+00	5.53E+01	1.69E+03	3.62E-02	3.00E+01	1.94E+01
11.80	34.58	8.38	29.23	2.19E-01	32.69	37.82	3.99E+03	0.00E+00	5.36E+01	1.67E+03	3.55E-02	2.96E+01	1.91E+01
12.00	34.47	8.36	28.84	2.20E-01	32.40	35.59	4.04E+03	0.00E+00	5.29E+01	2.44E+03	4.14E-02	3.84E+01	2.23E+01
12.20	34.36	8.34	28.40	2.21E-01	32.20	33.07	3.74E+03	0.00E+00	5.02E+01	1.62E+03	3.40E-02	2.88E+01	1.83E+01
12.40	34.26	8.32	27.98	2.23E-01	31.96	30.69	3.61E+03	0.00E+00	4.85E+01	1.60E+03	3.33E-02	2.84E+01	1.79E+01
12.60	34.16	8.29	27.51	2.24E-01	31.35	28.00	3.46E+03	0.00E+00	4.64E+01	1.54E+03	3.21E-02	2.74E+01	1.72E+01
12.80	34.08	8.28	27.07	2.25E-01	31.45	25.50	3.31E+03	0.00E+00	4.44E+01	1.52E+03	3.13E-02	2.70E+01	1.68E+01
13.00	34.00	8.26	26.62	2.26E-01	31.11	22.92	3.29E+03	0.00E+00	4.31E+01	2.23E+03	3.60E-02	3.50E+01	1.93E+01
13.20	33.93	8.24	26.12	2.28E-01	30.86	20.04	2.95E+03	0.00E+00	3.96E+01	1.48E+03	2.94E-02	2.63E+01	1.58E+01
13.40	33.86	8.23	25.66	2.29E-01	30.54	17.35	2.75E+03	0.00E+00	3.69E+01	1.46E+03	2.83E-02	2.59E+01	1.52E+01
13.60	33.81	8.22	25.14	2.31E-01	29.73	14.38	2.51E+03	0.00E+00	3.37E+01	1.44E+03	2.71E-02	2.56E+01	1.45E+01
13.80	33.76	8.21	24.67	2.32E-01	29.74	11.63	2.26E+03	0.00E+00	3.04E+01	1.43E+03	2.57E-02	2.53E+01	1.38E+01
14.00	33.73	8.20	24.20	2.33E-01	29.15	8.90	2.08E+03	0.00E+00	2.72E+01	2.07E+03	2.76E-02	3.26E+01	1.48E+01
14.20	33.70	8.20	23.70	2.34E-01	28.67	6.04	1.65E+03	0.00E+00	2.21E+01	1.38E+03	2.16E-02	2.45E+01	1.16E+01
14.40	33.69	8.19	23.29	2.35E-01	27.91	3.55	1.27E+03	0.00E+00	1.71E+01	1.38E+03	1.87E-02	2.46E+01	1.01E+01
14.60	33.68	8.19	22.88	2.37E-01	26.45	1.25	7.60E+02	0.00E+00	1.02E+01	1.40E+03	1.34E-02	2.48E+01	7.23E+00

LNTH	TR(I)	PR(I)	TW(I)	PW(I)	TWL(I)	X(I)	HR(I)	NTUR(I)	UR(I)	HW(I)	NTUW(I)	UW(I	UL(I)
14.80	32.89	8.19	22.59	2.38E-01	25.79	.00	1.05E+03	1.31E-01	1.42E+01	1.41E+03	1.68E-02	2.50E+01	9.03E+00
15.00	30.45	8.19	22.28	2.39E-01	25.21	.00	0.00E+00	0.00E+00	0.00E+00	0.00E+00	0.00E+00	0.00E+00	0.00E+00

Table A-6.15(b): The profiles of parameters for Run 44

SUMMARY OF RANGE OF POSSIBLE EVAPORATOR CONDITIONS ASSUMIMG 50% COMPRESSOR ISENTROPIC EFFICIENCY
COND. PRESS= 10.1 COND. TEMP= 42.20 ENT. H= 222412. ENT. S= 738.54 LEAV. TEMP= 31.34 LEAV. H= 65891. LEAV. S= 244.18

		EVAPORATOR				*	ENTRY		EXIT			*	EVAP	COMP	PRESS	VDOT	COPH
TEMP	PRESS	H(X=0)	H(X=1)	S(X=0)	S(X=1)	*	S	X	S	H	T	*	CAP	CAP	RATIO	CUM/H	
16.00	5.06	51028.	194168.	194.77	689.93	*	246.18	.1038	692.66	195039.	17.14	*	895.	190.	2.004	.86	5.718
18.00	5.36	52935.	194970.	201.26	689.23	*	245.77	.0912	696.85	197273.	21.18	*	910.	174.	1.891	.83	6.226
20.00	5.67	54851.	195764.	207.74	688.55	*	245.41	.0784	700.91	199483.	25.17	*	925.	159.	1.787	.79	6.826
22.00	6.00	56775.	196550.	214.20	687.89	*	245.10	.0652	704.84	201669.	29.11	*	940.	144.	1.689	.76	7.545
24.00	6.34	58708.	197327.	220.64	687.26	*	244.82	.0518	708.66	203830.	32.99	*	955.	129.	1.599	.72	8.423
26.00	6.69	60651.	198095.	227.07	686.64	*	244.59	.0381	712.36	205968.	36.83	*	970.	114.	1.514	.69	9.518
28.00	7.06	62604.	198854.	233.48	686.03	*	244.40	.0241	715.95	208081.	40.61	*	985.	99.	1.435	.66	10.922
30.00	7.45	64568.	199604.	239.89	685.44	*	244.25	.0098	719.43	210172.	44.35	*	999.	85.	1.361	.63	12.787
32.00	7.85	66542.	200343.	246.28	684.86	*	244.18	-.0049	722.80	212236.	48.04	*	1014.	70.	1.291	.61	15.380
34.00	8.26	68528.	201071.	252.66	684.30	*	244.18	-.0199	726.08	214279.	51.68	*	1028.	56.	1.227	.58	19.244
36.00	8.69	70526.	201788.	259.04	683.73	*	244.18	-.0353	729.26	216299.	55.28	*	1042.	42.	1.166	.56	25.601
38.00	9.14	72537.	202493.	265.41	683.18	*	244.18	-.0511	732.35	218296.	58.84	*	1056.	29.	1.109	.54	38.021
40.00	9.60	74562.	203186.	271.78	682.62	*	244.18	-.0674	735.35	220270.	62.35	*	1069.	15.	1.055	.51	73.063

SUMMARY OF RANGE OF POSSIBLE EVAPORATOR CONDITIONS ASSUMIMG 55% COMPRESSOR ISENTROPIC EFFICIENCY
COND. PRESS= 10.1 COND. TEMP= 42.20 ENT. H= 222412. ENT. S= 738.54 LEAV. TEMP= 31.34 LEAV. H= 65891. LEAV. S= 244.18

		EVAPORATOR				*	ENTRY		EXIT			*	EVAP	COMP	PRESS	VDOT	COPH
TEMP	PRESS	H(X=0)	H(X=1)	S(X=0)	S(X=1)	*	S	X	S	H	T	*	CAP	CAP	RATIO	CUM/H	
12.00	4.49	47237.	192543.	181.71	691.41	*	247.14	.1284	694.23	193397.	13.18	*	883.	201.	2.255	.97	5.394
14.00	4.77	49129.	193359.	188.25	690.66	*	246.64	.1162	697.82	195473.	17.00	*	898.	187.	2.124	.92	5.810
16.00	5.06	51028.	194168.	194.77	689.93	*	246.18	.1038	701.29	197527.	20.77	*	912.	172.	2.004	.88	6.290
18.00	5.36	52935.	194970.	201.26	689.23	*	245.77	.0912	704.67	199559.	24.50	*	926.	158.	1.891	.84	6.849
20.00	5.67	54851.	195764.	207.74	688.55	*	245.41	.0784	707.94	201568.	28.17	*	940.	144.	1.787	.80	7.509
22.00	6.00	56775.	196550.	214.20	687.89	*	245.10	.0652	711.13	203555.	31.80	*	954.	131.	1.689	.77	8.300
24.00	6.34	58708.	197327.	220.64	687.26	*	244.82	.0518	714.21	205520.	35.39	*	967.	117.	1.599	.73	9.266
26.00	6.69	60651.	198095.	227.07	686.64	*	244.59	.0381	717.21	207463.	38.93	*	981.	104.	1.514	.70	10.470
28.00	7.06	62604.	198854.	233.48	686.03	*	244.40	.0241	720.13	209384.	42.44	*	994.	90.	1.435	.67	12.014
30.00	7.45	64568.	199604.	239.89	685.44	*	244.25	.0098	722.96	211284.	45.90	*	1007.	77.	1.361	.64	14.065
32.00	7.85	66542.	200343.	246.28	684.86	*	244.18	-.0049	725.70	213161.	49.31	*	1020.	64.	1.291	.61	16.918
34.00	8.26	68528.	201071.	252.66	684.30	*	244.18	-.0199	728.37	215018.	52.69	*	1033.	51.	1.227	.59	21.168
36.00	8.69	70526.	201788.	259.04	683.73	*	244.18	-.0353	730.96	216854.	56.04	*	1046.	39.	1.166	.56	28.162
38.00	9.14	72537.	202493.	265.41	683.18	*	244.18	-.0511	733.48	218670.	59.34	*	1058.	26.	1.109	.54	41.823
40.00	9.60	74562.	203186.	271.78	682.62	*	244.18	-.0674	735.93	220465.	62.61	*	1071.	13.	1.055	.51	80.369

SUMMARY OF RANGE OF POSSIBLE EVAPORATOR CONDITIONS ASSUMIMG 60% COMPRESSOR ISENTROPIC EFFICIENCY
COND. PRESS= 10.1 COND. TEMP= 42.20 ENT. H= 222412. ENT. S= 738.54 LEAV. TEMP= 31.34 LEAV. H= 65891. LEAV. S= 244.18

		EVAPORATOR				*	ENTRY		EXIT			*	EVAP	COMP	PRESS	VDOT	COPH
TEMP	PRESS	H(X=0)	H(X=1)	S(X=0)	S(X=1)	*	S	X	S	H	T	*	CAP	CAP	RATIO	CUM/H	
8.00	3.98	43476.	190890.	168.55	693.01	*	248.30	.1521	696.67	191945.	9.54	*	873.	211.	2.546	1.09	5.137
10.00	4.23	45353.	191720.	175.14	692.20	*	247.69	.1403	699.73	193891.	13.17	*	887.	198.	2.395	1.04	5.488
12.00	4.49	47237.	192543.	181.71	691.41	*	247.14	.1284	702.70	195815.	16.76	*	900.	184.	2.255	.99	5.885
14.00	4.77	49129.	193359.	188.25	690.66	*	246.64	.1162	705.58	197718.	20.30	*	913.	171.	2.124	.94	6.338
16.00	5.06	51028.	194168.	194.77	689.93	*	246.18	.1038	708.38	199601.	23.80	*	926.	158.	2.004	.89	6.862
18.00	5.36	52935.	194970.	201.26	689.23	*	245.77	.0912	711.10	201463.	27.26	*	939.	145.	1.891	.85	7.471
20.00	5.67	54851.	195764.	207.74	688.55	*	245.41	.0784	713.74	203305.	30.67	*	952.	132.	1.787	.81	8.191
22.00	6.00	56775.	196550.	214.20	687.89	*	245.10	.0652	716.31	205126.	34.05	*	964.	120.	1.689	.77	9.055
24.00	6.34	58708.	197327.	220.64	687.26	*	244.82	.0518	718.80	206927.	37.39	*	977.	107.	1.599	.74	10.108
26.00	6.69	60651.	198095.	227.07	686.64	*	244.59	.0381	721.23	208708.	40.69	*	989.	95.	1.514	.71	11.422
28.00	7.06	62604.	198854.	233.48	686.03	*	244.40	.0241	723.58	210470.	43.96	*	1001.	83.	1.435	.67	13.106
30.00	7.45	64568.	199604.	239.89	685.44	*	244.25	.0098	725.88	212212.	47.19	*	1013.	71.	1.361	.64	15.344
32.00	7.85	66542.	200343.	246.28	684.86	*	244.18	-.0049	728.10	213932.	50.38	*	1025.	59.	1.291	.62	18.456
34.00	8.26	68528.	201071.	252.66	694.30	*	244.18	-.0199	730.27	215634.	53.54	*	1037.	47.	1.227	.59	23.092
36.00	8.69	70526.	201789.	259.04	683.73	*	244.19	-.0353	732.37	217318.	56.67	*	1049.	35.	1.166	.56	30.722
38.00	9.14	72537.	202493.	265.41	683.18	*	244.19	-.0511	734.42	218982.	59.77	*	1060.	24.	1.109	.54	45.625
40.00	9.60	74562.	203186.	271.79	682.62	*	244.19	-.0674	736.41	220627.	62.83	*	1072.	12.	1.055	.52	87.675

Table A-6.15(c): Summary of range of possible evaporator conditions for Runs 44

****** TUBE-BESIDE-TUBE CONDENSER SIMULATION ****** ASSUME TUBE WALLS HAVE INFINITE CONDUCTIVITY ******
GEOMETRY: SUBCOOLER 7.50M OF 5.75MM OD. CONDENSER: 7.50M OF 5.75MM OD. WATER SIDE 7.65MM OD. ALL WALLS .74MM THICK.
BOND CNDCTNCE 500.0W/M.C THML PWR 993.4W. WATER IN 25.9C. HOT GAS 72.5C. DEW POINT 48.2C. SUBCLD LIQD 39.2C.

ITERATION NUMBER: 15 USED I= 151 SEGMENTS. TRIAL WATER EXIT TEMP: 49.6620 CORRESPONDING TO TW(I)= 25.7862 & TR(I)= 38.3593

EXIT WATER TEMP 49.66C. FLOW RATE 10.0284 GRAM/SEC. WATER PRESS DROP .0870 BAR. PUMP PWR .0872 WATT (OR .0088%)
REFRIGERANT MASS FLOW RATE 6.560E+00 GRAM/SEC

SEPARATE RESULTS FOR THE THREE SEGMENTS	SUPE RHEAT	TWO-PHASE	SUBCOOLER	TOTAL/AVERAGE
LENGTH OF EACH SEGMENT IN METRES	2.3750E+00	1.2500E+01	1.2500E-01	1.5000E+01
MASS OF REFRIGERANT IN KG.	2.1878E-03	3.3256E-02	3.5796E-03	3.9023E-02
REFRIG SIDE HEAT TRANS COEFNT: W/SQ M C.	8.0601E+02	4.6804E+03	1.0146E+03	4.0161E+03
REFRIG SIDE LINEAR H.T.C.: W/M C.	1.0767E+01	6.2472E+01	1.3610E+01	5.3607E+01
REFRIGERANT SIDE REYNOLDS NUMBER	1.3557E+05	3.1645E+03	1.0076E+04	2.4301E+04
WATER SIDE HEAT TRANS COEFNT: W/SQ M C.	1.9355E+03	1.6053E+03	1.0722E+03	1.6507E+03
WATER SIDE LINEAR H.T.C. W/M C.	3.3474E+01	2.7617E+01	1.9032E+01	2.8434E+01
WATER SIDE REYNOLDS NUMBER	3.9865E+03	3.5483E+03	2.5824E+03	3.6051E+03
OVERALL LINEAR CONDUCTANCE: W/M C	8.1341E+00	1.8646E+01	7.9350E+00	1.6834E+01
NO. OF HEAT TRANSFER UNITS REFRIG. SIDE	3.6906	.1171	.2375	4.0452
NO. OF HEAT TRANSFER UNITS WATER SIDE	.4663	5.5658	.0378	6.0700
EFFECTIVENESS OF EACH SEGMENT (PERCENT)	96.4977	95.7121	20.8165	71.0087
REFRIGERANT SIDE PRESSURE DROP IN BAR	1.8639E-01	1.3993E+00	5.0006E-03	1.5907E+00
THERMAL POWER PICK-UP BY WATER (W & %)	129.8(13.0)	848.3(84.8)	22.1(2.2)	1000.2
THERMAL POWER TRANSFERRED BY R12 (W & %)	127.9(12.8)	848.9(85.0)	22.0(2.2)	998.8
TOTAL MAX THERMAL POWER WITHOUT LOSS (W)	127.94	848.88	22.03	998.85
THERMAL POWER LOSS FROM FREON (W & %)	.0000	.0000	.0000	.00(.0)
SPECIFIC ENTHALPY OF REFRIG (J/KG)	2.2515E+05	2.0565E+05	7.6257E+04	7.2900E+04
SPECIFIC ENTROPY OF R12 (J/KG.C)	7.3822E+02	6.8055E+02	2.7708E+02	2.6655E+02
REFRIGERANT TEMPERATURE (DEG.C)	7.2462E+01	4.7468E+01	4.1665E+01	3.8359E+01
REFRIGERANT PRESSURE (BAR)	1.1684E+01	1.1498E+01	1.0098E+01	1.0093E+01
WATER TEMPERATURE (DEG.C)	4.9662E+01	4.6561E+01	2.6313E+01	2.5786E+01

RATE OF LOSS OF EHTHALPY BY R12 9.9885E+02 WATTS RATE OF GAIN OF ENTHALPY BY WATER 1.0002E+03 WATTS
CORRESPONDING TO AN ENERGY IMBALANCE OF 1.3541E+00 WATTS OR .1363 % OF SPECIFIED POWER

THE POWER LOSS BY R12 TO OUTSIDE -5.3980E+00WATTS BY -.5434 % OF THE SPECIFIED POWER
THE POWER LOSS BY WATER TO OUTSIDE -6.7521E+00 WATTS BY -.6797 % OF THE SPECIFIED POWER

RATE OF LOSS OF ENTROPY BY R12 3.0943E+00 WATTS/C RATE OF INCREASE OF ENTROPY BY WATER 3.2190E+00 WATTS/C
NET RATE OF ENTROPY FLOW THRU SYSTEM BOUNDARY 1.2463E-01 WATT/C THERMAL ENTROPY CREATION RATE 7.9165E-02 WATT/C
R12 P.D. ENTROPY CREATION RATE 4.5463E-02 WATT/C RATE OF LOSS OF GROSS WORK 4.0047E+01 WATTS AT 48.18 C

RATE OF ENTROPY GAIN OF WATER HAD IT BEEN 10C HOTTER 3.1168E+00 WATTS/C. FOR SAME GROSS RATE OF ENTROPY INCREASE,
A COUNTER-FLOW WATER-WATER HEAT EICHANGER WOULD HAVE DELTA-T OF 12.2004 DEG C CORRESPONDING TO AN EFFECTIVENESS OF 66.18%
OR 1.957 HEAT TRANSFER UNITS, WHICH IS 32.24 % OF THAT FOR THE WATER SIDE OF THE PRESENT HT.XR.

Table A-6.16(a): Results in three segments for Run 58

LNTH	TR(I)	PR(I)	TW(I)	PW(I)	TWL(I)	X(I)	HR(I)	NTUR(I)	UR(I)	HW(I)	NTUW(I)	UW(I	UL(I)
.00	72.46	11.68	49.66	0.00E+00	61.06	100.00	8.22E+02	1.65E-01	1.10E+01	1.91E+03	1.99E-02	3.39E+01	8.33E+00
[illegible]	65.89	11.67	48.87	1.99E-03	53.18	100.00	8.39E+02	1.64E-01	1.13E+01	1.87E+03	2.01E-02	3.32E+01	8.41E+00
.40	61.06	11.65	48.28	2.75E-03	51.51	100.00	8.24E+02	1.60E-01	1.10E+01	1.84E+03	1.97E-02	3.27E+01	8.26E+00
.60	57.40	11.63	47.82	5.22E-03	50.02	100.00	8.14E+02	1.56E-01	1.09E+01	1.82E+03	1.95E-02	3.23E+01	8.16E+00
.80	54.80	11.62	47.50	5.97E-03	49.33	100.00	8.03E+02	1.53E-01	1.08E+01	1.80E+03	1.93E-02	3.20E+01	8.06E+00
1.00	52.84	11.60	47.25	6.72E-03	48.55	100.00	8.33E+02	1.62E-01	1.09E+01	2.62E+03	2.06E-02	4.12E+01	8.63E+00
1.20	51.32	11.59	47.05	8.17E-03	48.13	100.00	7.91E+02	1.49E-01	1.06E+01	1.78E+03	1.90E-02	3.16E+01	7.95E+00
1.40	50.20	11.57	46.91	9.92E-03	47.74	100.00	7.87E+02	1.48E-01	1.06E+01	1.78E+03	1.89E-02	3.15E+01	7.91E+00
1.60	49.32	11.56	46.80	1.24E-02	47.37	100.00	7.85E+02	1.47E-01	1.05E+01	1.77E+03	1.88E-02	3.14E+01	7.89E+00
1.80	48.67	11.54	46.72	1.31E-02	47.20	100.00	7.82E+02	1.46E-01	1.05E+01	1.77E+03	1.88E-02	3.14E+01	7.86E+00
2.00	48.16	11.53	46.65	1.38E-02	47.00	100.00	8.15E+02	1.56E-01	1.07E+01	2.58E+03	2.02E-02	4.06E+01	8.45E+00
2.20	47.76	11.51	46.60	1.63E-02	46.90	100.00	7.78E+02	1.44E-01	1.04E+01	1.72E+03	1.86E-02	3.06E+01	7.78E+00

LNTH	TR(I)	PR(I)	TW(I)	PW(I)	TWL(I)	X(I)	HR(I)	NTUR(I)	UR(I)	HW(I)	NTUW(I)	UW(I	UL(I)
2.40	47.47	11.50	46.56	1.70E-02	46.79	99.98	5.79E+02	0.00E+00	7.76E+00	1.72E+03	1.48E-02	3.05E+01	6.19E+00
2.60	47.42	11.48	46.52	1.94E-02	46.77	99.81	1.48E+03	0.00E+00	1.99E+01	1.72E+03	2.87E-02	3.05E+01	1.20E+01
2.80	47.34	11.46	46.47	2.02E-02	46.86	99.55	2.11E+03	0.00E+00	2.83E+01	1.72E+03	3.51E-02	3.05E+01	1.47E+01
3.00	47.27	11.44	46.40	2.09E-02	46.85	99.23	2.90E+03	0.00E+00	3.80E+01	2.57E+03	4.67E-02	4.04E+01	1.96E+01
3.20	47.19	11.42	46.33	2.34E-02	46.83	98.84	3.59E+03	0.00E+00	4.82E+01	1.71E+03	4.45E-02	3.04E+01	1.86E+01
3.40	47.12	11.40	46.24	2.41E-02	46.80	98.45	4.39E+03	0.00E+00	5.89E+01	1.71E+03	4.78E-02	3.03E+01	2.00E+01
3.60	47.04	11.38	46.15	2.65E-02	46.71	97.97	5.32E+03	0.00E+00	7.13E+01	1.70E+03	5.07E-02	3.02E+01	2.12E+01
3.80	46.97	11.36	46.05	2.72E-02	46.71	97.50	6.19E+03	0.00E+00	8.30E+01	1.70E+03	5.28E-02	3.01E+01	2.21E+01
4.00	46.89	11.34	45.95	2.80E-02	46.65	97.01	7.40E+03	0.00E+00	9.68E+01	2.54E+03	6.75E-02	3.99E+01	2.83E+01
4.20	46.81	11.31	45.83	3.04E-02	46.57	96.41	6.87E+03	0.00E+00	9.22E+01	1.69E+03	5.40E-02	3.00E+01	2.26E+01
4.40	46.73	11.29	45.73	3.11E-02	46.48	95.87	6.71E+03	0.00E+00	9.00E+01	1.68E+03	5.36E-02	2.99E+01	2.24E+01
4.60	46.65	11.27	45.60	3.35E-02	46.34	95.25	6.56E+03	0.00E+00	8.79E+01	1.68E+03	5.32E-02	2.98E+01	2.23E+01
4.80	46.57	11.25	45.48	3.42E-02	46.29	94.68	6.44E+03	0.00E+00	8.64E+01	1.67E+03	5.28E-02	2.97E+01	2.21E+01
5.00	46.48	11.23	45.37	3.49E-02	46.19	94.10	6.62E+03	0.00E+00	8.67E+01	2.50E+03	6.46E-02	3.93E+01	2.70E+01
5.20	46.39	11.20	45.23	3.73E-02	46.09	93.43	6.24E+03	0.00E+00	8.37E+01	1.66E+03	5.21E-02	2.95E+01	2.18E+01
5.40	46.31	11.18	45.10	3.80E-02	45.99	92.81	6.16E+03	0.00E+00	8.26E+01	1.66E+03	5.18E-02	2.94E+01	2.17E+01
5.60	46.21	11.16	44.96	4.04E-02	45.82	92.10	6.08E+03	0.00E+00	8.15E+01	1.65E+03	5.15E-02	2.93E+01	2.15E+01
5.80	46.12	11.13	44.83	4.11E-02	45.78	91.44	6.01E+03	0.00E+00	8.06E+01	1.64E+03	5.12E-02	2.92E+01	2.14E+01
6.00	46.03	11.11	44.69	4.18E-02	45.66	90.77	6.21E+03	0.00E+00	8.13E+01	2.45E+03	6.25E-02	3.86E+01	2.62E+01
6.20	45.93	11.08	44.53	4.42E-02	45.56	89.99	5.88E+03	0.00E+00	7.89E+01	1.63E+03	5.06E-02	2.90E+01	2.12E+01
6.40	45.83	11.06	44.39	4.49E-02	45.44	89.27	5.82E+03	0.00E+00	7.81E+01	1.63E+03	5.03E-02	2.88E+01	2.11E+01
6.60	45.73	11.03	44.22	4.72E-02	45.25	88.44	5.79E+03	0.00E+00	7.77E+01	1.62E+03	5.01E-02	2.87E+01	2.10E+01
6.80	45.63	11.00	44.06	4.79E-02	45.21	87.68	5.75E+03	0.00E+00	7.72E+01	1.61E+03	4.98E-02	2.86E+01	2.09E+01
7.00	45.53	10.98	43.90	4.87E-02	45.08	86.88	5.98E+03	0.00E+00	7.83E+01	2.40E+03	6.09E-02	3.78E+01	2.55E+01
7.20	45.43	10.95	43.71	5.10E-02	44.96	85.96	5.68E+03	0.00E+00	7.61E+01	1.60E+03	4.93E-02	2.83E+01	2.06E+01
7.40	45.33	10.92	43.54	5.17E-02	44.84	85.10	5.64E+03	0.00E+00	7.57E+01	1.59E+03	4.91E-02	2.82E+01	2.05E+01
7.60	45.22	10.89	43.34	5.39E-02	44.62	84.10	5.60E+03	0.00E+00	7.51E+01	1.58E+03	4.88E-02	2.80E+01	2.04E+01
7.80	45.11	10.87	43.15	5.47E-02	44.58	83.17	5.56E+03	0.00E+00	7.46E+01	1.57E+03	4.85E-02	2.79E+01	2.03E+01
8.00	45.01	10.84	42.95	5.54E-02	44.43	82.20	5.77E+03	0.00E+00	7.56E+01	2.34E+03	5.91E-02	3.68E+01	2.48E+01
8.20	44.89	10.81	42.72	5.76E-02	44.30	81.07	5.48E+03	0.00E+00	7.35E+01	1.55E+03	4.79E-02	2.76E+01	2.00E+01
8.40	44.79	10.78	42.50	5.83E-02	44.16	80.01	5.43E+03	0.00E+00	7.29E+01	1.54E+03	4.76E-02	2.74E+01	1.99E+01
8.60	44.67	10.75	42.25	6.05E-02	43.91	78.78	5.39E+03	0.00E+00	7.23E+01	1.53E+03	4.72E-02	2.72E+01	1.98E+01
8.80	44.56	10.73	42.02	6.12E-02	43.87	77.62	5.34E+03	0.00E+00	7.17E+01	1.52E+03	4.69E-02	2.70E+01	1.96E+01
9.00	44.45	10.70	41.77	6.19E-02	43.70	76.41	5.54E+03	0.00E+00	7.25E+01	2.22E+03	5.62E-02	3.49E+01	2.36E+01
9.20	44.34	10.67	41.48	6.41E-02	43.55	75.00	5.24E+03	0.00E+00	7.03E+01	1.50E+03	4.61E-02	2.66E+01	1.93E+01
9.40	44.23	10.64	41.21	6.48E-02	43.40	73.66	5.19E+03	0.00E+00	6.96E+01	1.49E+03	4.57E-02	2.64E+01	1.91E+01
9.60	44.11	10.61	40.89	6.59E-02	43.09	72.10	5.13E+03	0.00E+00	6.88E+01	1.47E+03	4.53E-02	2.62E+01	1.90E+01
9.80	44.00	10.58	40.59	6.65E-02	43.06	70.61	5.07E+03	0.00E+00	6.80E+01	1.46E+03	4.48E-02	2.59E+01	1.88E+01
10.00	43.89	10.56	40.27	6.72E-02	42.87	69.05	5.24E+03	0.00E+00	6.86E+01	2.13E+03	5.37E-02	3.34E+01	2.25E+01
10.20	43.78	10.53	39.91	6.83E-02	42.70	67.24	4.93E+03	0.00E+00	6.62E+01	1.43E+03	4.39E-02	2.54E+01	1.84E+01
10.40	43.67	10.50	39.56	6.89E-02	42.54	65.52	4.86E+03	0.00E+00	6.52E+01	1.39E+03	4.27E-02	2.46E+01	1.79E+01
10.60	43.55	10.47	39.15	6.99E-02	42.13	63.52	4.78E+03	0.00E+00	6.41E+01	1.37E+03	4.21E-02	2.43E+01	1.76E+01
10.80	43.45	10.44	38.77	7.06E-02	42.16	61.63	4.70E+03	0.00E+00	6.31E+01	1.36E+03	4.16E-02	2.41E+01	1.74E+01
11.00	43.34	10.42	38.37	7.13E-02	41.93	59.65	4.83E+03	0.00E+00	6.32E+01	2.01E+03	5.03E-02	3.16E+01	2.11E+01
11.20	43.23	10.39	37.89	7.23E-02	41.74	57.32	4.51E+03	0.00E+00	6.06E+01	1.32E+03	4.04E-02	2.35E+01	1.69E+01
11.40	43.13	10.36	37.45	7.29E-02	41.54	55.13	4.42E+03	0.00E+00	5.93E+01	1.30E+03	3.97E-02	2.32E+01	1.66E+01
11.60	43.02	10.34	36.93	7.39E-02	41.01	52.56	4.30E+03	0.00E+00	5.77E+01	1.28E+03	3.90E-02	2.28E+01	1.63E+01
11.80	42.92	10.31	36.44	7.46E-02	41.08	50.14	4.19E+03	0.00E+00	5.62E+01	1.27E+03	3.83E-02	2.25E+01	1.60E+01
12.00	42.83	10.29	35.93	7.52E-02	40.80	47.61	4.25E+03	0.00E+00	5.57E+01	1.83E+03	4.53E-02	2.88E+01	1.90E+01
12.20	42.73	10.26	35.34	7.62E-02	40.58	44.69	3.92E+03	0.00E+00	5.26E+01	1.22E+03	3.67E-02	2.17E+01	1.54E+01
12.40	42.65	10.24	34.78	7.68E-02	40.33	41.93	3.78E+03	0.00E+00	5.07E+01	1.20E+03	3.59E-02	2.14E+01	1.50E+01
12.60	42.56	10.22	34.14	7.78E-02	39.67	38.76	3.62E+03	0.00E+00	4.85E+01	1.18E+03	3.49E-02	2.10E+01	1.46E+01
12.80	42.48	10.20	33.54	7.84E-02	39.80	35.78	3.49E+03	0.00E+00	4.68E+01	1.14E+03	3.37E-02	2.02E+01	1.41E+01
13.00	42.41	10.18	32.92	7.91E-02	39.45	32.72	3.51E+03	0.00E+00	4.59E+01	1.67E+03	3.99E-02	2.63E+01	1.67E+01
13.20	42.34	10.17	32.21	8.00E-02	39.20	29.19	3.18E+03	0.00E+00	4.27E+01	1.10E+03	3.19E-02	1.95E+01	1.34E+01
13.40	42.28	10.15	31.55	8.06E-02	38.87	25.90	3.01E+03	0.00E+00	4.04E+01	1.08E+03	3.10E-02	1.92E+01	1.30E+01
13.60	42.22	10.14	30.80	8.16E-02	37.98	22.19	2.80E+03	0.00E+00	3.75E+01	1.06E+03	2.99E-02	1.88E+01	1.25E+01
13.80	42.18	10.13	30.11	8.22E-02	38.06	18.73	2.58E+03	0.00E+00	3.46E+01	1.04E+03	2.88E-02	1.85E+01	1.21E+01
14.00	42.14	10.12	29.40	8.28E-02	37.46	15.20	2.44E+03	0.00E+00	3.20E+01	1.49E+03	3.23E-02	2.35E+01	1.35E+01
14.20	42.10	10.11	28.63	8.38E-02	36.92	11.34	2.03E+03	0.00E+00	2.72E+01	1.01E+03	2.57E-02	1.79E+01	1.08E+01
14.40	42.08	10.10	27.93	8.44E-02	36.18	7.84	1.69E+03	0.00E+00	2.27E+01	1.01E+03	2.39E-02	1.79E+01	1.00E+01
14.60	42.07	10.10	27.21	8.53E-02	34.43	4.22	1.26E+03	0.00E+00	1.69E+01	1.02E+03	2.08E-02	1.81E+01	8.74E+00
14.80	42.06	10.10	26.61	8.60E-02	33.16	1.22	1.02E+03	0.00E+00	1.37E+01	1.06E+03	1.89E-02	1.88E+01	7.92E+00

LNTH	TR(I)	PR(I)	TW(I)	PW(I)	TWL(I)	X(I)	HR(I)	NTUR(I)	UR(I)	HW(I)	NTUW(I)	UW(I	UL(I)
15.00	39.95	10.10	26.04	8.66E-02	31.89	.00	1.02E+03	1.20E-01	1.37E+01	1.09E+03	1.91E-02	1.94E+01	8.02E+00

Table A-6.16(b): The profiles of parameters for Run 58

SUMMARY OF RANGE OF POSSIBLE EVAPORATOR CONDITIONS ASSUMING 50% COMPRESSOR ISENTROPIC EFFICIENCY

COND. PRESS= 11.7 COND. TEMP= 48.18 ENT. H= 225152. ENT. S= 738.22 LEAV. TEMP= 39.17 LEAV. H= 73723. LEAV. S= 269.14

		EVAPORATOR				+	ENTRY		EXIT			+	EVAP	COMP	PRESS	VDOT	COPH
TEMP	PRESS	H(X=0)	H(X=1)	S(X=0)	S(X=1)	+	S	X	S	H	T	+	CAP	CAP	RATIO	CUM/H	
20.00	5.67	54851.	195764.	207.74	688.55	+	272.13	.1339	690.81	196541.	20.94	+	806.	188.	2.061	.73	5.293
22.00	6.00	56775.	196550.	214.20	687.89	+	271.64	.1213	694.88	198725.	24.90	+	820.	173.	1.948	.70	5.730
24.00	6.34	58708.	197327.	220.64	687.26	+	271.18	.1083	698.83	200885.	28.81	+	834.	159.	1.844	.67	6.240
26.00	6.69	60651.	198095.	227.07	686.64	+	270.78	.0951	702.65	203021.	32.67	+	848.	145.	1.746	.64	6.842
28.00	7.06	62604.	198854.	233.48	686.03	+	270.41	.0816	706.36	205134.	36.49	+	862.	131.	1.655	.61	7.564
30.00	7.45	64568.	199604.	239.89	685.44	+	270.09	.0678	709.97	207222.	40.25	+	876.	118.	1.569	.59	8.446
32.00	7.85	66542.	200343.	246.28	684.86	+	269.82	.0537	713.46	209285.	43.96	+	889.	104.	1.489	.56	9.544
34.00	8.26	68528.	201071.	252.66	684.30	+	269.58	.0392	716.85	211327.	47.64	+	903.	91.	1.414	.54	10.953
36.00	8.69	70526.	201788.	259.04	683.73	+	269.38	.0244	720.14	213345.	51.26	+	916.	77.	1.344	.52	12.825
38.00	9.14	72537.	202493.	265.41	683.18	+	269.22	.0091	723.34	215341.	54.85	+	929.	64.	1.279	.50	15.434
40.00	9.60	74562.	203186.	271.78	682.62	+	269.14	-.0065	726.44	217314.	58.39	+	942.	51.	1.217	.48	19.319
42.00	10.08	76600.	203865.	278.14	682.07	+	269.14	-.0226	729.45	219264.	61.89	+	955.	39.	1.159	.46	25.718
44.00	10.58	78653.	204531.	284.51	681.52	+	269.14	-.0392	732.38	221192.	65.35	+	967.	26.	1.104	.44	38.241
46.00	11.10	80722.	205182.	290.89	680.96	+	269.14	-.0562	735.21	223098.	68.77	+	980.	13.	1.053	.42	73.727

SUMMARY OF RANGE OF POSSIBLE EVAPORATOR CONDITIONS ASSUMING 55% COMPRESSOR ISENTROPIC EFFICIENCY

COND. PRESS= 11.7 COND. TEMP= 48.18 ENT. H= 225152. ENT. S= 738.22 LEAV. TEMP= 39.17 LEAV. H= 73723. LEAV. S= 269.14

		EVAPORATOR				+	ENTRY		EXIT			+	EVAP	COMP	PRESS	VDOT	COPH
TEMP	PRESS	H(X=0)	H(X=1)	S(X=0)	S(X=1)	+	S	X	S	H	T	+	CAP	CAP	RATIO	CUM/H	
16.00	5.06	51028.	194168.	194.77	689.93	+	273.27	.1586	692.90	195104.	17.24	+	796.	197.	2.311	.82	5.040
18.00	5.36	52935.	194970.	201.26	689.23	+	272.68	.1464	696.38	197134.	20.98	+	810.	184.	2.181	.78	5.405
20.00	5.67	54851.	195764.	207.74	688.55	+	272.13	.1339	699.75	199142.	24.68	+	823.	171.	2.061	.75	5.822
22.00	6.00	56775.	196550.	214.20	687.89	+	271.64	.1213	703.03	201128.	28.33	+	836.	158.	1.948	.71	6.303
24.00	6.34	58708.	197327.	220.64	687.26	+	271.18	.1083	706.21	203091.	31.94	+	849.	145.	1.844	[illegible]	[illegible]
26.00	6.69	60651.	198095.	227.07	686.64	+	270.78	.0951	709.30	205033.	35.51	+	861.	132.	[illegible]	[illegible]	[illegible]
28.00	7.06	62604.	198854.	233.48	686.03	+	270.41	.0816	712.30	[illegible]	[illegible]	[illegible]	[illegible]	[illegible]	[illegible]	[illegible]	[illegible]
30.00	7.45	64568.	199604.	239.89	685.44	+	270.09	[illegible]	[illegible]	[illegible]	[illegible]	[illegible]	[illegible]	[illegible]	[illegible]	[illegible]	[illegible]
32.00	7.85	66542.	200343.	246.28	[illegible]	[illegible]	[illegible]	[illegible]	[illegible]	[illegible]	[illegible]	[illegible]	[illegible]	[illegible]	[illegible]	[illegible]	[illegible]
34.00	8.26	[illegible]	[illegible]	[illegible]	[illegible]	[illegible]	[illegible]	[illegible]	[illegible]	[illegible]	[illegible]	[illegible]	[illegible]	[illegible]	[illegible]	[illegible]	[illegible]
36.00	[illegible]	[illegible]	[illegible]	[illegible]	[illegible]	[illegible]	[illegible]	[illegible]	[illegible]	[illegible]	[illegible]	[illegible]	[illegible]	70.	[illegible]	[illegible]	[illegible]
[illegible]	[illegible]	[illegible]	[illegible]	[illegible]	[illegible]	[illegible]	[illegible]	[illegible]	[illegible]	[illegible]	[illegible]	[illegible]	[illegible]	59.	[illegible]	[illegible]	[illegible]
[illegible]	[illegible]	[illegible]	[illegible]	[illegible]	[illegible]	[illegible]	[illegible]	[illegible]	[illegible]	[illegible]	[illegible]	[illegible]	[illegible]	47.	1.217	.48	21.251
[illegible]	[illegible]	[illegible]	[illegible]	[illegible]	[illegible]	[illegible]	[illegible]	[illegible]	[illegible]	[illegible]	[illegible]	+	958.	35.	1.159	.46	28.290
[illegible]	[illegible]	[illegible]	[illegible]	[illegible]	[illegible]	[illegible]	[illegible]	[illegible]	733.44	221552.	65.83	+	970.	[illegible]	1.104	.44	42.065
[illegible]	[illegible]	[illegible]	[illegible]	[illegible]	[illegible]	+	269.14	-.0562	735.76	223285.	[illegible]	+	[illegible]	12.	1.053	.42	81.100

SUMMARY OF RANGE OF POSSIBLE EVAPORATOR CONDITIONS ASSUMING 60% COMPRESSOR ISENTROPIC EFFICIENCY

COND. PRESS= 11.7 COND. TEMP= 48.18 ENT. H= 225152. ENT. S= 738.22 LEAV. TEMP= 39.17 LEAV. H= 73723. LEAV. S= 269.14

		EVAPORATOR				+	ENTRY		EXIT			+	EVAP	COMP	PRESS	VDOT	COPH
TEMP	PRESS	H(X=0)	H(X=1)	S(X=0)	S(X=1)	+	S	X	S	H	T	+	CAP	CAP	RATIO	CUM/H	
[illegible]	4.23	45353.	191720.	175.14	692.20	+	275.36	.1938	692.69	191902.	10.21	+	775.	218.	2.761	.97	4.554
12.00	4.49	47237.	192543.	181.71	691.41	+	274.61	.1823	695.74	193825.	13.81	+	788.	206.	2.600	.92	4.834
14.00	4.77	49129.	193359.	188.25	690.66	+	273.92	.1705	698.70	195727.	17.37	+	800.	193.	2.450	.88	5.146
16.00	5.06	51028.	194168.	194.77	689.93	+	273.27	.1586	701.57	197608.	20.89	+	813.	181.	2.311	.83	5.498
18.00	5.36	52935.	194970.	201.26	689.23	+	272.68	.1464	704.37	199469.	24.37	+	825.	168.	2.181	.80	5.896
20.00	5.67	54851.	195764.	207.74	688.55	+	272.13	.1339	707.08	201310.	27.80	+	837.	156.	2.061	.76	6.351
22.00	6.00	56775.	196550.	214.20	687.89	+	271.64	.1213	709.72	203130.	31.20	+	849.	144.	1.948	.72	6.876
24.00	6.34	58708.	197327.	220.64	687.26	+	271.18	.1083	712.28	204930.	34.55	+	861.	133.	1.844	.69	7.488
26.00	6.69	60651.	198095.	227.07	686.64	+	270.78	.0951	714.78	206710.	37.87	+	872.	121.	1.746	.66	8.211
28.00	7.06	62604.	198854.	233.48	686.03	+	270.41	.0816	717.20	208470.	41.16	+	884.	109.	1.655	.63	9.077
30.00	7.45	64568.	199604.	239.89	685.44	+	270.09	.0678	719.56	210211.	44.40	+	895.	98.	1.569	.60	10.135
32.00	7.85	66542.	200343.	246.28	684.86	+	269.82	.0537	721.84	211930.	47.61	+	907.	87.	1.489	.57	11.452
34.00	8.26	68528.	201071.	252.66	684.30	+	269.58	.0392	724.07	213631.	50.79	+	918.	76.	1.414	.55	13.143
36.00	8.69	70526.	201788.	259.04	683.73	+	269.38	.0244	726.24	215313.	53.94	+	929.	65.	1.344	.53	15.390
38.00	9.14	72537.	202493.	265.41	683.18	+	269.22	.0091	728.35	216976.	57.06	+	940.	54.	1.279	.50	18.521
40.00	9.60	74562.	203186.	271.78	682.62	+	269.14	-.0065	730.40	218620.	60.14	+	951.	43.	1.217	.48	23.183
42.00	10.08	76600.	203865.	278.14	682.07	+	269.14	-.0226	732.39	220246.	63.20	+	961.	32.	1.159	.46	30.862
44.00	10.58	78653.	204531.	284.51	681.52	+	269.14	-.0392	734.33	221852.	66.22	+	972.	22.	1.104	.44	45.889
46.00	11.10	80722.	205182.	290.89	680.96	+	269.14	-.0562	736.22	223441.	69.22	+	982.	11.	1.053	.42	88.473

Table A-6.16(c): Summary of range of possible evaporator conditions for Run 58

****** TUBE-BESIDE-TUBE CONDENSER SIMULATION ****** ASSUME TUBE WALLS HAVE INFINITE CONDUCTIVITY ******
GEOMETRY: SUBCOOLER 7.50M OF 5.75MM OD. CONDENSER: 7.50M OF 5.75MM OD. WATER SIDE 7.65MM OD. ALL WALLS .74MM THICK.
BOND CNDCTNCE 500.0W/M.C THML PWR 963.6W. WATER IN 26.7C. HOT GAS 73.9C. DEW POINT 49.7C. SUBCLD LIQD 41.2C.

ITERATION NUMBER: 12 USED I= 151 SEGMENTS. TRIAL WATER EXIT TEMP: 51.5010 CORRESPONDING TO TW(I)= 26.4892 & TR(I)= 39.7606

EXIT WATER TEMP 51.50C. FLOW RATE 9.2976 GRAM/SEC. WATER PRESS DROP .0664 BAR. PUMP PWR .0618 WATT (OR .0064%)
REFRIGERANT MASS FLOW RATE 6.427E+00 GRAM/SEC

SEPARATE RESULTS FOR THE THREE SEGMENTS	SUPE RHEAT	TWO-PHASE	SUBCOOLER	TOTAL/AVERAGE
LENGTH OF EACH SEGMENT IN METRES	2.5750E+00	1.2400E+01	2.5000E-02	1.5000E+01
MASS OF REFRIGERANT IN KG.	2.4625E-03	3.4204E-02	1.7865E-03	3.8453E-02
REFRIG SIDE HEAT TRANS COEFNT: W/SQ M C.	7.9567E+02	4.5468E+03	1.0116E+03	3.8775E+03
REFRIG SIDE LINEAR H.T.C.: W/M C.	1.0623E+01	6.0691E+01	1.3570E+01	5.1758E+01
REFRIGERANT SIDE REYNOLDS NUMBER	1.3187E+05	3.0908E+03	9.9105E+03	2.5310E+04
WATER SIDE HEAT TRANS COEFNT: W/SQ M C.	1.7340E+03	1.4260E+03	9.8967E+02	1.4761E+03
WATER SIDE LINEAR H.T.C. W/M C.	2.9878E+01	2.4559E+01	1.7567E+01	2.5429E+01
WATER SIDE REYNOLDS NUMBER	3.8068E+03	3.3755E+03	2.4267E+03	3.4435E+03
OVERALL LINEAR CONDUCTANCE: W/M C	7.8220E+00	1.7065E+01	7.6561E+00	1.5411E+01
NO. OF HEAT TRANSFER UNITS REFRIG. SIDE	3.8851	.1167	.1167	4.1186
NO. OF HEAT TRANSFER UNITS WATER SIDE	.5240	5.4506	.0197	5.9943
EFFECTIVENESS OF EACH SEGMENT (PERCENT)	96.9752	96.4994	10.9189	68.1312
REFRIGERANT SIDE PRESSURE DROP IN BAR	1.8670E-01	1.2858E+00	2.4000E-03	1.4749E+00
THERMAL POWER PICK-UP BY WATER (W & %)	127.9(13.2)	832.7(85.7)	10.7(1.1)	971.4
THERMAL POWER TRANSFERRED BY R12 (W & %)	125.9(12.9)	836.5(86.0)	10.6(1.1)	973.1
TOTAL MAX THERMAL POWER WITHOUT LOSS (W)	125.91	836.52	10.64	973.07
THERMAL POWER LOSS FROM FREON (W & %)	.0000	.0000	.0000	.00(.0)
SPECIFIC ENTHALPY OF REFRIG (J/KG)	2.2571E+05	2.0612E+05	7.5974E+04	7.4319E+04
SPECIFIC ENTROPY OF R12 (J/KG.C)	7.3775E+02	6.8011E+02	2.7619E+02	2.7101E+02
REFRIGERANT TEMPERATURE (DEG.C)	7.3918E+01	4.8982E+01	4.1387E+01	3.9761E+01
REFRIGERANT PRESSURE (BAR)	1.2114E+01	1.1927E+01	1.0642E+01	1.0639E+01
WATER TEMPERATURE (DEG.C)	5.1501E+01	4.8204E+01	2.6764E+01	2.6489E+01

RATE OF LOSS OF ENTHALPY BY R12 9.7307E+02 WATTS RATE OF GAIN OF ENTHALPY BY WATER 9.7135E+02 WATTS
CORRESPONDING TO AN ENERGY IMBALANCE OF -1.7178E+00 WATTS OR -.1783 % OF SPECIFIED POWER

THE POWER LOSS BY R12 TO OUTSIDE -8.4401E+00WATTS BY -.8776 % OF THE SPECIFIED POWER
THE POWER LOSS BY WATER TO OUTSIDE -7.7220E+00 WATTS BY -.8014 % OF THE SPECIFIED POWER

RATE OF LOSS OF ENTROPY BY R12 2.9999E+00 WATTS/C RATE OF INCREASE OF ENTROPY BY WATER 3.1135E+00 WATTS/C
NET RATE OF ENTROPY FLOW THRU SYSTEM BOUNDARY 1.1366E-01 WATT/C THERMAL ENTROPY CREATION RATE 8.3157E-02 WATT/C
R12 P.D. ENTROPY CREATION RATE 3.0503E-02 WATT/C RATE OF LOSS OF GROSS WORK 3.6699E+01 WATTS AT 49.74 C

RATE OF ENTROPY GAIN OF WATER HAD IT BEEN 10C HOTTER 3.0154E+00 WATTS/C. FOR SAME GROSS RATE OF ENTROPY INCREASE,
A COUNTER-FLOW WATER-WATER HEAT EXCHANGER WOULD HAVE DELTA-T OF 11.5822 DEG C CORRESPONDING TO AN EFFECTIVENESS OF 68.35%
OR 2.160 HEAT TRANSFER UNITS, WHICH IS 36.03 % OF THAT FOR THE WATER SIDE OF THE PRESENT HT.XR.

Table A-6.17(a): Results in three segments for Run 60

LNTH	TR(I)	PR(I)	TW(I)	PW(I)	TWL(I)	X(I)	HR(I)	NTUR(I)	UR(I)	HW(I)	NTUW(I)	UW(I	UL(I)
.00	73.92	12.11	51.50	0.00E+00	62.71	100.00	8.11E+02	1.61E-01	1.09E+01	1.70E+03	2.06E-02	3.01E+01	7.99E+00
.20	67.61	12.10	50.69	6.14E-04	55.32	100.00	8.25E+02	1.59E-01	1.11E+01	1.66E+03	2.07E-02	2.95E+01	8.05E+00
.40	62.93	12.08	50.08	1.24E-03	53.59	100.00	8.11E+02	1.55E-01	1.09E+01	1.63E+03	2.04E-02	2.90E+01	7.91E+00
.60	59.33	12.07	49.60	3.25E-03	52.00	100.00	8.03E+02	1.52E-01	1.08E+01	1.61E+03	2.02E-02	2.86E+01	7.82E+00
.80	56.75	12.05	49.26	3.87E-03	51.30	100.00	7.93E+02	1.49E-01	1.06E+01	1.60E+03	1.99E-02	2.84E+01	7.74E+00
1.00	54.79	12.04	49.00	4.49E-03	50.47	100.00	8.24E+02	1.59E-01	1.08E+01	2.33E+03	2.15E-02	3.67E+01	8.33E+00
1.20	53.24	12.02	48.79	6.48E-03	50.00	100.00	7.83E+02	1.45E-01	1.05E+01	1.58E+03	1.97E-02	2.80E+01	7.64E+00
1.40	52.10	12.01	48.63	7.10E-03	49.58	100.00	7.79E+02	1.44E-01	1.05E+01	1.57E+03	1.96E-02	2.79E+01	7.60E+00
1.60	51.19	11.99	48.51	9.08E-03	49.17	100.00	7.77E+02	1.43E-01	1.04E+01	1.57E+03	1.95E-02	2.78E+01	7.58E+00
1.80	50.51	11.98	48.42	9.70E-03	48.99	100.00	7.74E+02	1.42E-01	1.04E+01	1.56E+03	1.95E-02	2.77E+01	7.55E+00
2.00	49.99	11.97	48.34	1.03E-02	48.76	100.00	8.07E+02	1.53E-01	1.06E+01	2.29E+03	2.11E-02	3.61E+01	8.17E+00
2.20	49.56	11.95	48.28	1.23E-02	48.63	100.00	7.71E+02	1.41E-01	1.03E+01	1.56E+03	1.94E-02	2.76E+01	7.52E+00
2.40	49.24	11.94	48.24	1.29E-02	48.51	100.00	7.70E+02	1.40E-01	1.03E+01	1.55E+03	1.94E-02	2.76E+01	7.51E+00

LNTH	TR(I)	PR(I)	TW(I)	PW(I)	TWL(I)	X(I)	HR(I)	NTUR(I)	UR(I)	HW(I)	NTUW(I)	UW(I	UL(I)
2.60	48.98	11.93	48.20	1.49E-02	48.40	99.94	8.90E+02	0.00E+00	1.19E+01	1.55E+03	2.15E-02	2.76E+01	8.33E+00
2.80	49.00	11.91	48.16	1.55E-02	48.48	99.76	1.57E+03	0.00E+00	2.11E+01	1.55E+03	3.08E-02	2.76E+01	1.20E+01
3.00	48.93	11.89	48.11	1.61E-02	48.49	99.51	2.29E+03	0.00E+00	2.99E+01	2.28E+03	4.20E-02	3.59E+01	1.63E+01
3.20	48.86	11.87	48.04	1.81E-02	48.49	99.20	2.77E+03	0.00E+00	3.71E+01	1.55E+03	4.07E-02	2.75E+01	1.58E+01
3.40	48.79	11.85	47.97	1.87E-02	48.47	98.87	3.42E+03	0.00E+00	4.59E+01	1.55E+03	4.42E-02	2.74E+01	1.72E+01
3.60	48.72	11.83	47.89	2.07E-02	48.39	98.48	4.18E+03	0.00E+00	5.61E+01	1.54E+03	4.74E-02	2.74E+01	1.84E+01
3.80	48.66	11.81	47.81	2.13E-02	48.39	98.09	4.91E+03	0.00E+00	6.59E+01	1.54E+03	4.98E-02	2.73E+01	1.93E+01
4.00	48.59	11.80	47.72	2.19E-02	48.34	97.67	5.92E+03	0.00E+00	7.74E+01	2.26E+03	6.27E-02	3.55E+01	2.43E+01
4.20	48.52	11.78	47.61	2.38E-02	48.29	97.18	6.54E+03	0.00E+00	8.78E+01	1.53E+03	5.35E-02	2.72E+01	2.08E+01
4.40	48.45	11.76	47.51	2.45E-02	48.24	96.70	6.73E+03	0.00E+00	9.03E+01	1.53E+03	5.37E-02	2.71E+01	2.08E+01
4.60	48.38	11.74	47.40	2.64E-02	48.11	96.15	6.55E+03	0.00E+00	8.79E+01	1.49E+03	5.23E-02	2.64E+01	2.03E+01
4.80	48.31	11.72	47.29	2.70E-02	48.07	95.65	6.42E+03	0.00E+00	8.61E+01	1.48E+03	5.20E-02	2.63E+01	2.02E+01
5.00	48.23	11.70	47.18	2.76E-02	47.98	95.13	6.58E+03	0.00E+00	8.62E+01	2.23E+03	6.42E-02	3.50E+01	2.49E+01
5.20	48.15	11.68	47.06	2.96E-02	47.89	94.54	6.19E+03	0.00E+00	8.31E+01	1.48E+03	5.13E-02	2.62E+01	1.99E+01
5.40	48.08	11.66	46.94	3.02E-02	47.80	93.99	6.10E+03	0.00E+00	8.19E+01	1.47E+03	5.10E-02	2.61E+01	1.98E+01
5.60	47.99	11.63	46.81	3.21E-02	47.65	93.35	6.02E+03	0.00E+00	8.07E+01	1.47E+03	5.07E-02	2.60E+01	1.97E+01
5.80	47.91	11.61	46.68	3.27E-02	47.61	92.76	5.94E+03	0.00E+00	7.97E+01	1.46E+03	5.04E-02	2.59E+01	1.96E+01
6.00	47.83	11.59	46.55	3.33E-02	47.51	92.16	6.14E+03	0.00E+00	8.03E+01	2.19E+03	6.22E-02	3.45E+01	2.41E+01
6.20	47.75	11.57	46.40	3.52E-02	47.41	91.45	5.81E+03	0.00E+00	7.79E+01	1.45E+03	4.99E-02	2.57E+01	1.94E+01
6.40	47.66	11.54	46.26	3.58E-02	47.31	90.80	5.75E+03	0.00E+00	7.71E+01	1.45E+03	4.96E-02	2.57E+01	1.93E+01
6.60	47.57	11.52	46.10	3.77E-02	47.14	90.03	5.68E+03	0.00E+00	7.62E+01	1.44E+03	4.93E-02	2.56E+01	1.91E+01
6.80	47.49	11.50	45.95	3.83E-02	47.10	89.33	5.63E+03	0.00E+00	7.55E+01	1.43E+03	4.90E-02	2.55E+01	1.90E+01
7.00	47.40	11.47	45.80	3.89E-02	46.98	88.60	5.86E+03	0.00E+00	7.67E+01	2.15E+03	6.04E-02	3.38E+01	2.35E+01
7.20	47.30	11.45	45.62	3.98E-02	46.88	87.74	5.56E+03	0.00E+00	7.46E+01	1.42E+03	4.86E-02	2.52E+01	1.89E+01
7.40	47.21	11.42	45.45	4.04E-02	46.77	86.94	5.52E+03	0.00E+00	7.41E+01	1.42E+03	4.83E-02	2.51E+01	1.88E+01
7.60	47.12	11.40	45.25	4.13E-02	46.56	86.00	5.48E+03	0.00E+00	7.36E+01	1.41E+03	4.81E-02	2.50E+01	1.87E+01
7.80	47.02	11.37	45.06	4.19E-02	46.53	85.12	5.45E+03	0.00E+00	7.31E+01	1.40E+03	4.78E-02	2.49E+01	1.86E+01
8.00	46.93	11.35	44.87	4.25E-02	46.39	84.21	5.66E+03	0.00E+00	7.41E+01	2.10E+03	5.88E-02	3.30E+01	2.28E+01
8.20	46.83	11.32	44.64	4.34E-02	46.27	83.13	5.37E+03	0.00E+00	7.20E+01	1.39E+03	4.72E-02	2.46E+01	1.83E+01
8.40	46.73	11.29	44.43	4.40E-02	46.15	82.12	5.33E+03	0.00E+00	7.15E+01	1.38E+03	4.69E-02	2.44E+01	1.82E+01
8.60	46.63	11.27	44.18	4.49E-02	45.90	80.94	5.28E+03	0.00E+00	7.09E+01	1.37E+03	4.66E-02	2.43E+01	1.81E+01
8.80	46.54	11.24	43.94	4.54E-02	45.87	79.82	5.24E+03	0.00E+00	7.03E+01	1.36E+03	4.63E-02	2.41E+01	1.80E+01
9.00	46.44	11.22	43.69	4.60E-02	45.72	78.65	5.43E+03	0.00E+00	7.11E+01	1.99E+03	5.59E-02	3.13E+01	2.17E+01
9.20	46.33	11.19	43.40	4.69E-02	45.58	77.27	5.14E+03	0.00E+00	6.90E+01	1.34E+03	4.55E-02	2.38E+01	1.77E+01
9.40	46.23	11.16	43.12	4.75E-02	45.44	75.96	5.10E+03	0.00E+00	6.83E+01	1.33E+03	4.52E-02	2.36E+01	1.75E+01
9.60	46.13	11.13	42.80	4.84E-02	45.13	74.42	5.04E+03	0.00E+00	6.76E+01	1.32E+03	4.47E-02	2.34E+01	1.74E+01
9.80	46.03	11.11	42.49	4.89E-02	45.12	72.96	4.98E+03	0.00E+00	6.68E+01	1.31E+03	4.43E-02	2.32E+01	1.72E+01
10.00	45.93	11.08	42.16	4.95E-02	44.94	71.43	5.15E+03	0.00E+00	6.74E+01	1.91E+03	5.35E-02	3.00E+01	2.08E+01
10.20	45.83	11.05	41.78	5.04E-02	44.78	69.62	4.85E+03	0.00E+00	6.51E+01	1.28E+03	4.34E-02	2.27E+01	1.68E+01
10.40	45.73	11.03	41.42	5.10E-02	44.61	67.90	4.79E+03	0.00E+00	6.42E+01	1.27E+03	4.29E-02	2.25E+01	1.67E+01
10.60	45.62	11.00	40.99	5.18E-02	44.22	65.88	4.71E+03	0.00E+00	6.32E+01	1.25E+03	4.23E-02	2.22E+01	1.64E+01
10.80	45.52	10.98	40.58	5.24E-02	44.24	63.96	4.63E+03	0.00E+00	6.21E+01	1.24E+03	4.18E-02	2.20E+01	1.62E+01
11.00	45.43	10.95	40.16	5.29E-02	44.01	61.94	4.76E+03	0.00E+00	6.23E+01	1.80E+03	5.01E-02	2.83E+01	1.95E+01
11.20	45.33	10.92	39.66	5.38E-02	43.86	59.59	4.45E+03	0.00E+00	5.97E+01	1.18E+03	4.00E-02	2.10E+01	1.55E+01
11.40	45.23	10.90	39.19	5.43E-02	43.66	57.37	4.36E+03	0.00E+00	5.85E+01	1.16E+03	3.93E-02	2.07E+01	1.53E+01
11.60	45.14	10.87	38.64	5.52E-02	43.13	54.77	4.25E+03	0.00E+00	5.70E+01	1.15E+03	3.86E-02	2.03E+01	1.50E+01
11.80	45.05	10.85	38.12	5.57E-02	43.22	52.32	4.14E+03	0.00E+00	5.55E+01	1.13E+03	3.79E-02	2.00E+01	1.47E+01
12.00	44.96	10.83	37.58	5.63E-02	42.94	49.75	4.21E+03	0.00E+00	5.51E+01	1.63E+03	4.51E-02	2.57E+01	1.75E+01
12.20	44.87	10.81	36.96	5.71E-02	42.74	46.77	3.88E+03	0.00E+00	5.21E+01	1.09E+03	3.64E-02	1.94E+01	1.41E+01
12.40	44.79	10.78	36.36	5.77E-02	42.49	43.96	3.75E+03	0.00E+00	5.03E+01	1.07E+03	3.56E-02	1.90E+01	1.38E+01
12.60	44.71	10.76	35.68	5.85E-02	41.82	40.72	3.59E+03	0.00E+00	4.81E+01	1.05E+03	3.46E-02	1.87E+01	1.35E+01
12.80	44.63	10.74	35.04	5.90E-02	41.93	37.67	3.46E+03	0.00E+00	4.64E+01	1.03E+03	3.38E-02	1.83E+01	1.31E+01
13.00	44.57	10.73	34.37	5.96E-02	41.59	34.50	3.48E+03	0.00E+00	4.55E+01	1.49E+03	3.98E-02	2.34E+01	1.55E+01
13.20	44.50	10.71	33.61	6.04E-02	41.34	30.87	3.16E+03	0.00E+00	4.24E+01	9.78E+02	3.17E-02	1.74E+01	1.23E+01
13.40	44.44	10.70	32.90	6.09E-02	41.05	27.50	3.00E+03	0.00E+00	4.02E+01	9.61E+02	3.08E-02	1.71E+01	1.20E+01
13.60	44.39	10.68	32.10	6.17E-02	40.15	23.68	2.80E+03	0.00E+00	3.75E+01	9.43E+02	2.98E-02	1.67E+01	1.16E+01
13.80	44.35	10.67	31.35	6.23E-02	40.25	20.11	2.59E+03	0.00E+00	3.47E+01	9.30E+02	2.88E-02	1.65E+01	1.12E+01
14.00	44.31	10.66	30.59	6.28E-02	39.66	16.47	2.46E+03	0.00E+00	3.22E+01	1.33E+03	3.26E-02	2.08E+01	1.27E+01
14.20	44.28	10.65	29.75	6.36E-02	39.12	12.45	2.06E+03	0.00E+00	2.76E+01	9.11E+02	[illegible]	[illegible]	[illegible]
14.40	44.25	10.65	28.98	6.42E-02	38.33	8.77	1.73E+03	0.00E+00	2.33E+01	9.13E+02	[illegible]	[illegible]	9.55E+00
14.60	44.24	10.64	28.18	6.50E-02	36.56	4.91	1.31E+03	0.00E+00	1.76E+01	9.16E+02	2.17E-02	1.63E+01	8.46E+00
14.80	44.23	10.64	27.50	6.55E-02	[illegible]	1.63	7.82E+02	0.00E+00	1.05E+01	9.59E+02	1.67E-02	1.70E+01	6.49E+00

LNTH	TR(I)	PR(I)	TW(I)	PW(I)	TWL(I)	X(I)	HR(I)	NTUR(I)	UR(I)	HW(I)	NTUW(I)	UW(I	UL(I)
15.00	41.39	10.64	26.76	6.61E-02	34.71	.00	1.01E+03	1.17E-01	1.36E-01	9.90E+02	1.97E-02	1.76E+01	[illegible]

Table A-6.17(b): The profiles of parameters for Run 60

SUMMARY OF RANGE OF POSSIBLE EVAPORATOR CONDITIONS ASSUMIMG 50% COMPRESSOR ISENTROPIC EFFICIENCY
COND. PRESS= 12.1 COND. TEMP= 49.74 ENT. H= 225714. ENT. S= 737.75 LEAV. TEMP= 41.20 LEAV. H= 75787. LEAV. S= 275.61

		EVAPORATOR				+	ENTRY		EXIT			+	EVAP	COMP	PRESS	VDOT	COPH
TEMP	PRESS	H(X=0)	H(X=1)	S(X=0)	S(X=1)	+	S	X	S	H	T	+	CAP	CAP	RATIO	CUM/H	
22.00	6.00	56775.	196550.	214.20	687.89	+	278.63	.1360	691.94	197868.	23.68	+	785.	179.	2.020	.69	5.384
24.00	6.34	58708.	197327.	220.64	687.26	+	278.13	.1232	695.92	200026.	27.59	+	799.	165.	1.911	.65	5.836
26.00	6.69	60651.	198095.	227.07	686.64	+	277.68	.1101	699.78	202160.	31.46	+	812.	151.	1.810	.62	6.365
28.00	7.06	62604.	198854.	233.48	686.03	+	277.27	.0968	703.53	204270.	35.28	+	826.	138.	1.715	.60	6.992
30.00	7.45	64568.	199604.	239.89	685.44	+	276.91	.0831	707.16	206356.	39.05	+	839.	124.	1.627	.57	7.745
32.00	7.85	66542.	200343.	246.28	684.86	+	276.58	.0691	710.68	208417.	42.77	+	852.	111.	1.544	.55	8.668
34.00	8.26	68528.	201071.	252.66	684.30	+	276.30	.0548	714.10	210457.	46.45	+	866.	98.	1.467	.53	9.827
36.00	8.69	70526.	201788.	259.04	683.73	+	276.06	.0401	717.42	212473.	50.08	+	879.	85.	1.394	.50	11.323
38.00	9.14	72537.	202493.	265.41	683.18	+	275.86	.0250	720.64	214467.	53.67	+	891.	72.	1.326	.48	13.331
40.00	9.60	74562.	203186.	271.78	682.62	+	275.69	.0095	723.77	216438.	57.22	+	904.	60.	1.262	.46	16.163
42.00	10.08	76600.	203865.	278.14	682.07	+	275.61	-.0064	726.81	218386.	60.72	+	917.	47.	1.201	.45	20.461
44.00	10.58	78653.	204531.	284.51	681.52	+	275.61	-.0228	729.76	220312.	64.19	+	929.	35.	1.145	.43	27.758
46.00	11.10	80722.	205182.	290.89	680.96	+	275.61	-.0396	732.62	222216.	67.62	+	941.	22.	1.091	.41	42.868
48.00	11.63	82807.	205818.	297.26	680.39	+	275.61	-.0571	735.40	224098.	71.01	+	953.	10.	1.041	.40	92.814

SUMMARY OF RANGE OF POSSIBLE EVAPORATOR CONDITIONS ASSUMIMG 55% COMPRESSOR ISENTROPIC EFFICIENCY
COND. PRESS= 12.1 COND. TEMP= 49.74 ENT. H= 225714. ENT. S= 737.75 LEAV. TEMP= 41.20 LEAV. H= 75787. LEAV. S= 275.61

		EVAPORATOR				+	ENTRY		EXIT			+	EVAP	COMP	PRESS	VDOT	COPH
TEMP	PRESS	H(X=0)	H(X=1)	S(X=0)	S(X=1)	+	S	X	S	H	T	+	CAP	CAP	RATIO	CUM/H	
16.00	5.06	51028.	194168.	194.77	689.93	+	280.42	.1730	690.37	194382.	16.18	+	762.	201.	2.396	.80	4.785
18.00	5.36	52935.	194970.	201.26	689.23	+	279.77	.1609	693.87	196410.	19.93	+	775.	188.	2.261	.76	5.116
20.00	5.67	54851.	195764.	207.74	688.55	+	279.18	.1486	697.27	198415.	23.64	+	788.	175.	2.136	.73	5.492
22.00	6.00	56775.	196550.	214.20	687.89	+	278.63	.1360	700.58	200399.	27.30	+	801.	163.	2.020	.69	5.923
24.00	6.34	58708.	197327.	220.64	687.26	+	278.13	.1232	703.78	202361.	30.91	+	814.	150.	1.911	.66	6.420
26.00	6.69	60651.	198095.	227.07	686.64	+	277.68	.1101	706.90	204301.	34.48	+	826.	138.	1.810	.63	7.002
28.00	7.06	62604.	198854.	233.48	686.03	+	277.27	.0968	709.92	206219.	38.01	+	838.	125.	1.715	.61	7.691
30.00	7.45	64568.	199604.	239.89	665.44	+	276.91	.0831	712.86	208116.	41.49	+	851.	113.	1.627	.58	8.520
32.00	7.85	66542.	200343.	246.28	684.86	+	276.58	.0691	715.71	209989.	44.94	+	863.	101.	1.544	.56	9.535
34.00	8.26	68528.	201071.	252.66	684.30	+	276.30	.0548	718.48	211844.	48.35	+	874.	89.	1.467	.53	10.809
36.00	8.69	70526.	201788.	259.04	683.73	+	276.06	.0401	721.18	213677.	51.72	+	886.	77.	1.394	.51	12.456
38.00	9.14	72537.	202493.	265.41	683.18	+	275.86	.0250	723.80	215489.	55.05	+	898.	66.	1.326	.49	14.664
40.00	9.60	74562.	203186.	271.78	682.62	+	275.69	.0095	726.34	217281.	58.35	+	909.	54.	1.262	.47	17.779
42.00	10.08	76600.	203865.	278.14	682.07	+	275.61	-.0064	728.82	219052.	61.61	+	921.	43.	1.201	.45	22.507
44.00	10.58	78653.	204531.	284.51	681.52	+	275.61	-.0228	731.22	220803.	64.84	+	932.	32.	1.145	.43	30.534
46.00	11.10	80722.	205182.	290.89	680.96	+	275.61	-.0396	733.56	222534.	68.03	+	943.	20.	1.091	.41	47.155
48.00	11.63	82807.	205818.	297.26	680.39	+	275.61	-.0571	735.83	224245.	71.20	+	954.	9.	1.041	.40	102.095

SUMMARY OF RANGE OF POSSIBLE EVAPORATOR CONDITIONS ASSUMIMG 60% COMPRESSOR ISENTROPIC EFFICIENCY
COND. PRESS= 12.1 COND. TEMP= 49.74 ENT. H= 225714. ENT. S= 737.75 LEAV. TEMP= 41.20 LEAV. H= 75787. LEAV. S= 275.61

		EVAPORATOR				+	ENTRY		EXIT			+	EVAP	COMP	PRESS	VDOT	COPH
TEMP	PRESS	H(X=0)	H(X=1)	S(X=0)	S(X=1)	+	S	X	S	H	T	+	CAP	CAP	RATIO	CUM/H	
12.00	4.49	47237.	192543.	181.71	691.41	+	281.85	.1965	693.58	193213.	12.91	+	755.	209.	2.696	.90	4.613
14.00	4.77	49129.	193359.	188.25	690.66	+	281.11	.1848	696.56	195113.	16.47	+	767.	197.	2.540	.85	4.899
16.00	5.06	51028.	194168.	194.77	689.93	+	280.42	.1730	699.46	196993.	19.99	+	779.	185.	2.396	.81	5.220
18.00	5.36	52935.	194970.	201.26	689.23	+	279.77	.1609	702.27	198852.	23.47	+	791.	173.	2.261	.78	5.581
20.00	5.67	54851.	195764.	207.74	688.55	+	279.18	.1486	705.00	200690.	26.91	+	803.	161.	2.136	.74	5.991
22.00	6.00	56775.	196550.	214.20	687.89	+	278.63	.1360	707.66	202509.	30.31	+	814.	149.	2.020	.71	6.461
24.00	6.34	58708.	197327.	220.64	687.26	+	278.13	.1232	710.24	204307.	33.67	+	826.	138.	1.911	.67	7.004
26.00	6.69	60651.	198095.	227.07	686.64	+	277.68	.1101	712.75	206085.	36.99	+	837.	126.	1.810	.64	7.638
28.00	7.06	62604.	198854.	233.48	686.03	+	277.27	.0968	715.19	207844.	40.28	+	849.	115.	1.715	.61	8.390
30.00	7.45	64568.	199604.	239.89	685.44	+	276.91	.0831	717.56	209583.	43.53	+	860.	104.	1.627	.59	9.294
32.00	7.85	66542.	200343.	246.28	684.86	+	276.58	.0691	719.86	211300.	46.75	+	871.	93.	1.544	.56	10.402
34.00	8.26	68528.	201071.	252.66	684.30	+	276.30	.0548	722.11	212999.	49.93	+	882.	82.	1.467	.54	11.792
36.00	8.69	70526.	201788.	259.04	683.73	+	276.06	.0401	724.29	214680.	53.08	+	893.	71.	1.394	.51	13.588
38.00	9.14	72537.	202493.	265.41	683.18	+	275.86	.0250	726.41	216341.	56.20	+	903.	60.	1.326	.49	15.997
40.00	9.60	74562.	203186.	271.78	682.62	+	275.69	.0095	728.48	217984.	59.29	+	914.	50.	1.262	.47	19.396
42.00	10.08	76600.	203865.	278.14	682.07	+	275.61	-.0064	730.48	219607.	62.35	+	924.	39.	1.201	.45	24.553
44.00	10.58	78653.	204531.	284.51	681.52	+	275.61	-.0228	732.44	221213.	65.38	+	935.	29.	1.145	.43	33.309
46.00	11.10	80722.	205182.	290.89	680.96	+	275.61	-.0396	734.34	222799.	68.38	+	945.	19.	1.091	.41	51.442
48.00	11.63	82807.	205818.	297.26	680.39	+	275.61	-.0571	736.19	224367.	71.36	+	955.	9.	1.041	.40	111.376

Table A-6.17 (c): Summary of range of possible evaporator conditions for Run 60